Proceedings of the 5th International Conference on Civil Engineering for Sustainable Development (ICCESD 2020), 7~9 February 2020, KUET, Khulna, Bangladesh (ISBN-978-984-34-8764-3)

FLOOD INUNDATION MAPPING ON TEESTA FLOODPLAIN USING HEC-RAS 1D/2D COUPLE MODEL

Tarannum Tabassum Islam[1], Mashrura Yeasmine Auditia[2], Purnima Das*[3] and Md. Sabbir Mostafa Khan[4]

[1]Student of Military Institute of Science and Technology (MIST), Dhaka, Bangladesh, e-mail: x1528.equilibria@gmail.com
[2]Student of Military Institute of Science and Technology (MIST), Dhaka, Bangladesh, e-mail: mashrura.auditia904@gmail.com
[3]Graduate Student of Bangladesh University of Engineering and Technology (BUET), Dhaka, Bangladesh, e-mail: pinkiwre10@gmail.com
[4]Professor of Bangladesh University of Engineering and Technology (BUET), Dhaka, Bangladesh, e-mail: sabbbirkhanbuet@gmail.com

***Corresponding Author**

ABSTRACT

Bangladesh is known as one of the highest flood prone countries in the world, being located at the convergence of the three major rivers named Ganges, the Jamuna and the Meghna. Bangladesh is a low-lying country which is situated on the lower elevation of Ganges Delta and the many distributaries which flow into the Bay of Bengal. Flood frequently takes place in Bangladesh, causing enormous losses in terms of property and life. A large amount of border monsoon runoff, together with its own runoff through a network of rivers, are drained out forcefully by Bangladesh. Most of the time the capacity of the drainage channels is exceeded by the volume of generated runoff, and this makes Bangladesh one of the most vulnerable countries in the world. Almost one fifth of our country is flooded every year. In case of severe flood, up to 68% of the total area remains inundated on average.

Teesta is one of the major rivers in the northern region of Bangladesh. From its entrance into Bangladesh to the Kamargani Moura of Gaibandha, it makes a total runoff of about 120 km where it meets the river Brahmaputra. In the months of June to September, the Teesta flow is greatest when there is massive monsoon rain and abundant meltwater supplied by the glaciers. The main objective of the study is to show the capacity of HEC-RAS 1D/2D coupled model to simulate the flood inundation of the Teesta river floodplain.

To create a HEC-RAS 1D/2D coupled model, GIS software and HEC-GeoRAS tool was used to produce an appropriate river geometry. The hydrological data were collected from the BWBD (Bangladesh Water Development Board). Discharge and water level data were defined for the boundary condition of upstream and downstream. After that, with the help of collected hydrological data, the channel calibration and validation were performed. Using RAS Mapper, the flood inundation map was generated after the model had been calibrated and validated for Manning's value n=0.031. A lateral structure was placed on a tentative mid-way of the river reach to connect with 2D mesh flow areas to the left and right. At the end of the study, the area which was inundated during the flood season was determined with respect to the total floodplain area.

Keywords: *Teesta, HEC-RAS, HEC-GeoRAS, Floodplain, Inundation.*

1.INTRODUCTION

Bangladesh is a low-lying country which is highly prone to cyclones, river erosions and floods. Among all, flood is the most prevalent one. Flood is one of the most subversive natural hazards in Bangladesh, and has a great impact on the society. The plate of Bangladesh is mostly flat, with an exception of some hilly regions located mostly to the south-east region of the country. As being located on the Ganges Delta and many tributaries flowing into the Bay of Bengal, flood occurs almost every year in Bangladesh. In summer from the month of June to October heavy monsoon rainfall occurs. The annual average rainfall varies from 1200 mm in the west to 5800 mm in the northeast. (Rahman,1996)

According to IPCC (2013), Bangladeshis are highly vulnerable to climate changes where both monsoon rainfall and sea level will be raised. Flood cataclysm will be invaded for increasing monsoon rainfall and raising sea level. Bangladesh has faced floods of an immense magnitude in 1974, 1984, 1987, 1988, 1998, 2000 and 2004 (FFWC 2005). In the year of 1988,1998 and 2004 the floods are inundated about 61%, 68% and 38% respectively of the total area of a country (Rahman et al. 2007). Recent disastrous flood took place in 1988, 1998, 2004, and 2007 which caused losses from one to over two million metric tons of rice, or 4–10 % of the annual rice production (Islam, et. al., 2009). Flood prone districts in Bangladesh serve to have consistently greater headcount ratios of poverty and that floods cause subsidence in poverty headcount ratio, especially in historically flood-prone areas (Dasgupta, 2007)

Teesta is the tributary river of Jamuna which is flowing through India and Bangladesh. It originates in Himalayas near Chungthang in Sikkims and flows to the South. The Teesta river flow initiates from Jalpaiguri (India) by the three channels, named the Karotoya, Punarbhaba and Atrai. The Teesta is one of the most significant rivers in Northern Region. Without provoking flood, the Teesta with huge amount of water left over, could not pass down the Atrai. The catchment areas of Teesta are the Sikkim, Darjeeling and northern part of Bangladesh. The Teesta subject area is the largest sub-regions of Bengal basin. It covers almost the entire Rangpur district.

The Teesta flood plain is bound by latitudes 25.30 to 26.18 N' and longitudes 88.52 to 89.45 E'. The present districts of Lalmonirhat, Nilphamari, Gaibandha, Kurigram and Rangpur are included in that boundary. An area of about 3861.5 square kilometers is covered by the 14 thanas located in the floodplain region of Teesta river. We can know, with this study, the amount of area that will be flooded for the given discharge. We need to know the amount of flood plain areas that will be flooded due to the increasing and decreasing discharge at various rates. A two-dimensional model is required for flood inundation modeling. For this, hydrodynamic model of one dimensional (1D) and two dimensional (2D) is used in combined. It includes the river as 1D and flood plain as 2D. Using the HEC-RAS software 1D/2D coupled model has been done which has given some special features. An implicit finite volume algorithm is used for the 2D unsteady equation solving. The detailed flood mapping is utilized in this software. By this along with the simulation of flood stage, the amount of flooding that has increased or decreased over the year can be evaluated.

2.METHODOLOGY

2.1 Data Collection

For the study, data of recent and previous years have been collected to develop the hydrodynamic model. These data are required for analysis of the hydrodynamic model and for further interpretation of the condition of the study area. Various hydrologic data, namely water level and discharge data were used along with topographic data, which includes river cross-sections and Digital Elevation Model (DEM). Pre-processing of the data in GIS was a necessary step for further developing the mathematical model for inundation mapping. The collected DEM data for Bangladesh is of 30 m x 30

m resolution. The DEM elevation has been measured taking the mean sea level as datum. All the data used in pre-processing has projected to Bangladesh Transverse Mercator (BTM).

2.2 Data Analysis

After taking the DEM of Bangladesh, the shape file of the floodplain identified for Teesta River in the North West Zone of Bangladesh has been superimposed. The DEM of the study area has been clipped using the clipping tool in Arc-GIS ArcToolbox (Figure-1). After the required DEM has been clipped from the original DEM file, it is converted from Raster type to TIN file by using the Raster to TIN tool in the Arc Toolbox. The purpose of using the Raster to TIN tool is to create a Triangulated Irregular Network (TIN) whose surface does not differ from the input raster by more than a specified Z value. To create 1D geometry of the river, we used only the bathymetric grid and excluded the river floodplain. This was done for developing the spatial data required to generate a HEC-RAS import file with a 3-D river network and 3-D cross sections. This extraction follows several steps before being completed, which are, creation of a river centreline, cross-sections, river banks, and flow path lines as shape files, keeping certain rules in mind which must be followed for proper execution of the work. After completing the extraction, the 1D geometric data was imported into HEC-RAS, where further processing was done (Figure-2).

The floodplain was then divided into two parts of the river and 2D mesh were created on each side of the river. The cell size used for creating the 2D mesh was 400 x 400. After the analysis of mesh, the cells were created. 1D and 2D model were coupled using a lateral structure on the upstream of river. The bank elevation and the elevation of the lateral structure were kept approximately close in the model. Later, the lateral structure was made to breach to depict actual flooding condition and then ran the geometric pre-processor from RAS-Mapper. Finally, boundary condition lines were drawn at the upstream and downstream part of the river flood plain. For the calibration and validation of unsteady flow data, different boundary conditions were applied for different time series. In case of 2D connection, additional boundary condition needs to be applied. Hence, in order to allow entrance of water flow from outside, discharge data was provided at the upstream boundary condition Data of year 2013 have been used to calibrate and of year 2016 have been used to validate the hydrodynamic model for Teesta river. After iterating calibration graphs for Manning's n ranging from 0.015 to 0.035, 0.031 was fixed as calibrated value and the graph was then verified with n value as 0.031.

2.3 Mapping and Visualization

The floodplain for Teesta river was delineated based on year 2004, as one the most recent devastating flood in Bangladesh occurred in 2004. The calibrated and validated model was used for generating water surface profiles for different flow conditions. Flood discharge water profile for 2004 was firstly generated, followed by water surface profiles with an interval of one-day for the duration June to October. The water surface profile which was generated, have been exported in GIS format for development of flood inundation map. Apart from this, the floodplain delineation which was done by HEC-RAS 5.0.3 software itself was shown in RAS Mapper. The inundation map was exported from HEC-RAS to ArcGIS, where the area inundated was re-drawn as a shapefile for evaluating the area which were flooded during the year 2004 during June to October.

3.RESULTS AND DISCUSSIONS

3.1 Digital Elevation Model, Study Area and River Reach

The DEM was clipped with respect to the extents of the floodplain region. As a part of post-processing, the river reach, bank stations, cross sections, flow lines and bank lines were drawn in Arc-GIS and then exported to HEC-RAS for further processing.

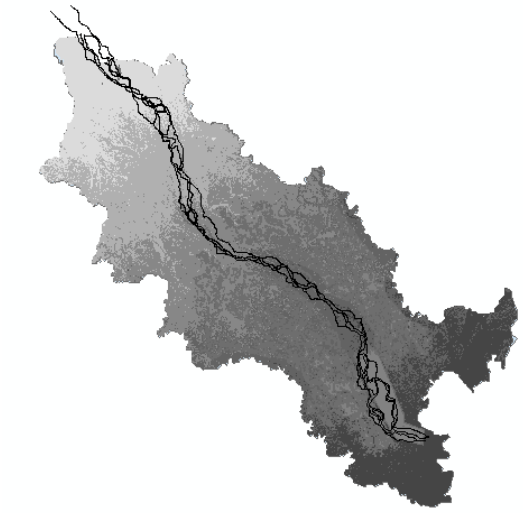

Figure 1: Study Area DEM and Teesta River

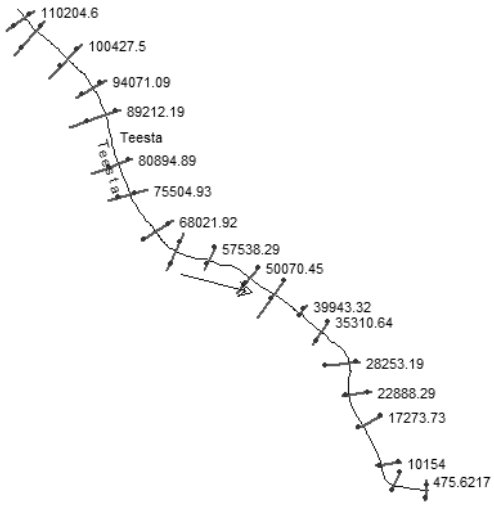

Figure 2: River Reach and Cross Sections

3.2 Calibration and Validation Graphs

The hydrodynamic model was calibrated for the year of 2013 and validated for 2016. For the purpose of calibration, the model was undergone 1-D simulation for various values of Manning's roughness coefficient (n) ranging from 0.015-0.035. A comparison two-line graph was generated for the duration of 1-D simulation against the observed water level and hydrodynamically simulated water level. After quite a number of trials, the graphs were calibrated and validated for n=0.31 as shown in the figure 3(a) and figure 3(b).

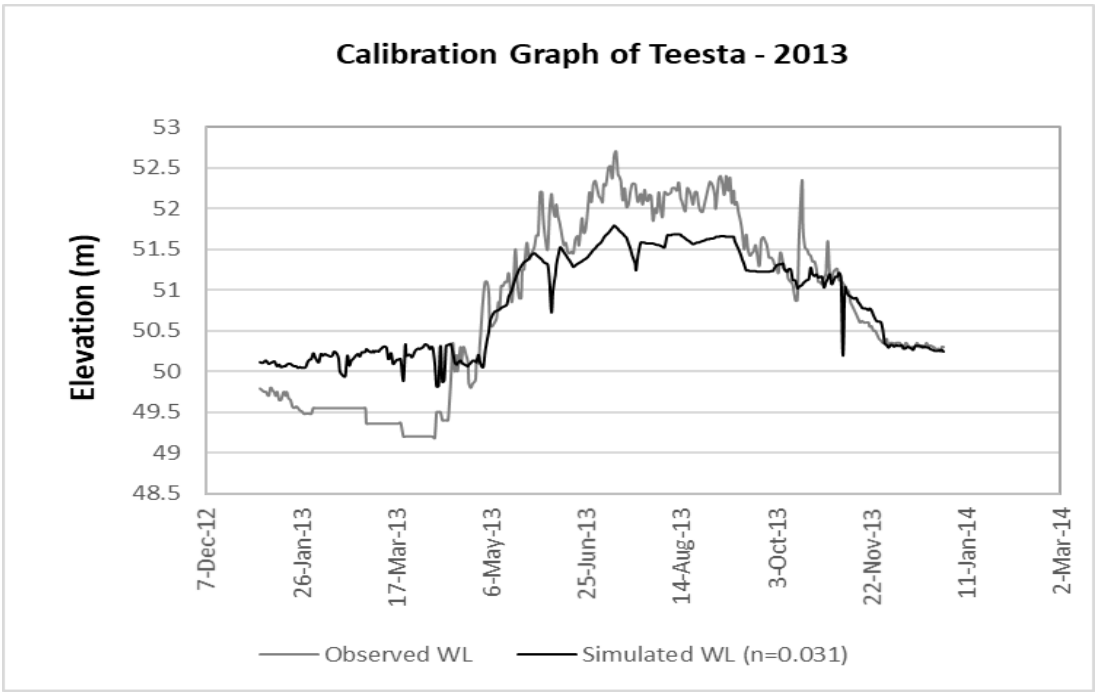

Figure 3(a): Calibration Graph for Teesta River - 2013

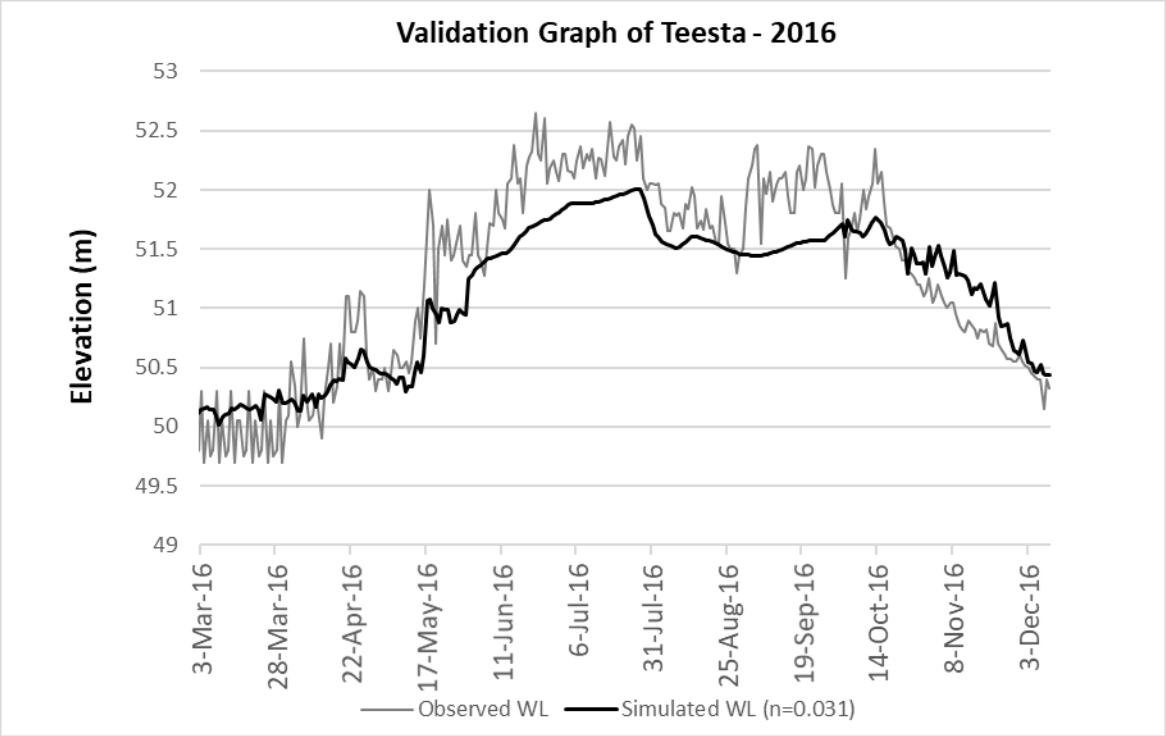

Figure 3(b): Validation Graph for Teesta River - 2016

3.3 Flood Inundation Map and Comparison with MODIS Satellite Imagery

MODIS Satellite Imagery was available for the day o 13th October 2004. For the sake of comparison, the inundation map of 13th October 2004 was compared to the available MODIS Satellite Image as shown in Figure 4. The places which shown similar inundation characteristics have been marked in circles.

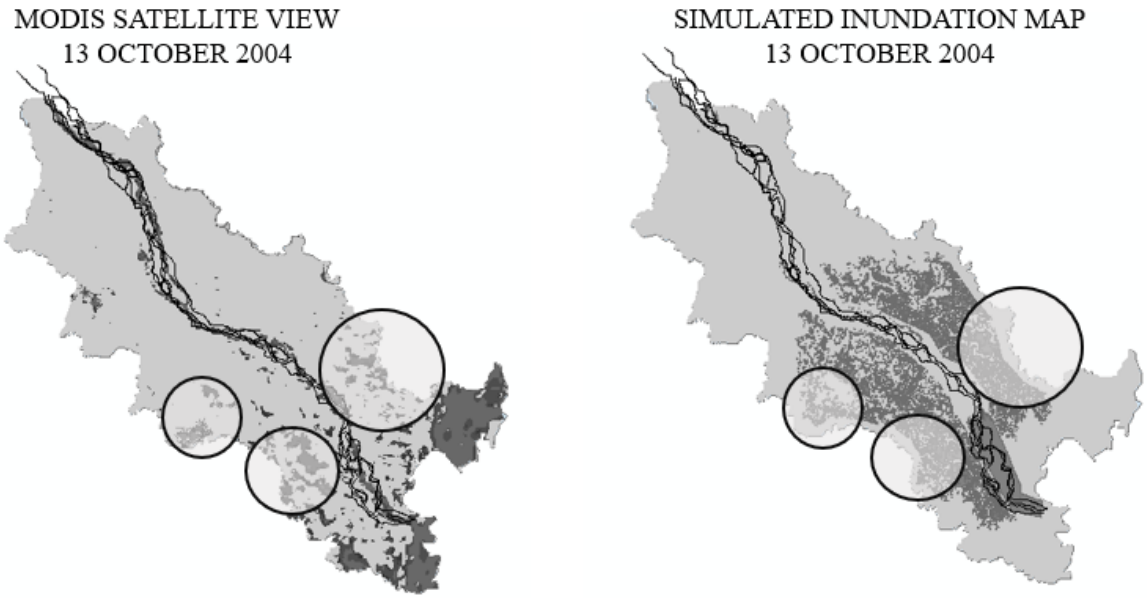

Figure 4: Comparison of Simulated Inundation Map and Modis Satellite Image

3.4 Flood Inundation Area

After the model was simulated for the months of June to October, a study was done based on how much land area of the total floodplain (3861.5 sq km) was inundated during the flood season. A summary has been done every 1st and 15th day of each month, through the months of June to October. Also, to get a better picture of the overall river flow, the flow hydrograph was generated for the year 2004 for Teesta River (Figure 5).

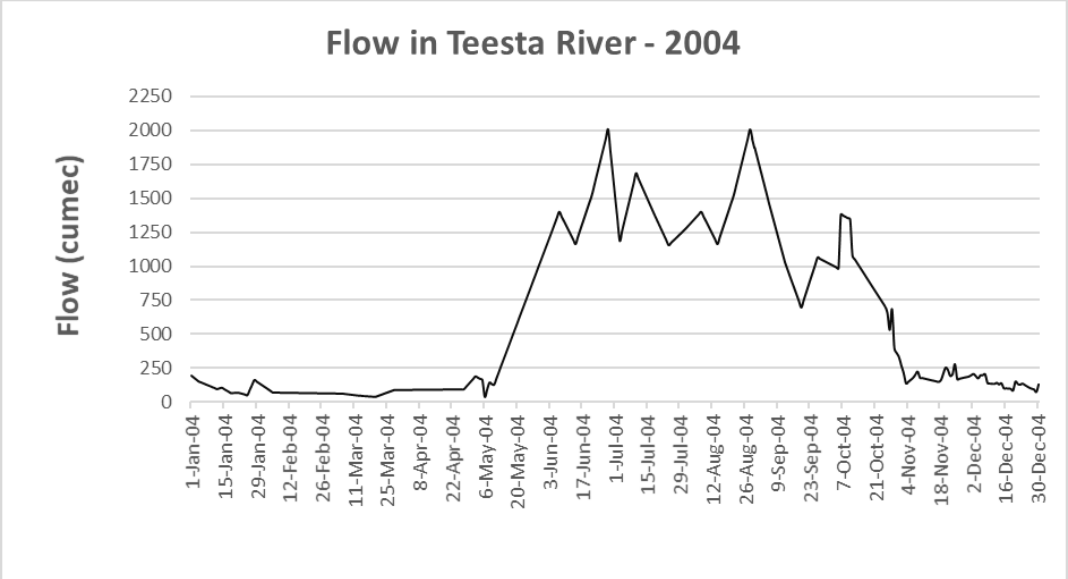

Figure 5: Flow Hydrograph for Teesta River (year 2004)

From the hydrograph it can be clearly stated that, the peak flow occurred during the months of June and September mainly. In accordance to this, our observation of the percentage inundation seems viable.

Table 1: Percentage of Area Inundated (Teesta, 2004)

Month	Date	% Area Inundated
June	1/Jun/2004	21.14
	15/Jun/2004	43.90
July	1/Jul/2004	20.09
	15/Jul/2004	12.19
August	1/Aug/2004	4.29
	15/Aug/2004	7.64
September	1/Sep/2004	14.21
	15/Sep/2004	45.26
October	1/Oct/2004	11.37
	15/Oct/2004	26.16

4. CONCLUSIONS

Hydrodynamic model for Teesta river was established through coupling of 1D and 2D flood plain. Calibration model for Teesta river was done for 2013 based on available sets of data. The model established was calibrated using Manning's n of value 0.028. The floodplain was delineated for the year 2004. From the inundated flood maps which have been developed, area inundated during the flood season was determined with respect to the total floodplain area.

Some of the prospective outcome from this study can be pointed out as follows:

a. Help in planning and management of floodplain area
b. Determining suitability structures like embankment, detention ponds, watershed etc.
c. Automated hydrologic analysis and floodplain mapping provides a better and more effective result.
d. Comparison of the result of this model with studies relating to 2D models can yield possibilities of overall process simplification and improvement through more trial and error.
e. Flood risk and hazard maps, impact of structures like flood control dam, reservoir etc. can also be studied with updated versions of the software and additional modeling tools.

ACKNOWLEDGEMENTS

The authors acknowledge the support from the Department of Civil Engineering, MIST during this study.It is also a great pleasure for the author to express her gratefulness to Sarder Udoy Raihan, Sub-Divisional Engineer, Flood Forecasting and Warning Center, Bangladesh Water Development Board for supporting author during her entire data and necessary maps collection period and for giving suggestions while needed.

REFERENCES

Dasgupta, A. 2007, 'Floods and poverty traps: Evidence from Bangladesh', *Economic and Political Weekly*, 3166-3171.

FFWC 2005, *Flood Annual Report 2005*. Consolidation and strengthening of flood forecasting and warning services, Flood forecasting and warning center, final report, volume ii monitoring and evaluation. Technical report. Bangladesh Water Development Board. Dhaka.

IPCC 2013. *Climate Change 2013*, The Physical Science Basis, Contribution of Working Group I to the Fifth Assessment Report of the Intergovernmental Panel on Climate Change [Stocker, T.F., D. Qin, G.-K. Plattner, M. Tignor, S.K. Allen, J. Boschung, A. Nauels, Y. Xia, V. Bex and P.M. Midgley (eds.)]. Cambridge University Press, Cambridge and New York. <https://doi.org/10.1017/CBO9781107415324>

Islam A. S., Bala SK, Haque A, 2009, 'Flood inundation map of Bangladesh using MODIS surface reference data'. *In: 2nd international conference on water & flood management*.

Mondal, M.S.H. & Islam, M.S. 2017, 'Chronological trends in maximum and minimum water flows of the Teesta River, Bangladesh, and its implications', *Jàmbá: Journal of Disaster Risk Studies* 9(1), a373. <https://doi.org/10.4102/jamba.v9i1.373>

Rahman, L. N. 1996, 'Present situation and future issues regarding river and hydrological database in Bangladesh'. *In Proc. Second Experts Conf. on River*

Rahman, M. M., Hossain M. A. and Bhattacharya, M. A., 2007, 'Flood management in the flood plain of Bangladesh', *International Conference on Civil Engineering in the New Millennium: Opportunities and Challenges (CENM).*

Proceedings of the 5th International Conference on Civil Engineering for Sustainable Development (ICCESD2020), 7~9 February 2020, KUET, Khulna, Bangladesh (ISBN-978-984-34-8764-3)

NUMERICAL MODELLING OF FLOW IN A 90° CHANNEL CONFLUENCE

Shafiqul Islam Shakil*[1], Md. Jahir Uddin[2] and Chandan Mondol[3]

[1]Department of Civil Engineering, Khulna University of Engineering & Technology, Khulna, Bangladesh, e-mail: shakil021295@gmail.com
[2]Professor, Department of Civil Engineering, Khulna University of Engineering & Technology, Khulna, Bangladesh, e-mail: jahiruddin@ce.kuet.ac.bd
[3]Ph.D. Scholar, Department of Civil Engineering, Khulna University of Engineering & Technology, email: chandance2k7@gmail.com

***Corresponding Author**

ABSTRACT

A confluence can be found where two streams join to form a river with a new name, or where two separate channels of a river join together at the downstream end, or at a point where a tributary meets a larger river. Open channel confluences are seen in many natural and man-made channels. There is a complex flow behavior in or around the junction. On the inner side immediately downstream of the junction, a separation zone is developed. The complex flow is a function of channel geometry, confluence angle, flow rate, boundary roughness and intensity of turbulence. A major influence on bed erosion and bank scouring is caused by channel confluence. A numerical simulation was performed in a 90-degree channel junction using River2D solver in iRIC to investigate the flow behavior. Velocity and surface elevation of water were computed for different flow ratios. From numerical simulation it was found that at upstream of the junction, water surface elevation was higher followed by a sudden drop of water levels immediately downstream of the junction. At outer bank velocity was higher and decreased towards the inner wall. The length and width of separation zone were decreased with increasing flow ratio. Numerical results of this investigation was compared with the experimental results of Kalyani Dissanayake (2009). The new data found from the current study can be used for the detailed analysis of flow dynamics. The application of this new knowledge can be used in improved design of river bank protection works and urban flood and erosion control structures.

Keywords: *Confluence, Water Surface Elevation, Separation zone, Flow ratio.*

1. INTRODUCTION

According to geography, a confluence is found where at least two streams of water join together to form a single water flow. A confluence can be found where two streams join for the formation of a river with a new name, or where two separate channels of a river join together at the downstream end. Confluences are studied in a variety of sciences. The flow pattern characteristics of bars, erosion and scour pools were studied in Hydrology (James L. Best,1986). The consequences and characteristics of water flow are often analyzed with mathematical models (Laurent Schindfessel et. al, 2015). The living organism distribution (i.e. ecology) depends on the channel confluence as well; "the general pattern (downstream of confluences) of increasing stream flow and decreasing slopes drives a corresponding shift in habitat characteristics (Beechie et. al., 2012). The overall aim of this research is to obtain a detailed description of flow behavior at a 90-degree channel confluence.

The specific objectives are to conduct a critical literature review of existing knowledge in open channel junction flows without sediment transport and identify the knowledge gaps in the research area, to perform Numerical simulations of junction flow, to compare experimental results with numerical simulations and to analyze the validity of the numerical simulations and predict the velocity profile. To achieve the above-mentioned objectives this study was carried out step by step. The literature reviews mainly focused on studies presented in journals, books and conference publications, to find out how previous studies in junction flows were conducted, and what conclusions were drawn from their results and experiments. This information helped to identify the knowledge gaps in junction flows and to set out the objectives for current study. Experimental result was taken from the experiments conducted by Kalyani Dissanayake, 2009. iRIC (International River Interface Co-operative) was used to simulate 90° open channel junction flow behavior with clean water. A steady-state two-dimensional numerical simulation was carried out. The water surface elevation and velocity are subsequently computed for different flow. Result of the numerical simulation is compared with the experimental result to analyze the validity.

Previous studies of channel junction flows were mainly based on laboratory scale model experiments with simplified flow conditions in which variables were controlled rather easily. Most laboratory experiments used fixed- bed channels and the key characteristics investigated were depth ratio, separation zone, effect of discordant beds, and location of shear layers, stagnation point and secondary flow current. In the most common and traditional approach, confluence characteristics have been determined in prismatic channels in laboratories (Taylor, 1944). However, subsequent predictions were based on several assumptions related to idealistic flow conditions using simplified channel geometries and small-scale physical models. Taylor studied the flow characteristics at a junction of two horizontal channels with rectangular cross sections. He applied the momentum equation to analyze the combined flow and verified the predictions with experimental data for junction angles of 45° and 135°. However, his theoretical predictions were applicable only for smaller junction angles. There was no acceptable agreement for large junction angle such as 135°. It was believed that this was due to the velocity distribution downstream of the junction that was distorted and the flow did not remain parallel to the channel walls. In Taylor's study (1944) he recognized that failure to measure the pressure on the walls of the branch channel or failure in the estimation of the momentum transfer from branch to main channel constitutes an important shortcoming.

Weber, et al. (2001) conducted experiments in an equal width, equal depth, and flatbed 90° laboratory open channel junction with rectangular geometry for different flow conditions. Velocities and water depth were measured in the vicinity of the junction using the Acoustic Doppler Velocimetry (ADV) technique and a point gauge respectively. A data set was compiled which fully describes the complex three-dimensional flow conditions present in an open channel junction for the selected flow conditions.

Compared to laboratory experiments, there is a shortage of data available from field studies on natural confluences. Field investigations are largely based on point measurements of the velocity field. Mamedov (1989) conducted field investigations measuring velocity field and sediment concentration

of the flow. He identified major characteristic zones such as separation zone and stagnation zone in the Kura River in Russia. Kenworthy and Rhoads, (1995) found that patterns of normalized sediment concentrations at a cross-section near the exit of the confluence are a function of the ratios of momentum flux and mean sediment concentration in the upstream channels. These patterns reflected a shift in the location of the shear layer toward the outer bank with increase in the momentum ratio. However, the data collected in this study consists of only depth-integrated sediment samples and measurements of bulk upstream hydraulic variables. Therefore, a rigorous analysis of the mixing process in terms of flow mechanics was not possible.

In numerical simulation, partial differential equations expressing the governing physical laws are solved incorporating the constitutive models based on numerical methods. It is a technique that allows the alteration of one variable at a time, so assessment of the relative importance and interaction of different controls becomes possible.Duan, J.G. and Nanda, S.K. (2006) used a two-dimensional depth-averaged hydrodynamic model to simulate suspended sediment concentration distribution in the Groyne-River. The governing equations were depth-averaged two-dimensional Reynolds' averaged momentum equations and the continuity equation in which the density of sediment laden-flow varied with the concentration of suspended sediment.

2. METHODOLOGY

2.1 Experimental Setup

An open channel junction was designed and constructed at the Hydraulics Laboratory of the University of Wollongong as part of a PhD project by K. Dissanayake (2009). The size of the experimental facility was adjusted to suit the constraints on the available space. The experimental facility consists of a 90° junction of two equal-width, equal-depth flatbed channels with two separate water recirculation systems, water height measuring system and a data acquisition system using the LabVIEW program, along with other experimental control devices.

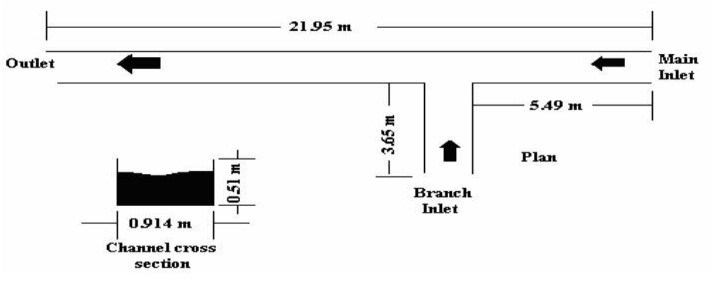

Figure 1: Experimental set up (K. Dissanayake, 2009)

The experimental setup was designed and constructed according to the dimensions given in Figure 1. The flume was fabricated using 6 mm thick Perspex sheets. It has a low Manning's value, around 0.009. The sharp corners at the junction were not rounded off. Clean water flow was established in the main channel.

2.2 Calibration

Dissanayake (2009) performed laboratory experiments in a 90° combining flow flume. The experimental facility was capable of establishing different flow conditions. The varying discharge on both channels (main and branch) were supplied by header tanks. Perforated plates and 100 mm thick honeycomb were placed at the main and branch channel inlets in order to reduce eddy generated at inlets. The transition pieces of channel were made smooth from vertical to horizontal while the entire floor of the facility was kept horizontal on bends in order to minimize losses. The length of main channel and branch channel were 21.95m and 3.66m respectively. The junction was 5.49m

downstream of the flume entrance. The width of branch channel, main and the downstream combined flow channel was 0.914 m and the depth were 0.51m. The total combined flow was 0.170 m^3/s, and the tail-water depth was 0.296m and both were held constant, yielding a constant downstream Froude number (0.37), and a constant average velocity (0.628 m/s) of tail-water.

The above-mentioned experimental condition is simulated by solver River2D of iRIC. In this numerical solution, Bousinessq type eddy viscosity is used for the transverse shear modeling. Secondary flows are not considered during calculation, which is the main reason for losing energy of flow near the channel boundary. Total numbers of grids are 2119. In the present study, concept of geometric similarity is applied for better result. During simulation by River2D, very shallow depth of flow as compared with (Dissanayake, 2009) brings erroneous result. The condition of geometric similarity is expressed in Figure 2.

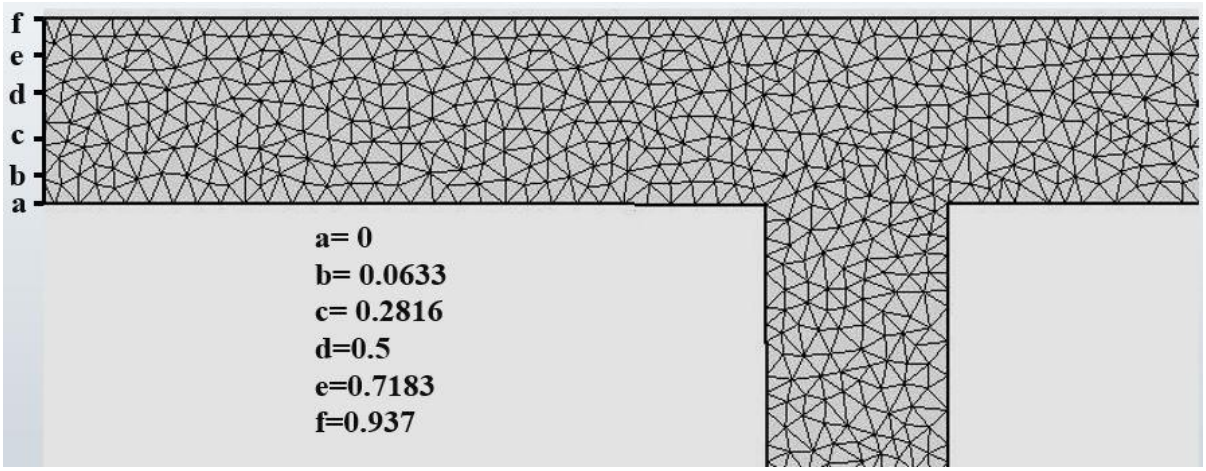

Figure 2: Computational Mesh for River2D Solver in iRIC

Discharge ratio was determined by $q^*= Q_{main}/Q_{total}$. Water height was normalized by h*=h/w. Distance along x-direction was normalized by x*=x/w. Distance along y-direction was normalized by y*=y/w. Here, "w" is the channel width.

3. RESULTS AND DISCUSSIONS

Water heights were measured at set locations using five-point gauges which were mounted on a simple sliding base. For each of two different flow conditions, the sliding base was moved along the channels recording the water heights at five different locations across the channels simultaneously. Figure 3 shows the Normalized water depth (h*) contours in the main channel.

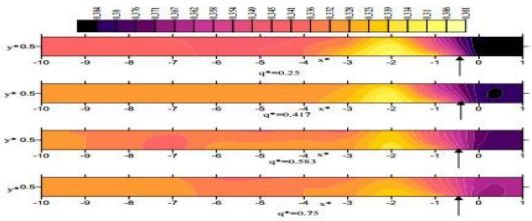

Figure 3: Normalized water depth (h*) contours in the main channel

Shown above water depth contour maps and water surface profiles in the main channel (Figure 3) it was observed that higher water depths were generated before the junction. The free surface profile along the main channel showed a sudden depression immediately after the junction, followed by recovery after about 7-8 channel widths from junction. Upstream to downstream depth deference was

higher for lower discharge ratios and highest difference was observed for q*=0.25 flow condition. Super elevation exists adjacent to outer bank after the junction for all flow conditions. This water depths pattern is generated due to the obstruction effect caused by the lateral stream associated with turbulence mixing and energy losses at the junction. Measured water depths for flow conditions q*=0.25 and q*=0.75 were then compared with iRIC simulation and found that they are in good agreement showing the similar pattern of free surface profile changes at the junction.

3.1 Validity Analysis & Velocity Prediction

Two-dimensional numerical modelling was carried out using River2D for 90° open channel junction to simulate flow conditions q*=0.25 and q*=0.75. Results of the numerical simulations were compared with experimental data from previous researchers (Dissanayake, 2009). Higher water depths were generated before the junction. The free surface profile along the main channel showed a sudden depression immediately after the junction, followed by recovery after about 7-8 channel widths from junction. Upstream to downstream depth deference was higher for lower discharge ratios and highest difference was observed for q*=0.25 flow condition. There is a drop-in surface elevation at the right corner of the junction. This zone is called the Stagnation zone. The relative velocity of water in this zone is zero. Figure 4 shows the color contour of water surface profile. The experimental result (Dissanayake, 2009) was compared with the result from River2D and both results show a very little variation (Figure 5 to 14).

(q*=0.25) (q*=0.75)

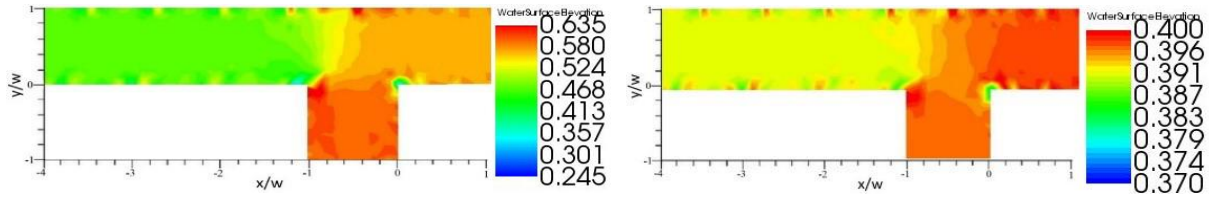

Figure 4: Water Surface Profile along the junction

It can be seen that the overall water depth patterns show very similar trends in both simulation and experiment. The depression of water at the junction downstream along and across the channels is shown clearly. The figures show further comparisons between experimental and computed dimensional water depths. At the upstream end, the agreement between experiment and simulation is very good. At further downstream locations, there is an increasing discrepancy between experimental observation and simulation within the high turbulence zone, although the free surface shape is accurately reproduced. A possible reason for this is a slight mismatch between the exact locations of the experimental data collection points, and the mid-points of the computational cells where the data is stored after calculations.

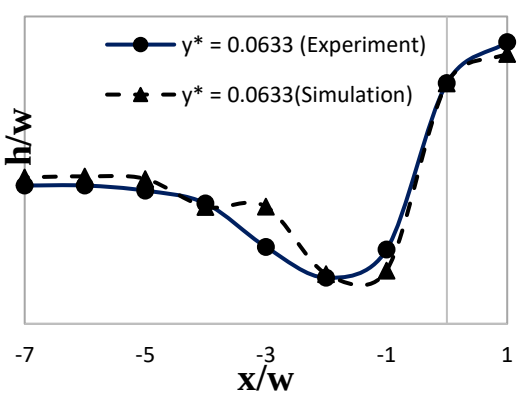

Figure 5: Water Surface Profile (q*=0.25, y*=0.0633)

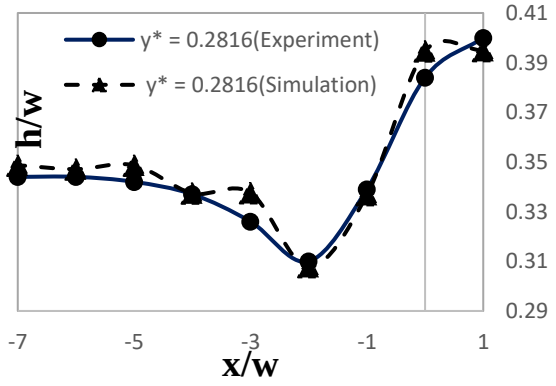

Figure 6: Water Surface Profile (q*=0.25, y*=0.2816)

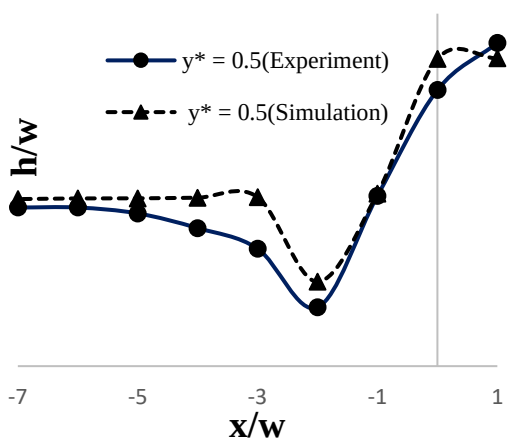

Figure 7: Water Surface Profile (q*=0.25, y*=0.5)

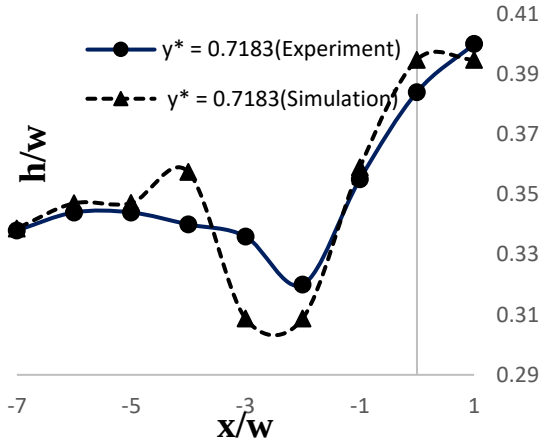

Figure 8: Water Surface Profile (q*=0.25, y*=0.7183)

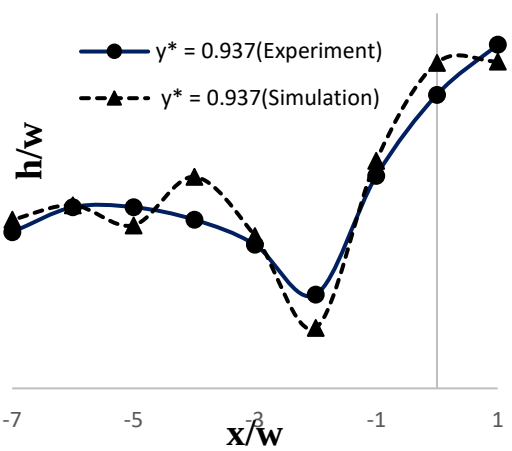

Figure 9: Water Surface Profile (q*=0.25, y*=0.937)

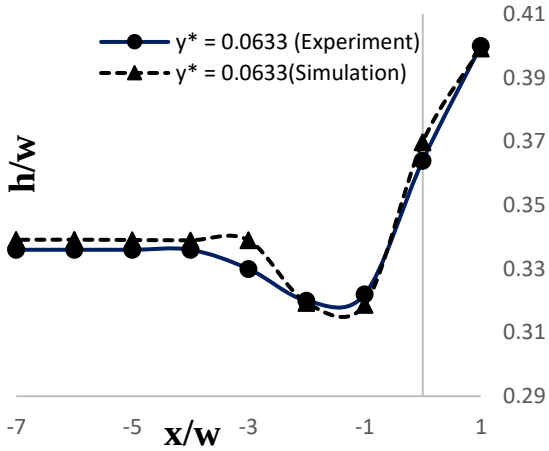

Figure 10: Water Surface Profile (q*=0.75, y*=0.0633)

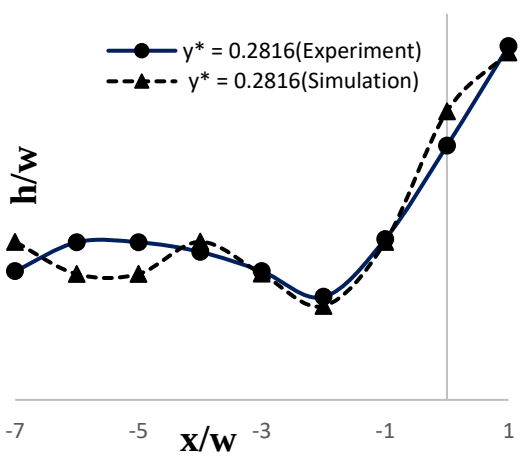

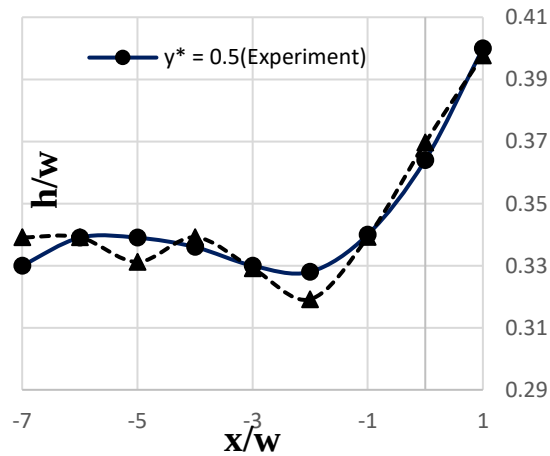

Figure 11: Water Surface Profile (q*=0.75, y*=0.2816)Figure 12: Water Surface Profile (q*=0.75, y*=0.5)

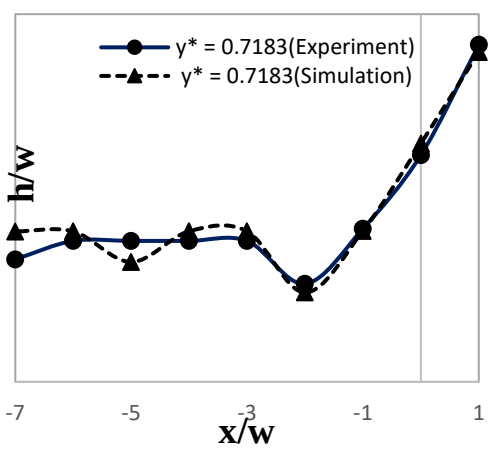

Figure 13: Water Surface Profile (q*=0.75, y*=0.7183)

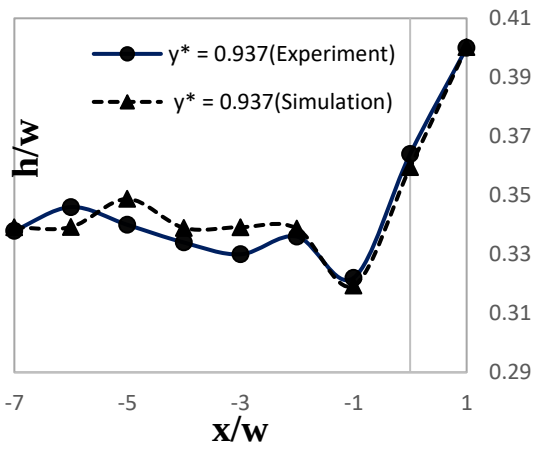

Figure 14: Water Surface Profile (q*=0.75, y*=0.937)

The maximum depth difference between upstream and downstream in the simulation is 0.08 m (73mm) whereas the maximum depth difference in the experiment is 0.07 m (64 mm). Therefore, the simulation results show 14% discrepancy in water heights. In reality it is virtually impossible to simulate exactly the actual flow conditions which exist in real situations. Furthermore, flow through open channel junctions is inherently three dimensional and unsteady. Therefore, appropriate assumptions were made to simplify the problem which results in discrepancy between predictions and experimental observations.

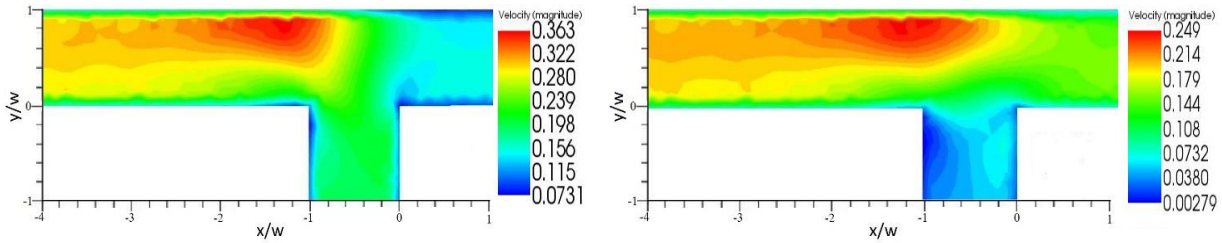

q*=0.25 q*=0.75

Figure 15: Color Contour of velocity distribution

The maximum velocity is distant from the inner bank of the main channel. The flow remaining in the main channel develops within the section after passing the intake entrance, but because of the effects of curved flow lines at the intake entrance, the maximum velocity will be deviated back towards the inner wall. Figure 15 shows the color contour of velocity distribution along the junction for different flow ratios.

The major cause of velocity loss near the outer boundary is the frictional resistance between the channel boundary and the flowing water. There is also some source of errors. The positions of the cross sections were not accurate. So, the result slightly deviates from the experimental one. There is a drop of velocity in the right corner of the branch channel at the junction. The velocity was nearly zero there. This zone is called the Stagnation zone. The highest static pressure is found at zero velocity and hence the maximum static pressure is at the stagnation points. This static pressure is known as the stagnation pressure. Flow separation occurs at the left corner of the branch channel at the junction where the boundary layer travels far enough against an adverse pressure gradient that the speed of the boundary layer relative to the object falls almost to zero. The fluid flow becomes detached from the surface of the object, and instead takes the forms of eddies and vortices. In this study, there is no significant result regarding the separation zone as the secondary flow was not considered. There were limitations on total number of elements in the computational domain based on the software type.

Therefore, there were limitations for further mesh refinements of the computational mesh. The quality of the mesh could effect on the accuracy of predictions. Dense cell population in areas of higher flow parameter changes were enabled to simulate accurate flow fields. The current study does not consider the effect of secondary current. The behavior of separation zone depends on the secondary current. Sediment transport was not taken into account in this present study. In natural river confluences sediment transportation is a major factor. The current study was based on a 90° open channel junction. Though this confluence angle produces maximum obstruction to the main channel flow among most channel configurations in nature are of small confluence angles such as 30º, 45º and 60º. Flow fields in such channel junctions are different. (Obtuse confluence angles also exist in nature. Most commonly those sites have hard rocks. Increased velocities will not be a crucial issue for such sites). Therefore, it is recommended to conduct further studies on such channel configurations investigating flow and sediment characteristics.

4. CONCLUSIONS

Considerable research on open-channel flows has been undertaken in the past and yet the description of flow behavior at channel junctions is incomplete. Therefore, the present study was aimed at further investigation of junction flow behavior without sediment transport through comprehensive numerical techniques. The current study provides new data, particularly on the geometry of the recirculation region immediately downstream of the junction, contributing to a better understanding of flow dynamics at open channel junctions.The studies conducted in this research provide greater insight towards the understanding of the flow and sediment transport characteristics. It is revealed that flow dynamics at open channel junctions may have important effects on the dispersal of dissolved or suspended substances in headwater areas of channel networks. Data obtained in this study is useful in controlling sediment erosion and deposition processors and flooding at channel junctions. The simulation can be perfected with the consideration of the secondary flow. Thus, a detailed investigation can be conducted on the separation zone characteristics. Sediment laden flows can also be investigated for a better understanding of the flow and sediment transport behavior on the open channel confluences.

REFERENCES

Beechie et al. (2012), who cite earlier work. Tim Beechie, John S. Richardson, Angela M. Gurnell, and Junjiro Negishi (2012) "Watershed processes, human impacts, and process-based restoration." In Philip Roni and Tim Beechie (eds.) (2012) Stream and Watershed Restoration: A Guide to Restoring Riverine Processes and Habitats, John Wiley & Sons

Best, J. L., (1986) "The morphology of river channel confluences",*Progress in Physical Geography 10:157–174*

Biron, P., Best, J. L., & Roy, A. G. (1996). "Effects of bed discordance on flow dynamics at open channel confluences",*Journal of Hydraulic Engineering, 122(12), 676-682.*

Dissanayake, K. (2009)"Experimental and numerical modelling of flow and sediment characteristics in open channel junctions", Doctorof Philosophy thesis, School of Civil Mining and Environmental Engineering, University of Wollongong, 2009. *https://ro.uow.edu.au/theses/3555*

Gurram, S. K., Karki, K. S., & Hager, W. H. (1997). "Subcritical junction flow", *Journal of Hydraulic Engineering, 123(5), 447-455.*

Laurent Schindfessel, Stéphan Creëlle and Tom De Mulder (2015) "Flow patterns in an open channel confluence with increasingly dominant tributary inflow",*Water 7: 4724–4751.*

Taylor, E. H. (1944). "Flow characteristics at rectangular open-channel junctions",*Transactions of the American Society of Civil Engineers, 109(1), 893-902.*

Weber L. J., Schumate E. D., and Nicola Mawer (2001). “Experiments on flow at a 90 0 open channel junction.” *Journal of Hydraulic Engineering, 127 (5).*

Proceedings of the 5th International Conference on Civil Engineering for Sustainable Development (ICCESD 2020), 7~9 February 2020, KUET, Khulna, Bangladesh (ISBN-978-984-34-8764-3)

GENERATING INUNDATION MAP OF ATRAI RIVER USING HEC-RAS 1D/2D COUPLED MODEL

Proma Maria Rozario[1], Kazi Mushfique Mohib[2], Sahika Ahmed[3], Purnima Das*[4] and Md. Sabbir Mostafa Khan[5]

[1]Graduate Student of Bangladesh University of Engineering and Technology (BUET), Dhaka, Bangladesh, e-mail: rozarioproma@gmail.com
[2]Graduate Student of Bangladesh University of Engineering and Technology (BUET), Dhaka, Bangladesh, e-mail: kazimushfique23@gmail.com
[3]Graduate Student of Bangladesh University of Engineering and Technology (BUET), Dhaka, Bangladesh, e-mail: sahika.buet14@gmail.com
[4]Graduate Student of Bangladesh University of Engineering and Technology (BUET), Dhaka, Bangladesh, e-mail: pinkiwre10@gmail.com
[5]Professor at Bangladesh University of Engineering and Technology (BUET), Dhaka, Bangladesh, e-mail: sabbbirkhanbuet@gmail.com

***Corresponding Auther**

ABSTRACT

Bangladesh is a densely-populated, low-lying and mainly riverine country located in South Asia at the downstream of three major river basins name by the Ganges, Brahmaputra, and Meghna. Straddling the Tropic of Cancer, Bangladesh has a tropical monsoon climate characterized by heavy seasonal rainfall, high temperatures, and high humidity. For these geographical characteristics it has become a flood prone country and in recent years the frequency of abnormal floods has increased substantially, causing serious damage to lives and property.

Besides other major rivers, Atrai River is one of the leading causes of flooding in certain areas. It flows in West Bengal and northern parts of Bangladesh covering Dinajpur and Naogaon district and serves as a perennial fishing ground. During rainy season (July to September) higher discharge can be observed ranging with 2000 to 3000 cubic meter per second in Atrai and flood occurs due to overflow of the river water along the riverbanks. The main purpose of the study is to setup a HEC-RAS 1D/2D coupled model for generating flood inundation map of lower Atrai River as an accurate flood mapping can help to indicate the vulnerable zones and to take proper measures that can reduce the flood damages. In this study, 1D/2D coupled hydrodynamic model as long as HEC-GeoRAS have been used to develop flood inundation model of Atrai River floodplain and simulated for 2004, 2012 and 2016. The study shows that the flooded area is maximum in September and October in the 2004 and 2016 flood event in the designated floodplain boundary. The overall analysis is actually helpful to describe the 2D flow simulation with 1D in HEC-RAS and the results of the whole study can be useful to create the facility of early warning system with sufficient lead time, hydrologic and hydrodynamic model will help to mitigate the effect of flooding in those surrounding high inundation areas of Atrai river and will help to visualize where flood protection is needed and where not.

Keywords: *HEC-RAS, HEC-GeoRAS, Atrai river, Discharge, Flood inundation.*

1. INTRODUCTION

Floods are the most significant natural hazard causing suffering to a large number of people and damage to property in Bangladesh. In recent years the frequency of abnormal floods in Bangladesh has increased substantially for many reasons (Khalequzzaman, 1994). As a natural phenomenon cannot be prevented totally so concern have to raise on how to mitigate that. Flood mapping is a great way to fulfil this purpose.

In this research, flood mapping has been done for Atrai River that flows in West Bengal and northern parts of Bangladesh. Specifically the Lower Atrai that renters Bangladesh through Naogaon district and falls upon Hurasagar River in Shirajgonj district (Figure 1). Length of the river is approximately 390 kilometer, Average width is 177 meter, maximum depth of the river is 30 m.

During January to April the discharge of the river becomes very low but in rainy season discharge becomes higher and flood occurs due to overflow of the river water along the riverbanks.(Information source: Wikipedia and Rivers of Bangladesh book by BWDB). It was observed that the 2017 floods broke the historic record crossing the danger levels in several stations of many river, Mohadebpur in Atrai was also one of them (Rahman, 2017). In 2017, during middle of August, water in the Atrai River was currently 214 cm above the danger level. Dams are breached in more than 100 villages across the district. Ten villages were flooded near the Dhamirhat border after the Atrai River broke through dams in the area (Islam, 2017).

Hence the main objective of the study is to deal with the flood propagation with time in monsoon season by generating map of the study area. As HEC packages are freeware, this study will apply HEC packages to develop flood inundation map by hydrological and hydro-dynamic analysis by using mainly HEC-RAS 1D/2D coupled model. 1D is used for creating the features of the river by providing necessary discharge and water level data, for proper calibration and validation. Then 2D part of HEC-RAS has been introduced to generate the floodplain of Atrai. So the ultimate combination of HEC-RAS 1D and 2D was capable to create the whole scenario of the flood map of Atrai River.

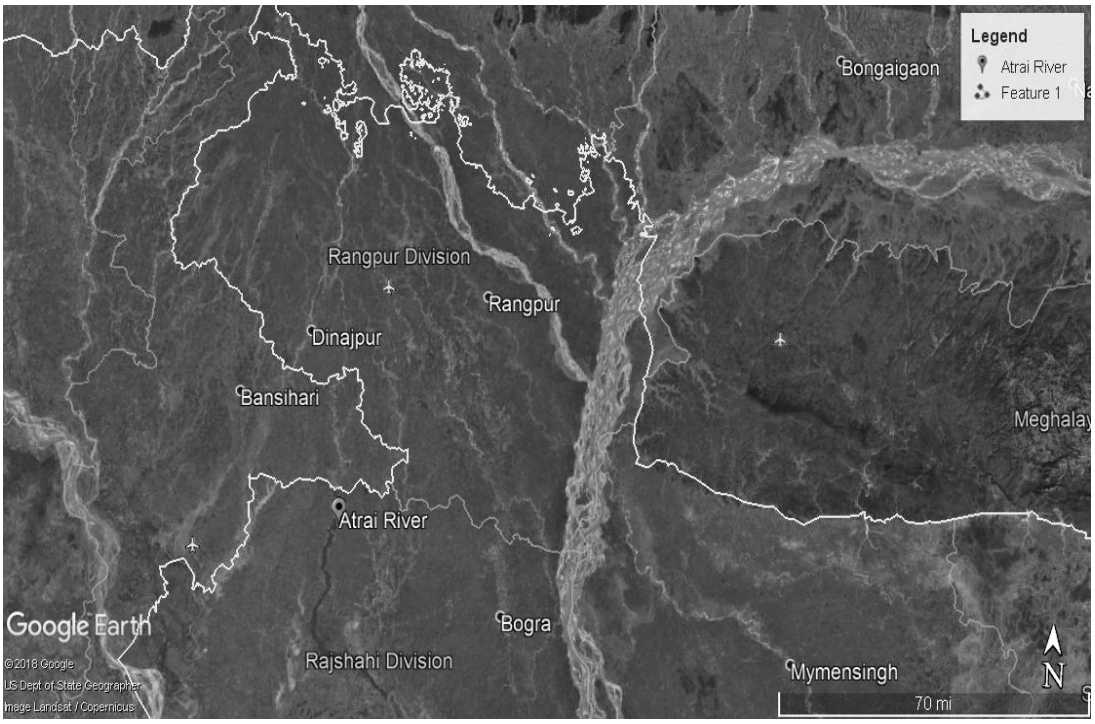

Figure 1: Google earth image of study area (Atrai River)

2. METHODOLOGY

2.1 Preparation Phase

In this study, ArcGIS 10.4.1, HEC-GeoRAS, HEC-RAS 5.0.5 etc. were the softwares that have been used here. At first a reach of Chakhariharpur to Atrai Rly Bridge was selected for the analysis. Then all hydrological data and necessary images of specific years were collected from BWDB, USGS website and from Google earth.

Now, the analysis was started with ArcGIS 10.4.1 by modification of Digital Elevation Model (DEM) of Bangladesh. As the DEM was in geographical coordinate system (GCS_WGS_1984), so it was converted into Bangladesh Transverse Mercator (BTM). And also as the elevation of the DEM is measured with respect to the mean sea level but the collected data of river cross sections, water surface elevation etc. have been considered are measured from Public Work Datum (PWD), so to adjust this difference in elevation, a slight modification of the collected DEM has been done.

After taking the modified DEM of Bangladesh, two districts- Naogaon and Rajshai which covers the floodplain area of Atrai, has been clipped from the modified digital elevation model using the Clipping Tool in Arc Toolbox. Further it was converted from raster to TIN. The purpose of the Raster to TIN tool is to create a Triangulated Irregular Network (TIN) whose surface does not deviate from the input raster by more than a specified Z tolerance. It is used to convert raster from a DEM to a TIN surface model. It is done by using the Raster to TIN tool in the Arc Toolbox. All the stages mentioned above have been shown in Figure 2.

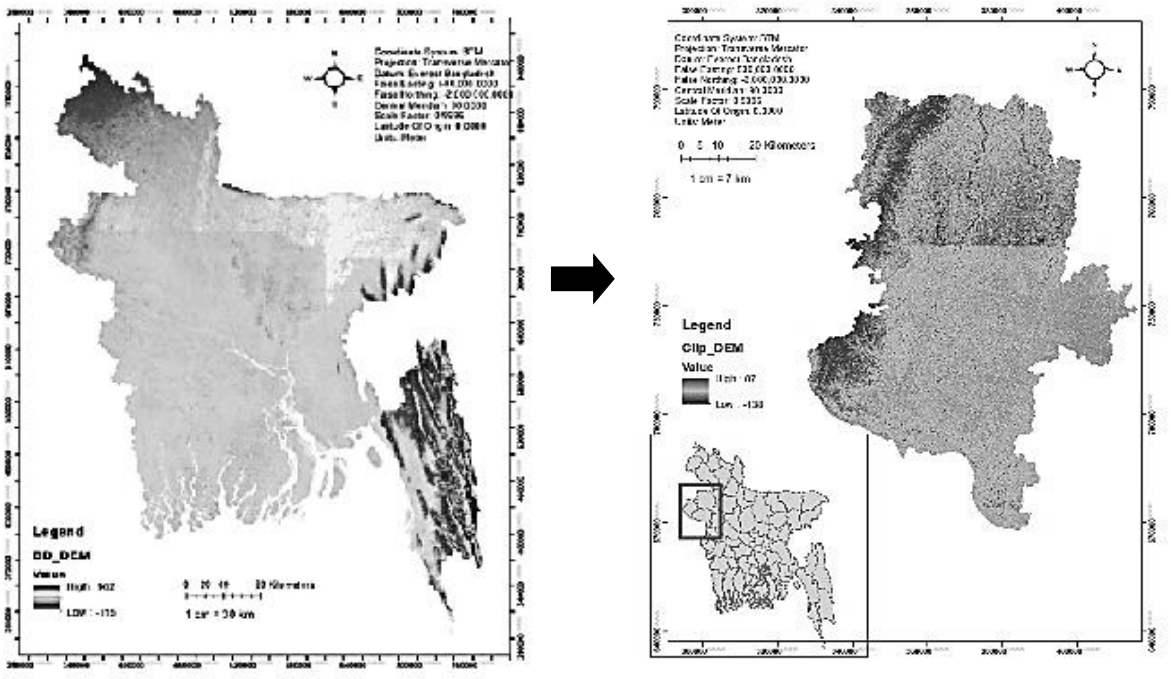

DEM of Bangladesh

DEM (Before modification)

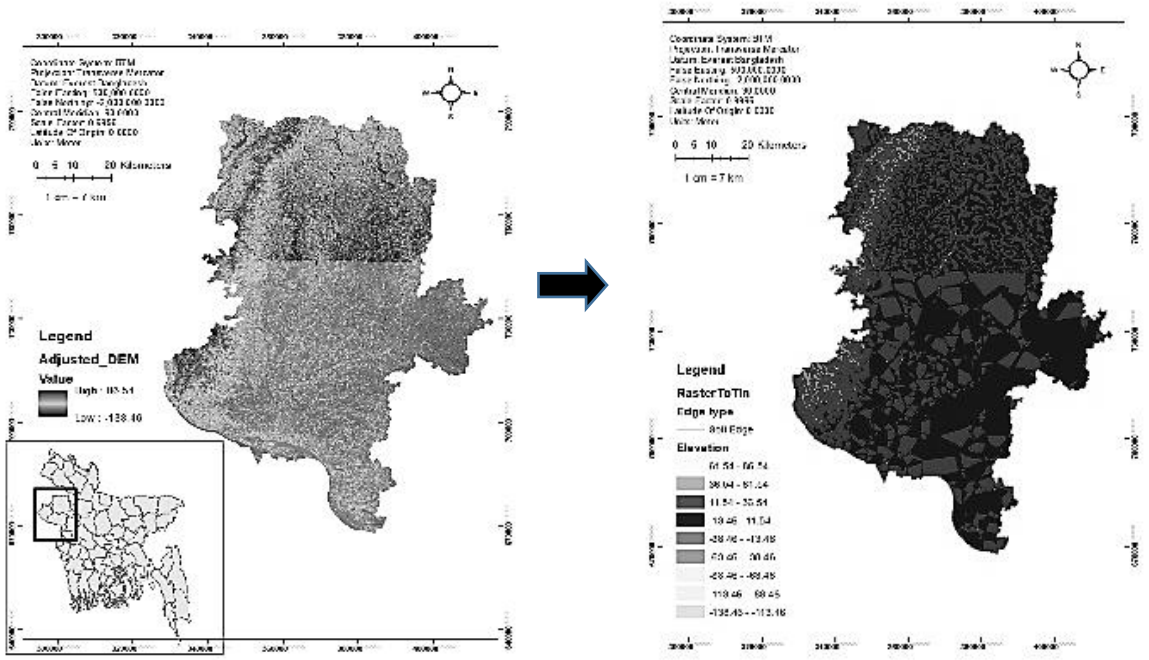

DEM (After modification)

Raster to TIN formation of

Figure 2: Different stages of Preparation Phase

2.2 Executive Phase

2.1.1 Pre-processing in HEC-GeoRAS

HEC-GeoRAS is an Arc GIS extension specifically designed to process geo spatial data to incorporate with the Hydrologic Engineering Center River's Analysis System (HECRAS). The extension allows users to create an HEC-RAS import file containing geometric attribute data form an existing digital terrain model (DTM) and complementary data sets. So, after converting the DEM from Raster to TIN, a complete modified bathymetry was prepared in Arc-GIS with the help of HEC-GeoRAS by developing river centreline, river banks, flow paths and cross sections as shape files with the help of Ras Geometry by all layers for the GIS model**.**

2.1.2 Processing in HEC-RAS

Then after importing the DEM from HEC-GeoRAS to HEC-RAS and providing required flow and stage hydrographs (Figure 3 and Figure 4), 1D hydrodynamic model was created.

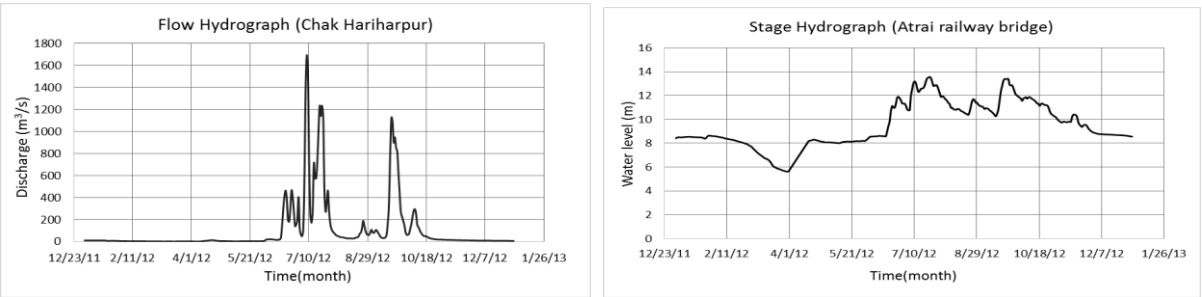

Figure 3: Flow and Stage hydrographs of Atrai River (2012)

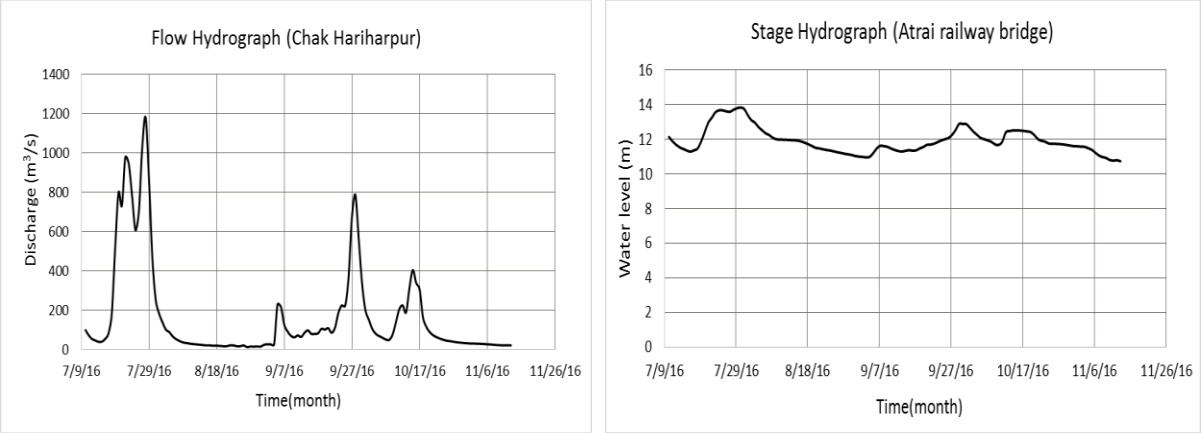

Figure 4: Flow and Stage hydrographs of Atrai River (2016)

To ensure the model's performance, the degree of accuracy of the model was checked by calibration and validation. The calibration was done for 2012 and validation was for 2016 for Manning's n=.026, shown in Figure 5.

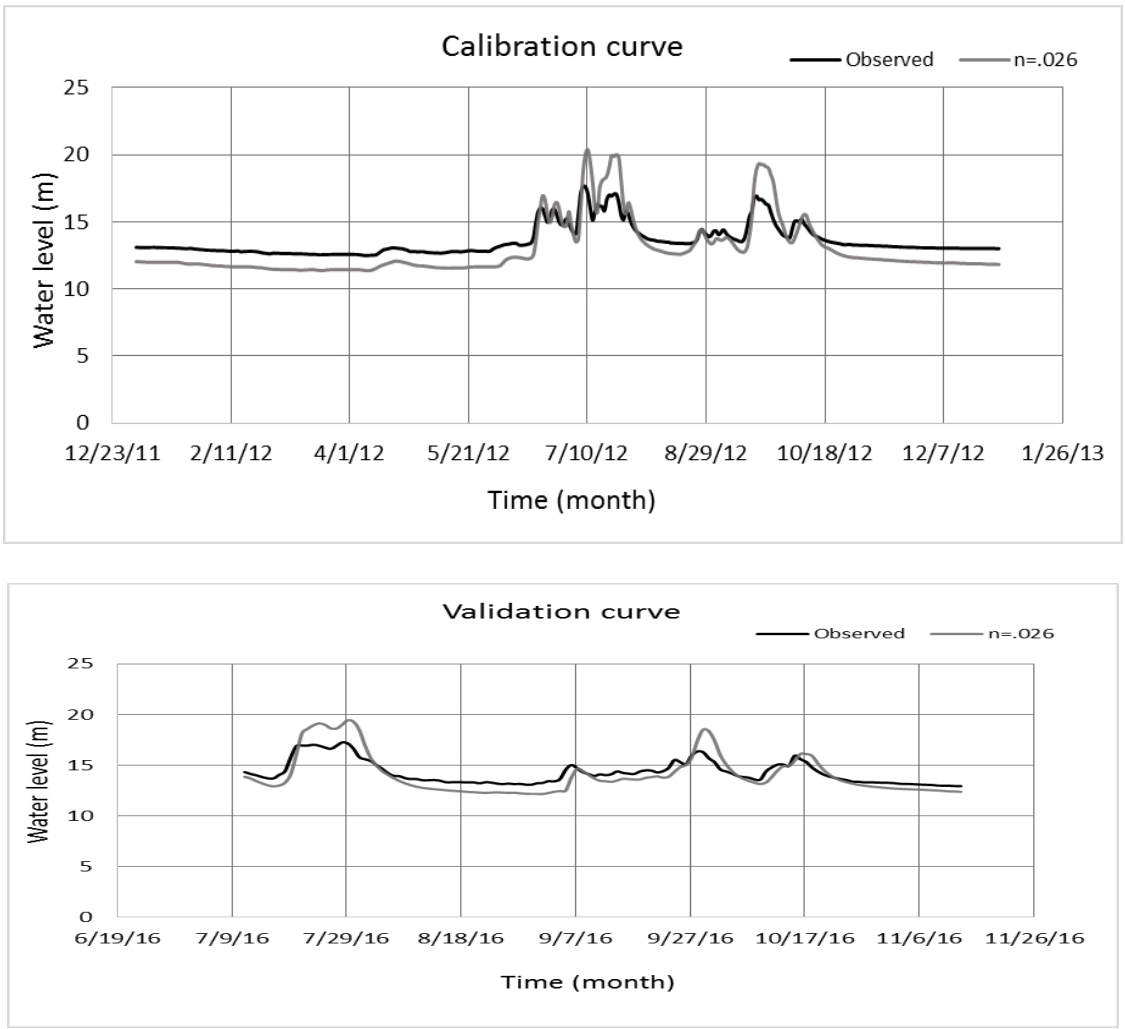

Figure 5: Calibration and Validation curve for Atrai River

Hence coupling of 1D and 2D model was done after assigning the floodplain area of Atrai River and inundation map was generated in RAS Mapper by developing the terrain of the existing DEM. While coupling, two levee as lateral structure were built in both banks of the upstream of Atrai. The height of the levees were slightly higher than the Ground level of the banks of the river. (Figure 6)

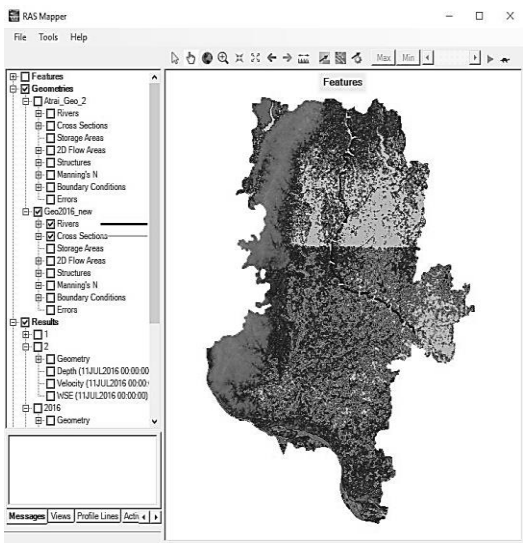

Creating Terrain in Ras Mapper

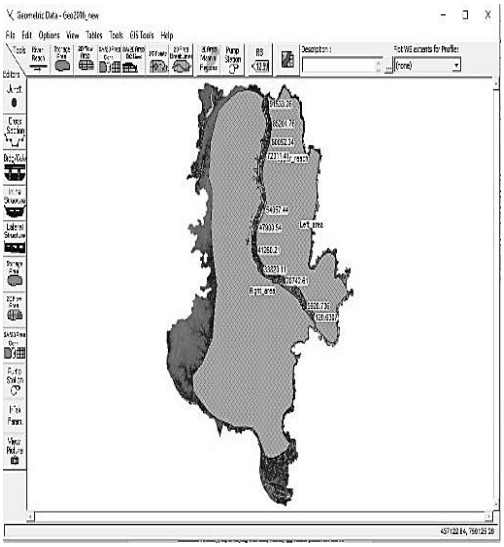

2D flow area computational mesh

Figure 6 Processing in HEC-RAS

Finally on total three models have been generated for year 2004, 2012 and 2016. In the final stage, inundated area for several months in different years were determined with respect to total floodplain area.

3. RESULTS AND DISCUSSIONS

3.1 Figures and Graphs

The model was calibrated for the year 2012 and Manning's roughness coefficient was found as 0.026. In unsteady calibration, the coefficient of determination R^2 have been found 0.9234 which indicate that the simulated value is closer to the observed value (Figure 7). This 'n' value was further rechecked by validation with the year of 2016 to analyse whether it was correct for that year too or not.

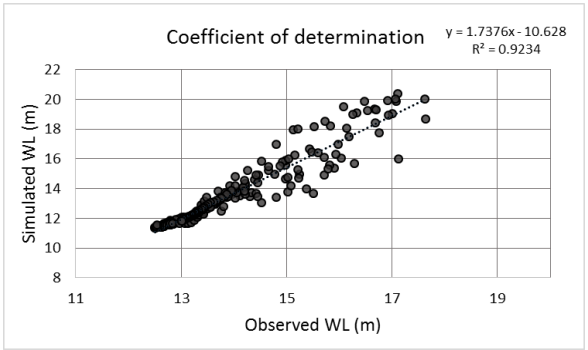

Figure 7: Measuring coefficient of determination

Then generation of flood inundation map of lower Atrai River is successfully done for 2004 and 2016 by creating map for several months (May to November) of these years. And percentage of inundated area were calculated by RAS Mapper. Inundation maps of 13th October for both 2004 and 2016 have been shown in Figure 8 and inundated areas have been given in following tables, Table 1 and Table 2.

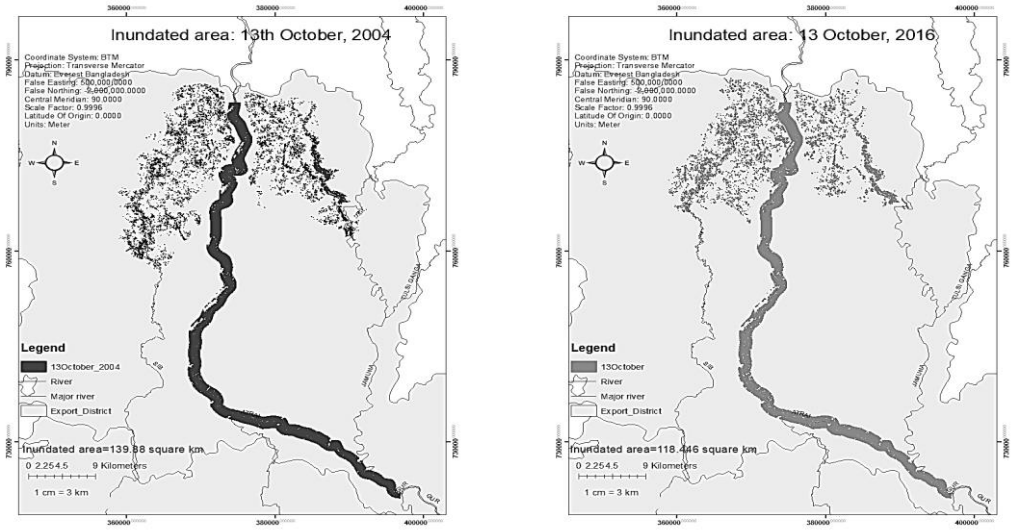

Figure 8: Inundation map for 13th October of 2004 and 2016

3.2 Tables

Table 1: Analysis of percentage of inundated area of 2004

Year	Inundated area	Inundated area	Area of Floodplain	Inundated area
2004	(square m)	(square Km)	(square Km)	(Percentage)
13th May	57123884.4	57.12	1484.79	3.85
13th June	75340927.22	75.34	1484.79	5.07
13th July	114247320.5	114.24	1484.79	7.69
13th August	117469300.9	117.46	1484.79	7.91
13th September	128435541.9	128.43	1484.79	8.65
13th October	139880852.5	139.88	1484.79	9.42
13th November	102338256	102.33	1484.79	6.89
Max	168035770.8	168.03	1484.79	11.32

Table 2: Analysis of percentage of inundated area of 2016

Year	Inundated area	Inundated area	Area of Floodplain	Inundated area
2016	(square m)	(square Km)	(square Km)	(Percentage)
13th July	84106809.02	84.11	1484.79	5.67
13th August	98974453.64	98.97	1484.79	6.67
13th September	102341860.4	102.34	1484.79	6.89
13th October	118445886.4	118.45	1484.79	7.98
13th November	92900605.58	92.9	1484.79	6.26
Max	148360377.3	148.36	1484.79	9.99

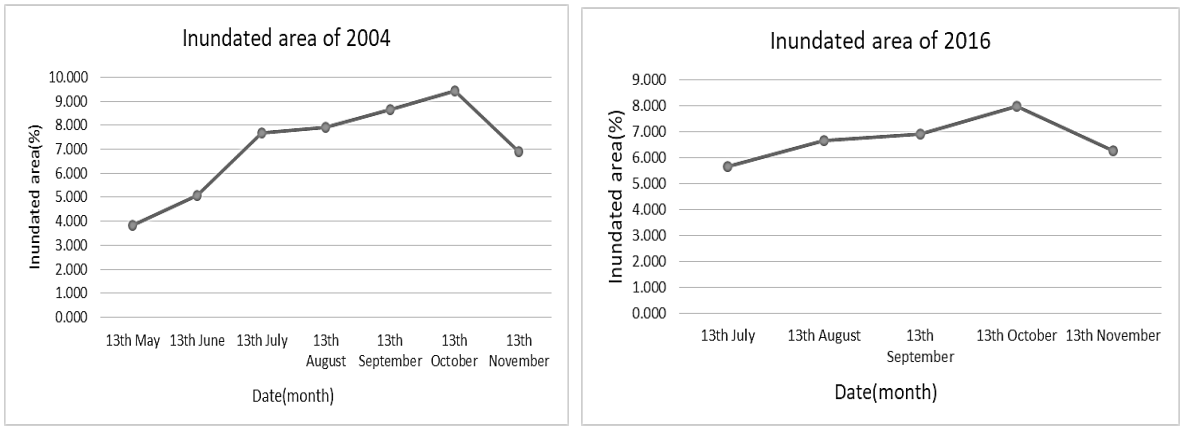

Figure 9: Percentage of inundated area for 2004 and 2016

The percentage of inundated area compared to the area of the two districts (Naogaon and Rajshahi) varies from 3-12% and the extent of the flood is in Dhamoirhat, Patnitala and Mahadebpur Thana. Here percentage value of inundated area are found very small as because the inundated area is comparatively too small then the total assumed floodplain area (1484.799 sqkm). But it can be clearly observed that the percentage of inundated are is smaller in 2016 than 2004 (flood year). And also from the following tables it can be observed that the inundated area (in square Km) gradually increase from May to October and decrease in November in both 2004 and 2012 because of the natural rain and discharge pattern of the environment. The tabulated forms of the analysis can be represented graphically as Figure9.

4. CONCLUSIONS

In this study, 1D/2D coupled hydrodynamic model has been used to develop flood inundation model of Atrai River floodplain and simulated for 2004, 2012 and 2016. The study shows that the flooded area is maximum in September and October in the 2004 and 2016 flood event in the designated floodplain boundary. The overall analysis is actually helpful to describe the 2D flow simulation with 1D in HEC-RAS and the results of the whole study can be useful to create the facility of early warning system with sufficient lead time, hydrologic and hydrodynamic model will help to mitigate the effect of flooding in those surrounding high inundation areas of Atrai river and will help to visualize where flood protection is needed and where not. Moreover this model can further be used for risk map analysis, sensitivity analysis and effect of the variation in levee height for measuring the proper height of the protection.

ACKNOWLEDGEMENTS

The authors acknowledge the support from the Department of Water Resources Engineering, BUET during this study.It is also a great pleasure for the author to express her gratefulness to Sarder Udoy Raihan, Sub-Divisional Engineer, Flood Forecasting and Warning Center, Bangladesh Water Development Board for supporting author during her entire data and necessary maps collection period and for giving suggestions while needed.

REFERENCES

Islam, S. (2017). *Flooding worsens in Naogaon, dams at risk.* bdnews24.com.

Khalequzzaman, M. (1994). RECENT FLOODS IN BANGLADESH: POSSIBLE CAUSES AND SOLUTIONS . *Natural hazards*, 65-80.

Rahman, M. (2017). *Bangladesh Needs to Shore up its Flood Defence.* Dhaka: Inter press service.

FLOOD INUNDATION MAPPING OF KUSHIYARA RIVER USING HEC-RAS 1D/2D COUPLED MODEL

Kazi Mushfique Mohib[1], Proma Maria Rozario[2], Sahika Ahmed[3], Purnima Das*[4] and Md. Sabbir Mostafa Khan[5]

[1]Graduate Student of Bangladesh University of Engineering and Technology (BUET),Dhaka, Bangladesh, e-mail: kazimushfique23@gmail.com
[2]Graduate Student of Bangladesh University of Engineering and Technology (BUET), Dhaka, Bangladesh, e-mail: proma_rozario@hotmail.com
[3]Graduate Student of Bangladesh University of Engineering and Technology (BUET), Dhaka, Bangladesh, e-mail: sahika.buet14@gmail.com
[4]Graduate Student of Bangladesh University of Engineering and Technology (BUET), Dhaka, Bangladesh, e-mail: pinkiwre10@gmail.com
[5]Professor of Bangladesh University of Engineering and Technology (BUET), Dhaka, Bangladesh, e-mail: sabbbirkhanbuet@gmail.com

***Corresponding Author**

ABSTRACT

Bangladesh is a flood-prone country.It consists of the flood plains of the Ganges, the Brahmaputra and the Meghna rivers and their numerous tributaries and distributaries. As a low-lying country, at least, 20 % areas are flooded every year and in case of severe flood 68% areas are inundated in Bangladesh.The north eastern part of Bangladesh is accountable to not only the monsoon flood but also the flash flood caused by the hilly regions of India. The Kushiyara River crossing through three districts (Shylet, MoulviBazar and Sunamganj) plays the major role in the flooding of this regions especially in the Shylet and Moulovibazar district. The most catastrophic flood event on this area was originated during the year 2004, and also in the year 1998. The major objective of the study is to generate floods maps of these years including the year 2015, and then to show the comparison of inundated area and the extent of the flood between 1998, 2004 and 2015 flood events. Another purpose of the study is to generate a calibrated 1D-2D model for the Kushiyara river floodplain.

To achieve the objectives the 1D model was generated using the Hec-GeoRAS and the HEC-RAS 5.0.5 model and the Manning's n was calibrated for the year 2015 and validated for 2004 and 2016. After generating a calibrated model of Kushiyara river,a 2D simulation was performed for the monsoon period (May-November).Boundary conditions for upstream and downstream were defined by discharge and water level for operating the 1D and 2D model. After the simulation of the 1D-2D coupled model, the flood inundation boundary was exported in GIS and flood inundation boundary map was generated using the map layers of GIS.

The study founded the Manning's n value as .020 after the calibration and validation was performed. The study has founded that the area of flood extent varies from 7-26 % of the total land area of the floodplain and the floodplain boundary consists of the area of the thana's through which the river flows .And the effect of the flood was comparatively catastrophic in 2004 than the other two years based on the available data of the first three months of the monsoon. And the comparative analysis shows that generally the flood extent is maximum in the later monsoon and the inundated area gradually increases from May to November in 2015 flood and maximum is August and September in 1998 flood in the respected floodplain.

***Keywords**: Kushiyara river, HEC-GeoRAS, HEC-RAS, Flood inundation.*

1. INTRODUCTION

Flood can be defined as the temporary overflow of a normally dry area due to overflow of a body of water, unusual build up, runoff of surface waters or abnormal erosion or undermining of shoreline. Flood can also be overflow of mud caused by build-up of water underground (BusinessDictionary, 2019). Bangladesh is under sub-tropical monsoon climate where annual average precipitation is 2300 mm, varying from 1200mm in the north-west to over 5000 mm in the north-east (FFWC, Flood Annual Report, 2015).The country is mostly flat with few hills in the southeast and the north-east part (Rahman & Hossain, 2014). It consists of the flood plains of the Ganges, the Brahmaputra and the Meghna rivers and their numerous tributaries and distributaries.

The Ganges, Brahmaputra and Meghna river systems together, drain the huge runoff generated from large area with the highest rainfall areas in the world (FFWC, Flood Annual Report, 2015). Country has experienced seventeen highly damaging floods in the 20th century (Rahman & Hossain, 2014).Since independence in 1971, Bangladesh has experienced floods of a vast magnitude in 1974,1984,1987, 1988, 1998, 2000 & 2004 (FFWC, Flood Annual Report, 2005). The largest recorded flood in depth and duration of flooding in its history was occurred in 1998 when about 70% of the country was under water for several months (FFWC, Flood Annual Report, 2015). The recent catastrophic floods had caused losses from one to over two million tons of rice, or 4-10% of the annual rice production (Islam, Bala, & Haque, 2010).

Floods are the most significant natural hazard causing suffering to a large number of people and damage to property in Bangladesh. Different reports estimate that the flood damage was US $ 1.4, 2.0, 2.3, and 1.1 billion in the 1988, 1998, 2004 and 2007 severe flood's year in Bangladesh respectively.

In the flood event of 1998, 32 of 64 districts in Bangladesh were affected, 1050 deaths reported, 30 million people were affected, 25 million people were homeless, 26000 live stocks lost, 575,000 hectares of crops were destroyed, 200000 schools and other educational facilities damaged, 300,000 tube wells damaged, 16,000 km of roads were flooded and 45000 km of river embankments damaged. (Aid, 1998). In the North Eastern region of Bangladesh aside the monsoon floods the flash flood is also a common phenomenon. Flash floods, which are caused by heavy or excessive rainfall in a short period over a relatively small area. During flash flooding, water levels rise and fall rapidly with little or no advance warning. Typically, they occur in areas where the upstream basin topography is relatively steep and the time needed for the water to flow from the most remote point point in the watershed is relatively short. The most flood affected areas are in the Hoar Basin of the northern belt of Bangladesh, which is made up of Sylhet, Sunamganj, Moulavibazar,Habigang and Netrokona Districts, as well as the southeast in the Chittagong, Cox's Bazar and the Bandarban Districts (BWDB, 2014).

Flash floods are most common from April to July and from September to October. Flash floods carry sediment that has eroded from hilly catchment areas. During heavy rainfall in the hilly regions, massive erosion occurs on exposed surfaces of the hills. When there is high rainfall, coarser sediment erodes and moves along the rivers. During a flash flood, sediment transport rates increase significantly in a disproportionate distribution of sediment and changes in channel sizes, shapes and even location (Bangladesh, 2018).

2. METHODOLOGY

2.1 Study Area

Kushiyara is a trans-boundary river. It originates from the Barak river of India and enters Bangladesh in the Boro Thakuria union of Jokigang upazilla of the Shylet district and and falss in the upper Meghna in the Kalma Union of Ostogram Upizilla of Kishorgang district. There is no significant historical change in the discharge, water level or the width of the Kushiyara River but the bank erosion increased with time.

The length of the Kushiyara River is 288 km, and the minimum width 196m and the maximum width is 347m and the average width is 268m. The characteristics of the flow of Kushiyara is meandering and the average slope is 6 cm per kilo-meter. The flow of the river is perennial, and the dry season is February-April where the approximate flow is 25.02 cubic meter and the maximum approximate flow is 2990 cubic meter recorded in the August in the Sheola Station. There is flood protection embankment 118.60 kilo-meter in the right bank. There are also two bank revetments in the left and right bank which are respectively 8.054 km and 1.069 km. There are also two spurs in the river of .30 km and .072 km long in the left and right bank of the river.

This river is used to transport stones to different regions of the country and sand is transported in Shylet. And according to BIWTA the navigation route of Kushiyara is of class 3.

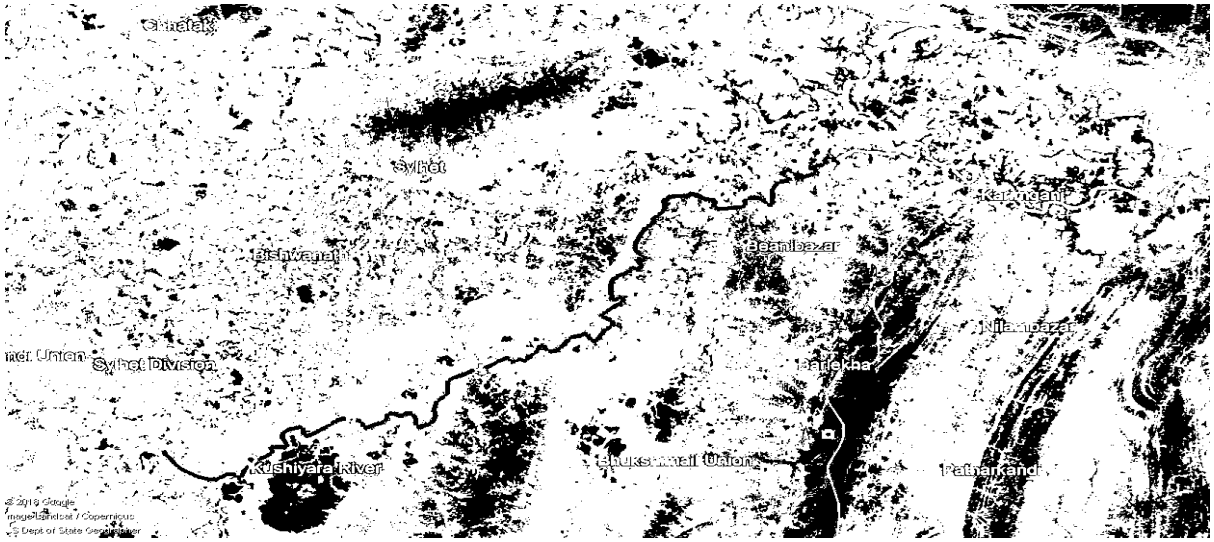

Figure 2-1: Reach of Kushiyara River for the Study

2.2 Data Collection

In order to develop the mathematical flood model, various kinds of data, recent and previous years have been collected and compiled. These data also form the basis for further analysis and interpretation of the model results leading to accurate assessment of hydrological condition of Kushiyara River floodplain. According to the modelling requirements, a significant amount of data includes water level, discharge, cross-section have been collected and setup flood model using this data.

Table no 2-1: Type & Sources of Data Sets

Data Type	Data Source	Data Location	Position	Periods (Year)
Discharge Data	BWDB	Sheola-173	Upstream	1980-2016
Discharge Data	BWDB	Sherpur-175.5	Downstream	1980-2016
Water Level Data	BWDB	Sheola-173	Upstream	1980-2016
Water Level Data	BWDB	Fenchugang-174	Mid Position	1980-2016
Water Level Data	BWDB	Sherpur-175.5	Downstream	1980-2016
Cross Section	BWDB	RMKUS 1 to RMKUS 12		2004
DEM	USGS	Bangladesh		2014
Satellite Image	Earth Explorer	North-East (NE) of Bangladesh		2018

2.3 Sequential Steps in Model Setup

The following steps was undertaken to setup the HEC-RAS 1D-2D coupled model. At first the Digital Elevation Model (DEM) was processed in GIS using HEC-GeoRAS, then the model was done by HEC-RAS & finally the output maps were generated by using GIS.

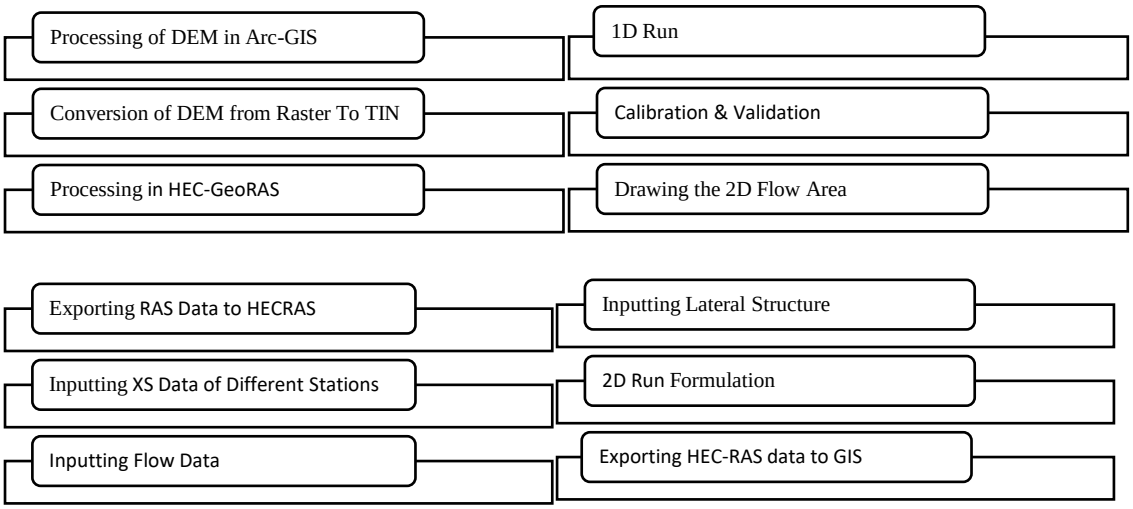

3. RESULTS & DISCUSSIONS

3.1 Calibration & Validation Result

The following Table 3-1 shows the calibration & validation result of the 1D-2D coupled model. The table also consists the BWDB station names that was used to carry out the calibration & validation It can be observed from the table that the Mannings roughness parameter was found to be 0.020 for the year 2015,2014 & 1998.

Table 3-1: Calibration & Validation Results

Model Run Year	Year of Comparision	u/s discharge Station	d/s Water Level Station	Calibrated With Station	Manning's n
2015	2015	SW 173	SW 175.5	SW 174	.020
2014	2014	SW 173	SW 175.5	SW 174	.020
1998	1998	SW 173	SW 175.5	SW 174	.020

The following Figure 3-1 shows the calibration curve, comparing the observed & simulated water level for the station SW 174. The calibration curve shows that the simulated water level follows the pattern of the observed water level founded from the BWDB station data & that indicates that the 1D model was well calibrated for the year 2015.

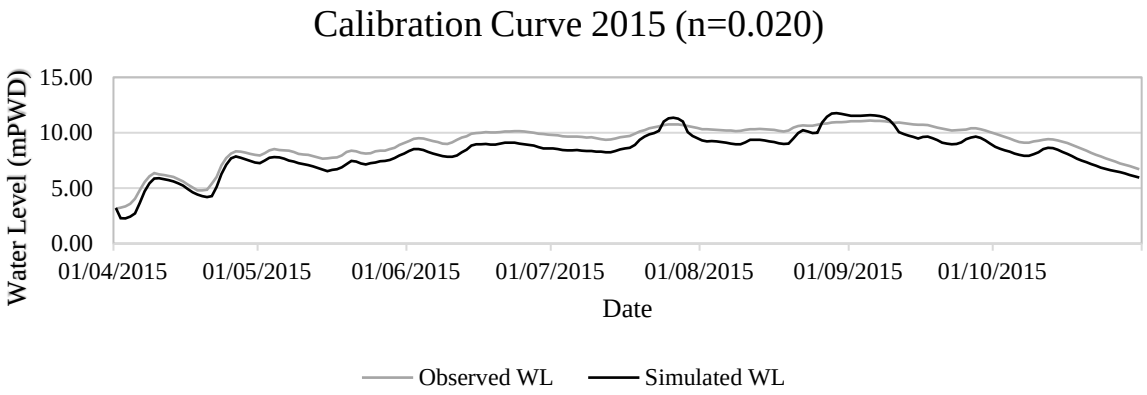

Figure 3-1: Calibration Curve for 2015

In order to find whether the Manning's 'n' value is well suited for the other years as well, a validation was done for the year 2014 & 1998. The following Figure 3-2 shows the validation curve between the observed & simulated water level values of the station SW 174. The figure shows that the Manning's n value remains merely the same in both of the years, that signifies that it took a good amount of time for the morphological change of any river.

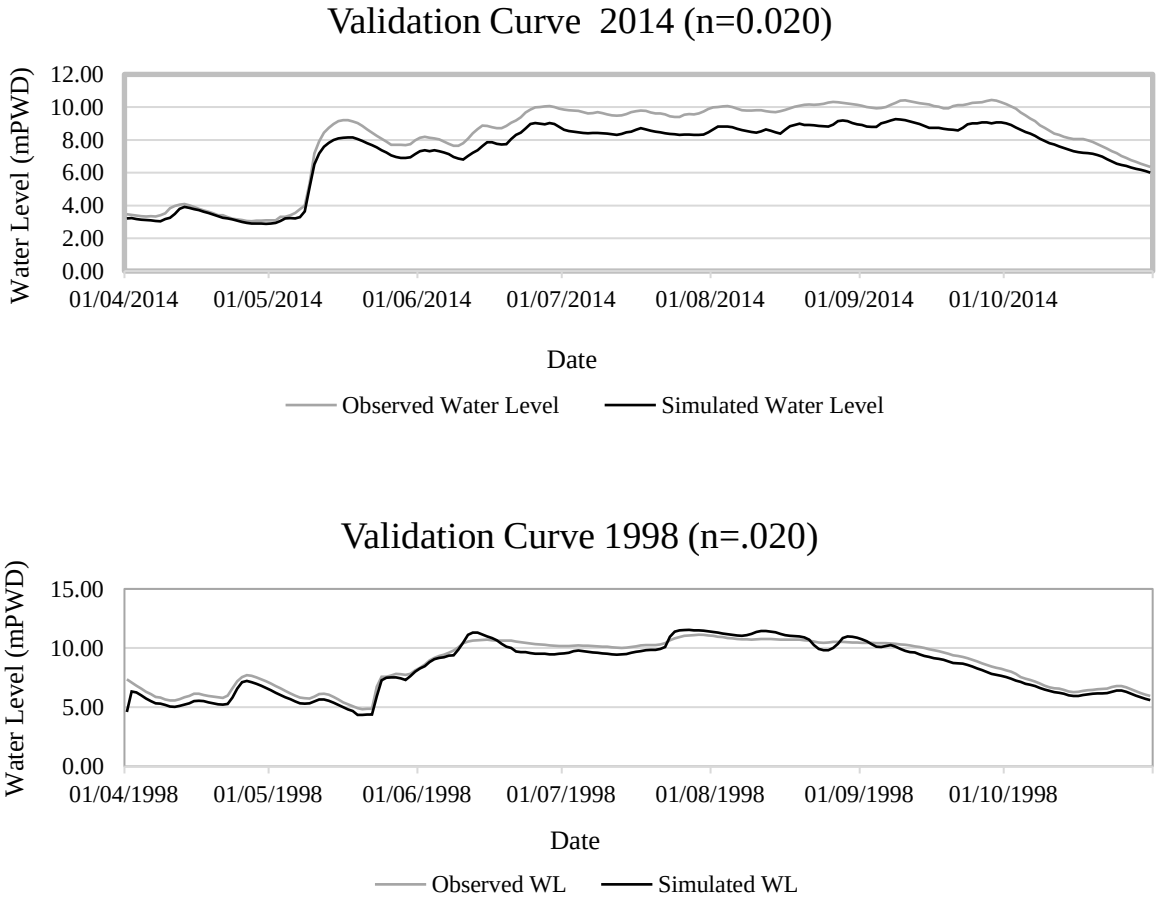

Figure 3-2: Validation Curve for 1998

3.2 Results of Flood Inundation Modeling

The following Figure 3-3 shows the inundation map of the Kushiyara River from the 1D-2D simulation using HEC-RAS 5.0.5. The details analysis of the inundation has discussed on section 3.3.1

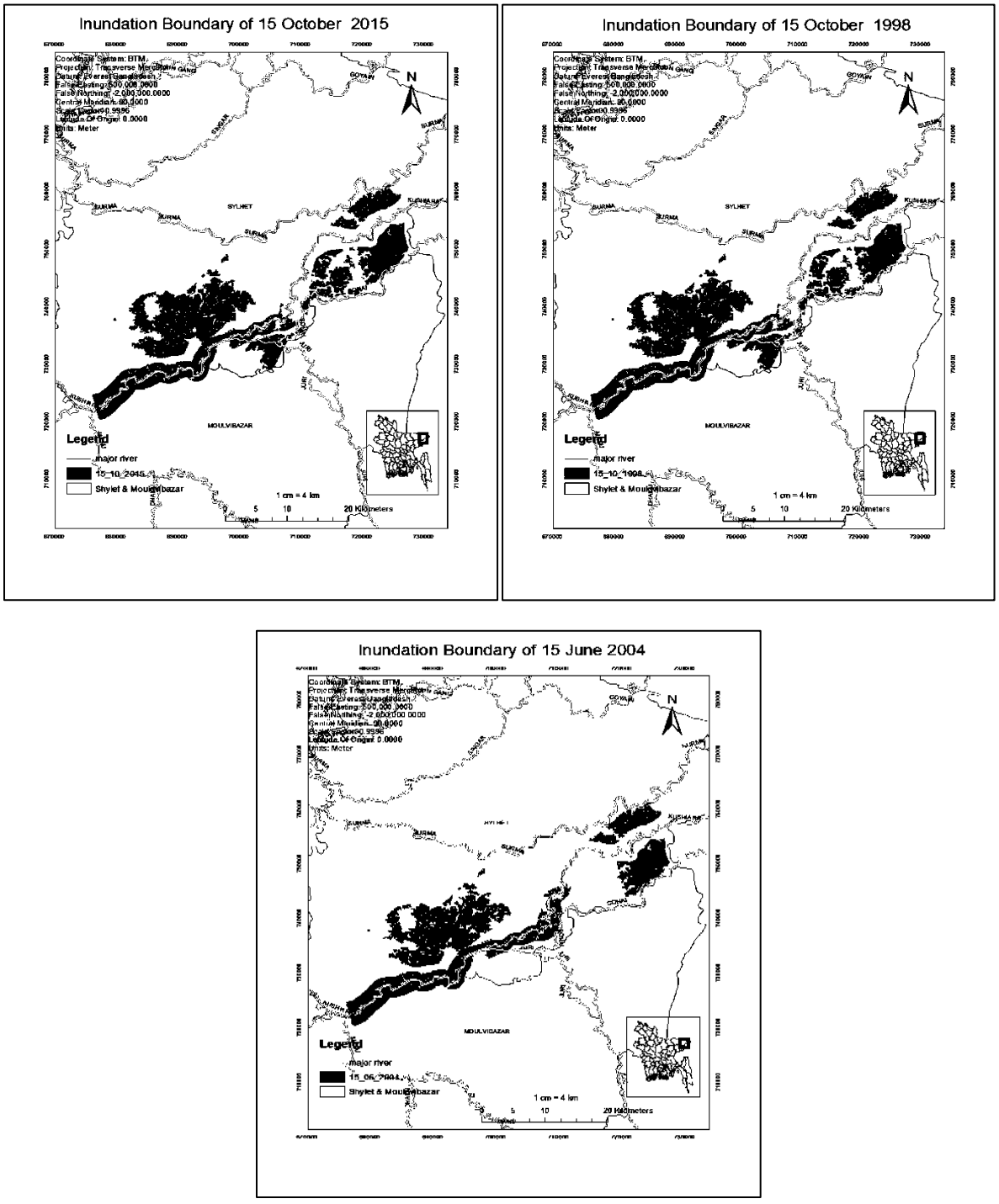

Figure 3-3: Inundation Maps of Year 2015, 2004 & 1998

The comparative analysis of the inundation areas for the different flood years are shown in the following Figure 3-4. It can be observed from the figure that the inundation area is higher for the flood events of 1998 & 2004 compared to the area of 2015.

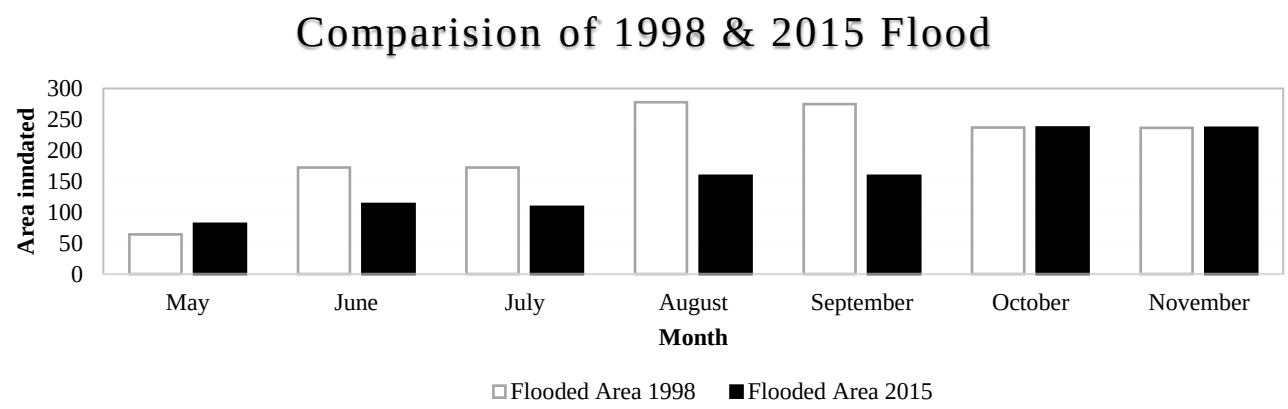

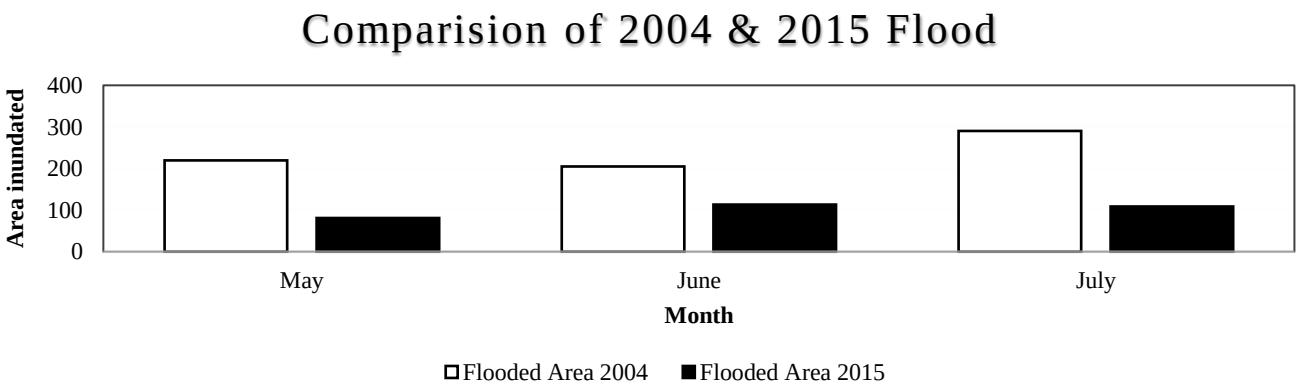

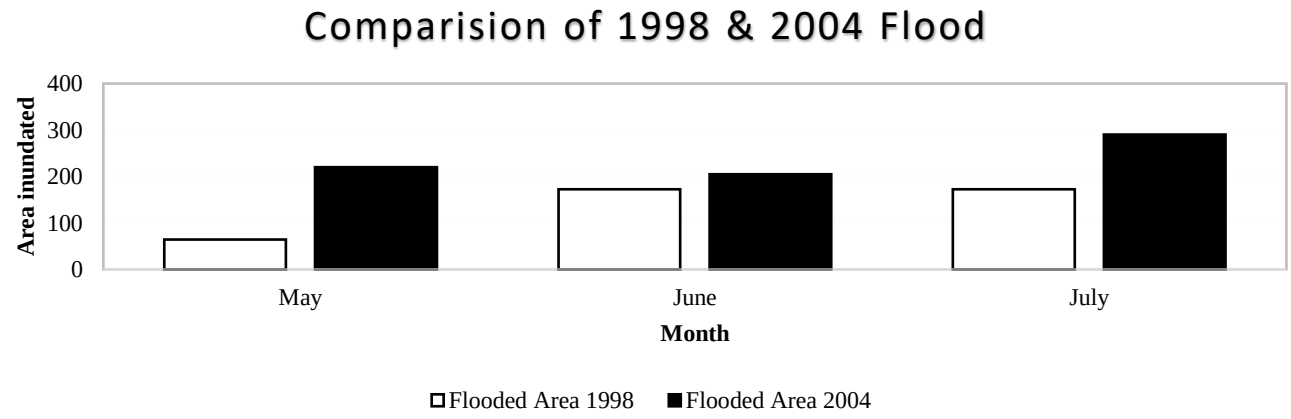

Figure 3-4: Comparative Representation of the Flooding Areas among the Respective Years

The comparison of the inundation areas of different years can be seen in the Figure 3-5, it shows that the 2004 flood was more catastrophic compared to the other to flood years.

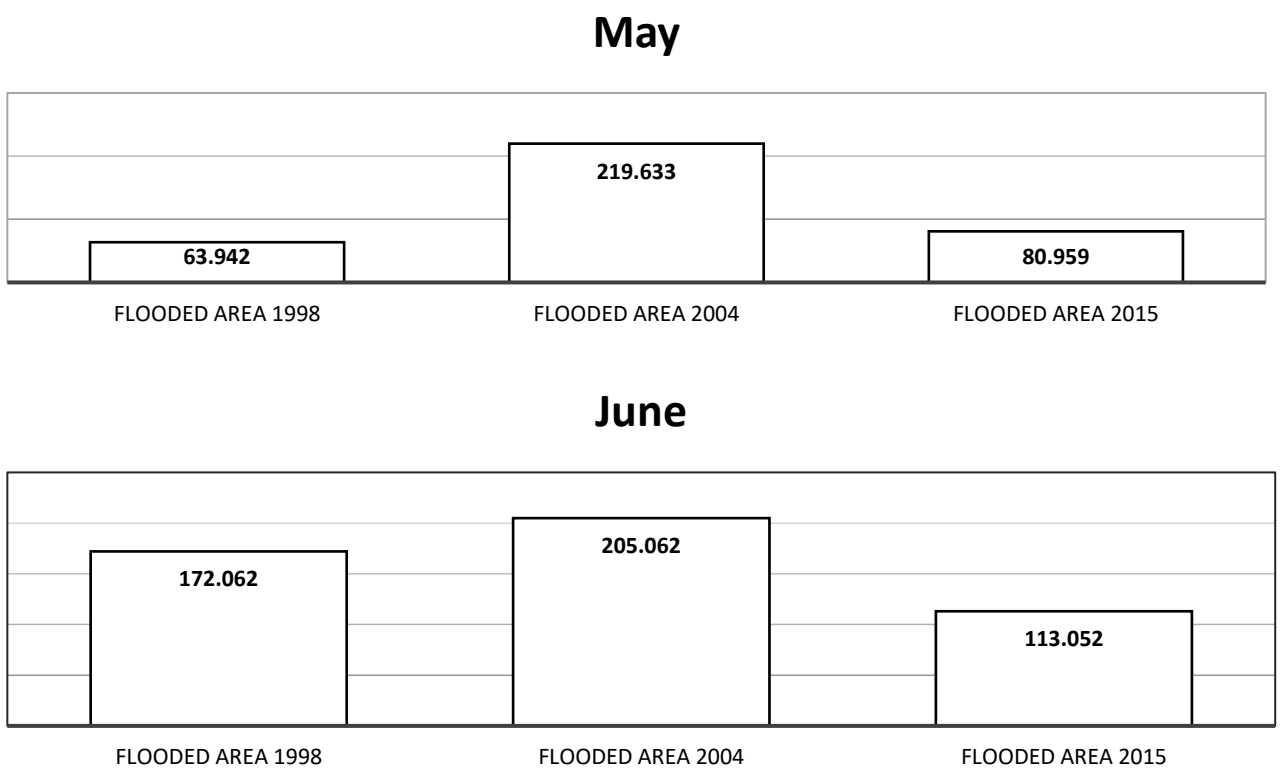

Figure 3-5: Monthly Comparison of Inundation Areas of the Respective Years

The following Table 3-2 shows the percentage of the area inundated in different months of different flood years. The total area of the floodplain was 1116.779 Square Kilometers that consists of Beanibazar, Golapgonj(Partial), Fenchuganj, Balaganj,Rajnarag(Partial) thana's.The table shows that about 26% of the total floodplain area was inundated during the July 2004 flood & more than 12% area was inundated for about 5 months during the 1998 flood event.

Table 3-2: Percentage of Inundation Area of different Flood Years

	Area Inundated (Square Kilometer)					
Month/ Year	**1998**	**Percentage of Total Area (%)**	**2004**	**Percentage of Total Area (%)**	**2015**	**Percentage of Total Area (%)**
May	63.94	5.72	219.63	19.66	80.95	7.24
June	172.06	15.40	205.06	18.36	113.05	10.12
July	172.39	15.43	290.38	26.00	108.52	9.71
August	277.53	24.85			158.69	14.21
September	274.89	24.61			158.69	14.21
October	236.98	21.22			236.98	21.22
November	236.43	21.17			236.43	21.17

3.3 Discussions

3.3.1 Analysis of Flood Inundation of Different Years

Analysing the Flood maps of 2015 shows the followings:

- The extent of flood is maximum in the later monsoon, in the October and November and the inundation area is maximum in these two months.
- The Flood extent or the inundated area is very negligible in the pre-monsoon period consisting of the month May, June and July and it gradually increases from the August to the November.

Analysing the Flood maps of 1998 shows the followings:

- The inundation pattern is almost quite similar in the middle of October and November that shows that the flood water stayed for about a month in the respected Floodplain.
- The Flood Maps shows that the upstream portion of the river flooded in the mid of the monsoon where the downstream portion of the river inundated in the later monsoon, that shows that the elevation of the downstream floodplain is higher than the upstream floodplain.

Analysing the Flood maps of 2004 shows the followings:

- The extent of flood in the following three months is comparatively higher than the other years, especially in the May. That shows the possibility of flash flood in the region in the May.
- The extent of the flood in the pre monsoon shows that the flood event of 2004 is most catastrophic and the inundation areas is higher in the later months, but the maps can't be generated due to unavailability of data.

3.3.2 Outcomes of the Study

- The Manning's roughness value is found to be .020 from the study after several trails of different values in the calibration year and was validated for two different years, that was approximately same or having a small change in the value. That signifies that the roughness of the reach remains quite unchanged through the years.
- The model was simulated for three different years. A comparatively low flood year 2015 and for the flood year of 1998 and 2004. The graphical representation shows that the flood event was most catastrophic in 2004 in comparison to other flood events.
- The comparison of 1998 and 2015 flood shows that, the extent of the 1998 flooding was gradually increasing in comparison to 2015 flooding but was nearly same in the later monsoon.
- The study shows that the flooded area is maximum in August and September in the 1998 flood event and in October and November in the 2015 flood event in the designated floodplain boundary.
- But there is a severe change in May 2004, the total inundated area is very high that could be the effect of combination of both the higher monsoon flood and the flash flood.
- The percentage of inundated area compared to the area of the three districts varies from 7-26% according this three year and the extent of the flood is maximum in the Shylet district rather than Moulovi-Bazar.
- This calibrated model can also be used for generating Risk Map of the area and also for future inundation mapping on the availability of generated hydrologic datasets.

  The calibrated model can also be used for determining the crest level of levee for the flood protection measure.

4. CONCLUSIONS & RECOMMENDATIONS

In comparison with the extent and effect of flooding in Bangladesh, the study modelling for flood inundation has not been done with a great extent so far. And especially for the flash flood in the north-eastern region of Bangladesh where flash flood is of great interest as well as the monsoon flood. This study has tried to generate the flood condition of the flood years conducting unsteady flow using discharge and water level data sets of different stations. The model is not capable of representing the actual scenario of the river, as only the hydrologic data and the cross-section data sets does not represent

the morphologic and bed characteristics of the river but can give a brief idea about the flood scenario of different years.

- The most important part of the model is the DEM (Digital Elevation Model) file, which has of spatial resolution of 30m*30m. The DEM of such spatial resolution does not represent the actual morphologic characteristics of the region, so DEM of higher spatial resolution should be used to get a better scenario of flood inundation.
- In this study the HECRAS 5.0.5 was used, though it is the latest version of HEC-RAS but the model gets unstable some of the time while computing a large number of datasets in a comparatively shorter interval. So, the simulation capacity of the model could be improved to get better results.
- The collected discharge and water level data were sometimes insufficient to run the model, as like there was no WL data in the d/s station in 2004 after August, hat keeps the mapping incomplete in an important flood year so the data sets should be complete and appropriate.

ACKNOWLEDGEMENTS

The authors acknowledge the support from the Department of Water Resources Engineering, BUET during this study.

REFERENCES

(2019, April 18). Retrieved from BusinessDictionary: http://www.businessdictionary.com/definition/flood.html

Aid, A. (1998). *Official Damage Statistics of Bangladesh Flood 1998.*

Bangladesh, S. F. (2018). *Bangladesh Flooding Disaster Summary Sheet.*

BWDB. (2014). *BWDB Annual Report.* Bangladesh Water Development Board.

FFWC. (2005). *Flood Annual Report.* Flood Forecasting and Warning Centre. Bangladesh Water Development Board, Government of the People's Republic of Bangladesh Ministry of Water Resources, Dhaka.

FFWC. (2015). *Flood Annual Report.* Flood Forecasting and Warning Centre.Bangladesh Water Development Board, Government of the People's Republic of Bangladesh Ministry of Water Resources, Dhaka.

Islam, A., Bala, S., & Haque, M. (2010). Flood inundation map of Bangladesh using MODIS time-series images. *Journal of Flood Risk Management*.

Rahman, D. M., & Hossain, M. A. (2014). *An Analytical Study of Flood Management in Bangladesh.* IOSR Journal of Engineering (IOSRJEN).

Proceedings of the 5th International Conference on Civil Engineering for Sustainable Development (ICCESD 2020), 7~9 February 2020, KUET, Khulna, Bangladesh (ISBN-978-984-34-8764-3)

CAUSES AND EFFECTS OF WATER LOGGING IN MIRPUR AREA, DHAKA CITY

Sk. Md. Imdadul Islam*[1], Sayed Shams-E-Rabbi[2] and Maria Shirin Anita[3]

[1] Lecturer ,World University Of Bangladesh, Dhaka, Bangladesh, e-mail: imdadulemon109@gmail.com
[2] Post-graduate Student, AEM, IPE, BUET, Bangladesh, e-mail: sayed.rabbi@outlook.com
[3] B.Sc., CE, KUET, Bangladesh, e-mail: mariashirin17@gmail.com

***Corresponding Author**

ABSTRACT

Dhaka is the capital city of Bangladesh, is one of the populous mega City in the world. As the growth of urban population is taking place at an exceptionally rapid rate, the city is unable to cope up with the changing situations due to their internal resource constraints and management limitations. In recent years Dhaka City is facing extensive water logging during the monsoon (May to October) as a common and regular problem of the city like water pollution, traffic congestion, air and noise pollution, solid waste disposal, black smoke, etc. This paper focuses on the rainfall-induced flooding that is caused by high-intensity storm rainfall runoff in the city area that is inundated for several days mainly due to lack of proper drainage system and inefficient management. It ascertains the inherent causes of such water logging and its effects on the city life from the perception of authorities of different development organizations, experts and people living in different parts of Dhaka City. Heavy downpour occurs in Dhaka City during monsoon, as it is located on the extensive floodplains of Ganges and Brahmaputra. But the unplanned spatial development activities and growth of habitation due to rapid population growth are causing encroachment on retention areas and natural drainage paths with little or no care of natural drainage system that creating obstacles to properly drained out the urban runoff. Therefore water logging is taking place as different parts of the city remain inundated for several days. Inadequate drainage sections, conventional drainage system with low capacity and gravity, natural siltation, absence of inlets and outlets, indefinite drainage outlets, lack of proper maintenance of existing drainage system, and over and above disposal of solid waste into the drains and drainage paths are accounted for the prime causes of blockage in drainage system and water logging. Also, seasonal tidal effects and the topography of the city area causing water logging. This water logging becomes a burden for the inhabitants of Dhaka City and creating adverse social, physical, economic and environmental impacts. Disruption of traffic movement and normal life; damage of structures and infrastructure; destruction of vegetation and aquatic habitats; loss of income potentials are the encountered effects of water logging on city life. The storm water becomes polluted as it mixes with solid waste, clinical waste, silt, contaminants, domestic wastes and other human activities that increase the water-borne diseases. The stagnant storm water leads to the creation of breeding sites for disease vectors that becomes a hazard to health as well as being unsightly and foul-smelling.

Management of drainage system of Dhaka City is presently a challenge for the urban authorities because of the rapid growth of population and unplanned development activities. Therefore, close coordination among urban authorities and agencies and collaboration between public and private sectors is needed for effective management and sustainable operation of the urban drainage system.

Keywords: *Water logging, Excessive rainfall, Mismanagement of waste ,Drainage, Mirpur.*

1. INTRODUCTION

Water logging is one of the prime urban problems that Dhaka suffering for decades. Even after a light rain many areas of the Dhaka turned out to be small islets with thousands stranded or wallowing through knee-deep dirty waters stuck up in roads and streets. If the rain lasts for hours it changes the view of the Dhaka city - most of the busy roads Mirpur-10 Kazi para Shewra para and streets become inundated because canals, being the primary drainage system of the city are blocked cannot carry the huge volume of storm water. This water logging is a problem creating adverse social, physical, economic and environmental impacts in life and living in Dhaka. Water logging becomes a burden for the inhabitants of Dhaka City and creating adverse social, physical, economic and environmental impacts. This Study will assess the causes and effects of water logging in Mirpur Area. Disruption of traffic movement and normal life; damage of structures and infrastructure; destruction of vegetation and aquatic habitats; loss of income potentials are the encountered effects of water logging on city life. The storm water becomes polluted as it mixes with solid waste, clinical waste, silt, contaminants, domestic wastes and other human activities that increase the water borne diseases. The stagnant storm water leads to the creation of breeding sites for diseases vectors that becomes a hazard to health as well as being unsightly and foul-smelling even death of pedestrians. (Tawhid, Causes and effects of water logging in Dhaka city, 2004)

Bangladesh is located on the extensive floodplains of the Ganges and Brahmaputra. Therefore, flooding is a natural part of the life of its inhabitants. Thus water logging in Dhaka City is not a new problem but the frequency of this problem is increasing day by day. Flooding due to rainfall is also a severe problem for Dhaka City that is inundated for several days mainly due to the drainage congestion (Haq & Alam, 2003). Dhaka metropolitan area has experienced water logging for last couple of years. Even a little rain causes a serious problem for certain areas, so that parts of Dhaka are inundated for several days. The water depth in some of the areas may be as much as 50-70 cm, which creates large infrastructure problems for the city and a huge economical loss in production for the city together with large damages of existing property and goods (Mark & Chusit, 2002). In addition, deceases are spread and gives problems to the population e.g. in terms of diarrhoea. Dhaka City is protected from river flooding by an encircled embankment called Buckland Flood Protection Embankment. During the monsoon (May to October), the water level of the surrounding rivers remains higher than the internal drainage level. Consequently, the drainage of the city depends very much on the water levels of the peripheral river system. At present, the drainage depends mostly on the difference in water level between the river and the drainage system in the city and when the water level in the river increases the drainage capacity to the river is reduced (Mark & Chusit, 2002). Flooding in Dhaka Metropolitan area can be classified into two types. One results from high water levels of peripheral river systems, thus rendering any natural drainage impossible.

1.1 Objectives of the Study

The Main objective of this paper is to identify the Water logging in Mirpur area. The ultimate goal of the study is to improve the drainage condition of the Mirpur area to remove the water logging problem of the area. However there are some specific objectives to full fill the goals. These are,

- To identify the causes of drainage congestion of the Mirpur area.
- To investigate the problem of drainage congestion on city life.
- To suggest some recommendation for improving the Water Logging on of Mirpur area.

basins, which in turn lead to shortening of the runoff concentration time and an increase of the peak flow.

1.2 Location

Mirpur is located at 23.8042°N 90.3667°E. It has a total area of 58.66 km2 (22.65 sq. mi) and is situated in the north-east of Dhaka city. Mirpur is one of the prominent regions of Dhaka city. Established in 1962, it is located to the north-east of the city (BRACK, 2016). If the rain lasts for hours it changes the view of the Dhaka city - most of the busy roads Mirpur-10 Kazi para, Shewra para and streets become inundated because canals, being the primary drainage system of the city are

blocked cannot carry the huge volume of storm water. This water logging is a problem creating adverse social, physical, economic and environmental impacts in life and living in Dhaka. Water logging becomes a burden for the inhabitants of Dhaka City and creating adverse social, physical, economic and environmental impacts. This Study will assess the causes and effects of water logging in Mirpur Area. Disruption of traffic movement and normal life; damage of structures and infrastructure; destruction of vegetation and aquatic habitats; loss of income potentials are the encountered effects of water logging on city life. The storm water becomes polluted as it mixes with solid waste, clinical waste, silt, contaminants, domestic wastes and other human activities that increase the water borne diseases. The stagnant storm water leads to the creation of breeding sites for diseases vectors that becomes a hazard to health as well as being unsightly and foul-smelling even death of pedestrians.

1.3 Water Logging Situation in Dhaka City

Water logging in urban areas is an inevitable problem for many cities in Asia. In Bangladesh, Mirpur area has serious problems related to water logging. The situation was highlighted in September 2017-2019 when residences experienced ankle to knee-deep water on the streets. Daily activities in parts of the city were nearly paralyzed and heavy traffic jams occurred due to stagnant water on the streets.
Given the severity of the problem, some organizations, including both private and public ones, have conducted several studies to identify the major causes of water logging in the city. Dhaka South City Corporation (DNCC) and Dhaka Water Supply and Sewerage Authority (Wasa) have recently jointly carried out such a study, the findings of which will be released around the middle of next month. The Dhaka Tribune obtained a copy of the study report that describes the causes and possible solutions at length. The draft report says sewage makes its way into nearby rivers, but the authorities are constructing a system of sewers that is not properly connected to the main streams or canals. “If a drain or a sewer pipe is not properly linked with another drain or pipe, water will never drain away. Most of the drains in Dhaka are not correctly connected with one another causing flood and water logging in the city.

1.4 Causes and Effect of Water Logging

1.4.1 Major Causes Identified

Extensive field observations in and around mirpur area, long discussions with officials of relevant organizations and analyses of available data suggest the followings to be the major causes of water logging in Metropolitan Dhaka.

- Poor discharge capacity of existing drainage pipes and canals.
- Clogging of existing drainage pipes due to inadequate collection of solid wastes, street sweepings and lack of maintenance.
- Impediment of canal waters due to encroachment of buildings and by problems caused by road and railway crossings.
- Insufficiency of drainage pipe length.
- Electrical breakdown of equipment at the existing pump stations.
- Encroachment of the natural drainage channels.

To find out inherent causes of water logging in Dhaka City, a field survey as a questionnaire survey, informal interviews and open discussion has been conducted with the authorities of different concerned organizations, experts and people living in different parts of Dhaka City.

1.4.2 Excessive Rainfall

Bangladesh is a tropical country and is located on the extensive floodplains of the Ganges and Brahmaputra. The Himalayas stands to the northeast of the country and the Bay of Bengal lies on the south of the country. As a result heavy downpour occurs on the country, especially in the monsoon season (May to October). In recent years the Dhaka Metropolitan area has been exposed to water logging due to heavy rainfall. During the 2018, 2019 , excessive rainfall occurred in Dhaka caused short duration flooding in different areas of the City namely Shantinagar, Nayapaltan, Rajarbag, Dhanmodi, Azimpur and Green Road (S. Huq and M. Alam, 2003). The most recent downpour

occurred from September 11th to 16th 2004 in Dhaka forced the City life standstill. 341 mm. of rain in 24 hours between September 14th and 15th is the heaviest ever rainfall. Dhaka's previous record of 274 mm of rain on September 16, 1966. Dumped with average 300 mm of rain in that week (MDB, September 2004), Dhaka was sloshing with floodwaters that sent many places, including Motijheel commercial heart, under chest-deep water. The devastating impact of the downpour that paralyzed Dhaka City is a salutary reminder of the severity of the problem.

According to survey, 74 percent of the respondent has been mentioned that heavy rainfall is one of the main reasons for water logging in Dhaka City. Relatively low intensity of rainfall causes serious water logging problems for certain areas of the City that are inundated for several days mainly due to the drainage congestion.

1.4.3 Disappearance of Natural Drainage System

The disappearance of the natural drainage system is one of main causes for water logging. Rapid population growth and unplanned development, unplanned land filling to develop new residential areas, uncontrolled and haphazard disposal of solid wastes and garbage into the existing drainage system, and encroachment on lakes, khals/canals and rivers with unauthorized construction are the summarized general man made physical and social activities related to the disappearance of natural drainage system. 95 per cent of the respondent claimed these activities for prime causes of water logging in Dhaka City.

1.4.4 Waste Management System

"Waste management system is one of the important factors for water logging in Dhaka City," said 82 per cent of the interviewers from different development organizations and inhabitants. The increased congestion of the city area, the high population density and the rapid growth all around it has made it impossible to clean the street and drains as fast as the waste thrown onto them. Dhaka, with a population about 18 million, generates a massive quantity of waste every day from various sources. The major sources of solid waste in Dhaka are residences, streets, market places, commercial establishment, and hospitals. Sources and characteristics of urban wastes in Bangladesh are shown in Table 1.

Table 1: Sources and Characteristics of Urban Waste in Dhaka

Types of Solid waste	Quantity (%)
Domestic	40-60
Commercial	5-2
Street Sweeping	20-30
Combustible	20-30
Non-combustible	30-40
Moisture	45-50

Source: Bangladesh Centre for Advanced Studies (BCAS), 2017

Due to urban development, population growth, and consumption increase, the volume of solid waste generation in Dhaka City increases every year. At present Dhaka City generates 3500-4000 tons solid waste per day, with a per capita generation of about 0.5 kg per day (Kazi, 2017). The composition of solid waste varies according to location, standard of living, energy sources and season. The quantity of waste generation increases during rainy season when many vegetables and fruits, especially mango and jackfruit, are available. Solid waste in Dhaka mainly consists of food, grass and plants, brick, dirt, paper and polythene materials (Table 2)

Table 2:Composition of Solid Waste in Dhaka City

Materials	Quantity (%)	
	Residential Areas	Commercial Areas
Food Waste (Organic)	84.37	79.49
Paper/cardboard	5.68	7.22
Textiles	1.83	1 .59
Plastics	1.74	1 .48
Glass/metals and construction debris	6.38	10.22

Source: Bangladesh Centre for Advanced Studies (BCAS), 2017

1.5 Effects of Water Logging

Urban runoff causes problems. These become obvious when a constructed drainage system fails. Urbanization disrupts natural drainage patterns; natural watercourses are destroyed; natural retention of runoff by plants and soil is removed and the creation of impervious surfaces increases the amount of runoff. This runoff becomes polluted as solid waste, silt and contaminants are washed off roads. The increase in volume and rate of runoff causes erosion and siltation. Therefore, it becomes a burden for the inhabitants of the city, leading to water logging and creating adviser social, physical, economical as well as environmental impacts. A field survey as questionnaire survey, informal interview and open discussion has been conducted with inhabitants of Dhaka City to know the problem faces due to water logging. The total sample was 100 in different parts of the city including authorities of different concerned organizations, experts and general people and their summarized opinions about the problem faces due to water logging are as follows.

Table 3: Types of Problems Faced due to Water Logging in Dhaka City

Problems	Percentage
Disruption of traffic movement	88
Disruption of normal life	93
Damage of roads	70
Damage of underground service lines	56
Damage of household goods	65
Water pollution	95
Water borne diseases	84
Damage of trees and vegetation	48
Increase of construction and maintenance cost	58

Source: Report from brac, 2018

1.5.1 Social Problem

Disruption of Traffic Movement

Disruption of traffic movement is an important identified impact according to 88 per cent of interviewers, which arises due to the traditional water logging problem. Normal traffic movement is hampered during rainfall over 25 mm, creating traffic jam in the city area and people lose their valuable time. Where the storm water cannot drain out, puddles will form. This is not just inconvenience for pedestrians but also dangerous for road users. Following pictures (Picture-2.1) illustrates that the heavy rainfall in August 2019 disrupted traffic movement in Mirpur area**.**

Disruption of Normal Life

Water logging seriously disrupts normal life and it has direct impacts on the poor, as they often live on unsuitable, low-lying and flood prone or steep, and unstable sites, have high-density housing (increasing the impermeability of the ground), poor urban planning and control and lack of investment

in urban infrastructure. 93 per cent inhabitants (according to field survey) mentioned that water logging hamper daily life of the city dwellers. The more affluent members of society have the option to move to less flood prone or less polluted areas or flood-proof their homes, e.g. through raising the ground level. But the poor bear the brunt of bad drainage, through direct flood damage, pollution of water supplies and the aquatic environment, the breeding of vectors and soil erosion, leading to direct financial costs, loss of income potential, as the home may also be the workplace, and adverse health impacts. Sometimes, they don't have access to potable water and so had to rely on surface or shallow groundwater sources that are polluted. Picture-6.2 illustrates an example that the heavy down pour disrupt the daily life of the city in different places in Dhaka**.**

Purabi-Kalishi road in Dhaka's Mirpur goes under water after rains – An article named "Water logging in city" by Mahmud Zaman Ovi. Published on August 14, 2019 in reader's forum of The New Nation (Bangladesh's Independent News Source) can be a practical example for disruption of traffic movement and normal life.

1.5.2 Environmental Impact

Water Pollution
Theoretically, Dhaka WASA maintains two separate sewer systems: one for domestic wastewater and another for storm water. However, in reality storm sewers also receive domestic wastewater, which causes unwanted deterioration of the storm water discharges. These discharges in turn pollute the receiving water bodies including the lakes, rivers and detention areas. According to survey, 95 per cent inhabitants said that storm water of Dhaka City becomes polluted as it is mix with solid waste, clinical waste, silt, contaminants, domestic waste water and other human activities, which contaminated ground water as well as the receiving water bodies. In recent years Dhaka City is facing extensive water logging during the monsoon (May to August) as a common and regular problem of the city like water pollution, traffic congestion, air and noise pollution, solid waste disposal, black smoke etc.

2. METHODOLOGY

2.1 Methodology

It has already been mentioned earlier that flooding in Dhaka Metropolitan area can be classified into two types. One is river flooding that results from high water levels of peripheral river systems and another is rainfall induced flooding that is caused by high intensity storm rainfall runoff in the city area. The study would be focus on the rainfall induced flooding treated as water logging due to storm water in this study. The methodological approaches of the study are as follows. 1. Selection of the study area.

2.2 Data Collection

To fulfil the objective of the study both primary and secondary data were needed. All the necessary data has been collected from various sources.

2.2.1 Collection of Maps

For the purpose of the present study, three different types of maps have been collected. These are Cadastral Survey (CS) map (1912-1915), Revenue Survey (RS) map (1965-1975) and Dhaka topographic survey maps (1998). First two types of maps have been collected from Directorate of Land Records and Survey (DLRS) the last map is from Survey of Bangladesh. The existing land use map has been collected from Rajdhani Unnayan Kartripakkha (RAJUK) and the land use of different periods has been collected from some relevant literatures and organizations. The existing drainage layout map was also needed and this has been collected form Institute of Water and Flood Management (IWFM), BUET.

2.2.2 Other Secondary Data

Rainfall data and the storm water drainage system data were needed for the study. The rainfall data has been collected from Meteorological Department of Bangladesh (MDE) and the drainage data has been collected from Drainage Department of Dhaka City Corporation (DCC). The past and present data on natural drainage system has been collected from different land use maps prepared by RAJUK. Some literature related to the topic has been reviewed for better understanding of the problem and their main objectives and outputs are attached at the end of this chapter.

2.2.3 Collection of Photographs

Lot of photographs was also needed to illustrate the situation of water logging, related obstacles into the smooth drainage of urban runoff and its effects on urban life. Some of these photographs have been collected directly from field survey and some other from daily newspapers as well as from internet websites.

2.3 Questionnaire Survey and Informal Interview

To find out inherent causes of water logging in Dhaka City and its associate impact on city life, a field survey as questionnaire survey, informal interview and open discussion has been conducted with the authorities of different concerned organizations, experts and people living in different parts of Dhaka City. The questionnaire was designed in such a way that it would track down the problem from the inception and the impact of the water logging in the locality. The sample questionnaire is given in Appendix A. The sample size of these survey activities was 100. Again the respondents were selected in different water logging prone area of the city with different professions. To identify the quality of environment certain environmental parameters were fixed. It also covered the people's perception on conservation/sustainable development of drainage system. Informal interview of official experts of different development agencies was also done in order to know their view of causes and effects of water logging in Dhaka city and sustainable solutions.

3. RESULTS & DISCUSSIONS

Dhaka city, the capital of Bangladesh, is located on the flat deltaic plain of the three major international rivers, the Ganges, Brahmaputra and Meghna and is surrounded by their tributaries. Flood waters overflowing the river banks - frequently inundate the low-lying areas of the city. On the other hand, heavy monsoon rains cause water logging in many places within the city creating manifold problems for the citizens.

3.1 Results

Experimental studies generally focus on the durability of the vehicle, dry and wet for water logging. Provides some of the earliest analysis to determine the required speed of a vehicle and a vehicle. However, the efficiency of the vehicle is calculated as a result of dry and wet movement. Those experimental tasks are now investigating the value of traffic congestion time and further studies economically reducing traffic congestion time.

Table 4: Data Sheet

Traffic Movement		
Name of road: Mirpur Area	Direction- from: Mirpur-10	To: Kazi Para
Place: Kazi para	Distance: 2.00 Km	Date: 27/07/2019

Data Calculation & Graph

Dry Traffic Movement Calculation (1Hour)		**Wet Traffic Movement Calculation(1Hour)**	
Time	Vehicle	Time	Vehicle
11:30 AM-11:40 AM	69	04:20 PM-04:30PM	40
11:40 AM-11:50 AM	159	04:30 PM-04:40 PM	65
11:50 AM-12:00 PM	191	04:40 PM-04:50 PM	92

12:00 AM-12:10 PM	195	04:50 PM-05:00PM	95
12:10 AM-12:20 PM	192	05:00 PM-05:10PM	105
12:20 AM-12:30 PM	222	05:10 PM-05:20 PM	125

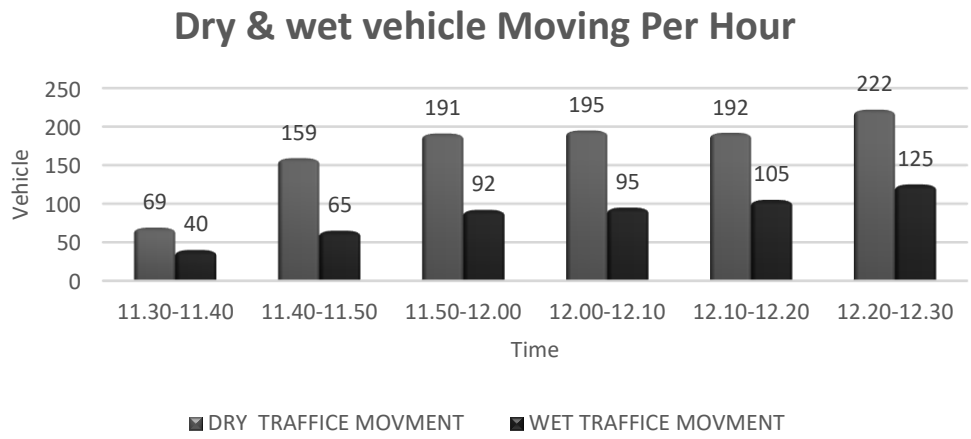

Figure 1: Dry & wet traffic movement

Table 5: Dry & wet traffic movement Calculation

1 hour Total Moving Vehicle				Efficiency	Decrease
Dry		Wet			
Time(1 hour)	Vehicle	Time(1 hour)	Vehicle		
11:30 AM-12:30PM	1028	04:20 PM-05:30	512	49.81%	50.19%

3.2 Discussions

Existing approaches to assessing the impact of Water logging on transport disruption do not capture the complexity of inter-actions between the Water logging hazard and transport system. Typically, assumptions can include.

- Traffic volumes and speeds are assumed to correspond to regional (or even national) average statistics;
- A road is assumed to be completely closed when its crown is covered by water logging, regardless of depth;
- Traffic on open roads continues to flow smoothly, perhaps at a slightly reduced maximum speed;
- Traffic volumes do not exceed the design capacity of a road;
- Traffic conditions do not change over the course of the day, or seasonally; and
- Diversion routes, and changes (or not) to driver behavior as a result of the flood, are often assumed without any clear rationale.

4. RECOMMENDATIONS

4.1 Permeable Pavement Design And Construction

Permeable pavements have gained very rapid use across North American in the past ten years. For new designs and retrofit projects, permeable pavements transform conventional, non-permeable pavement into a storm water management asset. Almost all permeable pavements use an open-graded aggregate base or sub base to store and infiltrate water into the soil sub grade. The asphalt, concrete and interlocking concrete pavement industries, as well as a number of other manufacturers of permeable surfaces, provide a variety of pavement surface options. Regardless of the surface,

permeable pavement systems include three design approaches. First, they are primarily used to promote complete or full infiltration of rainfall into the soil sub grade. Second, where soil sub grades have low infiltration rates, partial infiltration into the soil sub grade occurs and the remaining water exits via under drains. Third, for designs that require no infiltration, permeable pavement systems are enveloped with a geo membrane that prevents detained water from entering the soil sub grade and the stored water exits via under drains.

4.1.1 Key Permeable Pavement Design Features

A successful permeable pavement considers structural and hydrologic design. Structural design considers the pavement strength required to accommodate the vehicle loadings without the pavement failing. Hydrologic design considers the capacity required to infiltrate, store and release water in a manner that contributes positively to storm water management. Some key design, construction and maintenance considerations are as follows:

Site Drainage - Consider the overall site drainage and evaluate rainfall onto the pavement and water. That may drain onto the permeable pavement from surrounding areas. This could include adjacent pavements, grassed areas, building roofs, etc.

Contaminant Loading - Consider potential contaminants such as winter sand (for traction), biomass (tree leaves and needles, grass clippings, etc.) and sediment. Contaminants may reduce the long-term permeability of the pavement system and likely require maintenance such as vacuum sweeping.

Groundwater Depth - The top of the sub grade under a permeable pavement should be no less than 0.6 m from the seasonal high groundwater level.

Sub grade Type and Strength -The type of sub grade and its compaction/consolidation govern if water can be adequately infiltrated into the ground. Permeability values in the order of 12 mm/hr. permit full infiltration designs that accommodate rainstorm depths in most areas of North America. Lower permeability sub grade in high rainfall event areas may require supplemental under drains. Permeable pavements constructed over fine-grained soils (silts and clays) generally require thicker pavements than those constructed over coarse-grained soils (sands and gravels).

Traffic Type and Composition - Avoid using permeable pavements in high, concentrated traffic areas subjected to many heavy vehicles such as trucks and buses. While permeable pavements can be designed to accommodate very heavy loads.

Pavement Surface - Consider the type of surface most appropriate for the traffic and infiltration. Capacity conditions. For example, porous asphalt or pervious concrete may be more appropriate for some slope conditions whereas permeable interlocking concrete and grid pavements may be more suitable for situations where vehicles are turning. While some projects have steeper slopes, most permeable pavements should have slopes less than 5 percent.

Aggregate Base and Sub base - Permeable pavements typically utilize open graded aggregates to provide structural and hydraulic capacity for the pavement. The aggregates should be hard, durable and have a low percentage of material passing the 75 µm sieve size. Select durable, crushed aggregate materials to maximize structural capacity and porosity for water storage. For heavier traffic conditions, a cement- or asphalt-stabilized open-graded aggregate may be more suitable. Dense-graded aggregates for road bases are generally not used because of low water storage capacity and fines that can weaken them when saturated. To prevent migration of smaller base aggregate material into the larger sub base aggregate, aggregate gradations should satisfy the following criteria:

$$D50\ \text{Sub base}/D50\ \text{Base} < 25$$

$$D15\ \text{Sub base}/D85\ \text{Base} < 5$$

For example, the ratio of the D50 Sub base (sub base aggregate size at which 50 percent of the material is larger than this size and 50 percent is smaller) to D50 Base (base aggregate size at which 50 percent of the material is larger than this size and 50 percent is smaller) must be less than 25.

Subgrade Slope - Infiltration designs should minimize subgrade slope to promote water infiltration. Sites with subgrade slopes over 3 percent often require buffers,

Pavement Overflow - During high intensity/depth storm events, the pavement design should incorporate features such as curb cut outs, grading to supplementary drainage outlets such as catch basins, storm water ponds, etc. to prevent the pavement system from flooding.

Under drains - For partial or no infiltration designs determine the type, location and need for under drains. Specify outlet details and clean out provisions.

5. CONCLUSIONS

The findings of the study helped to conclude that water logging is affected by different significant factors including political & regulatory factors, drainage and waste management factors, unplanned development factors, population and development factors, etc. The study has also found that the residents of Dhaka city faced different problems due to water logging, most influential problems are; productivity loss, increase of construction and maintenance cost, environmental problem, sanitary problem, damage of roads, financial loss, health hazard, increase mosquito, disruption of normal life and economic loss etc. It is projected that this study will provide some useful thoughts for the water logging problems in Dhaka city and thus will help to solve water logging problems of the city. It is expected that this paper will give some valuable thoughts to the future researchers and policy makers to eradicate this problem. The major limitations of the paper are location, lack of secondary data and lack of time. Therefore, the future study may look at the extra variables. Whereas endorsing these limitations, next we expect that they do not notably diminish the significance of a comprehensive investigation of factors affecting the water logging in Dhaka city**.**

REFERENCES

Australia, G. o. (2004-07). *Stormwater management* . Government of Western Australia.

BRACK. (2016). *BRAC offers a variety of programmes including microfinance, education, and health.* Mirpur Dhaka.

COUNTS, M. C. (2017). *Government of the People's Republic of Bangladesh Ministry of Communications.* Dhaka.

Hasan, M. (2019). *Water Logging Situation in Dhaka City.* Dhaka: Dhaka Tribune.

Ismail, G. (2019). *Water logging in Dhaka City 2019.* Dhaka: bdnews24.com.

Maria Pregnolato ⇑, A. F. (2017). The impact of flooding on road transport.

RAHMAN, S. (1995). *CAUSES OF WATER LOCCINC IN DHAKA METROPOLITAN CITY.* Dhaka.

RAHMAN, S. (JUNE,2017). *CAUSES OF WATER LOCCINC IN DHAKA METROPOLITAN CITY.* Dhaka.

Tawhid, K. G. (2004). *Causes and effects of water logging in Dhaka city.* Dhaka.

Tawhid, K. G. (Stockholm 2004). *Causes and Effects of Water Logging in Dhaka City, Bangladesh.* Dhaka.

The daily Star. (2019, September). *Rain Water logging in Mirpur Area.* Dhaka.

Water), W. A. (2004–07). *Rainwater storage systems.* Australia.

Proceedings of the 5th International Conference on Civil Engineering for Sustainable Development (ICCESD 2020), 7~9 February 2020, KUET, Khulna, Bangladesh (ISBN-978-984-34-8764-3)

IMPACT OF WATER-LOGGING DUE TO CLIMATE CHANGE SCENARIOS INSIDE COASTAL POLDERS-24, 25 OF BANGLADESH

Hossain Md Jahid*[1], Haque M Aminul[2], Jamal M Haider[3] and Haque Anisul[4]

[1]Senior Scientific Officer, Water Resources Planning Organization, Dhaka, Bangladesh, e-mail: sso_gw@warpo.gov.bd
[2]Principle Scientific Officer, Water Resources Planning Organization, Dhaka, Bangladesh, e-mail: maminul05@yahoo.com
[3]Scientific Officer, Water Resources Planning Organization, Dhaka, Bangladesh, e-mail: sabbir87@gmail.com
[4]Professor, Institute of Water and Flood Management, Dhaka, Bangladesh, e-mail: anisul.buet@gmail.com

***Corresponding Author**

ABSTRACT

Coastal region of Bangladesh possesses a fragile ecosystem and is exposed to a number of hazards like cyclones, fluvial floods, tidal flood, storm surges, and water-logging. All these hazards shaped the lives and livelihood patterns of people in the region. Among these hazards, water-logging is characterized as a long-duration hazard that may last for at least three months, and may prolong up to 8-9 months or even become perennial. The depth of flooding varies, according to the topography of the area, and can reach up to 3m. A detail understanding on the impact of water-logging due to various natural, man-made and climate change scenarios is still lacking. Considering this research gap, the present research is aimed to study impacts of these scenarios inside polders-24 & 25 which are situated on the western part of the coastal region. As natural scenario, sedimentation in the Hari river (that flows in between these two polders) is considered. As man-made scenario, new polders in the south-central region (proposed in Bangladesh Delta Plan-2100) is introduced. As climate change scenario, an extreme sea level rise of 1.48m is considered. To study these impacts, long-term satellite images are analyzed, and numerical model is applied in the study area. The result shows that water-logging is more acute inside polder-25 compared to polder-24. Sedimentation in Hari River aggravates the water-logging condition. Dredging in Hari River does improve the situation, but the impact is confined within the floodplain of the river. If new polders are constructed in the south-central coastal region (at present there is no polder in this region), it will have little impact on the water-logging condition inside polders-24 and 25. Towards the end of century (2088 year) with a sea level rise of 1.48m, the entire system becomes insensitive to any physical intervention of the Hari river.

Keywords: *Polder, Water-logging, Sedimentation, Dredging, Climate change.*

1. INTRODUCTION

Waterlogging is the dominant hazard in the south-west region of Bangladesh. Among the prevailing 32 hazards recognized by Bangladesh, water logging is considered as the key water resources challenge by Bangladesh Delta Plan 2100.Southwest coastal region of Bangladesh has a unique brackish water ecosystem comprising the districts of Satkhira, Khulna, Bagerhat and the southern part of Jessore. Large portion of this region is coastal wetland which is formed by the rivers flowing to the sea. This region possesses a fragile ecosystem and is exposed to a number of natural calamities like cyclones, floods, tidal surges, repeated water logging, and land erosion, degradation etc. All these hazards shaped the lives and livelihood patterns of people in the region. Among these hazards, water-logging is characterized as a long-duration hazard that may last for at least three months, and may prolong up to 8-9 months or even become perennial. The depth of flooding varies, according to the topography of the area, and can reach up to 3m. Technically, water-logging refers to a situation when the level of ground water meets plants' root zone.

Water-logging in the western floodplain of the system came into existence during mid 80's. In earlier decades before 1960s, as Bangladesh is located at the lowermost reaches of three mighty river systems- Ganges, Brahmaputra and Meghna, low lying areas of coastal zone were frequently flooded by salt water during high tide (Islam Md. S. et al, 2013). In order to increase agricultural production, a series of polders enclosing the low-lying coastal areas was built (Bangladesh Water Development Board, 2003). This polder system from Dutch experiences was not fruitful (Masud & Azad, 2018b) in the long run due to lack of consideration of geo-physical settings and hydro-morphological characters of the south-west region (Roy et al., 2017). The presence of coastal polders de-linked the flood plain. Due to confinement of the rivers by the polders, rivers gradually started to be silted up one after another and created water-logging in the floodplain, and by 1980s, many of the river beds became higher than the adjacent crop lands and vast area under the polders became permanently water logged, rendering large tract of land uncultivable (Leender de Die 2013). Sediment could not be deposited in the flat tidal plain due to polder embankment and began to deposit on the river bed. As a result, flat sluice gate became inoperative; water in the polders could not flow out. Through these processes, more than one hundred thousand hectares of land became water-logged in a gradual process. One of the problems with water logging is to define the limits of water logging – a seasonal drainage problem – as distinct from perennial water bodies in south-western region of Bangladesh. One way to do this is to compare satellite images at different times of the year/hydrological cycle.

Besides these natural and man-made causes, climate change also aggravates the water logging problem in this region. Polders are generally believed to cause water-logging inside the protected land due to sedimentation in the peripheral rivers. But it is still unknown how these polders affect re-distribution of coastal floodplain sedimentation in the region. A detail understanding of the process of water-logging due to sedimentation of peripheral rivers is also lacking (WARPO and IWFM, 2019). Considering this research gap, the objectives of the paper are (1) to identify the water-logging process in the study area by analyzing satellite images and numerical model (2) to analyse the impact of water-logging inside polders due to sedimentation in peripheral rivers.

2. METHODOLOGY

2.1 Study Area

In the early 60s, 1566 km of embankments with 282 sluice gates were constructed in the southwest region to reclaim all the tidal influence coastal areas that lay below the highest tide levels for periodic inundation by saline water for crop production. 21 vents Bhabadaha sluice gate was one of the important structures which is now the source of the pains for millions of people. Within 15 years of the construction of embankments, siltation started at the water entrance point of the sluice gates and rivers and canals bed height began to increase. As a result, first the BeelDakatiainsidepolder 25 became water logged. Subsequently polder 24, 27 and 28 also became water-logged one after another. In this paper, the study area is comprised with the areas of polders 24 and 25. Four upazilas are within

the polder area. These are: Phultala, Khan Jahan Ali, Dumuria from Khulna District and Keshabpur from Jessore district. The main river flowing in between these two polders are Hari River which largely dictates the drainage from the polders. Several depression (beels) works as perennial water bodies within the polders. The study area is shown in Fig 1.

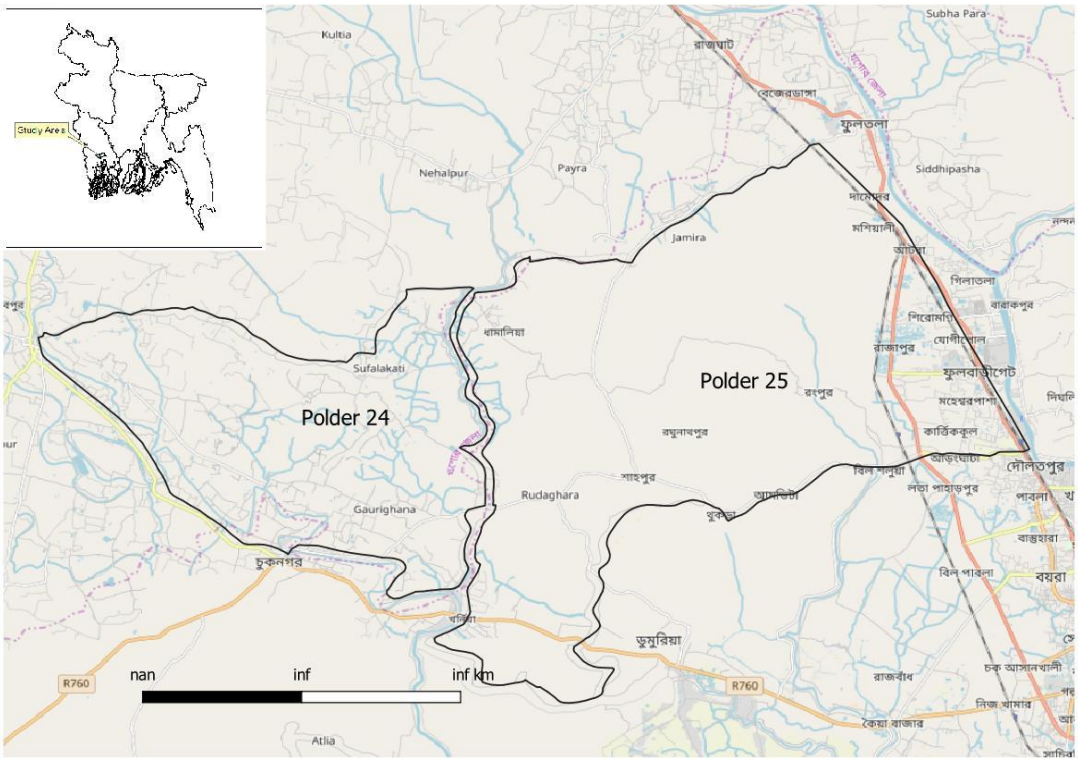

Figure.1. Study Area for Water Logging

2.2 Data Collection and Model

This research is conductedby considering natural, man-made and climate change scenarios to compute the water-logging process by analyzing satellite images and byapplying numerical model. As study area for model application, polders 24 and 25 are selected. The flow module of Delft 3D modeling suite is applied to computethe water-logging inside polders 24 and 25. This model requires a detail description of river and canal network, road network, depression (beels) and sluices that connects the main river with the polder domain inside. A detail of the water-logging model that shows canal network, road network, sluices is shown in Fig.2.

Land topographic input in the model is provided from Digital Elevation Model (DEM) which is currently available at WARPO.For the river bathymetry, combinations of secondary and primary data are used. Secondary data are collected from BWDB and primary data in 294 locations in the rivers/estuaries of coastal zone are measured. Ocean bathymetry is provided from the open access General Bathymetric Chart of the Oceans (GEBCO). Channel plan forms are assumed to remain the same over the model simulation period. Similar assumption is made for channel bed level and floodplain levels of rivers / estuaries.

Model receives fluvial flows from three major rivers in the region – the Ganges, Brahmaputra and Upper Meghna. For all the scenario runs – model simulated daily discharges from INCA hydrological model (Whitehead et al., 2015) are used as discharge boundary conditions. Tidal forcing in the model is provided by sea surface elevation in the Bay of Bengal. For all the scenarios runs – model simulated hourly sea surface by GCMOS ocean model (Kay et al., 2015) is provided as the downstream sea

level boundary. In micro-scale model, morphological changes are considered static (except subsidence) – so no additional sediment input is provided.

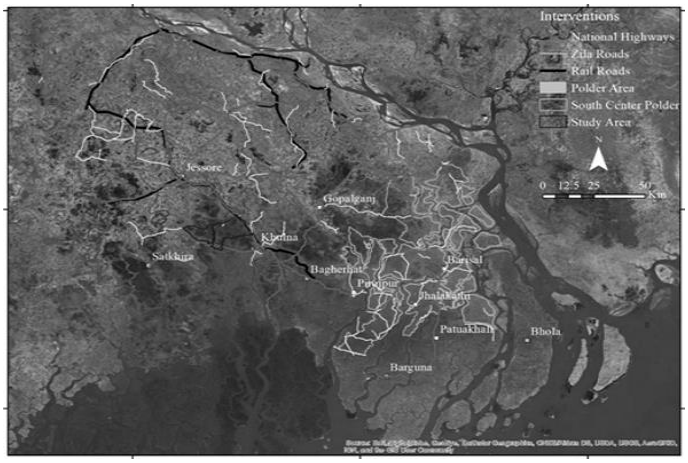

Figure.2. Details of Water-logging Model

As climate change scenario, eight different scenarios are constructed to analysis water-logging conditions in different combinations of morphological and climatic variables. Out of these 8 scenarios, 4 are for base condition and 4 are for future. Year 2000-2001 is used as thebase year and end-of-century is used as the future scenario. For end-century scenario, a sea level rise of 1.48m is used as sea level condition and a warmer & wetter climate is used as the climatic condition. A warmer and wetter climate increases the precipitation in the upstream basins during the monsoon and affects the upstream discharges of the major river systems. These combined effects are taken into considering during simulation of water-logging condition during end-century. Four base and future scenarios are constructed by considering (1) no intervention (2) sedimentation in the Hari River which is the main river system in the study region (3) dredging of the Hari River and (4) construction of new polders in the south-central region. New polders in south-central region are introduced by considering the fact that this region is flooded during the sea level rise and currently there is no polder in this region.

3. RESULTS AND DISCUSSIONS

To identify the extent of inundation inside polders 24 and 25, model simulated result for the average flood year scenario of the year 2000 is compared with MODIS satellite images (which is also the base year in this study) which is shown in Fig.3.

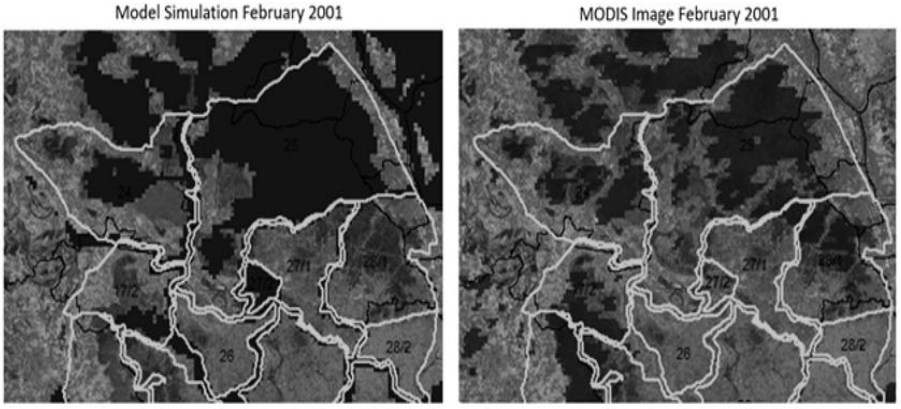

Figure.3**.** Comparison of inundation extent between model simulation (left) and MODIS Image (right) during dry season (February) of the year 2001. The comparison shows inundation inside polders 24 and 25.

Validated model is applied to simulate 8 different water-logging scenarios. Scenario descriptions and results from model simulations for each of the scenarios are described in Table-1 and in Fig.4 (a- n). The Fig. 4 (a-n) shows the base condition, end-century and water logged condition during monsoon and dry season of the study area.

Table-1: Model simulated result comprising 8 climate change scenarios using water logging model

Scenario no	Scenario Description	Assumptions for the scenario	Results from the scenario
1	Base scenario. Base condition is the average flood year 2000. Sea level rise is zero. The scenario is driven by the discharges of year 2000. To capture the completedrainage condition, model run is extended till March 2001.	In this scenario, no physical intervention is made. This is the base scenario for years 2000-2001.	• Flooding is mainly concentrated in the depression region. • Flooding is more pronounced inside polder-25 compared to polder-24. • After drainage during the entire dry season, water-logged condition is observed in most of the depressions inside polders 24 & 25. Results are shown in Figure 4(a).
2	Base scenario. Sedimentation in the Hari river (which is the main river between polders 24 & 25) is considered in base condition.	This is the base scenario where sedimentationis introduced in the Hari river. It is assumed that sedimentation reach of the river has decreased conveyance which has a length of about 30 km. The sedimentation has filled the river bed to a maximum of 1.5m. The sediment volume that has deposited inside the river is about 6750 ton.	• During monsoon, inundation inside polders 24 & 25 increases due to sedimentation of the Hari river. • Sedimentation in Hari river aggravates the water-logging condition. • Sedimentation mainly affects the region which is close to the Hari river. Results are shown in Figure 4(b).
3	Base scenario. Dredging in the Hari river (which is the main river between polders 24 & 25) is considered in base condition.	This is the base scenario where Hari river is dredged to improve the water-logged condition. A total of 30 km reach of the Hari river is dredged to a depth of 1.5m from its present bed level. Dredging is made uniformly keeping the bed slope same before and after dredged condition. In this way, a total of 6750 ton of soil is dredged from the river bed.	• During monsoon, inundation inside polders 24 & 25 decreases when Hari river is dredged. • Dredging in Hari river improves the water-logging condition. • Dredging mainly affects the region which is close to the Hari river. Results are shown in Figures 4(c) and 4(d).
4	Base scenario. New polders (SC polders) are introduced in south-central region in base condition.	In this scenario, new polders are introduced in south-central region in base condition. With the introduction of new polders in this region, the south-central region will be flood-free. But this intervention shifts the flood hazard to further west where polders 24 and 25 (present study area) are situated. Water has not entered inside these polders but affects the	• During monsoon, impact of SC polders inside polders 24 & 25 is not visible. • SC polders slightly aggravate water-logging condition. This shows SC polders mainly affect drainage. • Impact of SC polders are visible close to eastern border of polder 25. This border directly feels the shift of flood hazard due to construction of SC polders. Results are shown in Figures 4(e),

Scenario no	Scenario Description	Assumptions for the scenario	Results from the scenario
		flooding in surrounding region. This might have some impact on the water-logging condition inside polders 24 and 25.	4(f) and 4(g).
5	End-century scenario. The snapshot selected for end-century is the year 2088-2089. Sea level rise is 1.48m. Warmer and wetter climate drives increased inflow into the system.	This is the end-century scenario where sea level rise is 1.48m and flooding is driven by a warmer and wetter climate. The end-century scenario is represented by snapshot of the year 2088-2089. In this scenario, no intervention is considered.	Both the polders 24 & 25 are completely inundated. • During dry season, inundation depth decreases but the extent of inundation remains the same. • The entire region becomes perennial water body. • Result is shown in Figure 4(h).
6	End-century scenario. Sedimentation in the Hari river is considered in end-century.	This is the end-century scenario when the Hari river is sedimented. Comparison shows inundation patterns during monsoon when Hari river is sedimented and when it is not sedimented. This comparison is for end-century. Thisshows impact of sedimentation of Hari river on water-logging in end-century.	• Impact of sedimentation is not visible in monsoon. The entire area is completely inundated. • Water-logging remains almost same both for with and without sedimentation of the Hari river. Results are shown in Figures 4(i) and 4(j).
7	End-centuryscenario. Dredging in the Hari river is considered in end-century.	This is the futurescenario where Hari river is dredged to improve the water-logged condition. Comparison of inundation patterns during monsoon when Hari river is not dredged and when it is dredged isshown. This comparison is for end-century.	• Impact of dredging is not visible in monsoon. The entire area is completely inundated. • Water-logging remains almost same both for with and without dredging of the Hari river. Results are shown in Figures 4(k) and 4(l).
8	End-century scenario. New polders in south-central region are considered in end-century.	In this scenario, new polders are introduced in south-central region in end-century. At present, there is no polder in south-central region and the region will be flooded during sea level rise Comparison of inundation patterns during monsoon when SC polders is absent and when it is present isshown. This comparison is for end-century.	• Impact of SC polders is not visible in monsoon. The entire area is completely inundated. • Water-logging remains almost same both for with and without SC polders. Results are shown in Figures 4(m) and 4(n).

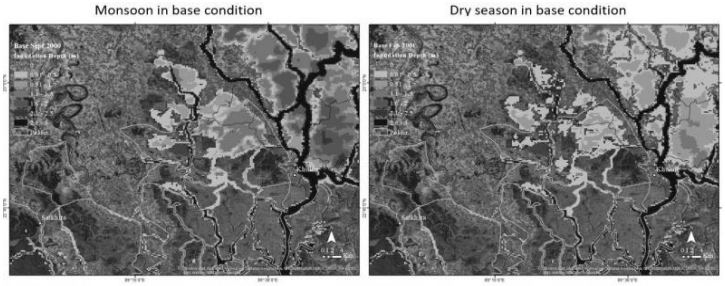

Figure-4(a): Scenario-1: Inundation in base condition during monsoon and dry season

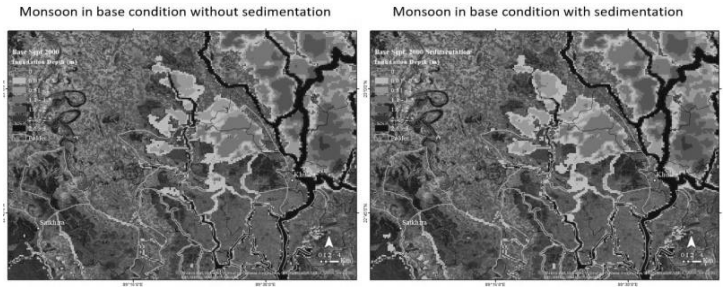

Figure-4(b): Scenario-2: Inundation during monsoon when Hari river is not sedimented (left) and when it is sedimented (right). This scenario is for base condition.

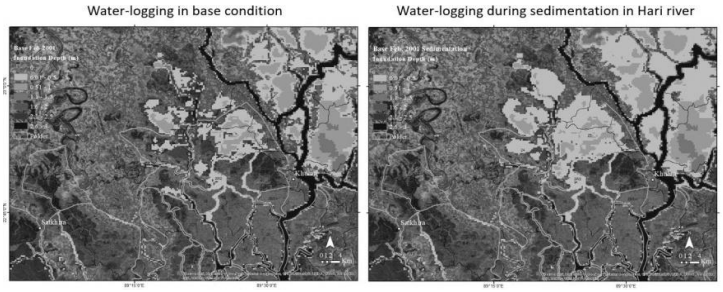

Figure-4(c): Scenario-3: Water-logging in the study area. Water-logged condition is created during dry season of base condition. The left image shows when there is no sedimentation in Hari river.The right image shows when Hari river is sedimented.

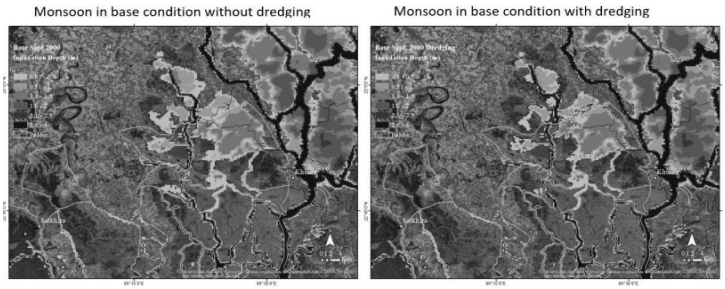

Figure-4(d): Scenario-3: Inundation during monsoon when Hari river is not dredged (left) and when it is dredged (right). This is for the base condition.

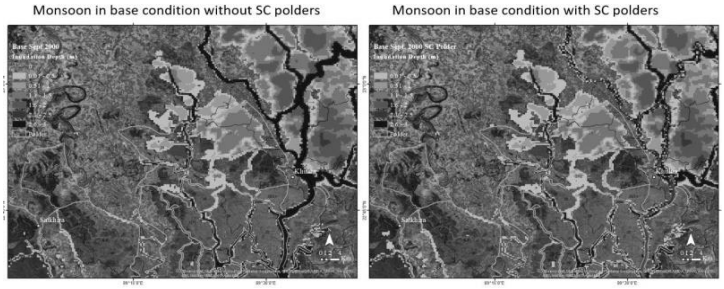

Figure-4(e): Scenario-4: Change of flooding pattern due to construction of new polders in south-centralregion. The red circled region shows polders 24 & 25 which is the study area of present study.

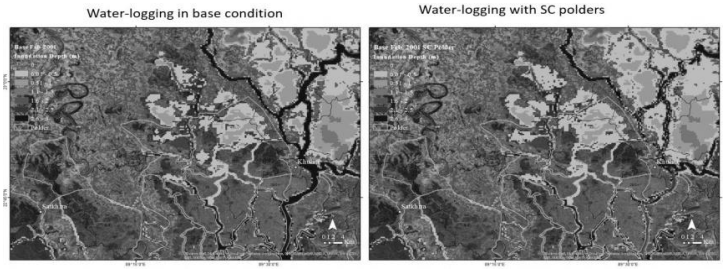

Figure-4(f): Scenario-4: Inundation during monsoon without SC polders (left) and with SC polders (right). This scenario is for base condition.

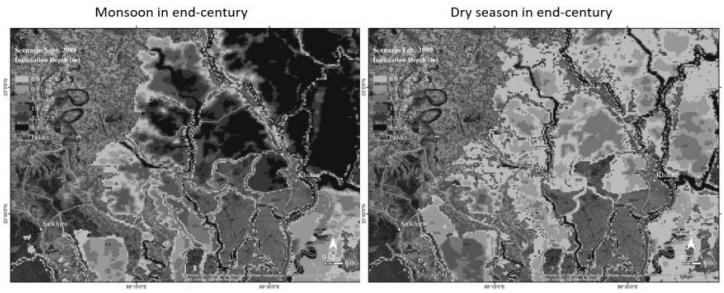

Figure-4(g): Scenario-4: Water-logging in the study area. Water-logged condition is created during dry season. The left image shows without SC polders. The right image shows with SC polders.

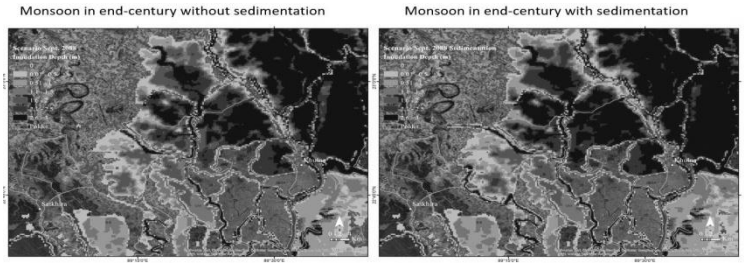

Figure-4(h): Scenario-5: Inundation in end-century during monsoon and dry season

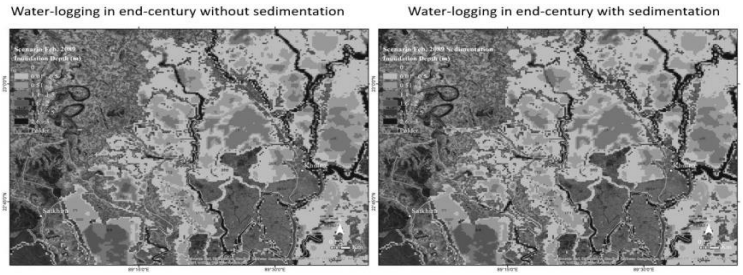

Figure-4(j): Scenario-6: Water-logging in the study area. Water-logged condition is created during dry season. The left image shows when there is no sedimentation in Hari River. The right image shows when Hari River is sedimented. The scenario is for end-century.

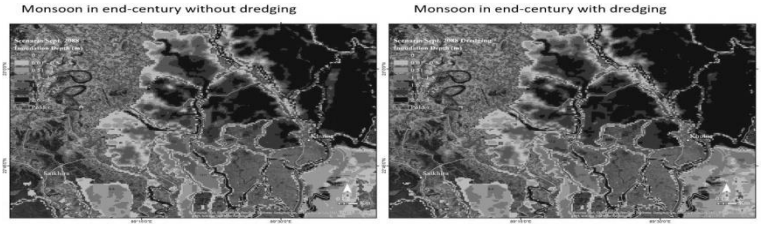

Figure-4(k): Scenario-7: Inundation during monsoon when Hari River is not dredged (left) and when it is dredged (right). This scenario is for end-century.

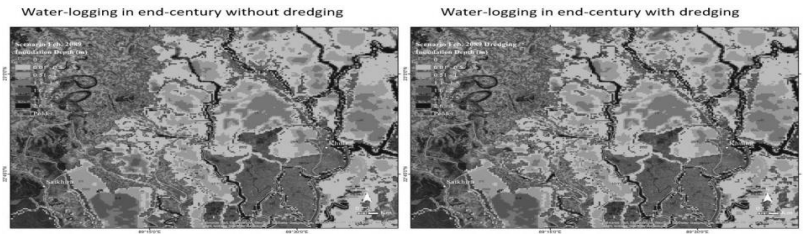

Figure-4(l): Scenario-7: Water-logging in the study area. Water-logged condition is created duringdry season of end-century. The left image shows when there is no dredging in Hari River. The right image shows when Hari River is dredged.

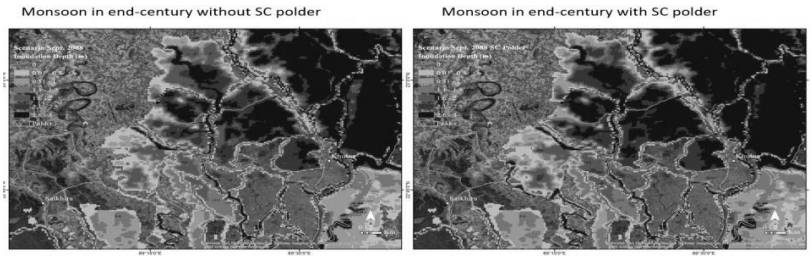

Figure-4(m): Scenario-8: Inundation during monsoon without SC polders (left) and with SC polders (right). This scenario is for end-century.

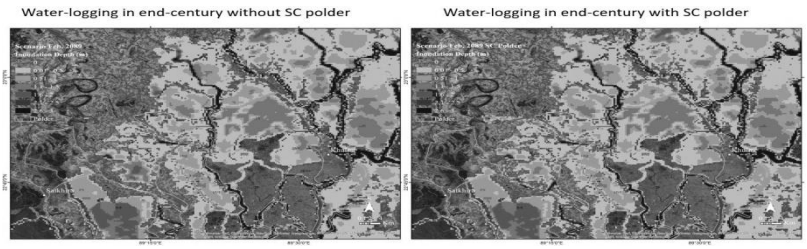

Figure-4(n): Scenario-8: Water-logging in the study area. Water-logged condition is created during dry season in end-century. The left image shows without SC polders. The right image shows with SC polders.

4. CONCLUSIONS

Water logging is more inside polder 25 compared to polder 24. Main cause of water-logging inside polders24 and 25 is sedimentation of the peripheral river. Model simulation results on 8 generated scenarios for water-logging inside polders24 and 25 reveals that sedimentation in the Hari River (the river which flows in between polders24 and 25) aggravates the water-logging situation inside the polders. Effect of sedimentation in the Hari River is confined within the floodplain of the river. Dredging of the Hari River does improve the water-logging, but the impact is confined within the floodplain of the river. If new polders are constructed in the south-central coastal region (at present there is no polder in this region), it will have little impact on the water-logging condition inside polders24 and 25. Towards the end of century with a sea level rise of 1.48m, the system becomes insensitive to any physical change of the Hari River.

ACKNOWLEDGEMENTS

The Authors is grateful to the WARPO Authority for taking the research project. It's also our pleasure to convey thanks to all those who helped us during the research with their mental and physical effort.

REFERENCES

Bangladesh Water Development Board (2003). "Khulna-Jessore Drainage Rehabilitation Project: Final Report Part A: Monitoring and Integration" Dhaka, Bangladesh.

Islam Md. S. et al (2013). "Methodology of crest level design of coastal polders in Bangladesh" 4th International Conference on Water & Flood Management (ICWFM), Dhaka, Bangladesh, 9-11 March, 2013.

Kay, S., Caesar, J., Wolf, J., Bricheno, L., Nicholls, R.J., Islam, A.K.M., Haque, A., Pardaens, A., Lowe, J.A. (2015). "Modelling the increased frequency of extreme sea level in the Ganges-Brahmaputra-Meghna delta due to sea level rise and other effects of climate change", Environ. Sci.: Processes Impacts, 2015, 17, 1311.

Kay, S., Caesar, J., Wolf, J., Bricheno, L., Nicholls, R.J., Islam, A.K.M., Haque, A., Pardaens, A., Lowe, J.A. (2015). Modelling the increased frequency of extreme sea level in the Ganges-Brahmaputra-Meghna delta due to sea level rise and other effects of climate change, Environ. Sci.: Processes Impacts, 2015, 17, 1311.

Leender de Die (2013). Tidal River Management: Temporary depoldering to mitigate drainage congestion in the southwest delta of Bangladesh MSc Thesis, Wageningen University & Research, the Netherlands

Masud, M.M.A and Azad A.K. (2018b). The role of the tidal river management for sustainable agriculture, Conference Proceedings, 2nd International Conference on Sustainable Development, 16-18 February,2018, United International University, Dhaka, pp.189-200

WARPO and IWFM, BUET, March (2019): Research on the Morphological processes under Climate Changes, Sea Level Rise and Anthropogenic Intervention in the coastal zone. Final Report, March 2019

Whitehead, P.G., E. Barbour, M. N. Futter, S. Sarkar, H. Rodda, J. Caesar, D. Butterfield, L. Jin, R. Sinha, R. Nicholls and M. Salehin (2015), Impacts of climate change and socio-economic scenarios on flow and water quality of the Ganges, Brahmaputra and Meghna (GBM) river systems: low flow and flood statistics, Environmental Science-Processes and Impacts, DOI: 10.1039/c4em00619d

Proceedings of the 5th International Conference on Civil Engineering for Sustainable Development (ICCESD 2020), 7~9 February 2020, KUET, Khulna, Bangladesh (ISBN-978-984-34-8764-3)

A COMPARATIVE STUDY ON MENONGCHARA AND BURAGHAT RUBBER DAM PROJECTS IN MYMENSINGH

Faisal Ahmed*[1], Asif Ahmed Rhythm[2], Zanit Ahmed Hridoy[3] and Md. Mirjahan Miah[4]

[1]Undergraduate Student, Department of Civil Engineering, Ahsanullah University of Science and Technology, Bangladesh, e-mail: faisal50.ce@gmail.com
[2]Undergraduate Student, Department of Civil Engineering, Ahsanullah University of Science and Technology, Bangladesh, e-mail: backgroundrhythm@gmail.com
[3]Undergraduate Student, Department of Civil Engineering, Ahsanullah University of Science and Technology, Bangladesh, e-mail: zinnatthasanzanith@gmail.com
[4]Professor, Department of Civil Engineering, Ahsanullah University of Science and Technology, Bangladesh, e-mail: mirjahan1951@gmail.com

***Corresponding Author**

ABSTRACT

Rubber dams are water retention structures. A large number of rubber dam projects have been implemented by LGED, BWDB and BADC are in operation in Bangladesh. The main purposes of these projects are to retain water for irrigation. The present study has been undertake as to compare the operation and management aspects and performance of two rubber dam projects implemented by different organizations. Performance of Menongchara and Buraghat projects has been evaluated considering technical, hydraulics, agricultural, environmental and socio economic indicators. Primary and secondary data were collected by field measurements and questionnaire survey conducted during 2018-19 crop season. In terms of actual irrigated area compared to design area, the performance of Buraghat project was better than Menongchara project. Irrigation efficiency and actual water productivity of two projects were almost same. Economic viability of both the project was found to be satisfactory. Profitability of farmer of Menongchara project was better than that of Buraghat project. Positive impact on fisheries, vegetation, livelihood, and wild life took place in both project areas. Few technical problems were identified in case of both projects. Project management committee of Buraghat project was found more active than that of Menongchara project. It was reported that LGED provides some financial and technical support in Buraghat project whereas no support is provided by BADC in Menongchara project. Based on this study it can be said that both Menongchara and Buraghat rubber dam projects are performing well. Certain problems were observed that are hindering optimal use of water. The uneven distribution of water in Buraghat project, lack of project management activity in Menongchara project, improper maintenance of canal are the problems faced by local people. If these problems were removed, more benefits could be obtained from the rubber dam projects.

Keywords: *Irrigation, Technical, Agricultural, Environmental, Socioeconomic.*

1. INTRODUCTION

Rubber dams are inflatable and deflatable hydraulic structures. Thousands of rubber dams have been installed worldwide for various purposes such as irrigation, water supply, tidal barrier, power generation, flood control, environmental improvement and recreations.

In 1957, the world first inflatable rubber dam appeared in Los Angeles, the United States, since then widely used all over the world. The rubber dam was installed in Australia and Japan in 1965, in Taiwan in 1977 and in Hong Kong in 1978. China built the first inflatable rubber dam in 1966 and that is the right door inflatable rubber dam in Beijing. More than 2000 rubber dams were built around the world, including Taiwan, Hong Kong, Japan, Australia (Saleh & Mondal, 2000).

In 1994 the Local Government Engineering Department with a joint technical team comprising experts from China Institute of Water resources and Hydropower Research (IWHR) in Beijing made a feasibility test for the first time on rubber dam construction. The joint technical team visited a number of areas at the field level and submitted a survey report titled "**Feasibility of rubber dam in Bangladesh.**" The report recommended construction of two rubber dams one on Idgaonkhal near Idgaon Bazar in Cox's Bazar and another on Bakkhali river about 5 km from Cox's Bazar on a pilot basis to assess some design parameters, performances, cost effectiveness and social acceptability. In the year 1995-96 these two pilot rubber dams were built and are being successfully used for agricultural purpose (LGED, 1994). Based on the success of two pilot rubber dams, the countries third rubber dam was constructed on the Bhogai river of Nalitabari thana of Sherpur district under the Ministry of Agriculture in the year 1996-97. The government of the People's Republic of Bangladesh has built 11 rubber dams in which 10 rubber dam construction projects are under the Ministry Finance for its own funding. LGED has built 52 rubber dams. Bangladesh Water Development Board also constructed two rubber dams in Pekua Cox's Bazar. Bangladesh Agricultural Development Corporation (BADC) involved with rubber dam project in 2009. They implemented eight rubber dams and few rubber dam are currently under construction.

A number of studies have been conducted to investigate into design aspects and to assess performance of individual rubber dam project. No study focuses on comparison of performance of projects under different management. The Menongchora and Buraghat rubber dam project, therefore, needs to be studied comparatively in order to investigate their performance in terms of the above mentioned aspects. So this comparative study on this rubber dam projects was undertaken.

1.1 Components of a Rubber Dam

Rubber dam comprises mainly of four parts: dam body or dam bag, anchorage of dam bag with concrete floor, control system (including water or air filling and emptying system, monitoring system and safety control system) and foundation (including foundation, top and side walls etc.). Some other parts: massive concrete base (dam base), vertical wall and slope wall, river bed inverted filter or block chamber, filter material and bench protection work. Schematic diagram of a rubber dam is shown in figure 1.

1.2 Expected Life of Rubber Bag

Dam bags usually have longevity of about 20 years (IWHR, 1994) and need full replacement after that period. In this regard, by loosening the anchorage, the used rubber bags are removed. New rubber bags are being placed in place and anchorage is being achieved again.

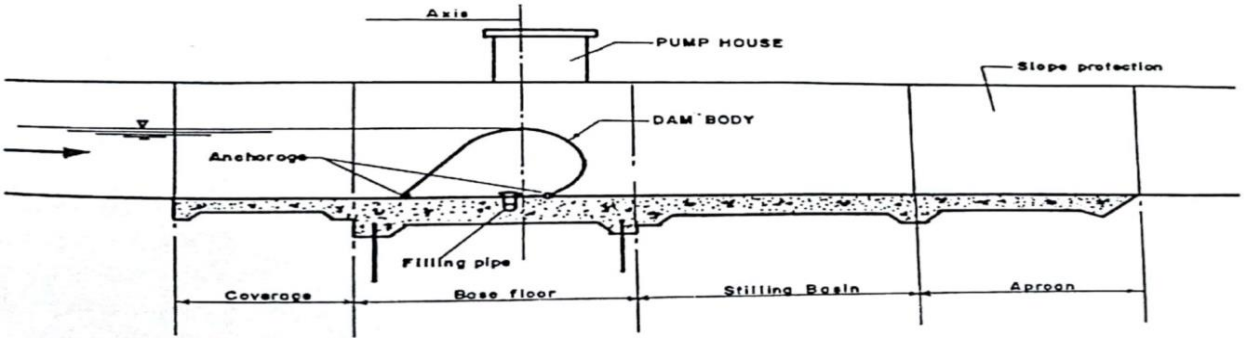

Figure 1: Cross-section of a Rubber Dam (Raquib, 1999)

2. METHODOLOGY

In this study Menongchara and Buraghat rubber dam projects were selected. Menongchara project was implemented by BADC and Buraghat project was implemented by LGED. In this study, evaluation of the performance of the two rubber dam projects was carried out using a standard set of performance indicators. The performance indicators such as water delivery performance, irrigation efficiency, yield efficiency, water productivity efficiency, fee collection efficiency, economic viability and profitability of farmer were used by Saleh and Mondal (2000). The command area efficiency was used by Ahmed (2014).

2.1 Water Delivery Performance

The indicator determines the degree to which water is delivered as arranged during the irrigation season. It is the ratio of the actual volume delivered to the target volume and is defined as

$$\text{Water delivery performance} = \frac{\text{Actual volume delivered}}{\text{Target volume}} \quad (1)$$

Actual volume of water delivered to the field was calculated by multiplying actual discharge with operating time. In the field discharge was determined by area-velocity method and the velocity was measured by floating method. Target volume data were obtained from feasibility report.

2.2 Irrigation Efficiency

Irrigation efficiency is also important indicator. It is the ratio of the amount of water consumed by the crop to the amount of water supplied through irrigation and is defined as

$$\text{Irrigation efficiency} = \frac{\text{Total demand of water}}{\text{Total supply of water}} \quad (2)$$

Net irrigation requirement of crop was calculated with the help of CROPWAT 8.0. Data were collected from BMD website. Total supply of water was calculated with the help of actual volume and actual irrigated area data.

2.3 Command Area Efficiency

Command area efficiency is the ratio of the actual irrigated area to the target area. In most cases the target area is taken as higher to show the project more attractive.

$$\text{Command area efficiency} = \frac{\text{Actual irrigated area}}{\text{Target irrigated area}} \quad (3)$$

2.4 Yield Efficiency

Yield efficiency is the ratio of the actual yield to the target yield

$$\text{Yield efficiency} = \frac{\text{Actual yield}}{\text{Target yield}} \quad (4)$$

2.5 Water Productivity Efficiency

Water productivity (kg of output per unit m^3 of water used) indicates the efficiency in use of water for producing the ultimate result, the crop yield.

$$\text{Water productivity efficiency} = \frac{\text{Actual productivity}}{\text{Target productivity}} \quad (5)$$

2.6 Fee Collection Efficiency

The operation and maintenance cost of the project come from the fees collected from the farmers and beneficiaries. Fee collection efficiency is the ratio of irrigation fee collected to the irrigation fees assessed.

$$\text{Fee collection efficiency} = \frac{\text{Irrigation fee collected}}{\text{Irrigation fee assessed}} \quad (6)$$

2.7 Economic Viability

The economic viability of a project indicates whether the amount of the investments made is going to be recovered over the life of the project. The expanse should include both capital and O&M costs. In public irrigation projects of Bangladesh the capital costs are not taken from the beneficiaries, just the O&M costs per ha per year of actual cultivated area have been considered. The indicator is defined as follows

$$\text{Economic viability} = \frac{\text{O\&M fee per ha}}{\text{O\&M Cost per ha}} \quad (7)$$

2.8 Profitability of Farmer

This indicator shows the benefit of farmers at the individual farm level. It is the ratio of benefit of irrigation per hectare to the irrigation fee per hectare. The benefit of rubber dam irrigation per hectare includes the difference between net benefit under irrigation with rubber dam and net benefit without the project. Net benefit of irrigation with rubber dam and without rubber dam was calculated by subtracting the total expanse of irrigation from the gross benefit. The indicator is defined as follows

$$\text{Profitability of farmer} = \frac{\text{Benefit of irrigation per ha}}{\text{Irrigation fee per ha}} \quad (8)$$

Other indicators are: technical problems, impact on fisheries, impact on ground water table, impact on wild life and animals, impact on vegetation and impact on livelihood. All of these indicators are evaluated through visual observations and discussions with local people.

3. DESCRIPTION OF STUDY PROJECTS

Menongchara project area is located at Lokkhikura union of Haluaghat Upazila. There are four villages within the subproject area. This project was constructed by BADC in 2012. The net irrigable land under the studied project is about 900 ha. But actual area covered by the project is about 100 ha.

Buraghat Rubber Dam project is under Gazir Bhita union of Haluaghat Upazila in Mymensingh district. There are eight villages within the sub project area. The project was constructed by LGED in

2007. The net irrigable land under the studied project is about 725 ha. But actual area covered by the project is about 150 ha.

Figure 2: Menongchara and Buraghat rubber dam

Salient features of Menongchara and Buraghat rubber dam projects are shown in table 1.

Table 1: Salient features of Menongchara and Buraghat rubber dam projects

	Menongchara dam	**Buraghat dam**
Length of Rubber Dam (m)	30	30
Dam height (m)	4.5	3.5
Maximum retention	4.3	3.5
Length of concrete floor	27	27
Material	Reinforced Rubber	Reinforced Rubber
Shell thickness (mm)	10	8.0
Thickness of Cover sheet (mm)	3.0	3.0
Bridge (m)	30	30
Guide bunds (km)	10 (Earthwork)	8.0 (Earthwork)
Approach road (km)	2.0	2.0
Pump house	1 no.	1 no.
Bag filling time	12-15 hrs.	12-15 hrs.
Pump Capacity	100 m^3/hr.	100 m^3/hr.
Scheme life	(15-20) yrs.	(15-20) yrs.

3.1 O&M Problems

O&M problems of Menongchara and Buraghat rubber dam projects are summarised in table 2.

Table 2: O&M problems of Menongchara and Buraghat rubber dam projects

Menongchara dam	**Buraghat dam**
Erosion of river embankment	Erosion of river embankment
Damage of outlet pipe	The LLP need to be repaired several times in a season
The threaded gate of pipe outlet becomes loose	The soil of downstream settled

4. RESULTS AND DISCUSSION

4.1Water Delivery Performance

Actual volume of water delivered to the field during the season was calculated by multiplying the actual discharge with the operating time. For Menongchara rubber dam actual discharge was determined by area-velocity method and the velocity was measured by floating method. Also 6 low lift pump of 3.5 HP and 1 low lift pump of 7.4 HP were operated during the season. The discharge was taken as 0.2265 cumec. The actual volume of water delivered during the crop season of 2018-19 is 1856156.54 cubic meter. For Buraghat rubber dam irrigation was done by operating 5 low lift pumps of 12 hp. Each pump was operated 24 hour in a day. The total discharge is 0.2832 cumec. Therefore the actual volume of water delivered during the crop season of 2018-19 was 2960686.08 cubic meter. Due to lack of target volume the water delivery performance could not be calculated in both the projects.

4.2 Irrigation Efficiency

The total demand of water of crop season 2018-19 was calculated with the help of CROPWAT software.NIR of crop season 2018-19 are shown in table 3.

Table 3: Calculation of Net Irrigation Requirement of crop

Month	ETc (mm)	Effective Rainfall, Re (mm)	NIR= ETc-Re (mm)
December	77.19	6.96	70.23
January	83.7	8.0	75.7
February	103.04	16.4	86.64
March	148.18	28.64	119.54
Total			352.11

For Menongchara rubber dam project total supply of water (in depth) = $\frac{1856156.54\ m^3}{101.25\times10^4 m^2}$ = 1.833 m. Using equation (2) irrigation efficiency = $\frac{0.35211\ m}{1.833\ m}$ = 0.1921 = 19.21%. For Buraghat rubber dam project total supply of water (in depth) = $\frac{2960686.08\ m^3}{153.9\times10^4 m^2}$ = 1.924 m. By using equation (2) irrigation efficiency is 18.30%. Based on result it can be said that irrigation efficiency of Menongchara and Buraghat rubber dam project seems to be low.

4.3 Command Area Efficiency

The actual and target irrigated areas of Menongchara rubber dam project are 101.25 ha and 900 ha respectively. In case of Buraghat rubber dam project the actual and target irrigated area is 153.9 ha and 725 ha respectively. By using equation (3) command area efficiencies of Menongchara and Buraghat rubber dam project are 11.25% and 21.23% respectively. The command area efficiency is very low. The reason is overestimation of target command area. The irrigated area is increasing in every season.

4.4 Yield Efficiency

According to farmers of Menongchara and Buraghat rubber dam projects the actual yield in the boro season was 5925.93 kg per hectare. From the feasibility report the target yields of Menongchara and Buraghat rubber dam project are 8450.62 kg per hectare and 7170 kg per hectare respectively. Using equation (4) yield efficiencies of Menongchara and Buraghat rubber dam project are 70.12% and 82.65% respectively. Yield efficiency of Menongchara and Buraghat rubber dam project seems to be good.

4.5 Water Productivity Efficiency

Actual productivity is the ratio between actual yield per square meter and actual depth of water supplied in the area. According to the farmers estimation the actual yield was 0.593 kg per square meter. Actual water productivities of Menongchara and Buraghat rubber dam project are 0.324 kg/m³ and 0.31 kg/m³ respectively. The actual productivity of water appears to be low. Due to lack of target productivity data, water productivity efficiency could not be calculated.

4.6 Fee Collection Efficiency

By using equation (6) fee collection efficiencies of Menongchara and Buraghat rubber dam project are 75% and 70% respectively. Fee collection efficiency of last few years is shown in figure 2.

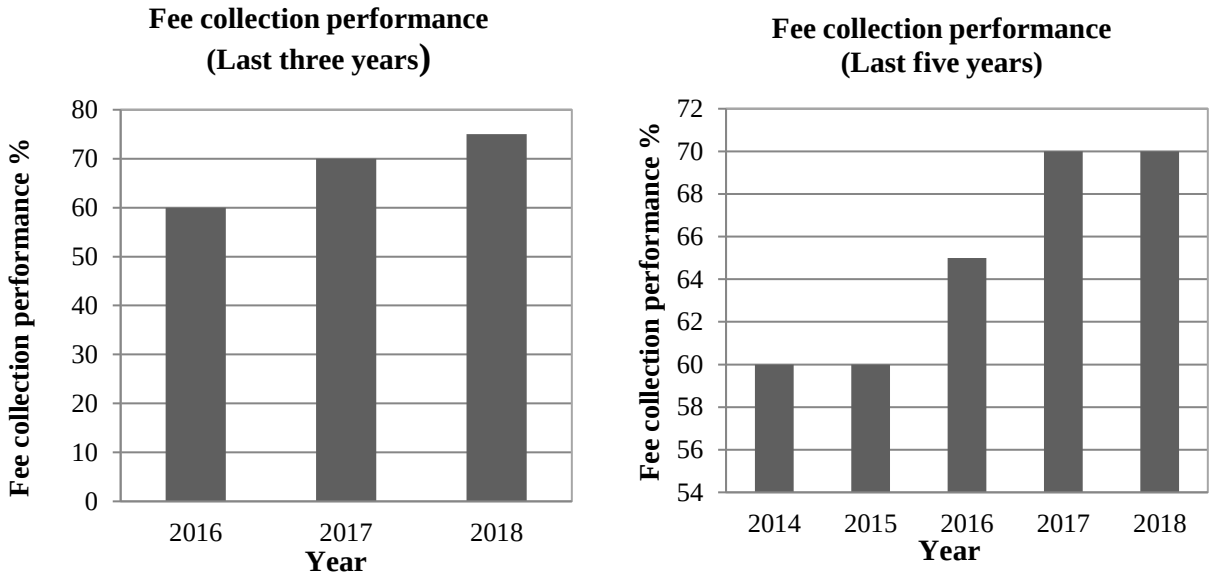

Figure 2: Fee collection efficiency of Menongchara and Buraghat rubber dam projects of last few years

4.7 Economic Viability

Economic viability determines how much of the investment made is going to be recovered over the life of the project. The irrigation fee including operation and maintenance fee are collected by the project management committee. The O&M service are provided by the project management committee. O&M fee of Menongchara and Buraghat rubber dam projects were taka 2470/ha and taka 3951/ha respectively. O&M costs of Menongchara and Buraghat rubber dam projects were 1838 taka/ha and 1854 taka/ha respectively. By using equation (7) economic viabilities of Menongchara and Buraghat rubber dam projects are 1.34 and 2.13 respectively.

4.8 Profitability of Farmer

For Menongchara and Buraghat rubber dam projects the gross return of boro crop season 2018-19 under irrigation was 88889 taka/ha. For Menongchara and Buraghat rubber dam projects total expanses of farmers including input cost, labor cost and irrigation fee were 66914 taka/ha and 70571 taka/ha respectively. The net benefit with rubber dam irrigation is 21975 taka/ha for Menongchara project and 18318 taka/ha for Buraghat project.As reported by the farmers of Menongchara and Buraghat rubber dam projects the gross benefits without rubber dam irrigation were 59260 taka/ha and 56297 taka/ha respectively. Total expanse of farmers including input cost and labor cost was 44445 taka/ha for Menongchara project and 45680 taka/ha for Buraghat project. So the net benefits without rubber dam irrigation of Menongchara and Buraghat projects were 14815 taka/ha and 10617 taka/ha respectively. The benefit of rubber dam irrigation per hectare is 7160 taka for Menongchara

project and 7701 taka for Buraghat project. According to farmersof Menongchara and Buraghat projects the total irrigation fee in the season were 3347 taka/ha and 3951 taka/ha respectively. Using equation (8) profitabilities of farmer of Menongchara and Buraghat projects are 2.14 and 1.95 respectively.

4.9 Technical Problems

According to Menongchara rubber dam operator the operating nut of rubber bag is loose so they cannot operate it properly. In Buraghat rubber dam project the outlet water sometime overflows which causes the operating valve tube submerged. As reported by local people other problems were frequent sliding of river bank, damage of outlet pipes and leakage of water through opening of gravity pipes. No leakage in rubber bag, no mechanical problem in filling pump and no anchorage problem were found in Menongchara and Buraghat rubber dam projects.

4.10 Comparison of Performance of Menongchara and Buraghat Rubber Dam Project

Table 4: Values of performance indicators for Menongchara and Buraghat rubber dam projects

Performance Indicator	Menongchara Project	Buraghat Project
Irrigation efficiency	19.21%	18.30%
Command area efficiency	11.25%	20.52%
Yield efficiency	70.12%	82.65%
Actual water productivity	0.324 kg/m³	0.31 kg/m³
Fee collection efficiency	75%	70%
Economic viability	134.4%	213%
Profitability of farmer	214%	195%

Table 5: Comparison of the performance of Menongchara and Buraghat rubber dam projects

Topic	Menongchara Project	Buraghat Project
Irrigation fee	2470 Taka/ha	3951 Taka/ha
O&M cost	1838 Taka/ha	1854 Taka/ha
Meeting	Very few in a crop season	Monthly in a crop season
Water distribution	Gravity and LLP	LLP
Irrigated area	101.25 ha	153.9 ha
Water management	Participated by all farmers	Farmers are not involved
Project committee	Less active	Active
Solving O&M problems	By local people and technician hired by committee	By local people and technician from LGED
Authorities involvement in O&M work	No	Yes
Social acceptance	Not good	Good
Impact on fisheries	Good	Good
Impact on vegetation	Good	Good
Impact on livelihood	Significantly positive	Significantly positive

Impact on ground water	Positive	Positive
Wild Life and Animals	Positive impact	Positive impact

5. CONCLUSIONS

The overall performance of Menongchara and Buraghat rubber dam project were assessed through field visits and observations of rubber dam bag, river, canal, condition of LLPs, rubber dam pump etc. The conclusions are summarized below.

Amount of water delivered to Menongchara and Buraghat rubber dam projects is satisfactory. Irrigation efficiencies of Menongchara and Buraghat rubber dam project is 19.21% and 18.3% respectively, which are less than national average value. Current irrigated areas of Menongchara and Buraghat rubber dam project are 101.25 hectare and 153.9 hectare respectively. The values are much less than target values. In every season irrigated area are increasing for both the projects. Yield efficiency of Menongchara project is 70.12% and Buraghat project is 82.65%. From the result it is seen that yield efficiency of both the project is satisfactory. Actual water productivity of Menongchara and Buraghat rubber dam projects are 0.324 kg/m³ and 0.31 kg/m³. Actual water productivities of Menongchara and Buraghat project appear to be satisfactory. Fee collection efficiencies of Menongchara and Buraghat rubber dam project are 75% and 70% respectively. From the study it can be said that fee collection efficiency of Menongchara and Buraghat project are increasing every year. The project management committee of Menongchara and Buraghat project performing well. Economic viabilities of Menongchara and Buraghat rubber dam project are 134.4% and 213% respectively. Both the projects show good performance in terms of economic viability of the management committee. Operation and maintenance cost per hectare of Menongchara and Buraghat rubber dam project are 1838 taka and 1854 taka respectively. It is seen that both the project committee collected O&M fee more than O&M cost. But according to the committee members of Menongchara and Buraghat rubber dam project, they are not able to save money due to maintenance work. It is to be noted that the management committees are paying only operation and maintenance cost. They are not contributing to cost recovery of the projects. From the study it is seen that profitability of farmer of Menongchara project is 2.14 and Buraghat project is 1.95. Based on result it can be said that the farmers are benefitted from the projects. From the field visit and discussion with the beneficiaries it can be said that BADC did not involve in O&M of the project, they only handover the project to the beneficiaries group. Whereas in Buraghat project LGED provides technical support in O&M of the project. Few technical problems are observed for both Menongchara and Buraghat project. Based on study it can be said that Menongchara and Buraghat project show positive impact on fisheries. Fish cultivations are increasing in both the project area. After Menongchara and Buraghat project was implemented vegetation are increased in both projects area. Based on result it can be said that no adverse impact was found on ground water level, wild life and animals, and livelihood due to Menongchara and Buraghat rubber dam project. According to farmer rubber dam is more preferable compared to earthen dam. Operation and maintenance is not very difficult and moreover it is not required to build in every year.

REFERENCES

Saleh, A.F.M. and Mondal, M. S. (2000). "*Performance Evaluation of rubber dam projects in irrigation development*". A publication under the Institute of flood control and drainage research, BUET, Dhaka.

LGED. (1994). *Feasibility of Rubber Dams in Bangladesh*. Institute of Water Conservancy and Hydroelectric Power Research, Chinaand Technical Design Unit, ISP, ESP, Local Government Engineering Department: Dhaka, Bangladesh.

IWHR. (1994). *Rubber Dam- a new type of flexible hydraulic structures*, a paper prepared by Institute of Water Conservancy and Hydroelectric Power Research and Beijing Keyu Water Engineering Technology Corporation, China.

Raquib, M.A. (1999). *Performance Evaluation of rubber dam projects in Bangladesh.* M. Engg. Thesis, Department of Water Resource Engineering, BUET, Dhaka.

Ahmed, S. (2014). *A study on the rubber dams in Bangladesh and performance evaluation of a selected rubber dam.* B.Sc. Engg. Thesis, Department of Water Resource Engineering, BUET, Dhaka.

Proceedings of the 5th International Conference on Civil Engineering for Sustainable Development (ICCESD 2020), 7~9 February 2020, KUET, Khulna, Bangladesh (ISBN-978-984-34-8764-3)

ASSESSMENT OF ENVIRONMENTAL FLOW REQUIREMENT OF TEESTA RIVER BY HYDROLOGICAL METHODS

Fardini Khandaker*[1] and Md. Ataur Rahman[2]

[1]Postgraduate student, Institute of Water and Flood Management (IWFM), Bangladesh University of Engineering and Technology (BUET), Bangladesh, e-mail: khandaker_f@yahoo.com
[2]Professor, Department of Water Resources Engineering, Bangladesh University of Engineering and Technology (BUET), Bangladesh, e-mail: mataur@wre.buet.ac.bd

***Corresponding Author**

ABSTRACT

Teesta River is one of the many transboundary rivers shared between India and Bangladesh. It is an important river for both India and Bangladesh. However, the river has also been an issue of debate between the two nations. Due to construction of a number of dam and barrages, the natural flow of the river has been highly utilized, diverted and controlled. But as the river is a transboundary river, it has never been easy to come to a satisfactory conclusion as to how much flow must be maintained in the river. Therefore assessment of environmental flow for Teesta River is of great importance not only for better negotiation but also to maintain the riverine ecosystem properly.The study assesses environmental flow of Teesta River by three hydrological methods- Tennant method, Flow Duration Curve method and Constant Yield method. The environmental flow is measured at Dalia station and Kaunia station which are upstream and downstream of Teesta barrage respectively. Therefore, the study aims at recommending a flow that has to be maintained upstream of the barrage and also to set recommendation of how much water must be maintained in the river downstream of the barrage. It should also be mentioned that in the study low flow period was considered from November to April and high flow period was considered from May to October. At Dalia, according to Tennant method environmental flow requirement was found to be 151 cumec (for good habitat quality) for the months of low flow. On the other hand, for high flow months environmental flow was found to be 302 cumec (good habitat quality) at Dalia. At Kaunia, EFR is 162 cumec (good habitat quality) and 324 cumec (outstanding habitat quality) for the low flow month. Again for high flow months at Kaunia EFR for good is 324 cumec. In flow duration curve method, the requirement range changed to 5 to 160 cumec for low flow and 422 to 1912 cumec for high flow at Dalia. For Kaunia it was found to be 10 to 314 cumec for low flow and 462 to 2111 cumec for high flow months. For constant yield method the requirement was found to be 41 to 284 cumec (low flow period)and 369 to 1844 cumec (high flow period) for Dalia. 81 to 307 cumec (low flow period) and 408 to 1940 cumec (high flow period) for Kaunia. In the study it was found that the prevailing flow is sufficient in high flow season (May to October) to meet the requirement derived by tenant and constant yield method. However in low flow season (November to April) the prevailing flow is found to be insufficient according to Tennant method.

As Tennant method is the common and accepted method for EFR assessment and low flow period is the main concern, the requirement found from the study can be stated as 151 cumec at Dalia and 162 cumec at Kaunia.

Keywords: *EFR, Hydrological method, Tennant method, Flow duration curve, Constant yield method.*

1. INTRODUCTION

1.1 Background:

Bangladesh is a riverine country. A network consisting of around 800 rivers flow through this land. Bangladesh Water Development Board (BWDB) has numbered 405 rivers, among which 57 are transboundary rivers. Bangladesh shares 54 transboundary rivers with India and 3 with Myanmar.

Teesta is one of the 57 transboundary rivers of Bangladesh. It originates in India and then crosses the India-Bangladesh border to meet Brahmaputra River at Kurigram district in Bangladesh. It is numbered as 52 number north-western river by Bangladesh Water Development Board.

Total length of the Teesta is about 315 km of which about 113 km falls inside Bangladesh (http://en.banglapedia.org/index.php?title=Tista_River). The river Teesta is one of the main Himalayan rivers and originates from the glaciers of Sikkim in North at an elevation of about 5,280 m (CISMHE, 2006). The glacial lake is located at the tip of the Teesta Khangse glacier, which descends from Pauhunri peak. The river rises in mountainous terrain in extreme north as Chhombo Chhu, which flows eastward and then southward to be joined by Zemu Chhu, upstream of Lachen village near Zema. The river takes a gentle turn in southeast direction and meets Lachung Chhu at Chungthang where it takes the form of a mighty Himalayan river. After the confluence of Teesta River and Lachung Chhu at Chungthang, the river gradually widens and takes a strong westward turn upstream of Tong and after flowing down to Singhik, the river drops from 1,550 m to 750 m (CISMHE, 2006).. The map of catchment area is shown in the Figure 1.1

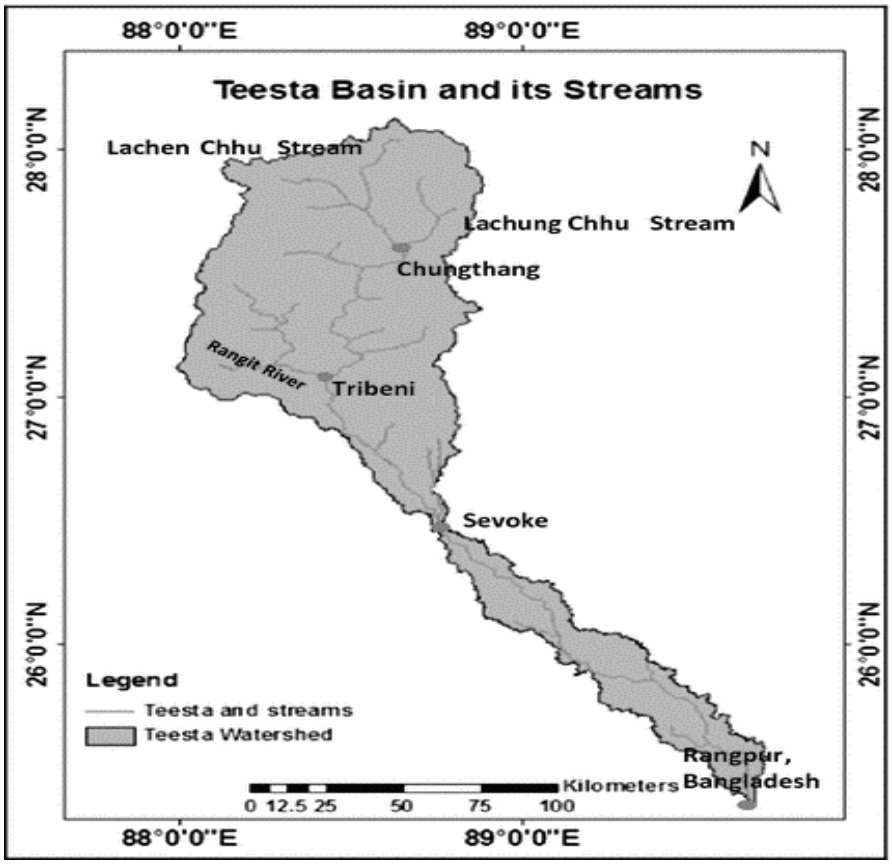

Figure 1.1: Map of catchment area of Teesta River

Teesta is an important river for both India and Bangladesh. Both the governments have created numerous structures and have proposed several projects throughout the years to utilize the water for irrigation and power generation. The large scale construction of dams in this area has been controversial.

One of the major two projects undertaken are Teesta Barrage at Gozaldoba, Jolpaiguri in West Bengal, India and Teesta barrage at Dalia situated in Lalmonirhat district, Bangladesh.

The water in Teesta has been regulated in India through the construction of irrigation barrage at Gozaldoba in 1987. Afterwards another irrigation barrage was established by Bangladesh at Dalia-Doani point in Lalmonirhat district in 1990 to supply water to Teesta Irrigation Project (TIP).

1.2 Study Area

The study focuses on determining the environmental flow for Teesta River which lies in Bangladesh portion (Figure 1.2). The river enters into Bangladesh at Dahagram village in Lalmonirhat and joins Brahmaputra (Jamuna) River near Chilmari Upazilla of Kurigram district (extending from 88055'40" E, 26018'N to 89038'59" E,2501'10" N)

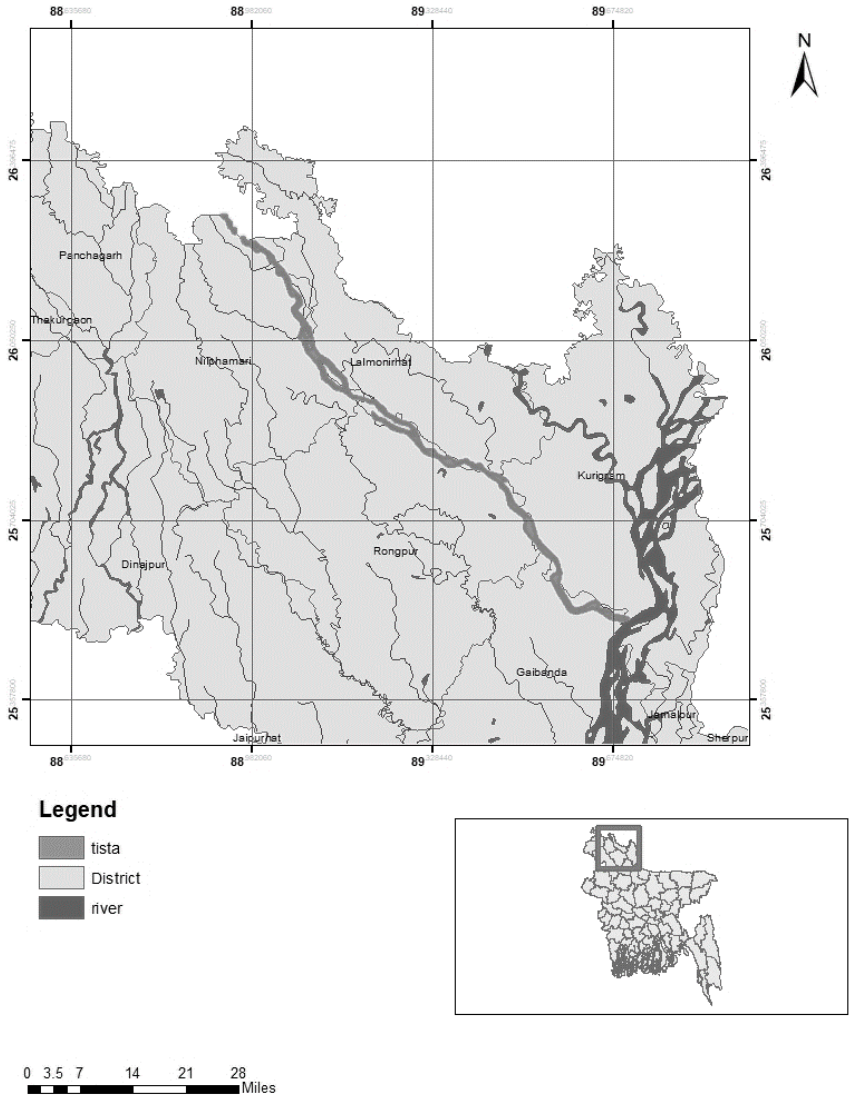

Figure 1.2: Location map of Teesta River in Bangladesh

Teesta River is the life line of the drought prone area of northern Bangladesh. It has always been at the centre point of the riverine ecosystem of the northern side of the country. However, subsequent construction of upstream structures, specially Gozaldoba and Dalia barrage, has drastically reduced its flow during dry period. Therefore, assessment of Teesta River environmental flow has been an important issue.

2. METHODOLOGY

2.1 Study Approach

Study approach is shown in figure 2.1

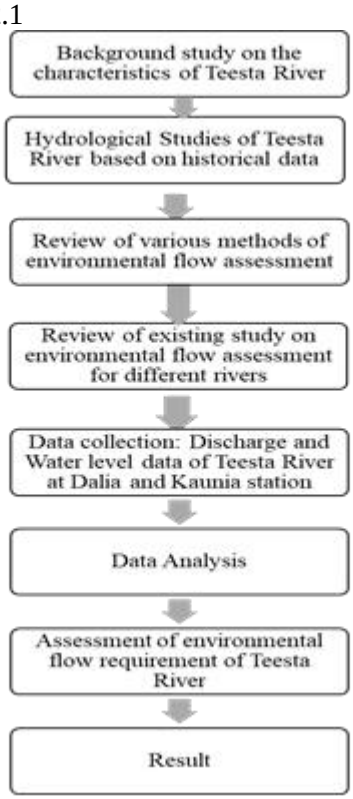

Figure 2.1: Study approach

The study approach is simple and sequential. To assess the environmental flow background study of the Teesta River characteristic (including physical and hydrological) is carried out. There are numerous ways of assessing environmental flow of a river. So to decide an appropriate method of environmental flow assessment for Teesta river, a literature review of various studies is performed. Finally through data analysis, environmental flow requirement is assessed according to the selected methods.

2.2 Data collection

Data has been collected from Bangladesh Water Development Board (BWDB) for the station Dalia and Kaunia. Dalia station is located upstream of Teesta barrage in Lalmonirhat district and Kaunia station is located downstream of the barrage in Rangpur. The distance between the two stations is about 70 km

2.3 Methods of Environmental Flow Assessment

As stated before, there are several methods used in determining environmental flow. In this study three hydrological methods have been used. They are:

1. Tennant Method
2. Flow duration Curve Method
3. Constant Yield Method

Tennant Method

According to Tennant method, required flow is a percentage of the mean annual flow of a river. For different habitat conditions (i.e. Flushing, excellent, good, etc.), the required flow varies from 10% to 200% of mean annual flow. Tennant method also uses different percentage of mean annual flow for low flow period and high flow. Tennant method is based on the reasoning that mean annual flow represents flow which has sustained the habitat of the flora, fauna and human activities of the river for several

years and hence various percentage of the mean annual flow can be used to determine environmental flow requirement. Table 2 shows Tennant's recommendation for environmental flow to support varying qualities of fish habitat.

Table 2: Percentage of MAF for various habitat quality (Source: Bari and Marchand, 2006)

Habitat Quality	Percent of Mean Annual Flow (MAF)	
	Low Flow Season	High Flow Season
Flushing or maximum	200	200
Optimum	60-100	60-100
Outstanding	40	60
Excellent	30	50
Good	20	40
Fair	10	30
Poor	10	10
Severe degradation	<10	<10

Flow Duration Curve Method

Flow duration curve method is another hydrological method. In this method environmental flow requirement is determined by observing the discharge and the percentage of time it is exceeded. In this method flow exceedance percentage is computed for each moth from the period 1985 to 2016. For months of high flow season, flow greater or equal to 50th percentile flow is recommended. For low flow season the recommendation is set at 90th percentile flow. Here 50th percentile flow refers to the flow which is exceeded 50% of the time. In other words, it is the value of discharge which is likely to occur or exceeded 50% of the time. Similarly, 90th percentile flow refers to flow which has 90% probability of occurring or exceeding.

In this study, flow duration curve for each month has been obtained using mean monthly discharge data from the years 1985 to 2016 of Dalia and Kaunia station. From there the 90th percentile flow is recommended for low flow season extending from the months of November, December, January, February, March, April. For high flow months (which includes May, June, July, August, September, October) 50th percentile flow is set as recommended discharge.

Constant Yield Method

In constant yield method, recommended flow is set at 100% of median flow of each month. For this purpose, the median flow for each month has been computed for each year from 1985 to 2016. Hence median monthly flow of each month was obtained and set as required environmental flow.

3. DATA ANALYSIS AND RESULTS

3.1 Flow characteristics of Teesta

Hydrological characteristics for Teesta River has been analysed from the years 1985 to 2016 based on data collected from Dalia and Kaunia station. Maximum, minimum and average discharge and water level variation has been analyzed from the collected data. In the following figures the variation has been shown graphically.

Water level: The variation of maximum, minimum and average water level from the years 1996 to 2018 have been shown in figure 3.1(a) and 3.1(b) for both the location Dalia and kaunia. The water level has not significantly decreased or increased over the years. From the figure it is clear that water level at Dalia is greater than Kaunia in general. Water level in Dalia varied from approximately 48 to 53 mPWD whereas in Kaunia water level was between the range 25 to 30 mPWD. Another observation is that at upstream of Teesta barrage, water level is rising. The trend lines shown in Figure 4.1 (a) all have a

positive slope and denote an overall increasing tendency of water level. However, the opposite scenario seems to be present at Kaunia. The water level here seems to have a declining trend, as shown in figure 4.1(b).

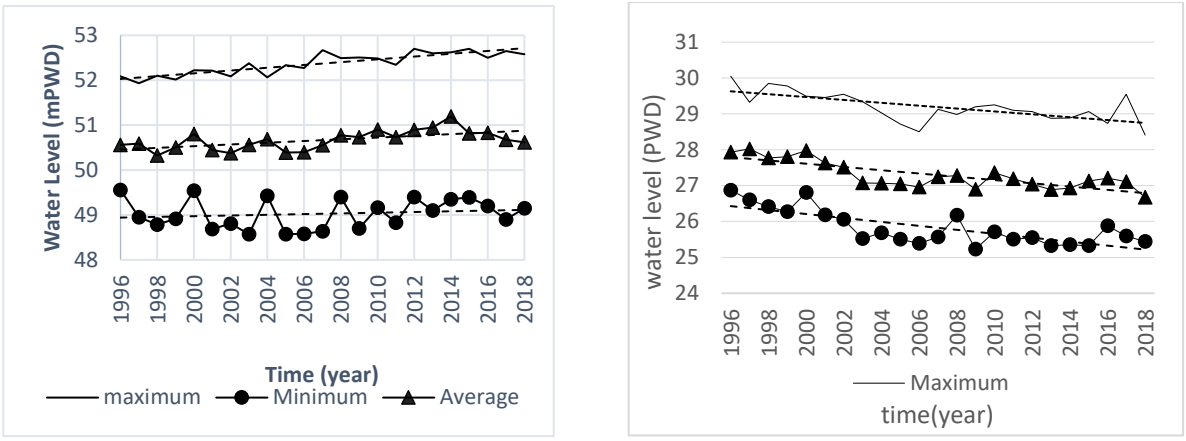

(a) (b)

Figure 3.1: Maximum, minimum and average water level at (a) Dalia station upstream of Teesta Barrage and (b) Kaunia station downstream of Teesta Barrage

The discharge at Dalia and Kaunia station has also been analyzed as maximum, minimum and average over the years 1985 to 2016. For Dalia, it is observed that the maximum value has been gradually decreasing since 2003 and the minimum value has also decreased drastically from1996 to 2003. After that the minimum flow values have increased. But overall the minimum flow is on the decreasing trend Maximum flow occurs during high flow season and minimum flow for any year occurs during low flow season. Therefore, it is observed that irrespective of whether the season is of high flow or low flow, flow is on the decreasing trend. Highest value of maximum discharge at Dalia is found to be 7420 cumec and lowest value of minimum flow is .20 cumec.

For Kaunia it is also seen that maximum, minimum and average flow for any year is also on the decreasing tendency. Similar to Dalia, it is also seen that minimum value of flow was drasctically decresed from 1999 to 2003. Highest value of maximum discharge at Dalia is found to be 8710 cumec and lowest value of minimum flow is 4.49 cumec. Hence it can be said that discharge at Kaunia seems to be higher than discharge at Dalia although water level at Kaunia is comparatively lower. The analysis has been shown in the figure 3.2 (a) to figure 3.2 (b).

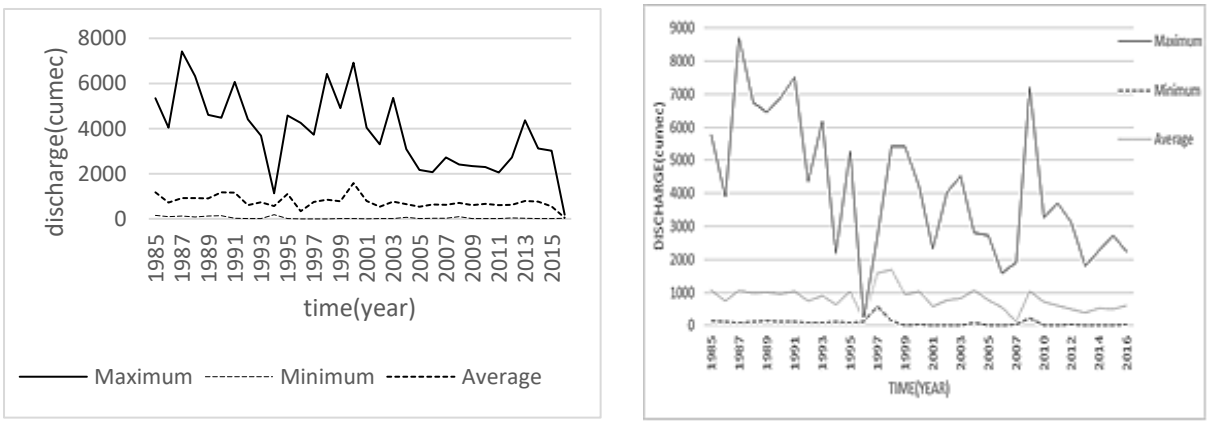

(a) (b)

Figure 3.2: Maximum, minimum and average discharge over the years 1985 to 2016 at (a) Dalia upstream of Teesta Barrage and (b) Kaunia station downstream of Teesta barrage.

3.2 Environmental Flow Requirement (EFR) of Teesta River

Environmental flow requirement has been assessed at Dalia (upstream of Teesta Barrage) and Kaunia (Downstream of Teesta Barrage). The requirement was estimated using hydrological methods which include – Tennant method, flow duration curve method and constant yield method. The acquired environmental flow requirements using these three methods have been tabulated in the following sections.

Tennant Method: Using different percentage of mean annual flow for different habitat quality, environmental flow requirement has been computed at Dalia and Kaunia. In the study, good and outstanding habitat quality is taken under consideration. For good and outstanding habitat quality the results from this method is given in Table 3.1

Table 3.1: Environmental flow requirement at Dalia and Kaunia station using Tennant method

Station: Dalia		
Environmental Flow requirement (cumec)		
Habitat Quality	Low flow Season	High Flow season
Good	151	302
Outstanding	302	454
Station: Kaunia		
Environmental Flow requirement (cumec)		
Habitat Quality	Low flow Season	High Flow season
Good	162	324
Outstanding	324	486

Flow Duration Curve Method: Environmental Flow requirement from flow duration curve has been tabulated in the following Table 3.2

Table 3.2: Environmental flow requirement at Dalia and Kaunia station using flow duration curve method

Month	**Jan**	**Feb**	**Mar**	**Apr**	**May**	**Jun**	**Jul**	**Aug**	**Sep**	**Oct**	**Nov**	**Dec**
Flow season	Low	Low	Low	Low	High	High	High	High	High	High	Low	Low
Station: Dalia												
EFR (cumec)	6	5	6	41	422	1231	1912	1761	1452	671	160	23
Station: Kaunia												
EFR (cumec)	33	15	10	50	462	1133	2111	1925	1436	785	314	211

Constant Yield Method: Environmental Flow requirement from flow duration curve has been tabulated in the following Table 3.3

Table 3.3: Environmental flow requirement at Dalia and Kaunia station using constant yield method

Month	**Jan**	**Feb**	**Mar**	**Apr**	**May**	**Jun**	**Jul**	**Aug**	**Sep**	**Oct**	**Nov**	**Dec**
Flow season	**Low**	**Low**	**Low**	**Low**	**High**	**High**	**High**	**High**	**High**	**High**	**Low**	**Low**
Station: Dalia												
EFR	95	41	53	162	369	1149	1844	1777	1386	670	284	170
Station: Kaunia												
EFR	141	81	106	192	408	1140	1940	1867	1411	712	307	208

3.3 Comparison between environmental flow requirement (EFR) and flow availability

Environmental flow requirement has been assessed for Dalia station and Kaunia Station as stated earlier. In this section of the study, the determined environmental flow is compared with flow that is currently present in the river. For this purpose, the determined environmental flow requirement from various methods has been compared against the mean monthly flow of each month for both stations.

Dalia Station: In Table 3.4 and Figure 3.3 (a) comparison between computed EFR using various methods and available flow has been shown. It is seen that available flow is higher than the required environmental flow according to Constant yield method. Available flow is also sufficient enough to meet the requirement for good and outstanding habitat quality in high flow season according to Tennant Method, however it is not sufficient in low flow season for either of the habitat qualities. On the other hand, according to flow duration curve method, the available flow fails to exceed EFR in high Flow season but is sufficient in low flow season.

Table 3.4: Comparison of computed environmental flow requirements by different methods with available flow (Dalia Station)

Month	Flow season	Environmental Flow requirement (cumec)				Available flow (cumec)
		Tenant Method		Flow Duration Curve Method	Constant Yield Method	
		Good Habitat Quality	Outstanding Habitat Quality			
January	Low	151	302	6	95	107
February	Low	151	302	5	41	78
March	Low	151	302	6	53	106
April	Low	151	302	41	162	239
May	High	302	454	422	369	443
June	High	302	454	1231	1149	1317
July	High	302	454	1912	1844	1988
August	High	302	454	1761	1777	1897
September	High	302	454	1452	1386	1488
October	High	302	454	671	670	772
November	Low	151	302	160	284	311
December	Low	151	302	23	170	181

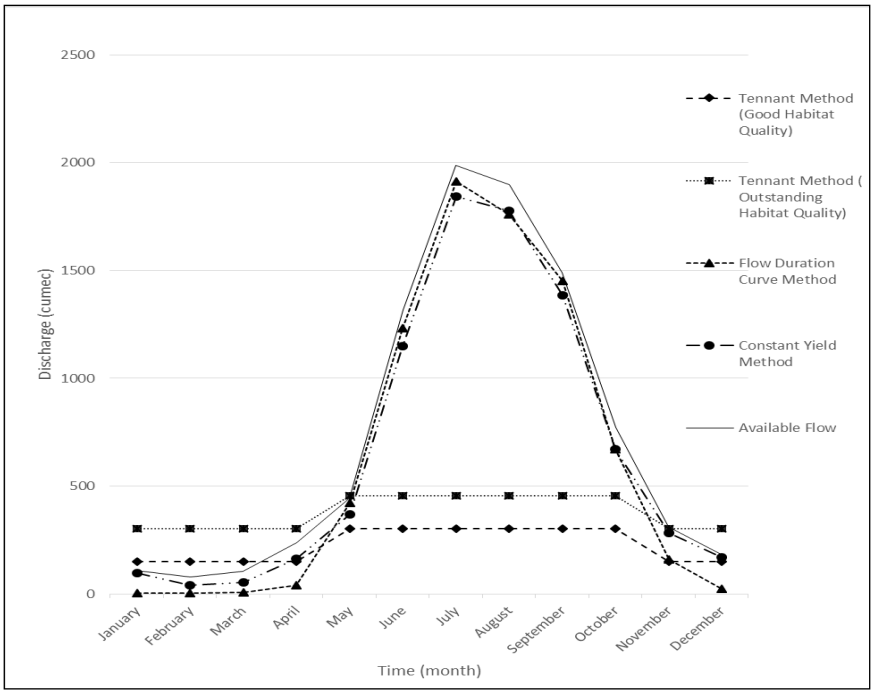

Figure 3.3 (a): Comparison of computed environmental flow requirements with available flow at Dalia Station

Kaunia Station: In Table 3.5 and Figure 3.3(b) comparison between computed EFR using various methods and available flow has been shown for Kaunia Station. In Table 4.8 and Figure 4.7 comparison between computed EFR using various methods and available flow has been shown. It is seen that available flow is higher than the required environmental flow according to Constant yield method and Flow Duration Curve method. Available flow is also sufficient enough to meet the requirement for good and outstanding habitat quality in high flow season according to Tennant Method, however it is not sufficient in low flow season for either of the habitat qualities which similar to the observation made in Dalia station.

Table 3.5: Comparison of computed environmental flow requirements by different methods with available flow (Kaunia Station)

Month	Flow season	Environmental Flow requirement (cumec)				Available flow (cumec)
		Tennant Method		Flow Duration Curve Method	Constant Yield Method	
		Good Habitat Quality	Outstanding Habitat Quality			
January	Low	162	324	33	141	121
February	Low	162	324	15	81	89
March	Low	162	324	10	106	98
April	Low	162	324	50	192	181
May	High	324	486	462	408	490
June	High	324	486	1133	1140	1268
July	High	324	486	2111	1940	2118
August	High	324	486	1925	1867	2025
September	High	324	486	1436	1411	1616
October	High	324	486	785	712	811
November	Low	162	324	314	307	320
December	Low	162	324	211	208	211

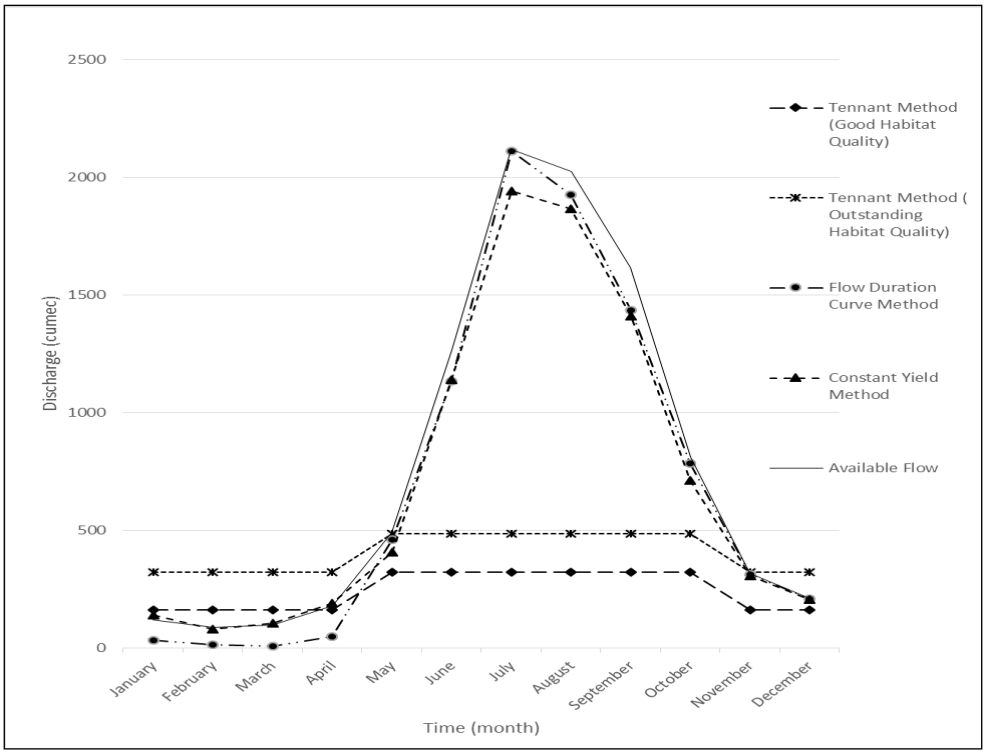

Figure 3.3 (b): Comparison of computed environmental flow requirements with available flow at Kaunia station

4. CONCLUSIONS

Teesta is an important river for both India and Bangladesh. Sharing of water of Teesta River has always been and still is a burning issue for both the nations. Assessment of environmental flow of such river can play a key role in determining rightful share and help in fruitful negotiation.

Environmental flow has been assessed of Teesta River at Dalia and Kaunia station where Dalia station is upstream of Teesta barrage and Kaunia station is at downstream of Teesta barrage. Therefore, the study is an effort to recommend a requirement of flow upstream and downstream of the barrage. The low flow period is the main concern for EFR assessment. As Tennant method is the common and accepted method for EFR assessment and low flow period is the main concern, the requirement was found as 151 cumec at Dalia and 162 cumec at Kaunia. In the study it was found that available flow is sufficient in high flow season to meet the derived requirements. However in low flow season the prevailing flow is found to be insufficient according to Tennant method.

REFERENCES

Bari, F. M., Marchand, M. (2006). *Introducing environmental flow assessment in Bangladesh: Multidisciplinary collaborative research.* BUET-DUT Linkage Project, Phase III, Research Project No. 2, BUET, Dhaka.

Centre for Inter Disciplinary Studies of Mountain and Hill Development (CISMHE). 2006. *'Carrying Capacity Study of Teesta Basin in Sikkim'.* Delhi, India: University of Delhi.

Proceedings of the 5th International Conference on Civil Engineering for Sustainable Development (ICCESD 2020), 7~9 February 2020, KUET, Khulna, Bangladesh (ISBN-978-984-34-8764-3)

ESTIMATION OF SURFACE RUNOFF USING SCS-CN METHOD IN GIS ENVIRONMENT: A CASE STUDY OF KHULNA CITY

Abdullah Al Mamun*[1], Samsuddin Ahmed[2] and Md. Esraz-Ul-Zannat [3]

[1]Graduate Student, Khulna University of Engineering & Technology, Bangladesh, abdullahmamunaman@gmail.com
[2]Student, Khulna University of Engineering & Technology, Bangladesh, samuddin.ce15@gmail.com
[3]Assistant Professor, Khulna University of Engineering & Technology, Bangladesh, esrazuz@gmail.com

Corresponding Author

ABSTRACT

Estimation of Surface runoff, a very important measure of rain water distribution, is essential to manage proper water balance within an area. This study was conducted to estimate surface runoff using SCS (Soil Conservation Service) –CN (Curve Number) method within political boundary of Khulna City Corporation (KCC) area. Runoff curve number, the key factor to determine surface runoff of this method, was established with the environment of Geographic Information System (GIS). ArcGIS technique was used to determine curve number using topographic map, land use map and soil map of the study area. Satellite image of the study area was collected from USGS. The catchment area of Khulna city is 40.79 km.2 where 1926 mm per year average precipitation was observed. Within the catchment area different curve numbers were obtained from land use and soil types. Finally, a relationship was established between rainfall and surface runoff and it was found that about 19% of rainfall is subjected to surface runoff. That's why it is easy to find out and calculate flow direction, flow accumulation, adjoin catchment of this area. Integration of GIS with the traditional SCS-CN method has been proved as a strong analytical tool for surface runoff estimation and helped to evaluate several land use policy to manage it.

Keywords: *Geographic Information System (GIS), SCS-CN method, Curve Number, Surface runoff, Khulna City Corporation (KCC).*

1. INTRODUCTION

Surface runoff is water, from rain, snowmelt, or other sources, that flows over the land surface, and is a major component of the water cycle. Runoff that occurs on surfaces before reaching a channel is also called overland flow. A land area which produces runoff draining to a common point is called a watershed. Urbanization increases surface runoff, by creating more impervious surfaces such as pavement and buildings do not allow percolation of the water down through the soil to the aquifer. First of all, surface runoff highly depends on precipitation. Surface elevation, texture, soil characteristics are highly related with surface runoff. When surface elevation or steepness is high, a potential amount of precipitation subjected to runoff. Again soil permeability is highly related to runoff. Different soil has different percolation capacity. When percolation is no longer possible then runoff occurs.

Surface runoff is subjected to rainfall where rainfall-runoff relationship is very complex, influenced by various storm and drainage characteristics (Seth et al. 1997). Rainfall induced runoff is very important for water resources development and management such as flood control and its management, Irrigation scheduling, design of drainage network, hydro power generation etc. (Mishra et al. 2013). Again surface runoff plays an important role in natural water balance. Ground water recharge is inversely related with surface runoff. It is worth mentioning that over the past two decades, the use of Remote Sensing and Geographic Information System (GIS) technologies in run-off estimation from urban watershed has gained increasing land use planning and watershed management can be done effectively and efficiently using SCS-CN number method with GIS (Ahmad et al. 2015). The major advantage of employing GIS in rainfall-runoff modelling is that more accurate sizing and catchment characterization can be achieved. Furthermore, the analysis can be performed much faster, especially when there is a complex mix of land use classes and different soil types (Shadeed and Almasri, 2010).

1.1 Study Area

Khulna is the 3rd large city and 2nd largest coastal zone of Bangladesh. It is also moderately high precipitated zone because of its geographical location. The geographical location of this area 22°49′0″N 89°33′0″E which is the south-western part of Bangladesh. Khulna city is situated at the western bank of the river Bhairov over a length of around 15 km. As of the 2011 census, the city has a population of 751.23 thousand and its total area is 64.78 km^2 (BBS, 2011).

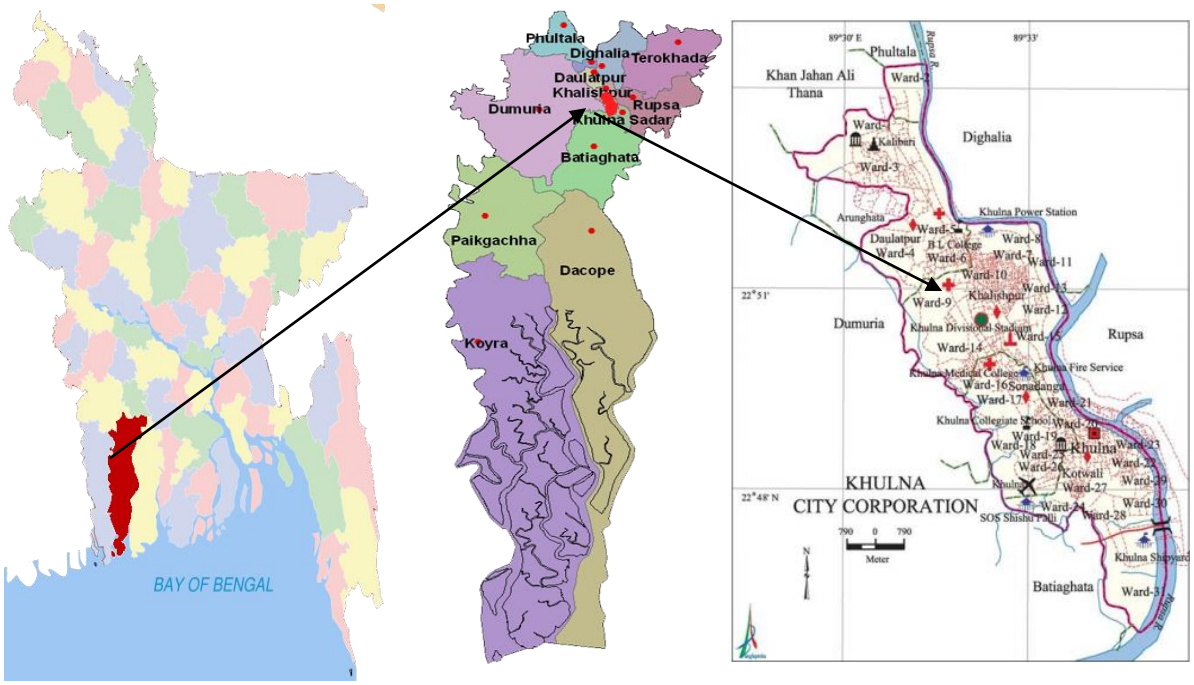

Figure 1: Study Map (Source: Google Map)

2. METHODOLOGY

2.1. Data Collection and Map Preparation

Data was collected from both primary and secondary sources. Most of the data required for the study were collected from the secondary sources. For the analysis purpose of GIS, data about topography, soil characteristics, study area image were collected from the secondary sources. Soil data of Khulna city was clipped from the soil map of Bangladesh and required topographic data was clipped from the DEM of Bangladesh. Data of land use and land cover was generated using ArcGIS through supervised classification and digitizing. Required study area image for that was collected from satellite image. Data of precipitation was collected from the meteorological station of Khulna in order to analyze the change of micro-climate. Different thematic map such as soil map, topographic map, land use and land cover map, CN map were prepared using ArcGIS.

2.2. Surface Runoff Calculation

The amount of surface runoff was estimated using SCS-CN method. The Soil Conservation Service Model also known as the Hydrologic Soil Cover Complex Model, is a widely used procedure for runoff estimation. The model uses a numerical value (Curve Number) varying between 0-100 to express runoff potentiality. The equation used for estimation of runoff depth is as follows,

$$Q = (P - .3S)^2 / (P + .7S) \qquad \text{Where} \quad S = 25400 / CN - 254$$

Here, Q = Runoff depth (mm). S = Maximum potential retention. CN = Curve Number. P = Rainfall depth (mm).

2.2.1. Computation of CN Value

Curve number depends on soil type, land use, Digital Elevation Model (DEM), Antecedent Moisture Condition of the study area.

2.2.2. Soil Map Generation

In the determination of CN, the hydrological soil classification was adopted. Here, soil was classified into three out of four classes named as A (Low Runoff Potential), B (Moderately Low Runoff Potential), C (Moderately High Runoff Potential), and D (High Runoff Potential). The classification was done based on runoff potential of different hydrological soil group.

2.2.3. Antecedent Moisture Condition (AMC)

Antecedent Moisture condition (AMC) refers to the moisture content present in the soil at the beginning of the rainfall-runoff event under consideration. It is well known that initial abstraction and infiltration are governed by AMC. For purpose of practical application three level of AMC are recognized by SCS as follows:

AMC-I: Soil are dry but not to wilting point. Satisfactory cultivation has taken place.

AMC-II: Average conditions.

AMC-III: Sufficient rainfall has occurred within the immediate past 5 days. Saturated soil condition prevails.

The limit of these three AMC classes, based on rainfall of the previous five days are given below,

Table 1: Antecedent moisture condition for determining the value of CN.

AMC Type	Total Rain in previous 5 days	
	Dormant Season	Growing Season
I	Less than 13 mm	Less than 36 mm
II	13 to 28 mm	36 to 53 mm
III	More than 28 mm	More than 53 mm

(Source: K. Subramanya, 2013)

2.2.4. Setting CN Look up Value

CN value is unique for different land use and land cover. After classifying the land use and land cover, there corresponding CN value was determined observing the hydrologic soil group. Increase in CN value denotes high runoff potential.

Table 2: CN value for different land use and soil type under AMC II.

Land Use and Land Cover	CN value of Hydrologic soil group			
	A	B	C	D
Agricultural Land	76	86	90	93
Vegetation	28	44	60	64
Open Space	49	69	79	84
Built Up Area	77	85	90	93
Water body and Wet land	0	0	0	0

(Source: K. Subramanya, 2013)

2.2.5. Curve Number Generation

HEcGeoMMS tool was used to generate curve number grid of the study area. After preparing all the needed criteria, Curve Number grid was obtained through the process shown in the flow diagram below:

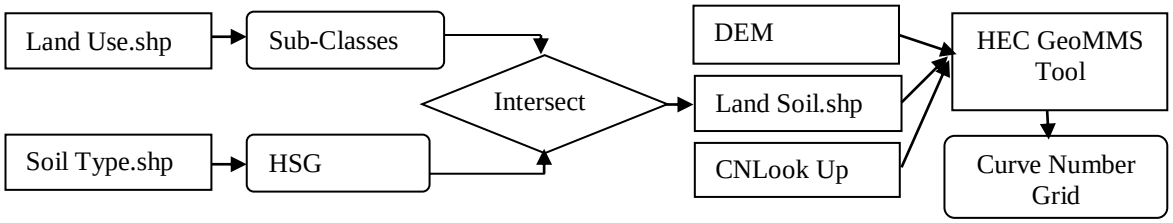

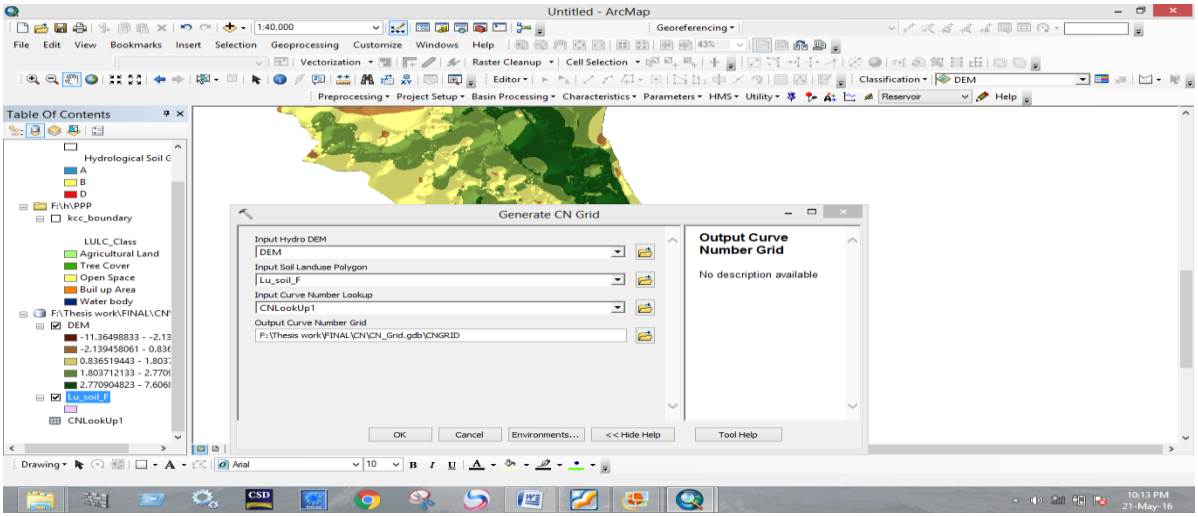

Figure 2: Curve Number Grid Generation through HEC GeoMMS Tool. (Source: Preparation on Arc GIS Environment)

Theissen polygons were established for each identified rain gauge station. For each theissen cell, area weighted CN (AMC II) and also CN (AMC I) and CN (AMC III) were determined. CN for AMC II is shown in Table 2. Area weighted composite curve number for various conditions of land use and hydrologic soil conditions were computed as follows:

$$CN = \sum_{i=1}^{i=n} \frac{CNi \times Ai}{A_i}$$

Weighted Curve Number,

Where Ai=A1, A2, A3, …., An represent areas of polygon having CN values CN1, CN2, CN3,…..,CNn respectively and Ai is the total area.

After calculation CN value for AMC II condition, CN value for AMC I and AMC III were obtained by the following equations:

$$CN_I = \frac{CN_{II}}{2.281 - 0.0128 CN_{II}} \qquad CN_{III} = \frac{CN_{II}}{.427 + 0.0128 CN_{II}}$$

Table 3: Curve Number and Soil Retention under Antecedent Moisture Condition.

Antecedent Moisture Condition	Weighted Curve Number	Maximum Retention (S)
AMC I	(CNI)= 47.60	279.57
AMC II	(CNII)= 67.45	122.56
AMC III	(CNIII)= 82.92	52.34

(Source: Derived from SCS-CN method)

3. ANALYSIS AND FINDING:

3.1. Precipitation Change of the Study Area

Khulna city has homogeneous climatic characteristics. The city area is small enough therefore the climatic variation at a particular time in different places is negligible. Normally Increase of precipitation means increase in run off. Figure 5.2 shows the change in precipitation within last ten

years (2005-2015). The amount of yearly precipitation was as much as 1926 mm for the year 2015 and as low as 801 for year 2010.

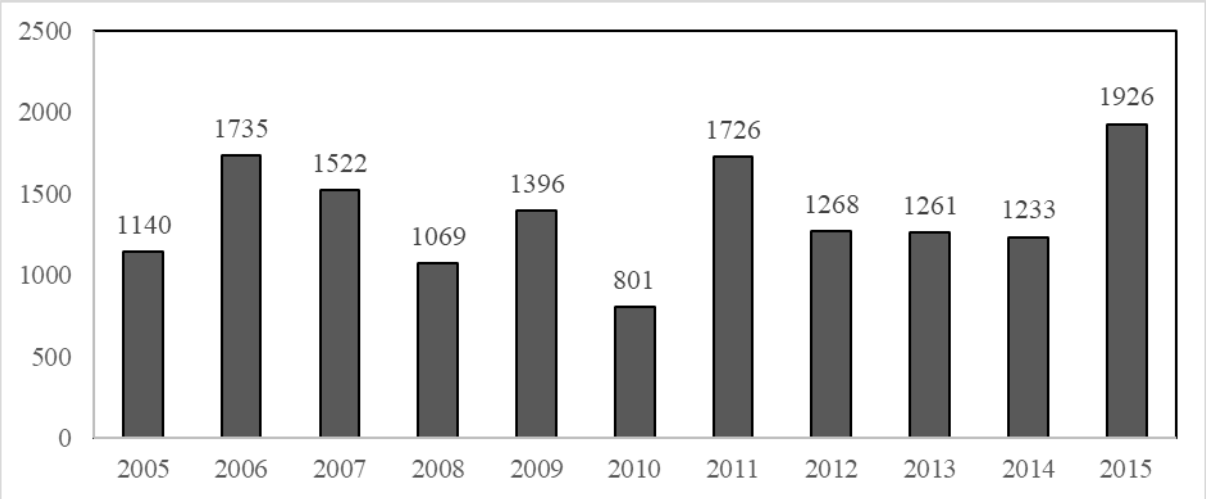

Figure 3: Change in precipitation (Source: BMD, 2016).

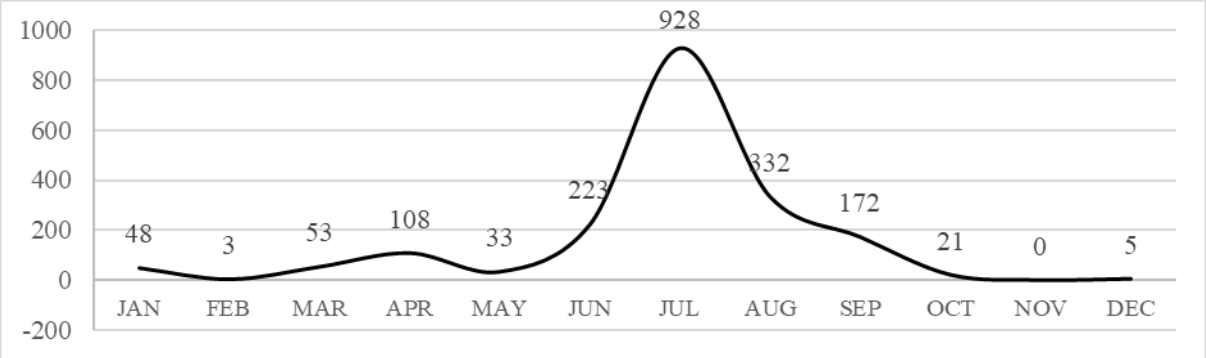

Figure 4: Variation of monthly precipitation in the study year (2015) (Source: BMD, 2016).

From the Figure 4, the potential precipitation amount was observed for only four months from June to September. Figure 4 also shows the negligible amount of precipitation for the months of October to February where precipitation of study year is as much as 928 mm for the month of July.

3.2. Analysis of Surface Runoff

Surface runoff was estimated using SCS-CN method. Surface runoff is highly related to the amount of precipitation, land use and land cover and topographic condition. All these parameter was evaluated in GIS environment which are described below.

3.2.1. Evaluation of Land Use of Khulna City

Land use plays an important role for identification of surface runoff. Khulna is an emerging city which land use is being changed with each passing year which will influence surface runoff potentiality.

Table 4: Land use of Khulna city.

Land use	Area (sq. m)	Percentage(%)
Agricultural Land	3686773.67	8.136225
Vegetation	7564165.85	16.69312
Open Space	5109758.83	11.27657
Built up Area	23920398.68	52.78918
Water body	5031975.95	11.10491

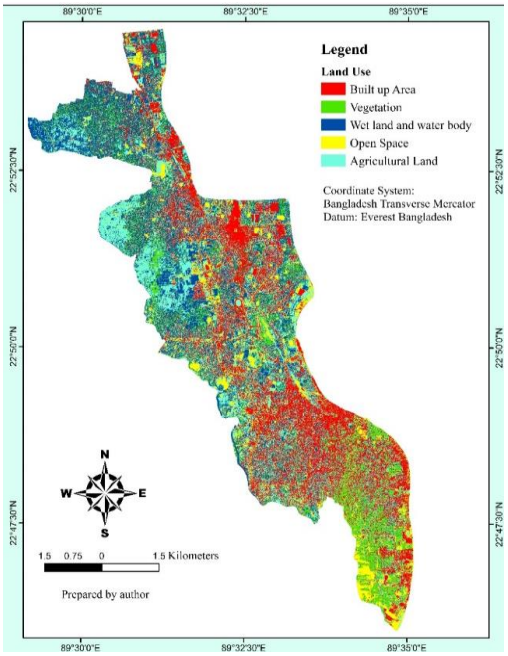

Figure 5: Land Use and Land Cover Map

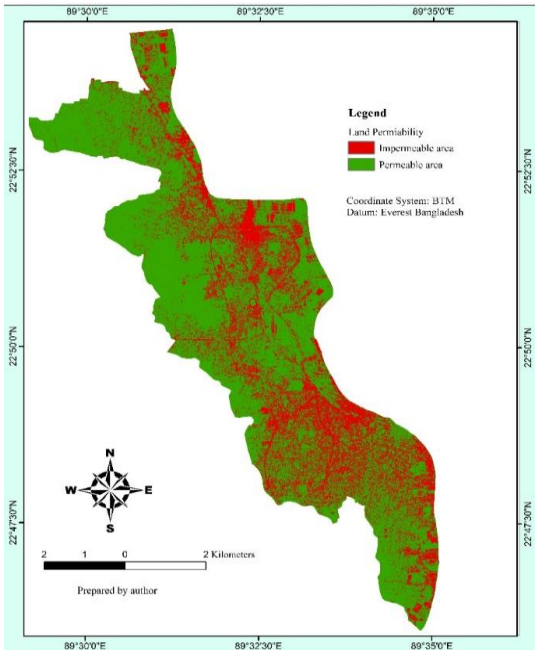

Figure 6: Permeable and impermeable area

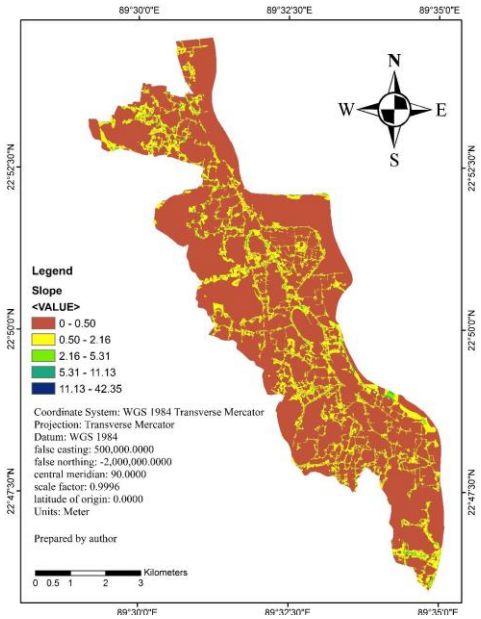

Figure 7: Topographic Map

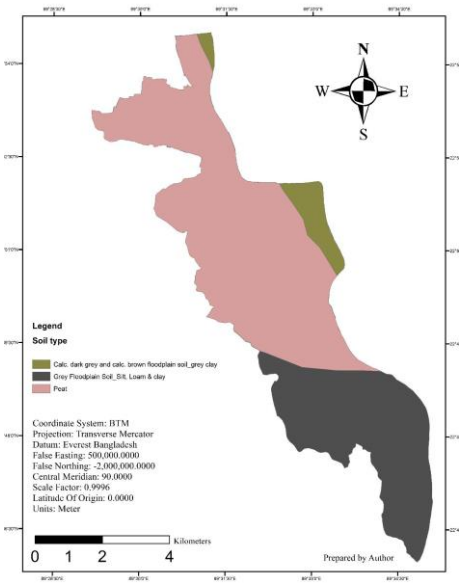

Figure 8: Soil Map

(Source: Preparation on ArcGIS Environment)

As per Table 4, 53 % area of Khulna city is covered by built up area which includes low and high density and 28.31% is impermeable.

3.2.2. Evaluation of Topographic Condition and Soil Characteristics of Khulna City

Variation of topography has impact on the runoff potentiality of an area. Topographic variation of Khulna city is not too much. Khulna is almost a flat area. Different soil type exist in Khulna city. Observed hydrological soil groups of Khulna city are A, B and D. Soil group A contains sand, loamy sand most of which found in peat soil. Within this soil type it is possible to maximize groundwater recharge. Soil group B contains silt loam or loam. Soil group D contains clay and is found on the bank of river at the outer part of the city corporation area.

Table 5: Hydrologic Soil type of Khulna city.

HSG	Area (sq m)	Percentage (%)
A	28247600	62.33
B	14786500	32.63
D	2278970	5.02

(Source: Calculation has done by Arc GIS tools.)

3.2.3. Runoff Curve Number of Khulna City

Curve number was calculated to find out the soil retention in the process of estimating surface runoff. The higher the value of curve numbers the higher the value of surface runoff. The highest range of curve number is 100.

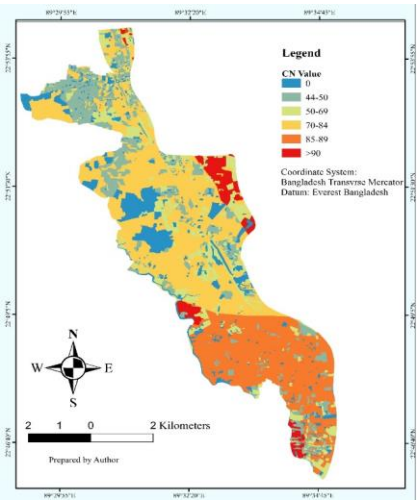

Figure 9: Curve Number Map (Source: Preparation on ArcGIS Environment)

Figure 9 shows the curve number map of Khulna city. Most of the area of the Khulna city has curve number around 70 to 85. This is because this area contain hydrologic soil group D which has highest runoff potential and also the topographic variation is noticeable here.

Table 6: Curve number and Surface retention value for different soil condition.

Soil Condition	AMC I	AMC II	AMC III
Curve Number	47.60	67.45	82.92
Surface Retention	279.5736	122.5662	52.33578

3.2.4. Monthly Surface Runoff of Khulna City

Using SCS-CN equation daily surface runoff was estimated for the year 2015. Surface runoff is highly related to the amount of precipitation. But the relation between precipitation and the surface runoff is a complex issue to evaluate. However, integration of Geographic information system with the traditional soil conservation service is proved very effective to find out the curve number in the process of runoff estimation. The relation between runoff and precipitation is shown in the figure 10 below,

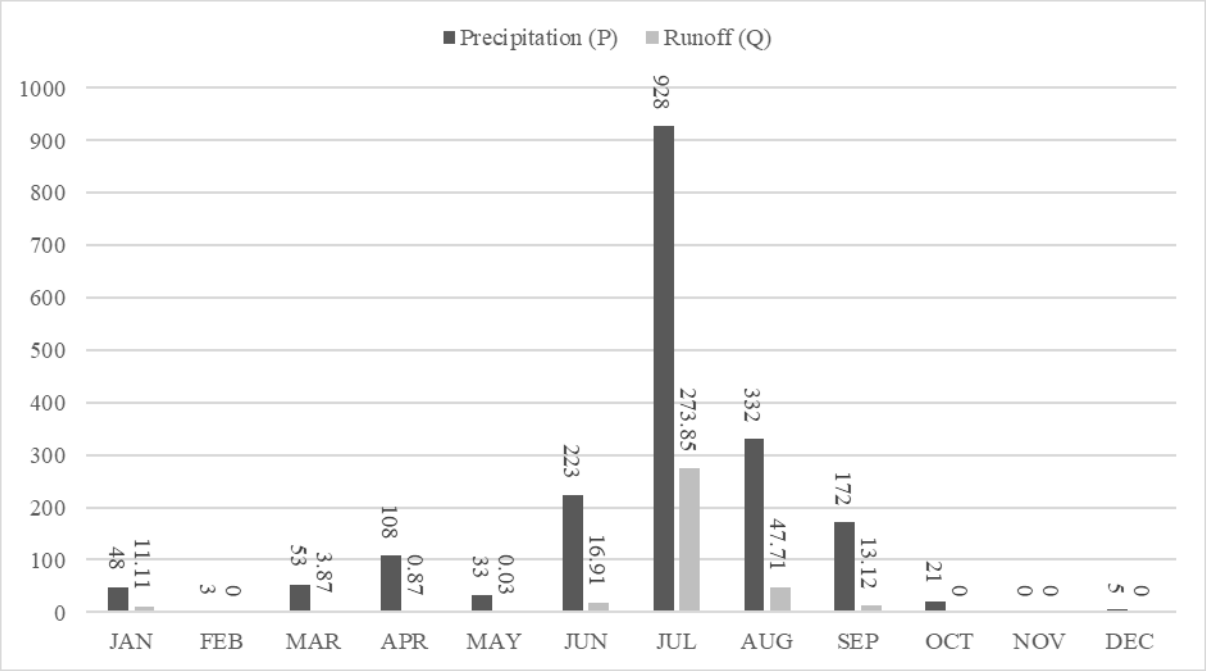

Figure 10: Surface runoff with respect to precipitation.

The total amount of runoff is 367.473753 (mm) in the respect of 1926 (mm) precipitation which is 19.08% of the total precipitation in the study year.

4. CONCLUSION

Runoff is the most imporant and the most challenging parts to estimate water cycle. It was observed that surface runoff is highly related with land use, topography and soil type. SCS-CN method was used with the integration of GIS for evaluating surface runoff. GIS technique is a very reliable alternative or a dependable support system to our conventional way of surveying, investigation, planning, monitoring, modelling, data storing and decision making process. However estimated surface runoff was about 19.08% of total precipitation. The volume of runoff can be used for the planning of land use and the careful management of soil, water and vegetation resources.

ACKNOWLEDGEMENT

All the praise to the almighty Allah, whose blessing and mercy succeeded us to complete this paper work fairly. We gratefully acknowledge the valuable suggestions, advice and sincere co-operation to express our heartiest and most sincere gratitude to a number of people who have helped us to complete this work. We would like to express our sincere appreciation to our friends for their insightful and valuable recommendations.

REFERENCES

Mishra, S. K., Sahu, R. K, Eldho, T. I., and Jain, M. K. 2006. An improved Ia-Srelation incorporating antecedent moisture in SCS-CN methodology. Water Resources Management, 20(5), 643-660. [Doi: 10.1007/s11269-005-9000-4]

Ahmad, I., Verma, V., & Verma, M. (2015). Application of Curve Number Method for Estimation of Runoff Potential in GIS Environment . 2015 2nd International Conference on Geological and Civil Engineering (pp. 16-20). India: IACSIT Press, Singapore.

SHADEED, S., & ALMASRI, M. (2010). Application of GIS-based SCS-CN method in West Bank catchments, Palestine . (pp. 1-13). Palestine: Water Science and Engineering.

Subramanya K (2013) Engineering Hydrology. Fourth Edition McGraw-Hill Education (India) Private Limited, New Delhi.

Gajbhiye, S. (2015). Estimation of Surface Runoff Using Remote Sensing and . International Journal of u- and e- Service, Science and Technology, 113-122.

Muthu, A. C., & M. Helen Santhi. (2015). Estimation of Surface Runoff Potential using SCS-CN Method Integrated with GIS. Indian Journal of Science and Technology, 1-5.

Topno, A., Singh A.K. , & Vaishya R.C. (2015). SCS CN Runoff Estimation for Vindhyachal Region using Remote . International Journal of Advanced Remote Sensing and GIS, 1214-1223.

(IWM), I. o. (2011). *TA 7385-BAN: Preparing the Khulna Water Supply Project* . Khulna.

Seth SM, Kumar Bhism, Thomas T, Jaiswal RK (1997) Rainfall-Runoff Modelling for Water Availability Study in Ken River Basin Using SCS-CN Model and Remote Sensing Approach. *Technical Reports, National Institute of Hydrology, Roorkee,* No. CS/AR-12/97-98.

Proceedings of the 5th International Conference on Civil Engineering for Sustainable Development (ICCESD 2020), 7~9 February 2020, KUET, Khulna, Bangladesh (ISBN-978-984-34-8764-3)

ASSESSMENT OF METEOROLOGICAL DROUGHT AND ANNUAL RAINFALL TRENDS OF DIFFERENT AREAS IN BANGLADESH

Rokshana Pervin*[1], Kalimur Rahman[1] and Ashraful Islam[1]

[1]Department of Civil Engineering,
Dhaka University of Engineering & Technology, Gazipur 1707, Bangladesh

***Corresponding Author**

ABSTRACT

In this assessment an effort has been set to calculate the condition of meteorological drought at different areas of Bangladesh by using Standardized Precipitation Index (SPI) method. For this investigation, the precipitation historical data of eight different rain gauge stations such as Dhaka, Sylhet, Mymensingh, Barisal, Chittagong, Rangpur, Khulna and Rajshahi areas were collected from Bangladesh Meteorological Department (BMD) over 30 years duration from 1988 to 2017. In Rajshahi area the meteorological drought was of nearly normal to severely dry, Barisal, Rangpur, and Mymensingh cities are nearly normal, Sylhet city moderately wet to extremely wet, Chittagong city nearly normal to severely wet, Dhaka and Khulna moderately dry to nearly normal over the last 30 years. It was found from the study that the northwest part (Rajshahi city) is the maximum drought prone and least annual rainfall area in the country. Also, It was established that Chittagong and Sylhet areas are the minimum drought prone area among all. By the rainfall trends analysis, it was visible that Khulna and Chittaging areas rainfall tends are increasing and remaining areas are declining.

Keywords: *Meteorological drought, Rainfall trends, Standard precipitation index.*

1. INTRODUCTION

Usually, Drought is a natural hazard due to scarcity of water in the soil for long period. This deficiency marks in a water inadequacy for various activities such as climatic influences the rising temperature, high wind and low relative humidity are responsible for drought. Drought is an interim of period, normally give privilege of months of years in a time, during which the genuine moisture supply of a definite place rather gradually reductions of the climatically anticipated or climatically appropriate moisture supply (Palmer, 1965). Overall, drought may be classified as meteorological, agricultural or hydrological depending on the intensity, duration and spatial coverage (World Meteorological Organization, 2012). Drought is a consistent climatic phenomenon which occurs in different parts of the world, with changing frequency, severity and time (Wilhite, 1993; Shatanawi et al., 2013). It is difficult to determine the beginning and ending of a drought. It develops slowly, and its impact may remain for years after end of the event (Morid et al., 2006).

Typically, in Bangladesh, drought happens once in each 2.5 years (Adnan, 1993; Hossain, 1990). In the year from 1960 and 1991, nineteen droughts occured at several areas inside Bangladesh (Mirza and Paul.1992). The key reason of drough in Bangladesh includes insufficient water accessibility due to not as much of rainfall than the amount required for crop production. It is important to note that Bangladesh is a country which is vulnerable to the impacts of climate change due to its geographical location (Mondol et al., 2017).

The current study intended to assess the trends of annual rainfall as well as meteorological drought at different areas in Bangladesh from the year 1988 to 2017.

2. Study Area

For this study, the obtainable data containing daily entire rainfall of eight different rain gauge stations in Bangladesh was collected from the Bangladesh Meteorological Department (BMD) for the year 1988 to 2017. The rain gauge stations at different areas of Bangladesh shown in Figure 1.

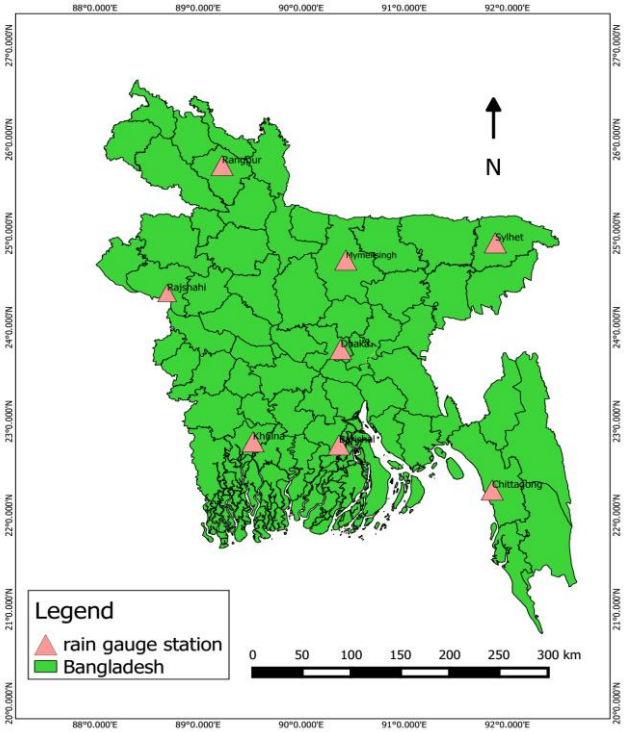

Figure 1: GIS map showing different rain gauge stations in Bangladesh.

2.1 Standardized Precipitation Index (SPI) and Meteorological Drought

The SPI was advised by (McKee et al., 1993) and has been used commonly throughout the past two decades (Hirschi et al., 2011; Vicente-Serrano et al., 2015). SPI is a extensive meteorological drought index that is merely recognized on rainfall data. Additional significant advantage is its suppleness in quantity of the drought for different time measures. In scheming of the standardized precipitation series, only the arithmetic average of the rainfall series and the standard deviation are needed. Standardized precipitation series for any x_1, x_2,… x_n precipitation time series, SPI value, is calculated using Eq. 1.

$$SPI = \frac{x_i - x_m}{S_x} \quad (1)$$

Where, x_i is precipitation record of the station; x_m is the arithmetic average of rainfall; and S_x is the standard deviation.

$$\boldsymbol{Sx} = \sqrt{\frac{\sum_{i=1}^{n}(x-\bar{x})^2}{n-1}} \quad (2)$$

SPI values are figured for each station on seasonally and annually time scales. Database is made for SPI consequences from 1988-2017 as exposed in Table 2. The SPI values and equivalent drought severity indices are shown in Table 1.

Table 1. The SPI ordering system according to McKee *et al*. 1993.

SPI value	Category
2.00 or more	Extremely wet
1.50 to 1.99	Severely wet
1.00 to 1.49	Moderately wet
−0.99 to 0.99	Near normal
−1.00 to −1.49	Moderately dry
−1.49 to −1.99	Severely dry
−2.00 or less	Extremely dry

3. RESULTS AND DISCUSSIONS

Figure 2 represents the trends of annual total rainfall for the study time of 30 years in different areas in Bangladesh. From this figure it can seen that the maximum rainfall occurs in Sylhet and the minimum rainfall occurs in Rajshahi city. A linear declining trends are detected for all considered raingauge stations excluding Chittagong and Khulna in the year 1988 to 2017. In Chittagong and Khulna stations, the trend line mounting upward that refers that rainfall at Chittagong and Khulna areas are increasing with time.

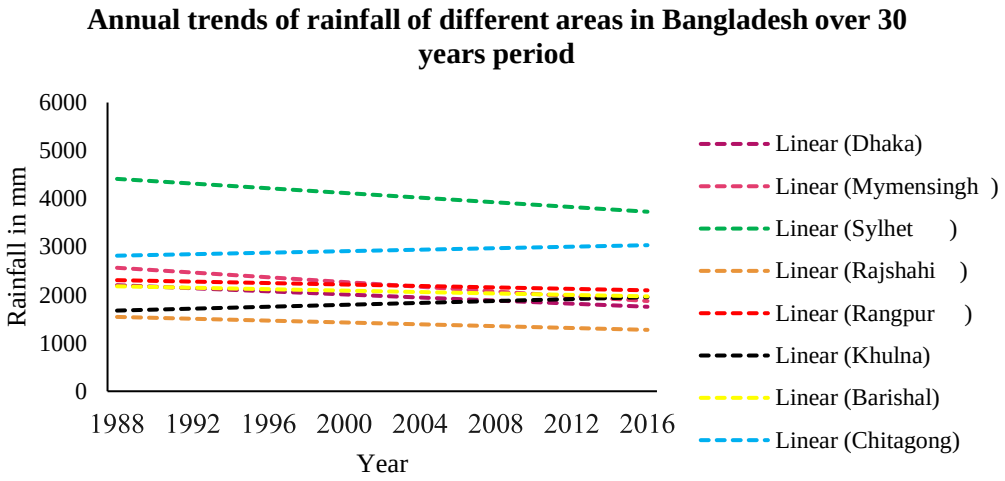

Figure 2: Annual rainfall trend lines for the studied raingauge stations in Bangladesh.

The maximum, minimum and average annual rainfall in all the area is within the last 30 years is given the figures 3 & 4, from this figures it is shown that the maximum precipitation occurs in Sylhet is in 2017 of almost six thousand millimeter (5944 mm) that means in year 2017, no chance to occurs drought in that region. The minimum rainfall occurs in Rajshahi is 792 mm in the year of 2010 which is exact less than the average value of 1412 mm. refers that the most drought occurs in Rajshahi is in 2010. The minimum rainfall occurred in Dhaka and Barisal in year 1992 and the minimum rainfall occurred in Rangpur, Khulna and Chittagong occurred in year 1994 that means the maximum drought occurred in that time in Bangladesh.

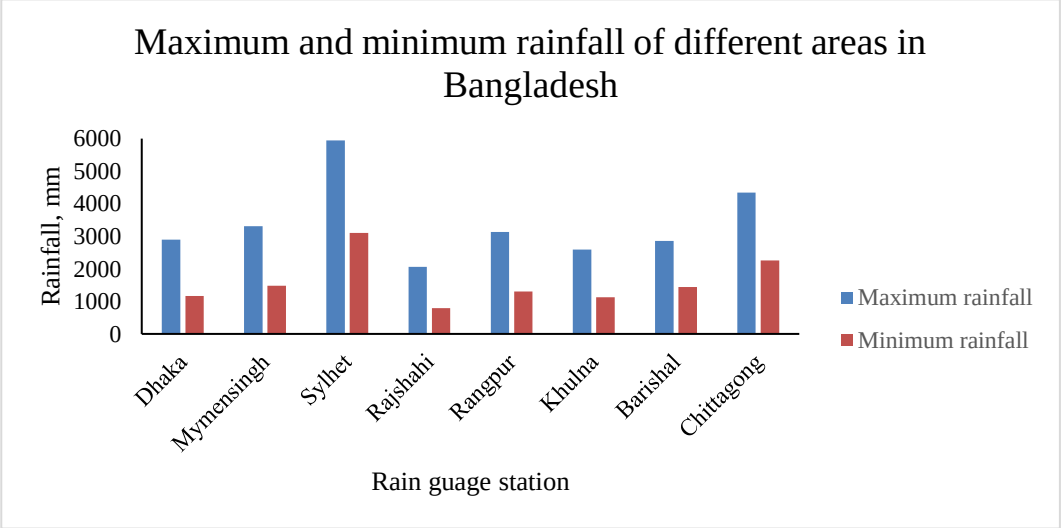

Figure 3. Annual maximum and minimum for the different raingauge stations in Bangladesh

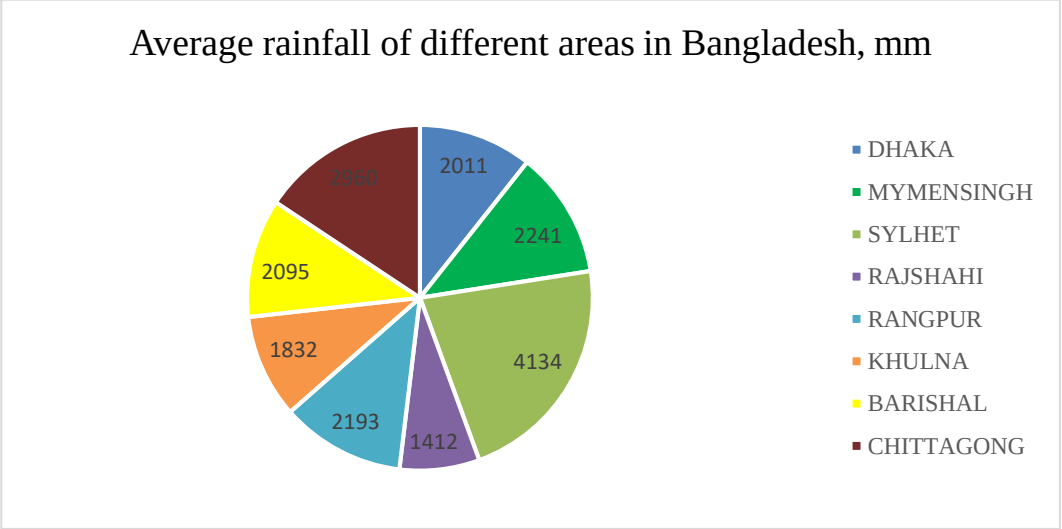

Figure 4: Annual average rainfall for the different raingauge stations in Bangladesh

Meteorological drought hazard detected by SPI during selected years of 1988 to 2017. From Table 2 SPI value can be easily observed that all five station except Sylhet, Rajshahi and Chittagong are as normal as SPI value within the normal range of -0.99 to 0.99. SPI value of Sylhet station is inside the value of 1.37 to 2.26 which references that the Sylhet city is in extremely wet or moderately wet condition in last 30 years. In Chittagong city the range of SPI value is within -0.2 to 1.56 which appears most of the year within that 30 years is in normal condition but several of few years are in moderately wet situation of the years are 1997 to 1998, 2007 to 2009, 2011, 2014 and 2015. In Rajshahi area the SPI value range is -1.55 to -0.70 that means the condition of Rajshahi is in severely dry to near normal condition in last 30 years.

Table 2: From the year 1988 to 2017 SPI values of different rain gauge stations in Bangladesh.

Year	Dhaka	Mymensingh	Sylhet	Rajshahi	Rangpur	Khulna	Barisal	Chittagong
1988	-0.312	0.278	2.232	**-1.040**	-0.278	-0.739	-0.326	0.184
1989	-0.519	-0.031	2.342	-0.746	-0.329	-0.688	-0.242	0.213
1990	-0.540	-0.125	2.243	-0.956	-0.065	-0.744	-0.200	0.386
1991	0.132	0.599	1.924	**-1.237**	-0.463	-0.972	-0.332	0.349
1992	-0.694	-0.203	2.073	**-1.080**	0.298	-0.636	-0.374	0.616
1993	-0.045	0.373	1.983	**-1.315**	-0.373	-0.831	-0.314	0.521
1994	-0.308	-0.228	2.193	-0.807	-0.607	-0.822	-0.012	0.591
1995	-0.840	0.385	2.068	**-1.277**	0.133	-0.435	-0.145	0.110
1996	-0.110	-0.580	2.073	-0.968	-0.154	-0.745	-0.359	0.843
1997	-0.594	-0.130	1.996	-0.347	-0.483	-0.713	-0.799	1.071
1998	-0.413	-0.374	1.762	**-1.219**	-0.355	-0.743	0.161	1.181
19999	-0.121	-0.431	1.366	-0.914	0.742	**-1.150**	-0.770	1.278
2000	-0.181	-0.108	2.153	-0.705	-0.653	-0.643	-0.629	0.766
2001	-0.702	-0.293	2.032	**-1.154**	0.535	-0.778	0.134	0.225
2002	**-1.060**	-0.169	1.648	**-1.549**	0.802	0.057	-0.023	0.295
2003	-0.599	-0.432	1.996	-0.990	0.388	-0.704	-0.457	0.798
2004	-0.368	-0.175	2.167	**-1.109**	0.073	-0.856	-0.127	0.395

2005	0.169	0.211	2.022	**-1.328**	0.431	-0.627	-0.674	-0.203
2006	-0.241	-0.179	2.115	**-1.376**	-0.588	-0.033	-0.125	0.427
2007	0.073	-0.027	1.494	**-1.126**	-0.755	-0.683	-0.471	1.496
2008	-0.004	0.026	1.532	**-1.226**	-0.424	-0.845	-0.482	1.422
2009	-0.240	-0.596	1.557	**-1.417**	0.139	-0.406	-0.387	1.349
2010	-0.469	-0.011	2.263	**-1.054**	-0.006	-0.602	-0.358	0.236
2011	-0.658	-0.049	1.517	**-1.153**	-0.402	-0.376	-0.440	1.561
2012	-0.665	-0.539	2.077	-0.803	-0.207	-0.401	-0.424	0.962
2013	-0.735	-0.501	2.166	**-1.129**	-0.275	-0.086	0.243	0.317
2014	-0.655	-0.019	1.692	-0.906	-0.375	-0.582	-0.590	1.435
2015	-0.481	-0.561	1.808	**-1.205**	-0.237	-0.334	-0.221	1.231
2016	-0.972	-0.311	2.239	-0.961	-0.095	-0.033	0.108	0.024
2017	-0.066	-0.101	2.109	**-1.081**	-0.778	-0.497	-0.257	0.671

From figure 5, it was seen that maximum times drought occured in Rajshahi area and others area are not remarkable.

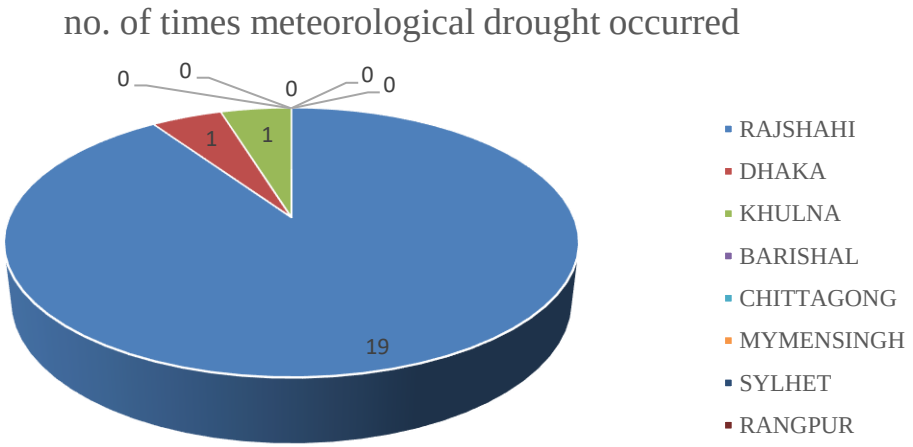

Figure 5. No. of times meteorological drought occurred of different raingauge stations in Bangladesh

4. CONCLUSIONS

The main objective of the study was to assess on the rainfall trends at different rain gauge stations of Bangladesh during the last 30 years and identify meteorological drought by Standardized Precipitation Index (SPI) method. From the investigation it is marked that the maximum precipitation occurred in Sylhet and the minimum precipitation occurred in Rajshahi city in the last 30 years (1988 to 2017). In Chittagong and Khulna areas annual rainfall are increasing and others areas are decreasing with time. In Rajshahi area annual drought occurred 19 times, whereas moderately drought occurred 18 times and severe drought occurred once in last 30 years. In Dhaka and Khulna regions drought occurred only once and for other regions, drought was insignificant.

ACKNOWLEDGEMENTS

Authors are thankful to the Bangladesh Meteorological Department (BMD) for providing the needed meteorological data.

REFERENCES

Adnan, S. (1993). Living Without Floods: Lessons from the Drought of 1992". Research and Advisory Services, Dhaka.

Hossain, M. (1990). Natural Calamities, Instability in Production and Food Policy in Bangladesh. Bangladesh Institute of Development Studies, Vol. 18(1).

Hirschi, M., Seneviratne, S.I., Alexandrov, V., Boberg, F., Boroneant, C., Christensen, O.B., & Stepanek, P. (2011). Observational evidence for soil-moisture impact on hot extremes in south eastern Europe. Nature Geoscience, Vol. 4 No. 1, pp. 17-21.

Mirza, M. Q., & Paul, S. (1992). Prakritik Durgojob O Bangladesh Paribesh (Natural Disaster and Environment in Bangladesh), Center for Environment Studies and Research, Dhaka.

McKee, T. B., Doesken, N. J., & Kleist, J. (1993). The relationship of drought frequency and duration to time scales. Preprints, 8th Conference on Applied Climatology, January 17–22, Anaheim, California.

Mondol, M.A., Ara, I., & Das, S. C. (2017). Meteorological Drought Index Mapping in Bangladesh Using Standardized Precipitation Index during 1981–2010. Advances in Meteorology, Hindawi Publishing Corporation, Cairo, Egypt.

Morid, S., Smakhtinb, V., & Moghaddasi, M. (2006). Comparison of seven meteorological indices for drought monitoring in iran. International Journal of Climatology, Vol. 26 No. 7, pp. 971-985, doi: 10.1002/joc.1264.

Palmer, W. C. (1965). Meteorological Droughts. Research paper No. 45, U. S. Weather Bureau, Washington, D. C., USA.

Shatanawi, K., Rahbeh, M., & Shatanawi, M. (2013). Characterizing, monitoring and forecasting of drought in Jordan river basin. Journal of Water Resource and Protection, Vol. 5 No. 12, pp. 1192-1202

Szinell, C.S., Bussay, A., & Szentimrey, T. (1998). Drought tendencies in Hungary", International Journal of Climatology, Vol. 24, pp. 1441-1460, doi: 10.1002/(SICI)1097-0088(199804)18:5.

Vicente-Serrano, S.M., Chura, O., López-Moreno, J.I., Azorin-Molina, C., Sánchez-Lorenzo, A., Aguilar, E., & Nieto, J.J. (2015). Spatio-temporal variability of droughts in Bolivia: 1955-2012. International Journal of Climatology, Vol. 35 No. 10, pp. 3024- 3040, doi: 10.1002/joc.4190.

Wilhite, D.A. (1993). Drought assessment, management, and planning: theory and case studies. Natural Resource Management and Policy Series, Vol. 2, Kluwer.

World Meteorological Organization (2012). Standardized Precipitation Index User Guide (M.Svoboda, M. Hayes and D. Wood, Eds). (WMO-No. 1090), Geneva, Switzerland.

Proceedings of the 5th International Conference on Civil Engineering for Sustainable Development (ICCESD 2020), 7~9 February 2020, KUET, Khulna, Bangladesh (ISBN-978-984-34-8764-3)

FLOOD INUNDATION MAPPING OF MAJOR RIVERS OF BANGLADESH USING HEC-RAS 2D

Md. Mukdiul Islam*[1] and Md. Ataur Rahman[2]

[1]*Lecturer, Chittagong University of Engineering & Technology, Bangladesh, e-mail: mukdiul1808@gmail.com*
[2]*Professor, Bangladesh University of Engineering & Technology, Bangladesh, e-mail: mataur@wre.buet.ac.bd*

***Corresponding Author**

ABSTRACT

Bangladesh lies at the downstream of GBM basin which is susceptible to large amount of precipitation resulting large amount of water to be drained out through Bangladesh each year. This draining water along with various other reasons causes frequent flooding with severe damage all over Bangladesh. Therefore, a mathematical model has been developed under this study, which is capable of simulating flood inundation area of the major rivers of Bangladesh and their associated flood plains. The study area has been selected based on the major rivers such as Ganges, Jamuna, Padma and Meghna of Bangladesh with the associated flood plains. For the analysis, two-dimensional hydrodynamic model software HEC-RAS 2D has been used. Bathymetry grid has been prepared using bathymetry data of the rivers collected from Institute of Water Modelling (IWM). DEM of the floodplain with resolution 30.87 m has been collected from USGS. Hydrographic data has been collected from BWDB. Combined bathymetry and topography grid have been prepared using ArcMap software. HEC-RAS 2D model has been set up based on the combined bathymetry and topography grid data of the study area and necessary boundary conditions. The calibration and validation of the model have been done against measured water level at Sengram (Ganges), Sirajganj (Jamuna), Mawa (Padma) and against measured discharge at Mawa (Padma). A flood inundation map for August 2, 2016, has been prepared based on the model simulation results and compared quantitively with the flood inundation map of that day prepared by Flood Forecasting and Warning Center (FFWC) of Bangladesh based on actual inundation data. The comparison shows good agreement of model simulated flood inundation area with that prepared by FFWC. Different flood parameters such as depth, arrival time etc. have been analyzed for the year of 2014 using the model simulated results. Manikganj district was the most flood affected district based on area of inundation with a percent of inundation 47.73 on 27 August 2014 is obtained from the inundation map prepared by model simulation.

Keywords: *Flood, HEC-RAS 2D, Inundation map.*

1. INTRODUCTION

Bangladesh is prone to flooding due to its location at the downstream of the GBM (Ganges-Brahmaputra-Meghna) river basin. The Ganges-Brahmaputra-Meghna (GBM) basin is approximately 1.6 million km2 and crosses five national boundaries: India, China, Nepal, Bhutan, and Bangladesh. The combined discharge of the GBM basin drains through Ganges, Brahmaputra and Meghna rivers and finally reaches the Bay of Benga (Curtis et al., 2017). Again heavy rainfall in the monsoon period is also responsible for floods in Bangladesh. Bangladesh is blessed with rivers. Padma, Meghna, and Jamuna are the major rivers of Bangladesh. The country Bangladesh is occupied with a network of about 405 rivers mostly alluvial in nature, spreading all over the country out of which 57 are transboundary (Pal et al., 2017). This low-lying country is an alluvial delta, and therefore, is extremely prone to flooding. It is one of the most susceptible countries to flood disasters. Flood occurs mainly during the monsoon season from June to September. The main causes of floods in Bangladesh are heavy rainfall in monsoon, snowmelt from the Himalayas, enormous upstream discharge and siltation of the river.

Flood Inundation Mapping is an important tool for engineers, planners, and the government agencies used for emergency action plans, flood risk assessment (economic, environmental, social, cultural and mankind). Flood inundation mapping provides important information like depth, and spatial extent of flooded zones, required by the authorities to inform the citizens about the major flood-prone areas and to adopt appropriate flood management strategies.

The Hydrologic Engineering Centre's River Analysis System (HEC-RAS) is a software package that is of great use for developing flood inundation map. An HEC-RAS model can be used for both steady and unsteady flows and supercritical flow regimes. Flood inundation mapping and analysis using HEC-RAS (2D) provides effective and standard results and saves time and resources.

Sumaiya (2017) developed a two-dimensional hydrodynamic model using HEC-RAS 5.0.3 of Jamuna River. Mozumder (2017) developed a 1D-2D coupled hydrodynamic model using HEC-RAS 5.0.3 of the Teesta River.

1.1 Study Area

A map of the study area focusing the flood plain of the major rivers system (Ganges, Jamuna, Padma, upper Meghna and lower Meghna) of Bangladesh is shown in Figure 1.

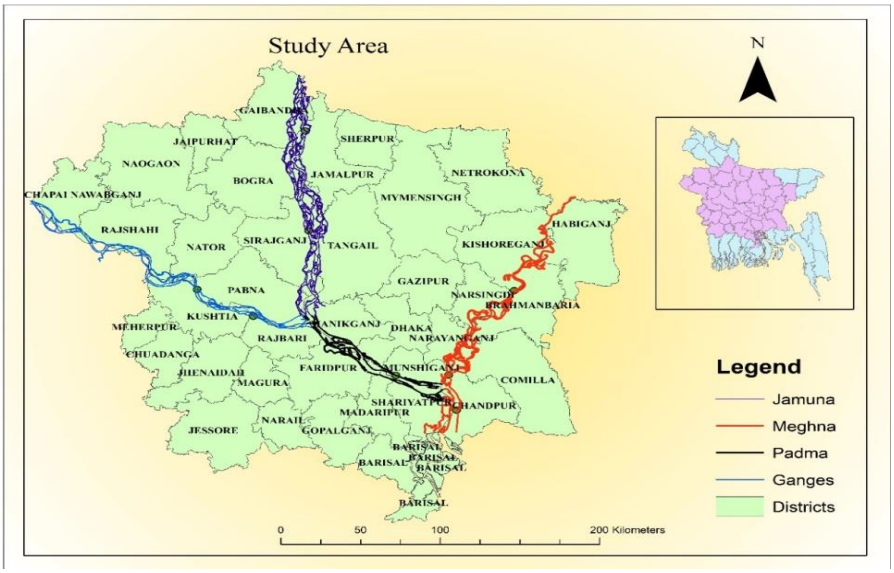

Figure 1: Map of the study area.

The Ganges is a transboundary river with a total length of 2,525 km (Mujiburrehman, 2015). The river rises in the western Himalaya basin the Indian state of Uttarakhand and flows south and east through the Gangetic Plain of North India into Bangladesh, where it empties into the Bay of Bengal. The Padma is the main distributary of the Ganges. It starts from the confluence of Jamuna and Ganges river and flows for 120 km. From the confluence of upper Meghna and Padma near Chandpur the river lower Meghna starts. The Brahmaputra-Jamuna is originated in the Himalayas, flowing through China, India and entering Bangladesh through the northern boundary. The Brahmaputra-Jamuna river has a basin area of approximately 1330 km^2 within Bangladesh (Rahman, 2015).

1.2 Data Collection

The collected data includes geometric data like river bathymetry, hydrologic data like discharge, water level and digital elevation model (DEM) as land topographic data. These data are collected from different sources. Table 1 represents the data collected for this study with their source and period.

Table 1: Collected data for this study with their source and period.

Data Type	Location	Data Source	BWDB Station Id	Period
DEM	Bangladesh	USGS	-	2014
Bathymetry Data at Rivers (x,y,z)	Ganges	IWM	-	2017
	Padma	IWM	-	2017
	Jamuna	IWM	-	2017
	Upper Meghna	IWM	-	2017
Discharge	Hardinge Bridge (Pakshi)	BWDB	SW90	2000-2017
	Bahadurabad	BWDB	SW46.9L	2000-2017
	Mawa	BWDB	SW93.5L	2000-2012
	Bhairabbazar	BWDB	SW273	2000-2017
	Chandpur	BWDB	SW277	2000-2017
Water Level	Sengram	BWDB	SW91.1	2000-2012
	Mawa	BWDB	SW93.5L	2000-2012
	Sirajganj	BWDB	SW49	2000-2012
	Badyar Bazar	BWDB	SW275	2000-2012
Flood Map	Bangladesh	FFWC	-	-

2. METHODOLOGY

Figure 2 represents a schematic diagram of the overall steps in the methodology of this study.

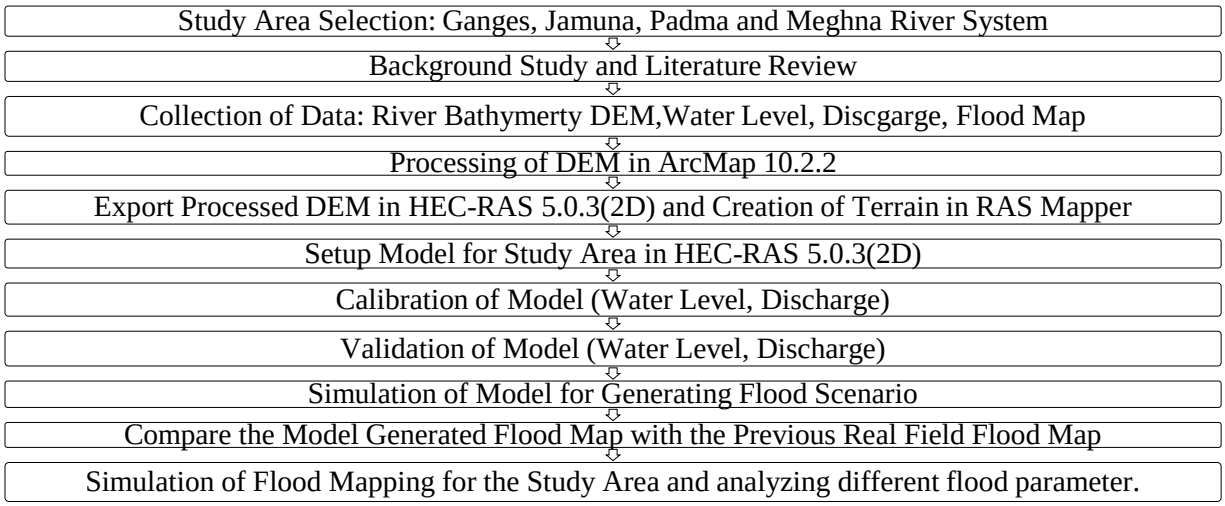

Figure 2: Schematic diagram of the overall steps in the methodology

To develop flood inundation map, the bathymetry data of the Ganges, Jamuna, Padma, Upper Meghna & Lower Meghna are processed in ArcMap. The processed bathymetry data are superimposed on the Digital Elevation Model of the study area to create a combined bathymetry & topography model. This model is exported to Ras-Mapper of HEC-RAS, the grid size is selected as 500m×500m. Assigning the boundary condition the model is simulated for unsteady flow. Flow hydrograph has been used as boundary condition at Hardinge Bridge(The Ganges), Bahadurabd (The Jamuna) & Badyarbazar (The upper Meghna). Stage hydrograph has been used as boundary condition at Chandpur (The lower Meghna). The model is then calibrated and validated at different locations against both discharge and water level. Finally, the calibrated and validated model is used to prepare flood inundation map using both HEC-RAS & ArcMap. Different flood parameters have been analyzed then using ArcMap.

3. ANALYSIS & RESULTS

3.1 Calibration & Validation of the model

The model has been calibrated against water level for the year of 2005 at different stations such as Sengram at the Ganges, Sirajganj at the Jamuna, Mawa at the Padma and Badyar Bazar at the Meghna. Table 2 represents the values of manning's roughness values at different river channels used for calibration and validation of the model.

Table 2: Calibrated values of manning's roughness value at different rivers.

River Name	Manning's roughness value
Jamuna	0.03
Ganges	0.027
Padma	0.025
Upper Meghna	0.03

Figure 3(a) and (b) show the calibration curve against water level at Sirajganj of Jamuna river & Badyar Bazar of Upper Meghna River respectively.

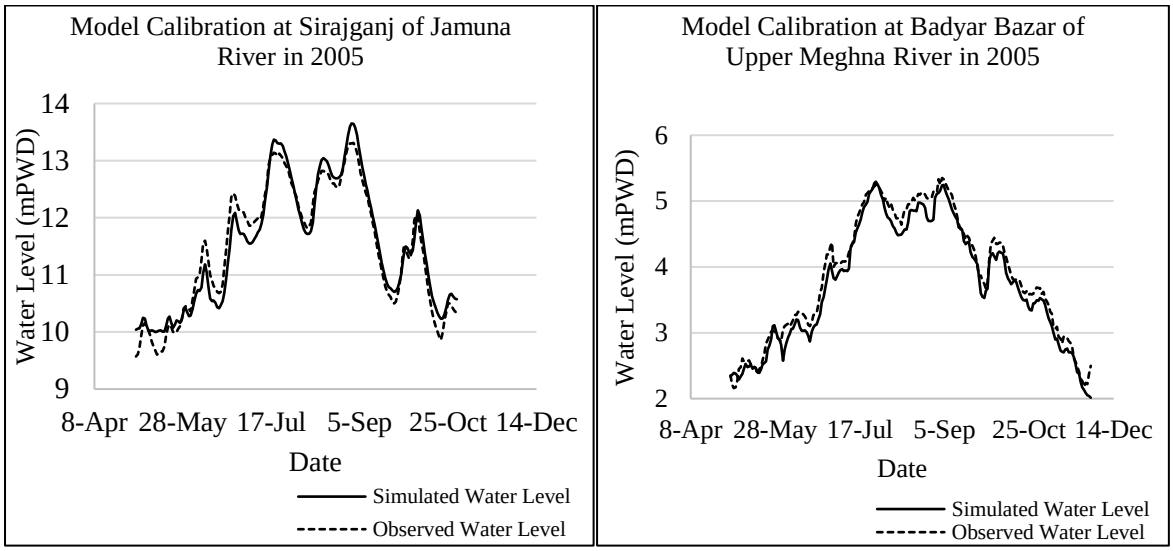

(a) (b)

Figure 3: (a) Model calibration at Sirajganj & (b) Model calibration at Badyar Bazar

The model has been also calibrated against discharge in Mawa at the Padma for the year of 2005. Figure 4 shows the calibration of the model against discharge at Mawa of Padma river in 2005.

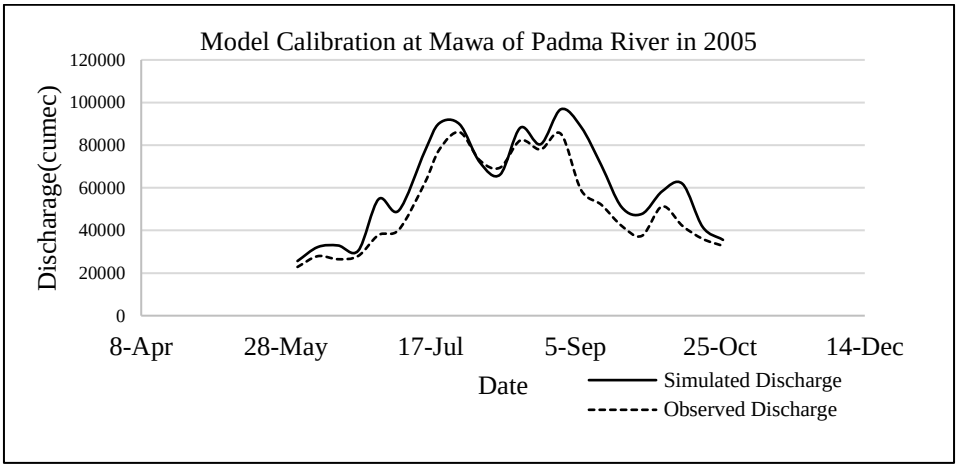

Figure 4: Calibration of the model against discharge at Mawa of the Padma river in 2005.

Figure 5 (a) & (b) represent the validation of the model against water level at Sirajganj of the Jamuna river in 2006 and against discharge at Mawa of the Padma river in 2006 respectively.

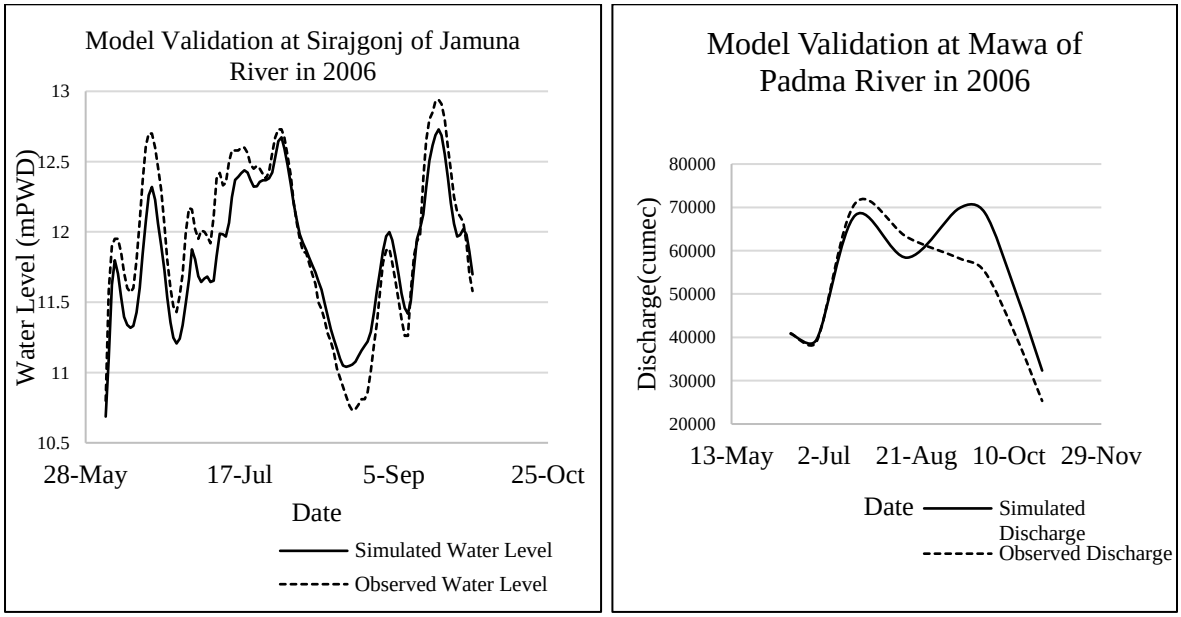

(a) (b)

Figure 5: (a) Model validation at sirajganj & (b) Model validation at Mawa.

3.2 Model Performance Evaluation for Calibration

Figure 6 (a) & (b) represent model generated water level vs observed water level at Sengram of the Ganges river in 2005 & model generated water level vs observed water level at Badyar bazar of Upper Meghna river in 2005. The correlation coefficient is obtained as 0.952 & 0.993 respectively.

3.3 Inundation Map

Inundation map gives an idea about which area are most vulnerable to flooding. Inundation maps are generated using both HEC-RAS and ArcMap. In this study inundation maps have been created for the year of 2014 & 2016.

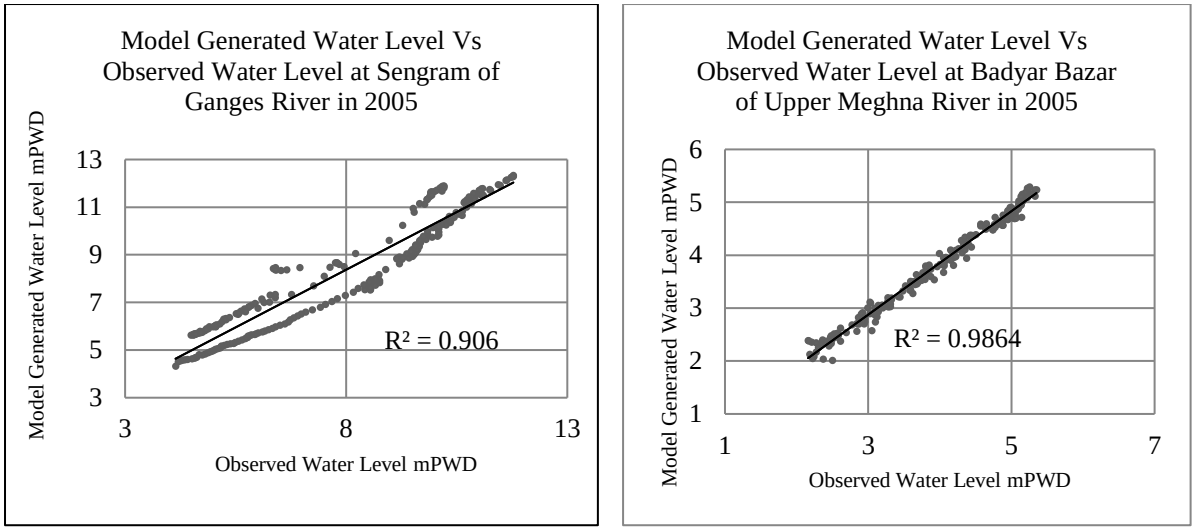

Figure 6: (a) Correlation at Sengram in 2005 & (b) Correlation at Badyar bazar in 2005.

Figure 7 (a) & (b) represent model generated flood inundation map and flood inundation map prepared by FFWC on 2 August,2016.

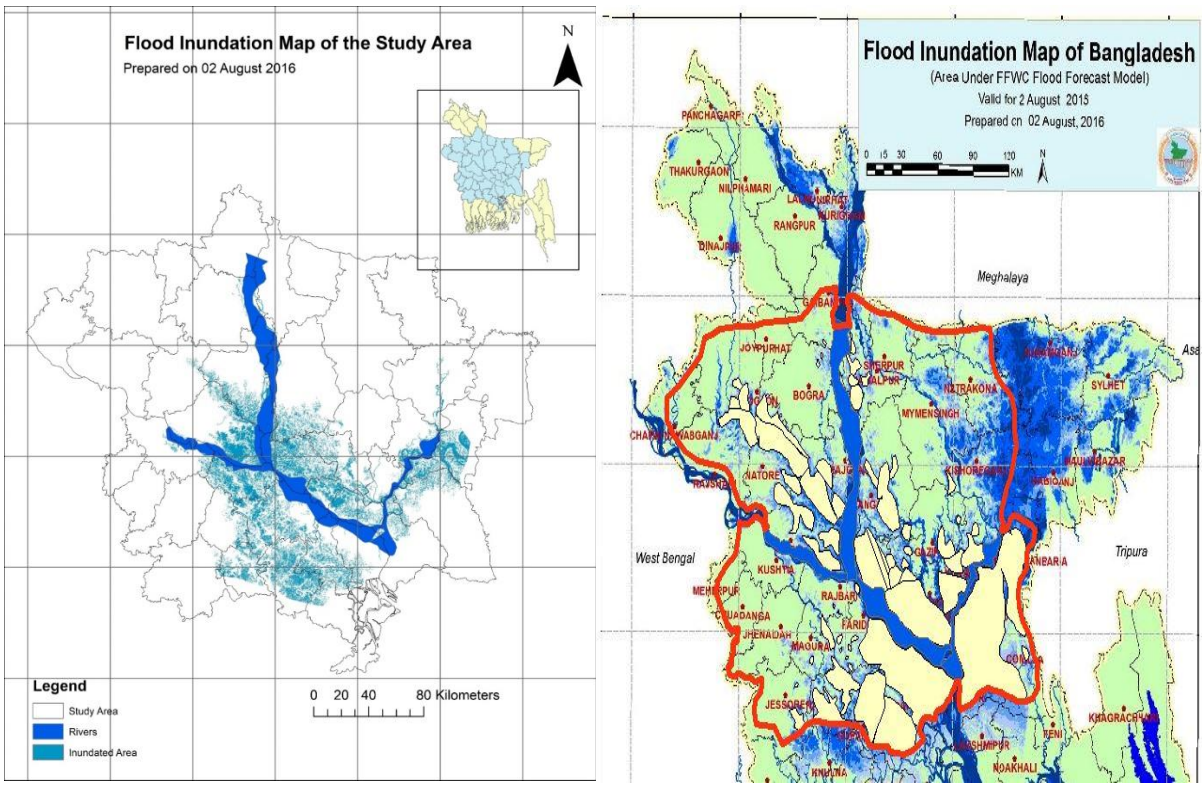

(a) (b)

Figure7: (a) Model generated flood inundation map & (b) FFWC flood inundation map.

Flood inundation map prepared by FFWC has been digitized to compare on the basis of inundated area with the model generated flood inundation map. Figure 8 represents the comparison on the basis of inundated area between the inundation map prepared by FFWC and model generated inundation map.

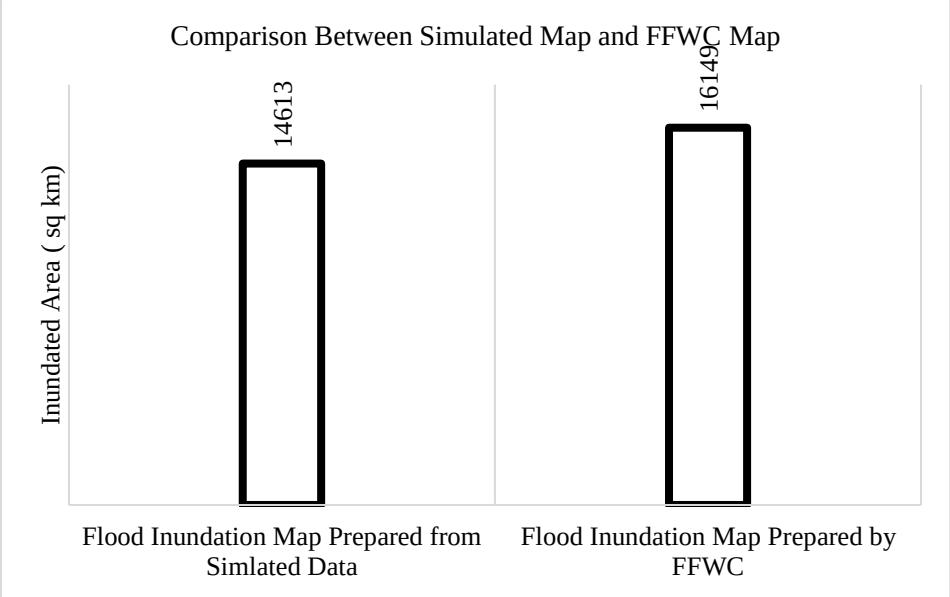

Figure 8: Comparison between simulated map & FFWC map on the basis of area of inundation.

3.4 Analysis of Different Flood Parameters for the Flood of 2014

3.4.1 Flood Arrival Time

Arrival time indicates the time required for the flood water to rise above threshold depth (0.1m) from the beginning of the simulation. Figure 9 represents the flood arrival time map for the year of 2014.

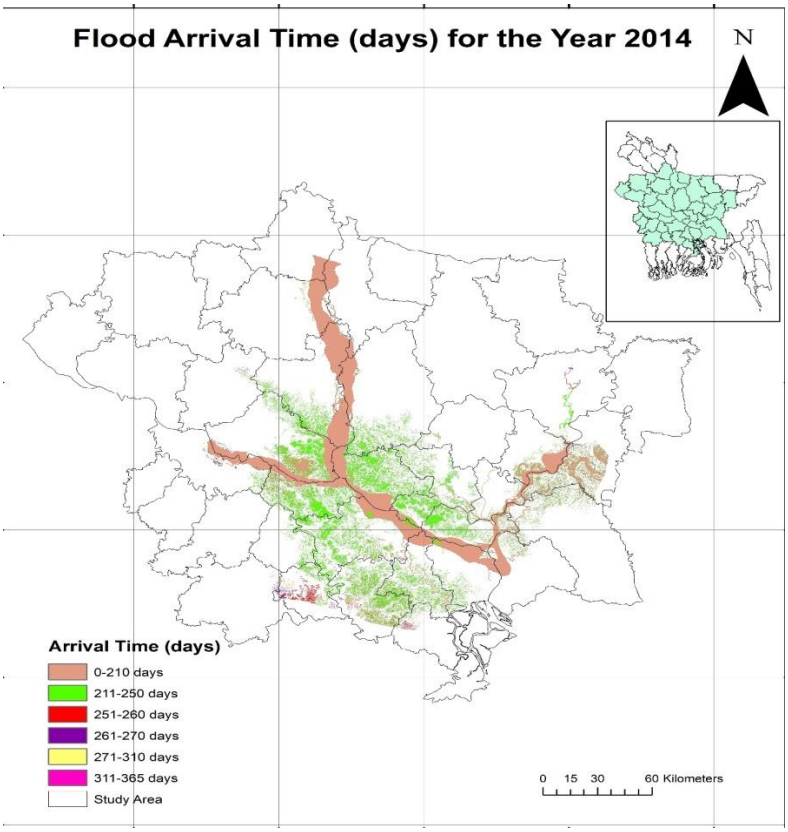

Figure 9: Flood arrival time (days) map for the year 2014.

It is seen that flood arrival time for most part of the study area is about 211-250 days, which means that the time required to rise the flood depth above the threshold depth (0.1m) is 211-250 days. So flood water will enter most part of the study area during 30th July to 7th September.

3.4.2 Date-wise Inundated Area

Table 3 represents date-wise total inundated area.

Table 3: Date-wise inundated area.

Date	Inundated Area (sq km)
16 June 2014	3176.124
27 August 2014	6149.132
17 September 2014	5486.849

3.4.3 District-wise Inundated Area & Percentage of Inundation

Table 4 represents district-wise inundated area and percentage of inundation.

Table 4: District-wise inundated area and percentage of inundation.

District Name	Inundated Area (sq km)	Percent Inundation
Narayanganj	89.58	11.49
Narshingdi	235.44	20.24
Pabna	717.38	29.76
Sirajganj	750.08	30.85
Tangail	345.81	10.03
Bogra	280.21	9.64
Brahmanbaria	359.07	18.75
Comilla	108.51	3.46
Munshiganj	271.44	29.13
Manikganj	655.99	47.73
Madaripur	250.46	22.46
Kushtia	317.28	18.83
Faridpur	396.52	19.19
Dhaka	223.54	14.71

The study shows that the Manikganj district was mostly affected by the flood of 2014 according to the percentage of inundation.

3.4.4 Area of Inundation Based on Depth of Manikganj District.

Figure 10 represents area of inundation based on depth of Manikganj district on 27 August,2014. It is seen that about 332.06 km^2 area of the Manikganj district had a flood depth above 3.6m & about 733.514 km^2 area had a flood depth below 0.1m.

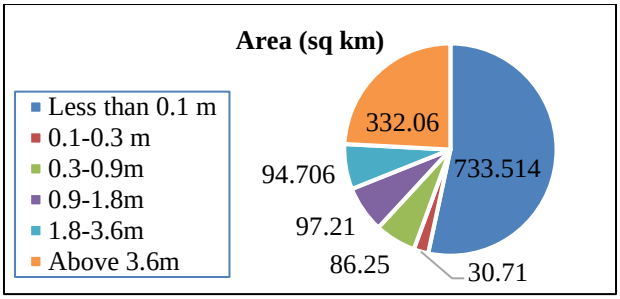

Figure 10: Area of inundation based on depth of Manikganj district on 27 August 2014.

4. CONCLUSIONS

In this study, HEC-RAS 2D has been used to prepare flood inundation maps of major rivers of Bangladesh including the Ganges, Padma, Jamuna, upper Meghna & lower Meghna rivers. Discharge and water level has been taken as the boundary condition. The model has been calibrated and validated with the help of iterating the calibration parameter Manning's roughness value 'n'. The verified model has been used to prepare flood inundation map of 02 August 2016 and has been compared with the flood inundation map prepared by Flood Forecasting and Warning Centre (FFWC). This comparison shows, the simulated flood map represents 90.4% of the inundated area represents in the map prepared by FFWC. Different flood parameters such as area of inundation, depth of inundation, arrival time etc. for the flood of 2016 has been analyzed. Area of inundation of the study area on 16 June 2014, 27 August 2014 and 17 September 2014 has been found as 3176.124 km^2, 6149.132 km^2, and 5486.849 km^2 respectively. On 02 August 2016 it has been found that the Manikjanj district was most affected according to area of inundation. A flood depth hazard map has been prepared for the Manikganj district and it has been found that almost 94.706 km^2 area had a water depth between 1.8m-3.6m.

This study shows the utility and effectiveness of using HEC-RAS 2D for the preparation of flood inundation map, identify the probable locations most affected by floodwater, depth of floodwater at different location and the time taken for flood water to rise above a threshold value which is of great use to reduce damage by flood to life and property.

ACKNOWLEDGEMENTS

Authors are gratefully acknowledging the deepest gratitude to Bangladesh Water development board (BWDB) and Institute of Water Modelling (IWM) for providing with the necessary data for conducting the study.-

REFERENCES

Curtis, S., Crawford, T., Munshi, K., & Paul, B. (2017). Monsoon Dynamics in the Ganges-Brahmaputra-Meghna Basin. In *The 1st Electronic Conference on Hydrological Cycle (CHyCle-2017)* (Vol. 1).

Pal, P. K., Rahman, A., & Yunus, A. (2017). Assessment of Morphodynamic Characteristics of Dudhkumar River Using Multi-temporal Satellite Images.

Mujiburrehman, K. (2015). Preparation of flood inundation map in Ganga River at Farakka Bridge, Malda, West Bengal, India. *Int J Res Geogr*, *1*(1), 1-17.

Rahman, M. (2015). Modeling flood inudation of the Jamuna river.

Sumaiya, U., (2017). "Flood inundation mapping of Jamuna River flood plain using HEC-RAS 2D", B.Sc. Engineering Thesis, Department of Water Resources Engineering, BUET.

Mozumder, T.R., (2017). "Study on Flood and its Management Along the Flood Plain on Teesta River", B.Sc. Engineering Thesis, Department of Water Resources Engineering, BUET.

Proceedings of the 5th International Conference on Civil Engineering for Sustainable Development (ICCESD 2020), 7~9 February 2020, KUET, Khulna, Bangladesh (ISBN-978-984-34-8764-3)

FLOW AUGMENTATION OF DHALESWARI RIVER USING AN UNSTEADY FLOW MODEL HEC-RAS

Md. Raiful Islam*[1] and Md. Abdul Matin[2]

[1]*Lecturer, Department of Water Resources Engineering, Bangladesh University of Engineering and Technology, Bangladesh, raiful.wre.buet@gmail.com*
[2]*Professor, Department of Water Resources Engineering, Bangladesh University of Engineering and Technology, Bangladesh, mamatin@wre.buet.ac.bd*

***Corresponding Author**

ABSTRACT

This study work has been conducted to assess the existing hydrodynamic condition of the Dhaleswari River and apply mathematical modeling for the hydrodynamic analyses for various dredging options. Dhaleswari River, one of the main distributaries of the Jamuna River, is the feeding River to the Buriganga-Turag-Balu-Shitalakshya river systems around Dhaka Metropolitan area. But the flow carrying capacity of the river has been reduced significantly over the past few decades. Because of gradual sedimentation, the conveyance capacities have been decreased causing no flow conditions during the dry season. Consequently, the navigational drafts have been reduced. In this situation, it will be impossible to recover the river water from its dying stage without augmenting the flow. Planed dredging works can be inevitable options to increase the carrying capacity of the river. Mathematical modeling analysis of the river can play an important role in the selection of suitable dredging options. The present study is based on the assessment of hydrodynamic analysis of Dhaleswari River by using a mathematical model namely HEC-RAS of version 5.0.7. The full length of the river is approximately 292 km. However, the present study covers a reach of 80 km starting from off-take Dhaleswari at Porabari to Savar. River cross-sections (RMD1 to RMD12), time series discharge data at the Tilli (SW 68), Water level data at Porabari (SW 50) and Jagir (SW 68.5) are collected from Bangladesh Water Development Board (BWDB) and Water Resources Planning Organizations (WARPO). The setup model has been successfully calibrated and validated against the data for the years 2016 and 2017 respectively. Computed water surface profile shows the least available water depth at different river stations range from 1.0 m to 1.1 m during the lean flow period. Therefore, navigation though the river at this period is a major challenge. To mitigate this issue, the hydrodynamic parameters of the river have been investigated based on dredging with the help of the channel modification module incorporated in HEC-RAS 5.0.7. Simulations have been performed with three different dredging sections that varied in base width, depth, and side slope. The simulated parameters are then compared before and after dredging to assess the functionality of each dredged bathymetry. The dredged section having a base width of 100 m, side slope of 1:5 and 1 m of average dredging depth shows the best hydrodynamic performance, specifically, the maximum flow augmentation. The first dredging strategy can be defined as the most efficient section with a velocity range of 0.41- 1.1 m/s. This study assessed only the hydrodynamic performance. However, morphological response to dredging is needed to investigate the overall stability of the river.

Keywords: *Flow augmentation, Dhaleswari river, Hydrodynamic, Mathematical model, Navigation, Dredging.*

1. INTRODUCTION

Bangladesh, the largest delta in the world, has been formed with sediment deposited by the three mighty rivers namely the Ganges, the Jamuna and the Meghna (GBM). These alluvial rivers are commonly featured with a lot of tributaries and distributaries (FAP24, 1996). The Dhaleshwari River (Figure 1) is one of the distributaries of the Jamuna River in central Bangladesh. It originates from the Jamuna River at the northwestern tip of Tangail District. Afterward, it split into two branches. The north branch retains the same name Dhaleshwari and merges with the Kaliganga River, the opposite branch at the southern a part of Manikganj District. This unified flow meets the Shitalakshya close to Narayanganj District and finally goes southward to merge into the Meghna River. The full length of the river is 292 km (BWDB, 2011). However, the length of the study reach is 80 km beginning from off-take Dhaleswari at Porabari to Savar (Figure 1). The flow rate of the river is very significant as the conveyance capacity of the Buriganga-Turag-Balu-Shitalakshya river systems is mainly depends on it (Khan, 2004). Therefore, the river route is expected to carry the necessary discharge through year-round (IWM, 2004). But the massive sediment coming from Jamuna River is eventually being deposited at the Dhaleswari offtake area as well as at the channel bed causing no flow conditions during the dry season. Consequently, navigational drafts have been reduced (Haque, 2018).

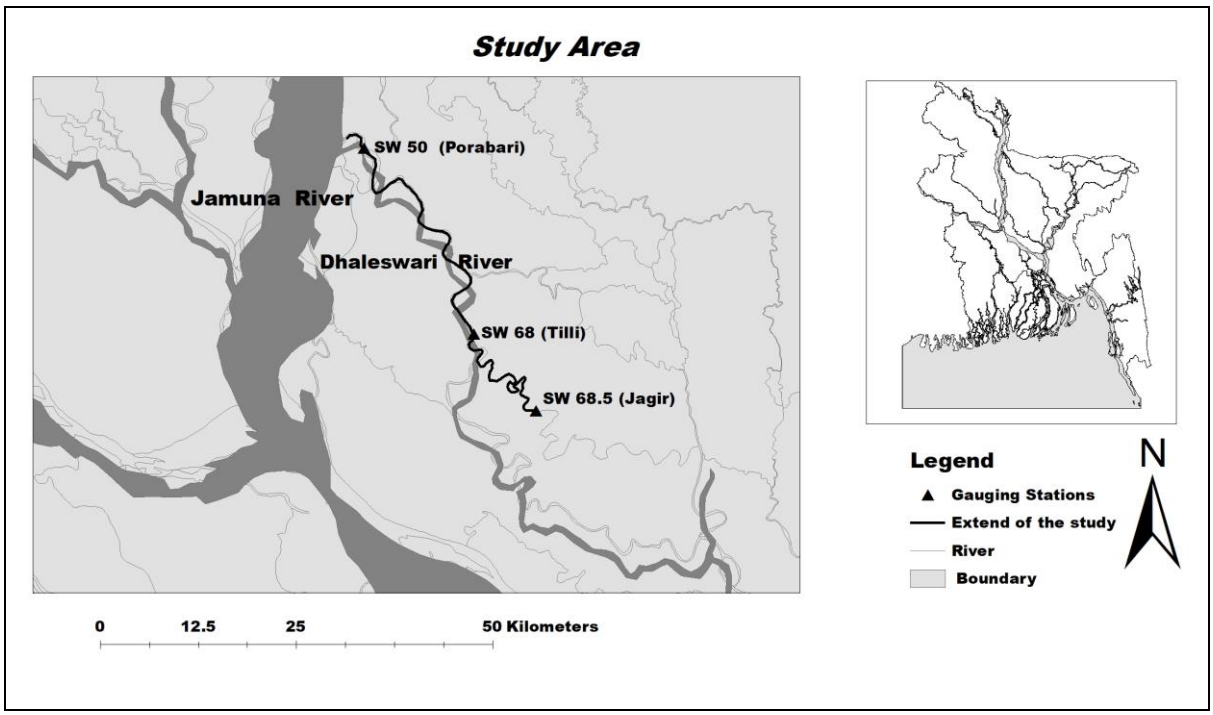

Figure 1: Map of the study area

Planed dredging works that involve the removal of bed materials can be inevitable options to increase the conveyance capacity and hence augmenting the river during the dry period (Paarlberg et al., 2015). Several studies have been made in this regard. Model studies are available indicating flow diversion at the Jamuna-Dhaleswari offtake. IWM (2004) had investigated the strategy for rehabilitating the Buriganga-Turag-Shitalakhya river system for flow augmentation. Still, further study is required to perform for a detailed understanding. The present study of the mathematical modeling aims to supplements the rehabilitation of the river system. In this regard, a one-dimensional numerical model (HEC-RAS 5.0.7) has been applied to perform one-dimensional unsteady flow calculations. HEC-RAS unsteady state simulation computes water surface from one cross-section to the next by solving the standard step iterative procedure to solve the St. Venant's equations of mass and momentum conservation (HEC RAS, 2010).

The present study is directed towards detail hydrodynamic analyses of the river using mathematical modeling with the recently collected flow, water level, and bathymetric data. Three different channel modifications have been made as a part of a solution of flow augmentation. Finally, hydrodynamic parameters including velocity and water level were compared before and after dredging and portrayed in the graphs and charts.

2. METHODOLOGY

The methodology of the study covers data collection, setting up a model of 80 km river reach of the upper Dhaleswari. Cross-section data (RMD1 – RMD12), time series discharge data at the Tilli (SW 68), Water level data at Porabari (SW 50) and Jagir (SW 68.5) are collected from Bangladesh Water Development Board (BWDB) and Water Resources planning organizations (WARPO) for the model setup. The types of data, location, and duration are shown in detail (Table 2).

Table 1: Model performance analysis

Types of Data	Location	Duration/ Time
Bathymetry Data	RMD1 to RMD12	2013, 2016
Discharge Data	SW 68.5	2013-2017
Water Level Data	SW 50; SW 68	2013-2017

2.1 1-D Model Setup, Calibration and Validation

The model setup is required bathymetry of the river network and two boundary conditions. Time series of discharge i.e. flow hydrograph had used as the upstream boundary condition and time series of water level i.e. stage hydrograph had specified as the downstream boundary condition. The distance between river stations was measured from BWDB maps and Google earth using ArcMap 10.2.2. The initial flow value for model computation had specified using opening discharge value in the respective flow hydrograph. The setup model had run for the period from 1st January 2016 to 31st December 2016. Computed water surface elevations had compared with the observed water surface elevations at an intermediate gauging station Tilli (SW-68). Roughness is the only parameter (calibration parameter) that can be changed to obtain an adequate match with the observed field conditions. Such fine-tuning for making a match of model output with real field observation is nothing but the calibration of the numerical model (Figure 2). Manning's roughness coefficient had adjusted after several trials of the model during calibration to an average value of n = 0.018.

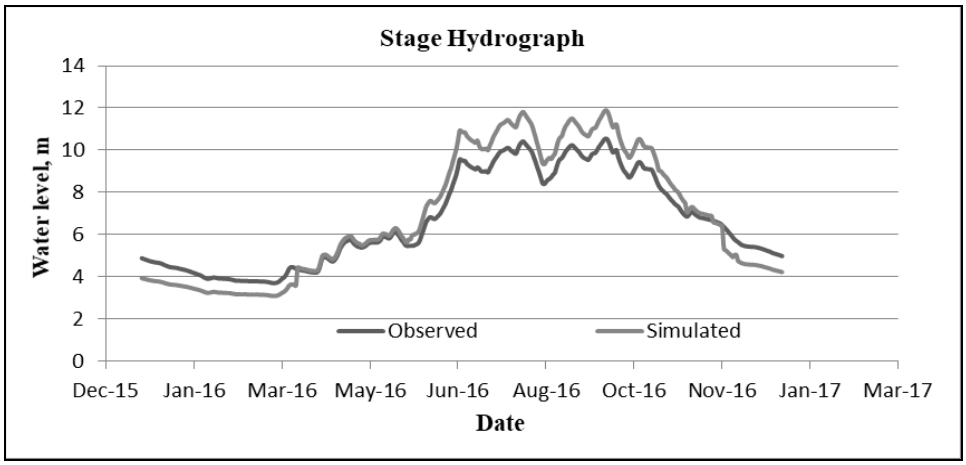

Figure 2: Calibration of water level at Tilli of Dhaleswari River

After estimating the model parameter (n =0.018), the model had been checked to assure that they adequately perform the functions satisfactorily. This verification of a calibrated model is known as validation (Figure 3). The model had been validated at the gauging station Tilli (SW 68) for the period 1st of January 2017 to 31st of December 2017.

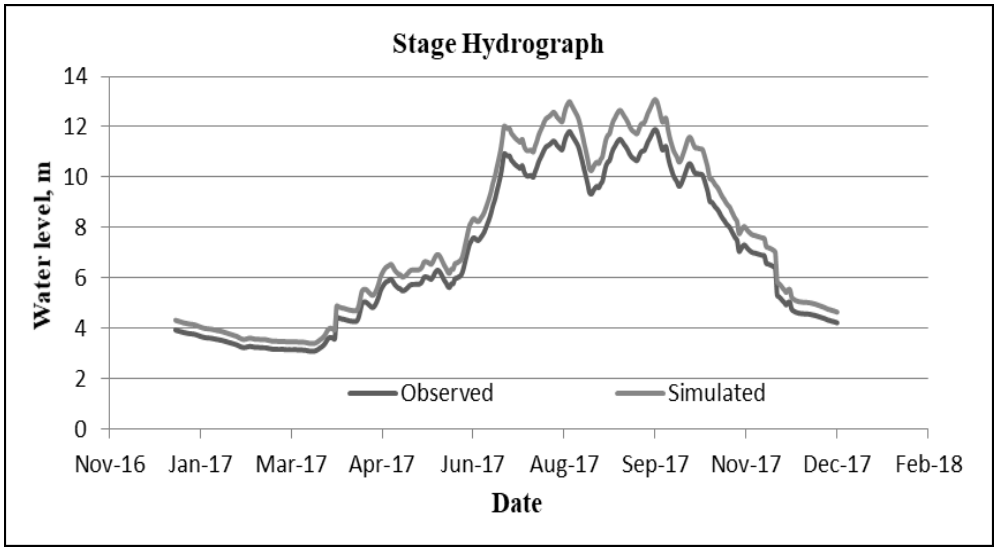

Figure 3: Validation of water level at Tilli of Dhaleswari River

From the calibration and validation curve of the hydrodynamic model, it figured that there are slight differences between observed and predicted water levels. RMSE-observations standard deviation ratio (RSR), Nash-Sutcliffe efficiency (NSE) used for determining the fitness of the calibration and validation curve. The values (Table 2) are indicating a good performance of the model.

Table 2: Model performance analysis

	RSR	**NSE**
Calibration	0.335	0.854
Validation	0.401	0.815

2.2 Selection of Dredging Section

The existing channel geometry is rigorously analyzed before selecting the design channel sections. It includes the comparative analysis through the plotting of all the cross-sections in a single figure (Figure 4). From the analysis, the average width of these cross-sections varies from 80 m to 200 m while the side slope varies from 1: 5 to 1: 35. Based on the existing geometry of the river three different dredge sections (Figure 5) have been introduced for channel modifications.

Strategy-1: Base width of around 100m with side slopes of 1:5
Strategy-2: Base width of around 150m with side slopes of 1:10
Strategy-3: Base width of around 200m with side slopes of 1:15

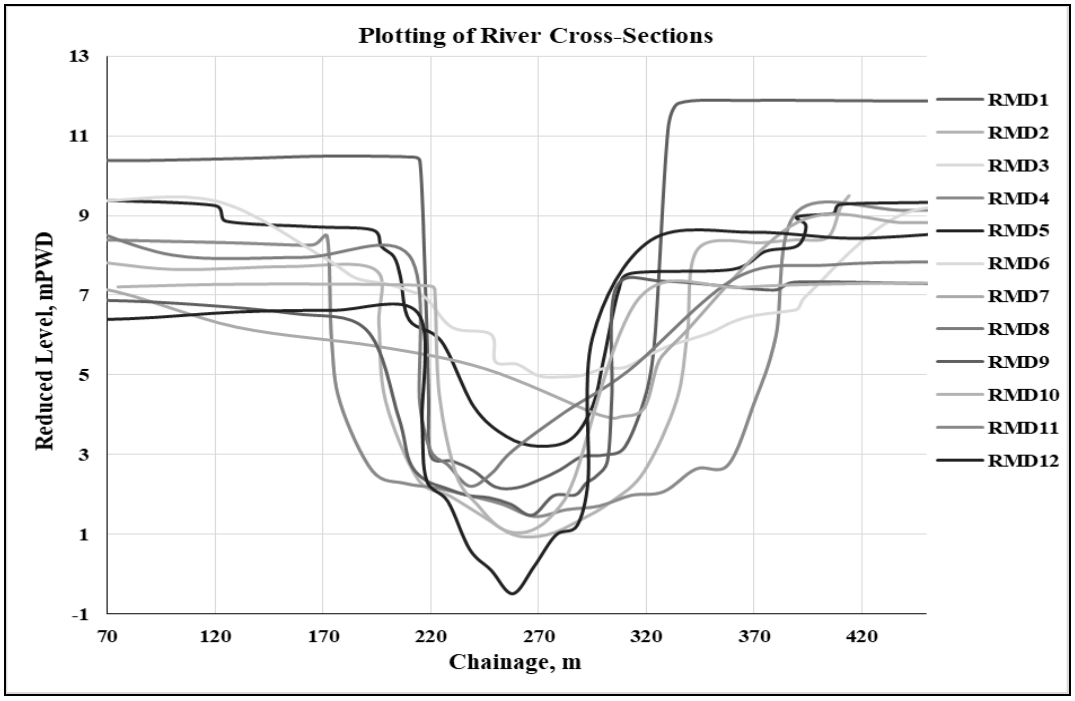

Figure 4: Plotting of original bathymetry

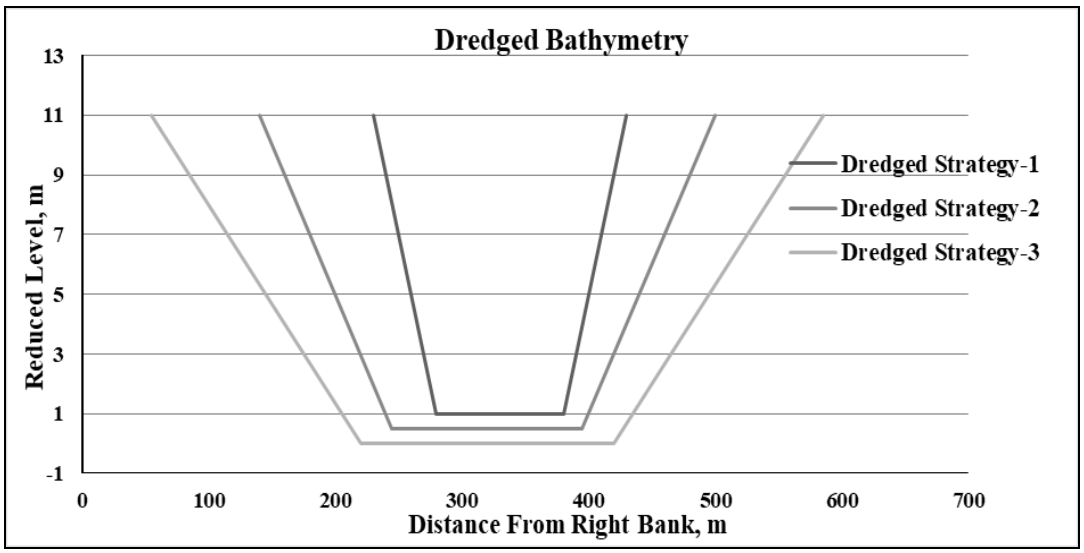

Figure 5: Channel section at three different dredging strategies

3. RESULTS AND ANALYSIS

3.1 Rating Curve Using Conveyance Analysis

A dredging strategy alters the bathymetry remarkably. This change in geometry triggers the conveyance capacity of the river. The rating curve has been developed (Figure 6) for the upstream cross-section using conveyance analysis. Maximum and minimum discharge calculated as 900 m^3/s and 200 m^3/s respectively. Manning's roughness and channel slope values were considered being 0.018 and 0.000025.

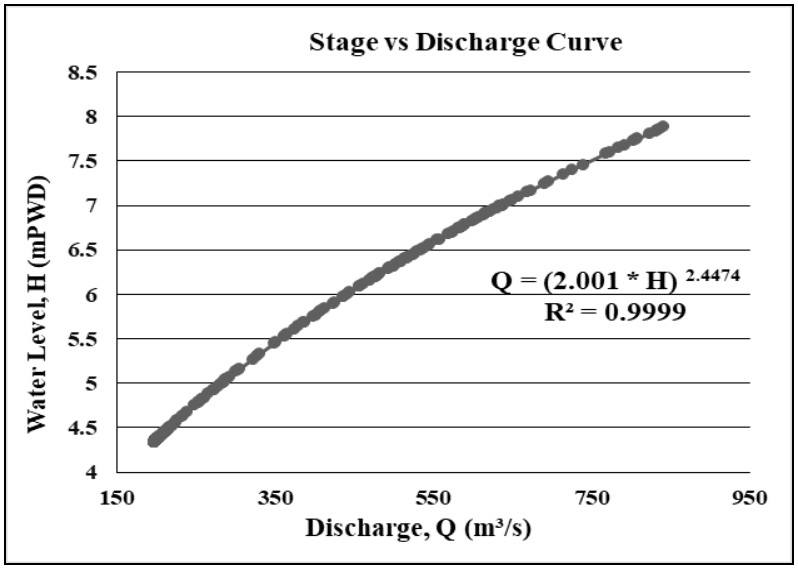

Figure 6: Rating curve using conveyance analysis

3.2 Response Due to Dredging

Dredging allows more water to flow through the main channel, thus conveyance capacity of the channel increased while water surface elevation may drop as dredging creates smooth passage of water flow. Water surface elevation of the study reach during dry and wet seasons had compared before and after dredging. Minimum available navigation depth at the different month of the year are shown in table (Table 3). During the lean flow period, minimum available depth is about 1.0-1.1 m for existing bathymetry, 2.85-2.87 m for the dredging option-1. Thus there is a significant increase in water depth compared to the original depth profile at this period. During the wet season there is lower water depth in the main channel of dredged bathymetry comparing with the original depth profile. Similar observations show for the second and third available dredging options.

Table 3: Response to different dredging strategies

	Minimum Available Water Depth (m)			
Month	**Existing bathy**	**Dredged strategy-1**	**Dredged strategy-2**	**Dredged strategy-3**
January	1.49	2.87	2.85	2.84
February	1.15	2.87	2.85	2.84
March	1.02	2.86	2.84	2.83
April	1.09	2.86	2.84	2.83
May	2.92	2.87	2.84	2.83
June	5.09	5.19	4.83	4.32
July	7.25	6.53	5.62	5.12
August	6.91	5.95	5.18	4.76
September	6.8	5.04	4.66	4.18
October	4.42	3.02	2.93	2.89
November	2.54	2.85	2.83	2.82
December	1.92	2.84	2.83	2.82

3.3 Comparison of Velocity Profiles

Dredging strategy changes the flow parameters by altering the bathymetry. A smoother passage for the flow occurred as dredging increases the bed slopes. Figure 7 shows a comparison of velocity at pre and post dredging conditions. During both the wet and dry season for the year 2017, there is a higher velocity of flow in the main channels and flood plains in case of dredged bathymetry. During

the wet season flow velocity varies from 0.42 m/s-1.1 m/s in dredged bathymetry while the velocity falls within the range of 0.37 m/s-0.41 m/s during the lean period flow. As the flow velocity increases due to dredging, it induces an increase in discharge along the study reach that augments both the dry and wet season flow.

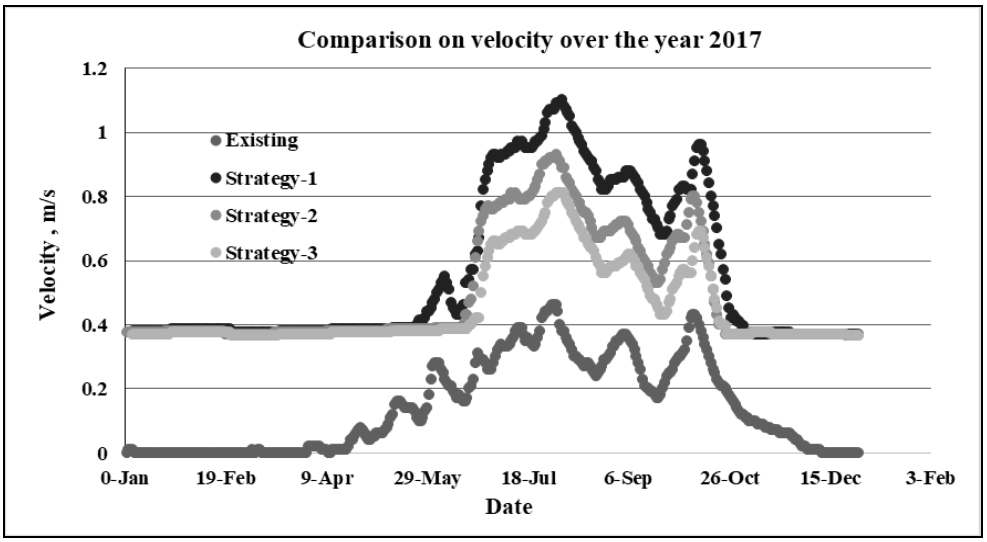

Figure 7: Velocity profile before and after dredging

3.4 Efficiency of Dredging Strategies

A comparative analysis has been performed to identify the most efficient dredging strategy among the proposed three. Minimum available water depth during the dry and wet season has been shown in figure (Figure 8a). During dry season all of these three options show approximately the same depth. Among these three strategies, option-1 gives the maximum available depth of 5.19 m. The variation in velocity is shown in figure 8(b). Maximum velocity exist in the option-1, varies from 0.41-1.1 m/s showing the fact that increase in velocity of flow is maximum in case of the dredging strategy-1 helps to divert more flow through the channel at the same time instant comparing with the other two.

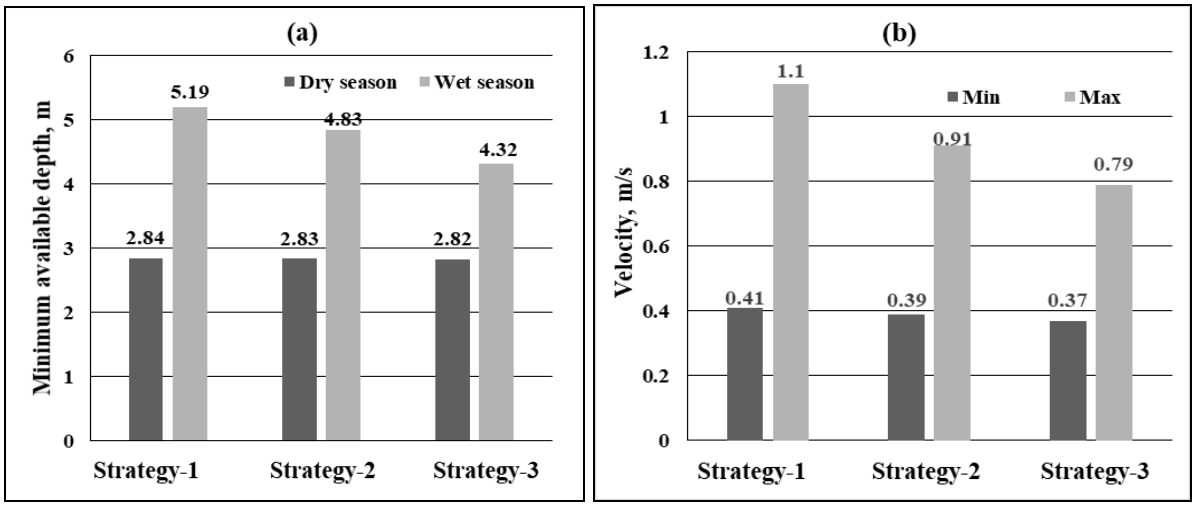

Figure 8(a): Minimum available navigation depth (b) Maximum and minimum velocity for the three proposed dredging strategies

Dredging works involves huge earth work (cutting and filling). Comparative cutting and filling volumes are shown in figure 8(c). Strategy-1 requires lees cutting volume compare to strategy-3.

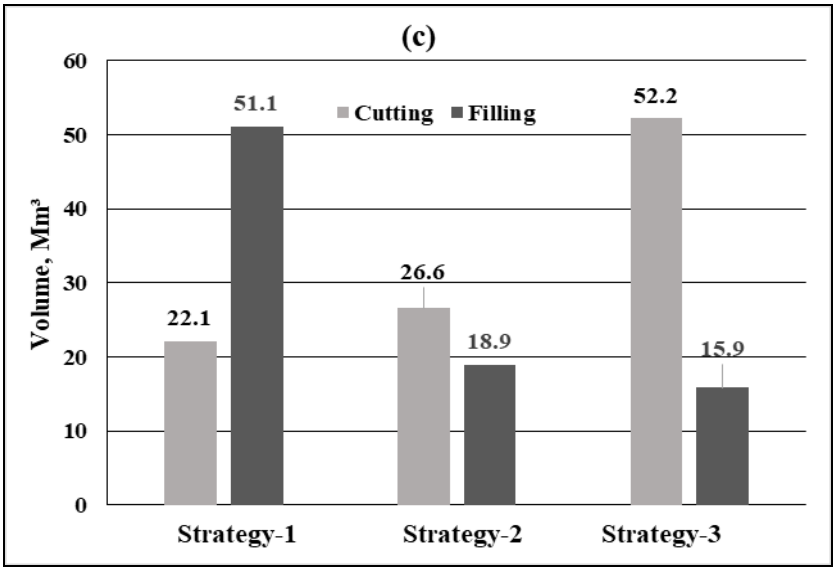

Figure 8(c): Cutting and filling volume for the three proposed dredging strategies

4. CONCLUSIONS AND RECOMMENDATIONS

The analysis has been done to assess the hydrodynamic response of the selected options for improving the dry season flow condition. It is found that for the dredging section having 100 m base width, side slope is approximately 1:5 and average dredging depth of 1.0 m hydrodynamic performance, specifically, flow augmentation is maximum. It has been found that Option-1 has the best functionality among others. Each dredged section has applied individually. But the geometry specifically the cross-sections are not constant in shape. Therefore, further study should perform considering different dredged sections in a single model setup for better realistic understanding.

REFERENCES

BWDB. (2011). *Bangladesh er nod-nodi*. Bangladesh Water Development Board (BWDB), Dhaka, Bangladesh.

FAP24. (1994). *Study report No. 3: Morphological studies phase 1, Available data and characteristics*. FAP24, Dhaka, Bangladesh.

HEC-RAS Applications Guide (2010). Hydrologic Engineering Center US Army Corps.

Haque, A., Z., M., S. (2018). Hydrodynamic and morphological analyses of new Dhaleswari River offtake using mathematical model (M. Sc. Thesis, Department of Water Resources Engineering, Bangladesh University of Engineering and Technology, Dhaka, Bangladesh). Retrieved from http://lib.buet.ac.bd:8080/xmlui/handle/123456789/126

IWM (2004). Feasibility & Mathematical Model Study of Approaching and Investigating Strategy for Rehabilitating the Buriganga-Turag-Shitalakhya River System and Augmentation of Dry Season Flow in the Buriganga River. Dhaka, Bangladesh

IWM. (2011). Mathematical modelling for offtake management of the new Dhaleswari River and hydraulic monitoring of new Dhaleswari-Pungli-BangshiTurag-Buriganga system: Prepared for Bangladesh Water Development Board, Dhaka, Bangladesh.

Khan, A., S. (2004). Augmentation of dry season flows in the peripheral rivers of Dhaka for improvement of water quality and round the year navigation. Institut für Wasserbau und THM der TU Dresden, pp. 237-247

Mushfequzzaman, M., Matin, M., A., & Noor, F. (2016). Response in the selected reach of Jamuna River due to dredging. Tech. Journal of River Research Institute, Vol.13, No.1, pp. 102-110.

Paarlberg, A., J., Guerrero, M., Huthoff, F., & Re, M. (2015). Optimizing dredge-and-dump activities for river navigability using a hydro-morphodynamic model. Water, 7(7), 3943-3962. https://doi.org/10.3390/w7073943

Proceedings of the 5th International Conference on Civil Engineering for Sustainable Development (ICCESD 2020), 7~9 February 2020, KUET, Khulna, Bangladesh (ISBN-978-984-34-8764-3)

ESTABLISHMENT OF RAINFALL INTENSITY-DURATION-FREQUENCY CURVES OF KHULNA

Sabrina Rashid Sheonty*[1] and G M Tarekul Islam[2]

[1]Lecturer, Military Institute of Science and Technology, Bangladesh, e-mail: sheonty077@gmail.com
[2]Professor, Bangladesh University of Engineering and Technology, Bangladesh, e-mail: tarek@iwfm.buet.ac.bd

***Corresponding Author**

ABSTRACT

The Intensity-Duration-Frequency (IDF) is one of the most important hydrologic tools used by engineers for designing drainage and flood control structures in urban areas. Local IDF equations are often estimated on the basis of records of intensities abstracted from daily rainfall depths of different durations, observed at a given recording rainfall gauging station. Because in developing countries like Bangladesh short duration rainfall is scarce and only daily rainfall data is available. In such cases, design rainfall approximation isn't accurate which can lead to failure of drainage system. Khulna is an important city of Bangladesh which is situated at the southern part of the country. It is the third-largest city in Bangladesh. It is the administrative seat of Khulna District and Khulna Division. Because of having the largest seaport of the country, it is an important hub for the industry and economy of Bangladesh. In this paper, the time scale invariance of rainfall of Khulna are investigated and Intensity-Duration-Frequency (IDF) curves for this city is determined. For this process, three empirical equations are used and the results are compared to find out the best fitted rainfall intensity method for the study area. This method allows for the determination of the design value of rainfall of selected return period and durations shorter than a day by using only the daily data. Firstly, 62 years of rainfall data (1948-2010) are collected from BMD and the quality of data is analyzed. The homogeneity, consistancy, randomness of data are checked and fitted to Gumbel Type 1 Extreme Value distribution function. The maximum rainfall intensities for 2 year,5 year, 10 year, 25 year, 50 year and 100 year return period were calculated using Gumbel distribution. Design rainfall from those analyses are used to calculate short duration rainfall intensity by using three different equations : Talbot, Sherman and Kimjima equation. Among these three empirical formulas, least-square method is applied to determine the best fitted rainfall intensity method for the study area. From the RMSE values of these three equations, it is concluded that Sherman equation is best fitted for this region. Finally, a 2hour-5year hyetograph is generated for Khulna region using the Sherman formula.

Keywords: *IDF curve, Gumble distribution, Khulna, RMSE value, Short duration data.*

1. INTRODUCTION

The Intensity-Duration-Frequency (IDF) is one of the most commonly used tools used by water resources engineers for planning, designing and operating drainage and flood control structures in urban areas. The establishment of such relationships was done before by Sherman (1905) and Bernard (1932). Since then, many relationships have been constructed for several parts of the globe. Hershfiled (1961) developed various rainfall contour maps to provide the design rain depths for various return periods and durations. Bell (1969) and Chen (1983) derived the IDF formulae for the United States, Kouthyari & Garde (1992) presented a relationship between rainfall intensity and duration for India.

Local IDF equations are generated from the records of intensities abstracted from rainfall depths of different durations, observed at a given recording rainfall gauging station. But only in some regions, these rainfall gauging stations are operating for a long time which produce a good amount and quality of data in order to produce reliable IDF relationship for the area. But mostly in developing countries, these rainfall gauging station doesn't exist or the sample size is too small to generate the IDF curve for the region. Specially in south asian subcontinent region and in Bangladesh, this problem is quite prominent. In this regard, research has focused on the mathematical representation of rainfall both in time and space, in which Gupta & Waymire (1990), Burlando & Russo (1996), Menabde et al. (1999), De Michele et al. (2002), Pao-Shan-Yu et al. (2004) and Nhat et al. (2006) showed the scaling invariance models to derive IDF characteristics of short duration rainfall from daily data.

Earlier, in Bangladesh different IDF curves were developed for different parts of Bangladesh. Matin et al. (1984) developed IDF curve for North-East region of Bangladesh. Recently, Rasel et al. (2015) developed IDF for for North-West region Bangladesh, Chowdhury et al. (2007), Rashid et al. (2012) developed IDF for Sylhet city, Afrin et al. (2015) developed IDF for Dhaka city. Khulna is also an important divisional city of Bangladesh shown in Figure 1. This paper aims to analyse the time scale invariance of rainfall of Khulna and develop Intensity-Duration-Frequency (IDF) relationships for this city.

Figure 1 : Map of Study Area (Khulna)

2. METHODOLOGY

For this study, 62 years of rainfall data (1948-2010) are collected from BMD for Khulna city and the quality of data is analyzed. The homogeneity, consistency, randomness of data is checked and fitted to Gumbel Type 1 Extreme Value Distribution function. The maximum rainfall intensities for 2 years, 5 years, 10 years, 25 years, 50 years and 100 year return period were calculated using Gumbel distribution. Design rainfall from those analyses are used to calculate rainfall intensity by using three different equations: Talbot, Sherman and Kimjima equation. Among these three empirical formulas, least-square method is applied to determine the best fitted rainfall intensity method for the study area. From the RMSE values of these three equations, it is concluded that Sherman equation is best fitted for this region.

2.1 Generalized IDF relationship

According to Koutsoyiannis et al. (1998), the generalized IDF relationships are shown in equation (1) where i is the rainfall intensity of duration d, and w, ν, θ, and η are non-negative coefficients.

$$i = \frac{w}{(d^{\nu} + \theta)^{\eta}} \tag{1}$$

Koutsoyannis et al. (1998) also showed that the errors resulting from imposing ν=1 in equation (1) are much smaller than the typical parameter and quantile estimation errors from limited size samples of data and considering ν≠1 as a model over parameterization. Thus, Koutsoyannis et al. (1998) suggested for a given return period the general IDF relationships as

$$i = \frac{w}{(d + \theta)^{\eta}} \tag{2}$$

The coefficients w, θ, and η are not independent on the return period and this dependence cannot be arbitrary. The IDF curves for different return periods cannot intersect each other. This restriction, the range of variation of parameters w, θ, and η are limited. If $\{w_1, \theta_1, \eta_1\}$ and $\{w_2, \theta_2, \eta_2\}$ denote the parameter sets for return periods T_1 and T_2 respectively, with $T_2<T_1$, Koutsoyannis et al. (1998) suggest the following restrictions shown in equation (3).

$$\theta_1 = \theta_2 = \theta > 0;\ 0 < \eta_1 = \eta_2 = \eta < 1;\ w_1 > w_2 > 0 \tag{3}$$

In these restrictions, the only parameter that can consistently increase with increasing return periods is w and these arguments justify the formulation of the following general model for IDF relationship shown in equation (4).

$$i = \frac{a(T)}{b(d)} \tag{4}$$

which exhibits the great advantage of expressing separable relations between i and T, and between i and d. In equation (4), $b(d)=(d+\theta)^{\eta}$ with $\theta>0$ and $0<\eta<1$, whereas a(T) is completely defined by the probability distribution function of the maximum rainfall intensities.

3. RESULTS AND CONCLUSIONS

3.1 Gumble Type 1 Extreme Value Distribution

The data quality was good and normally distributed and Gumble Type 1 Extreme value distribution fits well in the rainfall intensities of 24 hours. The frequency analysis was done by Gumble's distribution using following equations:

$$X_T = u + \alpha y_T \tag{5}$$

$$u = \bar{x} - 0.5772\alpha \quad (6)$$

$$\alpha = S_x (\sqrt{6}/\pi) \quad (7)$$

$$y_T = -\ln(-\ln(1-1/T)) \quad (8)$$

The frequency analysis was done for 2 years, 5 years, 10 years, 20 years, 30 years, 50 years and 100 year return period. For example, Gumble distribution for 100 year return period is shown in table 1.

Table 1: Gumble distribution for 100 years return period for Khulna

Days	Mean (mm)	Standard Deviation	α	u	T	y_T	X_T (mm)	Hours	Intensity (mm/hr)
1D	134.54	70.72	55.14	102.72	100.00	4.60	356.37	24.00	14.85
2D	179.35	84.35	65.76	141.39	100.00	4.60	443.91	48.00	9.25
3D	205.85	98.42	76.74	161.55	100.00	4.60	514.55	72.00	7.15
4D	226.84	102.04	79.56	180.92	100.00	4.60	546.91	96.00	5.70
5D	243.95	103.56	80.74	197.34	100.00	4.60	568.78	120.00	4.74
6D	257.97	107.26	83.63	209.70	100.00	4.60	594.42	144.00	4.13
7D	273.85	109.76	85.58	224.46	100.00	4.60	618.14	164.00	3.77

3.2 Khulna IDF curve from long duration data

From the daily rainfall data, Gumble's distribution is done 2 years, 5 years, 10 years, 20 years, 30 years, 50 years and 100 year return period and shown in table 2.

Table 2: Rainfall Intensity chart of Khulna for different return period

Hours	Intensity (2Year return period)	Intensity (5Year return period)	Intensity (10Year return period)	Intensity (20Year return period)	Intensity (30Year return period)	Intensity (50Year return period)	Intensity (100Year return period)
24	5.12	7.73	9.45	11.10	12.06	13.24	14.85
48	3.45	5.00	6.03	7.02	7.58	8.29	9.25
72	2.63	3.84	4.64	5.41	5.85	6.40	7.15
96	2.19	3.13	3.75	4.35	4.69	5.12	5.70
120	1.89	2.65	3.16	3.64	3.92	4.27	4.74
144	1.67	2.33	2.76	3.18	3.42	3.72	4.13
168	1.56	2.15	2.54	2.92	3.13	3.40	3.77

From this table long duration IDF curve is generated for Khulna which is shown in Figure 2. From this figure, it is seen that the highest rainfall intensity is 14.85mm/hr for 100 year return period for duration of 24 hours. For the same duration but 2 year return period the rainfall intensity is noted 5.12 mm/hr.

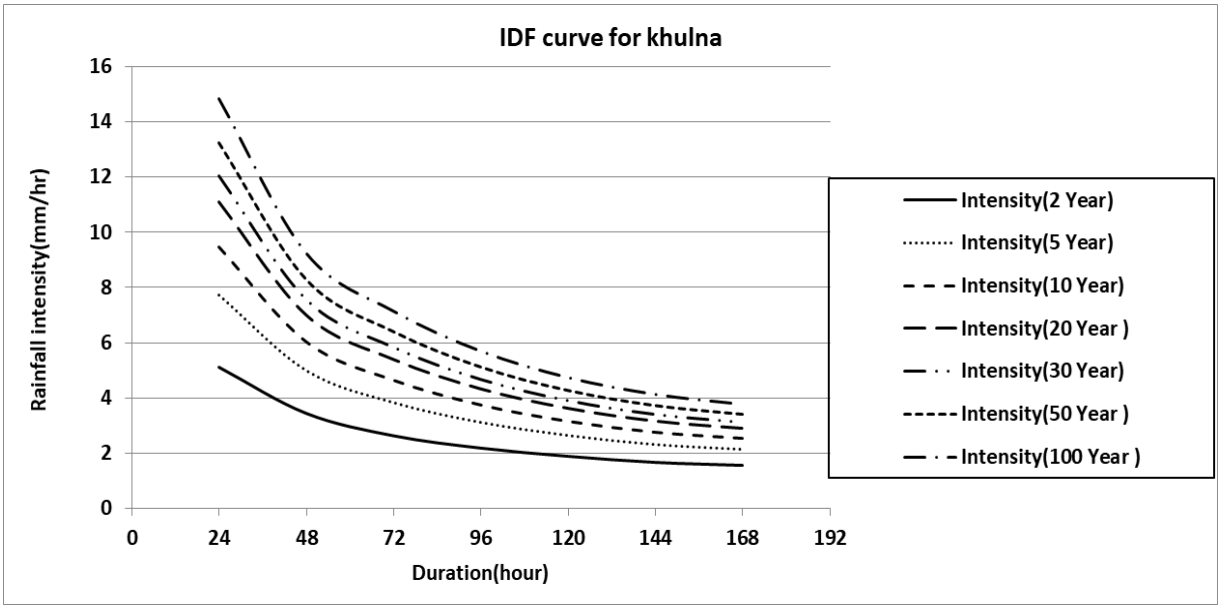

Figure 2 : IDF curve for Khulna for long duration data

3.3 Conversion of long duration data to short duration data using three empirical equations

The IDF formulas are empirical equations representing a relationship among maximum rainfall intensity (as dependent variable) and other parameters such as rainfall duration and frequency (as dependent variable). There are some commonly used formulas found in literature of hydrology applications (Chow et al., 1988). Some of the equations are shown in equation (9), (10), (11) which describe rainfall intensity duration relationship:

Talbot equation:

$$i = \frac{a}{d + b} \tag{9}$$

Sherman equation :

$$i = \frac{a}{(b + d)^e} \tag{10}$$

Kimjima equation:

$$i = \frac{a}{d^e + b} \tag{11}$$

Where i is the rainfall intensity(mm/hour), d is the duration(hour) and a, b, e are the constant parameters of related metrological conditions.

For Talbot, Sherman and Kimjima equation, the value of the constant parameters a, b,e are estimated using the long duration data for 2 year, 5 year, 10 year, 20 year, 30 year, 50 year, 100 year return period. From the estimated value of parameters for different return period, the rainfall intensity is converted to short duration data for 2 year, 5 year, 10 year, 20 year, 30 year, 50 year, 100 year return period. The results from Talbot and Sherman equation is shown in table 3 & 4.

Table 3 : Conversion of Short Duration data by Talbot formula for different return period

Hr	Intensity 2 RT	Intensity 5 RT	Intensity 10 RT	Intensity 20 RT	Intensity 30 RT	Intensity 50 RT	Intensity 100 RT
0.25	8.2461	13.5477	17.2110	20.7895	22.8693	25.4861	29.040
0.5	8.2451	13.5097	17.1587	20.7228	22.7939	25.3997	28.938
1	8.2432	13.4344	17.0551	20.5906	22.6448	25.2289	28.737
1.5	8.2413	13.3598	16.9528	20.4601	22.4975	25.0603	28.540
2	8.2394	13.1412	16.6531	20.0783	22.0670	24.5677	27.962
3	8.2356	12.7246	16.0843	19.3559	21.2537	23.6386	26.873
5	8.2280	12.3337	15.5532	18.6836	20.4981	22.7771	25.866
6	8.2243	11.9661	15.0559	18.0565	19.7945	21.9763	24.932
12	8.2016	9.6621	11.9896	14.2344	15.5296	17.1517	19.344
24	8.1568	7.4969	9.1839	10.8040	11.7366	12.9027	14.476

Table 4 : Conversion of Short Duration data by Sherman formula for different return period

Hr	Intensity 2 RT	Intensity 5 RT	Intensity 10 RT	Intensity 20 RT	Intensity 30 RT	Intensity 50 RT	Intensity 100 RT
0.25	89.5971	165.1596	218.1502	270.2414	300.6037	338.8674	390.907
0.5	58.1434	103.9776	135.7576	166.8429	184.9126	207.6463	238.511
1	37.7318	65.4599	84.4836	103.0062	113.7467	127.2385	145.527
1.5	29.2992	49.9366	64.0140	77.6867	85.6042	95.5418	109.001
2	24.4858	41.2108	52.5752	63.5944	69.9698	77.9674	88.793
3	19.0135	31.4380	39.8367	47.9625	52.6584	58.5448	66.507
5	13.8250	22.3538	28.0850	33.6162	36.8084	40.8067	46.210
6	12.3387	19.7921	24.7909	29.6113	32.3921	35.8742	40.579
12	8.0071	12.4602	15.4277	18.2816	19.9256	21.9825	24.759
24	5.1961	7.8445	9.6008	11.2868	12.2570	13.4701	15.107

3.4 RMSE value calculation

The RMSE value is estimated for Talbot, Sherman and Kimjima formula for all the mentioned return periods and the average RMSE values of the equations are shown in table 5.

Table 5: RMSE value comparison for different equations

Equation	RMSE value
Talbot	0.162724769
Sherman	0.093710522
Kimjima	0.176516145

From table 5, it is clear that the RMSE value is least for Sherman equation. From the RMSE value, it can be concluded that Sherman equation is best fitted for this region. The IDF curve using Sherman formula is shown for Khulna city in Figure 3. From this figure, it is seen that the highest rainfall

intensity is 390.9 mm/hr for 100 year return period for duration of 0.25 hour. For the same duration but 2 year return period the rainfall intensity is noted 89.59 mm/hr.

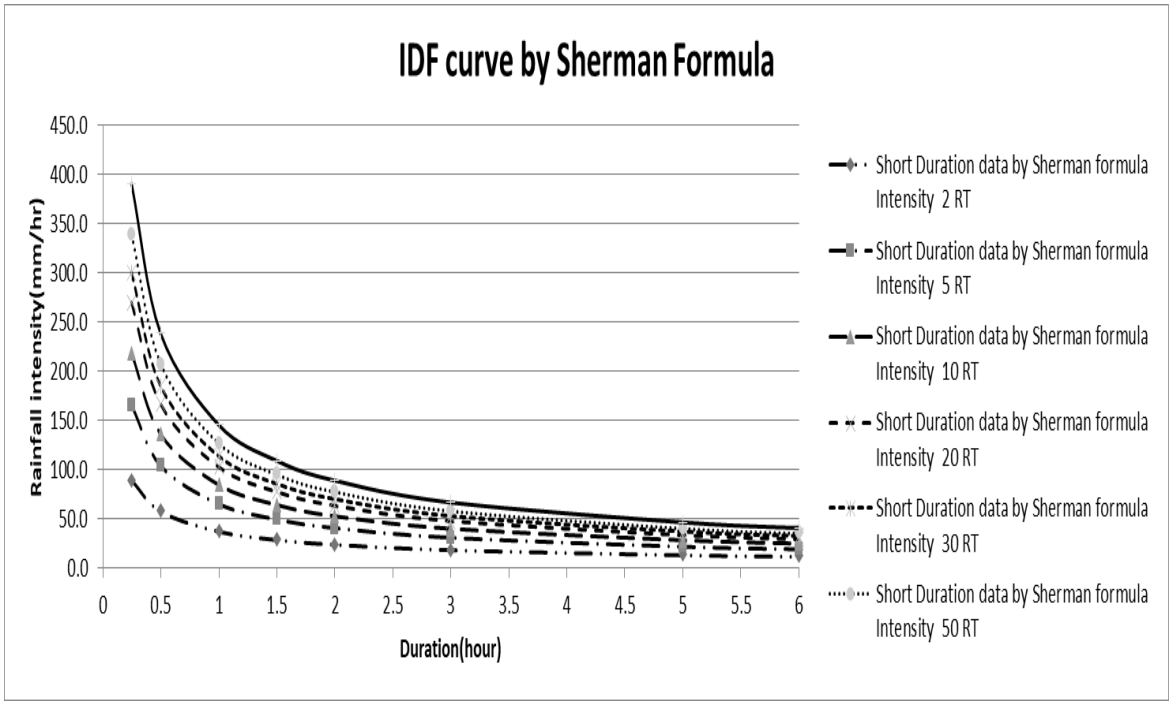

Figure 3 : IDF curve of Khulna using Sherman equation

Finally, a hyetograph of 2hr-5yr is generated for Khulna using the Sherman equation which is best fitted for this region. The hyetograph values are shown in table 6.

Table 6 : Generation of 2hr-5yr hyetograph for Khulna

Duration (min)	Intensity (mm/hr)	Cumulative Depth (mm)	Incremental Depth (mm)	Time	Precipitation (mm)
10	217.45	36.24	36.24	0-10	2.47
20	136.66	45.55	9.31	10-20	2.87
30	104.15	52.07	6.53	20-30	3.42
40	85.89	57.26	5.18	30-40	4.38
50	73.97	61.64	4.38	40-50	6.53
60	65.46	65.46	3.82	50-60	36.24
70	59.04	68.88	3.42	60-70	9.31
80	53.98	71.97	3.09	70-80	5.18
90	49.89	74.84	2.87	80-90	3.82
100	46.49	77.48	2.64	90-100	3.09
110	43.61	79.95	2.47	100-110	2.64
120	41.14	82.28	2.33	110-120	2.33

The 2hr-5yr hyetograph for Khulna city using the best fitted equation (Sherman equation) is shown in the following figure 4. In this figure it is seen that, the precipitation depth starts from 2.47 mm up to a peak of 36.24 mm then decreases to 2.33 mm.

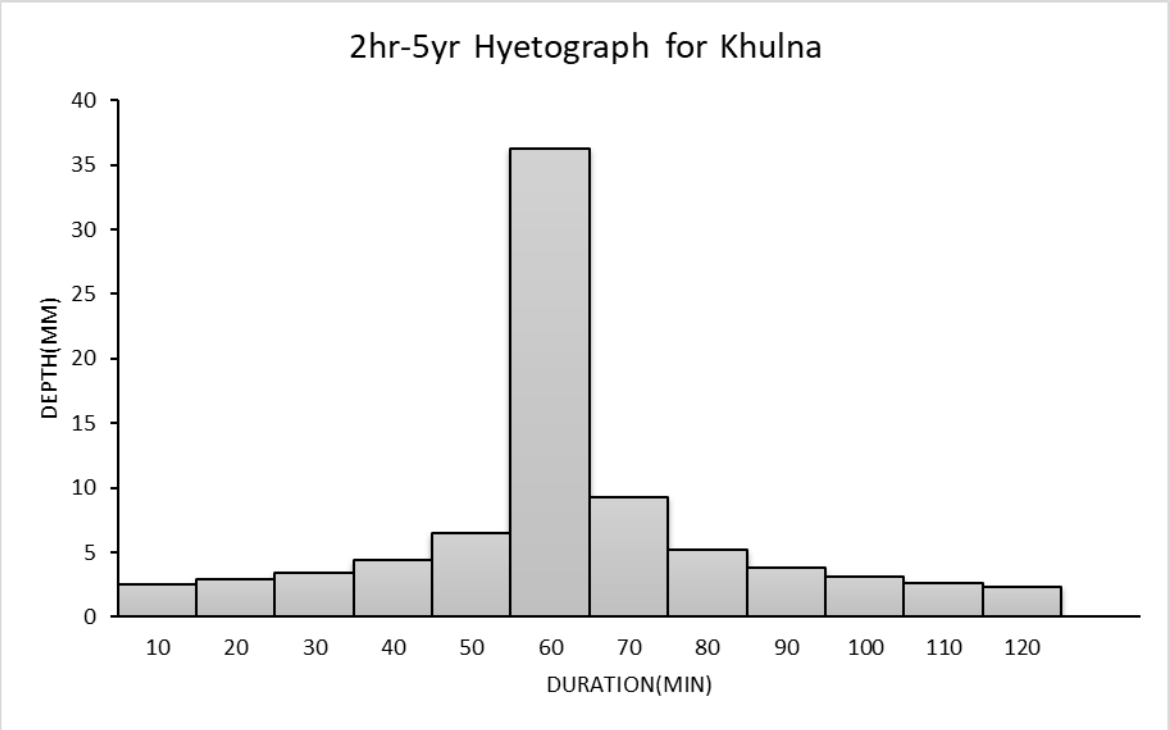

Figure 4 : 2hr-5yr hyetograph for Khulna

4. CONCLUSIONS

For drainage design and other practical applications, most hydrological studies require short duration rainfall data which are rare in developing countries. This study has been conducted to the formulation and construction of IDF curves of Khulna using daily rainfall data using the scaling properties with three different formulas. It is shown from the comparison of RMSE values that within these three formulas, Sherman formula is best suited for Khulna. Finally, a 2hr-5yr hyetograph is generated for the study area.

REFERENCES

Afrin S., Islam M. M., and Rahman M. M., 2015. Development of IDF Curve for Dhaka City Based on Scaling Theory under Future Precipitation Variability Due to Climate Change. *International Journal of Environmental Science and Development, Vol. 6, No. 5*

Bell F. C., 1969. Generalized rainfall-duration-frequency relationship. *ASCE Journal of the Hydraulic Division, Vol. 95, No. HY1, p. 311– 327.*

Bernard, M.M.,1932. *Formulas for rainfall intensities of long durations*. Transactions of the American Society of Civil Engineers, 96, 592– 624.

Burlando, P., Rosso, R., 1996. Scaling and multiscaling models of depth-duration-frequency curves for storm precipitation, *Journal of Hydrology,187, 45 – 65.*

Chen, C.L., 1983. Rainfall intensity– duration– frequency formulas. *Journal of Hydraulic Engineering – ASCE, 109, 1603 – 1621.*

Chow, V.T., 1964. *Handbook of Applied Hydrology*, McGraw-Hill, New York, pp. 1-1450.

Chowdhury R., Alam J. B., Das P. and Alam M. A. 2007. Short Duration Rainfall Estimation of Sylhet: IMD and USWB Method. *Journal of Indian Water Works Association. pp. 285- 292.*

De Michele, C., Kottegoda, N.T., Rosso, R., 2002. IDAF (intensity–duration–area–frequency) curves of extreme storm rainfall: a scaling approach. *Water Science and Technology, 25(2), 83– 90.*

Gupta, V.K., Waymire, E., 1990. Multiscaling properties of spatial and river flow distributions. *Journal of Geophysical Research, 95, D3, 1999– 2009.*

Hershfied, M., D., 1961. Estimating the Probable Maximum Precipitation, *Journal of the Hydraulic Division, Proceeding of the ASCE, HY5, 99-116*

Kothyari, U.C. and Grade, R.J., 1992. Rainfall intensity duration frequency formula for India, *J. Hydr. Engrg., ASCE, 118(2), 323-336.*

Koutsoyiannis, D., Kozonis, D., and Manetas, A., 1998. A mathematical framework for studying rainfall intensity: duration-frequency relationships. *J,. Hydrol., 206, 118-135*

Matin M. A. and Ahmed S. M. U. 1984. Rainfall Intensity Duration Frequency Relationship for the N-E Region of Bangladesh. *Journal of Water Resource Research. 5(1)*

Menabde, M., Seed, A. and Pegram, G.,1999. A simple scaling model for extreme rainfall. *Water Resources Research, Vol. 35, No. 1, p. 335-339*

Nhat, M., L., Tachikawa, Y., Sayama T., Takara, K., 2006. *Derivation of rainfall intensity-duration-frequency relationships for short duration rainfall from daily data*. Proc. of International Symposium on Managing Water Supply for Growing Demand, Bangkok, 16-20, October, 2006, IHP Technical Documents in Hydrology, no. 6, pp. 89-96.

Rasel M. M., and Islam M. M., 2015. Generation off Rainfall Intensity Duration Frequency Relationship for the North-West Region in Bangladesh. *IOSR Journal of Environmental Science, Toxicology and Food Technology. Vol-9, issue-9, Ver-I (Sep2014) p 4147.*

Rashid MM, Faruque SB and Alam JB. 2012. Modelling of short duration rainfall intensity duration Frequency (SDRIDF) equation for Sylhet City in Bangladesh. *ARPN Journal of Science and Technology. 2(2):92-95.*

Sherman, C. W., 1905. Maximum rates of rainfall at Boston, Trans. *Am. $oc. Civ. Eng., LIV, 173-181*

Yu, P.Sh., Yang, T.Ch. Lin, Ch.Sh., 2004. Regional rainfall intensity formulas based on scaling property of rainfall. *Journal of Hydrology, 295(1-4), 108 – 123*

Proceedings of the 5th International Conference on Civil Engineering for Sustainable Development (ICCESD 2020), 7~9 February 2020, KUET, Khulna, Bangladesh (ISBN-978-984-34-8764-3)

A STUDY ON PATTERN IDENTIFICATION OF BANK SHIFTING AROUND PADMA-UPPER MEGHNA CONFLUENCE USING MULTI-TEMPORAL SATELLITE IMAGES

Faria Nur*[1] and Mohammad Mostafa Ali [2]

[1]Postgraduate student, Department of Water Resources Engineering, BUET, Bangladesh,
e-mail: faria.wre14@gmail.com
[2]Professor, Department of Water Resources Engineering, BUET, Bangladesh,
e-mail: wremostafa@gmail.com

***Corresponding Author**

ABSTRACT

Padma-Upper Meghna confluence is widely acknowledged as an important geomorphological node that controls the downstream routing of water and sediment to the Bay of Bengal through Meghna Estuary. The present study aims at pattern analysis and forecasting of bank shifting around Padma-Upper Meghna confluence with spatial and geographic co-ordinate system based approach using GIS; and a deep learning approach based on long short-term memory (LSTM) network using MATLAB. Comparisons between different approaches are also divulged. Satellite images (LANDSAT MSS, TM and IRS) covering the period of 1973 to 2018 has been used to carry out the investigation. Maximum rate of bank migration has been found 59.25m/year for the left bank and 81.64m/year for the right bank for study reach of Padma River. Similarly, maximum migration rate for left bank is 8.17m/year and for right bank is 9.35m/year for the study reach of Upper-Meghna River, and the maximum migration rate for the Lower-Meghna reach is 64.39m/year for left bank and 146.55m/year for the right bank over 45 years.The present morphology at the confluence of Padma and Lower Meghna River is such that the width of cross-sections increases considerably at upstream of the confluence, leading to a decrease of stream velocity and consequently the generation of large chars elsewhere. Left bank of the Padma River is severely affected by erosion. Accretion was a dominant process from 1978-2002 in the Lower-Meghna but from 2002 erosion started to dominate and the net result is found to be accretion as dominant in the last 45 years.

Keywords: *Padma-Upper Meghna confluence, Satellite image, GIS; Bank shifting, Erosion-accretion.*

1. INTRODUCTION

In Bangladesh, river erosion is considered as one of the worst catastrophes to affect the country, almost on an annual basis, as it destroys productive land, livelihood and much needed infrastructures permanently. The present study, however, aims its analysis on the confluence of the Padma and the Meghna River and its downstream river reach of the Lower Meghna River. The vibrant morphological and hydrodynamic natures of such two large rivers make this region one of the most unstable and erosion prone area of the country. In fact, the erosion in the left bank of the lower Meghna River at Chandpur and further downstream has become a serious issue over the year. Bangladesh Water Development Board (BWDB) has taken several mitigation projects against this erosion problem including construction of embankments on the left bank of Lower Meghna River and developing hard point at Chandpur. On the other hand, as for being morphologically unstable and dynamic river like Padma and Lower Meghna, the islands and bars (locally called chars) in these rivers are changed its shape and size every year. Some of them are gone under severe erosion while some of them got deposited during monsoon and post-monsoon season. The huge amount of sediments coming from upstream (particularly sediments carrying by the Padma River flow) and the sediments formed by local scouring are deposited right bank of Lower Meghna River. Therefore, the very consequence of protecting the left bank from erosion and the curvature of the left bank of the Lower Meghna River upstream of Chandpur itself diverts the flow towards the right bank and the huge amount of sediment that this flow carrying deposits on that bank. As such during the last four decades the river at this location has lost it conveyance area considerably.

Previously Pegg and Galay (1974), Ali(1975), Rahman (1978), Ahmed (1989) studied the confluence shifting, movement of bank line of the Padma-Upper Meghna Confluence. Khan and Matin (1986) found that the Ganges carries about 30 percent of the suspended load as sand load, whereas, 90 percent of the suspended load of the Brahmaputra is sand, whose combined effects have influence on the morphology of Padma and around Chandpur Confluence.

Three approaches have been considered to realize the bankline shifting pattern in this study. Firstly, a common sinuous equation is introduced for different reaches which is based on spatio-temporal distances.Secondly, regression equation is evaluated based on geographic co-ordinate system. Finally, Recurrent Neural network (RNNs) namely, LSTM (Long-Short Term Memory) is considered to understand the bankline shifting pattern. Comparison between these studies have been discussed to make a better understanding of approaching on bankline shifting pattern.

2. METHODOLOGY

2.1. Study Area

The study area covers part of the Padma, the Upper Meghna, the Lower Meghna .The study area is considered from Mawa to Dighirpar of about 40km of Padma river reach, from Satnol to Chandpur of about 27.5km of Upper-Meghna River reach and From Chandpur to Haimchar of about 27.5km of Lower-Meghna reach (Figure 1). The Meghna joined at the present confluence about 150 years ago. The Lower Meghna had to adjust to carry the combined discharge of the Jamuna, Ganges and Meghna rivers, one of the largest rivers in the world, which conveys the combined discharge and sediment load of the three major rivers of Bangladesh into the Bay of Bengal.Over the past three decades, Padma river has changed from a relatively narrow, straight line to meandering to braided and most recently back to straight.Upper-Meghna river shows a meandering behaviour while Lower-meghna is straight, occasionally braided.

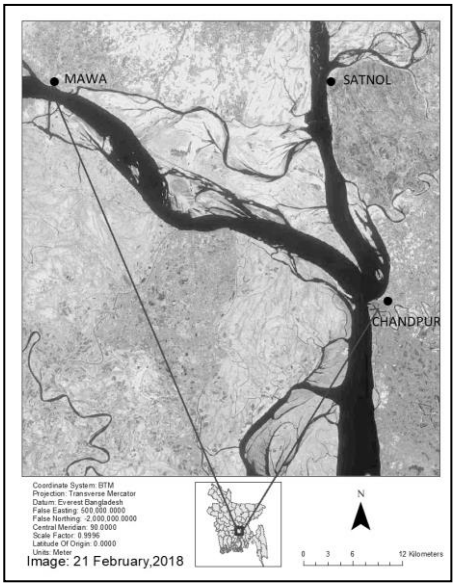

Figure 1: Location map of study area

2.2 Data Collection and Processing

A time-series satellite images of dry season for the Padma-Upper Meghna confluence have been collected from the website of United States Geological Survey (USGS). For this study, satellite images types of Landsat MSS,Landsat TM and IRS,LISS covering the period 1973-2018 were collected. The study has conducted diiferent steps which are given below:

- For estimation of erosion/accretion rate of bank line and identification of the pattern of bankline shifting, Padma river, Meghna river and Lower-Meghna river have been divided with four, one and two sections respectively which is imposed on image of 1973 (Figure 2).
- The Shifting of each point from bankline of 1973 to the bankline of specific year is estimated through the attribute table of ArcMap 10.3 and the data were processed for the further study.
- This study is based on three different approachs for bankline shifting observation: regression based analysis and geographic coordinate system based analysis are performed with Microsoft EXCEL, LSTM based study is performed with the help of MATLAB2018a.
- The developed equations from the regression and geographic coordinate system based analysis are used to forecast for the year of 2020 and also comparison between three approaches are observed appropriately..

3. RESULTS AND DISCUSSIONS

3.1 Bankline shifting analysis

In total, seven sections (P1, P2, P3, P4, M1, ML1 and ML2) are imposed on the Padma, Upper-Meghna and Lower-Meghna River where the sections are almost at 10 km interval. Considering 1973 as the base year, magnitude of left bank and right bank shifting has been determined (2 years interval) using GIS technique. The value of shifting is considered positive, if the digitized bank line of the specific year is in left side of the bank line of 1973 according to the flow direction. Similarly, the shifting value is considered negative, if the digitized bank line of the specific year is in right side of the bank line of 1973. Then all the values have been plotted in a graph for each section to observe the shifting pattern which is shown in figure 3.

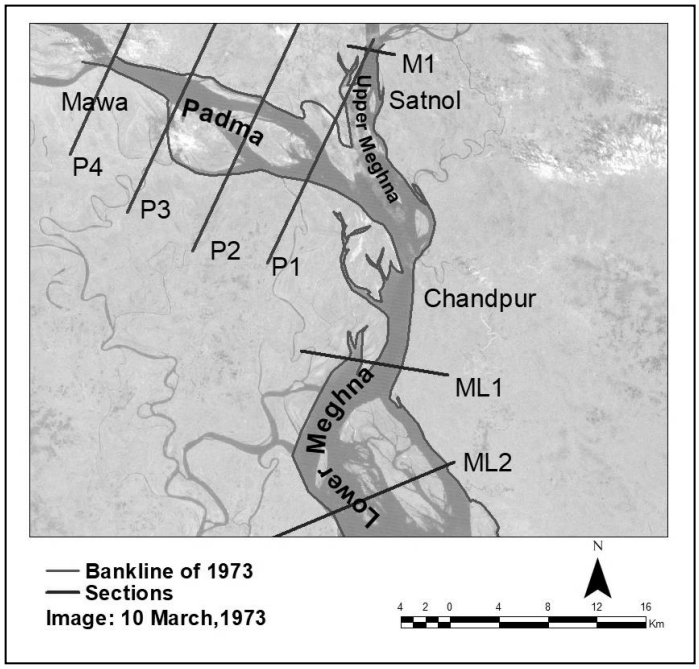

Figure 2: Sections imposed on 1973 image

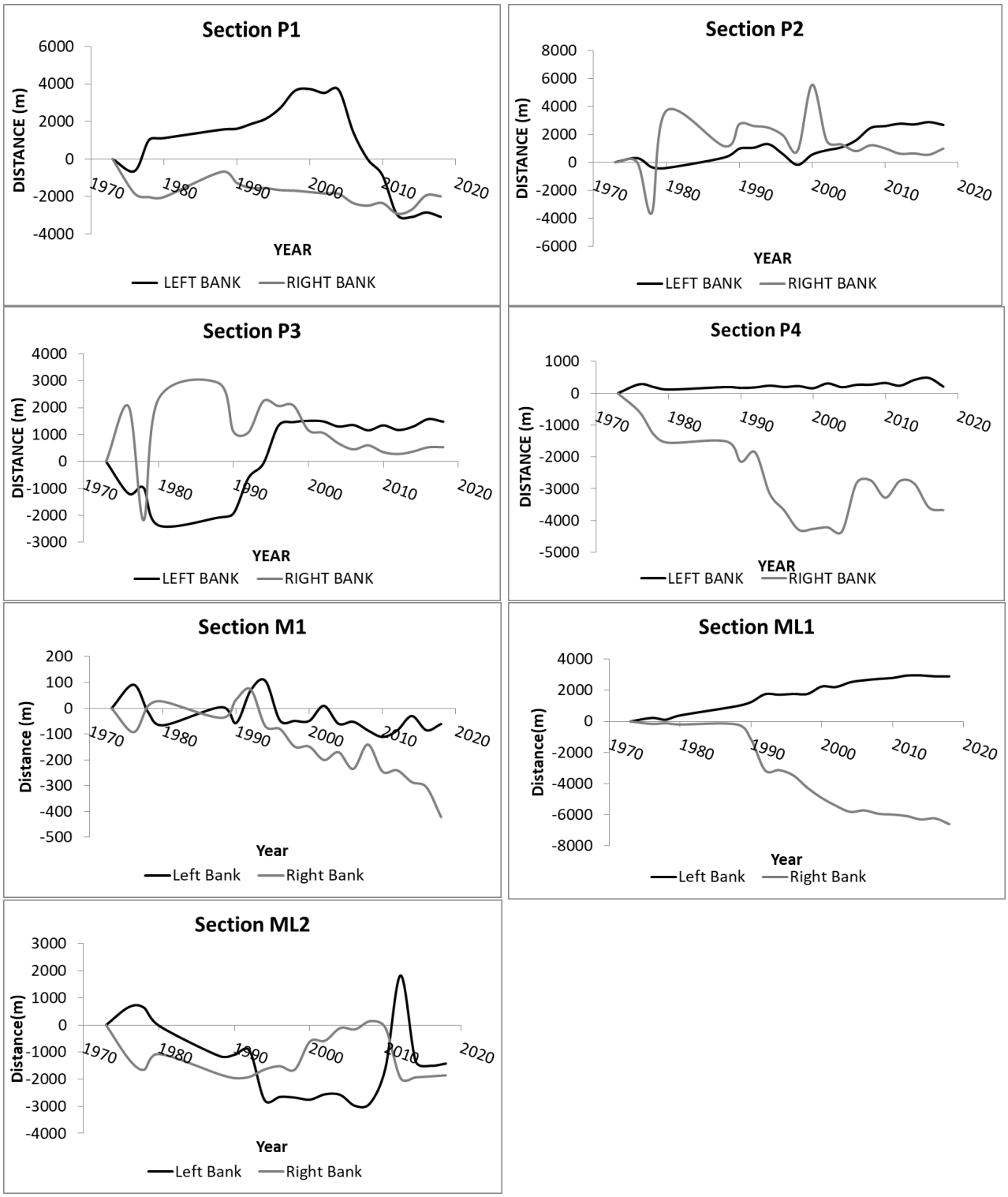

Figure 3: Bankline shifting from 1973 to 2018

3.1.1 Regression Based Analysis

To understand the pattern of bank shifting for the recent years, a sinuous equation $D= [(a_1\sin(b_1t+c_1) +a_2\sin(b_2t+c_2)+d)]$ is evaluated where D is the distance between the bank line of 1973 and the specific year and t is considered to be the last two digits of the corresponding year (e.g. 2012 is considered as 12) to avoid complexity. Regression analysis is done for the last 10 years for these seven sections.

Polynomial equations are derived for the sections who mismatched with the criterion. The regression equation and R^2 values are shown in Figure 4.

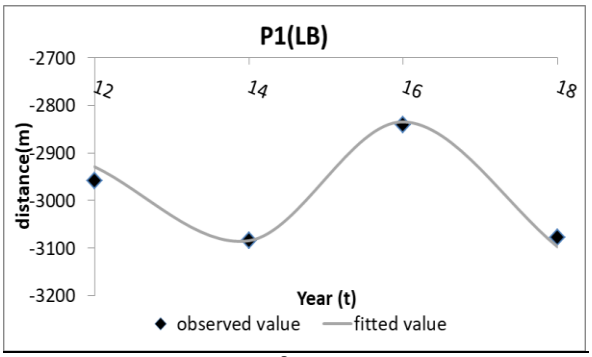

$D=a_1*\sin(b_1*t+c_1)+d$, $R^2=0.981328042$

a_1	b_1	c_1	d
140	-1.86	0.899	-3100

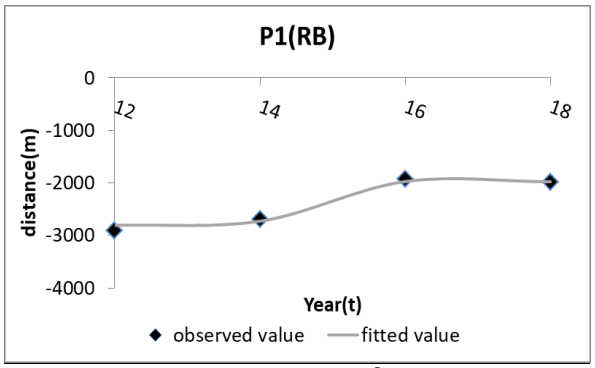

$D=a_1\sin(b_1t+c_1)+a_2\sin(b_2t+c_2)+d$, $R^2=0.9874760$

a_1	b_1	c_1	a_2	b_2	c_2	d
600	-40	1.305	70	80	0	-3150

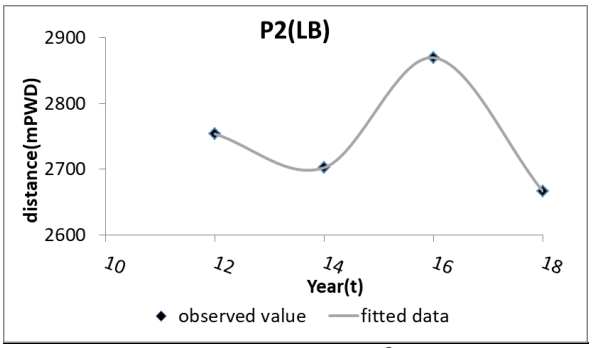

$D=a_1\sin(b_1t+c_1)+a_2\sin(b_2t+c_2)+d$, $R^2=1$

a_1	b_1	c_1	a_2	b_2	c_2	d
1533.73	0.123	442.7	183.02	0.834	442.7	442.74

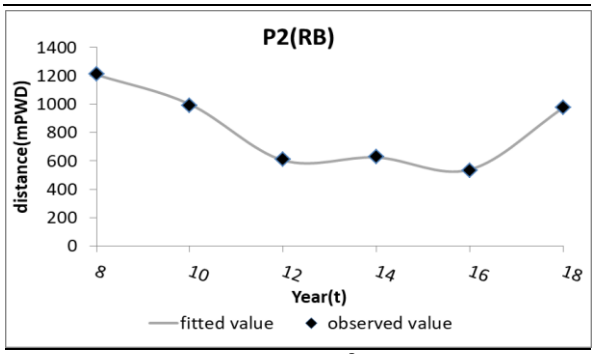

$D=a_1*\sin(b_1*t+c_1)+d$, $R^2=0.999619635$

a_1	b_1	c_1	d
479.2544	0.3313174	1025.6912	0

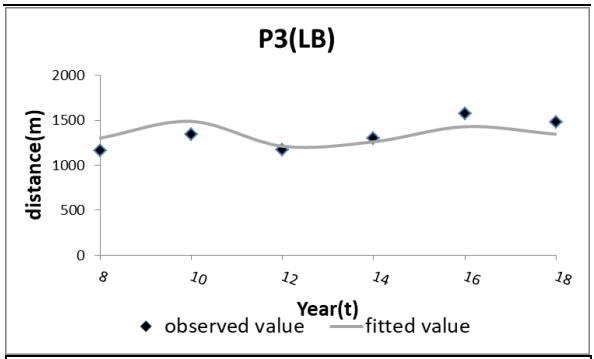

$D= -23.306x + 29.902$,
$R^2 = 0.8917$

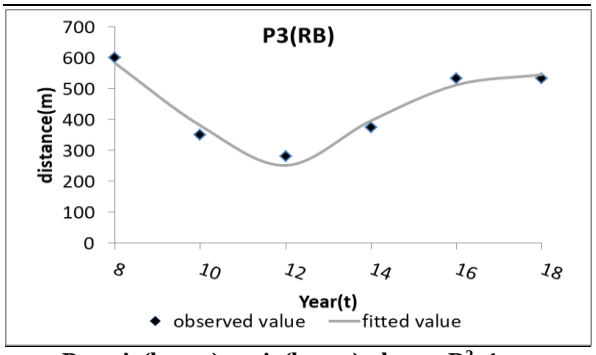

$D=a_1\sin(b_1t+c_1)+a_2\sin(b_2t+c_2)+d$, $R^2=1$

a_1	b_1	c_1	a_2	b_2	c_2	d
188.61	0.383	502.83	68.76	0.945	1.000	0

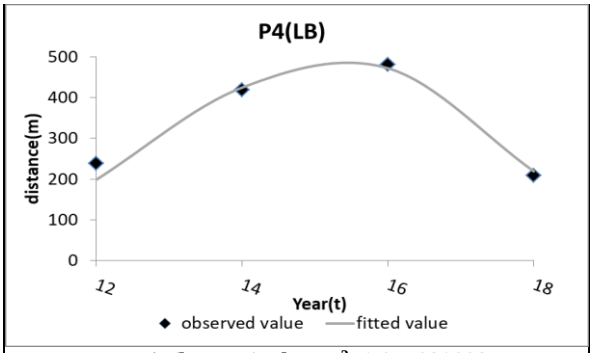

$D=a_1*\sin(b_1*t+c_1)+d, \quad R^2=0.974820992$

a_1	b_1	c_1	d
158.7897	0.93	355	0

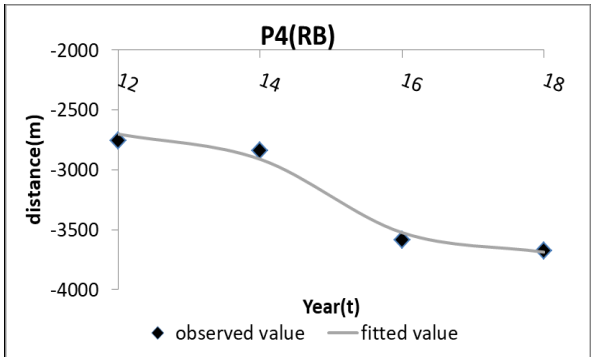

$D=a_1*\sin(b_1*t+c_1)+d, \quad R^2=0.983743638$

a_1	b_1	c_1	d
-520	-0.631	-3200	0

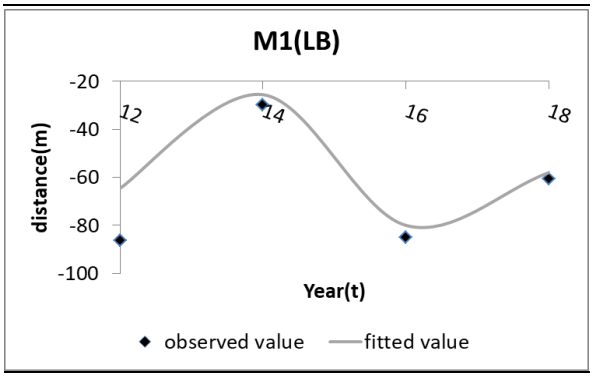

$D=a_1\sin(b_1t+c_1)+a_2\sin(b_2t+c_2)+d, \quad R^2=0.893483424$

a_1	b_1	c_1	a_2	b_2	c_2	d
-22	1.31	1.5	24	0.983	13.84	-45

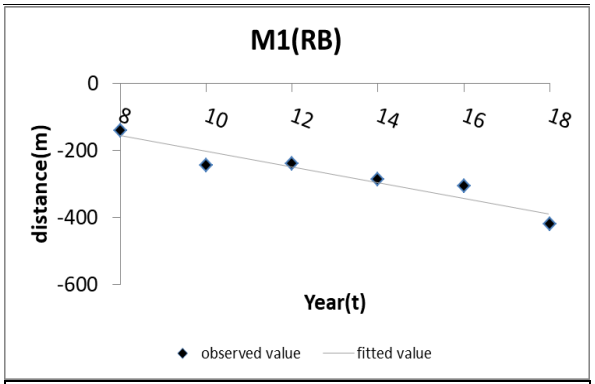

$D= -23.306x + 29.902,$
$R^2 = 0.8917$

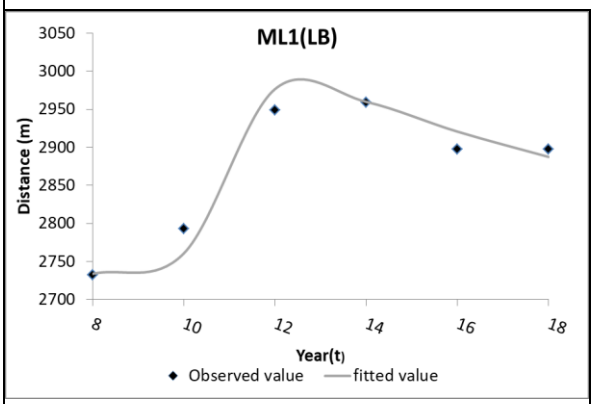

$D=a_1\sin(b_1t+c_1)+a_2\sin(b_2t+c_2)+d, \quad R^2=0.943180163$

a_1	b_1	c_1	a_2	b_2	c_2	d
104.6	0.5522	27.55	60	1.1559	-0.9999	0

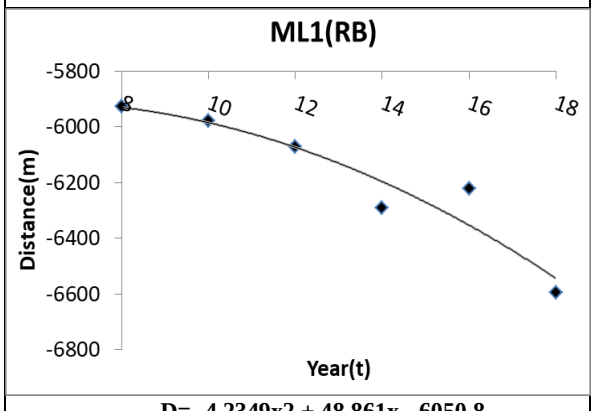

$D= -4.2349x2 + 48.861x - 6050.8$
$R^2 = 0.9038$

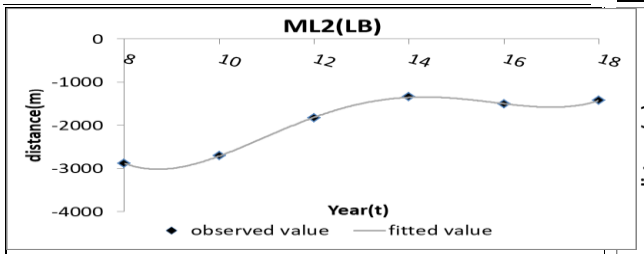

$D= -20.748x2 + 701.67x - 7320$
$R^2 = 0.9155$

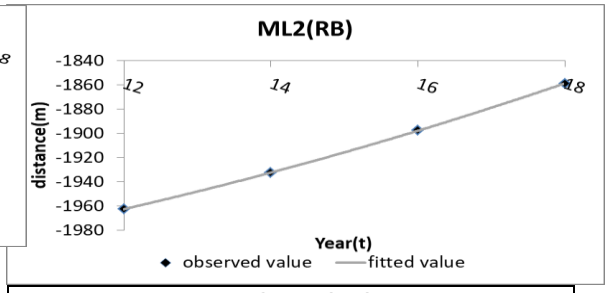

$D= 17.314x - 2172.5$
$R^2 = 0.9966$

Figure 4: Rgression based analysis

3.1.2 Geographic co-ordinate system based analysis

The spatio-temporal analysis is based on the base year of 1973. So, the coefficients of the equations derived from this study may vary if the base year is changed. Considering this consequence, a geographic coordinate system based study is evaluated in which the changes of latitude and longitude with respect to time can be brought under a pattern. Two sections of Padma, one section of Upper-Meghna and one section of Lower-Meghna is used to behold the study (figure 5).

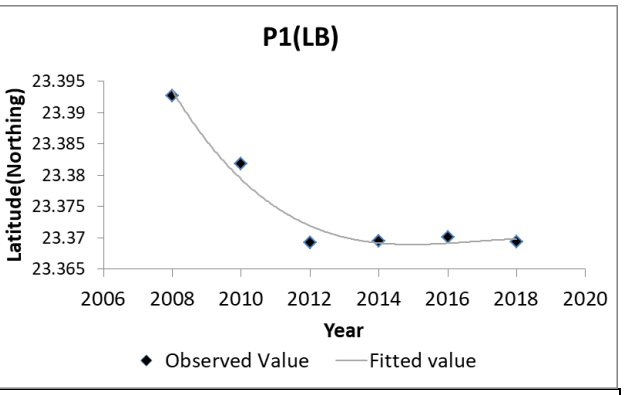

N = -4E-05x3 + 0.2495x2 - 503.18x + 338281
R^2 = 0.9683

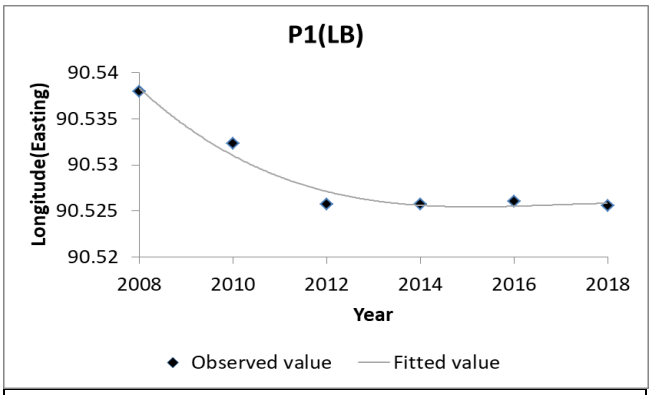

E = -4E-05x3 + 0.2495x2 - 503.18x + 338281
R^2 = 0.9683

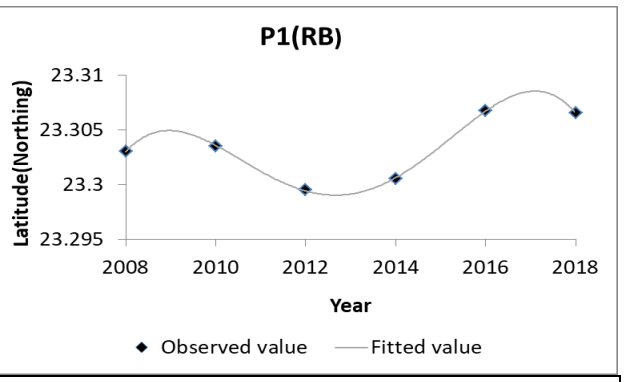

N= -3E-05x4 + 0.2227x3 - 672.34x2 + 902237x - 5E+08
R^2 = 0.9994

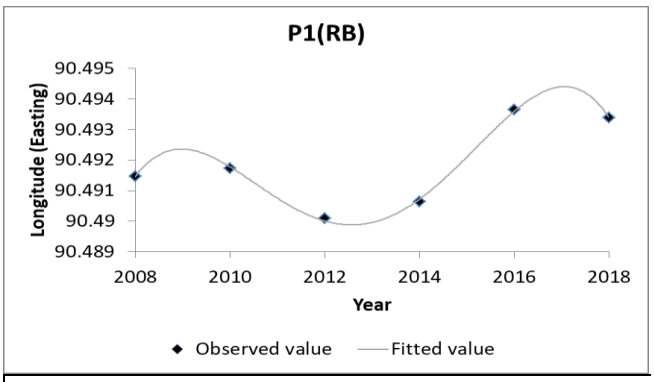

E = -1E-05x4 + 0.1032x3 - 311.47x2 + 417961x - 2E+08
R^2 = 1.0023

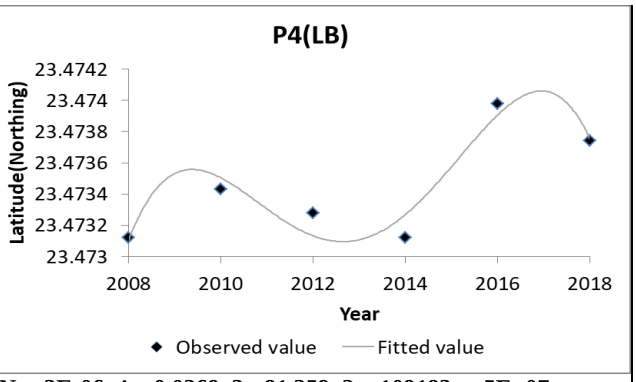

N= -3E-06x4 + 0.0269x3 - 81.359x2 + 109183x - 5E+07
R^2 = 0.9176

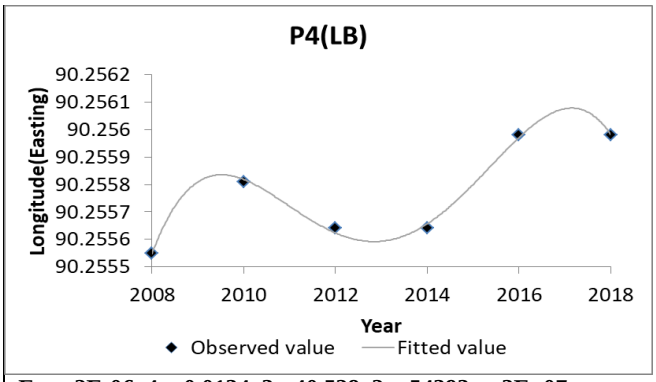

E = -2E-06x4 + 0.0134x3 - 40.528x2 + 54393x - 3E+07
R^2 = 1.2049

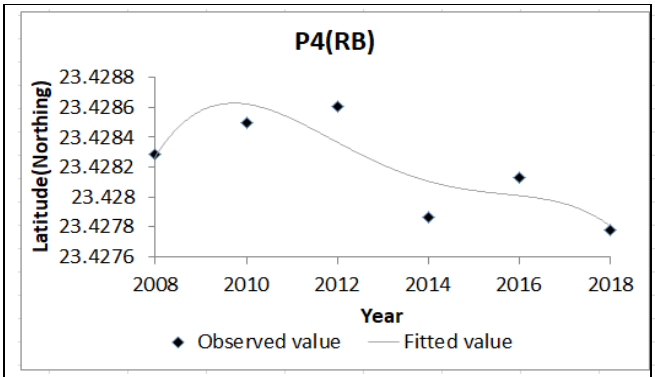

N= -3E-06x4 + 0.0269x3 - 81.359x2 + 109183x - 5E+07
R^2 = 0.9176

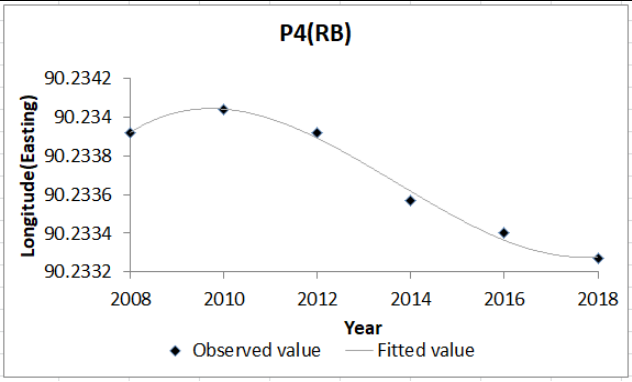

E = 3E-06x3 - 0.0184x2 + 37.03x - 24766
R^2 = 0.9977

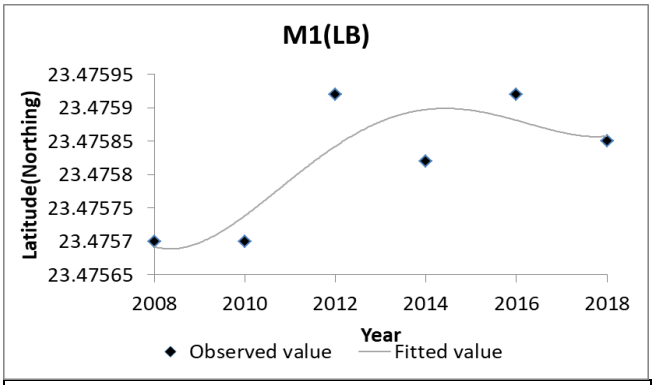

N= 2E-07x4 - 0.0018x3 + 5.3845x2 - 7227.8x + 4E+06
R^2 = 0.8598

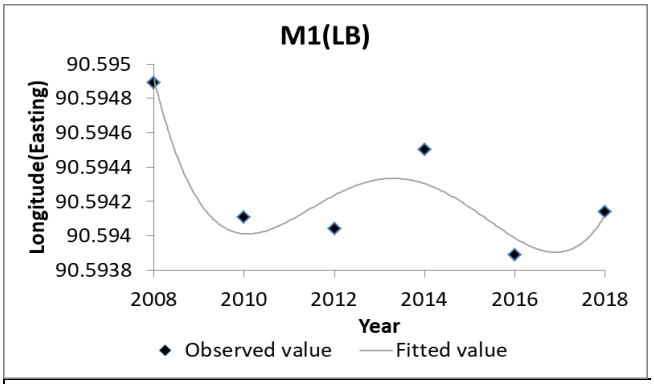

E = 3E-06x4 - 0.0221x3 + 66.826x2 - 89699x + 5E+07
R^2 = 0.9488

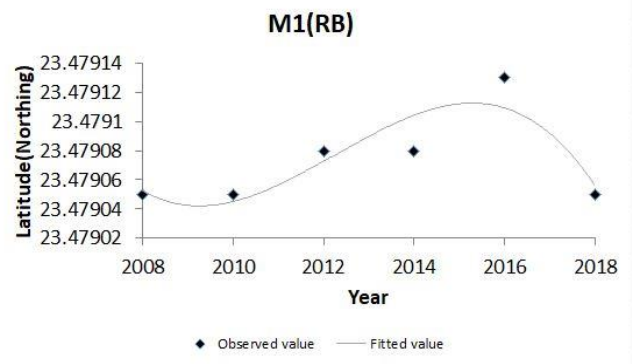

N= -6E-07x3 + 0.0039x2 - 7.8734x + 5304.6
R^2 = 0.764

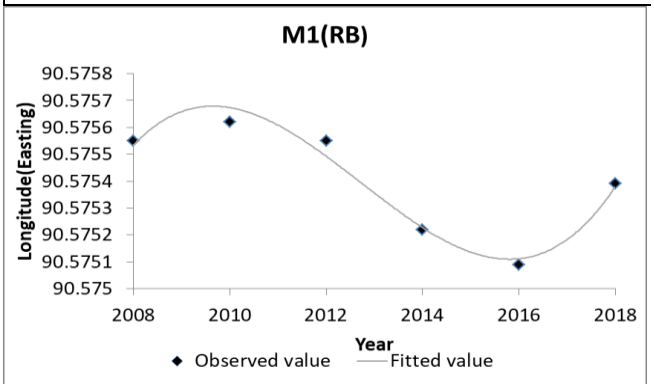

E = 5E-06x3 - 0.0296x2 + 59.5x - 39828
R^2 = 0.9763

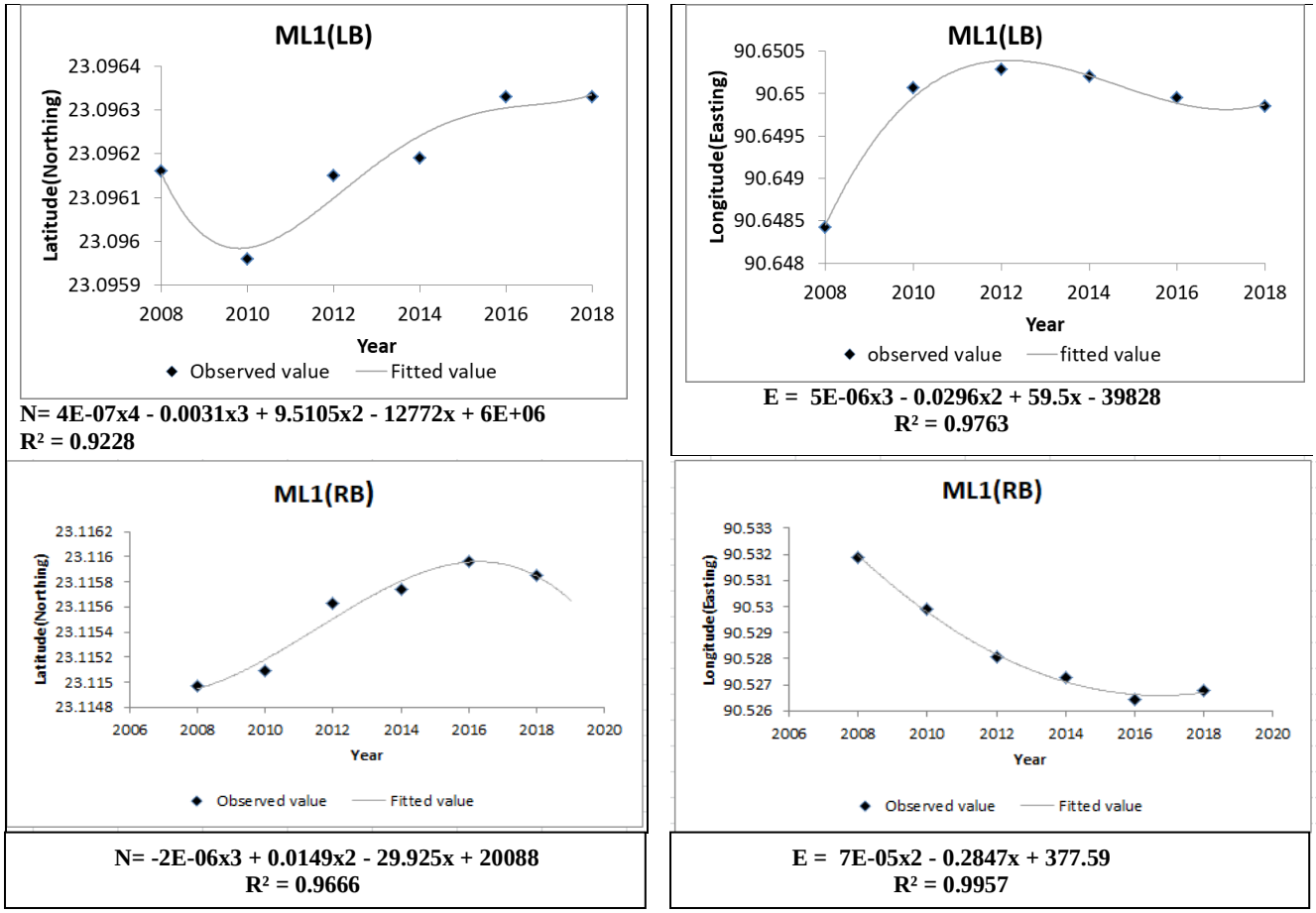

Figure 5:Geographic Coordinate system based analysis

3.1.3. Lstm based analysis

The LSTM program is implemented in MATLAB. The dataset is partitioned with 80% for training, 20% for the testing. The analysis is used for four sections only. The hyper-parameters used to train are carefully tuned and are given in Table 1 and the obtained Predicted value for 2018 and RMSEs (Root Mean Square Value) are shown in Table 2.

Table1. Dataset Partition, Parameters and Hyper-Parameters

Parameters and Hypermeters	Case study
Train data set	4 (80%)
Test data set	2(20%)
Max Epochs	250
time elapsed	4 sec
Initial learn rate	0.005
Gradient Threshold	1
Learn Rate Drop Period	125
Learn Rate Drop Factor	0.2
Verbose	0
Optimizer	Adam

Table 2: Results Obtained from LSTM

Sections	Observed value	Predicted value	RSME
P1LB	-3077.031832	-2.86E+03	164.7068
P1RB	-1982.172877	-2.43E+03	432.1116
P4LB	209.171909	213.3962	189.6368
P4RB	-3673.930572	-3.70E+03	81.4506
M1LB	-60.776865	-67.1754	13.4419
M1RB	-421.104105	-310.4744	66.7011
ML1LB	2897.367771	2.93E+03	29.0464
ML1RB	-6594.58581	-6.24E+03	199.2874

3.2 Comparison Between Approached Methods

The three methods described; Regression based study, Geographic Co-ordinate system based study and LSTM based study have shown their own predictions for different sections of the study area. All of them have shown satisfactory results.Regression based analysis has given the best results as it shows the least error. But LSTM based study has shown greater error because of the small amount of data sets. The error(%) obtained from the three methos are shown in figure 6.

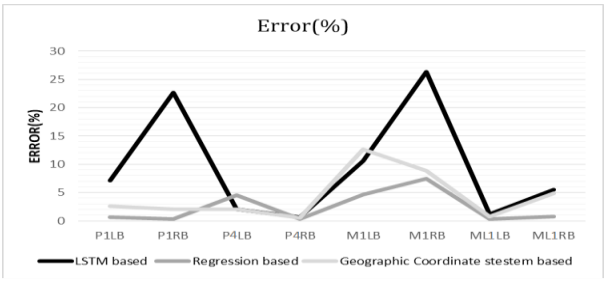

Figure 6: Error(%) from described three methods

3.3 Forecast

Using the regression equations described above, banline shifting for 2020 is forecasted with the regression based study and the geographic co-ordinate based study. It is shown that The results from both of the methods are nearly close to each other (figure 7).

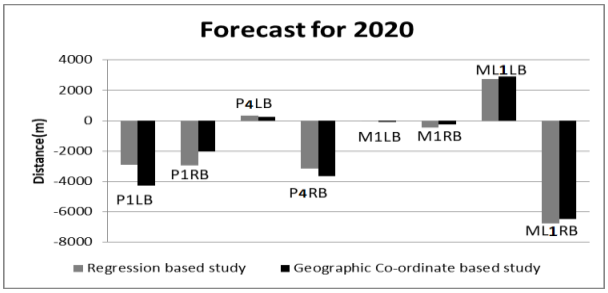

Figure 7: Forecast for 2020

4. CONCLUSIONS

The present morphology at the confluence of Padma and Lower Meghna rivers is such that the width of cross-sections increases considerably at upstream of the confluence, leading to a decrease of stream velocity and consequently the generation of large chars elsewhere. From the analysis of satellite images, it can be realized that major floods occurred in 1974, 1988, 1998 and 2004 impacted on char development and bank shifting of the whole area of interest.

- Over 45 years (1973-2018), the maximum erosion rate for both left bank and right bank are given in table below.The erosion rate is decreased over the last 10 years compared to the last 30 years.

	maximum erosion rate (m/yr)	
River	**Left Bank (m/yr)**	**Right Bank (m/yr)**
Padma	59.25	81.64
Upper-Meghna	8.17	9.35
Lower-Meghna	64.39	146.55

- From the bank line shifting analysis by regression, it is tried to evaluate a specific pattern of shifting, which follows a sinusoidal equation D=[(a1sin(b1t+c1)+a2sin(b2t+c2)+d)].This study is quite satisfactory as the R^2 value varies between 0.8 to 1, showing a little error.This analysis is quite suitable for small amount of data.

- The Geographic co-ordinate system based approach seems satisfactory too, as the R^2 values are in the range of 0.7-0.99.But the magnitude of latitude and longitude are very delicate to measure from the satellite images,nevertheless the analysis shows enough suitability.

- The LSTM based analysis also worked well enough to predict the bankline shifting process.But this process showed much error because of small amount of data. This process is highly helpful with a huge amount of data sets when regression based analysis is not very helpful.

REFERENCES

Ahmed. (1989). Study of some Bank Protection works in Bangladesh" M.Sc Engg.(WRE) Thesis, Dept of Water Resource Engineering, BUET, Dhaka.

Ali. (1975). Comprehensive Plan for protection of Chandpur town and Irrigation Project,CE, Planning,BWDB,Dhaka.

Galay, V. (1980).”Course of River Bed Degradation” Water resource Research,vol1.19,No.5,pp.1057-1090.

Khan, M. (1986). Morphological survey in sediment sampling in Bangladesh" Proceedings of Regional Workshop on erosion and sediment transport processes, UNESCO-BUET, Dhaka.

Pegg, V. G. (1974). Report on the Stabilization of Meghna River -Chandpur Irrigation Project" Bangladesh Water Development Board and Ministry of Flood Control & Govt. of Bangladesh

Rahman. (1978). A study on the erosion of river Padma", M.Sc. Engineering thesis, Department of water Resources Engineering, BUET, Dhaka.

Shume. (2008). A study on effect of char movement on river morphology around Upper Meghna-Dakatia confluence.

Proceedings of the 5th International Conference on Civil Engineering for Sustainable Development (ICCESD 2020), 7~9 February 2020, KUET, Khulna, Bangladesh (ISBN-978-984-34-8764-3)

NUMERICAL MODELLING FOR PLANNING AND HYDRAULIC DESIGN OF ROAD AND ASSOCIATED ROAD STRUCTURES IN COMPLEX PHYSICAL AND HYDROLOGICAL SETTINGS

Kanungoe Pintu*[1], Al Imran Abdullah[2] and Uddin Md. Alim[3]

[1]Chief Scientific Officer, River Research Institute, Bangladesh, e-mail: pintu_kanungoe@yahoo.com
[2]Scientific Officer, River Research Institute, Bangladesh, e-mail: imran0301086@gmail.com
[3]Director General, River Research Institute, Bangladesh, e-mail: rribd@yahoo.com

***Corresponding Author**

ABSTRACT

Sunamganj-Netrokona-Mymensingh road is a regional road of the Roads and Highways Department of Bangladesh. The road is indented to establish smooth roadway communication facility between the northeast and the northcentral regions of the country. However, because of complex physical and hydrological settings of the low-lying haor (wetland) area from Sachna Bazar to Golakpur Bazar of the Jamalganj upazila under Sunamganj district, the intended road communication could not be established yet. People of this region do not have easy access to national road network and largely depend on waterway communication. However, establishment of this road link is the most challenging task as it will run through an environmentally and hydrologically sensitive area. The river Surma flows along the likely road alignment and the road alignment has to cross either the Surma river or the Baulai river together with many other drainage routes. There is also distinct connectivity between rivers and haors. Since rainfall on the adjacent Indian state Meghalaya largely affects flooding in the study area, the rainfall pattern of the upstream catchment has great influence here. The Surma-Kushiyara basin receives water from the transboundary catchments of the Meghalaya, the Barak and the Tripura situated to the north, east and southeast respectively across the border in India. In view of the above mentioned facts a number of hydro-morphological and environmental aspects related to the proposed road project have been crucial for investigation.River Research Institute has conducted a comprehensive hydro-morphological study and EIA for construction of the road with appropriate alignment and road structures to minimize the adverse impacts of the road project on natural flooding, drainage and sedimentation. The study is based on extensive field survey data that include cross-sections of rivers and drainage routes, topographic data, data on infrastructure, surface and subsurface soil data, environmental data etc. The secondary data include historical hydrological data of the rivers, maps, time series satellite images etc. A two-dimensional model covering an extent of about 31km of the Surma river and parts of the Baulai and the Rakti rivers together with parts of their floodplains has been developed using modelling software MIKE21C. Flood frequency analysis has been done with historical hydrological data using General Extreme Value distribution and Extreme Value Type-1 distribution to determine different probable discharges and water levels at different gauge stations on the rivers. Based on the analyzed data two hydrological scenarios have been identified that are critical for the road project. Baseline hydrological and hydraulic conditions in the study area have been investigated for the selected critical hydrological scenarios. Based on baseline hydro-morphological and environmental conditions three alternative options of the proposed road alignment have been devised and assessed against a set of criteria. A standard screening process has been followed for selection of the preferred option. Hydraulic and hydrological assessment of the preferred option have been made for the two preselected critical hydrological scenarios and location and dimension of the road structures have been fixed following trial and error method. The study has come up with some important outcomes namely type, location and dimension of the road structures, locations and extents of road embankment slope protection works and their hydrologic and hydraulic design variables, design flood level, wave runup, road formation level, through bridge velocity, bridge scour etc.

Keywords: *Haor, Drainage, Scour, Wave runup, Flooding.*

1. INTRODUCTION

The study area is located in the North East Region (NER) of Bangladesh (Fig. 1). This region comprises an area about 22,000 km^2 which can be further subdivided into six distinct sub regions. The project area belongs to the Baulai sub region (5000 km^2) and the Surma sub region (4500 km^2). It means the total a result of excessive rainfall. The local and cross border flows and the internal rainfall influence the water level in the rivers and floodplains of the area. This is an interactive zone where flow area covered by these two sub regions is about 43% of the total area covered by the NER. These sub-regions are located in one of the depressed portions of the country. The topography of the study area along with other parts of the NER had undergone structural transformation creating depression in the remote past. The bowl-shaped depression is popularly known as haor and remains inundated for 6-7 months during the monsoon. Within the haor there are perennial and seasonal water bodies. Most of the rivers in these areas are originated from nearby hilly areas of India. These rivers are extremely flashy that is characterized by sudden and wide variation in flow as characteristics change with the rise and fall of water levels. The floodplain flows in the study area occur due to overflow of Surma, Baulai, Jadukata-Rakti and other small rivers. Therefore, during monsoon the study area remains deeply flooded. The flood water drains out with the fall of water level in the Surma-Baulai system. During normal flood period the rainwater is drained to the adjoining rivers through the link channels and small rivers following the flow directions. The average annual rainfall in the study area is 4000mm. One of the functions of flash floodwater is to carry sediments, which are eroded from the hilly catchment area. The sediments carried by the rivers are also deposited along the river banks resulting in an increase in the land elevation there compared to the surrounding low-lying areas. These elevated lands are inhabited by people. Therefore, patches of small villages almost all along the rivers and channels are visible in the study area. These village areas are densely vegetated with well grown trees.

Roads and Highways Department (RHD) of Bangladesh has decided to construct the missing stretch of the Sunamgonj-Netrokona-Mymensingh-Dhaka road by establishing road link between Sachna Bazar and Golakpur Bazar of Sunamganj district. If this road link can be established it would be easy to connect this road with existing Netrokona-Mymensingh-Dhaka road because establishment of this road link is the most challenging task as it will run through an environmentally and hydrologically sensitive low-lying haor (wetland) area. The river Surma flows along the likely road alignment and the road alignment has to cross either the Surma river or the Baulai river together with many other drainage routes. Understanding of the prevailing hydrological regime is of utmost importance to decide about appropriate road alignment and road structures

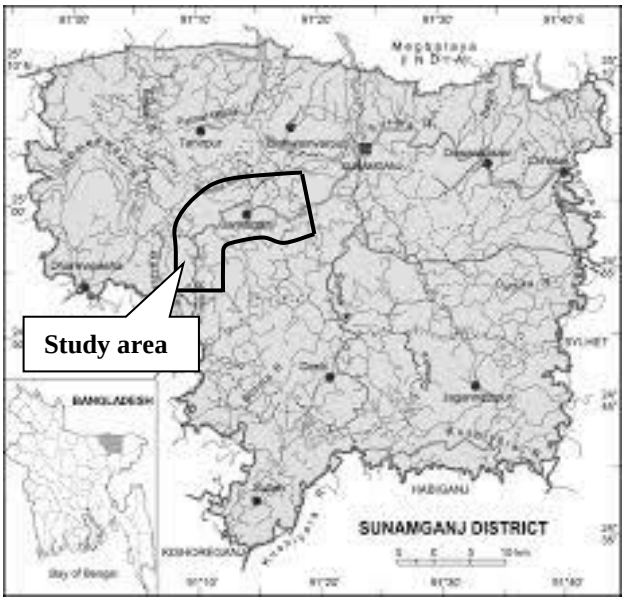

Figure 1: Location of the study area in the Sunamganj district

The Surma is the major river in the study area and there is distinct connectivity between rivers and surrounding haors. The connectivity between the Surma river and the haor area is a major issue for fixing the proper road alignment and road structure locations for establishing the proposed Sachna-Golakpur road link. Since rainfall on the adjacent Indian state Magalaya largely affects flooding in the study area, the rainfall pattern of the upstream catchment has great influence here. The Surma-Kushiyara basin receives water from the transboundary catchments of the Meghalaya, the Barak and the Tripura situated to the north, east and southeast respectively across the border in India.

Road embankment through the haors creates obstruction to natural flow of water and is subjected to wave actions. Also bridges and its accessory structures in general often constrict the flow area under the bridge and the bridge piers enhance this constriction resulting in increase of speed, acceleration of scouring process, backwatering of stage etc. Mathematical modeling is state-of-the-art technology applicable in planning and design and construction stages of the road embankment and road structures to ensure safe and economic design of the same. The technology can also be applied for devising suitable mitigation measures to counteract any negative impact of the road project.

Under this circumstance RHD has envisaged a comprehensive hydro-morphological study and EIA for construction of Sancha-Golakpur road with appropriate alignment to minimize the adverse impacts of the road project on natural flooding, drainage and sedimentation. The Surma is a sinuous river at and around the study reach. Since the structures like bridges across the river and road embankment in a hydrologically complex region (haor areas) will be constructed, a number of issues are there to be addressed properly before constructing the bridges/culverts and road embankment. The bridges/culverts and road embankment might have significant impacts on existing hydrological regime as well as environmental quality of the project area if not properly planned and designed.

River Research Institute (RRI), Faridpur, Bangladesh has conducted hydro-morphological study and EIA to support planning and hydraulic design of the road project. Necessary topographical, hydrological, hydrographic and sediment data have been collected through a field survey campaign. Historical hydrological data of the rivers concerned and satellite images of the study area have been collected from available sources.

The collected data have been processed and analysed to the extent of deriving necessary inputs for the MIKE21C model that has been developed for reproducing baseline hydrological and hydraulic conditions in the study area as well as for hydrological assessment and hydraulic analysis of the selected road alignment and road structures. The two-dimensional model covers the whole study area (rivers and floodplains). The tool (MIKE21C) is suited for river and floodplain hydro-morphological studies and includes modules to describe flow hydrodynamics, sediment transport, alluvial resistance, scour and deposition, bank erosion and planform changes (DHI, 2006). This paper highlights the application of the model in gaining understanding of the flow conditions in the study area for two critical hydrological scenarios and in deciding about appropriate road alignment and location, type and dimension of the road structures and their hydrological and hydraulic design parameters.

2. METHODOLOGY

In order to conduct the study needed primary and secondary data and other relevant information have been collected. The collected data include historical hydrological data (discharge and water level), digital elevation model (DEM) of the study area, cross-sections of the rivers, information on existing metalled and unmetalled roads and road structures, physical features on both sides of the Surma river in the project area, sediment samples, satellite images, maps, photographs etc. The secondary data have been collected from available sources whereas the primary data have been collected through field reconnaissance and field survey campaign (River Research Institute, 2017). A final road alignment survey has been conducted along the proposed road alignment covering a 100m corridor. Sub-soil investigation has been carried out at all proposed road structure locations. The collected data

have been processed and analyzed to the extent of gaining understanding of the present physical conditions of the rivers and the low-lying land surrounding the rivers in terms of their vertical and lateral stability and physical settings of the study area and also deriving information to use as model inputs. A two-dimensional model covering an extent of about 31km of the Surma river and parts of the Baulai and the Rakti rivers has been developed using modelling software MIKE21C. The initial bathymetry of the model is formed by use of the recently surveyed bathymetric and topographic data as well as DEM of the study area. The computational grid and initial bathymetry of the model is shown in Fig. 2 and Fig. 3 respectively. Practically flow enters into the model domain through two boundaries and leaves model domain through another two boundaries. The flow of the Surma river enters into the model domain through upstream boundary whereas flow from Meghalaya Hills enter into the same through right boundary. Water leaves the model domain through downstream boundary (Surma-Baulai river) as well as through left boundary into the haor. Since haors act as storage reservoir during monsoon, majority of the flow leaves the model domain through downstream boundary.

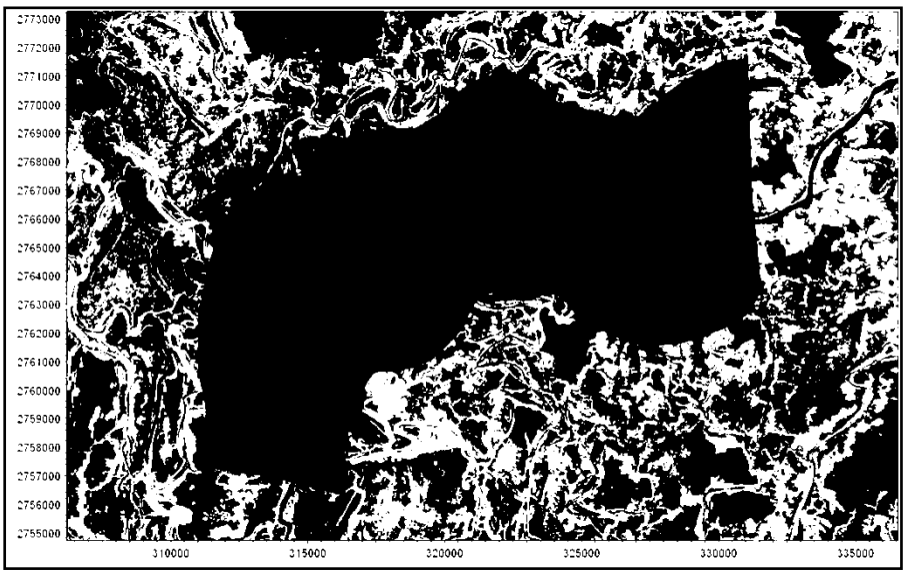

Figure 2: Curvilinear computational grid of the model

Figure 3: Initial bathymetry of the model

Downstream boundary data of the model are obtained from the recorded historical water level data at Sukdevpur, which is located at just downstream from the model downstream boundary. On the other hand, upstream boundary data of the model are obtained from the recorded historical discharge data at Sunamganj. It is to be noted here that the discharge gauge station at Sunamganj town is situated at about 12.5km (along the river) upstream of the model upstream boundary. During monsoon water enters into and leaves the river almost throughout this 12.5km stretch. There is no other discharge gauge station between Sunamganj town and model upstream boundary. Therefore, the discharge records at Sunamganj town have been used to determine the model upstream boundary. The right open boundary data of the model have been determined from historical discharge records of the Jadukata river at Laurerghar. Upon entering the Sunamganj plain from the Meghalaya Hills, the Jadukata river gets divided into a number of rivers. During monsoon flow enters into the model domain through these rivers as well as through overspill from these rivers. During generation of right boundary of the model this fact is taken into account.

Flood frequency analysis with available historical discharge and water level data at different gauge stations on the rivers that are hydrologically connected with the study area has been made for determination of different return period discharges and water levels. The GEV and EVI methods have been employed for frequency analysis of water level and discharge data. At first, the annual maximum water level and discharge is determined for each gauge station for the available years. It is found from the plots of the fitted GEV and EVI distributions together with 95% confidence limits for the water level and rated discharge data at Sunamganj, Sukdevpur and Laurerghar that GEV distribution fits the annual maximum water level and discharge data well relative to EVI distribution. Therefore, the water level and discharge obtained from GEV distribution for various return periods have been accepted. Since there is no water level or discharge gauge station in the model domain, the water level along the proposed road for different return period discharges including the design discharge have been determined from model simulation results. The water level at different road structures and discharges through them for different return period discharges have also been determined from model simulation results with structures in place.

As the flow conditions in the study area are very complex and depend on a number of factors namely magnitude of discharge and water level in the Surma river, magnitude of flash flood discharge from the Meghalaya Hills and water level of the Meghna river at the outfall of the Suma river. The extreme flow conditions result from the combination of these factors. But it is less likely that the peak discharges of the Surma river and the Jadukata river and peak water level of the Meghna river may occur at the same time. It is found from the hydrological data that simultaneous occurrence of an extreme event in the Surma river and large discharge from the Meghalaya Hills result in severe flood condition in the study area. During a flood event when flood stage goes up flow occurs not only through the rivers but also over the floodplain. Generally floodplain flow occurs in a direction more or less parallel to the Surma river flow direction. Therefore, such an occurrence has been considered as one critical hydrological scenario for the road project. Another critical hydrological scenario for the road project to decide about appropriate type, location and dimension of the road structures occurs if flash flood water from the Meghalaya Hills arrives in the study area during falling stage of Surma river flood or low stage of the Surma river. Based on these facts two critical hydrological scenarios have been developed for model simulation in base condition and with road and road structures in place.

On the basis of base line flow conditions in the study area, relevant factors controlling road alignment selection and identified issues and constraints three feasible alignment options of the road have been devised (Fig. 4). Alternative road alignment options are then assesses under a set of criteria and sub-criteria taking into account community and agency concerns. A two-step screening process namely advantages and disadvantages matrix and evaluation criteria matrix has been conducted for elimination and selection of options. Among the three road alignment alternatives, two options (Option-2 and Option-3) have been eliminated stating the reasons and Option-1 has been retained for further assessment as it provides a number of advantages and community attitude towards this road alignment is very positive.

Hydrological and hydraulic analysis of the selected road alignment is made for two pre-selected critical hydrological scenarios and type, location and dimension of the road structures have been selected following trial and error method. Four different arrangements of road structures have been tested to arrive at final decision as to appropriate type, location and dimension of the road structures. Based on model results wave runup, design water level and formation level of the road, design water level, discharge and maximum velocity for each road structure, scour depth at bridge piers and abutments, road stretches where road embankment slope protection works are needed etc. have been determined.

3. RESULTS AND DISCUSSIONS

The base line flow conditions in the study area have been investigated for two critical hydrological scenarios as mentioned earlier. Scenario one represents conditions when 50 year event (design event) occurs simultaneously in the Surma and the Jadukata rivers. On the other hand, scenario two represents conditions when a flash flood of 50 year return period suddenly occurs from the Meghalaya Hills during recession period of the Surma river. Both scenarios have been obtained by synthesizing recorded events. It is found that 50 year discharge of the Surma and the Jadukata river is 3567m3/s and 3184m3/s at Sunamganj town and Laurerghar respectively. On the other hand, 50 year water level of the Surma-Baulai system at Sukdevpur is 8.66mPWD;

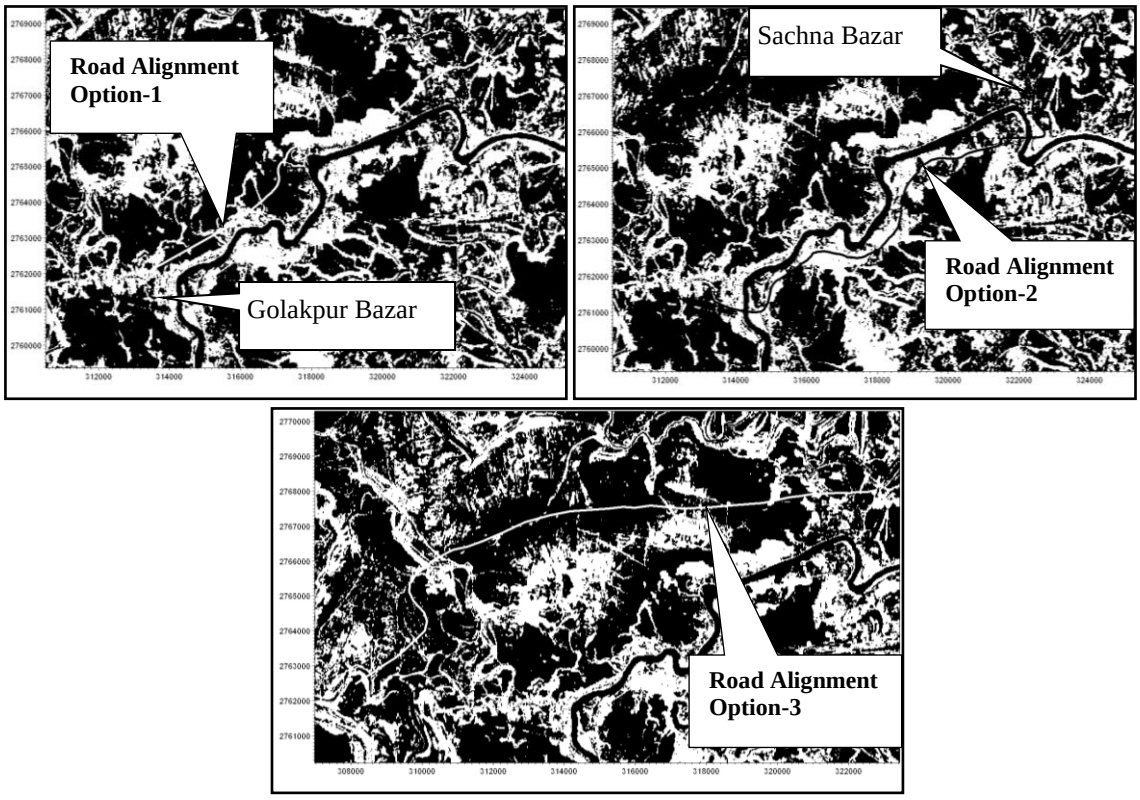

Figure 4: Devised road alignment options

3.1 Baseline Conditions

Velocity field and water depth in the study area for hydrological scenario one have been shown in Fig. 5 and Fig. 6 respectively. It is evident from the Fig. 5 that during an extreme event flow occurs both in the rivers and over the floodplain with a low velocity (<0.5m/s) and there is no noticeable difference between the magnitude of flow velocity in the river and over the floodplain. It is also noticeable from Fig. 5 that floodplain flow occurs more or less parallel to the Surma river. Since the selected road alignment runs more or less along the right bank of the Surma river it is less likely that the cross-flow

will occur through the road openings except for the upstream part of the road link where water from the river flows out over the river bank towards the low-lying floodplain. However, this is not the case for hydrological scenario two. A flash flood from the Meghalaya Hills during falling stage of the Surma river causes flow concentration at Baulai outfall as the river drains the north floodplain (haor area). As a result, flow velocity of the Surma river downstream of the outfall becomes higher than that upstream of the same. This occurrence is reported afterwards with road and road structures in place condition. It is found from the simulated water levels that the design water level (for 50 year discharge) of the proposed road varies from 8.52mPWD to 8.55mPWD from Golakpur end to Sachna Bazar end respectively. It is evident from the Fig. 6 that low water depth occurs over a narrow strip of land on both sides of the Surma river almost all along the river in the study area. The water depth along these strips of land having relatively higher elevation varies from 0m to 3m. On the other hand, relatively higher water depth occurs in the low-lying haor areas to the south, south-east and north-east of the Surma-Baulai confluence.

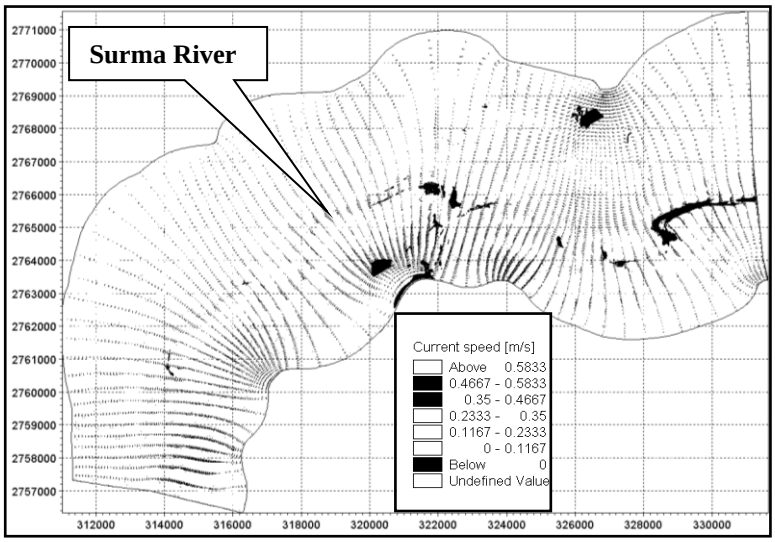

Figure 5: Velocity field in the study area for hydrological scenario one

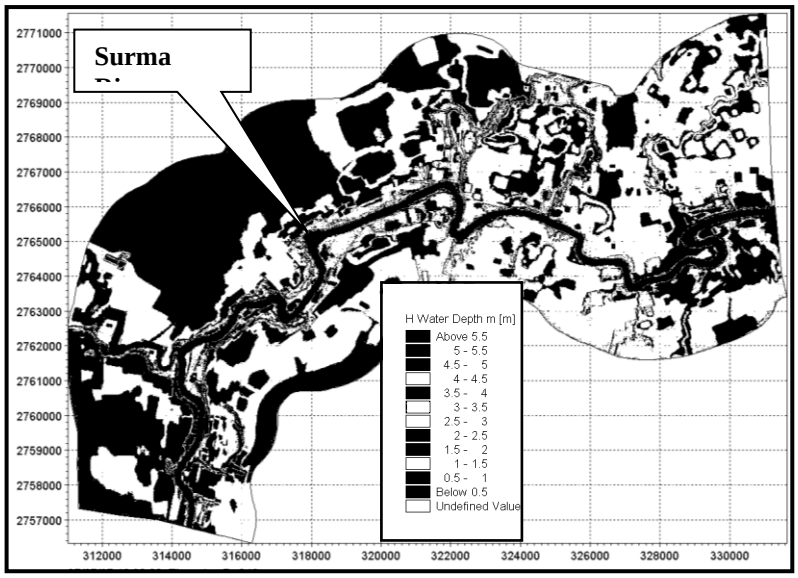

Figure 6: Water depth in the study area for hydrological scenario one

The Sachna-Golakpur road alignment is, therefore, selected in such a way so that the areas of high flood depth can be avoided. There are small villages and other community facilities and private properties on the elevated land (levee) along the Surma river. Therefore, the selected road alignment creates fewer disturbances to wetland biodiversity and ecosystem and integrates well with the existing community facilities. However, in order to ensure minimum disturbance to existing hydrological regime sufficient number of road openings have to be provided at appropriate locations.

3.2 Project Conditions

Based on the model simulation results in base condition and field information the type, location and dimension of the needed road structures have been determined and introduced in the model to assess their hydraulic performance. Hydrological assessment and hydraulic analysis of the road and road structures have been conducted for the two critical hydrological scenarios as is done in base condition. Initially 12 road structure (bridge) locations have been fixed to allow for smooth passage of flood flow as shown in Fig. 7. The length of the bridges varies from 25m to 190m. It is to be noted here that initially a total of 686m bridge opening throughout the road having length of about 12.2km has been considered. The percentage of considered road opening is about 5.62% of the total length of the road. Based on the performance of the structure's necessary modifications in the structure locations and dimensions have been made for reassessment of their performance. In this way after fourth trial the required type, location and dimension of the road structures have been determined. The effect of the road and road structures on existing hydrologic and hydraulic conditions has been assessed by

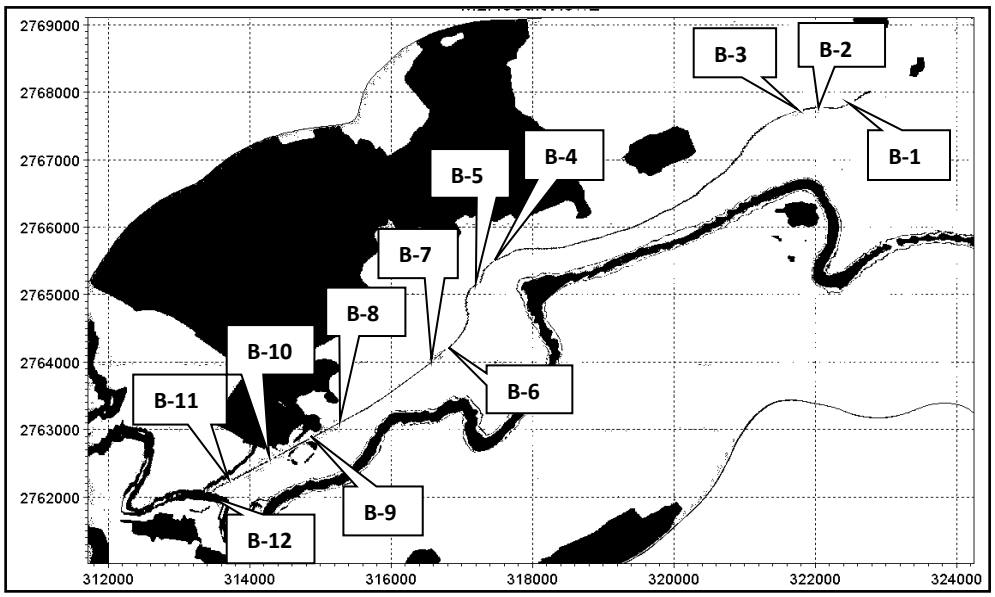

comparing the model results with that under base (without project) condition.

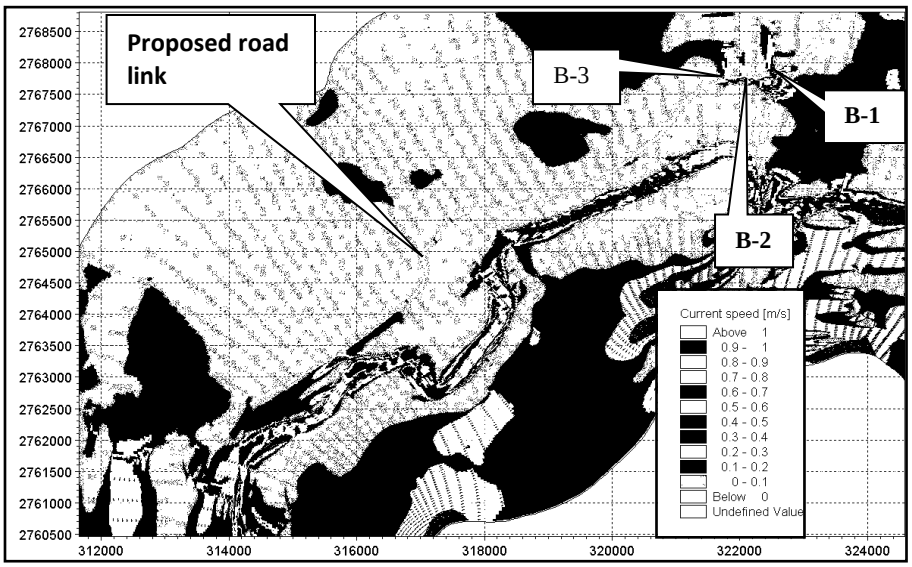

Figure 7: Location of initially considered bridges on the proposed road

The velocity field in the study area for hydrological scenario one and with initially considered bridges has been shown in Fig. 8. It is evident from the figure that under this hydrological scenario cross-flow occurs only through Bridge-1 to Bridge-3 (B-1 to B-3). There is very little or no cross flow through other considered bridges. However, exactly opposite condition is found for hydrological scenario two (Fig. 9). In this case, cross flow does occur through B-4 to B-12.

Bridge-12 (B-12) is situated over the Baulai which drains the haor area. Under hydrological scenario two substantial flood flows will enter into the Surma river through the Baulai river as well as over the nearby low-lying land. Since the proposed road obstructs this flow there should be sufficient road opening there. It is to be noted here that beyond southwest end of the proposed road link there is submersible road over the floodplain that has to be upgraded with sufficient road openings to establish the Sunamganj-Netrokona-Mymensingh road communication. It is found from the hydrological scenario one simulation results that about 3000m^3/s discharge may pass over the floodplain. Addressing this issue is beyond the scope of this study.

Figure 8: Velocity field for hydrological scenario one and initial arrangement of road structures

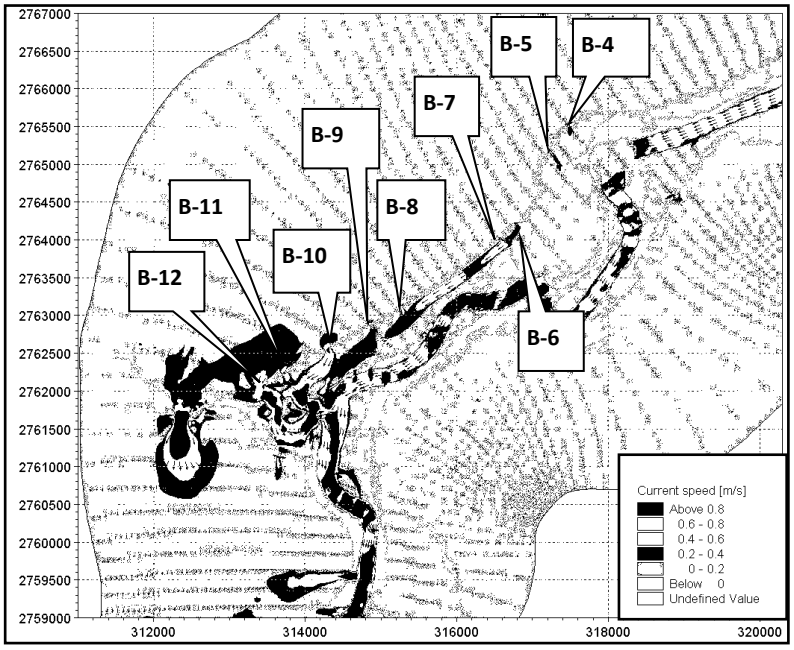

Figure 9: Velocity field for hydrological scenario two and initial arrangement of road structures

Based on the outcomes of the hydrological and hydraulic assessment of the initially considered arrangement of road structures, the number, location and dimension of the road structures have been changed for assessment, which is termed as first trial. In this way, four trials have been made to arrive at a decision as to appropriate number of road structures and their locations and dimensions. Analysis of model results shows that hydraulic performance of the road structures under fourth trial is satisfactory. The number and location of road structures under fourth trial are shown in Fig. 10.

The velocity field in the study area for hydrological scenario one and two is shown in Fig. 11. The discharge through each bridge has been determined from the model results and appropriate bridge length has been determined using Lacey's formula as shown in Equation (1).

$$W = 1.811C\sqrt{Q} \quad (1)$$

Where, W is effective width of waterway for the bridge (m), C is a co-efficient and Q is the design discharge (m^3/s).

Total length of road opening for finally decided ten bridges is 539m which is about 4.42% of the total length of the proposed road. It is found that one side of the road could be subjected to wave action at a number of locations. Therefore, wave runup has been calculated based on available wind speed record and information on average water depth, fetch length, angle of wave attack and slope of road embankment. Standard chart and formula have been used for wave runup computation. It is found that wave runup is 1.06m which is slightly higher than standard free board (1m). Therefore, formation level of the road has been computed by adding wave runup with design flood level.

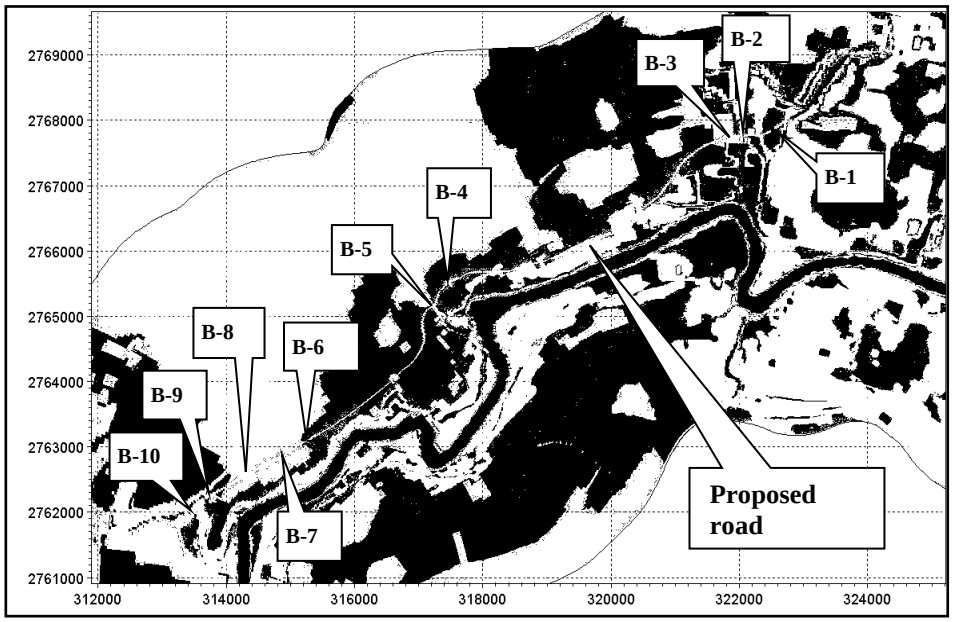

Figure 10: Final location of the road structures (bridges)

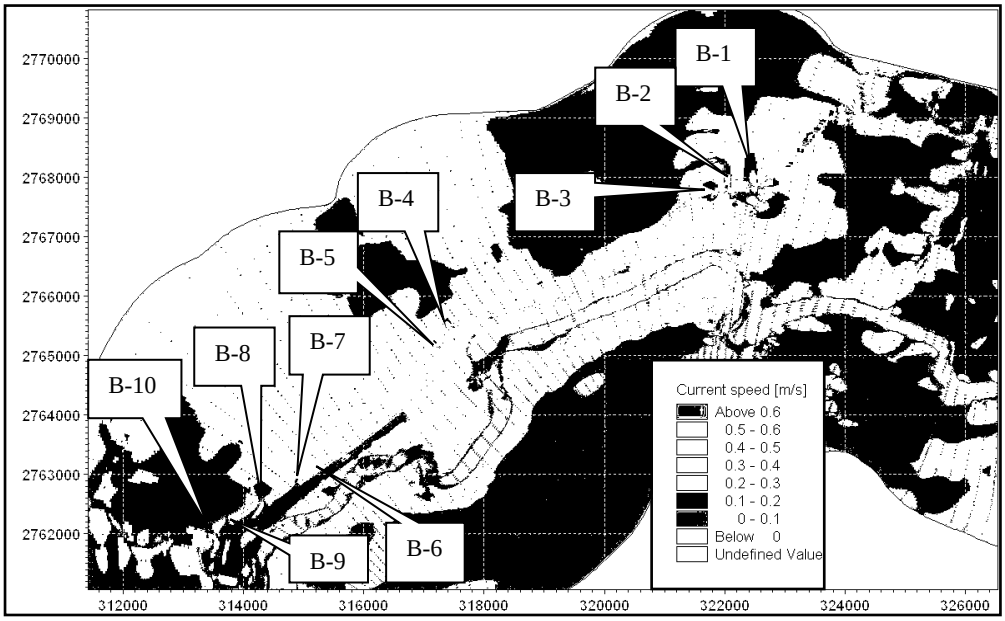

Figure 11: Velocity field for hydrological scenario one and final arrangement of road structures

Formation level of the road varies from 9.58mPWD at Golakpur end to 9.61mPWD at Sachna Bazar end. The expected minimum scour level at bridge piers and abutments for each bridge has been determined by using standard empirical formula and model generated hydraulic parameters. The hydrological and hydraulic design parameters of the bridges have been shown in Table 1. The chainages are from the starting point of the road at Sachna Bazar end (northeast end).

Table 1: Hydrologic and hydraulic design parameters of the road structures (bridges)

Road Structure description	Chainage (km)	Length (m)	Design discharge (m3/s)	Design water level (mPWD)	Maximum velocity (m/s)	Pier Scour level (mPWD)	Abutment scour level (mPWD)
Bridge-1	0.305	50	103	8.55	0.76	-2.59	-3.86
Bridge-2	0.725	50	88	8.55	0.56	-3.57	-3.26
Bridge-3	0.911	50	85	8.55	0.40	-4.50	-0.92
Bridge-4	6.092	31	26	8.54	0.63	-2.09	-2.70
Bridge-5	6.586	37.5	56	8.54	0.60	-4.25	-6.51
Bridge-6	9.554	28	33	8.54	0.76	-3.20	-3.87
Bridge-7	10.01	43.5	82	8.53	0.78	-4.95	-6.15
Bridge-8	10.65	93	245	8.53	0.97	-6.45	-7.50
Bridge-9	11.30	81	191	8.53	1.20	-6.78	-7.11
Bridge-10	11.722	75	168	8.53	0.88	-6.38	-1.16

It is found from the model result that during an extreme event water surface slope in the study area gets very mild. Maximum water level in the study area at and around the proposed Sachna-Golakpur road under hydrological scenario one has been shown in Fig. 12. It can be inferred from Fig. 12 that with proposed bridges in place afflux is negligible. It is also found from the model results that slope protection works along both sides of the road will be needed at some road stretches particularly where water depth is very high during the monsoon season.

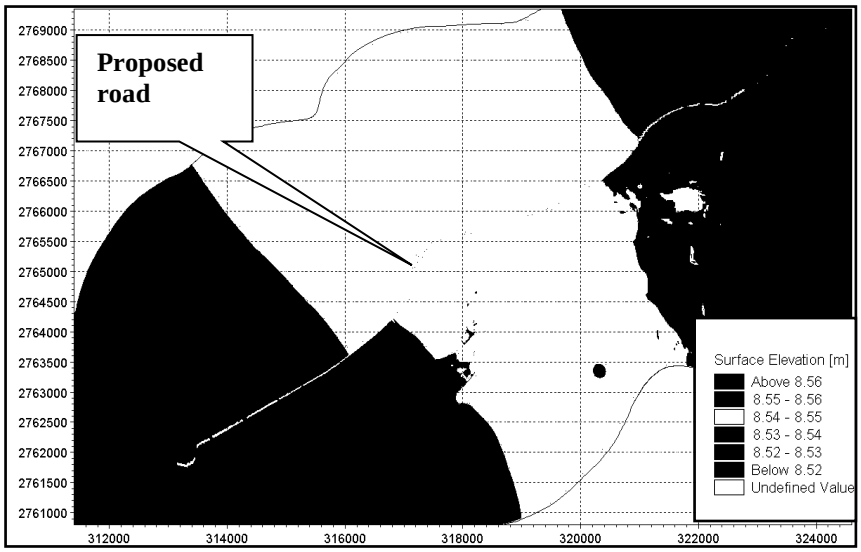

Figure 12: Design water level along the proposed road

The identified locations have been reported for taking necessary road embankment slope protection measures. It is revealed from the examination that all road approaches have to be protected from damage against parallel current by constructing slope protection works.

4. COCLUSIONS

The following key conclusions have been drawn from the study.

In order to establish the proposed Sachna-Golakpur road link in the low-lying haor area where hydrology is very much complex due to a number of factors, all relevant issues have to be taken into account. The Surma is the main river in the study area whereas the Baulai and the Rakti are important tributaries of the Surma. These rivers drain the haor area during recession period of the Surma river flood. The rivers are flashy in nature. 50 year return period discharge of the Surma and the Jadukata river is 3567m^3/s and 3184m^3/s at Sunamgonj town and Laurerghar respectively. On the other hand, 50 year return period water level of the Surma-Baulai system at Sukdevpur is 8.66mPWD.

The existing connectivity between the rivers and floodplain is very important for maintaining existing rich terrestrial and aquatic biodiversity in the haor region. Model results show that under hydrological scenario one Surma river water enters into the surrounding floodplain and flow occurs through the river as well as over the floodplain. During such an event, with a few exceptions flow velocity over the floodplain ranges from 0.1m/s to 0.2m/s. Flow velocity through the river also decreases in magnitude compared to that in bankfull discharge condition. Large inflow from the Meghalaya Hills during this time may cause an increase in the floodplain as well as river flow velocity to some extent. Model results under scenario two show that flash flood flow from the Meghalaya Hills will enter into the Surma river both through the Baulai and the Rakti rivers as well as over the floodplain. As a result, flow velocity at the outfall of these rivers will increase sharply. Flow velocity in the river downstream of the outfalls will also increase compared to that in the upstream of the same. Among three developed road alignment alternatives Option-1 is selected as preferred road alignment. The total length of the Sachna-Golakpur road link is about 12.2km. A number 10(ten) bridges on the proposed road link are needed to keep the existing hydrological regime undisturbed. The wave runup is 1.06m considering road embankment slope of 1:2. The design water level of the proposed road varies from 8.52mPWD to 8.55mPWD from Golakpur Bazar end to Sachna Bazar end respectively. Road embankment slope protection works will be needed at all road approaches and at some stretches of the road against parallel current and wave action.

ACKNOWLEDGEMENTS

The authors like to pay gratitude to Road Division, Sunamganj, Roads and Highways Department, Bangladesh for providing financial support and data and information available with them for successful completion of the study.

REFERENCES

River Research Institute. (2018*). Hydrological and Morphological Study Using Mathematical Model for the Proposed New Sachna-Golakpur Road under Sunamgonj Road Division*, Final Report, Faridpur.

DHI Water and Environment. (2006). MIKE21C, River Hydrodynamics and Morphology, User Guide.

Proceedings of the 5th International Conference on Civil Engineering for Sustainable Development (ICCESD 2020), 7~9 February 2020, KUET, Khulna, Bangladesh (ISBN-978-984-34-8764-3)

SUSTAINABLE SEDIMENT MANAGEMENT IN A SELECTED BEEL IN SOUTH-WEST REGION OF BANGLADESH

Md. Monirul Islam *[1], Umme Kulsum Navera [2] and Md. Rezanur Rahman [3]

[1]Senior Specialist, Irrigation Management Division, Institute of Water Modelling, Dhaka, Bangladesh, e-mail: mni@iwmbd.org
[2]Professor, Department of Water Resources Engineering, BUET, Dhaka, Bangladesh, e-mail: uknavera@gmail.com
[3]Junior Engineer, Flood Management Division, IWM, Dhaka, Bangladesh, e-mail: rezanur.buet@gmail.com

***Corresponding Author**

ABSTRACT

The southwest coastal region is highly vulnerable to erosion - siltation of river estuaries, water logging, coastal land subsidence and salt water intrusion etc. Excessive sedimentation by the incoming silts from the downstream sea with high tide adversely affect the river system of southwest region especially during the dry season. The Khulna-Jessore Drainage Rehabilitation project (KJDRP) is an example to mitigate water logging problems created by the coastal polders. It is of utmost importance to solve the drainage congestion and water logging problems in this area. A popular concept based on water management practice, known as Tidal River Management (TRM), which deals with natural tide movement in rivers, was adopted. From observation and monitoring of TRM processes inside East Beel Khukshia (EBK) and Beel Kedaria, it has been found that the sedimentation inside the tidal basins was not uniform and people were not satisfied to allow their land for TRM operations. So in order to find an effective as well as technically feasible TRM process, two management options have been analyzed in this paper by using MIKE 21 FM modelling simulation to verify the efficiency of these options for uniform sediment deposition. Beel Baruna was selected as a potential beel based on its location and operable area of tidal basin. In first option the beel has been divided into three compartments by constructing embankments and allowing sedimentation inside these compartments one after another by connecting to a river with an artificial link channel. Second one is constructing embankments along both banks of main khal through the beel and thereby allowing sedimentation by cutting the embankments part by part from upstream to downstream. Technical feasibility analysis of the two options have been performed through numrical modelling simulation. Non-uniform distribution of sediment was the major disadvantage of the current TRM practice. From mathmatical modelling simulation of two options, it is found that sediment distribution is more uniform in case of option 2. To the contrary, sediment deposition mainly takes place near the mouth of the link canal and volume of deposition is coparatively less in case of option 1. So option 2 is found more feasible to solve the water logging and drainage congestion problem and for proper sediment management in this area.

Keywords: *Southwest coastal region, Sedimentation, Tidal River Management (TRM), MIKE 21 FM.*

1. INTRODUCTION

Bangladesh has become one of the most climate vulnerable countries in the world due to climate change (BCCSAP, 2009, GermanWatch, 2011 and Islam et al., 2014). The coastal region in the southwest area of Bangladesh is considered to be maximum effected due to climate change. It will be directly affected by storm surges, drainage congestion, and sea level rise (Kibria, 2011 and Kibria et al., 2015). The problems of the southwest region including erosion - siltation of river estuaries, water logging, coastal land subsidence and salt water intrusion have become very severe (Islam et al., 2014). Salinity intrusion from the Bay of Bengal already penetrates 100 kilometers inland during the dry season (Huq et al., 2008).

The southwest region of Bangladesh is characterized by numerous morphologically active tidal rivers which form the main drainage network for coastal polders and low-lying beels (depressed land locally known as beels). The entire river network of this region is vulnerable to excessive sedimentation by the incoming silts from the Bay of Bengal with high tide especially during the dry season (Gain et al., 2017, Islam et al., 2014, IWM, 2010). The sedimentation effects of southwestern rivers and floodplain interventions were described by Sarker (2004). The reduction in flushing the fresh water flow from the upstream sources started to take place due to siltation up of the rivers in this region after the construction of coastal polders in the early 60s (Nowreen, 2014). To solve the long-standing water logging problems caused by such situation the KJDRP was implemented during 1994-2002 by BWDB (IWM, 2010). But this project could not solve the drainage problems effectively.

Later, a popular concept based on water management practice, known as Tidal River Management (TRM), was adopted. TRM deals with natural tide movement in rivers taking full advantage of the rise and fall of water within a tidal period. During flood tide, sediment borne tidal water is allowed to enter into an embanked low-lying area (tidal basin) where the sedimentation takes place during long storage period and thus acts as a sedimentation trap. During ebb tide, the water flows out of the tidal basin with greatly reduced sediment load eroding the downstream riverbed as well as increasing the drainage capacity. The natural movement of flood and ebb tide along the tidal basin and the surrounding river maintains a proper drainage capacity of the river in the above-mentioned way (Amir et al., 2013.).

TRM concept was practiced in Beel Bhaina and Beel Kedaria under Jessore and Khulna districts during 1997-2001 and 2002-2005, respectively (Figure 1). Beel Bhaina generated higher tidal volume inside its tidal basin than Beel Kedaria because of having higher tidal range compared to Beel Kedaria. The morphological changes of Teka-Hari River system due to closure of beel Kedaria tidal basin causes severe water logging in the Bhabodah and adjoining areas (IWM, 2007). Later on, operation of East Beel Khuksia for TRM was started in 2006 and monitoring results of East Beel Khukshia (EBK) TRM process showed that sedimentation inside the tidal basin was not uniform and people were not convinced to allow their land for TRM operation (IWM, 2010).

Local people allow their land to be used for TRM without any compensation, hoping that the land will rise after three or four years and they can cultivate more crops. But monitoring results of previous and present TRM practices revealed that sedimentation inside the tidal basin does not occur as expected almost in all cases. This results in people's unwillingness to allow their land for TRM (Amir, 2010). So, these areas require further attention for satisfactory and uniform sedimentation inside the beels during and after the TRM process. In this paper, an attempt has been made to verify the technical feasibility of two sediment management options by a cohesive sediment transport model using MIKE21 FM modeling system of beel Baruna in Jessore area.

2. METHODOLOGY

The methodology of this research work is arranged in a systematic way which includes study area selection, data collection, identification of sediment management options and development of a sediment management transport model.

2.1 Selection of the Study Beel

The study beel area which is Beel Baruna is located in between Latitudes 22° 49'40.3"N and 23° 6'27.1" N and Longitudes 89° 13'32.46" E and 89° 26'15.43" E (Figure 1). Beel Baruna is a very potential beel for TRM considering its location and operable area of tidal basin (IWM, 2010). It is in the southwestern region of Bangladesh under Jessore and Khulna districts. Beel Baruna is located just downstream of Bhabadah regulator and upstream of East Beel Khukshia. It is situated almost parallel and in the opposite bank of East Beel Khukshia. Beel selection was also guided by a set of criteria devised in line with the objectives of the study and considerations of availability of secondary data. The present TRM practice is verified with the help of a numerical model which will analyze the efficiency of that exercise.

2.2 Secondary Data Collection

The secondary data were collected from Institute of Water Modelling (IWM), Bangladesh Water Development Board (BWDB) and Centre for Environmental and Geographic Information Services (CEGIS).

2.3 Identification of Management Options with Development of Model

Two options have been selected for sediment management inside the beel during TRM operation. In Option-1 sedimentation is allowed in the divided compartment of the beel one after another. In this option divided three compartments has been connected with three different link canals according to location of compartments. When one compartment has been allowed for sedimentation, other compartments have been remained closed. Thus, this option has been selected to fill up the beel by different link canals. In Option-2 an embankment has been constructed along both banks of main khal in the beel. Then a link canal has been constructed to connect with the river. In this process sedimentation has been allowed by cutting the embankment part by part, gradually from upstream to downstream. Thus, this option has been selected to fill up the beel from upstream distance area to near the mouth of link canal.

A two-dimensional sediment transport model has been developed using MIKE21 FM Modeling system and duly calibrated to know the sedimentation inside the beel. The numerical model has been developed integrating the main Hari-Teligati-Gengrail river system and Beel Baruna tidal basin. Model has been calibrated with the observed data of Hari River and simulated for the identified options. Sedimentation inside the tidal basin has been assessed from the simulation results of cohesive sediment transport model for the identified options. Topographic data of beel baruna has been used to develop the bathymetry of Beel Baruna for the model.

3. RESULTS AND DISCUSSIONS

3.1 Schematization of Identified Options

In option 1, the areas of the compartments have been calculated 211 ha, 258 ha and 246 ha for compartment A, B and C respectively. For this Option, Noimuddir Khal has been used as a link canal for compartment A, Deakula Khal has been used as a link canal for compartment B and Tungir Khal has been used as a link canal for compartment C (Figure 2). All link canals are connected with the Hari river. In Option-2, embankment has been constructed along both banks of main khal in the beel. Link canal has been constructed along Noimuddir khal. At first step, embankment has been constructed for a length of 3800 m and sedimentation has been allowed for the first year. Then the embankment has been removed for 1000 m and sedimentation has been allowed for the second year. Similarly, in the third year the length of the embankment has been become as 1800 m and there was no embankment in the fourth year. Finally, sedimentation in the last year has been occurred as no embankment condition. Step by step construction of embankment with schematization for Option-2 are shown in Figure 2.

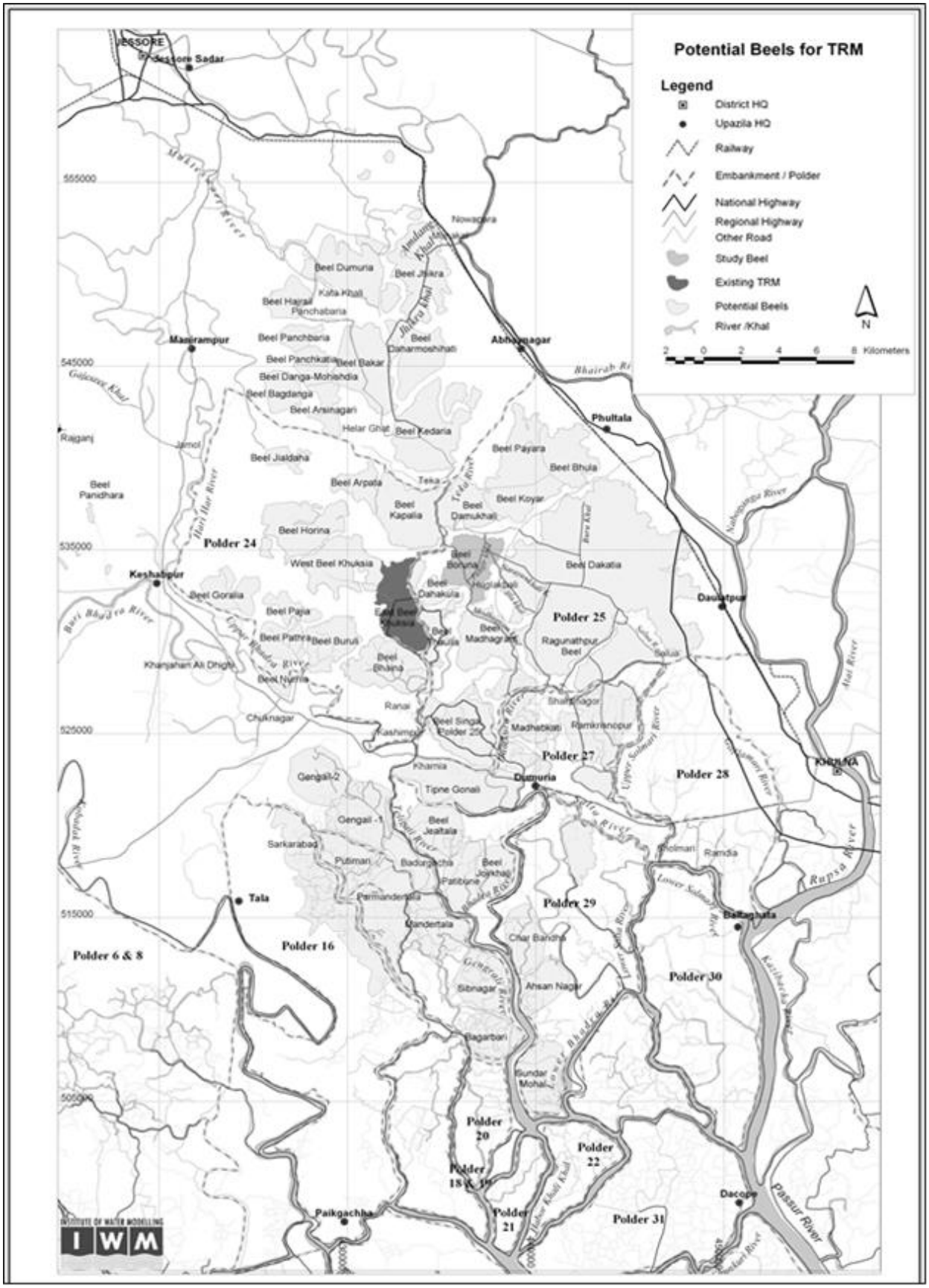

Figure: 1: Location Map of the study area (Source: IWM, 2010)

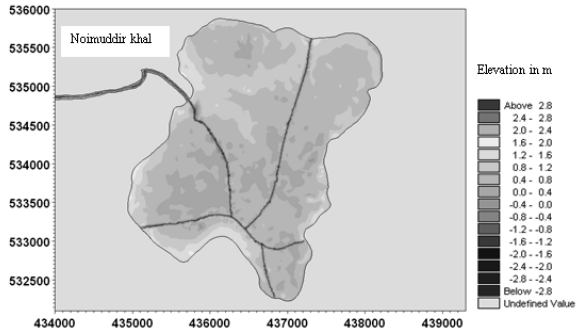

Base condition

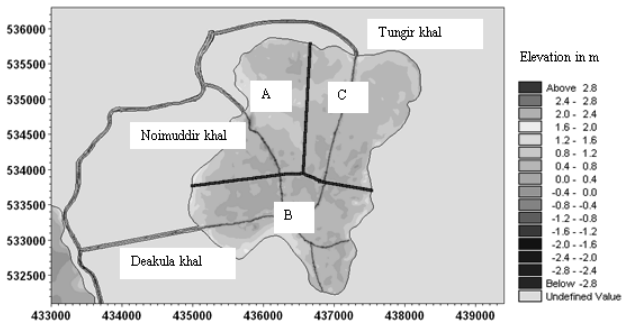

Option 1

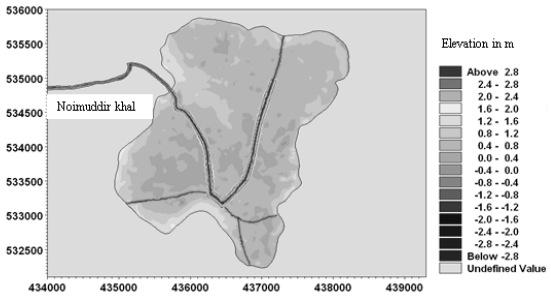

Option 2 with 3800 m embankment

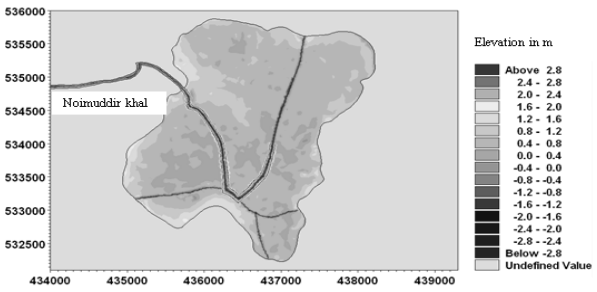

Option 2 with 2800 m embankment

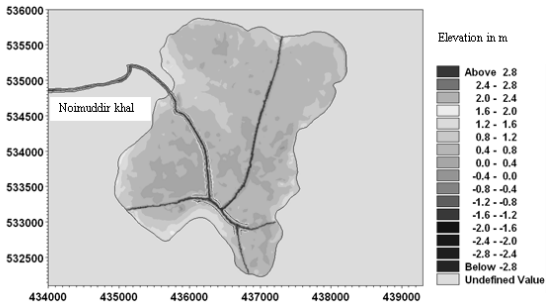

Option 2 with 1800 m embankment

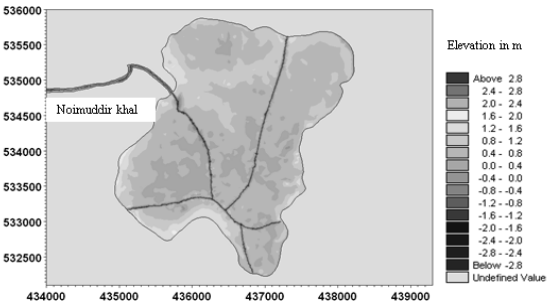

Option 2 with no embankment

Figure 2: Schematization of Beel Baruna for options 1 & 2

3.2 Analysis of Results from Option Simulation of Beel Baruna

After set up and calibration of the model, it has been simulated for the selected two options to find the most feasible option for sediment management and uniform deposition of the beel. The cohesive sediment transport model has been simulated for four years. Continuous 4 years model simulation for tidal river is quite complex and time consuming. For this reason, simulation has been done for the dry season as major sedimentation occurs in this season. Similarly, simulation for the next year has been done with the updated bed level of the previous year. Thus, total deposition inside the beel has been found for four years with respect to base condition.

Simulated results for option 1 & 2 have been presented in Figure 3 for consecutive 4 years.

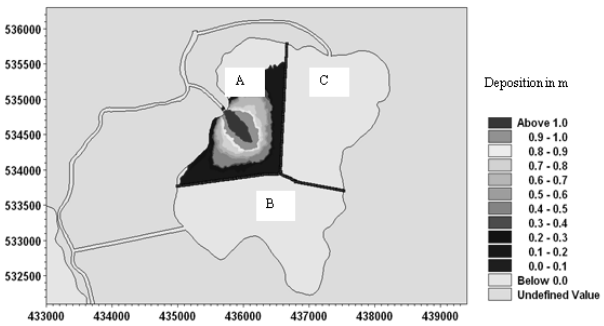

Option 1 (0-16 months); A is in operation,B & C closed

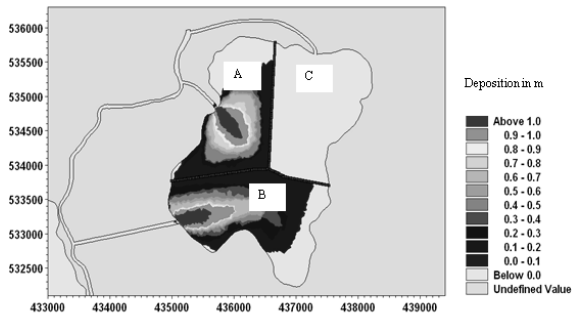

Option 1 (17-32 months); B is in operation, A & C closed

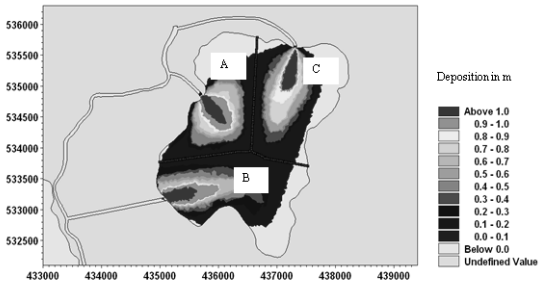

Option 1 (33-48 months); C is in operation, A & B closed

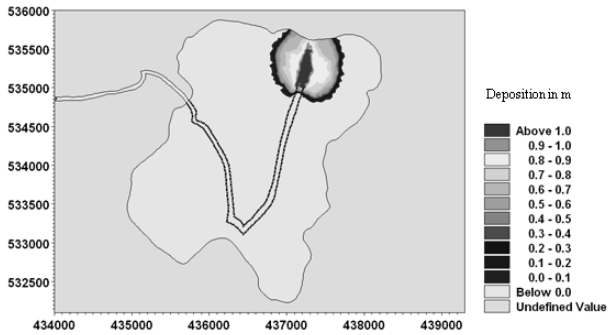

Option 2 after 1st year with embankment length 3800 m

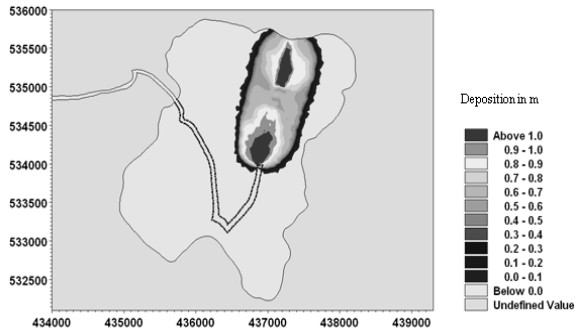

Option 2 after 2nd year with embankment length 2800 m

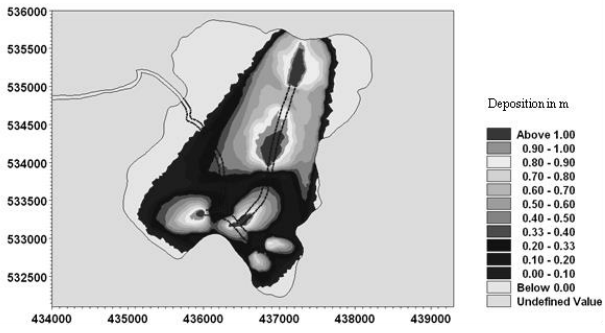

Option 2 after 3rd year with embankment length 1800 m

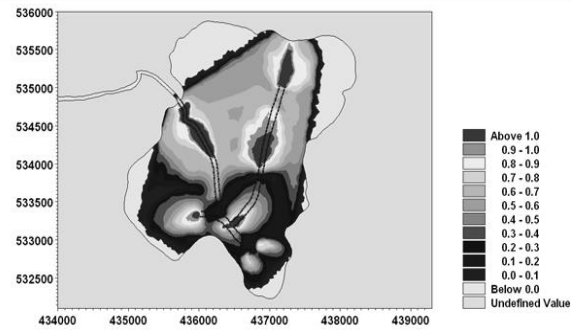

Option 2 after 4th year with no embankment

Figure 3: Simulated deposition pattern inside the tidal basin for option 1& 2 for 4 years

From the above simulated results, for option 1 it is seen that most sedimentation takes place at the mouth or near the mouth of the link canal and sediment distribution is not uniform. Thus, in this way silt cannot spread out in the areas far away from the link canal and also results in a non-uniform sedimentation in the basin. From the simulated results of options 2, it is seen that after fourth year simulation sediment spreads comparatively uniform and almost the whole area of the beel.

3.3 Deposition Volume

Deposition volume for Beel Baruna tidal basin after options simulation for the selected two options have been calculated according to change of bed thickness from the base condition. Provision of dredging is considered for all of options. Estimated deposition volume for Option-1 and Option-2 are shown in Table 1. More deposition is observed for Option-2 for the study beel.

Table 1: Deposited volume for the selected two options

Option	**Deposition Volume in Mm^3**			
1	After 16 months in Compartment-A	From 17-32 months in Compartment-B	From 33-48 months in Compartment-C	After 48 months in Compartments-A, B & C
	0.82	1.11	1.04	2.97
2	After 12 months	After 24 months	After 36 months	After 48 months
	0.52	1.26	2.42	3.12

3.4 Deposition Area

From the simulated results and deposition of sediment, two plots of deposited area versus time have been prepared for the two options (Figure 4). The plots are prepared for three level of deposition: net deposition greater than 0.50 m, net deposition greater than 0.80 m and net deposition greater than 1.0 m. Figure 4 show time versus deposition area plots for Option-1 & Option-2 respectively. It is seen from the plots that more deposition area (610 ha) covers for Option-2 comparing with the area (585ha) for Option-1.

Plots for Option-2 shows that for deposition depth greater than 0.80 m and 1.0 m, sediment deposition does not increase significantly after almost 36 months. But further deposition will occur under 48 months in areas where the net deposition depth is greater than 0.5 m.

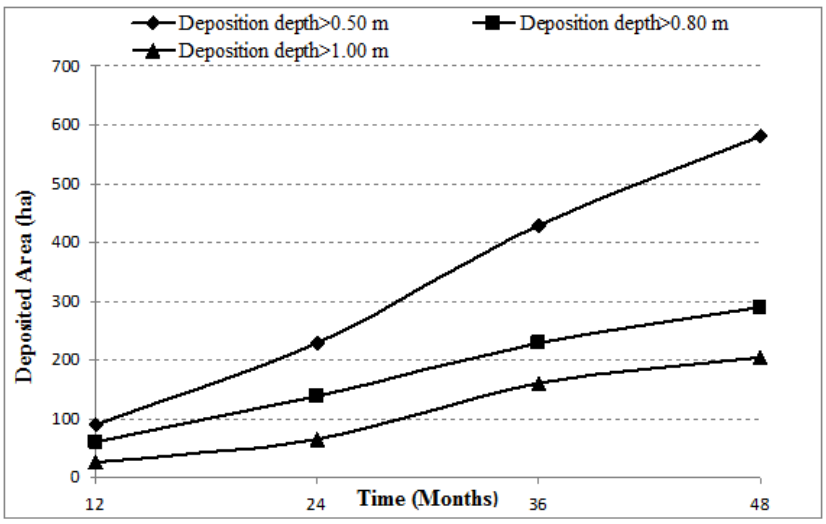

Option 1

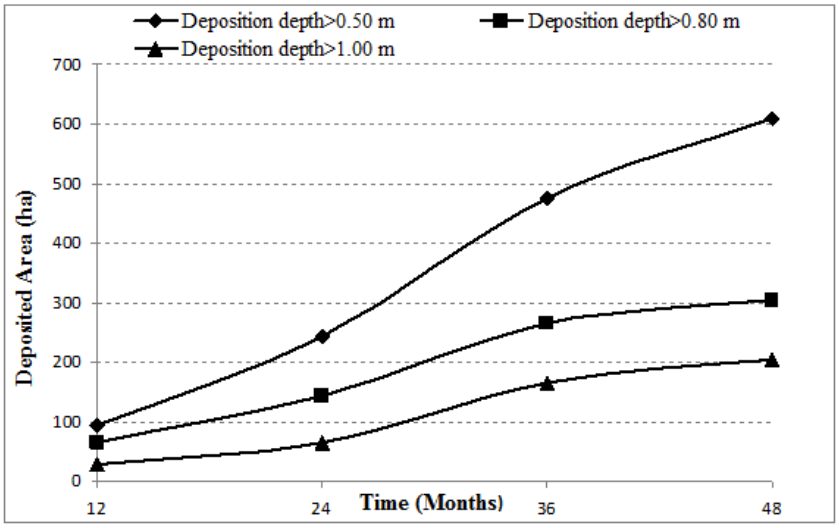

Option 2

Figure 4: Deposited area plot for Option 1 & 2

4. CONCLUSIONS

The techniques of Tidal River Management (TRM) is a popular and proven process to solve water logging problems in the tidal river area having low lying beels or tidal basins which has been simulated in this research paper for two different options in Beel Baruna. It has been found from the simulations of different options that sediment deposition inside the beel is not uniform in the present TRM practices which will make people unwilling to allow their land for TRM operation. Maximum deposition volume and area are found for Option-2 and comparatively less deposition area and volume are found for Option-1. Sediment deposition is more uniform in Option-2. So, in technical consideration, it appears that Option-2 is preferred in the area.

ACKNOWLEDGEMENTS

The author is highly grateful to Prof. Dr. M Monowar Hossain, Executive Director, Institute of Water Modelling for providing necessary supports to conduct the mathematical modelling simulation using MIKE software packages. The author is also grateful to Md. Zahirul Haque Khan, Director, Coast Port and Estuary Management Division, IWM and Md. Mobassarul Hasan, Associate Specialist, CPE, IWM for providing valuable guidelines related to numerical simulation throughout the study period.

REFERENCES

Amir, M.S.I.I., Khan, M.S.A., Khan, M.M.K., Rasul, M.G., Akram, F., (2013), "Tidal River Sediment Management-A Case Study in Southwestern Bangladesh.", World Academy of Science, Engineering and Technology, International Journal of Civil, Architectural, Structural and Construction Engineering, Vol-7, No-3.

Amir, M.S.I.I. (2010), "Socio-Technical Assessment of Sediment Management Options in Tidal Basins in Southwestern Bangladesh", M. Sc. Thesis, Institute of Water and Flood Management, Bangladesh University of Engineering and Technology.

BCCSAP (Bangladesh Climate Change Strategy and Action Plan), 2009, The Government of the People's Republic of Bangladesh.

Gain, Animesh. K., Benson, D., Rahman, R., Dattta, D.K., Rouillard, J. J., (2017), "Tidal river management in the south west Ganges-Brahmaputra delta in Bangladesh: Moving towards a transdisciplinary approach?", ELSEVIER, Environmental Science and Policy, Volume 75, September 2017, Pages 111-120.

GermanWatch, (2011), "Who Suffers Most from Extreme Weather Events? Weather Related Loss Events in 2009 and 1990 to 2009", Global Climate Risk Index.

Huq, Saleemul, Ayers and Jessica (2008), "Climate Change Impact and Responses in Bangladesh", Note Prepared by IIED for Policy Department Economy and Science, DG Internal Policies, European Parliament.

Islam, A.S. et al., (2014) "Climate Change Impacts, Vulnerability and Adaptation: Sustaining rice production in Bangladesh", Final Report, CEGIS, Dhaka.

Islam, A.S. et al., (2014) "Assessment of the impact of anticipated key drivers of change on water resources of the coastal zone", Final Report, Institute of Water Modeling (IWM), Dhaka.

IWM (2010), "Feasibility Study and Detailed Engineering Design for Long Term Solution of Drainage Problems in the Bhabodah Area", Final Report, Bangladesh Water Development Board.

IWM (2007), "Monitoring the Effects of Beel Khuksia TRM Basin and Dredging of Hari River for Drainage Improvement of Bhabodah Area", Final Report, Bangladesh Water Development Board.

Kibria, M.G., Saha, D., Kabir, T., Naher, T., Maliha, S. and Mondal, M.S. (2015). "Achieving Food Security in Storm Surge-prone Coastal Polders in South-West Bangladesh". South Asian Water Studies (SAWAS) Journal, Vol. 1, Issue 1, p. 26-42

Kibria, Z. (2011), "Tidal River Mangement (TRM): Community Based River Basin Management and Climate Change Adaptation in Southwest Coastal Region of Banngladesh", Uttaran, Dhaka, Bangladesh.

Nowreen, S., Jalal, M.R., Khan, M.S.A. (2014), "Historical Analysis of Rationalizing South-West Coastal Polders of Bangladesh", Water Policy 16 (2), IWA Publishing, Pages 264-279.

Sarker, M.H. (2004), "Impact of Upstream Human Interventions on the Morphology of the Ganges-Gorai System", The Ganges Water Diversion: Environmental Effects and Implications, M.M. Qader Mirza (ed.), Water Science and Technology Library Book Series, Springer Netherlands, Vol. 49, pp. 49-80.

Proceedings of the 5th International Conference on Civil Engineering for Sustainable Development (ICCESD 2020), 7~9 February 2020, KUET, Khulna, Bangladesh (ISBN-978-984-34-8764-3)

ESTIMATION OF GROUNDWATER RECHARGE FOR SELECTED URBAN AREAS OF BANGLADESH USING WATER TABLE FLUCTUATION METHOD

R. T. Khan*[1] and P. Chakma[2]

[1]Lecturer, Department of Water Resources Engineering, Chittagong University of Engineering & Technology, e-mail: rtk.cwre@cuet.ac.bd
[2]Lecturer, Department of Water Resources Engineering, Chittagong University of Engineering & Technology, e-mail: pollenchakma@cuet.ac.bd

***Corresponding Author**

ABSTRACT

Water supply in the densely populated urban areas of Bangladesh for domestic and industrial purposes is mainly dependent upon groundwater extraction.The abstraction of groundwater beyond the recharge rate may lead to unsustainability and eventually depletion of groundwater aquifers. This study aims at determining the annual groundwater recharge in highly industrialized and densely populated areas of Dhaka, Narayanganj, Munshiganj, Manikganj and Gazipur districts of Bangladesh for the time period 2002-2010 using water table fluctuation method. Ten GW observation wells with water table readings at weekly intervals were selected to observe the annual time series of groundwater table fluctuation. This method is based on the presumption that groundwater table fluctuates when recharge water from the unsaturated zone enters the underlying unconfined aquifer. It is the simplest method of GW recharge estimation with minimum data requirements, which involves only the specific yield values of aquifer materials and time series data of groundwater table elevation. The specific yield values for the aquifer materials for the study area were approximated based on the lithologic data obtained from Borelog Data Book, Dhaka Division, (DPHE), and the GW table data were obtained from observation wells of Bangladesh Water Development Board (BWDB). From analysis, it was found that mean annual groundwater recharge was highest in Dhaka District (about 3000 mm/year) and lowest in Narayanganj District (about 1500 mm/year). The results of this study would provide useful information on the allowable limit of annual groundwater extraction, and emphasize on the need for conjunctive use for sustainable water management.

Keywords: *Groundwater recharge, Urban area, Water table fluctuation method, Borelog data, Specific yield.*

1. INTRODUCTION

Groundwater is a vital source of domestic, industrial and agricultural water supply in Bangladesh because of high yielding characteristics of aquifers, presence of GW table at shallow depths, ease of drilling into the unconsolidated sediments and minimum treatment requirements (Shahid, et al., 2015). Municipal water supply relies on deep groundwater aquifers, whereas, the irrigation water requirement during the dry period is fulfilled mostly by the shallow aquifers (Nowreen, 2017). Being the most densely populated city of the world, with over 47,400 people living per square kilometer, Dhaka is facing tremendous burden upon its resources including groundwater (Amin, 2018). The prevailing dependency on groundwater resources (about 87 percent of the supplied water) causes depletion at the rate of 2.81 m/year which may result in up to 120m lowering of groundwater table by 2050 (Uddin & Baten, 2011).

Since gaining independence in 1971, Dhaka was the focus of industrial development until very recently. Currently industries are being shifted to the neighboring areas of the capital such as Narayanganj, Munshiganj, Gazipur, Savar, Dhamrai, etc. due to government policy of industrial re-locating, excessive population, pollution, and traffic congestion of Dhaka city (Hassan, Alenezi, & Good, 2019). As a result, the neighboring areas of Dhaka, which were previously agrarian, are currently being transformed into industrialized and urbanized districts. The increased water demand for industrial, domestic and agricultural purposes, and reduction of GW recharge zones may result in gradual depletion of the GW aquifers as a consequence.

The GWT fluctuation method of recharge estimation has been applied and discussed in numerous literatures in a wide range of aquifer formations and climatic conditions. The simplicity and minimum data requirements of this method facilitated its application dating back to the 1920's (Meinzer & Stearns, 1929), where weekly records of 22 observation wells of GWT for the period 1913 to 1916 were used to quantify the changes of water storage in the saturation zone in the Pomperaug Basin of Connecticut.

Healy & Cook (2002) discussed the underlying theory, methodology as well as the applicability and limitations of this method. To achieve greater accuracy, they recommended this method to be applied for short time intervals, ranging from hours to a few days. However, it was suggested that to estimate gross change in groundwater storage, this method can be applied for time periods extending over a season or a year. The major advantages of this procedure enlisted by them were, it is independent of the mechanism by which water flows through the unsaturated region, and the GWT data is representative of an area expanding over several square meters, making it an integrated approach rather than a point measurement. However, one of the main limitations of this technique derive from the uncertainty in approximation of the specific yield values for different aquifer formations. Also, due to large spatial extent of the wetting front of deeper aquifers, they may not readily show fluctuations in response to groundwater recharge, and as a result, may not yield satisfactory results.

Application of GWT fluctuation method has been carried out in context of Bangladesh by Adhikary, et. al., (2013) and Shahid, et al., (2015). The study conducted in Kushtia District of the Gorai River Basin by Adhikary, et. al., (2013) showed spikes in groundwater table in coherence of the rainfall periods occurring during the same time interval. This study concluded that over the time period of 16 years between 1992 to 2007, the annual average recharge was 1413 mm, constituting 74% of the average annual precipitation (1898 mm). Shahid, et al., (2015) addressed the issue of GW over-exploitation in the Northwestern districts of Bangladesh by juxtaposing the water abstraction for irrigation and domestic purposes with the GW recharge rate.

The objectives of the current study are:

- Determine the specific yield values of the aquifer materials of the study area based on lithologic data
- Record the highest fluctuation of the GWT in response to recharge from GW data observation wells

- Determine the annual GW recharge at selected sites for the years 2002-2010, and compare the GW recharge values among various years and various sites.

1.1 Study Area

The study area consists of Dhaka and its surrounding four districts of Gazipur, Munshiganj, Narayanganj and Manikganj. Their corresponding areas are enlisted in Figure 1 below:

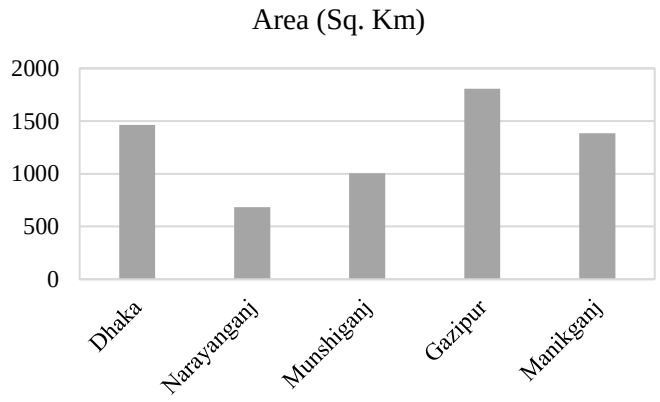

Figure 1: Areas of Selected Districts (Source: BBS 2013)

The selected areas are the focal points of various industrial, residential, commercial as well as agricultural activities. The major garments, textile, leather, jute, cement, steel and metal industries of the country are centered within these districts. Besides, remarkable portion of these districts are utilized as agricultural lands. The population densities vary from about 8229 persons per square kilometers in Dhaka to about 1007 persons per square kilometers in Manikganj.

Figure 2: Study Area Map Including Borelog and GW Data Stations

The study area falls within the tropical humid climate region, with average annual rainfall values varying from 1800 to 2200 mm. $year^{-1}$, and the bulk of the rainfall (about 80%) occurring during the tropical monsoon (May-September). Annual minimum and maximum temperature ranges between 12-34°C. In accordance with the dry and wet seasons, the troughs of the GW tables occurred in between the months of March-May and the peaks were observed in between August-November.

According to physiographic characteristics, Dhaka and Gazipur falls in the Pleistocene terraces in the Madhupur and Barind Tracts. The other districts of the study area fall within recent Holocene floodplains. Among them, Munshiganj and Narayanganj falls in the Old Brahmaputra Flood Plain, and Manikganj falls in the Brahmaputra-Jamuna Flood Plain. The Plio-Pleistocene aquifers of the Dupi Tila Formation account for 83% of the water supplied in Dhaka and Narayanganj cities by Dhaka WASA. (Zahid & Ahmed, Groundwater Resources Development in Bangladesh: Contribution to Irrigation for Food Security and Constraints to Sustainability, 2005) (Rahman, Wiegand, Badruzzaman, & Ptak, 2013). This aquifer formation is shown in Figure 3 below.

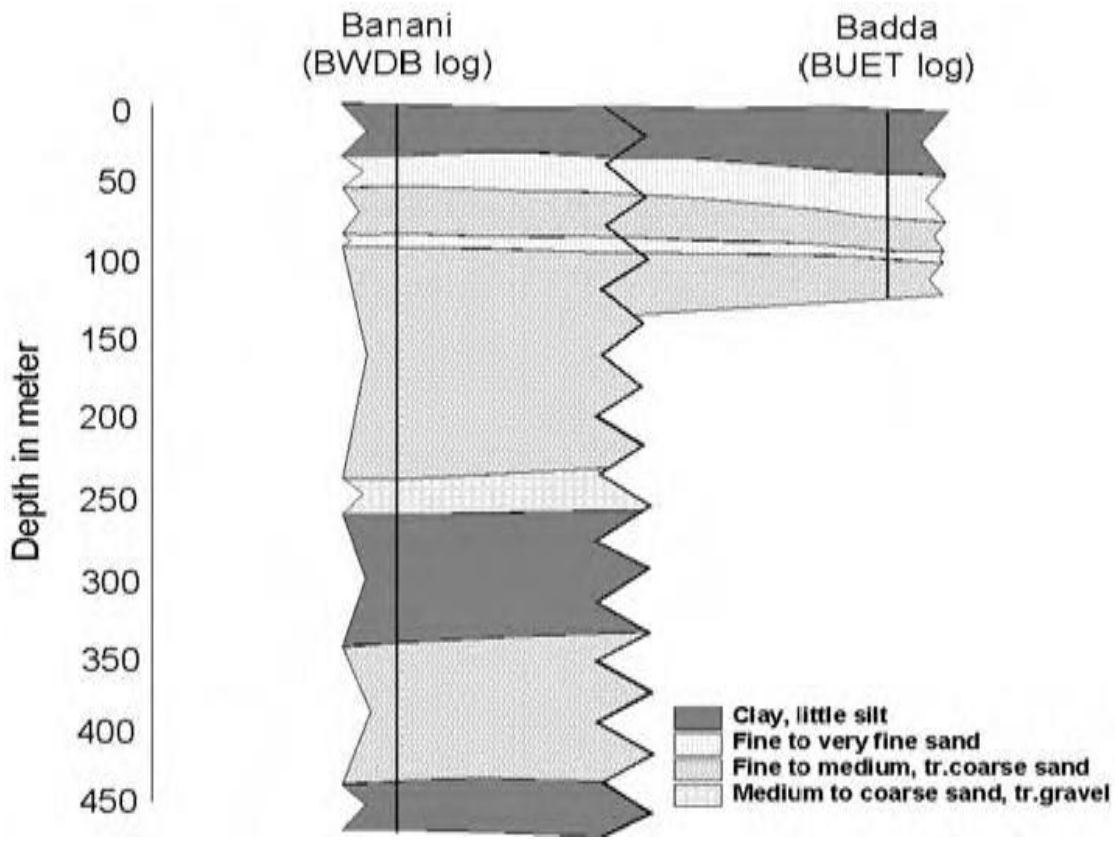

Figure 3: Peistocene Dupi Tila Aquifer of Dhaka City (Zahid, Hossain, Uddin, & Deeba, 2004)

In Manikganj District, the borelogs reveal that the upper aquifer materials consist predominately of fine to medium sand, up to depths of 50 meters. Coarse sand and silty clay could be found at depths exceeding 50m and 80m respectively. In Gazipur District, an upper aquitard layer consisting of clay was found up to 40 meters of depth, followed by silty clay (40-70m) and medium to coarse sand (70-160m). In Munshiganj, the upper aquifer consists of find sand up to depths of 40-60m, followed by medium to very coarse sands at larger depths. (Local Government Division, Ministry of LGRD & Co-operatives, Government of the People's Republic of Bangladesh, 2010).

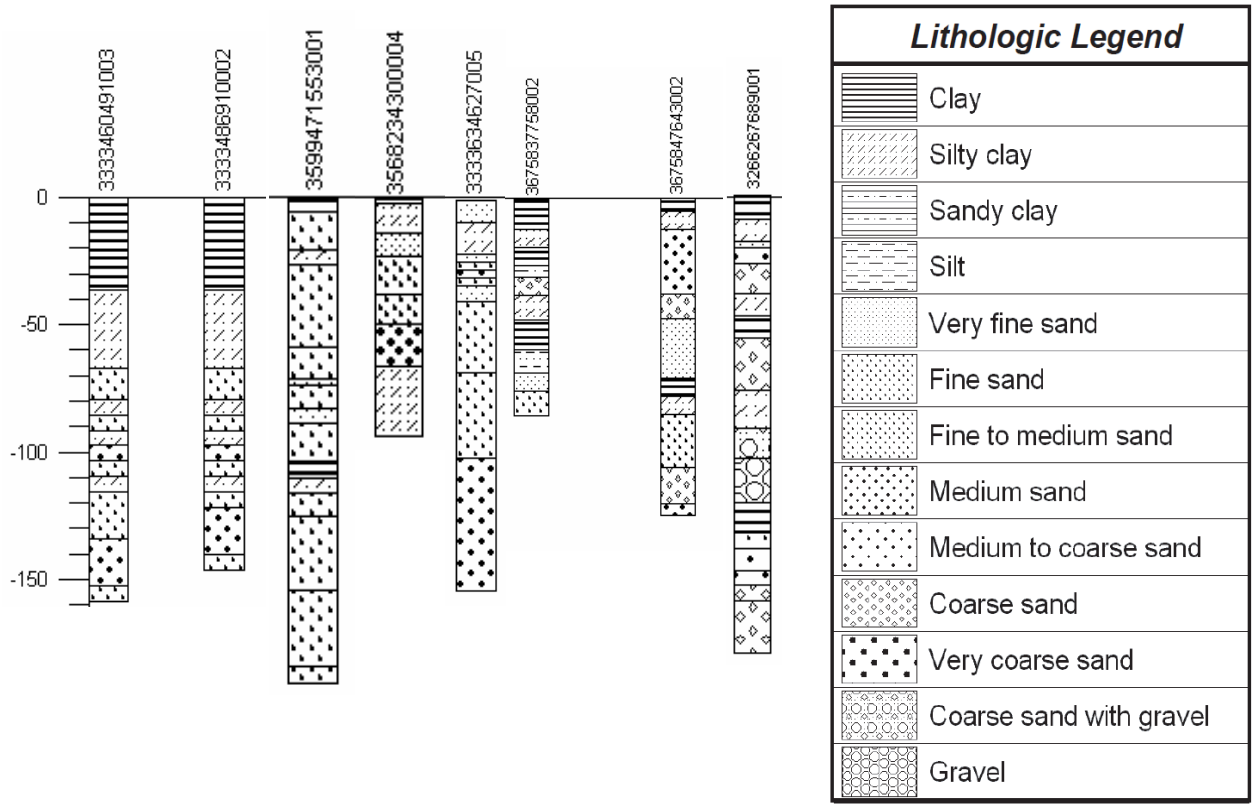

Figure 4: Lithology Data of the Selected Boreholes

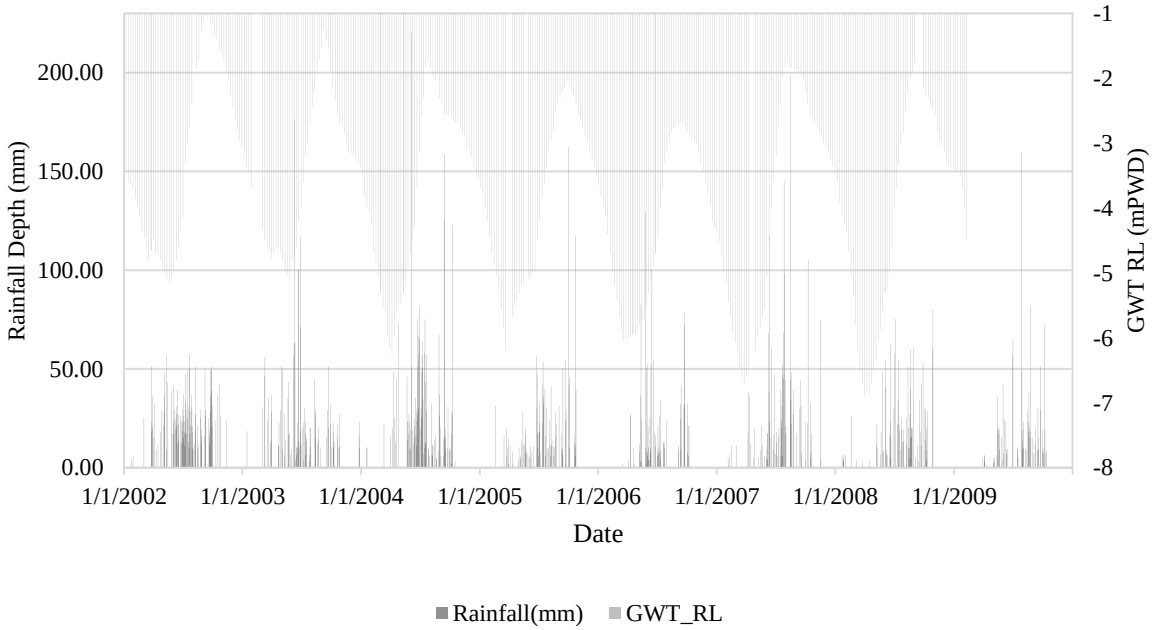

Figure 5: Fluctuation of GWT in response to rainfall at Kapasia Upazilla of Gazipur (Well ID GT3336012 and BWDB Rainfall Station ID CL37)

In the study area, 10 GWT observation wells of Bangladesh Water Development Board were selected. The lithologic data was obtained from the Bore log Data Book of Dhaka Division published by Department of Public Health Engineering (DPHE). The location of the GW observation wells and corresponding bore logs are given in Table 1 below:

Table 1: Location of Selected GWT Observation Wells and Borelogs

Sl. No.	District	Upazila	WellID	Latitude	Longitude	Borelog ID
1	Narayanganj	Narayanganj Sadar	GT6758005	23.65	90.51	5837758002
2	Narayanganj	Narayanganj Sadar	GT6758006	23.59	90.52	5847643002
3	Munshiganj	Tongibari	GT5994009	23.44	90.47	9471553001
4	Manikganj	Singair	GT5682015	23.77	90.14	8234300004
5	Gazipur	Kaliganj	GT3334009	23.96	90.54	3486910002
6	Gazipur	Kaliganj	GT3334010	24	90.58	3460491003
7	Gazipur	Kapasia	GT3336012	24.16	90.67	3634627005
8	Dhaka	Dhamrai	GT2614002	23.87	90.22	1453123000
9	Dhaka	Dhamrai	GT2614004	23.97	90.19	1477211001
10	Dhaka	Nawabganj	GT2662016	23.68	90.13	6267689001

2. METHODOLOGY

This method is based on the presumption that groundwater table fluctuates when recharge water from the unsaturated zone enters the underlying unconfined aquifer. The recharge (R) is determined using the following equation:

$$R = S_y \frac{dh}{dt} = S_y \frac{\Delta h}{\Delta t} \quad (1)$$

Where,
R = groundwater recharge (m/year)
S_y = specific yield (%)
dh = groundwater height between lowest and peak values (m)
dt = time (days)

In Equation 1, the specific yield value, S_y of a well was estimated by weighing the S_y values of each stratum against its corresponding depth, as given in Equation 2.

$$S_y = \frac{S_{y_1} \times thickness_1 + S_{y_2} \times thickness_2 + \cdots}{total\ thickness\ of\ the\ aquifer} \quad (2)$$

The specific yield values for various aquifer materials are enlisted in Table *2* below:

Table 2: Specific Yield Values of Various Aquifer Materials (Source: Johnson, 1967)

Material	Specific Yield (%)
Clay	2
Silt	8
Sandy clay	7
Fine sand	21
Medium sand	26
Coarse sand	27
Gravelly sand	25
Fine gravel	25
Medium gravel	23
Coarse gravel	22

The quantity Δh in Equation 1 reflects the difference in height between one trough and its succeeding crest, and Δt represents the corresponding time interval. These values were calculated from the GWT hydrographs. One sample calculation is shown below for GT2614004.

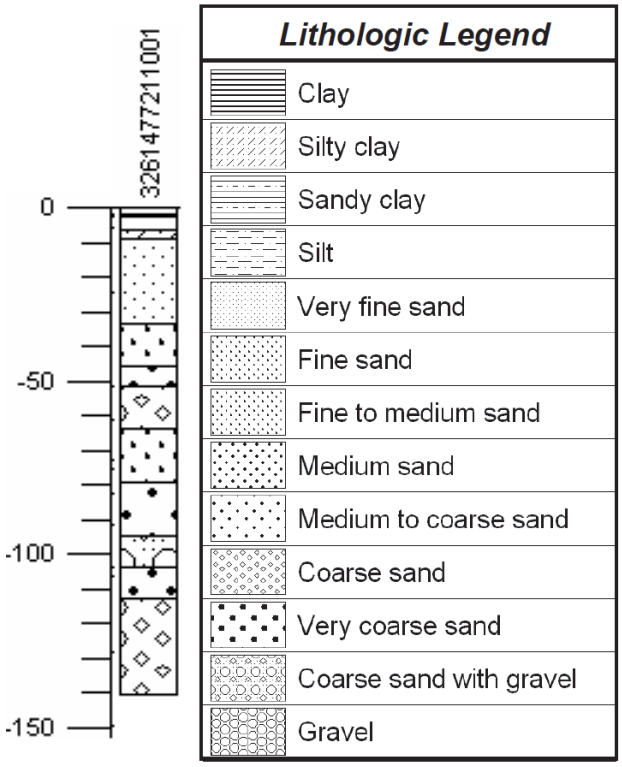

Figure 6: Lithology Data of Borehole of GT2614004

Table 3: Sample Specific Yield Calculation from Lithology Data

Depth(m)		Thickness(m)	Soil Type	Sy Value	Thickness*Sy
From	To				
0	6.5	6.5	Clay	0.02	0.13
6.5	9.03	2.53	Silty Clay	0.05	0.1265
9.03	33.34	24.34	Fine Sand	0.21	5.1114
33.34	45.52	12.15	Fine to Medium Sand	0.25	3.0375
45.52	51.27	5.75	Medium Sand	0.26	1.495
51.27	63.494	12.224	Coarse Sand	0.27	3.30048
63.494	78.864	15.37	Fine to Medium Sand	0.25	3.8425
78.864	94.214	15.35	Medium to Coarse Sand	0.265	4.06775
94.214	103.184	8.97	Coarse Sand with Gravel	0.25	2.2425
103.184	112.154	8.97	Medium Sand	0.26	2.3322
112.154	139.724	27.57	Coarse Sand	0.27	7.4439
Total		139.724			33.13

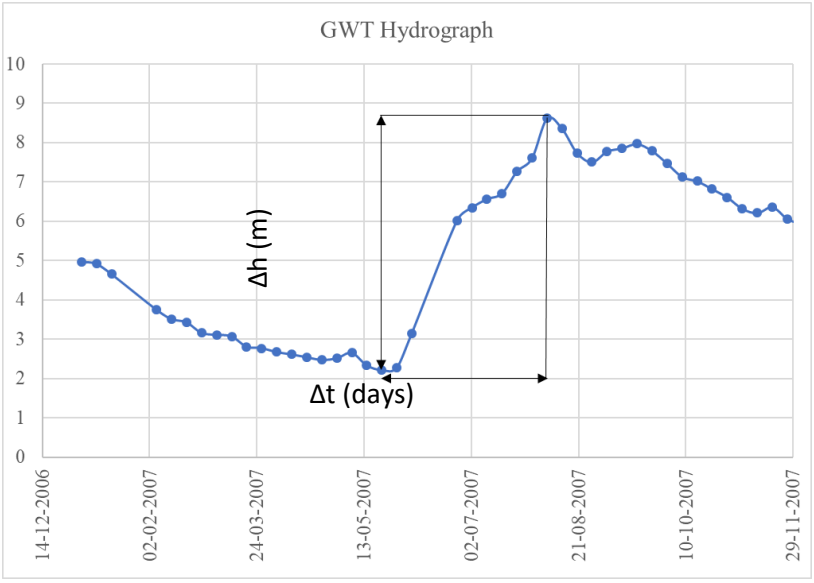

Figure 7: GWT Hydrograph for GT2614004 for the year 2007

S_y=33.13/139.724=0.237
From Figure 4,
Δh=8.62-2.21=6.41m;
Δt= (06-08-07) -(21-05-07) =77 days

Therefore, R=0.237x (6.41/77) =0.01973 m/day = 7201.26 mm/year

3. RESULTS AND DISCUSSIONS

1. From the 9 years' (2002-2010) 7-day hydrographs for different wells in the study area, it was observed that troughs of the hydrographs occurred in between April and May and peaks of the hydrographs occurred in between August and November, which is in accordance with the dry and wet periods of respectively.
2. From Figure 8, the maximum ground water recharge found for Gazipur district was 3500mm/year in the year 2004 in Kapasia Upazilla and the minimum yearly recharge was around 1500mm/year in the year 2005 in Kaliganj Upazilla. The average was found to be around 2200 mm/year.
3. In Dhaka District, GW recharge was observed to be maximum of about 7200 mm/year in the year 2007 in Dhamrai Upazilla and minimum of just below 1500 mm/year in Nawabganj upazilla. The mean annual GW recharge was about 3000 mm/year.
4. The overall annual groundwater recharge was found to be least in Narayanganj district. In 2010, the GW recharge fell as low as 110 mm/year in Narayanganj Sadar Upazilla whereas it reached its maximum in the year 2009 in Narayanganj Sadar Upazilla (GT6758006), with annual average recharge of about 1500 mm/year.
5. In Munshiganj, the groundwater recharge peaked in the year 2003 with about 3500 mm/year. It was minimum in the years 2002 and 2006, with a value of about 1900 mm/year. The mean annual recharge was about 2700 mm/year.
6. In Manikganj District, GW recharge was maximum in 2005 of about 1850 mm/year. The maximum value of 2550 mm/year was observed in the year 2002 and the mean value was observed to be around 2450 mm/year.
7. The annual GW recharge values did not follow any detectable trend.
8. The lowest annual GW recharge of Narayanganj Sadar Upazilla in GT6758005 can be attributed to its least conducive aquifer formation consisting mostly of clay and silty clay, with specific yield value of only 9.73%.

9. The large GWT fluctuation of 6.41m within a short time interval of 77 days gave rise to the highest groundwater recharge observed in Dhamrai, Dhaka in 2007. Although larger fluctuations of 7.10m was observed in Singair, Manikganj, within an interval of 119 days in 2007, the less conducive aquifer material (15% specific yield) resulted in much less groundwater recharge.
10. In the study area, the aquifers of Dhaka district were found to have higher specific yield values indicating their higher water yielding potential.
11. Although being located in close proximity, the recharge values at two GWT observation wells of Narayanganj District GT6758005 & GT6758006 showed large differences in annual GW recharge values due to sharp discontinuity in underlying hydrogeological formation, as evidenced from the borelog data.

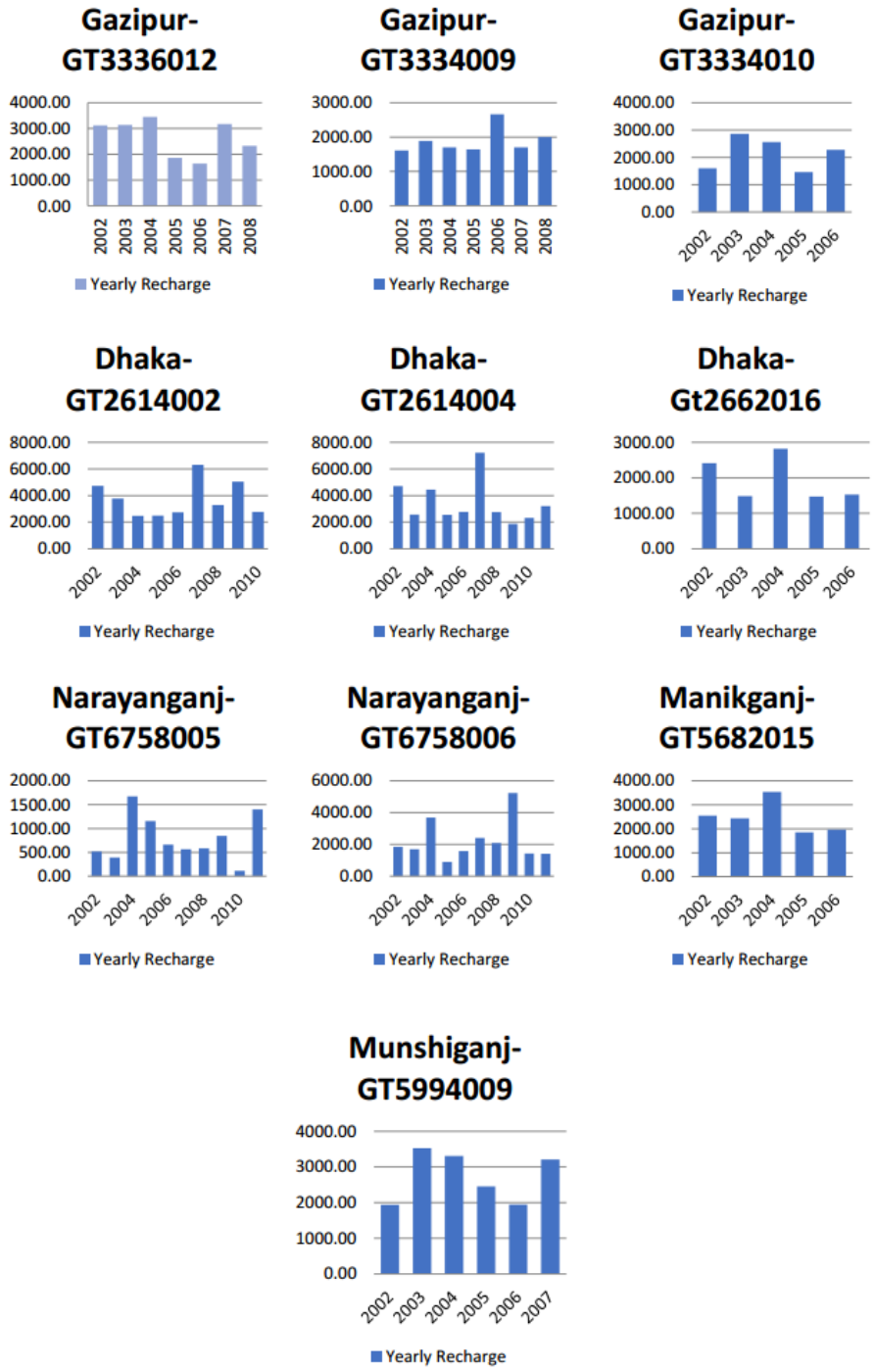

Figure 8: Annual GW Recharge Estimates at Various Locations of Study Area

4. CONCLUSIONS

1. From observation of the GW recharge patterns, it is evident that almost all the recharge occurs in the monsoon during the heavy rainfall period. The time of the rainfall recharge water to reach the GWT varied between 7 to 15 days. The rainfall occurring in the summer or winter periods are mostly converted to soil moisture or evaporation, and do not contribute to the GW recharge.
2. The annual GW recharge of the aquifers in Narayanganj were found to be significantly lower than the other districts, due to clayey lithology. As such, the aquifer in this area cannot be recommended for extraction of groundwater.
3. The aquifers of Dhamrai were seen to be recharged significantly, with annual GW recharge values exceeding 3000 mm/year. This can be a potential site for GW extraction for water supply in Dhaka city or the neighbouring semi-urban areas.
4. Based on the average annual GW recharge values, a safe yield value can be recommended for each of the aquifers of the selected districts. This safe yield value should be lower than the average annual GW recharge for sustainable groundwater exploitation.
5. At the time of conducting the study, time series data of GW level was available only up to 2010, with missing data values for periods greater than 3 months for some years, hence making the data of certain years unusable. Using recent data and longer time periods, the impact of land use change on GW recharge can be estimated. As all selected sub-districts of the study area are undergoing significant urbanization, the average annual GW recharge can be expected to decline in the recent and upcoming years.

5. RECOMMENDATIONS

1. A major drawback of the WTF method is the inaccuracy in estimation of the specific yield values. Similar geologic formations in different locations were seen to yield different specific yield values in previous studies. So, groundwater pumping test is required for accurate estimation of specific yield values, which was out of scope of the current study due to constraint of resources.
2. Besides GW recharge, GWT may fluctuate due to other causes such as air entrapment, GW pumping, changes in atmospheric pressure, etc. Also, a steady rate of recharge will not be reflected in the GWT hydrograph. In such cases, the WTF fluctuation method will not yield accurate results.

REFERENCES

Adhikary, S. K., Chaki, T., Rahman, M. M., & Gupta, A. D. (2013). Estimating Groundwater Recharge into a Shallow Unconfined Aquifer in Bangladesh. *Journal of Engineering Science, iv*(1), 11-22.

Amin, M. A. (2018, October 14). Dhaka remains the world's most densely populated city. *DhakaTribune*. Retrieved from https://www.dhakatribune.com/bangladesh/dhaka/2018/10/14/dhaka-remains-the-world-s-most-densely-populated-city

Bangladesh Bureau of Statistics. (2013). *District Statistics 2011.* Dhaka: Bangladesh Bureau of Statistics.

Hassan, M. M., Alenezi, M. S., & Good, R. Z. (2019). Spatial pattern analysis of manufacturing industries in Keraniganj, Dhaka, Bangladesh. *GeoJournal*, 1-15. doi:https://doi.org/10.1007/s10708-018-9961-5

Healy, R. W., & Cook, P. G. (2002). Using Groundwater Levels to Estimate Recharge. *Hydrogeology Journal, X*, 91-109. doi:10.1007/s10040-001-0178-0

Johnson, A. (1967). *Specific Yield-Compilation of Specific Yields for Various Materials.* California Department of Water Resources. Washington: U.S. Department of the Interior.

Local Government Division, Ministry of LGRD & Co-operatives, Government of the People's Republic of Bangladesh. (2010). *Borelog Data Book Dhaka Division.* Dhaka: Department of Public Health Engineering.

Meinzer, O. E., & Stearns, N. D. (1929). *A Study of Ground Water in the Pomperaug Basin, Connecticut.* U.S. Geological Survey, Department of the Interior. Washington: U.S. Geological Survey.

Nowreen, S. (2017). *Mechanism of Groundwater Response to Recharge and Its Quantification for Shallow Aquifers in Bangladesh.* BUET: Institute of Water and Flood Management, Bangladesh University of Engineering & Technology.

Rahman, M. A., Wiegand, B. A., Badruzzaman, A., & Ptak, T. (2013). Hydrogeological analysis of the upper Dupi Tila Aquifer, towards the implementation of a managed aquifer-recharge project in Dhaka City, Bangladesh. *Hydrogeology Journal, XXI*(5), 1071-1089. doi:https://doi.org/10.1007/s10040-013-0978-z

Shahid, S., Wang, X.-J., Rahman, M. M., Hasan, R., Harun, S. B., & Shamsuddin, S. (2015). Spatial Assessment of Groundwater Over-exploitation Spatial Assessment of Groundwater Over-exploitation. *Journal Geological Society of India, 85*, 463-470.

Uddin, A. A., & Baten, M. A. (2011). *Water Supply of Dhaka City: A Murky Future.* Dhaka: Unnayan Onneshan.

Zahid, A., & Ahmed, S. R. (2005). *Groundwater Resources Development in Bangladesh: Contribution to Irrigation for Food Security and Constraints to Sustainability.* Bangladesh Water Development Board, Groundwater Hydrology Division. Dhaka: Bangladesh Water Development Board. Retrieved from http://publications.iwmi.org/pdf/H039306.pdf

Zahid, A., Hossain, A., Uddin, M. E., & Deeba, F. (2004). Groundwater Level Declining Trend in Dhaka City Aquifer. *Proceeding of the International Workshop on Water Resources Management and Development*, (p. 133). Dhaka.

Proceedings of the 5th International Conference on Civil Engineering for Sustainable Development (ICCESD 2020), 7~9 February 2020, KUET, Khulna, Bangladesh (ISBN-978-984-34-8764-3)

LINEAR STABILITY ANALYSIS OF CORAL BED

Kaniz Farzana Rupa*[1] and Md. Jahir Uddin[2]

[1]M.Sc. Student, Department of Civil Engineering, Khulna University of Engineering & Technology, email: kanizfarzanarupa.2017@gmail.com
[2]Professor, Department of Civil Engineering, Khulna University of Engineering & Technology, email: jahiruddin@ce.kuet.ac.bd

***Corresponding author**

ABSTRACT

Coral is symbiotic with algae called zooxanthella, and grows by nutrients produced by photosynthesis of zooxanthella. It is assumed that a channel bed is composed of some kind of coral. In this study, linear stability analysis of coral bed is conducted by using three governing equations; Exner equation, Momentum equation, Continuity equation and the stability of coral bed is analyzed for the conditions without and with considering Reynolds stress. The governing equations are normalized to perform linear stability analysis. From the analysis, it is found that in the unstable region (without Reynold's stress), the growth rate increases monotonically with increasing wave number. For the condition (with Reynold's stress), it is revealed that the growth rate vanishes when the wave number goes to infinity. There is found a dominant wave number associated with a maximum growth rate. From the growth rate vs. Froude number curve, it is seen that the growth number is minimum when the Froude number is negative or the flow pattern is subcritical. On the other hand, the growth rate becomes neutral when the flow pattern is supercritical. From the growth rate vs wave speed curve, it is observed that the growth rate decreases with the increase of wave speed, and in a certain position, it becomes neutral.

Keywords: *Coral bed, Linear stability, Froude number, Wave number, Reynolds stress.*

1. INTRODUCTION

Coral is symbiotic with algae called zooxanthella and grows by nutrients produced by photosynthesis of zooxanthella. These beds (Figure 1) are formed of colonies of coral polyps held together by calcium carbonate. Most of the beds are built from stony corals, whose polyps cluster in groups. The coral bed serves ecosystem services for tourism, fisheries, and shoreline protection (Nagelkerken et al. 2002).

Figure 1: image of Coral bed

In fluid dynamics, the ambition of determining linear stability is to observe if a given flow is either stable or unstable, and if so, how these instabilities will affect the progress of turbulence is verified. The determination of linear stability is most particularly laid by Helmholtz, Kelvin, Rayleigh, and Reynolds. In this research, the linear stability of the coral bed will be defined, both respecting Reynold's stress and without considering Reynolds stress. The coral bed is very significant for many different motives aside from hypothetically comprising the most assorted ecosystem on the sphere. It defends coastlines from the harmful effects of wave conflicts and tropical storms and delivers locales and shelter for many marine creatures. It is the source of nitrogen and other vital nutrients for marine food chains supports in carbon and nitrogen setting and help with nutrient recycling.

In prior Linear stability has been analyzed in growth system of sand bars in anabranching rivers (Z.W, Li et al. 2013), meander development initiating from alternate bars (Fujita et al. 1985), gravel-bed river driven by vegetation (Y.Shimizu et al. 2013), river channel flows (Callandar, R.A et al. 1969), closed conduit (Hosoda et al. 2000) and so on. But linear stability analysis of coral bed is rarely found. As linear stability analysis is a very crucial function of fluid dynamics, research on the analysis of linear stability in coral beds has been shown in this paper.

It is supposed that necessary substances for photosynthesis such as carbon dioxide are abundant, and, as a result, photosynthesis is mainly controlled by light. In addition, coral is eroded if the flow velocity is higher than some critical velocity. Assuming that the availability of light decreases inversely proportionally to the flow depth and erosion rate is proportional to the flow velocity subtracted by the critical velocity. A simple sketch of a coral bed is shown in (Figure 2).

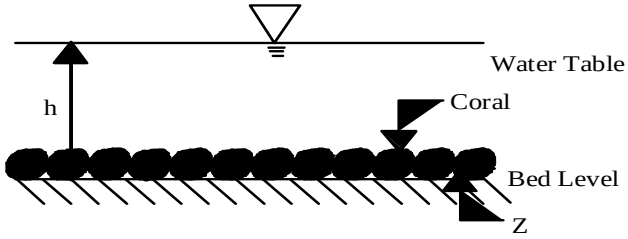

Figure 2: Simple sketch of coral bed.

In mathematics, in the concept of differential equations, if the resolution has the form, where A is a linear operative whose spectrum comprises eigenvalues with a positive real part. If all the eigenvalues have a negative real part, the solution is termed as linearly stable. An operating point of the system model is said to be linearly stable if, when perturbed from an operating point by a slight amount, the system model returns to that operating point (Sudhoff et al. 2003).

In this research, the three governing equations; Exner equation, Momentum equation, Continuity equation are normalized to make linear stability analysis, and the stability of coral bed is also analyzed for the conditions without and with considering Reynold's stress

2. METHODOLOGY

In this section, Exner equation, momentum equation, continuity equation, boundary condition, normalization of the governing equation, and asymptotic expansions are discussed.

2.1 Governing Equations

The governing equations Exner equation, Momentum equation and continuity equation are presented below:

Exner equation,

$$\frac{\partial \tilde{Z}}{\partial \tilde{t}} = \frac{\tilde{\alpha}}{\tilde{H}} - \tilde{\beta}(\tilde{U} - \tilde{U}_c) \tag{1}$$

Where $\tilde{Z}$ is the bed elevation, $\tilde{t}$ is time, $\tilde{\alpha}$ and $\tilde{\beta}$ are empirical constants with some dimensions, $\tilde{U}$ and $\tilde{H}$ is the flow velocity and depth respectively, $\tilde{U}_c$ is the critical flow velocity for the erosion of coral, and the tide denotes dimensional variables and are later removed to denote normalized equivalents

Flow in the channel is assumed to be described by Momentum equation for two conditions.

Without Reynold's stress:

$$\tilde{U}\frac{\partial \tilde{U}}{\partial \tilde{x}} = -g\frac{\partial \tilde{H}}{\partial \tilde{x}} - g\frac{\partial \tilde{Z}}{\partial \tilde{x}} + gS - \frac{\tilde{\tau}_b}{\rho \tilde{H}} \tag{2}$$

With Reynold stress:

$$\tilde{U}\frac{\partial \tilde{U}}{\partial \tilde{x}} = -g\frac{\partial \tilde{H}}{\partial \tilde{x}} - g\frac{\partial \tilde{Z}}{\partial \tilde{x}} + gS - \frac{\tilde{\tau}_b}{\rho \tilde{H}} - \tilde{\varepsilon}\frac{\partial^2 \tilde{U}}{\partial \tilde{x}^2} \tag{3}$$

Where $\tilde{x}$ is the streamwise coordinate, $\tilde{\tau}_b$ is the bed stress, ρ is the water density, g is the gravity acceleration, S is the bed slope, $\tilde{Z}$ is the bed elevation from the flat bed with a constant slope S, Reynold's stress $\tilde{\varepsilon} = 0.077\tilde{U}_f \tilde{H}_n$.

Where, $\tilde{\tau}_b = \rho C_f \tilde{U}^2$. (4)

Here, C_f is the friction coefficient which is assumed to be a constant for simplicity.

The Continuity equation is

$$\tilde{U}\tilde{H} = \tilde{q} \tag{5}$$

Where, $\tilde{q}$ is the net discharge. It is assumed that the growth rate of coral is balanced with the erosion rate, the equilibrium state is realized. Thus the bed remains flat with its constant elevation. The diagram of linear stability analysis with variables are shown in Figure 3, where, *Z* is the bed level, *U* and *H* are the flow velocity and depth respectively (dimensional).

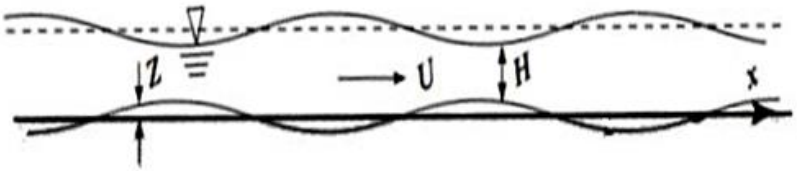

Figure 3: Diagram of linear stability analysis

2.2 Normalization

The following normalization has been used for normalization of the Exner equation, Momentum equation and continuity equation.

The equations (1), (2), (3), (4), (5) are normalized using the following equations (6), (7), (8), (9)

$$(\tilde{U},\tilde{U}_c)=\tilde{U}_n(U,U_c) \tag{6}$$

$$(\tilde{x},\tilde{H},\tilde{Z})=\tilde{H}_n(x,H,Z) \tag{7}$$

$$\tilde{t}=\frac{\tilde{H}_n{}^2}{\tilde{\alpha}}t \tag{8}$$

$$\tilde{\beta}=\frac{\tilde{\alpha}}{\tilde{q}}\beta \tag{9}$$

The normalized form of Exner equation.

$$\frac{\partial Z}{\partial t}-\frac{1}{H}+\beta(U-U_c)=0 \tag{10}$$

The normalized form of Momentum equation

$$U\frac{\partial U}{\partial x}+F^{-2}(\frac{\partial H}{\partial x}+\frac{\partial Z}{\partial x})-C_f(1-\frac{U^2}{H})=0 \tag{11}$$

$$U\frac{\partial U}{\partial x}+F^{-2}(\frac{\partial H}{\partial x}+\frac{\partial Z}{\partial x})-C_f(1-\frac{U^2}{H})+\varepsilon F^{-1}\frac{\partial^2 U}{\partial x^2}=0 \tag{12}$$

Equation (6) and (7) are the normalized form of momentum equation without and with the Reynold's stress respectively.

The normalized form of Continuity equation.

$$UH-1=0 \tag{13}$$

2.3 Linear Stability Analysis

For performing linear stability analysis, we have employed the asymptotic expansions of the sinusoidal form as,

$$u=A\hat{u}\exp[ik(x-\omega t)] \tag{14}$$

$$h=A\hat{h}\exp[ik(x-\omega t)] \tag{15}$$

$$z=A\hat{z}\exp[ik(x-\omega t)] \tag{16}$$

Where, A, k and ω are the amplitude, wavenumber and complex growth rate of perturbation ($\omega=\omega_r+i\omega_i$), respectively.

By performing linear stability analysis the following equations are obtained,

$$\omega=(F^{-2}\frac{U_c}{1-U_c})\frac{3C_f+ik(1-F^{-2})}{9C_f{}^2+k^2(1-F^{-2})^2} \tag{17}$$

From equation (17) separating the real and imaginary part we find,

$$\omega_r=(F^{-2}\frac{U_c}{1-U_c})\frac{3C_f}{9C_f{}^2+k^2(1-F^{-2})^2} \tag{18}$$

$$\omega_i=(F^{-2}\frac{U_c}{1-U_c})\frac{k(1-F^{-2})}{9C_f{}^2+k^2(1-F^{-2})^2} \tag{19}$$

After Linear stability analysis the complex growth rate of perturbation ($\omega = \omega_r + i\omega_i$) with considering Reynold's stress is goven below.

$$\omega = (F^{-2}\frac{U_c}{1-U_c})\frac{3C_f + ik(1-F^{-2}+\frac{k^2\varepsilon}{F})}{9C_f{}^2 + k^2(1-F^{-2}+\frac{k^2\varepsilon}{F})^2} \tag{19}$$

After separating the real and imaginary part from equation (19) it is perceieved that,

$$\omega_r = (F^{-2}\frac{U_c}{1-U_c})\frac{3C_f}{9C_f{}^2 + k^2(1-F^{-2}+\frac{k^2\varepsilon}{F})^2} \tag{20}$$

$$\omega_i = (F^{-2}\frac{U_c}{1-U_c})\frac{k(1-F^{-2}+\frac{k^2\varepsilon}{F})}{9C_f{}^2 + k^2(1-F^{-2}+\frac{k^2\varepsilon}{F})^2} \tag{21}$$

Here, ω_i = growth rate of perturbation.

3. RESULT AND DISCUSSIONS

To analyze the linear stability of coral bed, the variation of Froude number and wave number for both Reynold's stress and without Reynold's stress 'MATHMATICA 9' software has been used.

3.1 Instability diagram

Instability diagram without considering Reynold's stress and considering Reynold's stress is shown below.

3.1.1 For Without Reynold's Stress

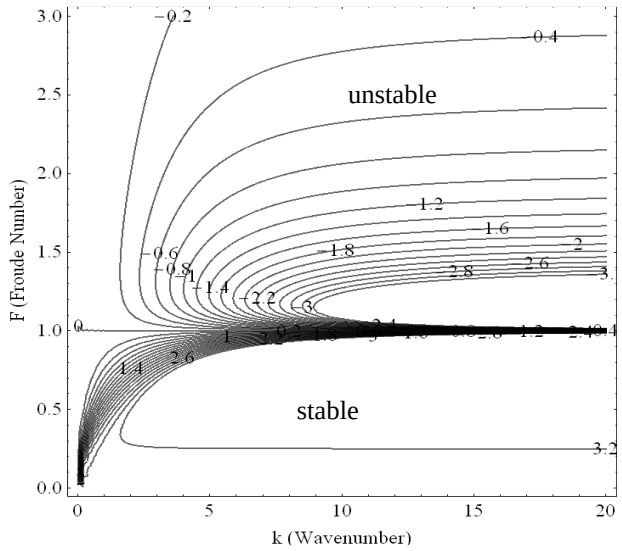

Figure 4: The contours of growth rate of perturbation (without Reynold's stress)

Figure 4 shows the contours of the growth rate of perturbation in the case for without Reynolds stress (variation of Froude number with wave number). In figure 4, ω_i is negative when $F \geq 1$. From Figure 4, it can be said that the flat bed is unstable when the Froude number is larger than unity. Because ω_r is always positive, the bed waves migrate downstream. The imaginary part of the angular frequency ω_i corresponds to the growth rate of perturbation so that the flat bed becomes unstable when F is greater than unity. In the unstable region, the growth rate ω_i increases monotonically with increasing wave number k, as k goes to infinity the growth rate asymptotically approaches to a constant value gradually.

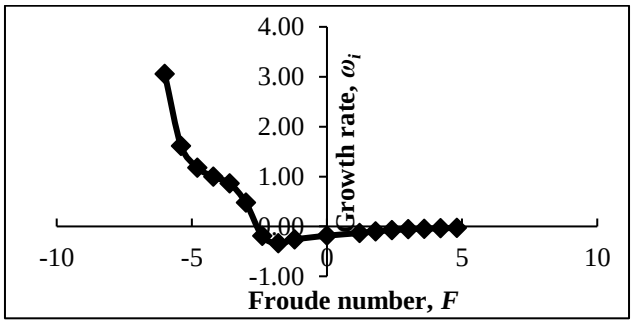

Figure 5: Variation of growth rate with Froude number (without Reynold's stress)

Here, in Figure 5, Growth rate ω_i is gradually decreasing with the increasing Froude number F. Growth rate is minimum when Froude number is approximately (-2). After that the growth rate starts to increase up to Froude number is approximately 5. Then the growth rate gradually becomes neutral with the increase of Froude number.

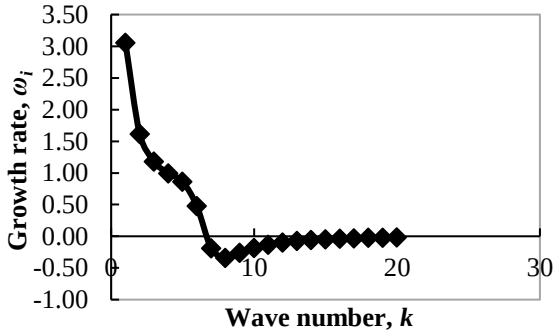

Figure 6: Variation of growth rate with wave number (without Reynold's stress)

Figure 6 indicates that, Growth rate ω_i is gradually decreasing with the increasing wave number k. Growth rate is minimum when wave number is approximately 7. After that growth rate starts to increase up to growth rate is approximately 15. Then the growth rate gradually becomes neutral with the increase of wave number.

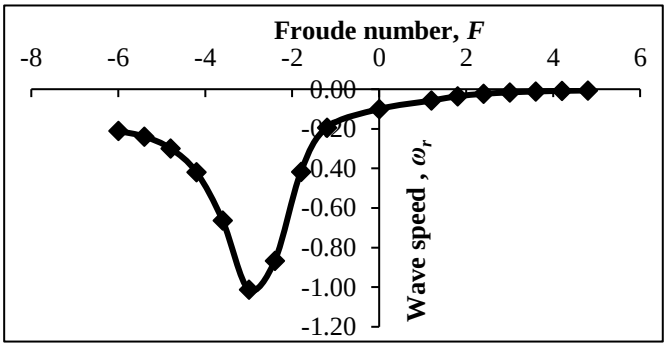

Figure 7: Variation of wave speed with Froude number (without Reynold's stress)

It is observed in Figure 7, wave speed ω_r is gradually decreasing with the increasing Froude number F. Wave speed is minimum Froude number is approximately (-3). After that wave speed starts to increase up to Froude number is approximately (+3). Then the wave speed gradually becomes neutral with the increase of wave number.

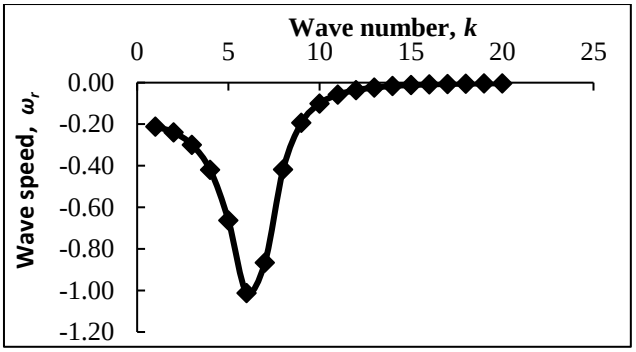

Figure 8: Variation of wave speed with wave number (without Reynold's stress)

Here, in Figure 8, wave speed ω_r is gradually decreasing with the increasing wave number k. Wave speed is minimum when wave number is approximately 6. After that wave speed starts to increase up to wave number is approximately 15. Then the wave speed gradually becomes neutral with the increase of wave number.

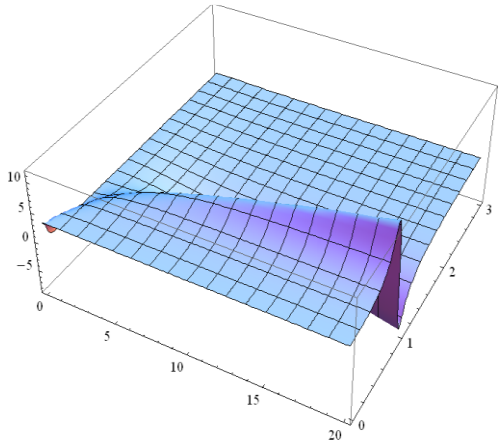

Figure 9: 3-D view of growth rate of perturbation (without Reynold's stress)

3.1.2 For Reynold's Stress

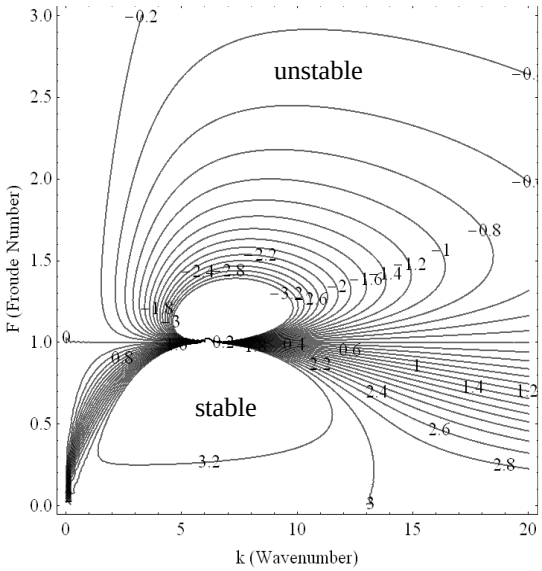

Figure 10: The contours of growth rate of perturbation (with Reynold's stress)

Therefore, from this Figure 10, it is found that ω_i is negative when $F \geq 1$ and the bed is unstable. In the unstable region the growth rate ω_i increases with increasing wave number, k in the small range of k. As, k goes to infinity, however, ω_i vanishes in this case because of the additional term originated from the Reynolds stress. There is a dominant wave number associated with a maximum growth rate.

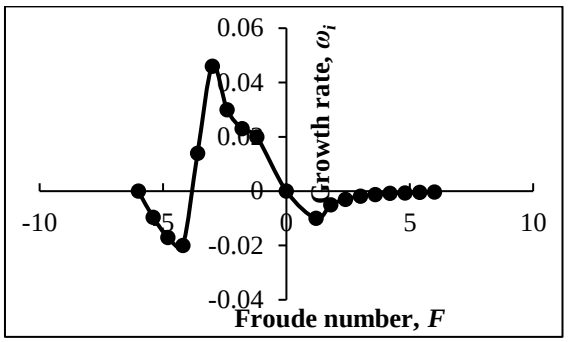

Figure 11: Variation of growth rate with Froude number (with Reynold's stress)

In this Figure 11, growth rate, ω_i is decreasing with the increase of Froude number, F. Growth rate decreases up to Froude number is approximately (-4). Then it starts to increase up to Froude number is approximately (-2.5). Then the growth rate again starts to decrease. When the Froude number is approximately 4 the growth rate becomes neutral gradually.

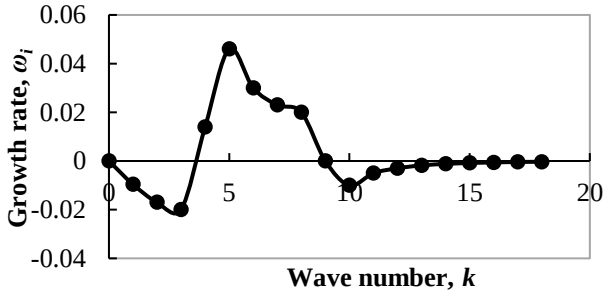

Figure 12: Variation of growth rate with wave number (with Reynold's stress)

In this Figure 12 growth rate, ω_i is decreasing with the increase of wave number, k. Growth rate decreases up to wave number is approximately 4. Then it starts to increase up to wave number is approximately 5. Then the growth rate again starts to decrease. When the wave number is approximately 15 the growth rate becomes neutral gradually.

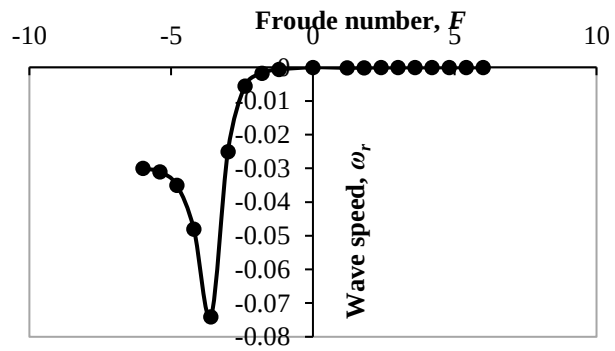

Figure 13: Variation of wave speed with Froude number (with Reynold's stress)

In Figure 13, wave speed, ω_r is decreasing with the increase of Froude number. The wave speed decreases up to Froude number is approximately (-4). Then it starts to increase up to the Froude number is approximately (-1) and then the wave speed becomes neutral gradually.

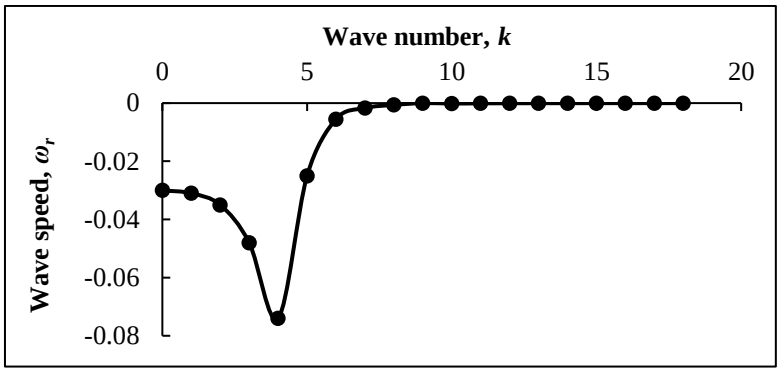

Figure 14: Variation of wave speed with wave number (with Reynold's stress)

From the above figure it is observed, wave speed, ω_r is decreasing with the increase of wave number. The wave speed decreases up to wave number is approximately 4. Then it starts to increase up to the wave number is approximately 7 and then the wave speed becomes neutral gradually.

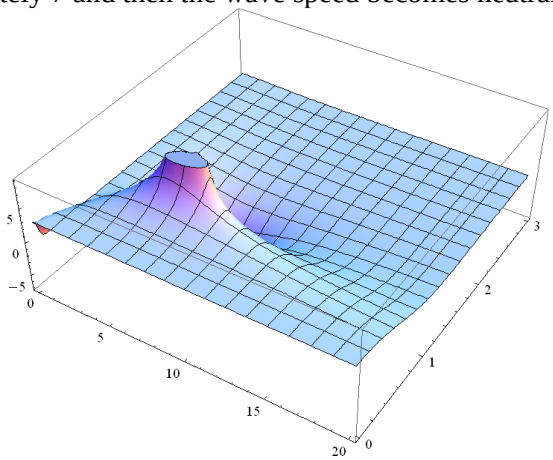

Figure 15: 3-D view of growth rate of perturbation (with Reynold's stress)

4. CONCLUSIONS

In this study, linear stability analysis of coral bed is conducted. Exner equation, Momentum equation, Continuity equation are used. Perturbation technique has been used to analyze the equations for stability analysis. From this analysis some conclusions are made. They are, stability of coral bed depends on Froude number and Wave number. Unstable region in the instability diagram expands in the direction of increasing wave numbers. Growth rate is negative and bed is unstable when Froude number is greater than unity. When wave number goes to infinity growth rate approaches to a constant position when Reynolds stress is absent. Growth rate vanishes when wave number goes to infinity when Reynold's stress is present.

REFERENCES

Callander, R. A. (1969). Instability and river channels. Journal of Fluid Mechanics, 36(3), 465-480.

Fujita, Y., & Muramoto, Y. (1985). Studies on the process of development of alternate bars.

Nagata, N., Hosoda, T., & Muramoto, Y. (2000). Numerical analysis of river channel processes with bank erosion. Journal of Hydraulic Engineering, 126(4), 243-252.

Nagelkerken, I., Roberts, C. V., Van Der Velde, G., Dorenbosch, M., Van Riel, M. C., De La Moriniere, E. C., & Nienhuis, P. H. (2002). How important are mangroves and seagrass beds for coral-reef fish? The nursery hypothesis tested on an island scale. Marine ecology progress series, 244, 299-305.

Shimada, R., Shimizu, Y., Hasegawa, K., & Iga, H. (2013). Linear Stability Analysis on the Meander Formation Originated by Alternate Bars (Japanese Title: Journal of Japan Society of Civil Engineers, Ser. B1 (Hydraulic Engineering), 69.

Sudhoff, S. D., Glover, S. F., Zak, S. H., Pekarek, S. D., Zivi, E. J., Delisle, D. E., & Clayton, D. (2003, April). Stability analysis methodologies for DC power distribution systems. In 13th International Ship Control Systems Symposium (pp. 7-9).

Zou, W., Yu, K. P., Arndt, R. E., Zhang, G., & Li, Z. W. (2013). On the shedding of the ventilated supercavity with velocity disturbance. Ocean Engineering, 57, 223-229.

Proceedings of the 5th International Conference on Civil Engineering for Sustainable Development (ICCESD 2020), 7~9 February 2020, KUET, Khulna, Bangladesh (ISBN-978-984-34-8764-3)

SIMULATING FLOOD RISK DUE TO CLIMATE CHANGE IN THE PADMA RIVER SYSTEM USING THE 2D HEC-RAS MODEL

Subir Biswas*[1], M. Shahjahan Mondal [2] and Md. Rashedul Islam[3]

[1]Research Associate, Institute of Water and Flood Management, BUET, Dhaka, Bangladesh, e-mail: subir_buet@yahoo.com
[2]Professor, Institute of Water and Flood Management, BUET, Dhaka, Bangladesh, e-mail: mshahjahanmondal@iwfm.buet.ac.bd
[3]Assistant Professor, Institute of Water and Flood Management, BUET, Dhaka, Bangladesh, e-mail: rashed_rakib@iwfm.buet.ac.bd

***Corresponding Author**

ABSTRACT

Bangladesh is in a unique geographic location with the dominance of floodplains, low land elevation, proximity to the sea and overwhelming dependence on nature. These characteristics have made the country highly vulnerable to climate change. Due to climate change, it is experiencing several consequences like irregular monsoon climate, untimely rainfall and heavy rainfall over a short period of time. This results in increased river flow and inundation during monsoon, increased frequency, intensity and recurrence of floods. Information about flood risk is usually available at the boundaries of major rivers. But it is usually unknown the flood risks at different points in the floodplain. Flood risks in the floodplain are determined using that river information. In this study, we have set up a two-dimensional hydrodynamic model called HEC-RAS for the Padma River system to simulate flood hydrographs at different locations. The Padma River and its adjoining areas are included in the model setup. Digital land elevation data from WARPO and river cross-section data from BWDB and our own survey are used to prepare the two-dimensional surface of the model. The model is calibrated and validated using observed water level (at the Padma and the Arial Khan River) and discharge (at Baruria Transit on the Padma river) data from BWDB and BIWTA. The model is calibrated for 2004 and validated for the largest flood of 1998 that occurred in the area. It is found that the model can simulate the observed variation of flood quite satisfactorily at different locations. To assess the impact of climate change on the flood, the discharge hydrographs at model boundaries (Baruria Transit on the Padma River) were changed according to climate change scenarios and the HEC-RAS model was rerun. The flood hydrographs under the base condition and changed climate were compared to assess the impact of climate change. The result reveals that the peak flood level in the Padma River can be increased by 60cm on average due to climate change.

Keywords: *Climate change, Flood, Deterministic simulation, HEC-RAS model, Padma river.*

1. INTRODUCTION

Throughout history, the global climate has been changed and its effects have already found on the environment. Climate Change has become a major issue nowadays. With a unique geographic location and geological characteristics, Bangladesh is highly vulnerable to climate change. Kreft, Eckstein and Melchior (2016) analyzed the most reliable data sets available on the impacts of extreme weather events and associated socio-economic data for the last 20 years (1996-2015) and made a Global Climate Risk Index for the year 2017. According to them, Bangladesh is in the sixth position among the world's top 10 countries most affected by extreme weather events (Kreft, Eckstein & Melchior, 2016). Among the hydro-climatic hazards, flooding is considered one of the devastating, widespread and frequent one (Teng et al., 2017). It is the most significant natural hazard in Bangladesh as the country lies on the downstream part of the GBM rivers basin. Every year Flood inundates about 20.5 percent of the country while floods with a return period of 100 years inundate more than 60 percent of the country. During1998 floods the affected area was about 70 percent of the country (FFWC, 2005).

Many Climate experts have suggested from their analysis (e.g. General Circulation Models (GCM) analysis) that flooding will be increased in future due to climate change in terms of both extent and frequency (Mirza, 1997; Mirza, Warrick & Ericksen, 2003 and Mohammed et al., 2017). Some of them also suggest an increase in monsoon rainfall (ADB, 1994). Such rainfall will play a key role in the runoff generation processes and eventually exacerbate the flooding problem. Mirza (1997) found an increase of about 69% in the mean annual flow of the Ganges River at Farakka by doubling of CO_2 scenario. He assessed a runoff-climate model with observational and GCM data for the nine sub-basins of the Ganges River basin where all basins showed an increase in runoff in the climate change scenario (Mirza, 1997). In another study, Mirza et al. (2003), have found that if temperature rise about 6^0C the mean flooded area may increase in the range of 20–40%. Depending on the general circulation model he predicted 55% of the flooded area could be deeply flooded (Mirza et al., 2003).

So, there is a possibility of more serious flooding in Bangladesh. Thus, it is very important to analyze flood risk in a changed climatic condition. The available information about flood risk at boundaries of major rivers can be used to simulate the risk at any point in the floodplain, also the risk under a changed climatic condition. The objective of this study is to assess the flood risk at a different point within the floodplain in terms of maximum water surface elevation, flood depth, flow velocity and direction under a changed climatic condition. For that, we have set up a two-dimensional hydrodynamic model called HEC-RAS for the Padma River along with its floodplains to simulate flood hydrographs at different locations. HEC-RAS is developed by the US Army Corps of Engineers. It is a freeware tool, basically a hydrodynamic mathematical model. This model simulates water movement by solving the Full Saint-Venant equations or the Diffusion Wave equations.

2. METHODOLOGY

The success of a 2D hydrodynamic model depends on the level of digital representation of the river and floodplain geometries through DEM. Also, the accurate description of the model parameters is needed to predict the flow magnitude and water levels accurately. In this study, digital land elevation data from WARPO and river cross-section data from BWDB and our own survey data are used to prepare the two dimensional surface of the model. In Figure 1, a schematic is showing the spatial extent of the 2D area and the river network used in this model.

2.1 Preparation of the DEM

Two dimensional (2D) hydrodynamic models require the geometric description of river bathymetry. A total of 26 cross-sections over a length of 98.7 kilometers in the Padma River, 12 cross-sections over a length of 81.4 kilometers in the Arial Khan River and 14 cross-sections over a length of 107.1 kilometers in small distributary rivers of the Padma River were used to make a Terrain surface for the river bathymetry in HEC-RAS environment. Most of the bathymetric information was collected from different projects in the Institute of Water and Flood Management (IWFM) of BUET over the last few

years and some were collected from BWDB. Some bathymetries of the Padma have also been obtained very recently. River cross-sections at reasonable spacing were interpolated to satisfy the requirements of cross-section spacing. Sometimes cross-section cut lines were adjusted the better representation of the rivers, especially at junctions. This adjusted has produced a considerable improvement in the model outputs. A 20 meters spatial resolution Terrain was prepared from the river cross-section.

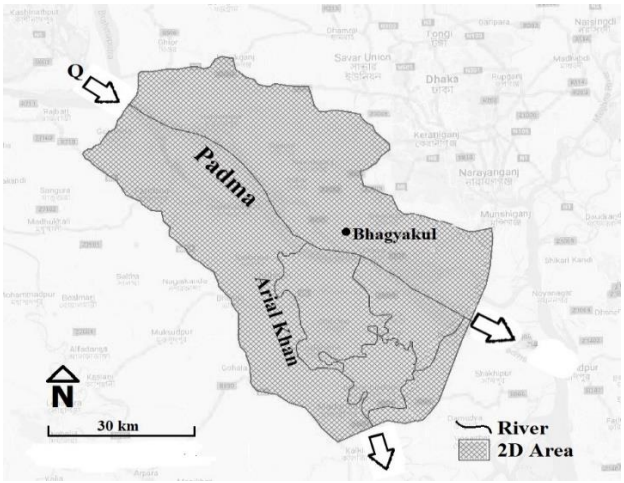

Figure 1: Model domain with 2D Mesh and River network

For floodplain bathymetry, a 500 meters DEM from WARPO was resampled into 50 meters raster file in the Arc-GIS environment through Inverse Distance Weighted (IDW) interpolation technique. The raster file was saved in float file format and then merged together with the rivers Terrain in HEC-RAS with the first priority for river Terrain and second for the raster DEM to integrate river bathymetry with the surrounding topography. The final processed DEM is shown in Figure 2. Before merging all necessary features projected into the same projection system as per HEC-RAS requirement.

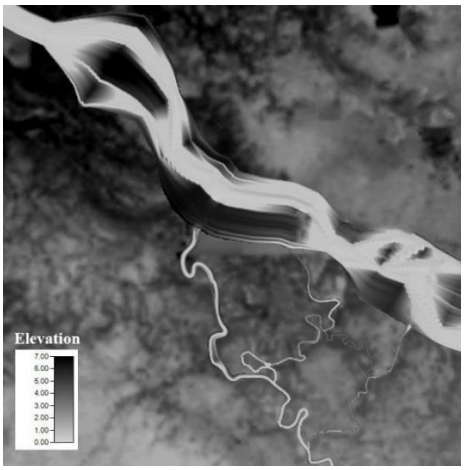

Figure 2: Image of the final processed DEM

2.2 Model Setup

In this 2D hydrodynamic model, a length of 87.4 kilometers of the Padma River spanning from Baruria Transit to down of Sureswar was modeled. The 2D area covers about 3890 kilometers^2 and a 200*200 meter^2 mesh cell size was used for the computation. The natural barriers such as roads, highways and Terrain contour lines were used as a guide to select the 2D area extent as suggested by HEC-RAS User Manual. It is found through several unsteady flow simulation that little change in 2D area vertex at floodplain have no impact in model output such as maximum water level, velocity. The model was set for 2004 and calibrated, and then validated for 1998.

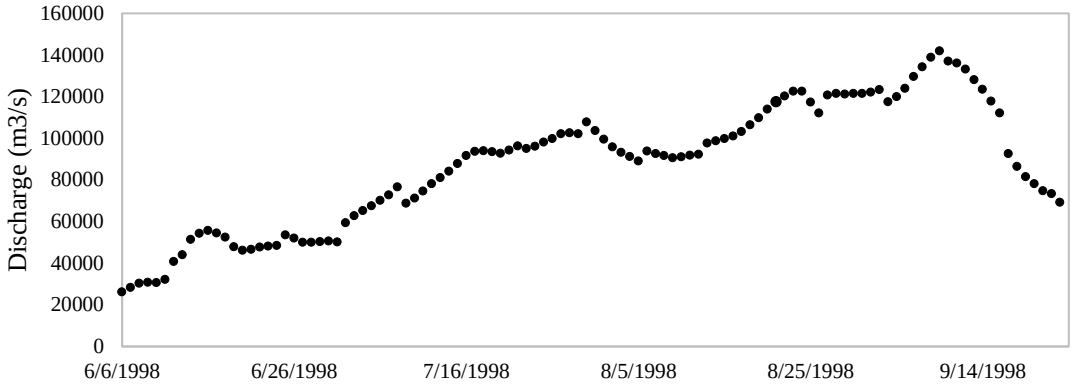

Figure 3: Mean daily discharge at Baruria Transit (SW91.9L) for 1998

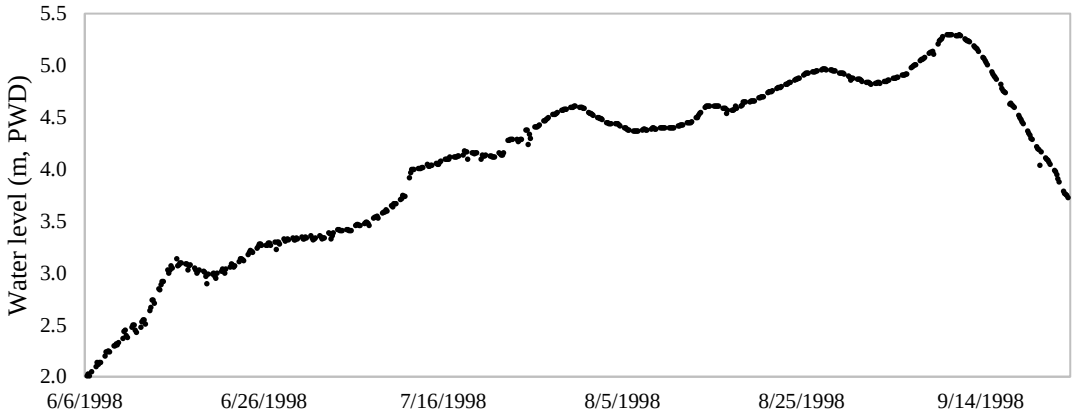

Figure 4: Water level of the downstream boundary at the Arial Khan River for 1998

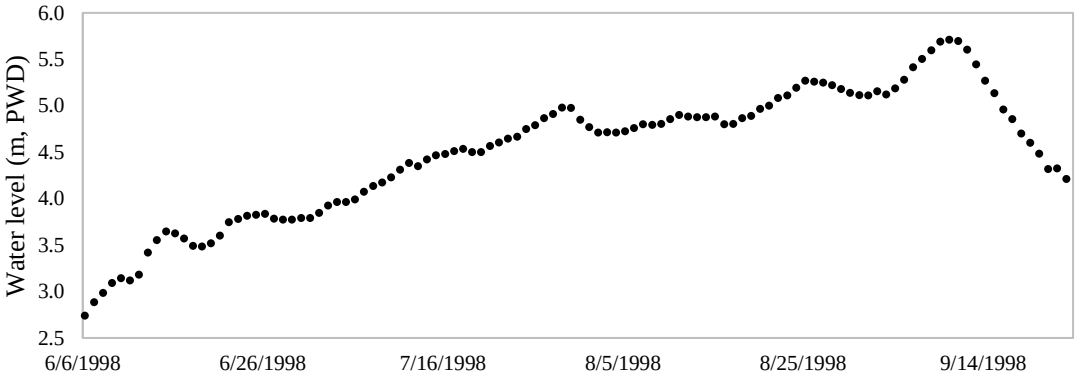

Figure 5: Water level of the downstream boundary at the Padma River for 1998

As it is an unsteady flow simulation, the model requires boundary and initial conditions. The upstream boundary condition of this model was set with a flow hydrograph at Baruria Transit (SW91.9L) on the Padma River with mean daily discharge (MDD). Figure 3 shows the flow hydrograph at the upstream boundary for 1998. For the downstream boundary condition, such as Madaripur (SW5) on the Arial Khan and Sureswar (SW95) on the Padma River, the water levels were used. The model boundary at the Arial Khan river is about 18 kilometers downstream of the Madaripur station. The water level at this location is determined from Madaripur station by water-surface slope analysis of the Arial Khan River. Figure 4 shows the water level of the downstream boundary at the Arial Khan River. Figure 5 shows the water level of the downstream boundary at Sureswar in the Padma River for 1998. Observed

discharge at Baruria Transit and water level at the Padma and Arial Khan were used as an initial condition.

2.3 Model Simulations

After the model setup, the simulation was performed from 5 June to 23 September for the year 2004 and then for 1998 to simulate the flood peak with a computational interval of 30 munites. As the model calculates water level at all points within the 2D area, we have compared the simulated water level with the observed water level at Bhagyakul river station (SW 93.4L) in the Padma River to calibrate the model for 2004. Manning roughness coefficient is used as a calibration and validation parameter. A land-use data layer with different Manning's n values is incorporated to define the surface resistance to flow using the RAS Mapper and Geometric window. Then, the model was rerun multiple times using different sets of Manning's n values for rivers and floodplains to get a proper matching in water levels. After the calibration, the model was rerun by changing the boundary conditions to simulate the flood of 1998 keeping other things the same. The validation was done by comparing the simulated water level and the observed water level at Bhagyakul river station for1998. A final fine-tuning in Manning's n values were done to get a satisfactory calibrated and validated model.

Due to climate change, the streamflow in different rivers would be changed as the rainfall pattern and intensity changes. There are literature based on modeling, give predictions about the amount of streamflow increase in different rivers in Bangladesh. It has been analyzed that the flow peak would increase due to climate change (Mondal et al., 2018). In this study, to simulate the climate changed scenario, the upstream flow at Baruria Transit was changed by increasing the flow of the 1998 flood as summarized by Mondal et al. (2018). Then the HEC-RAS model was rerun by changing the upstream boundary flows of the Padma River at Baruria Transit keeping other things the same as the year 1998. After the simulation, the climate change impact on the water level in different locations within the 2D area has been analyzed.

3. RESULT AND DISCUSSIONS

3.1 Model Calibration and Validation

The model was calibrated using the water level data at Bhagyakul river station (SW 93.4L), an intermediate gage station on the Padma River for the year 2004 and validated for the year 1998. In both years, there were floods in the study area and the 1998 flood was the most extreme one. The comparison of model-simulated and the observed water level is shown in Figure 6 and Figure 7. A Manning's n value 0.017 for the Padma River, 0.025 for the Arial Khan River and other distributary rivers, and 0.030 - 0.035 for the floodplain, from low elevation to high elevation, is used for the final setup. It is found that the model captures the variation in the stage hydrograph at Bhagyakul reasonably well.

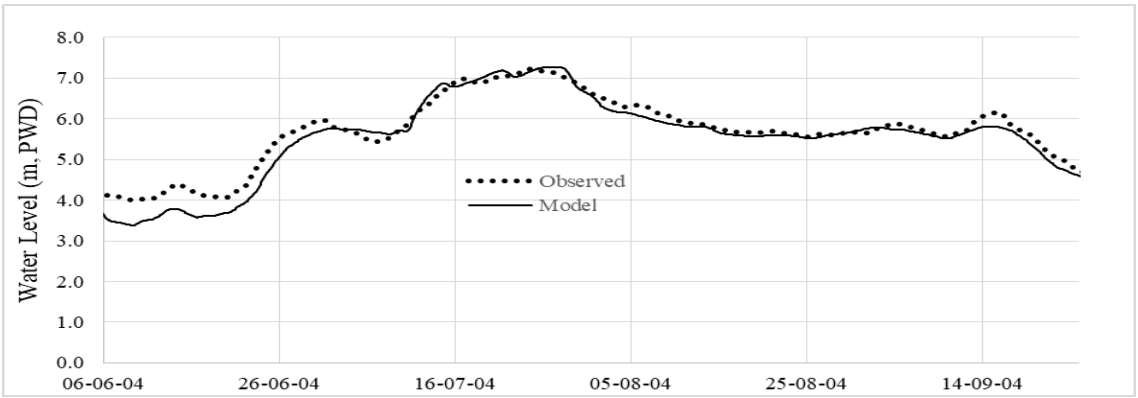

Figure 6: Comparison of model-simulated and observed water level at Bhagyakul on the Padma River for 2004

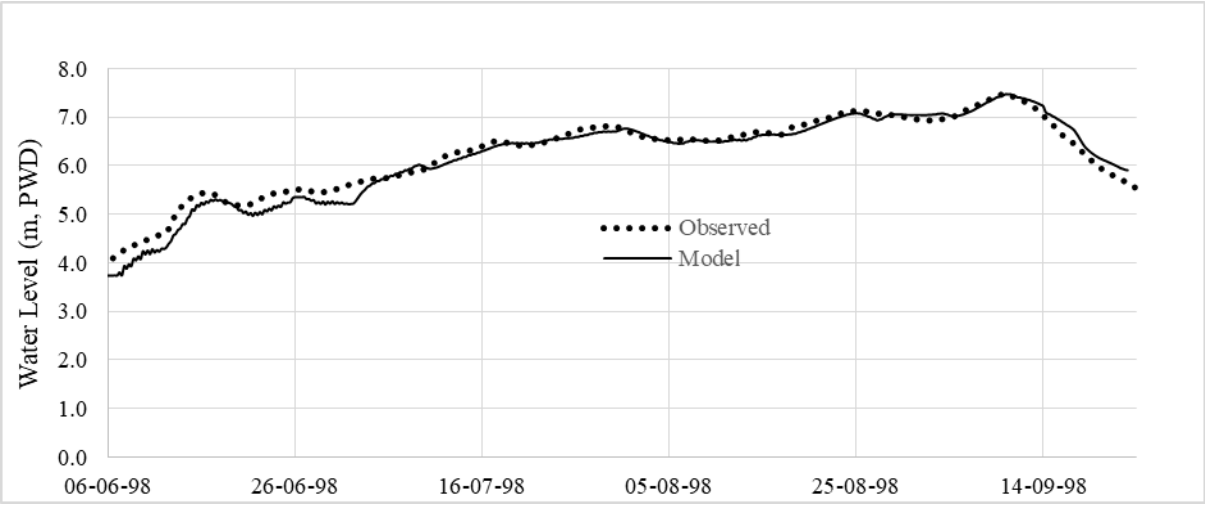

Figure 7: Comparison of model-simulated and observed water level at Bhagyakul on the Padma River for 1998

In the year 1998, the highest measured water level was found to be 7.50 m, PWD on the 10th of September and the highest simulated water level was 7.47 m, PWD on the same day. However, a closer view of the simulated hydrograph revealed that the model can simulate flood peak very well but underestimate the water level in low flow conditions at initial stages. From this model, such stage hydrograph is available at any point within the 2D area. Thus, flood risk can be easily determined at any point in both rivers and floodplains. But, at the edge of the 2D mesh, the results are not representative sometimes. So, it is suggested to keep the 2D mesh boundary away from the location of interest.

A survey was conducted by IWFM on maximum flood level in 1998 in Shariatpur and Madaripur district in two locations covering an area about 80-kilometer square. Age-old people who have experienced the flood in 1998 were asked about the highest flood level by showing some references. Those points are within this model domain. A relation between the surveyed maximum flood level and model maximum flood level is shown in Figure 8.

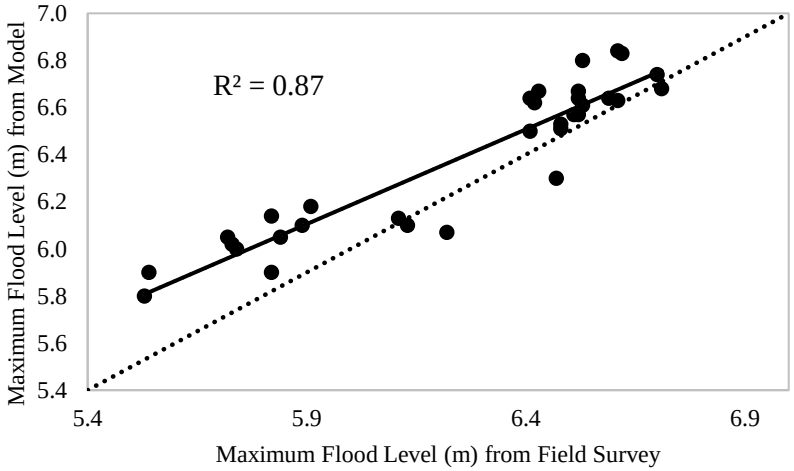

Figure 8: Correlation between maximum flood level from field survey and model

This surveyed area only covers a small portion of the total floodplain modeled in this study. But, it requires huge resources to collect such information about flood levels at such a huge scale. With this

limited information, it is found that the model simulated maximum flood water level is 15cm higher on average than the survey data.

3.2 Impact of Climate Change

It is expected that future streamflow would change due to climate change. Mohammed et al. (2017) have used the SWAT model to generate daily streamflow time series for three major transboundary rivers (the Ganges, the Brahmaputra and the Meghna). In that study, 11 different streamflow time series were available for 1980-2099 based on 11 climate projections. The simulated streamflows varied from one projection to another projection. A representative projection was identified by comparing the highest observed and modeled flows during the base period (1980-2009) for every river. From the analysis, a 29% increase in flow peak of the Ganges, 10% in the Brahmaputra and 22% in the Meghna are indicated by comparing the highest flow of the 2080s (1970-2099) with that of the base condition (1980-2009) (Mondal et al., 2018). The climate change condition was simulated in this model by adopting this increase in streamflow. The results are summarised through the comparison of the maximum water level at different locations in Table 1. The maximum water level is found on 10th September for both 1998 and climate changed condition.

Table 1: Comparison of maximum water level at different locations

Location	Observed maximum water level in 1998 (m)	Model maximum water level in 1998 (m)	Maximum water level due to climate change (m)	Increase in water level due to climate change (m)
Bhagyakul	7.50	7.47	8.09	0.62
Arial Khan Offtake	7.58	7.55	8.20	0.65
Mawa	7.14	7.05	7.63	0.58

After the simulation with climate changed condition, it is found that the peak flood level of 1998 magnitude has increased by 65cm at Offtake of the Arial Khan, 62cm at Bhagyakul and 58cm at Mawa in the Padma. The magnitude of flood level also increased in the floodplain by 41cm to 64cm with an average of 53cm in previously mentioned surveyed locations. From this model, flood levels at different locations of the Padma River system are available under the climate changed condition.

The model sensitivity has been tested by changing the Manning's n value for the Padma River and comparing the change in maximum water level at Bhagyakul river station. The relation between Manning's n value and corresponding maximum water level at Bhagyakul is shown in Figure 9. A change in Manning's n value of 0.001 of the Padma River results on average 0.083 meters change in maximum water level at Bhagyakul. Also, the change in water level reduces for a higher Manning's n value.

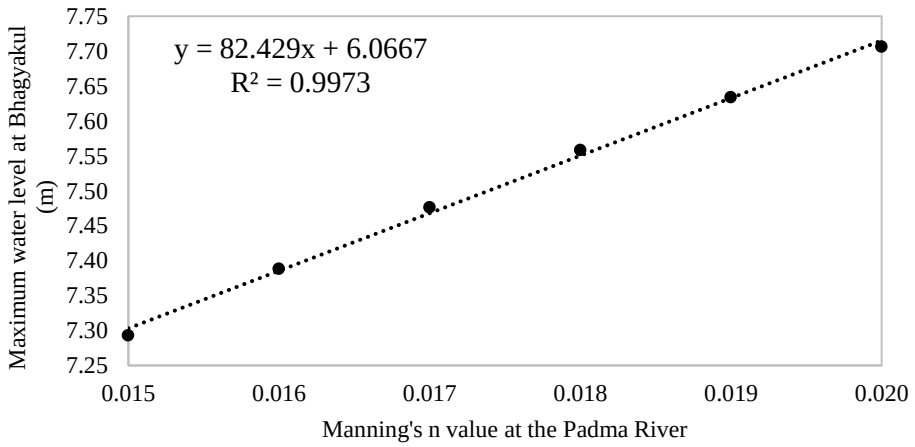

Figure 9: Water level change due to change in Manning's n value at the Padma River

4. CONCLUSIONS

In a country like Bangladesh, where data is very limited and scarce, different modeling approaches can give reasonable predictions of required scenarios. Flood risk in the Padma River along with its distributaries and floodplains due to climate change impacts were evaluated using the HEC-RAS model in this study. The flood peaks might increase by approximately 60cm in the Padma River system under a changed climate condition. The flood peaks might be higher if the potential rise in sea level is considered. As the model can provide stage hydrograph at any point within the 2D mesh, it would be useful in infrastructural planning and design, such as economic zone, power plant, airport, bridge, flood control embankment, river training work and road, in the floodplain of the rivers modeled.

ACKNOWLEDGMENTS

The authors would like to thank all the survey respondents at Shariatpur and Madaripur district for their valuable information about the highest flood level in that area.

REFERENCES

Asian Development Bank (1994). *Climate Change in Asia: Bangladesh Country Report*, ADB, Manila, the Philippines.

FFWC (2005). *Consolidation and strengthening of flood forecasting and warning services, Final Report, Volume II – Monitoring and evaluation*, Bangladesh Water Development Board, Dhaka.

Kreft, S., Eckstein D., and Melchior, I. (2016). *Global Climate Risk Index - 2017*, Germanwatch e.V., Retrieved from https://germanwatch.org/de/download/16411.pdf.

Mirza, M.M.Q. (1997). The runoff sensitivity of the Ganges river basin to climate change and its implications. *Journal of Environmental Hydrology*, 5, 1-12.

Mirza, M.M.Q., Warrick, R.A., and Ericksen, N.J. (2003). The implications of climate change on floods of the Ganges, Brahmaputra and Meghna rivers in Bangladesh. *Climate Change*, 57, 287-318.

Mohammed, K., Islam, A.K.M.S., Islam, G.M.T., Alfieri, L., Bala, S.K., & Khan, M.J.U. (2017). Impact of high-end climate change on floods and low flows of the Brahmaputra River. *Journal of Hydrologic Engineering*, 22(10), 04017041

Mondal, M.S., Islam, A.K.M.S., Haque, A., Islam, M.R., Biswas, S., & Mohammed, K. (2018). Assessing High-End Climate Change Impacts on Floods in Major Rivers of Bangladesh Using Multi-Model Simulations. *Global Science and Technology Journal*, 6(2), 1-14.

Teng, J., Jakeman, A.J., Vaze, J., Croke, B.F.W., Dutta, D., & Kim, S. (2017). Flood inundation modeling: A review of methods, recent advances and uncertainty analysis. *Environmental Modelling & Software*, 90, 201-216.

Proceedings of the 5th International Conference on Civil Engineering for Sustainable Development (ICCESD 2020), 7~9 February 2020, KUET, Khulna, Bangladesh (ISBN-978-984-34-8764-3)

SIMULATING FLOOD RISK DUE TO CLIMATE CHANGE IN THE PADMA RIVER SYSTEM USING THE 2D HEC-RAS MODEL

Subir Biswas*[1], M. Shahjahan Mondal [2] and Md. Rashedul Islam[3]

[1]Research Associate, Institute of Water and Flood Management, BUET, Dhaka, Bangladesh, e-mail: subir_buet@yahoo.com
[2]Professor, Institute of Water and Flood Management, BUET, Dhaka, Bangladesh, e-mail: mshahjahanmondal@iwfm.buet.ac.bd
[3]Assistant Professor, Institute of Water and Flood Management, BUET, Dhaka, Bangladesh, e-mail: rashed_rakib@iwfm.buet.ac.bd

***Corresponding Author**

ABSTRACT

Bangladesh is in a unique geographic location with the dominance of floodplains, low land elevation, proximity to the sea and overwhelming dependence on nature. These characteristics have made the country highly vulnerable to climate change. Due to climate change, it is experiencing several consequences like irregular monsoon climate, untimely rainfall and heavy rainfall over a short period of time. This results in increased river flow and inundation during monsoon, increased frequency, intensity and recurrence of floods. Information about flood risk is usually available at the boundaries of major rivers. But it is usually unknown the flood risks at different points in the floodplain. Flood risks in the floodplain are determined using that river information. In this study, we have set up a two-dimensional hydrodynamic model called HEC-RAS for the Padma River system to simulate flood hydrographs at different locations. The Padma River and its adjoining areas are included in the model setup. Digital land elevation data from WARPO and river cross-section data from BWDB and our own survey are used to prepare the two-dimensional surface of the model. The model is calibrated and validated using observed water level (at the Padma and the Arial Khan River) and discharge (at Baruria Transit on the Padma river) data from BWDB and BIWTA. The model is calibrated for 2004 and validated for the largest flood of 1998 that occurred in the area. It is found that the model can simulate the observed variation of flood quite satisfactorily at different locations. To assess the impact of climate change on the flood, the discharge hydrographs at model boundaries (Baruria Transit on the Padma River) were changed according to climate change scenarios and the HEC-RAS model was rerun. The flood hydrographs under the base condition and changed climate were compared to assess the impact of climate change. The result reveals that the peak flood level in the Padma River can be increased by 60cm on average due to climate change.

Keywords: *Climate change, Flood, Deterministic simulation, HEC-RAS model, Padma river.*

1. INTRODUCTION

Throughout history, the global climate has been changed and its effects have already found on the environment. Climate Change has become a major issue nowadays. With a unique geographic location and geological characteristics, Bangladesh is highly vulnerable to climate change. Kreft, Eckstein and Melchior (2016) analyzed the most reliable data sets available on the impacts of extreme weather events and associated socio-economic data for the last 20 years (1996-2015) and made a Global Climate Risk Index for the year 2017. According to them, Bangladesh is in the sixth position among the world's top 10 countries most affected by extreme weather events (Kreft, Eckstein & Melchior, 2016). Among the hydro-climatic hazards, flooding is considered one of the devastating, widespread and frequent one (Teng et al., 2017). It is the most significant natural hazard in Bangladesh as the country lies on the downstream part of the GBM rivers basin. Every year Flood inundates about 20.5 percent of the country while floods with a return period of 100 years inundate more than 60 percent of the country. During1998 floods the affected area was about 70 percent of the country (FFWC, 2005).

Many Climate experts have suggested from their analysis (e.g. General Circulation Models (GCM) analysis) that flooding will be increased in future due to climate change in terms of both extent and frequency (Mirza, 1997; Mirza, Warrick & Ericksen, 2003 and Mohammed et al., 2017). Some of them also suggest an increase in monsoon rainfall (ADB, 1994). Such rainfall will play a key role in the runoff generation processes and eventually exacerbate the flooding problem. Mirza (1997) found an increase of about 69% in the mean annual flow of the Ganges River at Farakka by doubling of CO_2 scenario. He assessed a runoff-climate model with observational and GCM data for the nine sub-basins of the Ganges River basin where all basins showed an increase in runoff in the climate change scenario (Mirza, 1997). In another study, Mirza et al. (2003), have found that if temperature rise about 6^0C the mean flooded area may increase in the range of 20–40%. Depending on the general circulation model he predicted 55% of the flooded area could be deeply flooded (Mirza et al., 2003).

So, there is a possibility of more serious flooding in Bangladesh. Thus, it is very important to analyze flood risk in a changed climatic condition. The available information about flood risk at boundaries of major rivers can be used to simulate the risk at any point in the floodplain, also the risk under a changed climatic condition. The objective of this study is to assess the flood risk at a different point within the floodplain in terms of maximum water surface elevation, flood depth, flow velocity and direction under a changed climatic condition. For that, we have set up a two-dimensional hydrodynamic model called HEC-RAS for the Padma River along with its floodplains to simulate flood hydrographs at different locations. HEC-RAS is developed by the US Army Corps of Engineers. It is a freeware tool, basically a hydrodynamic mathematical model. This model simulates water movement by solving the Full Saint-Venant equations or the Diffusion Wave equations.

2. METHODOLOGY

The success of a 2D hydrodynamic model depends on the level of digital representation of the river and floodplain geometries through DEM. Also, the accurate description of the model parameters is needed to predict the flow magnitude and water levels accurately. In this study, digital land elevation data from WARPO and river cross-section data from BWDB and our own survey data are used to prepare the two dimensional surface of the model. In Figure 1, a schematic is showing the spatial extent of the 2D area and the river network used in this model.

2.1 Preparation of the DEM

Two dimensional (2D) hydrodynamic models require the geometric description of river bathymetry. A total of 26 cross-sections over a length of 98.7 kilometers in the Padma River, 12 cross-sections over a length of 81.4 kilometers in the Arial Khan River and 14 cross-sections over a length of 107.1 kilometers in small distributary rivers of the Padma River were used to make a Terrain surface for the river bathymetry in HEC-RAS environment. Most of the bathymetric information was collected from different projects in the Institute of Water and Flood Management (IWFM) of BUET over the last few

years and some were collected from BWDB. Some bathymetries of the Padma have also been obtained very recently. River cross-sections at reasonable spacing were interpolated to satisfy the requirements of cross-section spacing. Sometimes cross-section cut lines were adjusted the better representation of the rivers, especially at junctions. This adjusted has produced a considerable improvement in the model outputs. A 20 meters spatial resolution Terrain was prepared from the river cross-section.

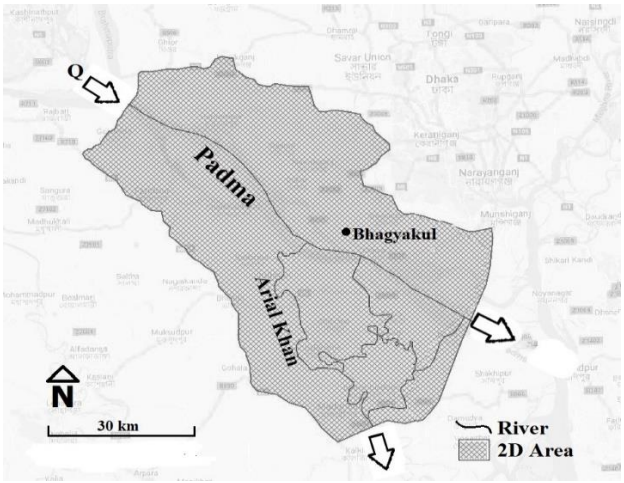

Figure 1: Model domain with 2D Mesh and River network

For floodplain bathymetry, a 500 meters DEM from WARPO was resampled into 50 meters raster file in the Arc-GIS environment through Inverse Distance Weighted (IDW) interpolation technique. The raster file was saved in float file format and then merged together with the rivers Terrain in HEC-RAS with the first priority for river Terrain and second for the raster DEM to integrate river bathymetry with the surrounding topography. The final processed DEM is shown in Figure 2. Before merging all necessary features projected into the same projection system as per HEC-RAS requirement.

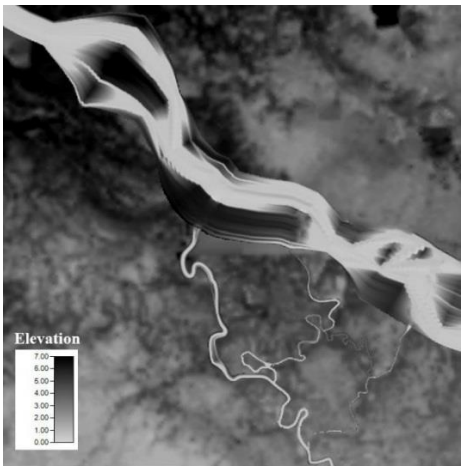

Figure 2: Image of the final processed DEM

2.2 Model Setup

In this 2D hydrodynamic model, a length of 87.4 kilometers of the Padma River spanning from Baruria Transit to down of Sureswar was modeled. The 2D area covers about 3890 kilometers^2 and a 200*200 meter^2 mesh cell size was used for the computation. The natural barriers such as roads, highways and Terrain contour lines were used as a guide to select the 2D area extent as suggested by HEC-RAS User Manual. It is found through several unsteady flow simulation that little change in 2D area vertex at floodplain have no impact in model output such as maximum water level, velocity. The model was set for 2004 and calibrated, and then validated for 1998.

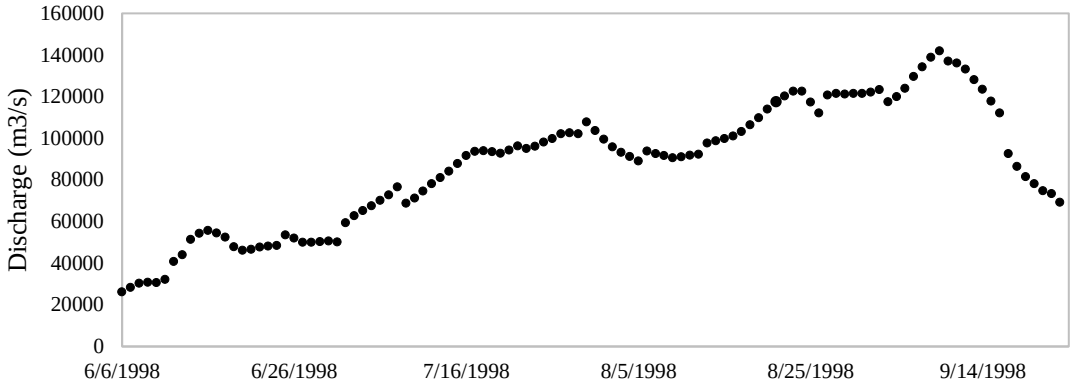

Figure 3: Mean daily discharge at Baruria Transit (SW91.9L) for 1998

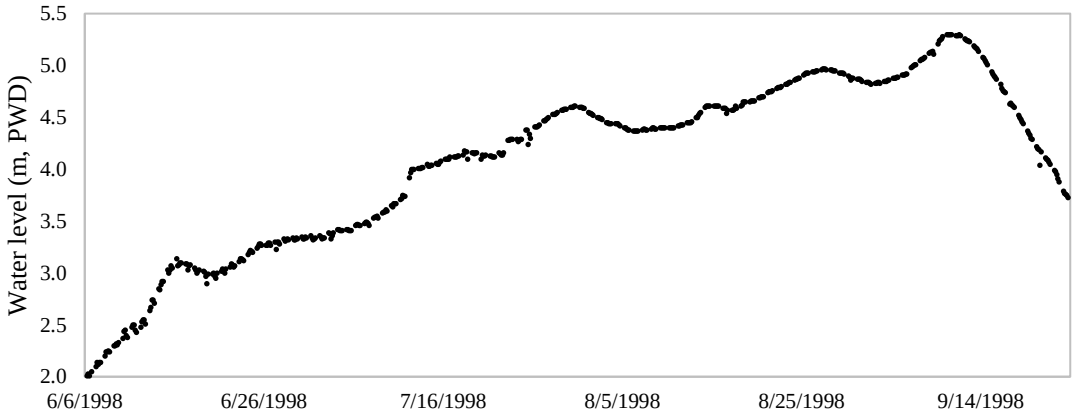

Figure 4: Water level of the downstream boundary at the Arial Khan River for 1998

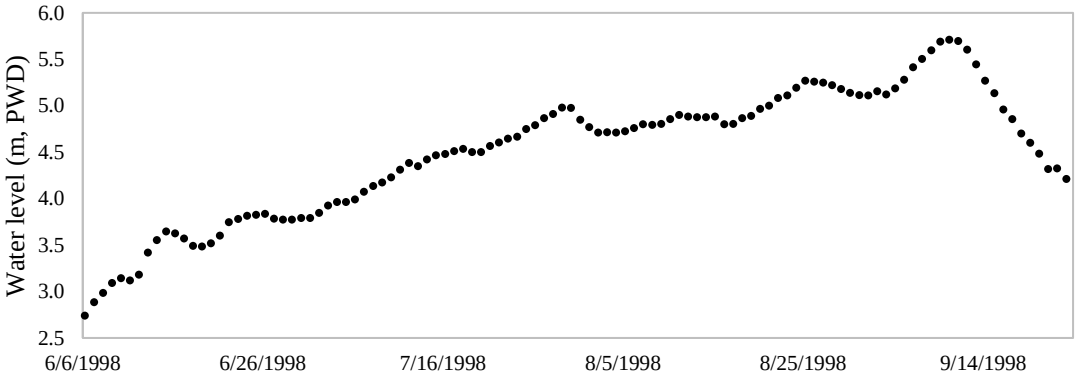

Figure 5: Water level of the downstream boundary at the Padma River for 1998

As it is an unsteady flow simulation, the model requires boundary and initial conditions. The upstream boundary condition of this model was set with a flow hydrograph at Baruria Transit (SW91.9L) on the Padma River with mean daily discharge (MDD). Figure 3 shows the flow hydrograph at the upstream boundary for 1998. For the downstream boundary condition, such as Madaripur (SW5) on the Arial Khan and Sureswar (SW95) on the Padma River, the water levels were used. The model boundary at the Arial Khan river is about 18 kilometers downstream of the Madaripur station. The water level at this location is determined from Madaripur station by water-surface slope analysis of the Arial Khan River. Figure 4 shows the water level of the downstream boundary at the Arial Khan River. Figure 5 shows the water level of the downstream boundary at Sureswar in the Padma River for 1998. Observed

discharge at Baruria Transit and water level at the Padma and Arial Khan were used as an initial condition.

2.3 Model Simulations

After the model setup, the simulation was performed from 5 June to 23 September for the year 2004 and then for 1998 to simulate the flood peak with a computational interval of 30 munites. As the model calculates water level at all points within the 2D area, we have compared the simulated water level with the observed water level at Bhagyakul river station (SW 93.4L) in the Padma River to calibrate the model for 2004. Manning roughness coefficient is used as a calibration and validation parameter. A land-use data layer with different Manning's n values is incorporated to define the surface resistance to flow using the RAS Mapper and Geometric window. Then, the model was rerun multiple times using different sets of Manning's n values for rivers and floodplains to get a proper matching in water levels. After the calibration, the model was rerun by changing the boundary conditions to simulate the flood of 1998 keeping other things the same. The validation was done by comparing the simulated water level and the observed water level at Bhagyakul river station for1998. A final fine-tuning in Manning's n values were done to get a satisfactory calibrated and validated model.

Due to climate change, the streamflow in different rivers would be changed as the rainfall pattern and intensity changes. There are literature based on modeling, give predictions about the amount of streamflow increase in different rivers in Bangladesh. It has been analyzed that the flow peak would increase due to climate change (Mondal et al., 2018). In this study, to simulate the climate changed scenario, the upstream flow at Baruria Transit was changed by increasing the flow of the 1998 flood as summarized by Mondal et al. (2018). Then the HEC-RAS model was rerun by changing the upstream boundary flows of the Padma River at Baruria Transit keeping other things the same as the year 1998. After the simulation, the climate change impact on the water level in different locations within the 2D area has been analyzed.

3. RESULT AND DISCUSSIONS

3.1 Model Calibration and Validation

The model was calibrated using the water level data at Bhagyakul river station (SW 93.4L), an intermediate gage station on the Padma River for the year 2004 and validated for the year 1998. In both years, there were floods in the study area and the 1998 flood was the most extreme one. The comparison of model-simulated and the observed water level is shown in Figure 6 and Figure 7. A Manning's n value 0.017 for the Padma River, 0.025 for the Arial Khan River and other distributary rivers, and 0.030 - 0.035 for the floodplain, from low elevation to high elevation, is used for the final setup. It is found that the model captures the variation in the stage hydrograph at Bhagyakul reasonably well.

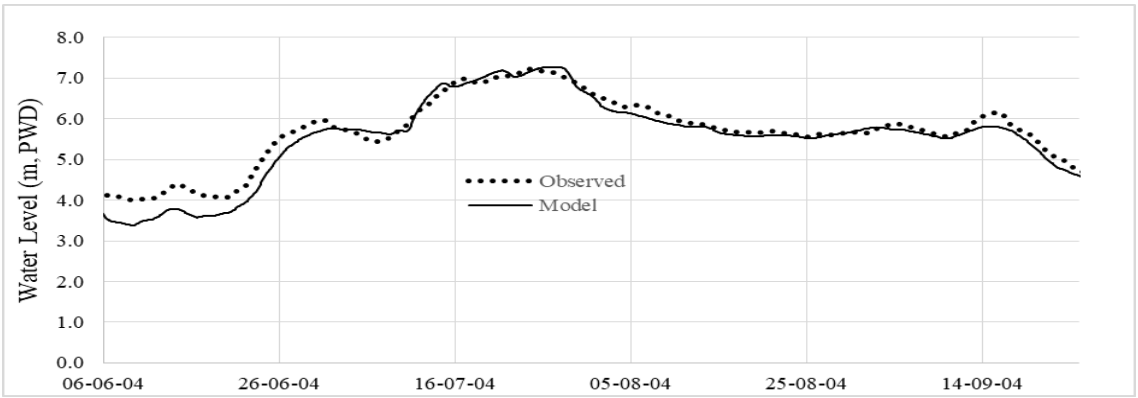

Figure 6: Comparison of model-simulated and observed water level at Bhagyakul on the Padma River for 2004

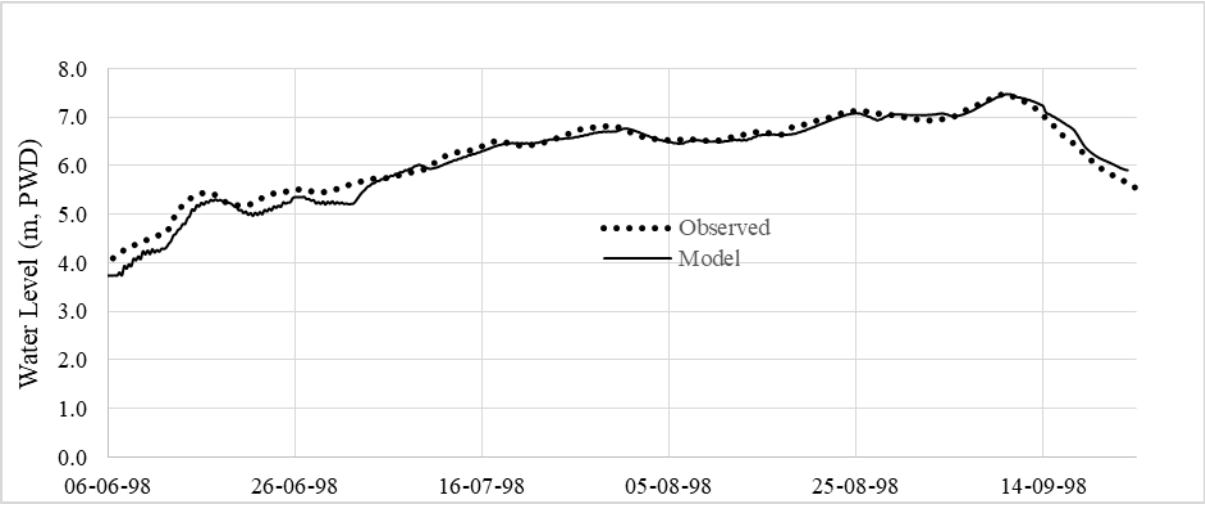

Figure 7: Comparison of model-simulated and observed water level at Bhagyakul on the Padma River for 1998

In the year 1998, the highest measured water level was found to be 7.50 m, PWD on the 10th of September and the highest simulated water level was 7.47 m, PWD on the same day. However, a closer view of the simulated hydrograph revealed that the model can simulate flood peak very well but underestimate the water level in low flow conditions at initial stages. From this model, such stage hydrograph is available at any point within the 2D area. Thus, flood risk can be easily determined at any point in both rivers and floodplains. But, at the edge of the 2D mesh, the results are not representative sometimes. So, it is suggested to keep the 2D mesh boundary away from the location of interest.

A survey was conducted by IWFM on maximum flood level in 1998 in Shariatpur and Madaripur district in two locations covering an area about 80-kilometer square. Age-old people who have experienced the flood in 1998 were asked about the highest flood level by showing some references. Those points are within this model domain. A relation between the surveyed maximum flood level and model maximum flood level is shown in Figure 8.

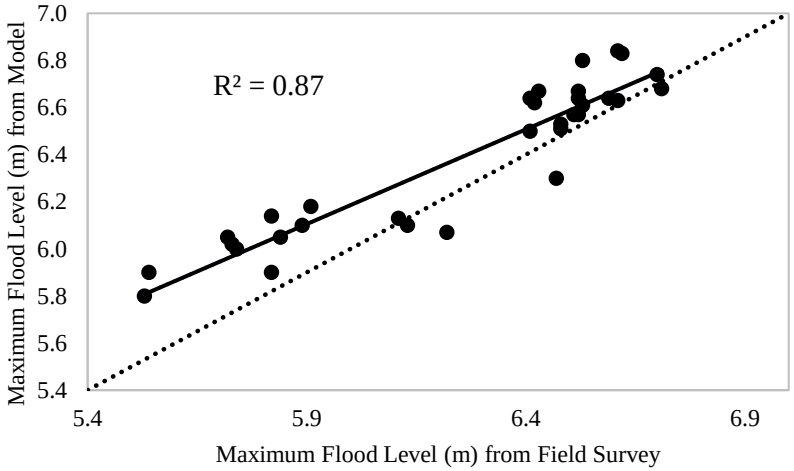

Figure 8: Correlation between maximum flood level from field survey and model

This surveyed area only covers a small portion of the total floodplain modeled in this study. But, it requires huge resources to collect such information about flood levels at such a huge scale. With this

limited information, it is found that the model simulated maximum flood water level is 15cm higher on average than the survey data.

3.2 Impact of Climate Change

It is expected that future streamflow would change due to climate change. Mohammed et al. (2017) have used the SWAT model to generate daily streamflow time series for three major transboundary rivers (the Ganges, the Brahmaputra and the Meghna). In that study, 11 different streamflow time series were available for 1980-2099 based on 11 climate projections. The simulated streamflows varied from one projection to another projection. A representative projection was identified by comparing the highest observed and modeled flows during the base period (1980-2009) for every river. From the analysis, a 29% increase in flow peak of the Ganges, 10% in the Brahmaputra and 22% in the Meghna are indicated by comparing the highest flow of the 2080s (1970-2099) with that of the base condition (1980-2009) (Mondal et al., 2018). The climate change condition was simulated in this model by adopting this increase in streamflow. The results are summarised through the comparison of the maximum water level at different locations in Table 1. The maximum water level is found on 10th September for both 1998 and climate changed condition.

Table 1: Comparison of maximum water level at different locations

Location	Observed maximum water level in 1998 (m)	Model maximum water level in 1998 (m)	Maximum water level due to climate change (m)	Increase in water level due to climate change (m)
Bhagyakul	7.50	7.47	8.09	0.62
Arial Khan Offtake	7.58	7.55	8.20	0.65
Mawa	7.14	7.05	7.63	0.58

After the simulation with climate changed condition, it is found that the peak flood level of 1998 magnitude has increased by 65cm at Offtake of the Arial Khan, 62cm at Bhagyakul and 58cm at Mawa in the Padma. The magnitude of flood level also increased in the floodplain by 41cm to 64cm with an average of 53cm in previously mentioned surveyed locations. From this model, flood levels at different locations of the Padma River system are available under the climate changed condition.

The model sensitivity has been tested by changing the Manning's n value for the Padma River and comparing the change in maximum water level at Bhagyakul river station. The relation between Manning's n value and corresponding maximum water level at Bhagyakul is shown in Figure 9. A change in Manning's n value of 0.001 of the Padma River results on average 0.083 meters change in maximum water level at Bhagyakul. Also, the change in water level reduces for a higher Manning's n value.

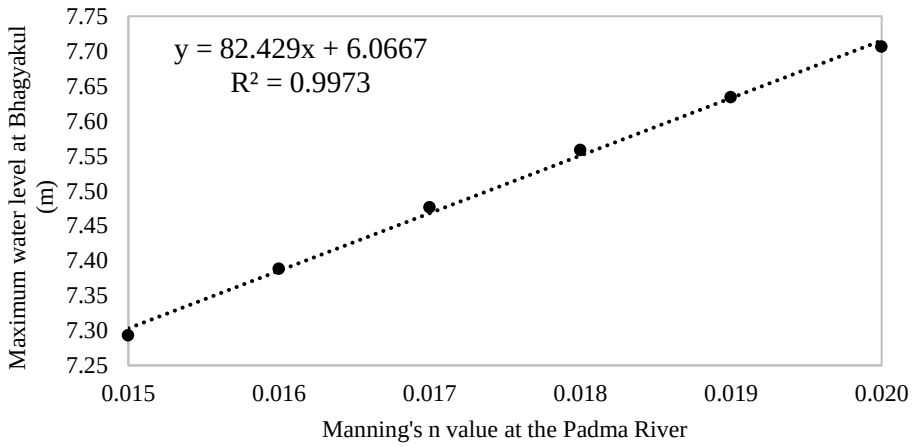

Figure 9: Water level change due to change in Manning's n value at the Padma River

4. CONCLUSIONS

In a country like Bangladesh, where data is very limited and scarce, different modeling approaches can give reasonable predictions of required scenarios. Flood risk in the Padma River along with its distributaries and floodplains due to climate change impacts were evaluated using the HEC-RAS model in this study. The flood peaks might increase by approximately 60cm in the Padma River system under a changed climate condition. The flood peaks might be higher if the potential rise in sea level is considered. As the model can provide stage hydrograph at any point within the 2D mesh, it would be useful in infrastructural planning and design, such as economic zone, power plant, airport, bridge, flood control embankment, river training work and road, in the floodplain of the rivers modeled.

ACKNOWLEDGMENTS

The authors would like to thank all the survey respondents at Shariatpur and Madaripur district for their valuable information about the highest flood level in that area.

REFERENCES

Asian Development Bank (1994). *Climate Change in Asia: Bangladesh Country Report*, ADB, Manila, the Philippines.

FFWC (2005). *Consolidation and strengthening of flood forecasting and warning services, Final Report, Volume II – Monitoring and evaluation*, Bangladesh Water Development Board, Dhaka.

Kreft, S., Eckstein D., and Melchior, I. (2016). *Global Climate Risk Index - 2017*, Germanwatch e.V., Retrieved from https://germanwatch.org/de/download/16411.pdf.

Mirza, M.M.Q. (1997). The runoff sensitivity of the Ganges river basin to climate change and its implications. *Journal of Environmental Hydrology*, 5, 1-12.

Mirza, M.M.Q., Warrick, R.A., and Ericksen, N.J. (2003). The implications of climate change on floods of the Ganges, Brahmaputra and Meghna rivers in Bangladesh. *Climate Change*, 57, 287-318.

Mohammed, K., Islam, A.K.M.S., Islam, G.M.T., Alfieri, L., Bala, S.K., & Khan, M.J.U. (2017). Impact of high-end climate change on floods and low flows of the Brahmaputra River. *Journal of Hydrologic Engineering*, 22(10), 04017041

Mondal, M.S., Islam, A.K.M.S., Haque, A., Islam, M.R., Biswas, S., & Mohammed, K. (2018). Assessing High-End Climate Change Impacts on Floods in Major Rivers of Bangladesh Using Multi-Model Simulations. *Global Science and Technology Journal*, 6(2), 1-14.

Teng, J., Jakeman, A.J., Vaze, J., Croke, B.F.W., Dutta, D., & Kim, S. (2017). Flood inundation modeling: A review of methods, recent advances and uncertainty analysis. *Environmental Modelling & Software*, 90, 201-216.

Proceedings of the 5th International Conference on Civil Engineering for Sustainable Development (ICCESD 2020), 7~9 February 2020, KUET, Khulna, Bangladesh (ISBN-978-984-34-8764-3)

HOW MUCH VALUE DO PEOPLE PLACE ON CONSERVING THE COASTAL FRESHWATER WETLAND IN BANGLADESH?

Muhammad Mainuddin Patwary*[1], Md. Al Amin[2], Sadia Ashraf[3] and Faysal Kabir Shuvo[4]

[1]MS, Environmental Science, Khulna University, Bangladesh, e-mail: raju.es111012@gmail.com
[2] MS Student in Environmental Science, Khulna University, Bangladesh, e-mail: alamin.nesa@gmail.com
[3]MS, Environmental Science, Khulna University, Bangladesh, e-mail: sadiaes11@gmail.com
[4]PhD Candidate, Population Wellbeing and Environment Research Lab, University of Wollongong, Australia, e-mail: fkshuvo@yahoo.com

***Corresponding Author**

ABSTRACT

Wetland ecosystems are among the world largest biological productive system that provides wide range of ecosystem services and support livelihoods of local communities. However, their mulitple benfits and conservation values are often negelcted in decision making that resulted in overexploitation of resources. Bangladesh is a land with surrounded by numerous wetlands. Wetlands of Bangladesh have great siginificane to support rich biodiversity and provide the livelihood of local rural people through employment, commercial fishing, seasonal agriculture, livestock, wood collection and recreation. Beel Dakatia, such a coastal freshwater wetland, located in the southwest hydrological region of Bangladesh provide a large amount of ecosystem services to the people living near the beel. However, the rapid land use change, water logging and inundation condition, siltataion in nearby river, poor sluice gate managmeent and conflicts among the beel users has posed seirous challenges to the existence of beel. Quantifying the economic value of wetlands can inform decision-makers to design solutions for the sustainable use of wetlands resources. Therefore, this study attempted to place a value on the conservation of Beel Dakatia.

The present study conducted a CV survey by using a payment card questionnaire. The survey was performed during 1-30 November 2018. A reconnaissance survey of 50 local peoples living around the wetland was performed during 10-15 November 2018. Face to face interview was conducted for data collection during November, 2018. A total of 150 households residing near the wetland were selected for the final CV interviews. Stratified random sampling method was followed during interviews.

Results reveal that local people supported the wetland management proram and willing to pay money for the Beel Dakatia conservation. More than 80% respondents thought that water-logging, canal filling and poor management of sluice gate were the most threating factor to the existence of Beel Dakatia. The results show that households were willing to pay for Beel Dakatia conservation at an average of 0.65$ per month. This study also examined the effect of socio-economic factors on willingness to pay (WTP). The results of estimates of Ordinary Least Square (OLS) model show that socioeconomic factor such as age, income and education significantly influences the WTP level. The R^2 value for present study is 0.26 that seems to be reasonable good. Therefore, the present study can be considered to be reliable for CV estimation.

Thus, findings provide positive evidence of public monies to protect the environmental value of the resources and thus help policymakers and natural resource managers to make a better decision for sustainable management of coastal freshwater wetlands of Bangladesh.

Keywords: *Beel Dakatia, Economic value, Coastal wetland, CVM, WTP.*

1. INTRODUCTION

Wetlands are among the worls's most productive ecosystem that provides environmental, economic and social benefits to the human being (Islam and Gnauck, 2007; Islam, 2010). Wetlands are functioned as "kidneys" of the earth that plays major role to maintain biodiversity depend on this ecosystems for sustaining, as it serves habitat for a range of species flora, fauna, fish and endangered species (Bai et.al., 2013; Nishat, 1993). Globally, wetland is estimated to cover 5-10% of Earth's terrestrial surface (Mitsch and Gosselink, 2009). Many of the author recently given an actual extent of global wetlands that ranges from 600 million to 1.2 billion ha. Freshwater wetland comprises about 85–95% of the total (Burton and Tiner 2009). Wetland acts as transition between terrestrial and aquatic ecosystem that plays significant role in supporting high biodiversity and providing livelihood security to the people living in the area (Rebelo et. al. 2009). A recent study estimted that worldwide over 1 billion people directly dependent on wetlands for their livelihood such as fishing or farming (Finlayson et. al. 2005). Globally, wetlands contribute to be about USD 70 billion per year (Brander and Schuyt 2004). Conservation of wetlands is necessary as they play major role in sustainable development and poverty reduction by providing subsistence and livelihood of poor people (Finlayson et. al. 2005). However, their multiple roles and conservation priority is often neglected in policy decision that resulted in overexploitation of wetland resources.Therefore, it is imperative to incorporate the value of wetland conservation in environmental decision making.

Approximately 50% (70000 to 80000 km^2) of the total land area is covered by wetlands in Bangladesh (Khan et.al., 1994). They have great importance for supporting the rich biodiversity and proividing the livelihood of rural communities through employment, commercial fishing, agriculture, seasonal livestock, wood collection and ecotourism (Nishat, 1993). Despite the immense significance of these ecosystems, wetlands of Bangladesh have been facing serious challenges from anthropogenic and natural changes (Ahmed et.al., 2008). Anthropogenic activities like drainages for agriculture, application of pesticide and herbicide in agricultural activities, land use changes, construction activities, industrial waste, sewage effluents, and large scale extraction of wetlands resources are the major threats to the survival of wetlands in Bangladesh (Siew et al., 2015). In addition, rapid expansion of roads and houses, agricultural activities has significant contribution to wetland degradation (Haq, 2016). According to Khan et.al. (1994) about 2.1 million ha of wetlands have been lost due to development activities in the GangesBrahmaputra-Meghna floodplain.

Economic valuation has been widely used in both developed and developing countries to assess environmental goods and services. Absence of adequate knowledge on economic value of wetlands services and proper understanding of potential revenue opportunities associated with it might led to make way for other developmental activities. Therefore, these concerns have necessitated the implications of wetland valuation to evaluate the public preferences on how much they willing to pay for conservation activities (Siew et.al., 2015; Jack, 2009). There are several methods that have been used to value the wetlands including market price method (Raphael & Jaworski, 1979), the contingent valuation method (e.g. Bateman and Langford, 1997), hedonic pricing method (e.g. Doss and Taff 1996), travel cost method (e.g. Cooper and Loomis 1993), and replacement cost method (e.g. Breaux et al. 1995). Among them, the contingent valuation method is most widely used technique to value economic benefits of wetland (Bateman et.el., 1992).

Beel Dakatia, a freshwater floodplain wetland, located in southwest hydrological region of Bangladesh and falls within the Ganges tidal deltaic plain, has a rich biodiversity and provides important ecosystem services that support the local livelihood (Kabir and Aftab, 2017). However, natural and anthropogenic activities such as water-logging, siltation n nearby river, poor maintenance of sluice gates and conflicts among beel users have been posed serious threat to the existence of Beel Dakatia in its natural condition (Ali and Syfullah 2016). A number of studies have been conducted on Beel Dakatia to assess its resource use, management strategies and associated livelihoods (e.g. Kabir and Aftab, 2017; Ali and Syfullah 2016). However, no study has been done so far to assess the

environmental benefits derived from the freshwater wetland. This study therefore made an attempt to quantify the values of Beel Dakatia conservation by Contingent Valuation Method (CVM).

2. METHODOLOGY

2.1 Study area

Beel Dakatia is a freshwater floodplain, located in the southwest costal region of Bangladesh. It is the second largest beel (smallest depression in floodplain) of Bangladesh. It covers a total area of about 17,400 hectares or 174,000,000 square metres. It lies between longitudes 89°20'E and 89°35'E and latitudes 22°45'N and 23°00'N under the administrative boundaries of Dumuria and Phultala sub-districts of Khulna district (Rahman 1995). The area is characterized with low elevation and having almost flat topography. Solmari, Hamkura and Salta are the three main rivers in this area that interconnected with the beel. The Beel Dakatia has experienced increasing degradation due to water-logging and inundation. Furthermore, the area has undergone a rapid land use change that affects the livelihood of the beel communities (Ali and Syfullah 2016). Fig 1 shows the geographic location of Beel Dakatia.

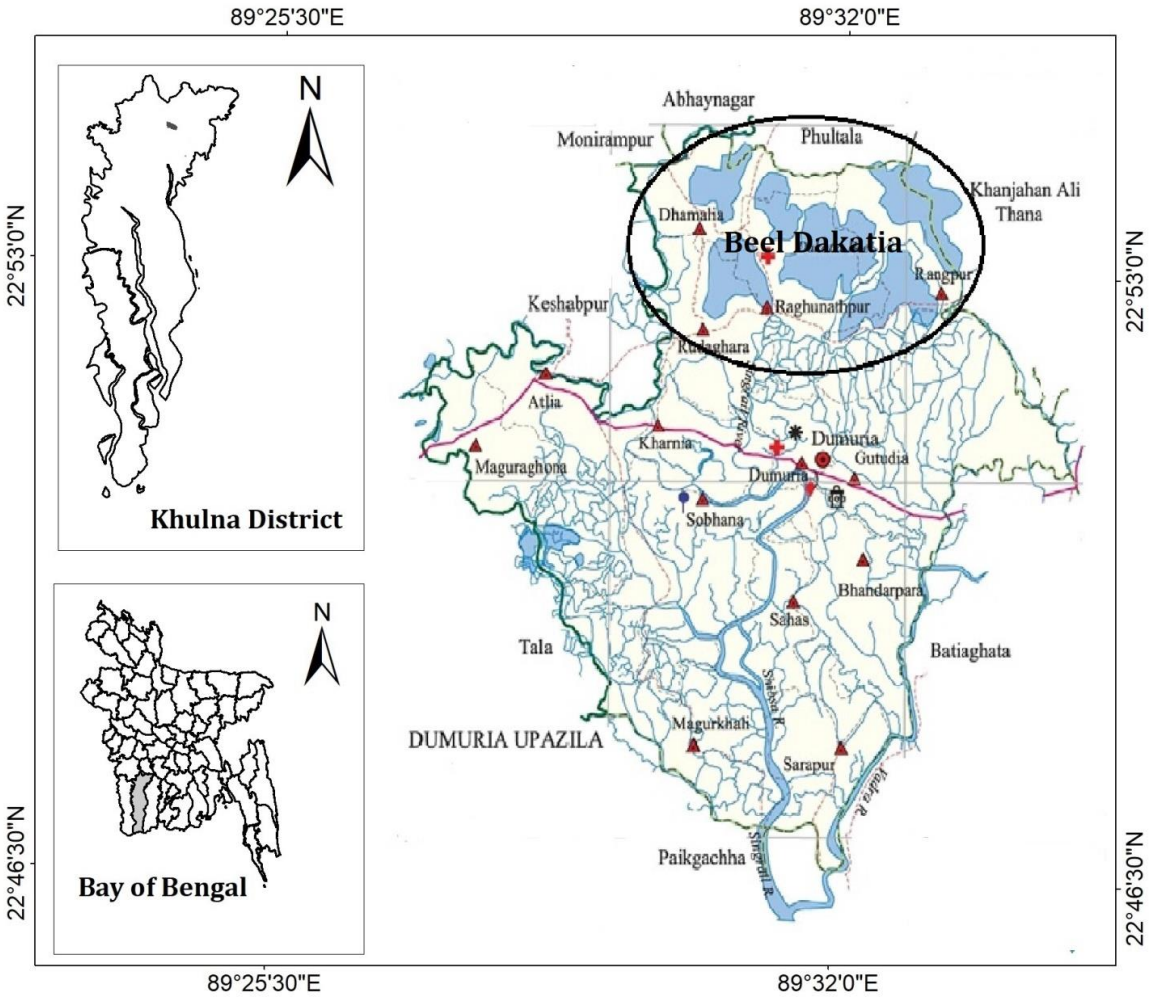

Figure 1: Study area location

2.2 Contingent valuation (CV) approach

In recent years, the CV technique has been widely used in developing countries to measure economics benefits of environmental goods and services (Kim et.al. 2018; Huh and Shin, 2018). Similarly, the present study used a CV survey to elicit public preferences to conserve Beel Dakatia. In CV survey, respondents are directly asked to determine their willingness to pay (WTP) for the use or conservation of natural goods and services. The CV survey is appropriate when no market data or their proxies are available. A major strength of using CV technique is that it does not rely on actual market behavior. According to Arrow et. al. (1993) CV survey is valid and accurate because it provides understandable and meaningful explanation of goods of concern to people.

2.3 Survey design

The present study conducted a CV survey by using a payment card questionnaire. The survey was performed during 1-30 November 2018. A reconnaissance survey of 50 local peoples living around the wetland was performed during 10-15 November 2018. The final questionnaire was designed by following National Oceanic and Atmospheric Administration (NOAA) Panel guidelines. Face-to-face interview was conducted for each of the respondents. The length of the interview was lasted for no longer than 20 minutes to maintain the respondent's attention during interview. The questionnaire was divided into three sections. The first section assessed the respondent's willingness to take part in CV survey, second section contained questions on demographic and economic information and the third section focused on the perceptions, attitudes and awareness of the respondents towards the present condition of the wetland. A hypothetical wetland management program was explained to respondents whether they would be willing to pay for Beel Dakatia conservation. The statement of paying is expressed as follows:

"Considering your current income and expenses would you be willing-to-pay for proposed program at x BDT?"

Where, x ranges from BDT 4 to BDT 120. If the respondents stated "YES", the WTP is elicited and they were later asked to distribute their maximum value based on their income and expenditure. A total of 150 households residing near the wetland were selected for the CV interviews. Stratified random sampling method was followed during interviews. The survey was started randomly from any side of the village and every 10^{th} household was selected for the interview. If the respondent of 10^{th} household refused to participate, the nearest household was considered. Only head of the households were interviewed.

2.4 Willingness to pay estimation

In theoretical model, the income-compensating function is used to explain the individual's WTP for a CV survey. In this study, the Ordinary Least Square (OLS) method was used to reveal the mean WTP and identify factors that affect stated WTP. The explanatory variables used in this study are age of the household head (AGE), gender (GENDER), household size (HHS), monthly household income (INC), level of the formal schooling of the respondents (EDU), employment status of the respondents (OCU). The OLS model for the general individual WTP function is as follows:

$$WTP = \alpha + \beta_1 GENDER + \beta_2 AGE + \beta_3 INC + \beta_4 HHS + \beta_5 EDU + \beta_6 OCU + \varepsilon \quad (1)$$

where α and βi's are the estimated parameters and ε is the random error.

3. RESULTS AND DISCUSSIONS

3.1 Respondent characteristics

Table 1 shows the socioeconomic profile of the respondents of the studied villages. Of the sample interviewed, 88% were male and only 12% female. About 92.1% of the respondents were reported

married. The mean age of the respondent was 57.85 ± 11.06. The mean household size was 4.80 ± 1.72. With regard to education, about eighty-seven percent were literate and had studied at least till the primary level. About 44.4% of people lives in tin shed (semi-pucca) house while only 11.1% in bamboo and 14.3% in mud houses. The average landholding size was 1.24 ± 0.16 ha, with more than 90% of the families owning up to 4 ha of agricultural land. The monthly mean family income was 113.82 ± 79.69 US$. Majority of the respondents in surveyed villages were engaged primarily in fishing (51%) and agricultural (32%) activities. However, there were low numbers of respondents with other occupational activities including small business, laborer and services. The average duration of living near the wetland was 34 (± 12.34).

Table 1: Socio-demographic profile of the respondents (N=150)

Features		Percentage	Features	Mean (±SD)
Male		88	Age (yr)	57.85 (±11.06)
Married		92.1	Household size	4.80(±1.72)
Literate		87.3	Income (US$)	113.82(±79.69)
Housing pattern			Land (ha)	1.24 (±0.16)
	Bamboo	11.1	Duration of living (yr)	34 (±12.34)
	Mud	14.3		
	Semi-pucca	44.4		
	Pucca	30.2		
Occupation				
	Fishing	51		
	Farming	32		
	Business	9		
	Laborer	3		
	Others	5		

3.2 Perception towards wetland conservation

Approximately 52% of the total respondents said that food production e.g fish, crop, vegetables showed an increasing trend in Beel Dakatia. However, 35.6% said that Beel Dakatia has experienced a decreasing trend of food production since last decades. Only 12% said that food provision from Beel Dakatia remain same as before. More than 50% of respondents agreed that people are not getting economic benefit from the beel as many years ago. Most of the respondents (63%) respond that wetland environment has been degrading at an increasing rate. About 43% of total respondents said that Beel Dakatia has no more state of use as recreational purposes. Factors such as food production and economic benefit of mean scores had more than 3.5 suggesting respondents were more inclined to the economic aspects of beel.

Table 2**:** Benefits perceived from the Beel Dakatia

Services	Increase	Unchanged	Decrease	Mean
Food production	52.4	12	35.6	4.10
Economic benefit	36	6	58	3.67
Recreation	32	25	43	2.88
Environmental Benefits	26	11	63	3.46

More than 80% respondents thought that water-logging, canal filling and poor management of sluice gate were the most threating factor to the existence of Beel Dakatia. Most of the respondents believed that overexploitation (71.9%), reduction of beel resources (77.3%), shrimp cultivation (65%) had moderate to very high impact to degrade the Beel Dakatia. In contrast, urban development (84%), salinity intrusion (67.1%), industrial waste (94%) and cyclone-flood (66.3%) had none to very little impact on the Beel degradation.

Table 3: Factors threating the existence of Beel Dakatia

Factors	**Threat (%)**					**Mean Score**
	None (1)	**Very little (2)**	**Moderate (3)**	**High (4)**	**Very high (5)**	
Water-logging			2	10	88	4.15
Poor management of Sluice gate			4	12	84	4.00
Canal Filling			12	6	82	3.89
Shrimp cultivation	10	25	45	13	7	2.78
Urban development	56	28	12	4		2.34
Salinity intrusion	18.2	48.9	31.1	1.8		1.89
Overexploitation	5	23.1	67.9	2.8	1.2	2.98
Reduction of Beel resources	10	12.7	12.3	46.3	18.7	3.14
Use of chemicals & insecticides		29.4	45.6	23.4	1.6	2.67
Industrial waste (effluent)	78.3	15.7	6			2.01
Cyclone-flood	6.4	59.9	31.1	3.6		2.31

The study also demonstrated the respondent's opinions of who should pay for the conservation of Beel Dakatia. Majority (64%) of the respondents believed that the Government solely should pay for the conservation activities. About 24% respondents thought that those who directly benefitted from the beel should pay. Only 7% of the total respondents believed that Government with private partnership should pay. Only a few numbers (3%) respond that polluter pay principle can be an option for conservation. This indicates that those who are causing pollution should be liable to pay damage cost. Only 2% believed that conservation of Beel Dakatia is a voluntary work.

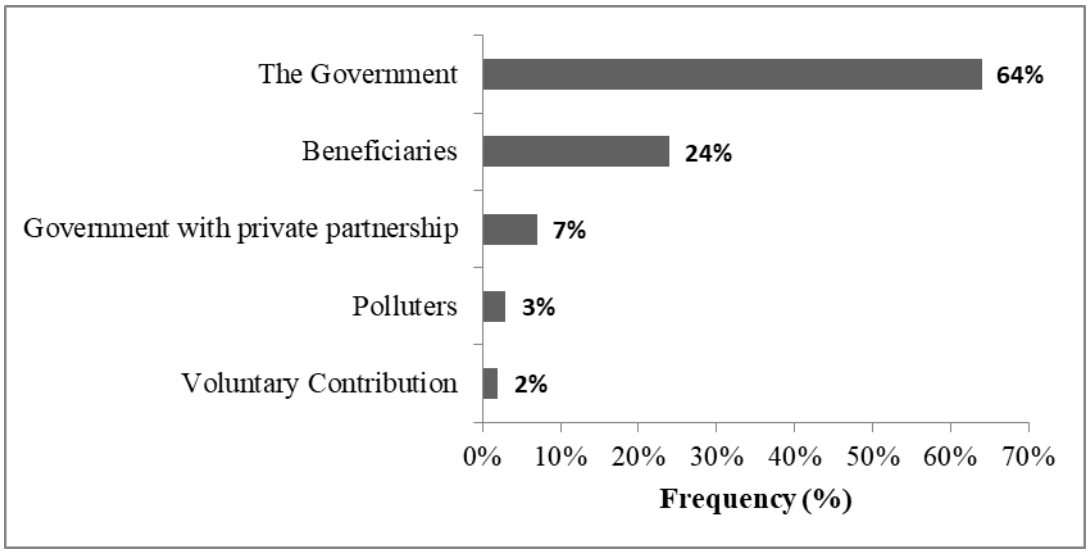

Figure 2: Respondent perception who should pay to conserve the Beel Dakatia

3.3 Estimation of WTP

Out of the 150 surveyed households, 92% were willing to pay for Beel Dakatia conservation. The respondent who did not agree to pay (zero WTP) for Beel Conservation were asked follow up question regarding their reason not willing to pay. The results show that about 23.6% of respondents showed their monetary incapability not to pay for the proposed program, 34.4% thinks that this is the sole responsibility of the government, 21.9% said that they would not get any benefit from the proposed program, 12.1% said that people who degrade the Beel should pay and about 8% responds that they would contribute to the program in labor. The results reveal that minimum WTP value per month per household is BDT 4.50 and maximum WTP is BDT 119. Therefore, the mean monthly WTP per household was estimated BDT 53.3± 25.6 (US$ 0.65). A similar study was conducted by Gosh and Mondal (2012) where mean WTP was estimated BDT 13.69 (US$ 0.20) per month per household of Chanda Beel, Bangladesh. Table 3 summarizes the mean WTP per month per household for Beel Dakatia conservation.

Table 4: Mean WTP (BDT* per month per household) for Beel Dakatia conservation (N=150)

WTP	**Statistics**
Mean	53.3 BDT
Minimum-maximum	4.50-119
Standard deviation	25.6
No of protest bids	12
% of total respondents	8

*BDT=Bangladeshi Taka, US$ 1 = 82 BDT (as of November 2018)

The Ordinary Least Square (OLS) method was used to identify the factors affecting the WTP and also to examine the reliability and validity of CV result. The results of regression showing factors affecting WTP for Beel Dakatia is given in Table 5. Results show that age, income and education were significant to determine the WTP. The coefficient of variable AGE (respondent age) was statistically significant at 5% significant level but with a negative sign. This suggests that younger people are more willing to pay than older ones. The coefficient of income variable was statistically significant at 5% significant level and positively influences the WTP. It seems that WTP is highly dependent on economic condition of the respondent. This finding is in line with Gosh and Mondal (2012) and Oglethorpe and Miliadou (2000). The coefficient variable education was also found positively and statistically significant at 1% significant level and it indicates that people with higher education tend to more willing to pay than lower education. According to Mitchell & Carson (1989), the simplest way to test the reliability of WTP amount is to obtain an acceptable R^2 value (R^2>0.15). The R^2 value for present study is 0.26 that seems to be reasonably good. Therefore, the present study can be considered to be reliable for CV estimation.

Table 5: Estimates of OLS regression model for the determinants of WTP

Explanatory Variables	**Coefficient**	**Standard Error**	**t-statistics**	**P value**
Constant	87.67	35.23	3.00	0.005**
Gender	2.34	5.564	0.67	0.45
Age	-1.56	0.002	2.56	0.004**
Income	2.93	0.034	2.87	0.005**
Household size	2.05	5.634	0.98	0.78
Education	2.12	0.015	2.89	0.00***
Occupation	3.13	6.578	1.56	0.987

Note: Number of observations = 150; R^2= 0.29, Adj. R^2= 0.26; **significant at p <0.05, ***significant at p< 0.01.

4. CONCLUSIONS

This study estimated the conservation value of Beel Dakatia freshwater wetland, using CVM. The results reveal that local communities support the program and willing to contribute money for the conservation of Beel Dakatia. This study also identified the socioeconomic factors that affect the level of WTP. Results show that respondents were willing to contribute monthly BDT 53.3 (US$ 0.65) per household that results in an aggregate value of US$ 7.8 yearly per household. The results of Ordinary Least Square model show that age of the household head, income and education has significantly influenced the households to pay for Beel Dakatia conservation. The findings of the study can assist the government and decision maker to incorporate public funds in freshwater wetland management decisions.

REFERENCES

Ahmed, I., Deaton, B. J., Sarker, R., and Virani, T. (2008). Wetland ownership and management in a common property resource setting: A case study of Hakaluki Haor in Bangladesh. *Ecological Economics*, 68(1–2), 429–436.

Ali M.S., and Syfullah, K. (2016). Effect of Sea Level Rise Induced Permanent Inundation on the Livelihood Of Polder Enclosed Beel Communities In Bangladesh: People's Perception. *Journal of Water and Climate Change*, 8(2), 219-234.

Arrow, K., Solow, R., Portney, P.R., Leamer, E.E., Radner, R. and Schuman, H. (1993). Report of the NOAA panel on contingent valuation. *Federal register*, *58*(10), 4601-4614.

Bai, J., Cui, B., Cao, H., Li, A. and Zhang, B. (2013). Wetland degradation and ecological restoration. *The Scientific World Journal*, *2013*.

Bateman, I., and Langford, I.H. (1997). Non-users willingness to pay for a national park: an application of the contingent valuation method. *Regional studies*, 31, 571–582.

Bateman, I.J., Willis, K.G., Garrod, G.D., Doktor, P., Langford, I. and Turner, R.K. (1992). Recreation and Environmental Preservation Value of the Norfolk Broads: A Contingent Valuation Study, Technical Report (Norwich, Environmental Appraisal Group, University of East Anglia).

Brander, L. and Schuyt, K. (2004). The economic values of the world's wetlands.

Breaux, A., Farber, S.C., and Day, J. (1995). Using natural coastal wetlands systems for wastewater treatment: an economic benefit analysis. *Journal of environmental management*, 44, 285–291.

Burton, T.M., and Tiner R.W. (2009). Ecology of Wetlands, in Encyclopedia of Inland Waters.

Cooper, J. and Loomis, J. (1993). Testing whether waterfowl hunting benefits increase with greater water deliveries to wetlands. *Environmental and resource economics*, 3, 545–561.

Doss, C.R., and Taff, S.J. (1996). The influence of wetland type and wetland proximity on residential property values. *Journal of agricultural and resource economics*, 21, 120–129.

Finlayson, C. M., Horwitz, P., & Weinstein, P. (Eds.). (2015). *Wetlands and human health* (Vol. 5). Springer.

Ghosh, P. K., & Mondal, M. S. (2013). Economic valuation of the non-use attributes of a south-western coastal wetland in Bangladesh. *Journal of environmental planning and management*, *56*(9), 1403-1418.

Haq, T. (2016). A Violent Threat to Conservation of Wetlands and the Existing Laws of Bangladesh: A Critical Analysis. *Philosophy and Progress*, 113-126.

Huh, S. Y., & Shin, J. (2018). Economic valuation of noise pollution control policy: does the type of noise matter?. *Environmental Science and Pollution Research*, *25*(30), 30647-30658.

Islam, S. (2010). Threatened wetlands and ecologically sensitive ecosystems management in Bangladesh. *Frontiers of Earth Science in China*, 4(4), 438-448.

Islam, S. N., & Gnauck, A. (2007). Effects of salinity intrusion in mangrove wetlands ecosystems in the Sundarbans: an alternative approach for sustainable management. *Wetlands: Monitoring, Modelling and Management*, 315.

Jack, B. K. (2009). Upstream–downstream transactions and watershed externalities: Experimental evidence from Kenya. *Ecological economics*, *68*(6), 1813-1824.

Kabir, K. H., & Aftab, S. (2017). Exploring management strategies for freshwater wetland: Policy options for southwest coastal region in Bangladesh. *Asian Development Policy Review*, *5*(2), 70-80.

Khan, S.M., Haq, E., Huq, S., Rahman, A. A., Rashid, S. M. A., and Ahmed, H. (1994). Wetlands of Bangladesh. Dhaka: Holiday Printers Limited, 1–88.

Kim, H. J., Jin, S. J., & Yoo, S. H. (2018). Public assessment of releasing a captive indo-pacific bottlenose dolphin into the wild in South Korea. *Sustainability*, *10*(9), 3199.

Mitsch, W. J., Gosselink, J. G., Zhang, L., & Anderson, C. J. (2009). *Wetland ecosystems*. John Wiley & Sons.

Nishat, A. (1993). Freshwater wetlands in Bangladesh: status and issues. *Freshwater Wetlands in Bangladesh-Issues and Approaches for Management. IUCN*, 9-22.

Oglethorpe, D.R. and Miliadou, D. (2000). Economic valuation of the non-use attributes of a wetland: a case-study for lake Kerkini. *Journal of environmental planning and management*, 43 (6), 755–767.

Rahman, A. (1995). *Beel Dakatia: The Environmental Consequences of a Development Disaster*. University Press.

Raphael, C. N., & Jaworski, E. (1979). Economic value of fish, wildlife, and recreation in Michigan's coastal wetlands. *Coastal Management*, *5*(3), 181-194.

Rebelo, L. M., McCartney, M. P., & Finlayson, C. M. (2010). Wetlands of Sub-Saharan Africa: distribution and contribution of agriculture to livelihoods. *Wetlands Ecology and Management*, *18*(5), 557-572.

Siew, M. K., Yacob, M. R., Radam, A., Adamu, A., & Alias, E. F. (2015). Estimating willingness to pay for wetland conservation: a contingent valuation study of Paya Indah Wetland, Selangor Malaysia. *Procedia Environmental Sciences*, *30*, 268-272.

Proceedings of the 5th International Conference on Civil Engineering for Sustainable Development (ICCESD 2020), 7~9 February 2020, KUET, Khulna, Bangladesh (ISBN-978-984-34-8764-3)

HISTORICAL FLOOD INUNDATION STUDIES AT SEVERAL IMPORTANT LOCATIONS OF DHAKA CITY UNDER DHAKA MASS RAPID TRANSIT DEVELOPMENT PROJECT LINE – 1

Md. Rashedul Islam*[1], M. Shahjahan Mondal[2] and Subir Biswas[3]

[1]Assistant Professor, Institute of Water and Flood Management, BUET, Dhaka, Bangladesh, e-mail: rashed_rakib@iwfm.buet.ac.bd
[2]Professor, Institute of Water and Flood Management, BUET, Dhaka, Bangladesh, e-mail: mshahjahanmondal@iwfm.buet.ac.bd
[3]Research Associate, Institute of Water and Flood Management, BUET, Dhaka, Bangladesh, e-mail: subir_buet@yahoo.com

***Corresponding Author**

ABSTRACT

The capital of Bangladesh, Dhaka is located in the center of Bangladesh. The area of the present city is around 350 km^2 bounded by the Buriganga River in the south, the Demra in the east, the Tongi Khal in the north and the Turag and Buriganga rivers in the west. The metropolitan city is bounded by Gazipur in the north, Manikganj in the west, Rupganj in the east, Narayanganj in the southeast and Keraniganj in the south. Recently Government of Bangladesh has initiated the Dhaka Mass Rapid Transit Development Project to solve the extreme amount of traffic congestions that occur throughout the entire city each and every day. Among the proposed six MRT lines throughout the city, the alignment of MRT line-1 will be from Kamalapur to Hazrat Shahjalal International Airport via Malibagh, Rampura, Badda and Kuril Bishwa road. There would be 12 underground stations on its route, located in the densely populated urban areas of Dhaka City. For fixing the ground elevations of these stations, the proper understanding of flooding and drainage system surrounding each station are mandatory. Primary data and information on inundation depth, river bathymetry and land elevation were needed for this study. Under this study, primary data on inundation depth due to historical floods such as the 1988 and 1998 floods and due to heavy rainfall were collected based on local water marks and people's perception. The availability of permanent water marks, the age of the local people providing the information, the permanency of residency in the area, the level of education of the person, etc., were the prime factors to determine the reliability of the data. Land elevations were collected at those locations where flood surveys were made with reference to available benchmarks of the Survey of Bangladesh. Then, the flood level at those locations was estimated from the land elevations and flood depths. Obtained flood level data by this method was then compared with the secondary flood level data based on the frequency analysis of the gage station data located in the surrounding rivers of the Dhaka city. After this comparison and some adjustments, design flood level for these locations were estimated. Finally, a spatial map of flood inundation over each candidate site was constructed in Geographic Information System (GIS) platform. These type of maps are useful to understand the general inundation scenarios at those important locations.

Keywords: *MRT Line-1, Historical floods, People perceptions, Inundation depth, Spatial maps.*

1. INTRODUCTION

Dhaka located in the centre of Bangladesh between longitude 90°20'E and 90º30'E and latitude 23º40'N and 23º55'N, is the busiest city of Bangladesh. Although Dhaka's area is less than 1% of the country's total land area, it supports about 10% of the total population and 30% of the total urban population. (Rahman, 2008). It is the 9th largest city in the world by population which covers 360 km^2 bearing more than 15 million people. (Azam et al., 2016). The present transportation system of the city is incapable of satisfying the demand resulting in huge traffic jam every day. With the shortage of land and limited area to expand the present road network, Government of Bangladesh has initiated the Dhaka Mass Rapid Transit Development Project to introduce a new apposite mode of transportation and to utilize the underground and elevated spaces in Dhaka city. As Bangladesh is flood prone area with inundation problems in urban areas, so without proper studies on flooding and drainages can make the whole process of utilizing the underground spaces vulnerable. Previously, several researches were conducted on flooding of Dhaka city and suggested some mitigation options (Faisal et al., 1999; Mark et al., 2001; Huq et al., 2003; Khan, 2006; Dewan et al., 2008; Gain, 2015)

In Bangladesh, depth of inundation over the floodplain is not systematically monitored and recorded by any organization. We know only the flood level at the gage stations, which are located on the rivers. While these rivers are responsible for the strategic location and the fertile soils of the region, they also carry with them the threat of destructive flooding for the city, all of which lies at relatively low elevation (Hafiz, 2011). But, a high-water level in a river may not necessarily correspond to a high-water level in a locality. A number of factors including flood characteristics, distance of the locality from the river, vegetation and physical obstructions influence the local inundation depth. An assessment of the local inundation depth, based on local people's experience on past floods and their depths in the area is necessary to understand the overall inundation scenario in that certain area. In order to fix the ground elevations of the underground stations, same approach was taken for the proper understanding of flooding and drainage system surrounding each station.

2. METHODOLOGY

MRT Line-1 will have 12 underground stations, 7 elevated stations, 1 transition section (heading to Purbachal) and 1 depot area. In this study, we will focus on the 12 underground stations that are located in the central part of Dhaka city. These stations are Kamalapur, Rajarbagh, Malibagh, Rampura, Hatir Jheel, Badda, Uttar Badda, Notun Bazar, Future Park, Khilkhet, Airport Terminal 3 and Airport Area. For further discussion, Kamalapur is considered as station 1 and this way Airport is considered as station 12. Figure 1 illustrates the layout plan of MRT Line-1 where green circles denote the underground stations.

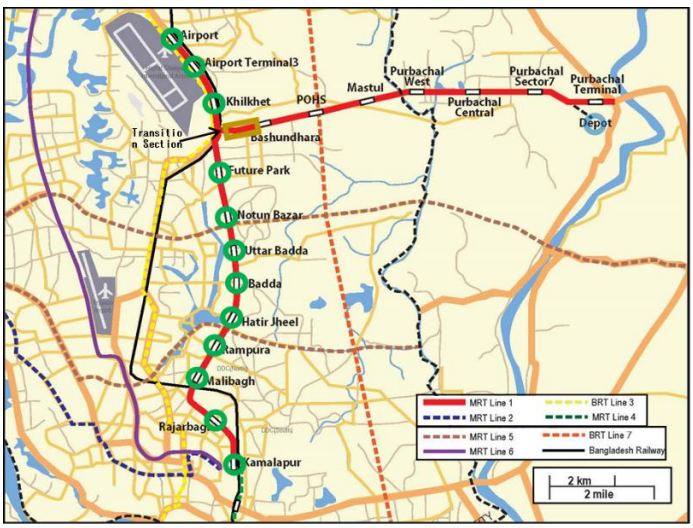

Figure 1: Layout plan of MRT Line-1

For each station, flood depths were collected at 20 points near the location with a radius of 500m surrounding the station. The initial task was to collect relevant flood and drainage information from these locations. Intensive interactions were made with the local people regarding this. The local people were specifically asked about the history of floods in the area, the highest flood year, the last flood year, known flood marks on houses, trees, etc., and the difference between the highest and recent flood levels. While collecting such information, a handheld GPS was carried to record coordinates.

2.1 Incorporation of Flood depth with Ground Level Data

A professional survey team was engaged to estimate the land levels at the locations where flood surveys were made. Ground level information were measured exactly at the same points where flood depths were collected with high accuracy. By combining the ground level data and flood depth data for certain point, flood level of that particular point was calculated (in m, PWD format) by adding these two.

2.2 Data Reliability Checking

The data for all these points were not equally reliable. So, screening out of the unreliable data was needed. The first level of screening was done by making a box plot of the collected flood level data at each station and noting the outliers and extremes in the data set. Outliers are values which are more than 3 box-lengths from the upper or lower edge of the box, and extremes are values with more than 1.5 box-lengths. These identified outliers and extremes were dropped from further analyses.

The second level of reliability checking was done by making a station-wise plot of all the data and then noting the overall regional pattern in the data. The data in which there was a large deviation from the regional pattern was considered to be unreliable and dropped.

The third level of screening was done based on the information while collecting the field data. If water mark was shown by a local respondent, the data was considered to be reliable. Also, if the respondent were an aged person, lived in the area during the said flood, is educated and has knowledge on local flooding pattern, the information provided by the respondent was considered to be reliable.

The fourth and final level of checking was made with the secondary data collected from BWDB. Considering all the stations, about 61% of the data was retained after these four levels of rigorous checking. The above four levels of checking provided reliable flood information at each station based on local people's perception. It is to be noted that, since this approach is based on local people's experience and information, it is likely to be fairly good. Figure 2 shows the view of the flood marks shown by the local people.

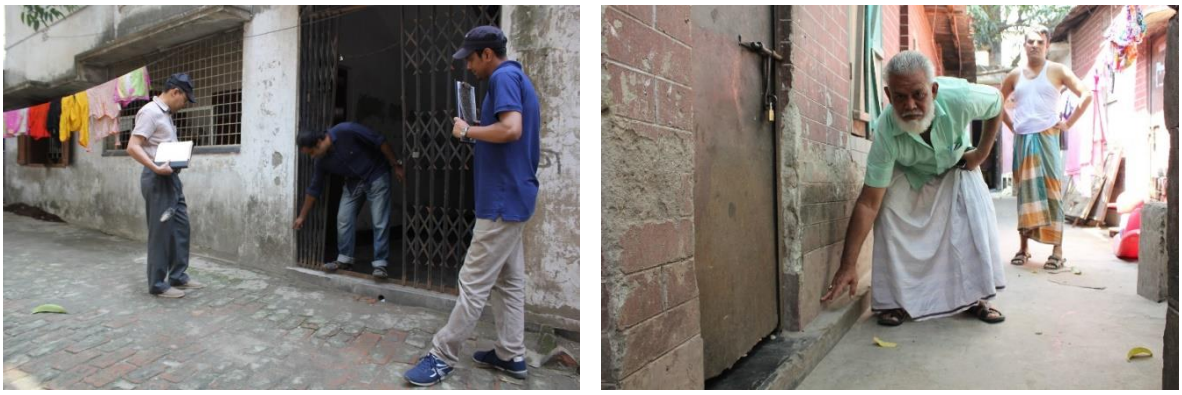

Figure 2: Flood marks shown by the local people

2.3 Comparison of Measured Flood Level Data with the Secondary Data

There are a number of gage stations maintained by the Bangladesh Water Development Board (BWDB) on the rivers surrounding Dhaka City. Figure 3 shows the locations of these stations. Frequency analysis was carried out with the annual maximum water level data using a number of probability distribution

functions. The gage stations are located at different distances from the MRT Line 1 stations. Thus, using the U.S. National Weather Service Method, the water levels at the different MRT stations were estimated. Then these estimated flood level data were compared to the flood level data obtained from the primary survey data.

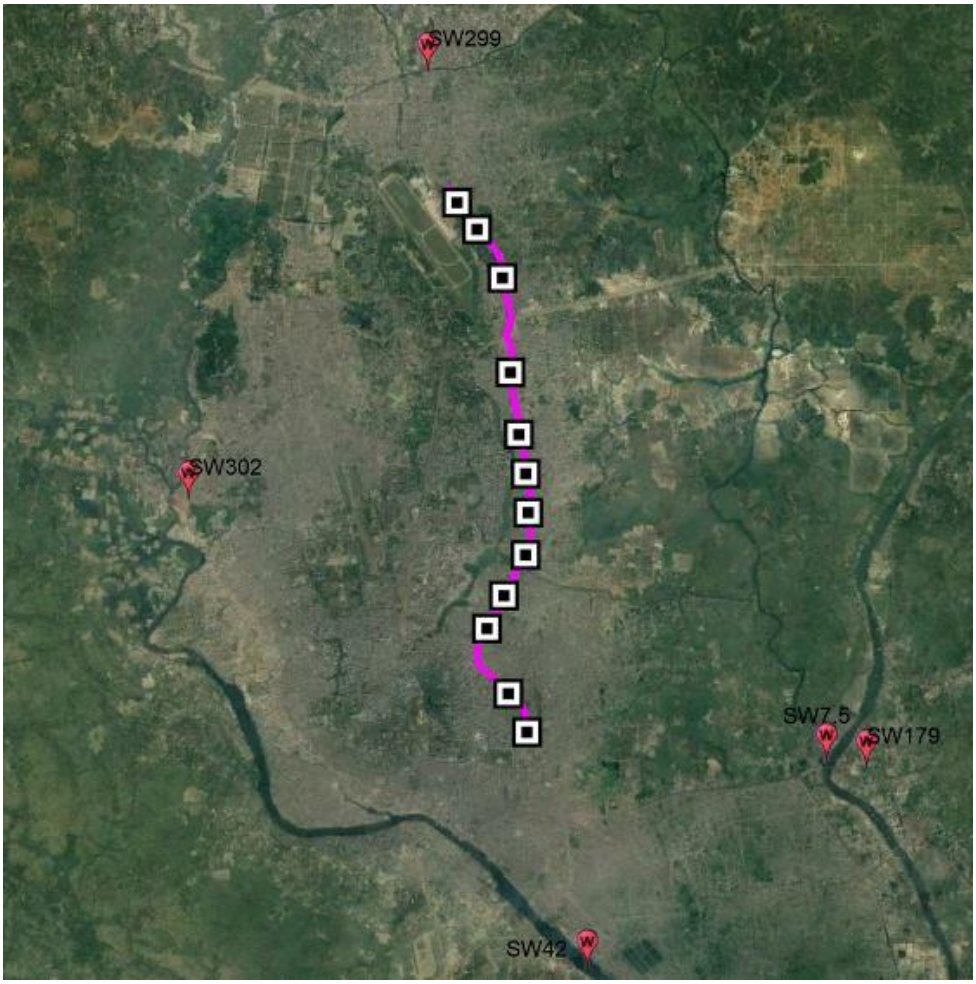

Figure 3: Locations of the gage stations surrounding Dhaka City (Source: Google Earth)

2.4 Preparation of Spatial Maps for Each Station

With ground level data provided by the survey team for each station, at first, ground level (GL) maps were prepared in Geographic Information System (GIS) platform to understand the land topography and identity high, medium and low lands. After incorporating collected flood depth data with the ground level, flood level map for all the stations were also done. The ground level maps and flood level maps are then used for fixing the ground elevation of those underground stations.

3. RESULTS AND DISCUSSIONS

3.1 Data Reliability Analyses

As mentioned in the methodology part, first level of reliability check was done by dropping out outliers and extreme values in the flood level data set. Figure 3 shows a box plot of the flood level data from the Rajarbagh Area (station 2 of MRT Line-1) as an example. The plot shows that there are three outliers in the data. Hence, these three outliers were dropped from further analysis. It is to be noted that the process of identification of outliers and extremes, dropping them from the data, and making the box plot again was repeated until the plot showed no outlier or extreme in the data set.

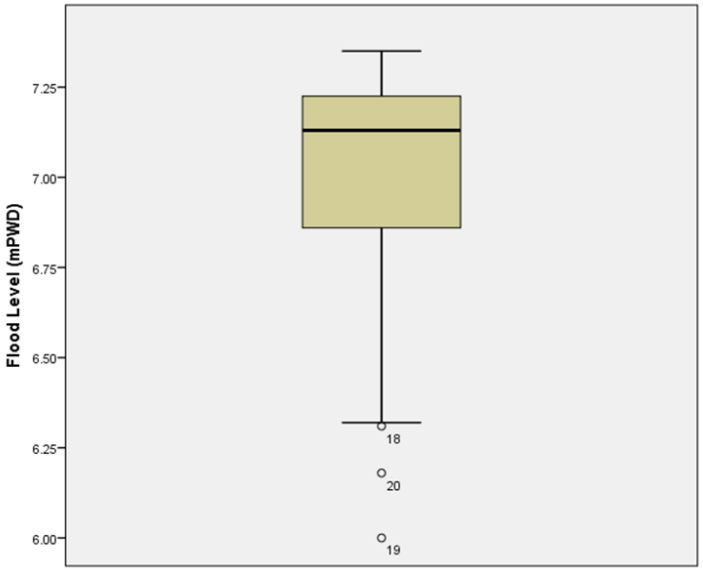

Figure 3: Box plot of the flood level data collected for the Malibagh Area

During second level of reliability check, for a data with large deviation from the regional pattern was considered to be unreliable and dropped from further analysis. Figure 4 shows such a plot. It is seen from the figure that the flood levels at the first four stations and at station 7 are more or less the same. The stations around Hatirjheel area (stations 5 and 6) show slightly higher flood level. The northern stations (stations 8-12) have the highest flood levels among the stations as they are close to the Tongi Khal in the north. Among the surveyed stations, station 9 provides the most reliable results. As seen in the figure, there are a few stations, such as stations 5, 6 and 11, which have long tails in the data. The lower long tail may lead to an under-estimation in flood level and upper long tail may lead to an over-estimation. To reduce the tail length, the reliability of the large and small data were checked further with the actual field information.

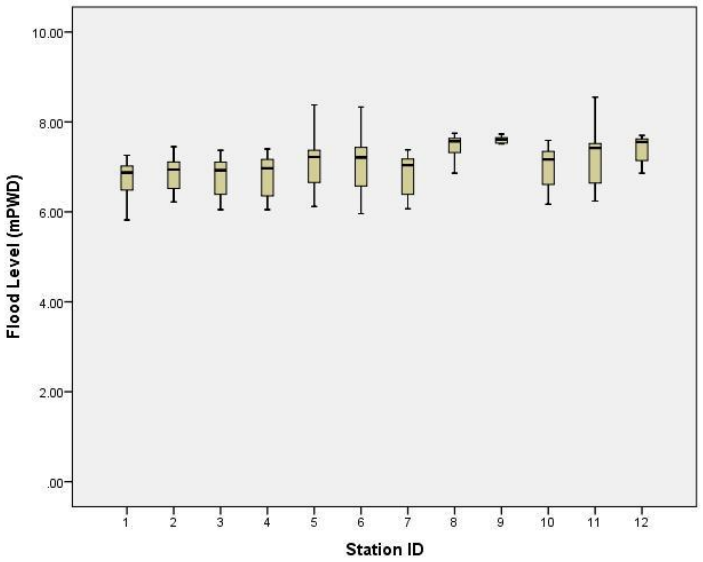

Figure 4: Station-wise Box plot of the flood levels after second level of reliability check

The third level of reliability was based on the level of people's perception regarding the flood depth. If water mark was shown by an aged local respondent, the data was considered to be reliable. In figure 5, as an example of the third level of screening, the field information revealed that the data for 6 points at the station 4 may not be very reliable though there was no outlier or extreme in this data set. So, the data from these 6 points were treated as 'doubtful' and ultimately dropped.

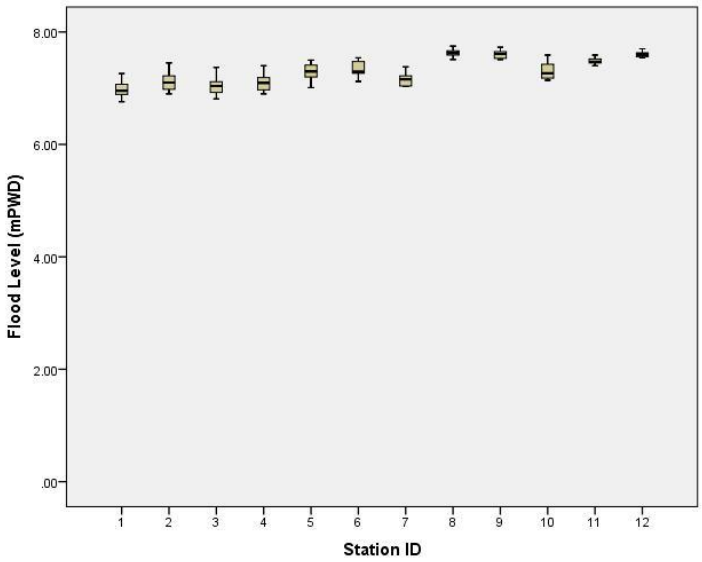

Figure 5: Station-wise Box plot of the screened flood levels

The fourth and final level of checking was made by comparing with the secondary data collected from Bangladesh Water Development Board. The highest flood level of the Balu at Demra was about 7.09 m PWD in 1988 and that of the Tongi Khal at Tongi was 7.84 m PWD. The highest flood levels from the survey data varied between 7.26 m and 7.75 m PWD at the MRT Line-1 stations. Thus, the filtered surveyed flood levels appear to be reasonable.

3.2 Flood Level from Secondary Data

As mentioned in the article 2.3, highest water level at the gage stations maintained by BWDB on the rivers surrounding Dhaka City were collected. Table 2 shows the highest flood level and its year of occurrence for each gage station. It is seen from the table that the highest flood level occurred in the year of 1988, except for Demra on the Shitalakhya. However, the difference between the 1988 water level at Demra on the Balu and the 1998 water level at Demra on the Shitalakhya is only 2 cm.

Table 1: Available hydrologic gage stations surrounding Dhaka City

River Name	Gage Station Name	Station ID	Type of Station	Available Period of Record	Observed Highest Flood Level (mPWD)
Turag	Mirpur	SW302	Tidal	1981-2018	8.35 (1988)*
Tongi Khal	Tongi	SW299	Tidal	1985-2018	7.84 (1988)*
Balu	Demra	SW7.5	Tidal	1985-2018	7.09 (1988)*
Buriganga	Mill Barrack	SW42	Tidal	1985-2018	7.58 (1988)*
Shitalakhya	Demra	SW179	Tidal	1985-2018	7.11 (1998)*

* The value within parentheses indicates the year of occurrence of the highest flood.

Then, frequency analysis was carried out for these rivers with the annual maximum water level data using a number of probability distribution functions, such as Two Parameter Log Normal (LN2), Three Parameter Log Normal (LN3), Pearson Type III (P3), Log Pearson Type III (LP3) and Gumbel's Extreme Value Type 1 (EV1). As, the gage stations are located at various distances from the MRT stations, in order to find the high flood level and different return period flood levels for each of these locations, U.S. National Weather Service Method (equation 1) was used in which the inverse of squared distance of a gage station is used as weightage.

$$X = \sum_{i=1}^{n} W_i X_i \quad (1)$$

where, W_i is the weight for station i, X_i is the water level at station i and n is the number of stations.

The maximum flood levels at different stations thus estimated are given in Table 2. It is seen from the table that the highest flood level varies from 7.55 m PWD at Kamalapur to 7.89 m at Future Park.

Table 2: Maximum and different return period flood levels obtained from secondary data at different MRT stations

Station No./Id.	Station Name	Highest Flood Level (mPWD)	2.33-Year Flood Level (mPWD)	5-Year Flood Level (mPWD)	10-Year Flood Level (mPWD)	20-Year Flood Level (mPWD)	50-Year Flood Level (mPWD)	100-Year Flood Level (mPWD)
1	Kamalapur	7.55	5.68	6.14	6.54	6.98	7.51	7.90
2	Rajarbagh	7.61	5.72	6.19	6.59	7.05	7.59	7.99
3	Malibagh	7.72	5.79	6.26	6.67	7.17	7.74	8.17
4	Rampura	7.72	5.80	6.26	6.67	7.18	7.74	8.16
5	Hatir Jheel	7.77	5.93	6.38	6.79	7.29	7.83	8.23
6	Badda	7.81	5.93	6.39	6.80	7.31	7.85	8.26
7	Uttar Badda	7.84	5.94	6.41	6.82	7.33	7.88	8.30
8	Notun Bazar	7.87	5.94	6.41	6.83	7.34	7.90	8.33
9	Future Park	7.89	5.94	6.42	6.84	7.34	7.90	8.32
10	Khilkhet	7.88	5.94	6.42	6.84	7.30	7.83	8.24
11	Airport T-3	7.87	5.93	6.42	6.84	7.27	7.80	8.20
12	Airport	7.86	5.93	6.42	6.84	7.26	7.78	8.17

3.3 Summary of Probable Flood Level

Based on inundation survey and secondary data analysis, a summary of probable flood levels at different stations of MRT Line 1 was prepared and is given in Table 3. From this Table, it is seen that, highest flood level from inundation survey varies from 7.26 to 7.59 mPWD whereas from secondary data analysis varies from 7.55 to 7.89 mPWD.

Table 3: Probable flood levels at different stations of MRT Line 1

Station No./Id.	Station Name	Flood Level from Inundation Survey (mPWD)	Flood Level from Secondary Data (mPWD) (Table 2)	Recommended Highest Flood Level (mPWD)
1	Kamalapur	7.26	7.55	7.29
2	Rajarbagh	7.12	7.61	7.35
3	Malibagh	7.18	7.72	7.45
4	Rampura	7.40	7.72	7.45
5	Hatir Jheel	7.50	7.77	7.50
6	Badda	7.49	7.81	7.54
7	Uttar Badda	7.38	7.84	7.54
8	Notun Bazar	7.57	7.87	7.59
9	Future Park	7.59	7.89	7.59
10	Khilkhet	7.59	7.88	7.59
11	Airport T-3	7.59	7.87	7.59
12	Airport	7.56	7.86	7.59

Table 3 shows that the survey flood level is lower than the secondary data driven flood level. This could be due to the fact that the MRT Line 1 stations are on floodplains, whereas the BWDB gage stations are on the rivers. During flood time, the river water level is usually higher than the corresponding floodplain level during a rising flood phase when the water flow is from the river towards the floodplain. To take this factor into account, the secondary flood level needed to be adjusted. The adjustment was made by looking at the relation between the two data sets and divided these MRT stations into two groups. For the first group, there is a general increasing trend in flood level from station 1 to station 7. This trend was also maintained in the adjusted highest flood level shown in the last column of Table 3. Stations 8 to 12 in the second group have almost the same flood level and the highest surveyed flood level was 7.59 m PWD. This level was maintained for the adjusted highest flood level in the last column.

3.4 Survey Results into Spatial Maps

Spatial maps are produced for each station location with a radius of 500m taking the station as a centre. Ground level maps were prepared based on the survey data provided by the surveyor. For flood level maps, at first, flood depths were added to respective ground level data to measure the flood levels. Then after four levels of reliability check with the flood level data, finally flood level maps were created. For generating both the ground level maps and the flood level maps, Geographic Information System (GIS) tool was used. Figure 6 shows the existing ground level map and flood level map for the Khilkhet area (station 10). Although, there are 20 measured points in the ground level map, after the reliability check, the number of reliable flood level data are 12 for this site.

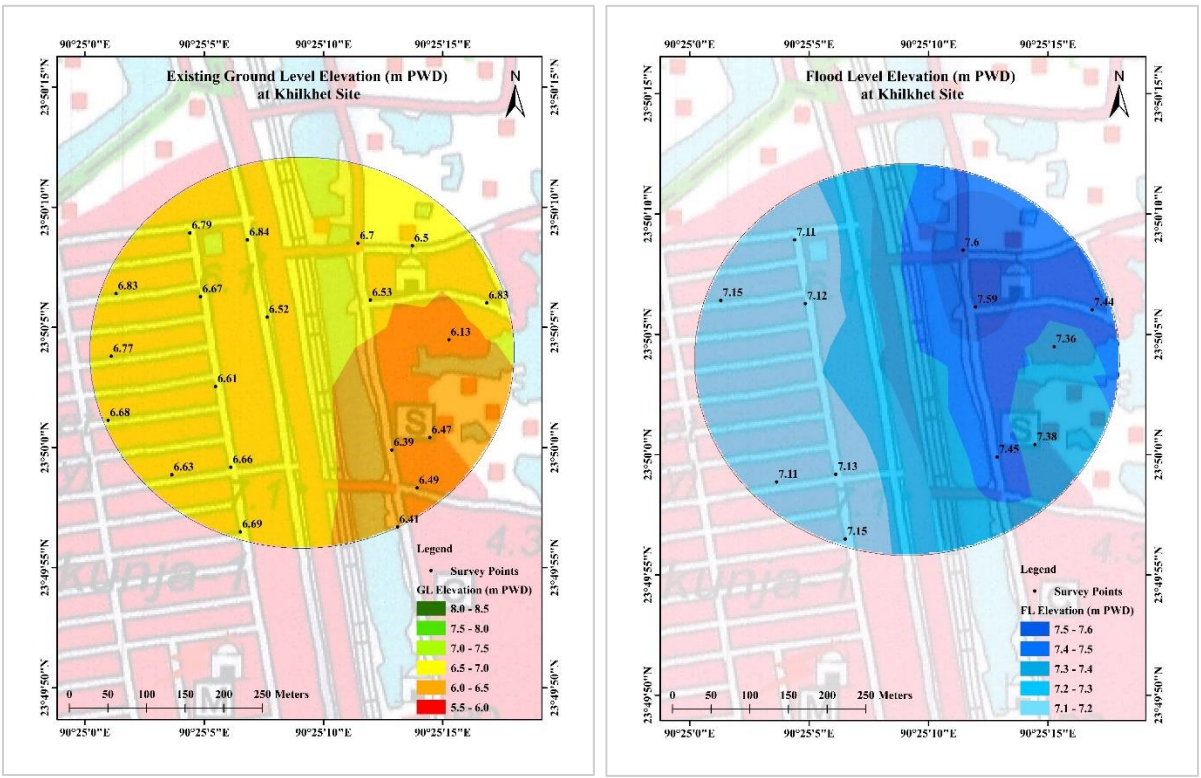

Figure 6: Ground level map and flood level map for the Khilkhet area (station 10)

4. CONCLUSIONS

This study estimates the design flood levels at different locations of MRT Line-1 after comparing the surveyed inundation data and secondary data. For this, primary field data on flood level from 12 underground stations were gathered. Secondary water levels at different available gage stations were collected from BWDB for making comparisons with the flood level obtained from field survey. Primary survey of flood depths at 20 points of each station was done on the basis of local water marks and

people's perception. Then land levels at these 20 locations of each station were obtained by a professional survey team. These together provided flood information for each station. A number of reliability checking was done with the collected data. The surveyed flood level included both riverine and rainfall floods. The highest flood level varied between 7.26 m PWD at station 1 to 7.59 m PWD at station 11 and was comparable with the flood level from the secondary data. As MRT stations are located at the floodplain whereas secondary flood level data were obtained based on the frequency analysis of the gage stations located in the surrounding rivers, relatively higher values were obtained by this method compared to the primary surveyed data. By considering all of these and after making some adjustments, highest flood levels for these important locations were proposed. Finally, prepared spatial maps of flood level at different station locations can be used for understanding the common flooding scenario in these places.

ACKNOWLEDGEMENTS

As this study is based on primary field survey, the authors are grateful to the local residents of the locations studied. Their cooperation and valuable information regarding the flood inundation make this study successful.

REFERENCES

Azam, F., Islam, M. S., & Shahin, H. M. (2016). Study on Tunneling for Underground Metro Rail System in Dhaka City. *International Journal of GEOMATE, 11*(20), 1776-1783.

Dewan, A. M., & Yamaguchi, Y. (2008). Effect of land cover changes on flooding: example from Greater Dhaka of Bangladesh. *International Journal of Geoinformatics, 4*(1), 11-20.

Faisal, I. M., Kabir, M. R., & Nishat, A. (1999). Non-structural flood mitigation measures for Dhaka City. *Urban Water*, *1*(2), 145-153.

Gain, A. K., Mojtahed, V., Biscaro, C., Balbi, S., & Giupponi, C. (2015). An integrated approach of flood risk assessment in the eastern part of Dhaka City. *Natural Hazards*, *79*(3), 1499-1530.

Hafiz, R. (2011). Urban Hazards in Dhaka. In 400 Years of Capital Dhaka and Beyond: Urbanization and Development. *Dhaka: Asiatic Society of Bangladesh*, 3.

Huq, S., & Alam, M. (2003). Flood management and vulnerability of Dhaka City. *Building Safer Cities*, *121*.

Khan, M.S.A. (2006). Stormwater flooding in Dhaka city: causes and management. *Journal of Hydrology and Meteorology, 3*(1), 77-85.

Mark, O., Apirumanekul, C., Kamal, M. M., & Praydal, G. (2001). Modelling of urban flooding in Dhaka City. In *Urban Drainage Modeling* (pp. 333-343).

Rahman, M. (2008). Future mass rapid transit in Dhaka city: Options, issues and realities. *Jahangirnagar Planning Review*, *6*, 69-81.

Proceedings of the 5th International Conference on Civil Engineering for Sustainable Development (ICCESD 2020), 7~9 February 2020, KUET, Khulna, Bangladesh (ISBN-978-984-34-8764-3)

INFLUENCE OF VERTICAL PLATES ON FORCE COEFFICIENTS OF SQUARE CYLINDER BY NUMERICAL SIMULATION

Md. N Haque*[1]

[1]Assistant Professor, Department of Civil Engineering, East West University, Bangladesh, e-mail: naimul@ewubd.edu

***Corresponding Author**

ABSTRACT

The aim of this study is to investigate the influence of attaching vertical plates on force coefficients of square cylinder. Four vertical plates of equal height are attached at the middle position on four sides of square cylinder to control the flow and investigate its effect on force coefficients. The normalized height w.r.t. to the depth of the square cylinder is varied from 0.01 to 0.14. Direct Numerical Simulation (DNS) is adopted to calculate the responses of the cylinder. Second order accurate numerical schemes are utimized to dicretize the flow both in space and time. Reynolds number is kept constant at 100. Aerodynamic force coefficients such as drag, lift and moment are predicted and flow filed are analyzed. The calculated force coefficients are compared in between various cases. It is found that due to attachment of vertical plate the force coefficients of the square cylinder altered noticeably and showed specific trend in the result due to variation of plate height. For a specific value of a normalized plate height, the drag coefficient showed a minimum value which is also lower than the square cylinder without any attachment. Similar to the force coefficients, the strouhal number of the square cylinders also showed very high sensitivity to the height of vertical plate.

Keywords: *Drag coefficient, Square cylinder, Flow field, Vertical plate, Flow control.*

1. INTRODUCTION

Flow around bluff bodies has drawn the attention of engineers of various fields such as civil, mechanical, chemical, naval and aerospace engineering etc. due to its huge practical application. Reduction of force coefficients, especially the drag force coefficient by understanding the flow mechanism is one of the main interests to optimize the design. Past researchers explored various active and passive control systems to reduce the force coefficients and improve the flow field. Among the passive control systems, the effectiveness for wake control of circular cylinder by attaching a horizontal plate (splitter plate) at the downstream side of the circular cylinder was shown by Roshko (1954). The mechanism of splitter plate for square cylinder was different as the leading edge separated flow goes at the downstream with large side bubbles (Doolan 2009). Over the time, a number of other effective passive control systems have also been invented for square cylinder and their effectiveness have been investigated at various Reynolds number.

Shiraishi et al. (1986) experimentally investigated the influence of corner cut on square cylinder and found that corner modification significantly reduced the drag and fluctuating lift coefficient. The influence of corner cut, recession and roundness was experimentally investigated by Kawai (1998). Among the three methods, the corner roundness was the most effective to suppress the aeroelastic instability. Tamura and Miyagi (1999) found that the square cylinder with corner cut and roundness have lower drag both in smooth and turbulent flows. Suppression of fluid force on square cylinder by putting a small bluff body was achieved by number researchers. Lesage and Gartshore (1987) placed a small rod, Igarashi and Ito (1993) placed a square prism, Sakamoto et al. (1997) placed a flat plate the upstream of the square prism and successfully decreased the fluid forces on the square cylinder. A variant of this method, by placing a control cylinder at the shear layer for forced reattachment of

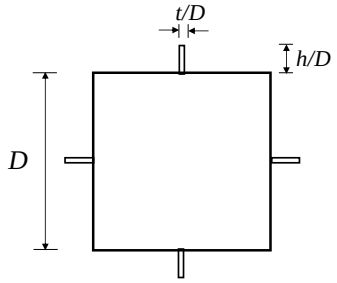

Figure 1: Side view of the square cylinder with vertical plate

flow to reduce the drag coefficient was achieved by Igarashi and Tsutsui (1989) and Shakamoto et al. (1991). A reduction of both in drag a lift force coefficient was obtained by Dey and Das (2015) by attaching a triangular thorn at the upstream face of the square prism. The reduction in drag was obtained mainly due to the weakening pressure and friction drag. By placing multiple small square prisms around the square cylinder, the reduction of drag force was obtained by Islam et al. (2017 and 2018).

In relation to this, in the present study vertical square plates are attached at the side faces of a square cylinder to improve the aerodynamic responses. Fig. 1 shows the side view of the square cylinder. As the plate is attached at the all four side faces of the cylinder, the dependency of performance on the direction of the flow has reduced. The normalized height (*h/D*) of the cylinder was varied from 0 to 0.14. The thickness of the plate is constant at 0.005 for all the cases. The aerodynamic responses are predicted numerically at Reynolds number 100. The mean and RMS values of the force coefficients are calculated to observe the influence of attaching the vertical plate at the side face of the square cylinder. Along with the force coefficients, the time dependent vorticity fields are also explored.

2. METHODOLOGY

The flow around the cylinders was assumed as two dimensional and simulated by solving the unsteady incompressible Navier-Stokes Equations as presented below.

$$\nabla \cdot u = 0 \tag{1}$$

$$\frac{\partial u}{\partial t} + (u \cdot \nabla)u = -\nabla p + \frac{1}{R_e}\nabla^2 u \tag{2}$$

where u is the velocity vectors and p denote the pressure. These dimensionless governing equations are integrated in time using second order accurate backward differentiation method. The convective and diffusive terms are discretized with a second-order accurate central differencing scheme. In space, the governing equations are discretized by the finite volume approach in an unstructured grid system. The pressure-velocity coupled discretized equations are solved by pimpleFoam algorithm which combines the conventional PISO (Pressure Implicit with Splitting of Operator) and SIMPLE (Semi-Implicit Method for Pressure Linked Equations) methods. The domain was sufficiently large. In the horizontal direction, the domain was stretched up to 61*D* (where, *D* is the height of the cylinder) and 25D was stretched in the vertical direction. Non-slip boundary condition was applied on the cylinders surface. The domain was divided into two parts. In the inner domain, finer mesh and in the outer domain, coarser mesh was utilized. A grid size of 0.05D and 0.02D were utilized around the square cylinder and vertical plate, respectively. The grid system, boundary condition and domain dimensions are shown in Fig. 2. A validation study was carried out to examine the reliability of the numerical setup for a square cylinder at Re 100. Force coefficients are compared with past numerical results and very good agreement was found which is not presented here.

3. RESULTS AND DISCUSSION

In two-dimensional analysis, the mean value of drag and rms value of lift force coefficients are two important parameters. All the force coefficients are calculated based on a characteristic length of (*d+2h*). The influence of vertical plate on mean drag coefficient is summarized in fig. 3. As can be seen the addition of vertical plate has great influence on the mean drag force coefficient. With the variation of plate height (*h*), the mean drag coefficient varies a lot. First the drag force decreases gradually with the increase in plate height (*h*), then increases again with the increase in plate height (*h*). For a normalized plate height of 0.09, the magnitude of drag force coefficient is significantly lower than bare square cylinder. The rms value of the lift force coefficient is summarized in fig. 4. Similar to the mean drag force coefficient, the rms of lift force coefficient also shows very high sensitivity to the addition of plate to square cylinder. Unlike mean drag force coefficient, the minimum rms value of lift force coefficient was found for a normalized plate height (*h*) of 0.05. The behaviour of shedding frequency is summarized in fig. 5. As can be seen there are two distinct zone in the shedding frequency. For normalized plate height (*h/d*) from 0.02 to 0.07, the shedding frequency decreases gradually and then increases again with decreasing trend. The instantaneous vorticity plot for normalized plate height (*h/d*) of 0.0, 0.04, 0.09 and 0.14 are summarized in fig. 6. Clear after-body vortex shedding can be seen for all four cases without any distinct variation. To reveal the flow mechanism, especially the reduction of drag force coefficient, further detail flow analysis is required.

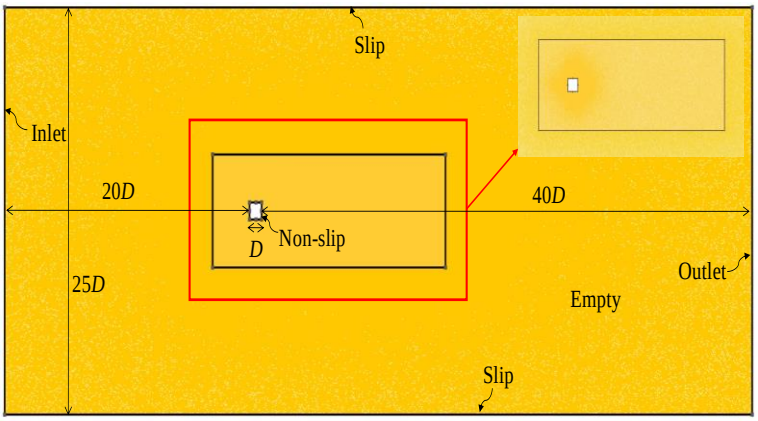

Figure 2: Flow domain and grid system utilized in the simulation

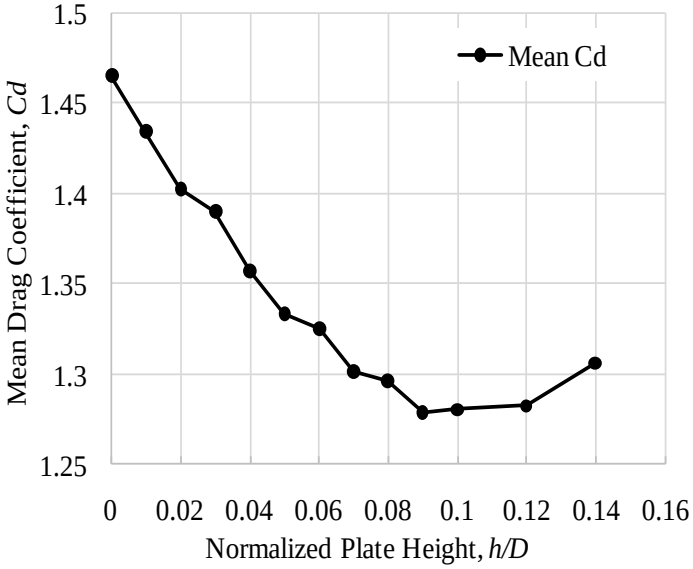

Figure 3: Influence of vertical plate on Mean Drag Force Coefficient

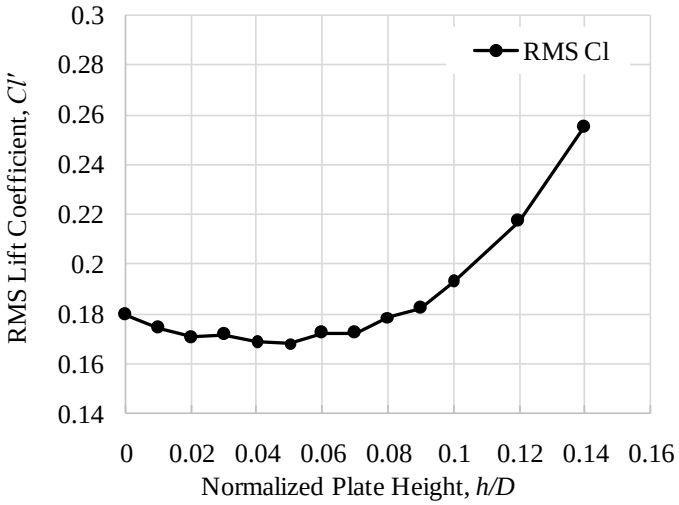

Figure 4: Influence of vertical plate on RMS of lift force coefficients

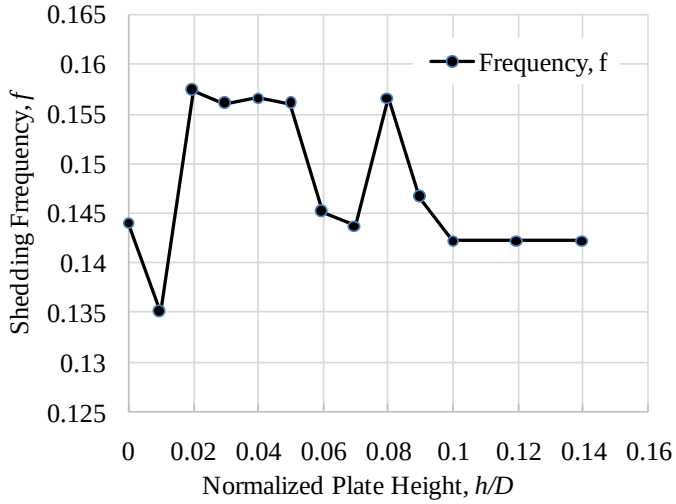

Figure 5: Influence of vertical plate on shedding frequency of square cylinder

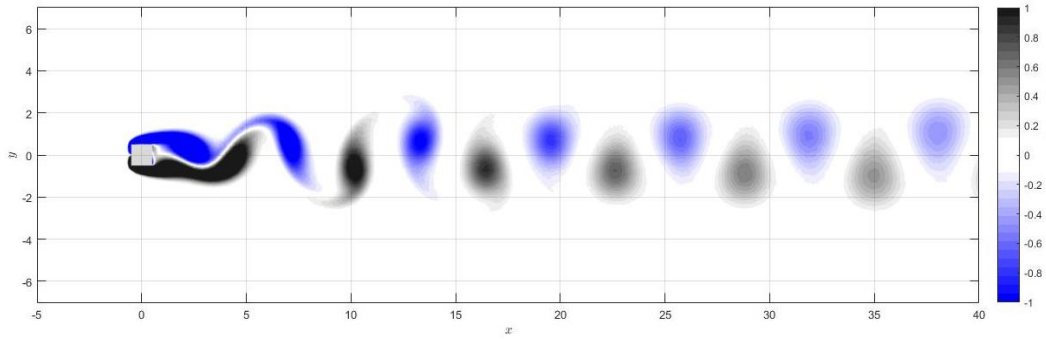

(a) Square cylinder with *h/D*=0.0

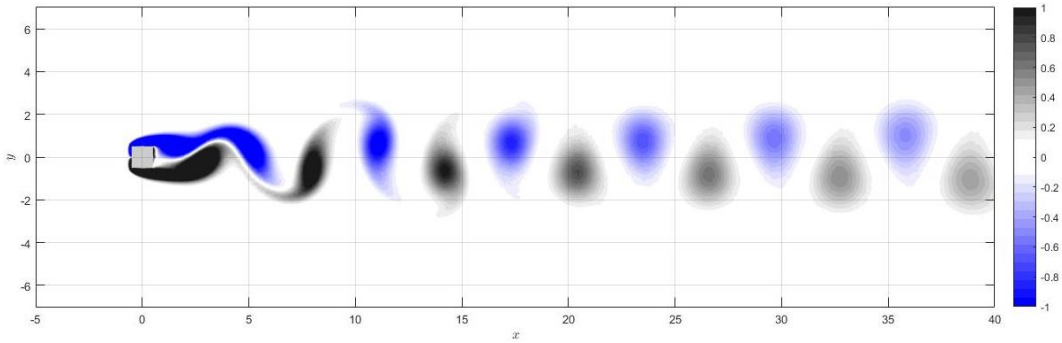

(b) Square cylinder with *h/D*=0.04

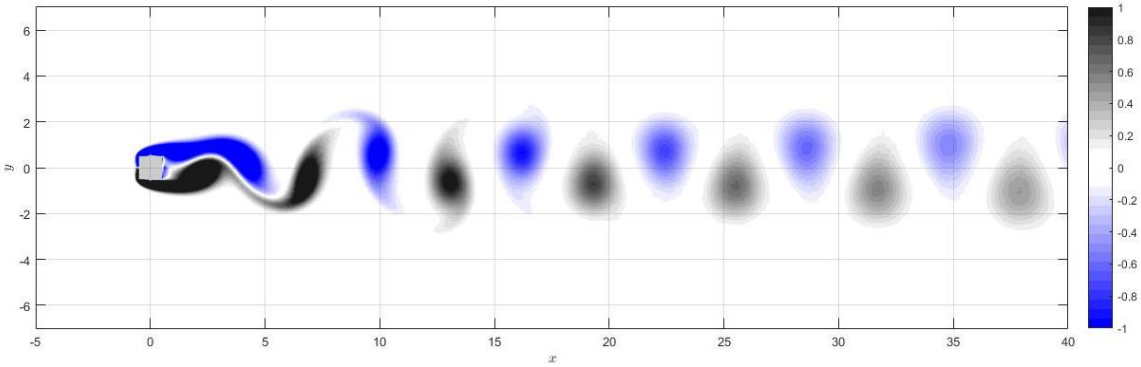

(c) Square cylinder with *h/D*=0.08

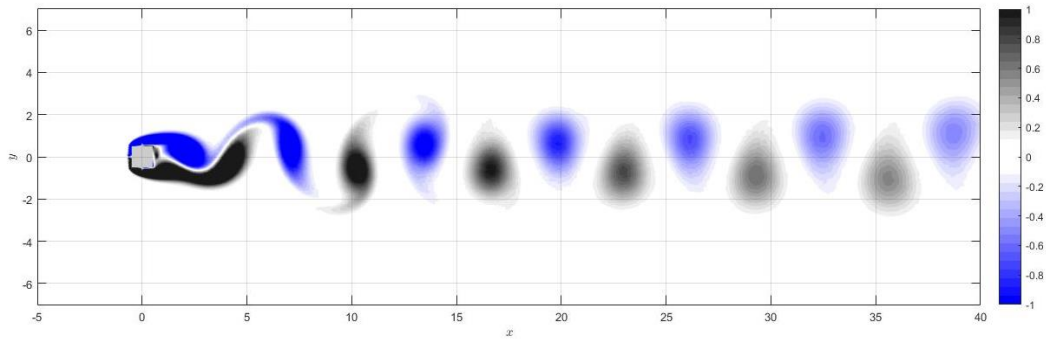

(d) Square cylinder with *h/D*=0.14

Figure 6: Instantaneous Z-vorticity for square cylinder with vertical plate of various height

4. CONCLUSIONS

The paper presented important force statistics of square cylinder with vertical plates. Vertical plates of various heights were attached at the four sides of the square cylinder. It was found that the addition of vertical plate significantly affected the mean drag and RMS of lift force coefficients. For a normalized plate height (*h/D*) of 0.09, the drag coefficient reduced and reached to a minimum value. On the other hand, the RMS of lift force coefficient became smallest for a normalized plate height (*h/D*) of 0.05. The shedding frequency also showed two distinct zones for various plate height. Important force statics and shedding frequency showed some interesting trends in results due to addition and variation of vertical plate in the square cylinder. The flow mechanism should be properly understood to grasp the reason behind the trends in the results. In future, the pressure filed, after body wake, the boundary layer flow and the velocity field will be explored in detail for understanding the flow mechanism.

REFERENCES

Roshko, A. (1954) On the drag and shedding frequency of two-dimensional bluff bodies. NACA Technical Note, No. 3169.

Doolan, C.J. (2009) Flat-plate interaction with the near wake of a square cylinder. AIAA J., 47, 475.

Shiraishi, M., Matsumoto, M., Shirato, H., Ishizaki, H. Nagata, H., Matsui, T. (1986) "On aerodynamic stability effects for bluff rectangular cylinders by their corners cut." Proc. 9th National Symp. on Wind Engineering, 193-198 (in Japanese).

Kawai, H. (1998) Effect of corner medications on aeroelastic instabilities of tall buildings. *Journal of Wind Engineering and Industrial Aerodynamics*, 74-76, 719-729.

Tamura, T. and Miyagi, T. (1999) The effect of turbulence on aerodynamic forces on a square cylinder with various corner shapes. *Journal of Wind Engineering and Industrial Aerodynamics,* 83, 135.

Lesage, F., Gartshore, I.S. (1987) A method of reducing drag and fluctuating side force on bluff bodies. *Journal of Wind Engineering and Industrial Aerodynamics*, 25, 229–245.

Igarashi, T. & Ito, S., (1993) Drag reduction of a square prism, 1st Report, Flow control around a square prism using a small vortex shedder. *Transactions of JSME*, 59 (568), 3701-3707.

Sakamoto, H., Tan, K., Takeuchi, N., Haniu, H. (1997) Suppression of fluid forces acting on a square prism by passive control. *ASME Journal of Fluids Engineering*, 119, 506–511.

Sakamoto, H., Tan, K., Haniu, H. (1991) An optimum suppression of fluid forces by controlling a shear layer separated from a square prism. *ASME Journal of Fluids Engineering*, 113 (2), 183-189.

Igarashi, T., Tsutsui, T. (1989) Flow control around a circular cylinder by a new method, 1st Report, Forced reattachment of the separated shear layer. *Transactions of JSME*, 55 (511), 701–706.

Dey, P. and Das, A.K. (2015) Numerical analysis of drag and lift reduction of square cylinder, *Engineering Science and Technology, an International Journal*, 18(4), 758-768.

Islam, S., Manzoor, R., Islam, Z., Kalsoom, S. & Ying, Z.C. (2017) A computational study of drag reduction and vortex shedding suppression of flow past a square cylinder in presence of small control cylinders. *AIP ADVANCES*, 7, 045119.

Islam, S. Manzoor, R. Khan, U., Nazeer, G. & Hassan, S. (2018) Drag Reduction on a Square Cylinder using Multiple Detached Control Cylinders. *KSCE Journal of Civil Engineering*, 22(5):2023-2034.

Proceedings of the 5th International Conference on Civil Engineering for Sustainable Development (ICCESD 2020), 7~9 February 2020, KUET, Khulna, Bangladesh (ISBN-978-984-34-8764-3)

APPLICATION OF HYDROLOGICAL METHODS TO ASSESS THE ENVIRONMENTAL FLOW OF GORAI RIVER IN BANGLADESH

Md. Mahmudul Hasan*[1] and Md. Shahjahan Ali[2]

[1]*Graduate Student, Department of Civil Engineering, Khulna University of Engineering & Technology, Khulna-9203, Bangladesh, email: hasan03ce@gmail.com*

[2]*Professor, Department of Civil Engineering, Khulna University of Engineering & Technology, Khulna-9203, Bangladesh, email: bablu41@yahoo.com*

***Corresponding Author**

ABSTRACT

Environmental flow requirement certifies natural condition prominence of a river. Due to terrestrial position, the rivers in Bangladesh have to face very high flow in wet season and low flow in dry season. Since the present condition of a river flow characteristics has proven on historic flow data, the estimation of environmental flow requirements (EFR) for the rivers are censoriously important for Bangladesh. The purpose of the study is to assess the EFR of Gorai River and to evaluate the change in flow characteristics in recent time compared to past. Two stations are selected to assess the environmental flow circumstance for Gorai River system. The selected stations are Gorai Railway Bridge and Kamarkhali Transit. There are several methods for calculating the environmental flow requirements of a river system. Three popular methods namely Mean Annual Flow (MAF), Flow Duration Curve (FDC) and Constant Yield (CY) methods are used here for estimation of the environmental flow of the selected stations. These methods are appropriate for hydrological attitude and in use of chronological flow data.

Daily discharge data of selected stations were collected from Bangladesh Water Development Board (BWDB) and analyzed for two periods i.e. G1 period (for the year 1984 to 1999) and G2 period (for the year 2000 to 2016), and IHA software (version 7.1) has been applied. It is found that the estimated environmental flows of Gorai River at Gorai Railway Bridge station are 202.4 Cumec and 195.9 Cumec for MAF and CY methods, respectively. Here, the average EFR is estimated as 199.15 Cumec. In the Kamarkhali transit station of Gorai River, the environmental flows are estimated as 159 Cumec and 217 Cumec for MAF and CY methods, respectively. Thus, the average value of environmental flow was estimated as 188 Cumec. Deficient flow situation was observed from December to May in both of the stations according to the estimated environmental flow requirement. For both of the stations, the highest and lowest flowing months were found as August and March, respectively. It is observed that, the river condition is good at high flow season but the flows in low flow season became lower than the environmental flows required for good habitat quality.

Keywords: *Environmental Flow Requirement, Mean Annual Flow, Flow Duration curve, Constant Yield, Indicators of Hydrologic Alteration.*

1. INTRODUCTION

The Rivers afford several belongings and amenities for nature. The river comprises a source of water used for domestic, trade and agricultural purposes, a means of power generation and unwanted discarding, directions for navigation and locates for recreational and spiritual accomplishments. In the recent time, river flow system in freshwater discharge is reflected as a main variable by the river scientists due to its durable guidance on the environmental aspects. But hydrologic systems show a foremost task in shaping the biotic configuration, function of aquatic, wetland, and riparian ecologies (Richter et al., 1996). The Environmental flow requirement is an assessment for how much of the original flow establishment of a river should endure to flow down it and onto its floodplains in order to sustain indicated valued geographies of the ecosystem, hydrological commands for the rivers.

The future circumstances of the ecosystem are largely dependent on the environmental flow requirement. In this study, The EFR for Gorai river has been estimated; it is a river in south west region of Bangladesh that carries its flow from Ganges River. The upstream part of the Gorai river carries freshwater and then brackish water in the estuary. It is the main source of upland freshwater supply in this region (Moly et al., 2015). The Environmental flow requirement is different for different regions. Moreover, the impact of the identical flow requirement is not same for all the areas. However, for the awareness and protection against threat as well as for the mitigation of danger, it is necessary to assess the temporal and spatial changes in flow characteristics of Gorai River and to estimate the Environmental Flow Requirement (EFR) of the river that can be used for future orientation in management purposes. The River used to expulsion into the Bay of Bengal through the Madhumati and Baleswar Rivers and thus attends as a essential appliance for conserving both the environment and economy of the region (Islam and Gnauck, 2011). Due to excessive extraction from the Ganges River in its upstream inside India, its distributaries inside Bangladesh are gradually fallen to death for not receiving their dry season flow. Implementation of the Farakka Barrage results in reduction of flow through the Gorai River and deposition started ensuing in the off-take. As a result, two types of environmental impacts have been created in the Gorai catchment area. The sediment particles are settling down on the river bed rapidly, which is one of the major problems of Gorai River morphology. On the other hand, the saline sea water is pushed up in the upstream area due to capillary upward movement. The main objective of this study is to assess the flow characteristics of Gorai River and to estimate the Environmental Flow Requirement (EFR) of the river that can be used for future reference in management purposes.

2. METHODOLOGY

The research is outlined as to study the changes of flow characteristics for two stations in Gorai river system (Gorai Raiway Bridge station and Kamarkhali station) through the comparison between past and recent times and the environmental flow requirement was estimated to sustain natural ecosystem. The analysis of discharge on Gorai river system were carried out through Mean Annual Flow (MAF), Flow Duration Curve (FDC) and Constant Yield (CY) methods. All the methods belong to hydrological approach and use historical flow data. For determination of EFR, IHA (Indicators of Hydrologic Alteration) software is used (IHA, 2009), where the software quickly processed daily hydrologic records to enable characterization of natural water conditions and facilitate evaluations of human-induced changes to flow regimes.

The IHA software contains 67 parameters, which are sectioned into two groups, 33 IHA parameters and 34 EFC (Environmental Flow Component) parameters. Mean daily discharge (Cumec) data have been collected from the Bangladesh Water Development Board (BWDB) for the years 1984 to 2016. All hydrologic indices have been calculated from daily mean flow records using the Indicators of Hydrologic Alteration (IHA) software (version 7.1). A common approach to assess hydrologic alteration involves a comparison of flow regimes between past and more recent time. The flow for last thirty years was analyzed using IHA Software for two periods: G1 period (for the year 1984 to 1999) and G2 period (for the year 2000 to 2016).

Moreover, the classification of seasons based on discharge reported in Moly et al. (2015) is applied in the analysis of the present study. Depending on mean monthly flow, Gorai flows were categorized in three separate seasons named low flow season for the months of February to May (mean annual flow ≤100 Cumec), high flow season from July to October (mean annual flow ≥1000 Cumec) and intermediate flow season from November to January and June (mean annual flow from > 100 to < 1000 Cumec).

In this study of Gorai river system, the seasonal variation approach used in the Teesta River case by Mullick (2010) is adopted. The seasons are categorized as high flow season for the months of June to September, intermediate flow season for October, November, April and May and low flow season for the months of December to March.

3. RESULTS AND DISCUSSIONS

3.1 General Features of the Gorai River Flow

The river data had been analysed using IHA software in two different ways, first is single period analysis (1984-2016) and second as a two-period analysis: G1 period (1984-1999) and G2 period (2000-2016). The river characteristics of G1 period were compared with G2. For further investigation of the flow data, annual flow has been categorized in three dispersed seasons subjected on the amount of mean monthly discharge. The seasons are categorized as high flow season (HFS) for the months of June to September, intermediate flow season (IFS) for October, November, April and May and low flow season (LFS) for the months of December to March. For the investigation of flow data, Range of Variability Approach (RVA) method is also used which offers a flow target that resembles the expected flow regime with the primary objective of protecting natural ecosystem (Mullick et al., 2010). The flow characteristics and RVA are analyzed by the IHA software.

In the LFS, the discharge is the lowest in the Gorai River system. By considering mean monthly annual flows of Gorai railway Bridge station, it is found that August has the highest discharge of 5089 Cumec as a single period analysis as shown in Table 1. For two period analyses, it is found 5633 Cumec for G1 period (1984-1999) and 4577 Cumec for G2 period (2000-2016) as shown in Table 2. Here the March is found to be the lowest flowing month having a discharge of 23.22 Cumec as a single period analysis and 11.26 Cumec for G1 period and 34.47 Cumec for G2 period.

On the other hand, in the mean monthly annual flows at Kamarkhali Transit station, August has the highest discharge of 3467 Cumec as a single period analysis as shown in Table 1. For two period analyses, it is found 3942 Cumec for G1 period (1984-1999) and 3159 Cumec for G2 period (2000-2016) as shown in Table 3.2. Here the March is found to be the lowest flowing month having a discharge of 14.05 Cumec as a single period analysis and 19.08 Cumec for G1 period and 10.8 Cumec for G2 period.

Some other general characteristics are also shown in Table 1 and 2. The mean annual flow for Gorai Railway Bridge is found as 1012 Cumec and for Kamarkhali transit 795 Cumec. The extreme lowest flowing season is found in March and highest flowing season found in August. For Gorai Railway Bridge station the low flow threshold estimated by IHA is 5.783 Cumec and high flow threshold is 1390 Cumec. Whereas for Kamarkhali Transit station, the low flow threshold estimated by IHA is 12.54 Cumec and high flow threshold is 1128 Cumec. March is the lowest flowing month where flows are far lower than high flow threshold. The annual CV found for both the stations are nearly same; for Gorai Railway Bridge it is 1.5 and for Kamarkhali Transit station it is 1.45. The flow predictability is also nearly same as 0.46 and 0.48; the constancy/predictability is same for both as 0.29, percent of flood in 60-day period is found 0.88 for Gorai railway Bridge station and 0.91 for Kamarkhali Transit station. Flood free season is also nearly same 236 and 238; one day minimum flow is 23.22 for Gorai railway Bridge station and for Kamarkhali Transit station it is found 14.02. One day maximum flow for Gorai railway Bridge station is 5089 Cumec and Kamarkhali Transit

station is 3467 Cumec, and rise rate is slightly higher for Gorai railway Bridge station (44.86) than the Kamarkhali Transit station is (30.03). The fall rate for Gorai railway Bridge station is 33.93 and for Kamarkhali Transit station is 26.08. The high flow threshold for the Gorai railway Bridge station is found as 1390 Cumec whereas for Kamarkhali Transit station it is found as 728 Cumec, this is lower than the Gorai railway Bridge station.

Table 1: General Characteristics of flows in Gorai Railway Bridge and Kamarkhali Transit stations as a single Period analysis

River Characteristics	Gorai railway bridge	Kamarkhali Transit
Period	**Total**	**Total**
Mean annual flow (Cumec)	1012	795.1
Annual C.V.	1.5	1.45
Flow predictability	0.46	0.48
Constancy/Predictability	0.29	0.29
% of flood in 60d period	0.88	0.91
Flood-free season	236	238
1-Day minimum flow	23.22	14.025
1-Day maximum flow	5089	3467
Base flow index	0.0348	0.0366
Rise rate	44.86	30.03
Fall rate	-33.93	-26.08
High flow threshold	1390	1128
Extreme low flow threshold	5.783	12.54

Table 2: General Characteristics of flows in Gorai Railway Bridge and Kamarkhali Transit stations as two-period analyses

River Characteristics	Gorai railway bridge		Kamarkhali Transit	
Period	**G1**	**G2**	**G1**	**G2**
Mean annual flow (Cumec)	1086	942.6	888.7	734.5
Annual C.V.	1.55	1.42	1.54	1.34
Flow predictability	0.53	0.49	0.5	0.53
Constancy/Predictability	0.31	0.27	0.29	0.28
% of flood in 60d period	0.91	0.91	0.83	0.88
Flood-free season	253	247	252	270
1-Day minimum flow	11.26	34.47	19.08	10.8
1-Day maximum flow	5633	4577	3942	3159
Base flow index	0.0281	0.0413	0.0587	0.0223
Rise rate	53.93	36.86	34.6	27.34
Fall rate	-41.11	-27.18	-34.67	-20.52
High flow threshold	1593	1593	957	957
Extreme low flow threshold	1.36	1.36	17.55	17.55

Table 3 shows the mean monthly flows for Gorai railway bridge station. It shows that the flows in January to May are lower than 100 Cumec for G1 period (1984-1999) and the flows in February to April are lower than 100 Cumec for G2 period (2000-2016). Whereas for total period (1984-2016) analysis the flows in February to May are lower than 100 Cumec. According to (Mullick et al. (2010) the flows in December to March are low flow seasons for Gorai railway bridge station. The flow values in June found slightly higher than 100 Cumec; and July to September flows are the high flow season. These mean monthly flows are higher for Gorai railway bridge station as HFS occurs in the month of June to September. The flow again starts decreasing in October and November. The Intermediate flow season occurs in the month of April, May, October and November.

Table 3: Mean monthly flows for different flow season at Gorai railway bridge station

Month	Season	G1 period (1984-1999) Cumec	G2 period (2000-2016) Cumec	Total period (1984-2016) Cumec
April	IFS	37.18	70.55	54.37
May		54.06	106.6	81.13
June	HFS	290.8	441.4	368.4
July		2239	1942	2086
August		3972	2925	3432
September		3925	2831	3362
October	IFS	1686	1784	1736
November		464.6	580.6	524.3
December	LFS	141.5	253.3	199.1
January		59.97	150.6	106.7
February		42.17	86.5	65.01
March		34.89	68.49	52.2

It is found for Gorai railway bridge station that, mean monthly flows satisfies LFS in November to June months. Whereas July to October flows are the high flow seasons. It is also observed in Table 3 that the March is the lowest flowing month and the flow is 34.89 Cumec in G1 period (1984-1999), 68.49 Cumec in G2 period (2000-2016), and for total period (1984-2016) the March flow is 52.2 Cumec in Gorai railway Bridge station. August is the highest flowing month and the flow is 3972 Cumec in G1 period (1984-1999), 2925 Cumec in G2 period (2000-2016), and for total period (1984-2016) the August flow is 3432 Cumec in Gorai railway Bridge station. The mean monthly flows of Gorai railway bridge station shows that HFS duration is 4 months and LFS duration is 8 months. In the 8 months of LFS duration, the June, November and December flows can be considered as intermediate flow season as per the mean monthly flows.

Table 4 shows the mean monthly flows of Kamarkhali Transit station. It shows that the flows in January to March are lower than 100 Cumec for G1 period (1984-1999) and the flows in January to April are lower than 100 Cumec for G2 period (2000-2016). Whereas for total period (1984-2016) analysis the flows in January to April are lower than 100 Cumec. According to Mullick (Mullick et al,. 2010) the flows in December to March are low flow seasons for Kamarkhali Transit station. The flow values in June found slightly higher than 100 Cumec; and July, August, September flows are the high flow season. These mean monthly flows are higher for Kamarkhali Transit station as HFS occurs in the month of June to September. The flow again starts decreasing in October and November. The Intermediate flow season occurs in the month of April, May, October and November.

Table 4: Mean monthly flows for different flow season at Kamarkhali Transit Station

Month	Season	G1 period (1984-1999)	G2 period (2000-2016)	Total period (1984-2016)
April	IFS	137.3	44.64	81.05
May		154.1	100.4	121.5
June	HFS	324.5	397.2	368.6
July		1741	1580	1643
August		3177	2460	2742
September		2923	2197	2483

October	IFS	1496	1201	1317
November		397.5	459.6	435.2
December	LFS	112.4	182	154.6
January		54.35	68.09	62.7
February		39	38.66	38.8
March		40.15	28.25	32.93

It is found for Kamarkhali Transit station that, mean monthly flows satisfies LFS in November to June months. Whereas July to October flows are the high flow seasons. It is also observed in Table 4 that the March is the lowest flowing month and the flow is 40.15 Cumec in G1 period (1984-1999), 28.25 Cumec in G2 period (2000-2016), and for total period (1984-2016) the March flow is 32.93 Cumec in Kamarkhali Transit station. August is the highest flowing month and the flow is 3177 Cumec in G1 period (1984-1999), 2460 Cumec in G2 period (2000-2016), and for total period (1984-2016) the August flow is 2742 Cumec in Kamarkhali Transit station. The mean monthly flows of Kamarkhali Transit station show that HFS duration is 4 months and LFS duration is 8 months. In the 8 months of LFS duration, the May, June, November and December flows can be considered as intermediate flow season as per the mean monthly flows.

3.2 Environmental Flow Requirement of Gorai River

The Environmental Flow Requirement of Gorai River is calculated in three different methods. The estimation of flows is describing as follows.

3.2.1 Mean annual flow (MAF) method

Table 3 and Table 4 shows summary of Mean monthly flows at low flow season (LFS), Intermediate flow season (IFS) and high flow season (HFS). It is observed that the lowest flow of Gorai Railway bridge station occurs in March as 34.89 Cumec in G1 period; and for Kamarkhali it is also observed in the March that is 28.25 Cumec in G2 period. The highest flow occurs for Gorai railway bridge Station in the month of August as 3972 Cumec in G1 period and for the kamarkhali station it is observed as 3177 Cumec in G1 period in the month of August as well.

According to MAF method, November to June is found as the low flow season (LFS) in both the stations. Whereas the high flow season (HFS) According to MAF method are July to October in both the stations. The June and November are the month of Intermediate flow seasons (IFS) or flow transition season in both the stations. In these months the flows are changing their patterns. The high flow comes to decrease at the month of November after which low flow season starts. Whereas low flow comes to increase at the month of April and May after which high flow season settles. It is observed that the flow in pre-monsoon starts increasing in June. The peak highest flow is found in monsoon period in the month of August, and then it again starts decreasing in the month of October. After the monsoon, the flow comes to a minimum level in the month of March.

Figure 1 describes the Comparison of Mean Monthly Flows with EFR in MAF method at Gorai Railway Bridge station. It shows that, mean annual flow of Gorai Railway Bridge station is 1012 Cumec during 1984 to 2016. The EFR value in MAF method for Gorai Railway Bridge is found as 202.4 Cumec. Mean monthly flows for April and May are lower than the environment flow required but the flows in June to November are more than the EFR by mean annual flow method. Again the flows in December to March are less than the required EFR value by mean annual flow method. Generally high flow seasons satisfies the EFR required flow but the flows in low flow seasons are normally less than the EFR by MAF method.

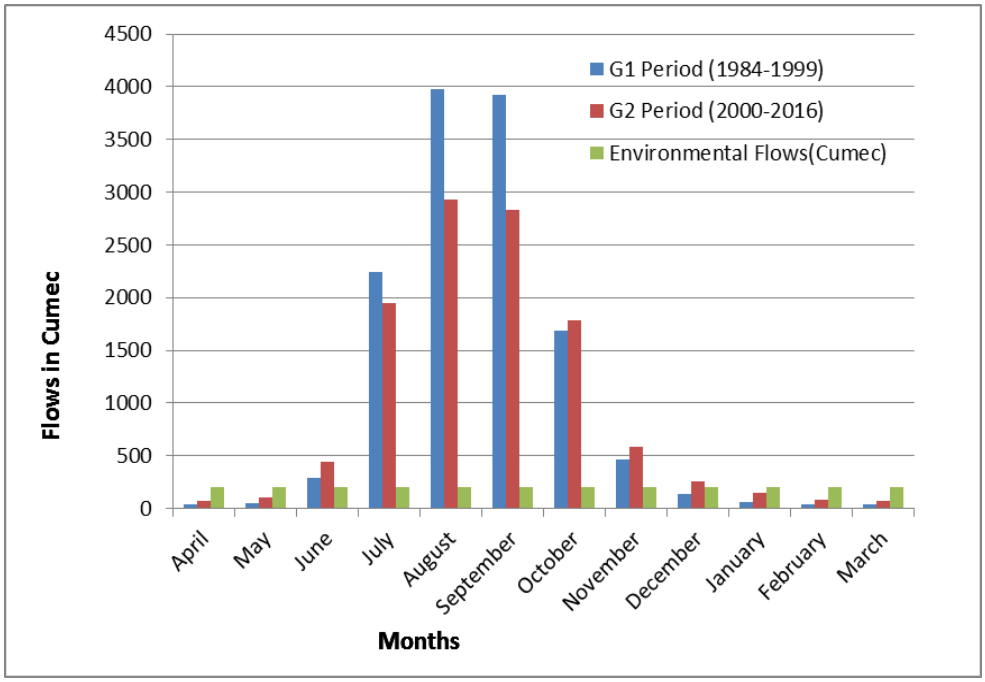

Figure 1: Comparison of Mean Monthly Flows with EFR in MAF method at Gorai Railway Bridge station

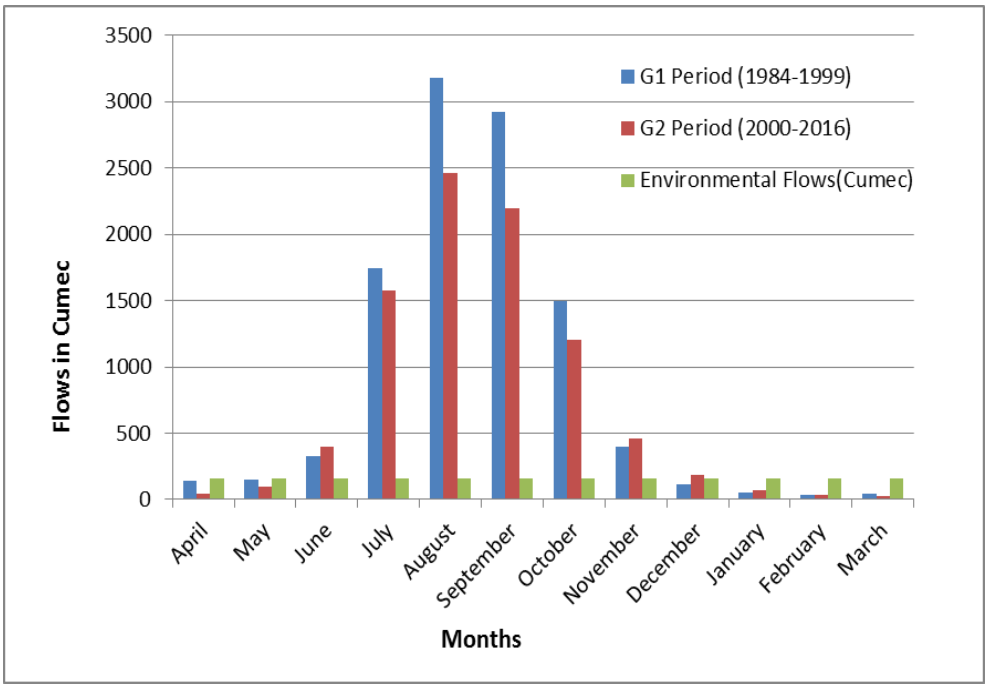

Figure 2: Comparison of Mean Monthly Flows with EFR in MAF method at Kamarkhali Transit station

Figure 2 describes the Comparison of Mean Monthly Flows with EFR in MAF method at Kamarkhali transit station. Mean annual flow of Kamarkhali transit station is 795.1 Cumec during 1984 to 2016. According to habitant quality, environmental flow requirement in MAF is found as 159.02 Cumec for kamarkhali transit station. Mean monthly flows for April and May are lower than the environment flow required but the flows in June to November are more than the EFR by mean annual flow method. Again the flows in December to March are less than the required EFR value by mean annual flow

method. Generally high flow seasons satisfies the EFR required flow but the flows in low flow seasons are normally less than the EFR by MAF method.

3.2.2 Flow Duration Curve (FDC) method

Table 5 shows summary for FDC values at different flow seasons. For the EFR in low flow season, this FDC values are taken at 90% value, for Intermediate flow season this FDC values are taken at 50% value and for high flow season it is taken 50% values of FDC. The lowest flow of Gorai Railway bridge station in FDC method is found in March as 127.1 Cumec in G1 period; and for Kamarkhali Transit station it is also observed in March flow that is 83.8 Cumec in G1 period. The highest flow occurs for Gorai Station in the month of August is 4051 Cumec in G1 period and for the kamarkhali station it is observed 3743 Cumec in G1 period in the month of August as well. According to FDC method, November to June is found as the low flow season (LFS) in both the stations. Whereas the high flow season (HFS) According to FDC method are July to October in both the stations. The June, November and December are the month of Intermediate flow seasons (IFS) or flow transition season in both the stations. In these months the flows are changing its patterns. The high flow comes to decrease at the month of November after which low flow season starts. Whereas low flow comes to increase at the month of April and May after which high flow season settles. It is observed that the flow in pre-monsoon starts increasing in June. The peak highest flow is found in monsoon period in the month of August, and then it again starts decreasing in the month of October. After the monsoon, the flow comes to a minimum level in the month of March.

Table 5: Percentile flow of monthly FDC (90% for LFS and 50% for IFS and HFS)

Months	**Season**	**Gorai railway bridge**			**Kamarkhali Transit**		
		G1 (1984-1999)	**G2 (2000-2016)**	**Total (1984-2016)**	**G1 (1984-1999)**	**G2 (2000-2016)**	**Total (1984-2016)**
April	IFS	9.589	51.5	44.27	46.6	16.13	33.98
May		31.51	92.09	66.53	81.55	50.24	59.73
June	HFS	197.2	273	246.9	217	216.9	217
July		2517	2107	2247	1720	1597	1717
August		4051	3037	3516	3743	2366	2564
September		3785	3195	3529	2866	2444	2581
October	IFS	1481	1404	1438	1290	1124	1132
November		447.6	572.5	473.9	276.6	381.9	337
December	LFS	369.4	514.2	395.2	273.2	394.1	281.5
January		164.2	395.2	260.1	153.3	182.3	180.6
February		132.4	189.7	167	116.5	129.2	124.4
March		127.1	150.6	134.4	83.8	83.81	83.29

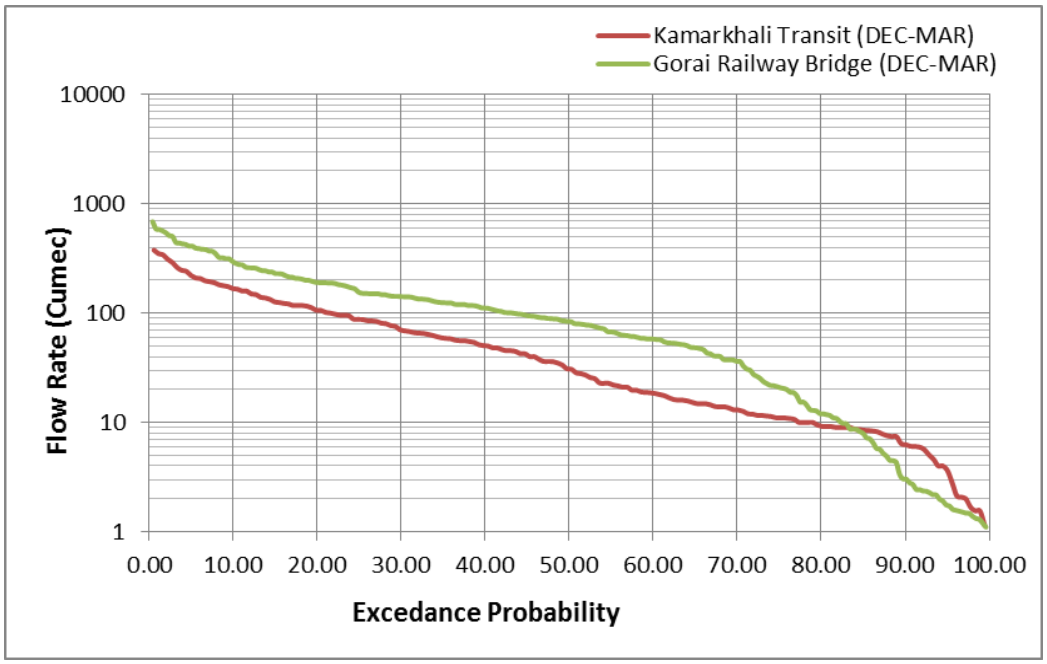

Figure 3: Flow Duration Curve at LFS for Gorai Railway Bridge and Kamarkhali Transit stations

Figure 3 shows the Flow Duration Curve for Gorai Railway Bridge and Kamarkhali Transit stations at LFS. From the Figure it is observed, for the Gorai railway bridge FDC values are higher than the Kamarkhali Transit stations FDC values through all the years. The FDC values crosses the Gorai Railway Bridge when the value of flow is nearer to 10 Cumec and it occurs at 83% of exceedence probability. According to FDC method the LFS requires 90th percentile flow as EFR. The 90th Percentile value on FDC for Gorai Railway Bridge station flow is found as 290 Cumec and the 90th Percentile value on FDC for Kamarkhali transit station flow is found as 167 Cumec.

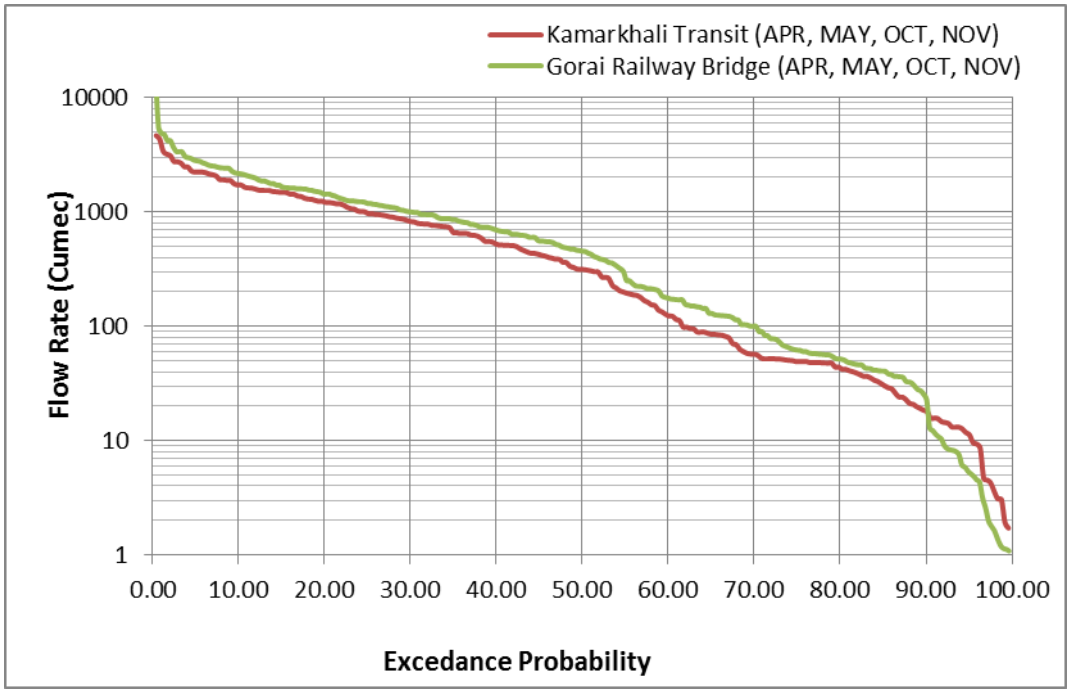

Figure 4: Flow Duration Curve at IFS for Gorai Railway Bridge and Kamarkhali Transit stations

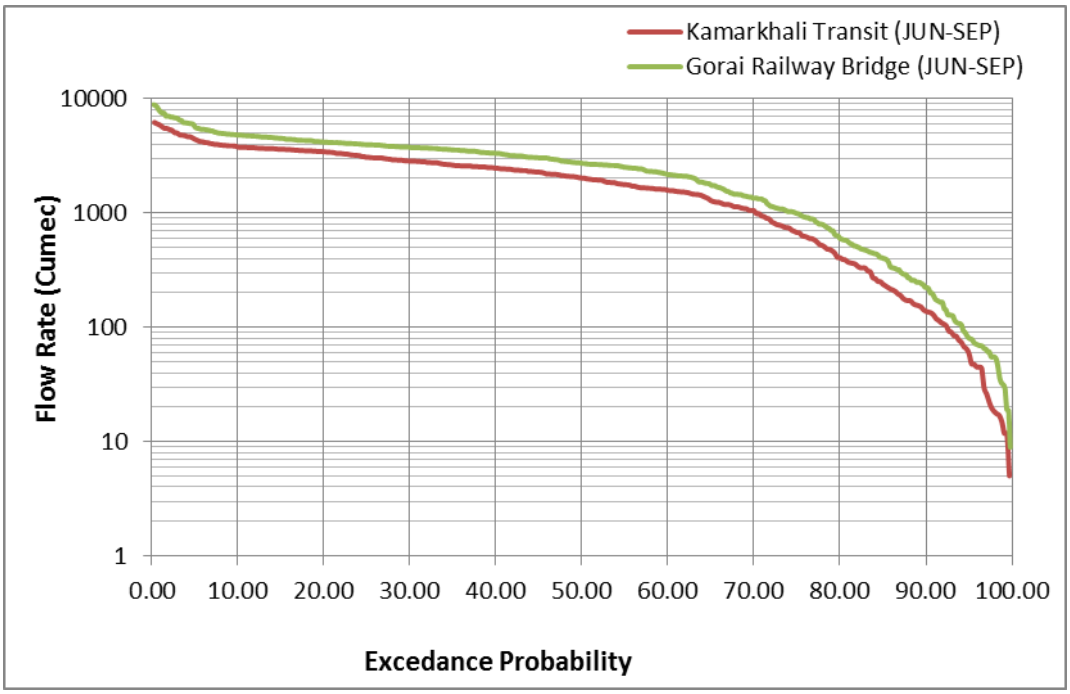

Figure 5: Flow Duration Curve at HFS for Gorai Railway Bridge and Kamarkhali Transit stations

Figure 4 shows the Flow Duration Curve for Gorai Railway Bridge and Kamarkhali Transit stations at IFS. From the Figure it is observed, for the gorai railway bridge FDC values are higher than the Kamarkhali Transit stations FDC values through all the years. The FDC values crosses the Gorai Railway Bridge when the value of flow is nearer to 18 Cumec and it occurs at 90% of exceedance probability. According to FDC method the IFS requires 50th percentile flow as EFR. The 50th Percentile value on FDC for Gorai Railway Bridge station flow is found as 455 Cumec and the 50th Percentile value on FDC for Kamarkhali transit station flow is found as 315 Cumec.

Figure 5 shows the Flow Duration Curve for Gorai Railway Bridge and Kamarkhali Transit stations at HFS. From the Figure it is observed, for the gorai railway bridge FDC values are higher than the Kamarkhali Transit stations FDC values through all the years. According to FDC method the HFS requires 50th percentile flow as EFR. The 50th Percentile value on FDC for Gorai Railway Bridge station flow is found as 2715 Cumec and the 50th Percentile value on FDC for Kamarkhali transit station flow is found as 2026 Cumec.

Table 6: Environmental flow Requirements based on FDC method

Flow season	Percentile value on FDC	Gorai Railway Bridge station Flow (Cumec)	Kamarkhali transit station Flow (Cumec)
High Flow	50th	2715	2026
Intermediate Flow	50th	455	315
Low Flow	90th	290	167

Table 6 shows the environmental flow requirement for the Gorai Railway Bridge station and Kamarkhali transit station based on FDC method. In case of Bangladesh Mullick et al. (2010), Hossain and Hosasin (2011) and Rahman et al. (2013) have used 90% (or 90th percentile) for low flow season and 50% (or 50th percentile) for Intermediate and high flow season to calculate environmental flow requirement of Teesta, Dudhkumar and Turag River respectively.

3.2.3 Constant Yield (CY) method

Table 7 shows summary for Constant Yield at low flow season (LFS) Intermediate flow season (IFS) and high flow season (HFS). It is observed that the lowest flow of Gorai Railway bridge station occurs in February as 3.073 Cumec in G1 period; and for Kamarkhali it is found in the month of March as 15.29 Cumec in G2 period. The highest flow occurs for Gorai railway bridge Station in the month of August as 4051 Cumec in G1 period and for the kamarkhali station it is observed as 3743 Cumec in G1 period in the month of August as well.

According to CY method, November to June is found as the low flow season (LFS) in both the stations. Whereas the high flow season (HFS) According to CY method is July to October in both the stations. The June and November are the month of Intermediate flow seasons (IFS) or flow transition season in both the stations. In these months the flows are changing its patterns. The high flow comes to decrease at the month of November after which low flow season starts. Whereas low flow comes to increase at the month of April and May after which high flow season settles. It is observed that the flow in pre-monsoon starts increasing in June. The peak highest flow is found in monsoon period in the month of August, and then it again starts decreasing in the month of October. After the monsoon, the flow comes to a minimum level in the month of March.

Table 7: Summary of Constant Yield at LFS, IFS and HFS

Months	**Season**	**Gorai railway bridge**			**Kamarkhali Transit**		
		G1 (1984-1999)	**G2 (2000-2016)**	**Total (1984-2016)**	**G1 (1984-1999)**	**G2 (2000-2016)**	**Total (1984-2016)**
April	IFS	9.589	51.5	44.27	46.6	16.13	33.98
May		31.51	92.09	66.53	81.55	50.24	59.73
June	HFS	197.2	273	246.9	217	216.9	217
July		2517	2107	2247	1720	1597	1717
August		4051	3037	3516	3743	2366	2564
September		3785	3195	3529	2866	2444	2581
October	IFS	1481	1404	1438	1290	1124	1132
November		447.6	572.5	473.9	276.6	381.9	337
December	LFS	89.58	226.9	195.9	61.87	113.6	108.7
January		27.83	120.7	88.99	21.69	25.82	23.76
February		3.073	79.8	49.29	20.69	16.95	17.26
March		12.06	59.5	41.18	38.79	15.29	20.23

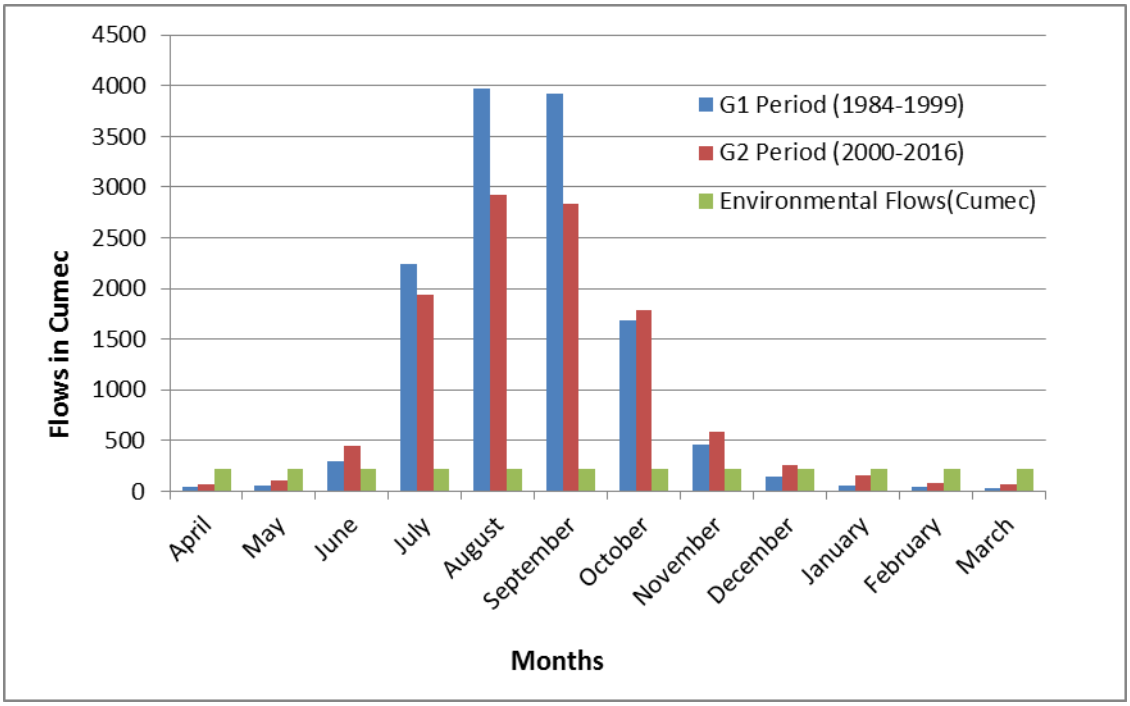

Figure 6: Comparison of Mean Monthly Flows with EFR in CY method at Gorai Railway Bridge station

Figure 6 describes the Comparison of Mean Monthly Flows with EFR in CY method at Gorai Railway Bridge station. The EFR value in CY method for Gorai Railway Bridge station is found as 221.4 Cumec. For this flow in the month of April and May the mean monthly flows are lower than the environment flow required but in June to November the flows are more than the EFR in CY method. Therefore, although the high flow season satisfies the flow required, the low flow season does not support this. Basically the flows in June and November are intermediate flow season where the flow season changes. Again the flows in December to March are less than the required EFR value in CY method. Generally high flow seasons satisfy the EFR required flow but the low flow seasons are normally less than the EFR flow by CY method at Gorai Railway Bridge station.

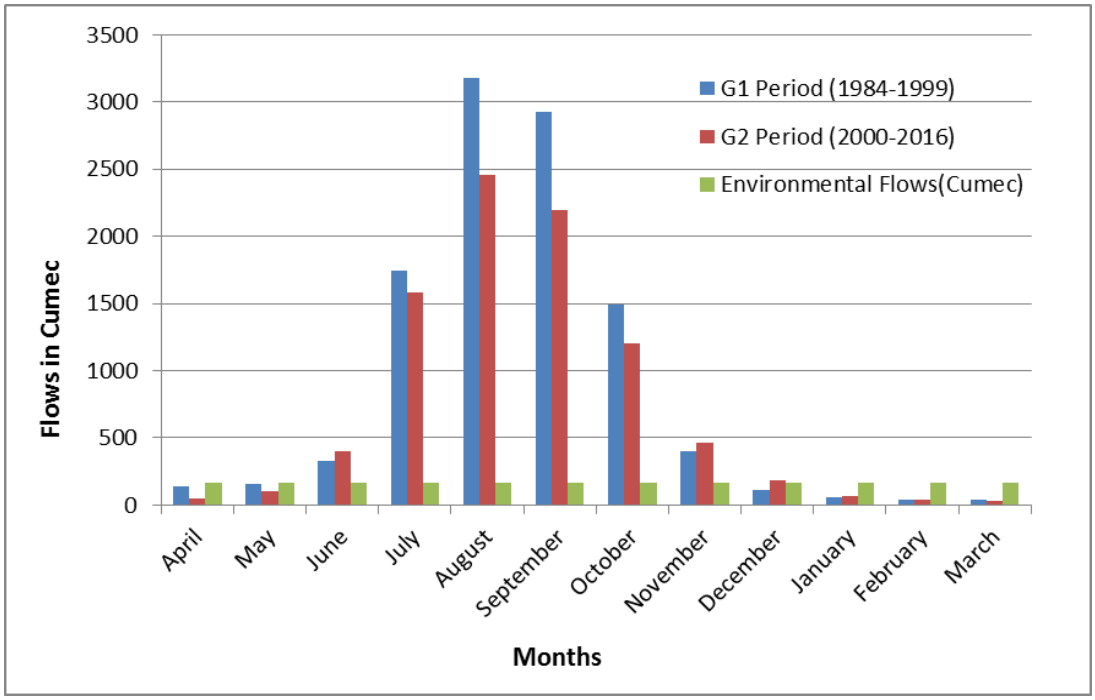

Figure 7: Comparison of Mean Monthly Flows with EFR in CY method at Kamarkhali Transit station

Figure 7 describes the Comparison of Mean Monthly Flows with EFR in CY method at Kamarkhali transit station. The EFR value in CY method for Kamarkhali transit station is found as 162.85 Cumec. For this flow in the month of April and May the mean monthly flows are lower than the environment flow required but in June to November the flows are more than the EFR in CY method. Therefore, although the high flow season satisfies the flow required, the low flow season does not support this. Basically the flows in June and November are intermediate flow season where the flow season changes. Again the flows in December to March are less than the required EFR value in CY method. Generally high flow seasons satisfy the EFR required flow but the low flow seasons are normally less than the EFR flow by CY method at Kamarkhali transit station.

Table 8 shows Summary of monthly Flow values computed by three methods for Gorai Railway bridge station, here in MAF method lowest flow occurs in March which is found as 52.2 Cumec, and the flow start increasing from April. The increasing rate is very slow from April to May, in June the flow has rapid increase and in July the flow has a high frequency. it continue the rapid high flow up to September, after September the flow again start decreasing and in October it has a downward slope of decrease. In November it has started drop the flow and decreases up to March. The low flow season (LFS) is December to March. Whereas the high flow season (HFS) found are June to September and the April, May, October and November are the month of Intermediate flow seasons (IFS) or flow transition season. In these months the flows are changing its patterns. The high flow comes to decrease at the month of October and November after which low flow season settles. Whereas low flow comes to increase at the month of April and May after which high flow season settles. In FDC method the lowest flow observed in April which is 44.27 and highest flow found in September which is found as 3529 Cumec and in CY method the lowest flow occurs in March is found as 41.18 Cumec and high flow found in September is found as 3529 Cumec. Among all methods the highest flow is 3529 found in September and the lowest flow is 41.18 found in March the overall flow condition are nearly same in above three described methods.

Table 8: Summary of monthly Flow values computed by three methods for Gorai Railway bridge station

Months	Season	MAF Method	FDC Method	CY Method
		Total	Total	Total
April	IFS	54.37	44.27	44.27
May		81.13	66.53	66.53
June	HFS	368.4	246.9	246.9
July		2086	2247	2247
August		3432	3516	3516
September		3362	3529	3529
October	IFS	1736	1438	1438
November		524.3	473.9	473.9
December	LFS	199.1	395.2	195.9
January		106.7	260.1	88.99
February		65.01	167	49.29
March		52.2	134.4	41.18

Table 9: Summary of monthly Flow values computed by three methods for Kamarkhali Transit station

Months	Season	MAF Method	FDC Method	CY Method
		Total	Total	Total
April	IFS	81.05	33.98	33.98
May		121.5	59.73	59.73
June	HFS	368.6	217	217
July		1643	1717	1717
August		2742	2564	2564
September		2483	2581	2581
October	IFS	1317	1132	1132
November		435.2	337	337
December	LFS	154.6	281.5	108.7
January		62.7	180.6	23.76
February		38.8	124.4	17.26
March		32.93	83.29	20.23

Table 9 shows summary of monthly Flow values computed by three methods for Kamarkhali Transit station, here in MAF method lowest flow occurs in March which is 32.93 the flow start increasing from April. The increasing rate is very slow from April to May, in June the flow has rapid increase and in July the flow has a high frequency. it continue the rapid high flow up to September, after September the flow again start decreasing and in October it has a downward slope of decrease. In November it has started drop the flow and decreases up to March. The low flow season (LFS) is December to March. Whereas the high flow season (HFS) found are June to September and the April, May, October and November are the month of Intermediate flow seasons (IFS) or flow transition season. In these months the flows are changing it patterns. The high flow comes to decrease at the month of October and November after which low flow season settles. Whereas low flow comes to increase at the month of April and May after which high flow season settles. In FDC method the low flow observed in April which is 33.98 and high flow found in September which is 2581 and in CY method the lowest flow occurs in February is 17.26 and high flow found in September is 2581 among

all methods the highest flow is 2742 found in August and the lowest flow is 20.23 found in March the overall flow condition is nearly same in above three described methods.

3.5 Assessment of Environmental Flow

It is observed from the analysis that, the Mean annual flow of Gorai Railway bridge station is 1012 Cumec during 1984 to 2016, and Mean annual flow of Kamarkhali transit station is 795.1 Cumec during 1984 to 2016. As low flow season is the main concern, about 202.4 Cumec flow is required to maintain good condition for Gorai Railway bridge station and 159 Cumec flow is required for Kamarkhali transit station in MAF method. The relationship between the magnitude and duration of stream flows is presented by flow duration curve (FDC). FDCs are used mainly to set environmental flow purposes. Flow duration intervals are stated as percentage of exceedance, with zero corresponding to the highest stream discharge in the record (i.e. flood conditions) and 100 to the lowest (i.e. drought conditions). As low flow season is the main concern, the environmental flow requirement based on FDC in LFS is found as 290 Cumec for Gorai Railway bridge station and 167 Cumec flow is required for Kamarkhali transit station in FDC method. During the low flow season the minimum requirement based on FDC method is retained during both intermediate and high flow seasons but not for low flow season which is the main concern. Environmental flow considering CY method for Gorai Railway bridge station is found as 221.4 Cumec and for Kamarkhali transit station it is found as 162.85 Cumec. The flow found in CY method is close enough to environmental flow requirement obtained from MAF and FDC methods.

The calculated environmental flow requirement based on Tennant method (MAF), FDC method and CY method are 202.4 Cumec, 290 Cumec and 221.4 Cumec respectively for Gorai Railway bridge station, whereas for Kamarkhali transit station it is found as 159 Cumec, 167 Cumec and 162.85 Cumec, respectively. By taking the average of these three values, the needed environmental flow of the Gorai Railway bridge station is found as 237.93 Cumec for Gorai Railway bridge station and for Kamarkhali transit station it is found as 162.95 Cumec. The river flow meets the environmental flow requirement in high flow season and intermediate flow season.

Table 10 shows the Flow requirement according to habitat quality for Gorai Railway Bridge and Kamarkhali Transit station. Here the flow requirement according to habitat quality are shown in high flow season and low flow season for both the Gorai Railway Bridge and Kamarkhali Transit station, the percentage of mean annual flow for flushing flow is 200%. For Gorai Railway bridge station it is found as 2024 Cumec. For high flow season and low flow season both the requirement is same and for Kamarkhali Transit station it is found as 1590.2 Cumec. The optimum range is 60% to 100% for both low flow and high flow season and outstanding flow at HFS 60% and LFS will be 40% of the mean annual flow and for the excellent flow it is required 50% of high flow season and 30% at low flow season of the MAF and for a good quality of flow it is required 40% at HFS and 20% at LFS. For a fair quality of flow it is required 30% at HFS and 10% at LFS. The quality will be Poor if the flow is 10% in both HFS and LFS. Severe degradation is occurred if the flow less than 10% for both the seasons. Considering the habitat quality, it is found that, for Gorai Railway bridge station the severe degradation is occurred if the flow is less than 101.2 Cumec and for Kamarkhali transit station the severe degradation is occurred if the flow is less than 79.51 Cumec. The severe degradation is occurred if the flow is less than the lowest flow after which the river can be lost its environmental habitat quality below this flow level.

Table 10: Flow requirement according to habitat quality for Gorai Railway Bridge and Kamarkhali Transit station

Flow Requirement	High Flow Season (HFS) (Cumec)		Low Flow Season (LFS) (Cumec)	
(% of MAF)	**Gorai station**	**Kamarkhali station**	**Gorai station**	**Kamarkhali station**
Flushing flow (200%)	2024	1590.2	2024	1590.2
Optimum range (60-100%)	607.2 - 1012	477.06 - 795.1	607.2 - 1012	477.06 - 795.1
Outstanding (60% at HFS, 40% at LFS)	607.2	477.06	404.8	318.04
Excellent (50% at HFS, 30% at LFS)	506	397.55	303.6	238.53
Good (40% at HFS, 20% at LFS)	404.8	318.04	202.4	159.02
Fair (30% at HFS, 10% at LFS)	303.6	238.53	101.2	79.51
Poor (10%)	101.2	79.51	101.2	79.51
Severe degradation (<10%)	<101.2	<79.51	<101.2	<79.51

It is observed that, the river condition is good at the high flow season but when the flow comes in low flow season it becomes lower than the environmental flows required for good habitat quality. The flows in the month of January to May are less than the EFR required. The flows of these months are less than the severe degradation flow. It shows severe problems for both the stations. For the Gorai river, it is necessary to maintain the flow values more than the severe degradation throughout the year to sustain the habitat quality for the river. The three methods show different values for environmental flow requirement. The flow requirements in the low flow season for three methods are found lower than the required flow in both stations. It shows that the river is endangered for habitat quality in low flow seasons. In every method it proved that, the Gorai River has flow scarcity because of the low flows from upstream. The reason is the construction of farakka barrage in the upstream. It causes to decrease the flow in the low flow season. The other factors are the cultivation and water use of the local people from river. Construction of houses in the river bank and dumping of garbage in river side causes the narrowing of the flow channel which causes reduction of flow from upstream to downstream. This wide ranging difference of EFR is due to the variation of habitat quality and flow seasonality. A flushing habitat quality requires the largest amount of flow whereas a 'fair' habitat quality requires the minimum amount of flow.

Observing all three methods it is found that, the discharge of G1 period is generally lower than G2 period in the month November to June, whereas the discharge of G1 period is generally higher than G2 period in the month July to October at Gorai railway Bridge station. On the other hand for Kamarkhali transit station, the discharge of G1 period is generally lower than G2 period in the month November to January, whereas the discharge of G1 period is generally higher than G2 period in the month February to October.

4. CONCLUSIONS

The estimated environmental flow for the Gorai Railway bridge station is found as 237.93 Cumec, which is the average of calculated environmental flow determined by MAF method (202.4 Cumec), Flow duration curve method (290 Cumec) and constant yield method (221.4 Cumec). The flows in June to November month meet the environmental flow requirement. From December to May, the river does not have sufficient discharge to meet environmental flow requirement. In the Gorai Railway bridge station, low flow season suffers in severe water shortage due to significant flow reduction in recent time.

The estimated environmental flow for the Kamarkhali Transit station is found as 162.95 Cumec, which is the average of calculated environmental flow determined by MAF method (159 Cumec), Flow duration curve method (167 Cumec) and constant yield method (162.85 Cumec). The flows in

June to November month meet the environmental flow requirement. From December to May, the river does not have sufficient discharge to meet environmental flow requirement.

Observing MAF, FDC and CY methods it is found that, the discharge of G1 period is generally lower than G2 period in the month November to June, whereas the discharge of G1 period is higher than G2 period in the month July to October at Gorai railway Bridge station. On the other hand, for Kamarkhali Transit station, the discharge of G1 period is generally lower than G2 period in the month November to January, whereas the discharge of G1 period is higher than G2 period in the month February to October.

It is observed that, the river is endangered for habitat quality in low flow seasons. In every method it proved that, the Gorai River has flow scarcity because of the low flows from upstream. The estimated environmental flow requirement found in FDC method is highest among three methods for both the Gorai Railway Bridge station and Kamarkhali Transit station. So considering the flow conservancy, the FDC method is the best for estimation of environmental flow requirement of a river. Again the EFR of LFS, IFS and HFS can be estimated in FDC method which is absent in MAF and CY methods.

REFERENCES

BWDB (2017). Bangladesh water development board, yearly data, Ministry of Water Resources, Govt. of the Peoples Republic of Bangladesh.

IHA (2009) The Nature Conservancy, 2009. Indicators of Hydrologic Alteration Version 7.1User's Manual.

Islam SN, Gnauck A (2011). Water shortage in the gorai river basin and damage of mangrove wetland ecosystems in sundarbans, Bangladesh. 3rd International Conference on Water & Flood Management (ICWFM-2011), Dhaka, Bangladesh.

Mullick RA, Babel MS, Perret SR (2010). Flow characteristics and environmental flow requirements for the Teesta River, Bangladesh, Proceedings of international conference on environmental aspects of Bangladesh (ICEAB10), Japan.

Moly, SQ, Mirza ATM R, Saadat AHM (2015). Environmental Flow Characteristics of the Gorai River Bangladesh, International Journal of Scientic Research in Environmental Sciences, 3(6), 208-218.

Richter BD, Baumgartner JV, Wigington R, Braun DP (1997). How much water does a river need? Freshwater Biology, 37: 231-249.

Proceedings of the 5th International Conference on Civil Engineering for Sustainable Development (ICCESD 2020), 7~9 February 2020, KUET, Khulna, Bangladesh (ISBN-978-984-34-8764-3)

PERFORMANCE OF GEO BAG AND CEMENT CONCRETE BLOCK TO PROTECT RIGHT BANK OF PADMA RIVER AT SHARIATPUR DISTRICT

Kazi Furkan Hossain*[1] and Md. Jahir Uddin[2]

[1]M.Sc. Student, Department of Civil Engineering, Khulna University of Engineering & Technology, email: kazifurkance@gmail.com
[2]Professor, Department of Civil Engineering, Khulna University of Engineering & Technology, email: jahiruddin@ce.kuet.ac.bd

***Corresponding Author**

ABSTRACT

River Bank erosion is an acute problem for Bangladesh which intensity rising day by day. A remarkable amount of riverside land is being eroded during the monsoon period for which many people eradicated, destitute and finally affecting on socio economic sides of Bangladesh. Bangladesh water development Board (BWDB) funding a huge amount of money to prevent river erosion works under different places of Bangladesh but there is no remarkable change till now. This research aimed to effectiveness comparison of geo bag and cement concrete (CC) blocks in the river protection works. Geo bag and CC Block area were visited and mentionable information have been collected from the office of the engineers of BWDB and local people regarding the geo bag dumping, CC block dumping and Placing. Finally collected estimated cost of identified area and images of different places of river bank protection works. Based on field data and collecting information analyzed which collect from BWDB engineers and local people. In this research observed geo bag use shows the positives and negative effects on bank erosion and found main causes of failure of geo bag. Mentionable that CC Block much better from geo bag to protect the river bank protection works.

Keywords: *River Bank, Erosion, Protection, CC Block & Geo bag.*

1. INRODUCTION

Rivers in Bangladesh are morphologically very dynamic. Erosion process are highly unpredictable and unexpected so that a huge amount of agricultural land losses of Bangladesh. Bank erosion has been an acute problem in Bangladesh. It is also a great signal to the people especially who are living in the coastal and vulnerable area. Around 10,000 of hectares land are eroded by river per year in Bangladesh and about one million people are being affected From 1989 to 1992 the maximum erosion rate of the river Jamuna was 21km^2 per year and also found average rate 13.51 sq. km per year during 1980 to 1989 (Oberhagemann & Hossain 2011, ISSN 2349-4476).Thus a huge amount of properties losses of Bangladesh which effect on Bangladesh economic structure. However, complex flow, sediment transport, channel geometry, longitudinal slope, groundwater level, characteristics of bed and bank materials, seepage characteristics, natural and manmade interface in the river bed are main issues for river bank erosion. Generally Bank erosion damages a lot of agricultural lands resulting in flooding and other socio-economic problems in the country. Those people who are affected by river bank erosion take shelter another slum area in cities (Uddin & Basak, 2012).

Bank erosion assessment is the prime objective prior to take sustainable protective measures against erosion. It is the vital source of sediment deposited at the downstream backwater areas. The erosion process is very active in the Padma River, especially during the pre and post monsoon period and during flooding time. Every year large croplands and numerous habitation and infrastructure experience erosion. Studies find that an increase of 10 percent maximum discharge of the Padma river generates approximately 25 percent increase in riverbank erosion (Islam, M. & Islam, A. 1985). The Padma River is a multi-channel braided river system that frequently develops sand bars and changes in river flow direction. Geographic Information Systems (GIS) and Remote Sensing (RS) are essential tools for detecting changes along coastlines and river bank erosion. The cost of the river bank protection along the Padma river is very expensive.

The Bangladesh Water Development Board (BWDB) has been tried to protect the river bank with its limited resources. Since the early 1970, Bank protection works in the Padma river have been practiced civil engineering techniques by using concrete or geo bag filling protections. Whereas these techniques proved to be resistant to the flow shear stress in many situations, they are often oversized especially in mountainous streams and reduce considerably the ecological values of the protected bank. BWDB, whose one of the important responsibility is to arrest bank erosion throughout the country. The organization has implemented a number of river training and bank protection projects on the Padma river(Cavaillé et al. 2013, 2015). Through the migration due river bank erosions people are losing their social bonding as well as their economic sources becoming impoverished and vulnerable day by day (Chatterjee & Mistri, 2013). Most of the people of India has migrated due to bank erosion of river (Iqbal, 2010; Islam, 2016). Many river training institute of Bangladesh to solve the river bank erosion problems. At present popularity of CC block to protect river erosion increasing day by day. The cement concrete (CC) blocks and sand filled geo bag are used since 1994 as a low cost effective..

2. STUDY AREA

The study area is the right bank of padma river of Janjira and Noria Upazila under Sharitpur district which one of the most vulnerable regions of Bangladesh in terms of riverbank erosion. The Padma river along the Janjira and Noria Upazila has been suffering from river bank erosion since long time. The research was conducted in the definite Location at Noria and Janjira Upazila of Shariatpur District. The Bangladesh Water Development Board (BWDB) was taken a necessary steps to protect the right bank of Padma river.

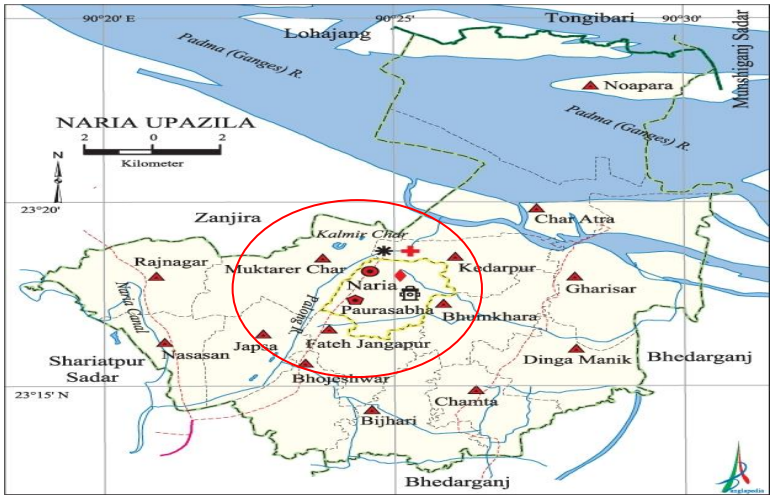

Figure 1: Location Map of Noria & Janjira Upazila, Shariatpur district, Bangladesh

3. METHODOLOGY

This research was carried out using on the field survey, interviews of local Engineering division of BWDB and some local people were involved during the construction and maintenance of bank erosion works. Some working sites were visited to collect the information about processing, preparation, transportation, placing and dumping of geo-bag and concrete blocks. The volume and covering surface area of geo-bags and CC blocks have been calculated in terms of cost.

Figure 2: Primary stage of Geo Bag Filling Mulfatganj, Shariatpur district (10 March 2000)

Figure 3: Final settlement of Geo Bag Filling Chandipur, Shariatpur district (05 March 2001)

In the figure 2 & 3 it is shown that the Initial and Final position of geo bag. The position of geo bag have been changed due to wave action of water. Sometimes geo bag damages due to environmental effect.

Figure 4: Primary stage of CC Block, Shuressor, Shariatpur District (15 Novemeber 2000)

Figure 5: Final stage of CC Block, Shuressor, Shariatpur District (15 Novemeber 2006)

In the figure 4 & 5 it is shown that the Initial and Final position of CC block. Although the cost of manufacturing and installing CC blocks is high, it will yield good results in the long run. So it can be said that CC block is better than geo bag in terms of longevity as a bank protective materials.

4. RESULTS AND DISCUSSIONS

Based on field surveys, image analysis and interviews, this survey found some positive and negative aspects of both bank security materials and their suitability in certain cases. Also, there is no change for the physical damage to the cement concrete block, the washing and the separate settlement such as geo-bags, but CC blocks are not suitable for emergency dumping. Geo bags filling is very effective for emergency dumping. Cement concrete blocks are used to protect the river banks as they have a higher resistance against scouring or bank erosion process. Sometimes CC blocks has been used like groin or spur are formed as a volumetric structure with a higher surface resistance using and geo-bags to divert the flow direction in order to save the valuable area of the downstream area. On the basis of surface area covering, uses of comparatively smaller sized CC blocks will be more economical than their counterparts. Geo-bags get set physically damaged within few days if they are dumped in the open air where solar radiation can hit them directly.

If sand filled geo-bags are dumped only under the water or they are covered with sand after placing in the river banks then they may last for 10 to 50 years whereas they may not sustain more than two years if they are dumped in the open air or partially in the air and water. In our country geo bag dumping in the sun and monsoon is very regular practice. In dry periods when the water levels in the rivers drop down, geo-bags get exposed to the open air though it was placed under the water during monsoon. Also covering the geo-bags with sand after placing in the field level is not feasible which leads to reduced life span of geo-bags.

If it can be ensured that geo-bags are protected from the solar radiation or dumped only under water, geo-bags are likely to turn out much better than CC blocks in all respects. On the other hand, CC blocks can hold out much longer time than the sand filled geo-bags and geo bags are displaced by heavy wave actions due to own self weight. CC Blocks are very expensive but its longevity is very

high compare to geo bag. However, this study did not deal with bank erosion processes and the interaction of geo-bags or CC block with the flowing streams along the banks.

Table 1: Physical properties and cost of CC blocks (Source- BWDB, Shariatpur, Site Office-2006).

Size (in cm^3)	Volume (m^3)	Coverage Area (m^2)	Mixing Ratio	Manufacturing Cost (BDT)	Average Dumping Cost (BDT)	Total Cost (BDT)
50X50X50	0.125	0.250	1:3:6	1200.27	164.92	1365..19
45X45X45	0.091	0.202	1:3:6	1175.25	155.36	1330.61
40X40X40	0.064	0.160	1:3:6	1155.25	148.25	1303.50

Table 2: Physical properties and cost of geo-bags (Source-BWDB, Shariatpur, Site Office- 2006)

Weight (KG)	Volume (m^3)	Coverage Area (mm^2)	Thickness (mm)	Manufacture Cost (BDT)	Filling cost (BDT)	Average Dumping Cost (BDT)	Total Cost (BDT)
275	0.1825	1325x1050	3	450.75	125.00	40.00	615.75
250	0.166	1200X950	3	435.55	123.30	38.00	596.55
175	0.116	1075X850	3	395.45	118.00	35.00	548.45

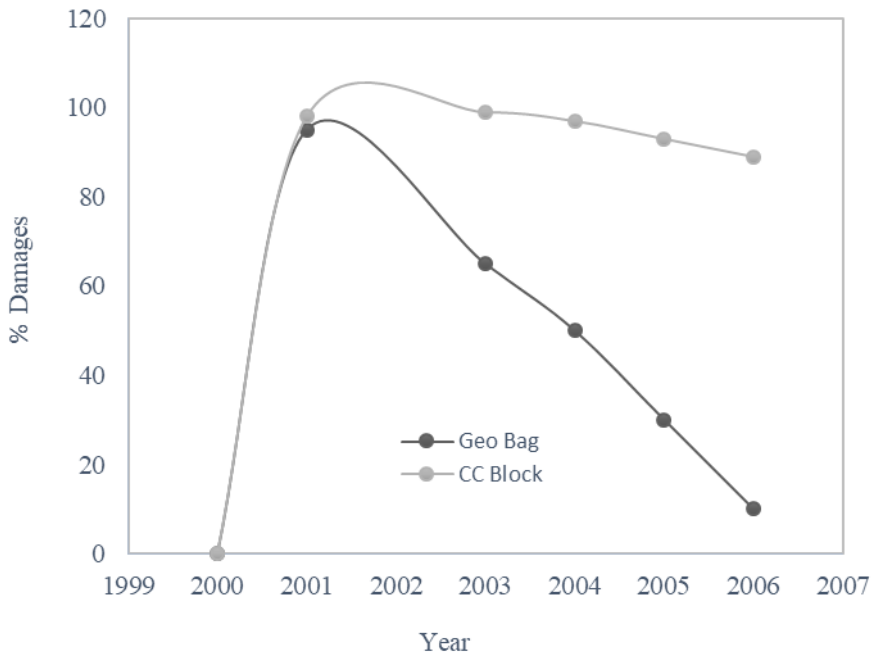

Figure 6: Percentage damages of CC block and Geo bag

Figure 6 presents that the performance of CC Block and geo bag varies over time. It gives effective results for protecting riverbank protection works. One of the main benefits of concrete blocks is its longevity. Concrete blocks are infected with high pressure and vibration, which makes the blocks very strong and able to withstand high levels of load. Concrete blocks are easy to install due to their uniform size and shape. Concrete blocks are very environmentally friendly.

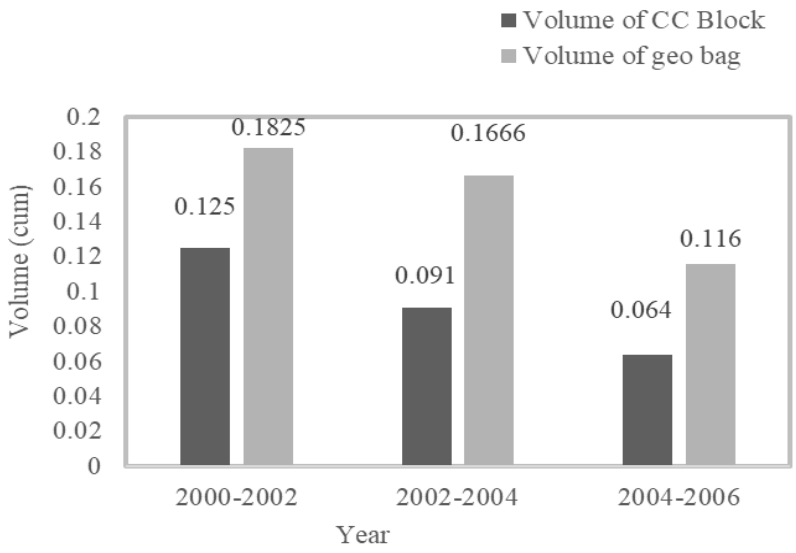

Figure 7: Volume of Geo bag and CC block

In the figure 7 shows that the comparison between volume of geo bags and CC block.

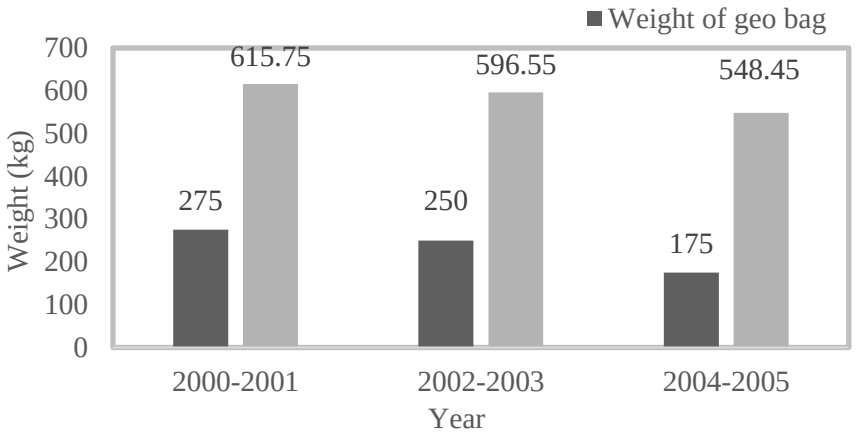

Figure 8: Weight of Geo bag

In the figure 8 it is shown that the changing condition of geo bag and CC block with rate.

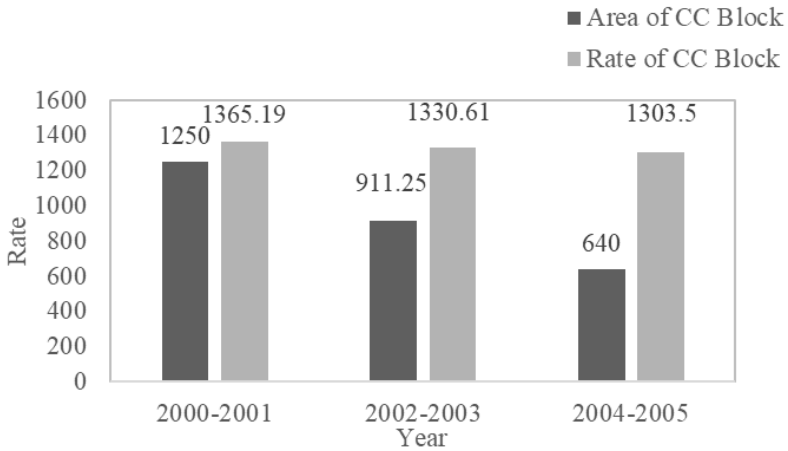

Figure 9: Rate of CC block

In the figure 9 it is shown that the rate of CC block depends on its size. Although the CC block rate is very high, it gives a good and effective result for defending bank security operations. Concrete blocks popularity as a bank protective materials increasing day by day.

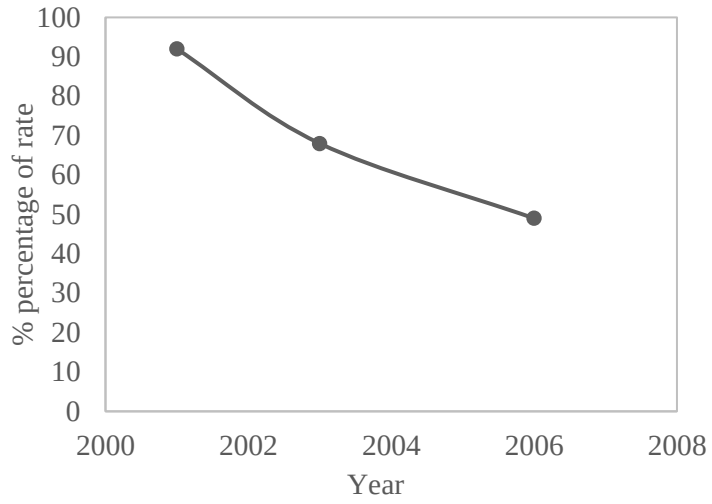

Figure 10: Percentage rate of Geo bag

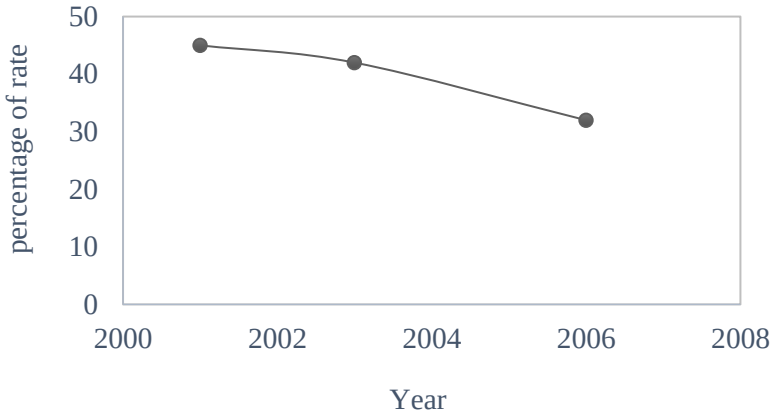

Figure 11: Percentage rate of CC block

In the figure 10 & 11 it is shown that the percentage rate of geo bag and CC block. CC block has been considered as the longevity of most of Bangladesh's projects related to riverbank security.

5. CONSLUSIONS

The main object of this research was to compare the performance between geo bag and cement concrete blocks as a protective-materials. Geo bag and CC Block both are well experienced protective materials but geo bag is effective only for short term or emergency purpose. On the other hand CC blocks is very effective and well balanced for long life.

ACKNOWLEDGEMENTS

The authors would like to give very special thanks to the related representative of BWDB along with their different site offices for providing necessary information, related images of site and supplying documents. The authors also appreciate to the local people for giving the necessary information about different failure modes of both bank protection materials.

REFERENCE

Chatterjee, S., &Mistri, B. (2013). Impact of river bank erosion on human life: a case study in Shantipur Block, Nadia District, West Bengal. International Journal of Humanities and Social Science Invention, 2(8), 108-111.

Cavaillé, P.; Dommanget, F.; Daumergue, N.; Loucougaray, G.; Spiegelberger, T.; Tabacchi, E. &Evette, A. Biodiversity assessment following a naturality gradient of riverbank protection structures
in French prealps rivers Ecological Engineering, Elsevier BV, 2013, 53, 23-30

Cavaillé, P.; Ducasse, L.; Breton, V.; Dommanget, F.; Tabacchi, E. &Evette, A. Functional and taxonomic plant diversity for riverbank protection works: Bioengineering techniques close to natural banks and beyond hard engineering Journal of Environmental Management, Elsevier BV, 2015, 151, 65-75

International Journal of Engineering Technology, Management and Applied Sciences
www.ijetmas.com December 2016, Volume 4, Issue 12, ISSN 2349-4476

Islam, A. R. M. T. (2016). Assessment of fluvial channel dynamics of Padma River in Northwestern Bangladesh. *Universal Journal of Geoscience*, *4*(2), 41-49.

Iqbal, S. (2010). Flood and erosion induced population displacements: a socio-economic case study in theGangetic riverine tract at Malda District, West Bengal, India. Journal of Human Ecology, 30(3), 201-211.

Islam, M. and Islam, A. (1985) A Brief Account of Bank Erosion, Model Studies and Bank Protective Works in Bangladesh. REIS Newsletter,2, 11-13

Nath, B. Naznin, S.N. and Paul, A. (2013) Trends Analysis of River Bank Erosion at Chandpur, Bangladesh: A Remote Sensing and GIS Approach. International Journal of Geomatics and Geosciences, 3,454-463.

Oberhagemann, K., & Hossain, M. M. (2011). Geotextile bag revetments for large rivers in Bangladesh.
Geotextiles and Geomembranes, 29(4), 402-414.

Uddin, A. F. M. A., &Basak, J. K. (2012). Effects of riverbank erosion on livelihood. Unnayan Onneshan-The Innovators: Dhaka, Bangladesh.

Proceedings of the 5th International Conference on Civil Engineering for Sustainable Development (ICCESD2020), 7~9 February 2020, KUET, Khulna, Bangladesh (ISBN-978-984-34-8764-3)

SALINITY MODELING OF KOBADAK- SIBSA RIVER SYSTEM BY HEC-RAS

Akramul Haque*[1] and K.M. Ahtesham Hossain[2]

[1]M.Sc Engineering Student, Dept. of Water Resources Engineering, Bangladesh University of Engineering and Technology, Dhaka-1000, Bangladesh, Email: akramul109183@gmail.com
[2]Assistant professor, Dept. of Water Resources Engineering, Bangladesh University of Engineering and Technology, Dhaka-1000, Bangladesh, Email: ahtesham@wre.buet.ac.bd

***Corresponding Author**

ABSTRACT

Salinity intrusion is a major problem and is found increasing day-by-day in the south-western parts of Bangladesh. Due to the commission of Farakka Barrage on the Ganges river in 1975 and siltation of the Gorai River mouth, flow has been drastically reduced in the downstream of South-West region. Salinity intrusion on the areas near the tidal rivers create severe problem in agriculture and drinking water source. This study focuses on 1-D salinity modeling of the Kobadak-Sibsa River by HEC-RAS. Work is carried out in simulation of salinity concentration in different location which helps to identify which location exceed water drinking limit 1000 ppm and agricultural water limit 1500 ppm . The hydrodynamic model is calibrated using the data of June,2016 . Then this model is validated using the data of July, 2015.Model simulated tidal range showed good agreement with the observed values for Manning's roughness coefficient as 0.021.Once the hydrodynamic model is calibrated and validated, the salinity model is performed and calibrated for the year 2016 for different dispersion coefficient (D) for different reaches as tuning parameter. It has been found that for Kobadak upstream D=25 m^2/s, downstream D=780 m^2/s, Paikgacha D=2000 m^2/s, Sibsa upstream D=300 m^2/s and downstream D=9000 m^2/s which showed good agreement between simulated and observed salinity data. It has been found that from the month of December salinity gradually increases and reaches it's peak in April or May. Maximum salinity concentration is found in different location such as in Jhikargacha 130 ppm, Tala Magura 325 ppm ,Godaipur 4600 ppm, Paikgacha 7600 ppm ,Bishnipur 8600 ppm,Sutarkhali 12200 ppm, Nalian 12450 ppm. Also, this study focuses on statistical analysis of salinity and water level over the year of 2000-2017.

Keywords: *Hydro-dynamic modelling , Salinity, Kobadak-Sibsa, Statistical analysis, HEC-RAS.*

1. INTRODUCTION

Bangladesh is riverine country and was formed by deltaic deposits of the Ganges-Brahmaputra-Meghna. Due to the commission of Farakka Barrage on the Ganges river in 1975 and carrying large amount of silt and human intervention such as construction of bridge, abstractions for agriculture, drainage return flows, structures for flood control causes the natural flow of Kobadak-Sibsa river has been drastically reduced and altered (Azbina,2014).In at last twenty years, flow volume in the dry-season (December – April) has been declining. So, surface salinity in downstream of Kobadak and Sibsa river begin to increase rapidly from December and reaches the peak in late March or early April. It has a serious environmental impact: specially along the coastal areas around the sanctuary forests where the salty water has increasingly been intruding(saran,2017). In the recent years, groundwater based water supply in coastal area is suffering from a number of major problems mainly arsenic contamination, lowering of the water table, salinity and non-availability of suitable aquifers(PDO-ICZMP, 2004).The Mathabhanga River is one of the most important distributaries of the Ganges River. The Kobadak River originates from the Mathabangha at Alamdanga, Chuadanga and falls into the Sibsa at Paikgacha, Khulna. The morphology of the Kobadak is governed by sedimentation process and the human induced influences.Over times, the river has lost its drainage capacity.Now overbank spillage is a common phenomenon during each peak monsoon. Consequently, the entire catchment becomes water logged during the monsoon (Mehzabin, S., 2015). The recent 262-crore Kobadak River dredging project will allow to lead a comfortable life along the banks of the river as there will be no water-logging in their areas and more fresh water will flow through Kobadak-Sibsa river.

SWR is composed of 15 sections, occupying 17 % of the suburban areas of Bangladesh. The land's 62 % is farmland, its 15 % is covered with mangrove forests (Sundarbans), and its 13% is water areas (Mehzabin, S.,2015). Sundri top dying disease will occur if salinity exceeds 15000 ppm, water becomes less useful as salinity increases to 1000 ppm(WHO,2011), irrigation water becomes undoubtful if salinity exceeds 1500 ppm (Ayers &Westcot, 1985).So in upstream of the river there requires a minimum flow which prevents excess salinity intrusion.The specific objective of this study are-

1. To setup hydrodynamic model of Kobadak-Sibsa river system using HEC-RAS and its calibration, validation and simulation.
2. To setup of water quality model and performing a water quality calibration and simulation of Kobadak-Sibsa river system using HEC-RAS.
3. Simulation of salinity concentration at different locations of study area using HEC-RAS.
4. Trend analysis of salinity and water level over the year of 2000-2017.

1.1 Study area

For the present study, Kobadak-Sibsa river is chosen due to it is the most important source of fresh water supply in the downstream in South West region and recently completion of Kobadak dredging project will allow the researchers to contribute to restore the environmental flow and prevent salinity intrusion.Figure 1-1(https://www.google.com/earth/) shows study area which was conducted on the 130km of Kobadak-Sibsa River stretching between the Jhikargacha river station in the upstream and the Sibsa River in the downstream named Nalianala Hadda river station.The average width of Kobadak river is 400 m including its floodplain. Kobadak River flows in the southern periphery and meets Sibsa near Jhikargacha and important source of Sibsa river. The average width of Sibsariver is 1250 km and is about 100 km long.The river forms much of the boundary between Paikgachha and Dacopeupazila. Inside the Sundarbans Reserve Forest, it meets the Passur River, then separates again near Mongla, before reaching the Bay of Bengal (Wikipedia).

`

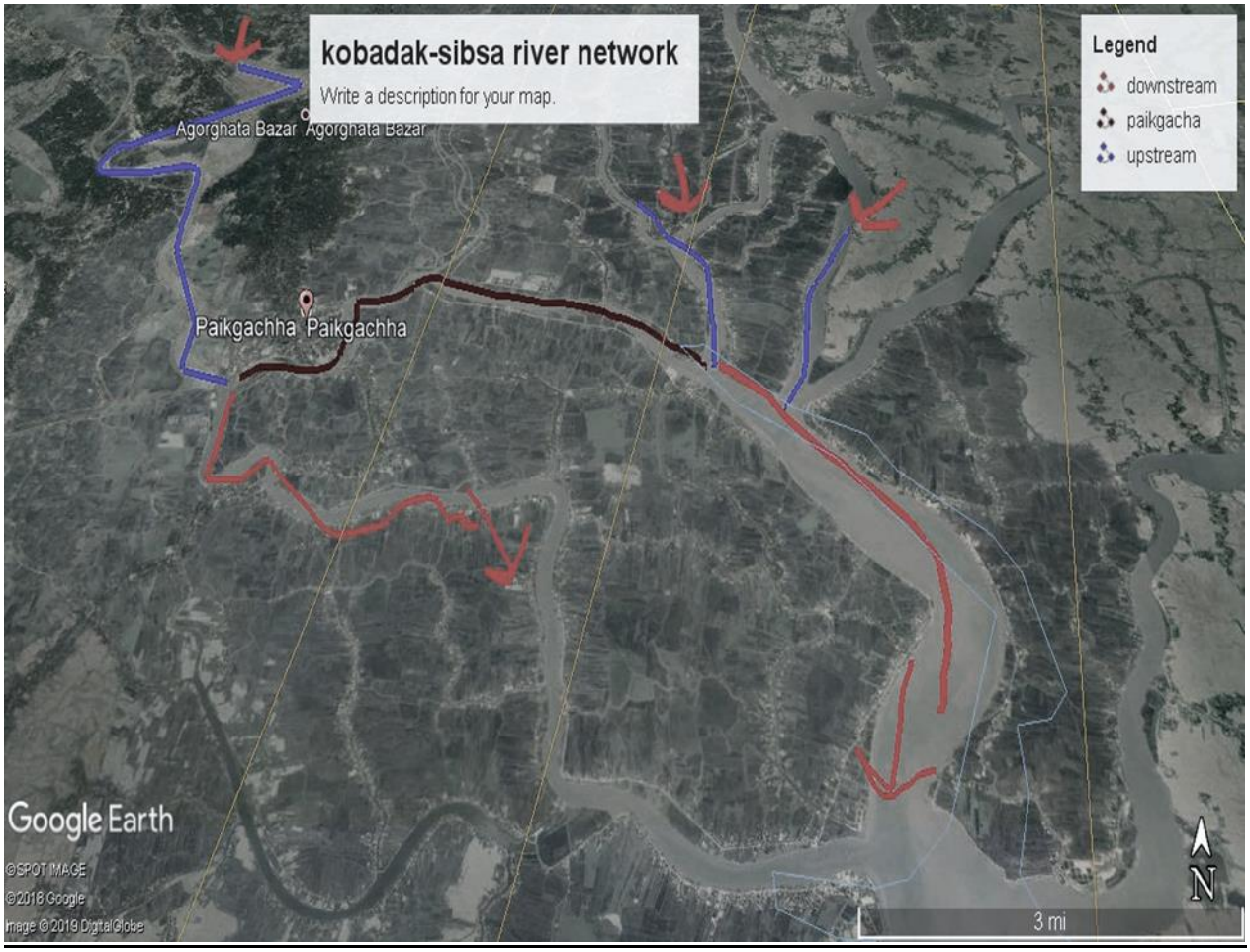

Figure 1-1: Kobadak-sibsa full network

2. METHODOLOGY

2.1 Data collection

For the development of hydrodynamic and salinity model of Kobadak-Sibsa River, data of bathymetry,discharge,stage hydrograph and salinity concentration at different stations have been collected from relevant sources which are shown in Table 1-1.30 cross section data (19 of Kobadak,6 of Passur river and other 5 are interpolated) of Rupsha-Passur river were collected.

Table 1-1: Data collection

Data type	Source	Data location	Period
Bathymetry	BWDB	Kobadak-Sibsa	2000-2017
Discharge	BWDB	Jhikargacha	2015,2016
Water level	BWDB	SW-162-164,258-259	2000-2017
Salinity	BWDB	SW-162,258,259	2000-2017

2.2 Model setup

Two steps are involved in HEC-RAS modelling:

- Hydrodynamic modelling
- Water quality analysis

`

In hydro-dynamic model setup, flow hydrograph of Jhikargacha SW-162 and stage hydrographSW-258, 242 for another upstream branch have been inserted as upstream boundary condition. For downstream branch, two stage hydrograph SW-259,164 have been inserted as downstream boundary condition. Data for January 2016 to December 2016 are used. SW-29 stage hydrograph is used for calibration and validation for the month of June, 2016 and July, 2015 respectively.

In water quality analysis, arbitrary constituent was selected as Water Quality constituents. Tracer was mentioned as conservative. Minimum cell Length was given 200. Salinity concentration data for upstream branch and downstream branch river have been inserted as boundary condition. No branch is neglected asupstream flow is very important for salinity analysis. Paikgacha station is used for calibration of salinity graph for January 2016 to December 2016.

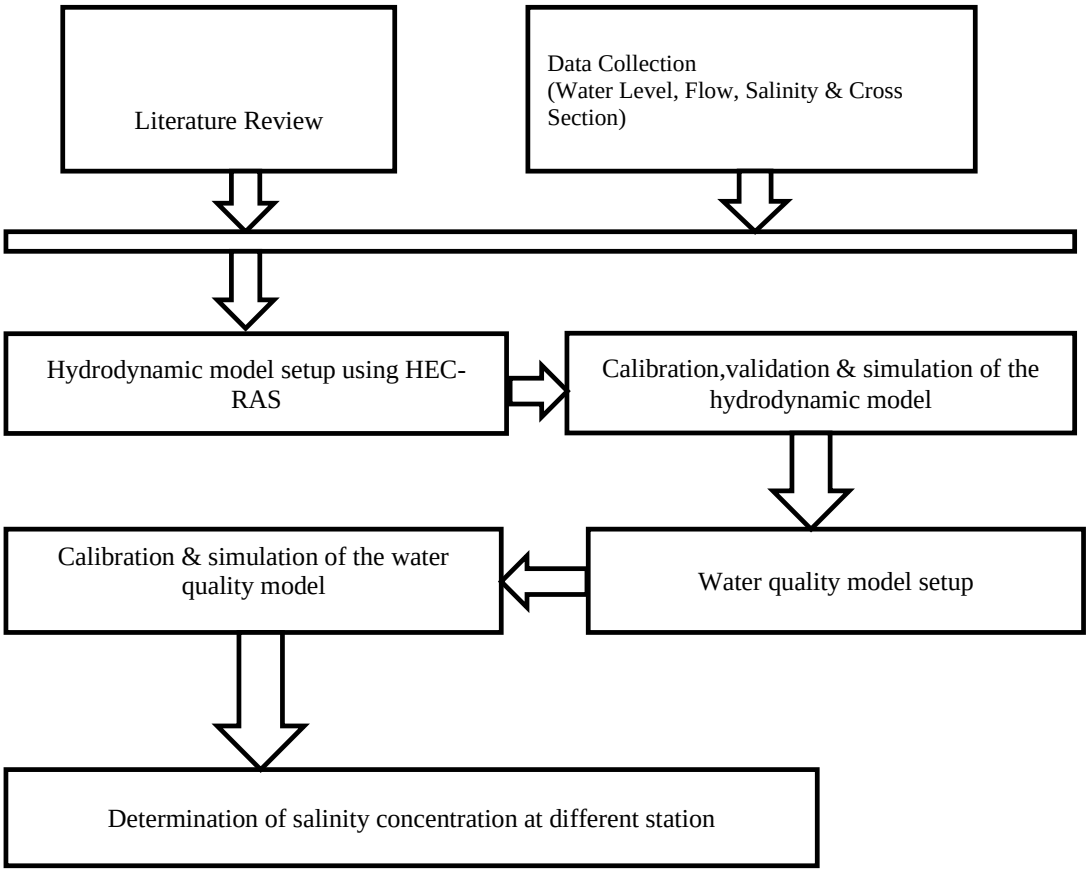

Figure 2-1: Diagram of methodology

3. DATA ANALYSIS AND RESULTS

3.1 Calibration and Validation of Hydrodynamic and Salinity Model

The hydrodynamic model is calibrated using the data of June,2016 (Figure 3-1). Then this model is validated using the data of July, 2015(Figure 3-2).Model simulated tidal range showed good agreement with the observed values for Manning's roughness coefficient as 0.021.Once the hydrodynamic model is calibrated and validated, the salinity model is performed and calibrated for the year 2016 for different dispersion,the coefficient (D) for different reaches as tuning parameter. It has been found that for Kobadak upstream dispersion co-efficient D=25 m^2/s,Kobadak river downstream D=780 m^2/s, Paikgacha D=2000 m^2/s, Sibsa upstream D=300 m^2/s and downstream D=9000 m^2/s which are shown in Table 3-1.

`

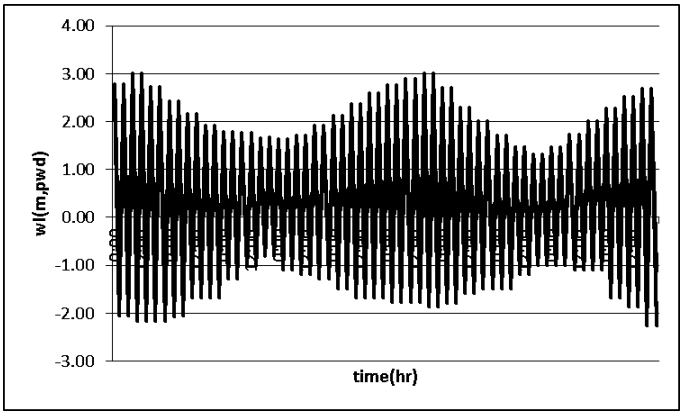

Figure 3-1: Calibration graph for n=0.021 (June 2016, SW-29, Sutarkhali Forest Office)

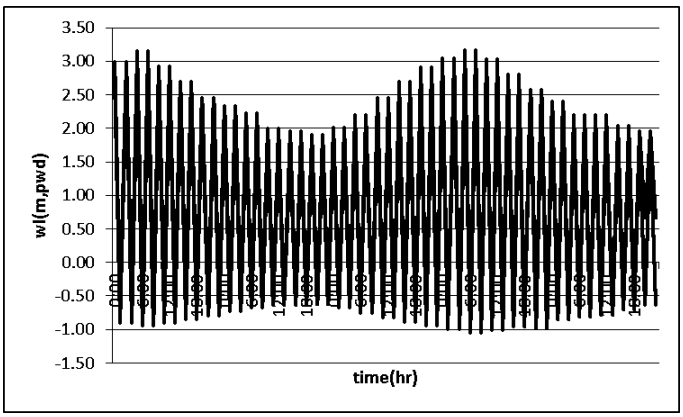

Fig 3-2: Validation stage hydrograph for n=0.021 (July,2015, Sutarkhali Forest Office)

The salinity concentration value of the River is determined by Water Quality Analysis through HEC-RAS. The salinity concentration differs with the advection dispersion coefficient used in the model. For the reach Paikgacha (station no:39), the salinity concentration value determined from model is compared to the original salinity concentration value of the Paikgacha SW-258.

Salinity concentration is given and computed in mg/L. Unit of the dispersion coefficient is in m^2/s. Calibration is done for January 2016 to December 2016 which is shown in Figure 3-3. The maximum possible value of dispersion coefficient is determined through analysis.

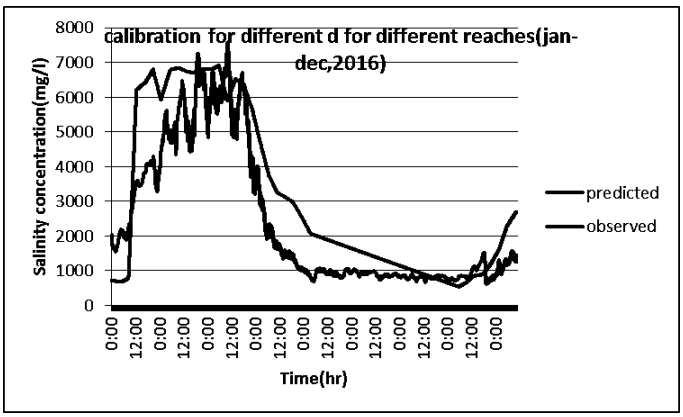

Figure 3-3: Salinity concentration graph for different d at SW-258(paikgacha)

`

Table 3-1: Fixed dispersion at different reaches

River	Reach	RS	Fixed dispersion(m^2/s)
Kobadak-Sibsa	Paikgacha	40	2000
Kobadak	Upstream	60	25
Kobadak	Downstream	30	780
Sibsa	Upstream	52.5	300
Sibsa	Intermediate	39	548
Sibsa	Upstream	70	105
Sibsa	Downstream	5	9000

Table 3-1 provides the dispersion co-efficient used for different reaches.So when considering main channel with branches it will be better to use different co-efficient value for different reach because dispersion co-efficient depends on velocity,top width,frictional slope,shear velocity,depth of the channel.

3.2 simulation of salinity concentration at different locations

It has been found that from the month of December salinity gradually increases and reaches its peak in April or May.Maximum salinity concentration is found in different location such as in Jhikargacha 130 ppm,TalaMagura 325 ppm,Godaipur 4600 ppm, Paikgacha 7600 ppm ,Bishnipur 8600 ppm,Sutarkhali 12200 ppm, Nalian 12450 ppm.

Figure 3-4 is for Agorghata where salinity concentration does not measure.It indicates that the maximum salinity is 1700 mg/l which occurs in the month of mid- April.As this location locates far upstream of Paikgacha the salinity concentration is in satisfactory range for agricultural and water drinking use.

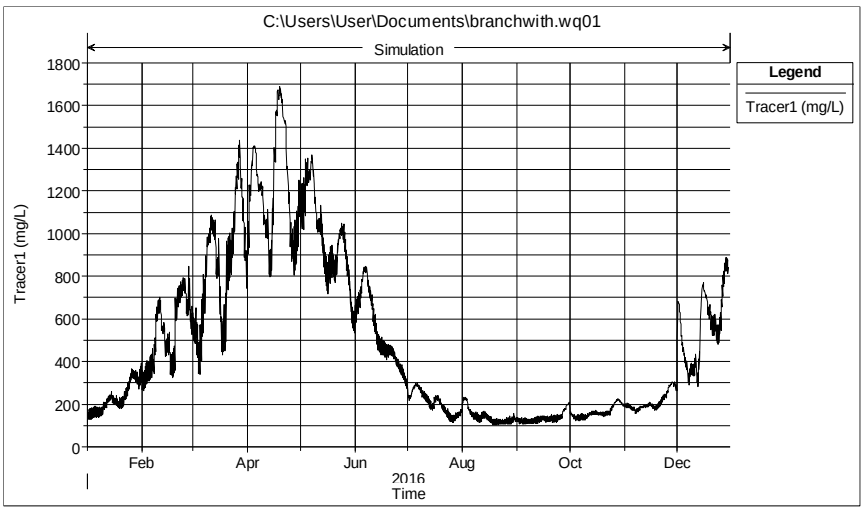

Figure 3-4: Salinity graph at Agorghata

At Godaipur, in figure 3-5, It indicates that the maximum salinity is 4600 mg/l which occurs in the month of mid-April. As this location locates near upstream of Paikgachaand low flow from upstream, the salinity concentration is not in good range for agricultural and water drinking use. The fluctuation of concentration is also very high.

`

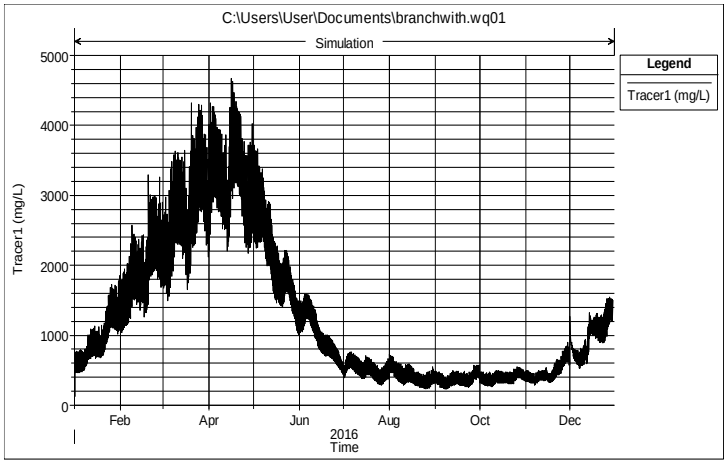

Figure 3-5 : Salinity graph at Godaipur

The figure 3-6 is for Paikgacha. It shows that the maximum salinity is 7600 mg/l which occurs in the month of mid -April.As this location locates near the tidal river name Sibsa the salinity concentration is very high .

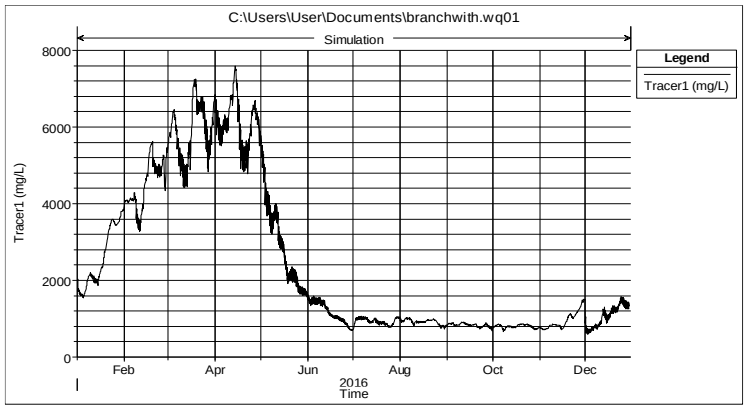

Figure 3-6 : Salinity graph at Paikgacha

The figure 3-7 and 3-8 is for Bishnipur and Sutarkhali respectively. That shows that the maximum salinity is 8600 mg/l and 12400 mg/l which occurs in the month of March.As those location locate in the tidal river the salinity concentration is usually very high.

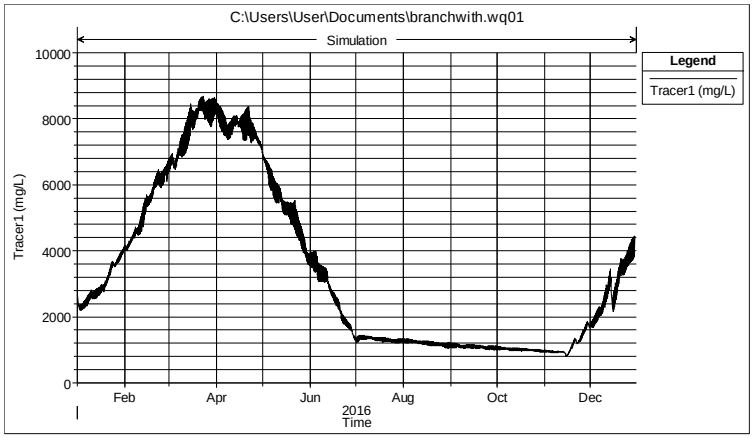

Figure 3-7 :Salinity graph at Bishnipur

`

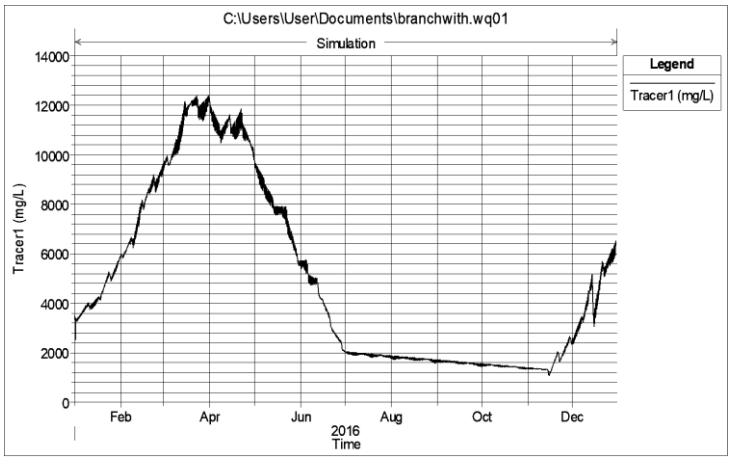

Figure 3-8 : Salinity graph at Sutarkhali

3.3 Statistical analysis

Salinity: graphs showing the variation of salinity and water level over the last 18 years:

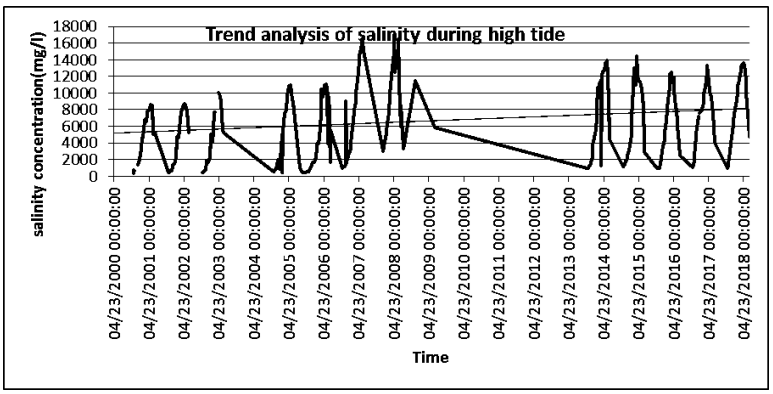

Figure 3-9 : Salinity variation during high tide at Nailina Hadda(SW-259)

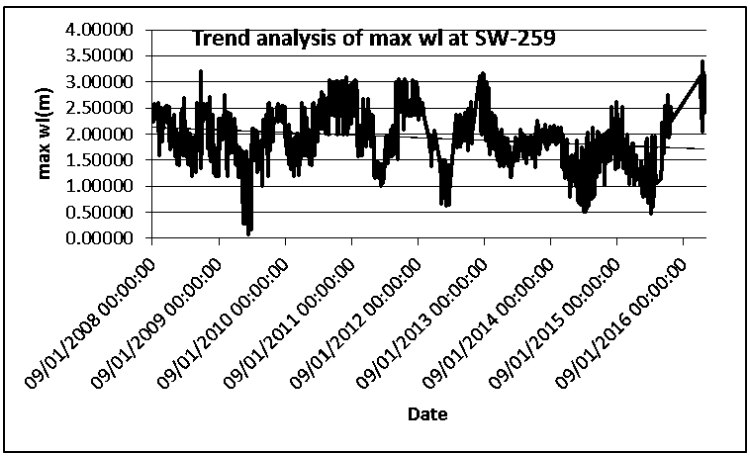

Figure 3-10: Max wl (m) variation over the year at Nailina Hadda (SW-259)

From above, we can say that there is relationship between water level and salinity. With decreasing water level salinity increases and vice-versa.

`

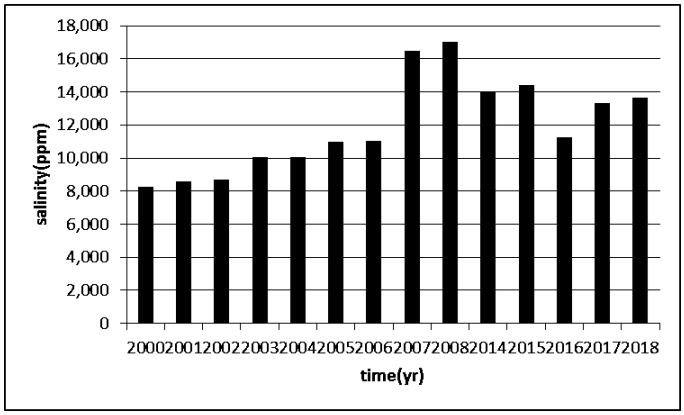

Figure 3-11:Maximum yearly salinity variation at Nailina_hadda(SW-259)

From above bar chart (Figure 3-11), we conclude that with the time salinity is increasing.But we see that in 2007 and 2008 the salinity is so high compare to other year.This is because 2007 tropical cyclone SIDR.

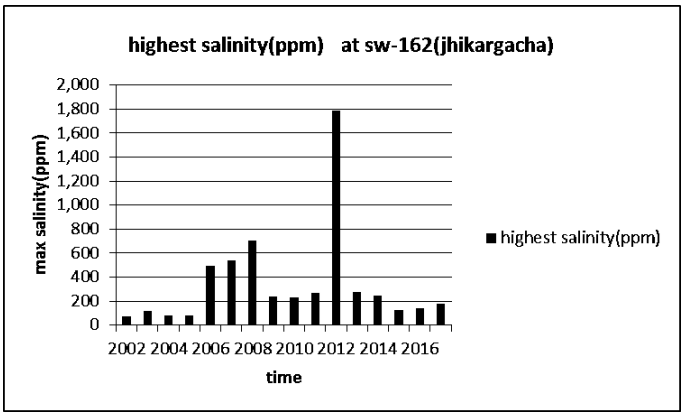

Figure 3-12:Maximum yearly salinity variation over at Jhikargacha (SW-258)

At Jhikargacha though salinity increases in 2007 at the time of SIDR but in 2012 the salinity concentration is higher than any other year because of low upstream flow in that year which is shown in Figure 3-12.

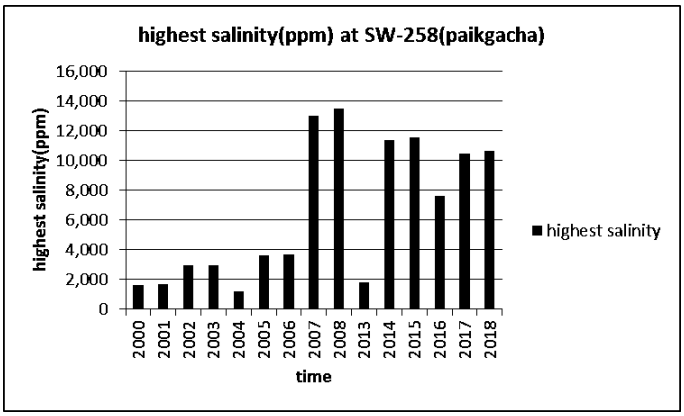

Figure 3-13: Yearly maximum salinity variation at Paikgacha(SW-258) from the year 2000 to 2016

At Paikgacha, in figure 3-13, the highest salinity occur at the time 2007-2008 because of SIDR.But we see that after 2013 the salinity was drastically increased compare to 2000-2006.

`

4.CONCLUSIONS

In this study, an attempt was made to analyze salanity concentration at different location and statistical analysis of variables:

- The hydrodynamic model is calibrated using the data of June , 2016 . Regression analysis is carried out and co-relation (R^2) is found 0.956. Then this model is validated using the data of July, 2015.Model simulated tidal range showed good agreement with the observed values for Manning's roughness coefficient as 0.021 and R^2 is found 0.9652 .Once the hydrodynamic model is calibrated and validated, the salinity model is performed and calibrated for the year 2016 for different dispersion coefficient (D) for different reaches as tuning parameter. It has been found that for Kobadak upstream D=25 m^2/s, downstream D=780 m^2/s, Paikgacha D=2000 m^2/s, Sibsa upstream D=300 m^2/s and downstream D=9000 m^2/s which showed good agreement between simulated and observed salinity data and R^2 is found 0.856 .

- Usually the maximum salinity occurs in April and May, at the end of dry season, During December to May.Water is neither usable as a source of drinking water nor for irrigation nearly paikgacha and it's downstream as salinity concentration exceeds water drinking limit 1000 ppm and agricultural water limit 1500 ppm (WHO,2011).The salinity intrusion zone has increased and is more than any previous years. Salinity in Jhikargacha, Hazirbaagh, Ujjalpur, Bankra, Deara, Digdana, Mathshia, Chakla, Nowali remain in safe limit throughout the year.But it has been found that found that maximum salinity in Agorghata is 1600 ppm, in Godaipur is 4000ppm,in Paikgacha is 6500ppm and downstream of Paikgacha such as in Bishnipur is 8000ppm,in Sutarkhali is 12000ppm,in Nalian is 12500ppm for the year of 2016.
- From statistical analysis it is seen that salinity is increasing with decreasing water level.The maximum salinity occur in Paikgacha and Naliana are 12500 ppm and 16500 ppm in 2007-2008 due to SIDR.

REFERENCES

BWDB. (2011). Rivers of Bangladesh. Bangladesh Water Development Board,Ministry of Water Resources.

Boa,E.R, & Rahman,M.A. (2015). Sundri top dying symptoms and cause. Bangladesh Forest Research Institute.

Google Earth Engine. (n.d.). Retrieved April 20, 2019, from https://www.google.com/earth/

Jahid, S. (2016). Assessing environmental flow for the Kobadak River and developing a framework for its maintenance. M.Sc. Thesis,Institute of Water and Flood Mangement, Bangladesh University Engineering and Technology,Dhaka,Bangladesh.

Mehzabin, S. (2015). Trend Analysis of variables and Modeling of Flow and Salinity of the Gorai River using HEC-RAS model. B.Sc Thesis,Department of Water Resources Engineering,Bangldesh University Of Engineering and Technology,Dhaka,Bangladesh.

Pal1, A., Hossain1, M. Z., Hasan2, M. A., Molla1, S. R., & Asif3*, A. A. (2016). Disaster(SIDR) causes salinity intrusion in the south-western parts of Bangladesh. Asian-Australasian Journal of Bioscience and Biotechnology, 301-302.

PDO-ICZMP. (2004). Areas with special status in Coastal Zone. warpo.portal.gov.bd.

Rahman, M. A., & Dipa, S. J. (2016). A study on river system, hydrology and surface water salinity of sundarbans rivers. Proceedings of 3rd International Conference on Advances in Civil Engineering, 21-23 December 2016, CUET, Chittagong, Bangladesh , (pp. 824-825).

Rahman, M. Z. (2015). Modeling of the Surface Water Salinity in the Southwest Region of Bangladesh. M.Sc Thesis,Department Of Water Resources Engineering, Bangladesh University Engineering and Technology,Dhaka,Bangladesh.

saran, S. H. (2017). Modeling of Flow and salinity characteristics of the rupsha-passur river system. B.Sc Thesis,Department Of Water Resources Engineering, Bangladesh University Engineering and Technology,Dhaka,Bangladesh.

`

Westcot, & Ayers. (1985). Guidelines for interpretation of mater quality for irrigation. The Food and Agriculture Organization of the United Nations.

WHO. (2011). Guidelines for Drinking-water Quality. Retrieved February 2019, from https://apublica.org/wp-content/uploads/2014/03/Guidelines-OMS-2011.pdf

Wikipedia. (n.d.). Retrieved 2019, from https://en.wikipedia.org/wiki/Shibsa_River

`

Proceedings of the 5th International Conference on Civil Engineering for Sustainable Development (ICCESD 2020), 7~9 February 2020, KUET, Khulna, Bangladesh (ISBN-978-984-34-8764-3)

DISCHARGE, RAINFALL AND POLLUTION LOAD ON DHALESHWARI RIVER: A STUDY ON TREND ANALYSIS

Md. Abdul Momen*[1], Md. Ekram Uddin[2] and Mehedi Hasan[1]

[1]Department of Civil Engineering, Bangladesh University of Engineering and Technology (BUET), Bangladesh
[2]Institutet of Water and Flood Management, Bangladesh University of Engineering and Technology (BUET), Bangladesh, e-mail: abdulmomen2k13@gmail.com

***Corresponding Author**

ABSTRACT

River flows are changing when hydro-meteorological variables are changing, water resources are losing the natural discharge capacity from upper stream as well as increasing rate of pollution load. This study has been conducted to discharge, rainfall and pollution of the Dhaleshwari river at savar station. 21 years of rainfall and discharge data have been collected. The time period of discharge and rainfall is 1998 to 2018. Mann-Kendall test and sen's slope estimator has been conducted to determine trend. Annual trend of discharge is a decreasing trend. Summer and monsoon discharge are decreasing trend but winter discharge is increasing trend. Annual rainfall is upward trend. Summer rainfall is upward but monsoon and winter both are downward trends. Pearson coefficient of correlation has been used to find the relation between hydro-meteorological variables. The dependency of rainfall on discharge is very low. So there is no strong relationship between rainfall and discharge. According to findings, it seems the discharge condition of Dhaleshwari river is always changing and rainfall at Savar is also changing. P^H, TDS, Salinity, chloride as some pollution loading parameters were studied for several years thus results frequent discharge and improper industrialization at bank of Dhaleshwari river.

Keywords: *Rainfall, Discharge, Dhaleshwari river, Pollution load, Change.*

1. INTRODUCTION

Surface water is an essential element for natural and artificial environment which is carried by rivers and provides the life generating-fuel to civilizations (Islam & Sikder, 2017). River is a large stream that begins from mountain or lake. A large stream consists of many small streams. River generally receives water from rainfall, snowmelt, etc. The river is a large stream of water. If a country is considered a human body then water is the blood of body and river is vein (Ekram et al, 2018). Dhalesshori river is locate in savar. There are 2 stations has been selected for discharge and rainfall which are jagir and savar respectively. Dhaleshwari river is a distributary of Jamuna river. It starts off the Jamuna near the north-western tip off tangail district. It is a meandering river having two branches. The mainstream flows north of manikganj and joins the other branch, the Kaliganga, south of Manikganj. The Kaliganga again joins with the Dhaleshwari. Study about river discharge and rainfall are pertinent to know the river flow conditions, surface water flow, irrigation etc. One of the most important variables used for observing the hydrological cycle over the land surface is the flow of river. River discharge is powerful integrating tools and its monitoring can provide accurate and timely data to response of the land surface to atmospheric forces. It is also one of the accurately measured components of the hydrological cycle (Shiklomanov et al, 2006) and therefore can provide more estimates of water cycle trends and variability. Variability in rainfall characteristics (type, amount, frequency, intensity and duration) is among the important climate change impacts. Rainfall variability affects water resources sustainability which includes the availability, management, and utilization of water resources. This may inversely affect ecosystems, land productivity, agriculture, food security, water quantity and quality, and human health (EPA, 2014). Rainfall is an important variable that underlies both droughts and floods (Coscarelli and Caloiero, 2012). Annual discharge at jagir station is downward and rainfall at savar station is upward. Climatic variability and surface water situation are changing all over the world, Bangladesh is not isolated from this phenomenon. Four assessment report of (IPCC, 2007) showed that, long term trend analysis of precipitation from 1900 to 2005 found drier situation in southern Asia. In this study, Dhalesshori river has been considered as study area. Hydro-meteorological data considered as rainfall at Savar station and river discharge at jagir station. Rainfall and discharge data are conducted for this research. Trend is a General direction in which something is developing of changing. The purpose of trend testing is to determine if values of a random variable generally increase (or decrease) over same period of time in statistical terms (Helsel and Hirsch, 1992). Rainfall and discharge trend have been analyzed here. 21 years of rainfall and discharge data (1998 to 2018) has been considered. Relation between rainfall and discharge has been studied in this research. Annual and seasonal trend and relation have been studied here. Dependency of rainfall on discharge is very low. Trend, relation variability has been discussed in this study, not impacts on human or wildlife.

2. METHODOLOGY

Research methodology is a way to systematically solve the research problem (Kothari, 2004). It may be understood as a science of studying how research is done scientifically. Research methodology is a science of studying how research is done scientifically. In short, methodology is the study or description of methods (Baskervile, 1991).

2.1 Sampling location

Dhalesshori river at Dhaka district is the study area of this project. Because one discharge station and one rainfall station are situated in there. Discharge and rainfall station of jagir and savar respectively are situated in Dhaka district. Rainfall station located near the discharge station of jagir. Both two station are shown in the following map.

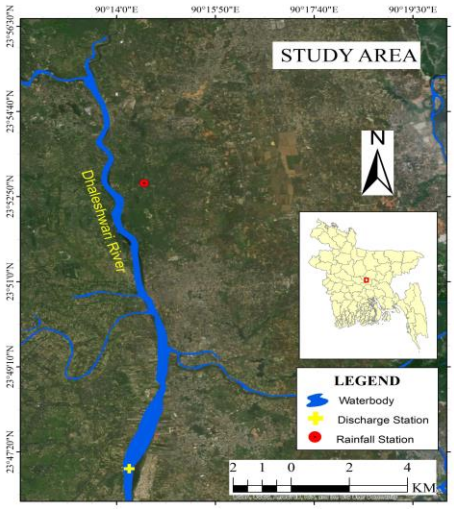

Fig 1: Sampling location

Daily time series data of streamflow or discharge at jagir (1998 to 2018). Total period of discharge data is 21 years at jagir station. In other hand, daily time series data of rainfall at Savar station have been analyzed. Discharge (from 1998 to 2018) of jagir station and rainfall (from 1998 to 2018) of Savar station have been collected from Flood Processing and Forecasting Circle (FPEC) of Bangladesh Water Development Board (BWDB).

2.2 Data processing

Processing implies editing, coding, classification and tabulation of collected data so that they are amenable to analysis (kothari, 2004). Collected discharge and rainfall data from NWRD was daily time series data. Discharge data purveyed for FPFC was observed data and rainfall was daily time series data. There are some missing data in collected time series of data set. All of the missing value was interpolated by some statistical formula. Two statistical formulas have been used for interpolation.

2.2.1 Linear interpolation method

Linear interpolation is often used to fill the gaps in a table. Linear pattern means the points created a straight line. Linear interpolation method use when gap of data is short. It lies between one or two days not more than two days. In case of discharge, the value of stream flow is closely related to previous or following days. Linear interpolation method use to fill up gap before last value and after first value. Formulas of linear interpolation is

$$y = y_1 + \frac{(x - x_1) \times (y_2 - y_1)}{(x_2 - x_1)} \qquad (1)$$

Here, y= new discharge, y_1= previous discharge, y_2= discharge of following days, x= new year, x_1= previous year, x_2= following years.

2.2.2 Interpolation by regression

Interpolation is a method of constructing new data points within the range of a discrete set of known data points. This can be achieved by regression. When gap of data is more than two variables or longer gaps then regression analysis is used to fill up missing data. Formula of regression is

$$y = bx + a \qquad (2)$$

Here, y= discharge, x= time period/year (independent), b= regression coefficient or changing rate for one-unit change in 'x', a= intercept.

2.3 Data processing

There are two types of trend test which one is parametric test and another one is non-parametric test. Non-parametric test is conducted to this research. Mann-Kendall Test (MK) and Sen's Slope Estimator method are used as non-parametric test. Non-parametric data is more reliable for hydrologic data. Pearson's Coefficient of Correlation is used to show the relationship between variable. Discharge-discharge, discharge-rainfall relation is determined by correlation. Relation is spectacled by percentage. Coefficient of correlation is calculated to determine the dependency rate.

2.3.1 Data analysis methods

I) Mann-Kendall test

The purpose of the Mann-Kendall (MK) test (Mann 1945, Kendall 1975) is to statistically assess if there is a monotonic upward or downward trend of the variable of interest over time. The hypotheses of Mann and Kendall's trend test is

H_0: Time series values are independent and identically distributed i.e. there is no trend.

H_A: There is a monotonic (not necessarily linear) trend.

So, it is a teo-tailed test. The test statistic, S (score) is then computed as

$$S = \sum_{i=1}^{n-1} \sum_{j=i+1}^{n} \text{sign}\ (y_j - y_i) \qquad (3)$$

Where, sign $(y_j - y_i)$ is equal to +1, 0, or -1, n is the total number of observations. A positive value of S indicates an 'upward trend' and a negative value of S indicates 'downward trend'.
The variance statistic is given as

$$V(s) = \frac{n(n-1)(2n+5)}{18} \qquad (4)$$

Therefore, the test statistic z is calculated as

$$Z = \begin{cases} \frac{(s-1)}{\sqrt{V(s)}} & \text{where } 0, S = 0 \\ \frac{(s+1)}{\sqrt{V(s)}} & \text{where } S < 0 \end{cases} \qquad (5)$$

Z follows standard normal distribution with mean zero and variance unity. A positive value of test statistic indicates a positive association means upward trend, a negative value of test statistic indicates a negative association means downward trend and test statistic w equal zero means no association(no trend). The null hypothesis of no trend is rejected when S and Z are significantly different from zero. It is highly recommended for general use by World Meteorological Organization (Mitchell et al., 1966).

II) Sen's Slope estimator test

This test computes both the slope (i.e. linear rate of change) and intercepts according to Sen's method. First, a set of linear slopes is calculated as follows:

$$T_i = \frac{x_j - x_k}{j - k} \qquad \text{for } i = 1, 2, 3, \ldots\ldots N \qquad (6)$$

Where, x_j and x_k are considered as data value at time j and k (j>k) correspondingly. The median of these N values of T_i is represented as Sen's estimator of slope which is guven as:

$$Q_i = \begin{cases} \frac{T_N + 1}{2} & \text{N is odd} \\ \frac{1}{2}\left(\frac{T_N}{2} + \frac{T_{N+1}}{2}\right) & \text{N is even} \end{cases} \qquad (7)$$

Sen's estimator is computed as $Q_{med} = T_{(N+1)/2}$ if N appears odd, and it is considered as $Q_{med} = [T_{N/2} + T_{(N+2)/2}] /2$ if N appears even. At the end, Q_{med} is computed by a two-sided test at 100 (1-α) % confidence interval and then a true slope can be obtained by the non-parametric test. Positive value of Q_i indicates upward or increasing trend and a negative value of Q_i gives a downward or decreasing trend in the time series.

III) Pearson's Coefficient of Correlation

Coefficient of correlation is a numerical measure of the correlation between two fluctuating series, and is denoted by r. The numerical expression of the degree of correlation existing between two variables. Let, $x_1, x_2, \ldots\ldots x_n$ and $y_1, y_2, \ldots\ldots y_n$ be two data sets. Coefficient of correlation between two data set can be expressed as

$$r = \frac{\sum_i (x_i - \bar{x})(y_i - \bar{y})}{\sqrt{\sum_i (x_i - \bar{x})^2 (y_i - \bar{y})^2}} \qquad (8)$$

Major characteristics of "r" are as follows:

1. The value of r lies between -1 to +1
2. When r = +1, there exists perfect positive correlation.
3. When r = -1, there exists a perfect negative correlation.
4. When r = 0, there is no correlation.

2.4 Coefficient of Determination

The coefficient of determination is the square term of coefficient of correlation (r). It is usually denoted by r^2 (or R^2). It expresses the proportion of the total variation of the dependent variable has been explained by the independent variable (Aziz, 2008). The value of Coefficient of Determination is 0 to 1. It is the proportion of the variance in the dependent variable that is predictable from the independent variable(s).

3. ILLUSTRATIONS

3.1 Trends in annual mean discharge

Within 21 years times (1998 to 2018) period of discharge has been calculated. Non-parametric tests have been applied here to detect trend. Mann-Kendall test and Sen's slope estimator has been conducted to find out the trend. Table 1 indicates Mann-Kendall and Sen's slope values and it has been depicted that value of z of discharge at jagir station is -0.94 and -0.164 respectfully. So, it seems that trend of discharge at jagir station is downward.

Table 1: Mann-Kendall test and Sen's slope value of annual discharge.

Station	Mann-kendalls slope (z)	Sen's slope (z)
Jagir	-0.94	-0.164

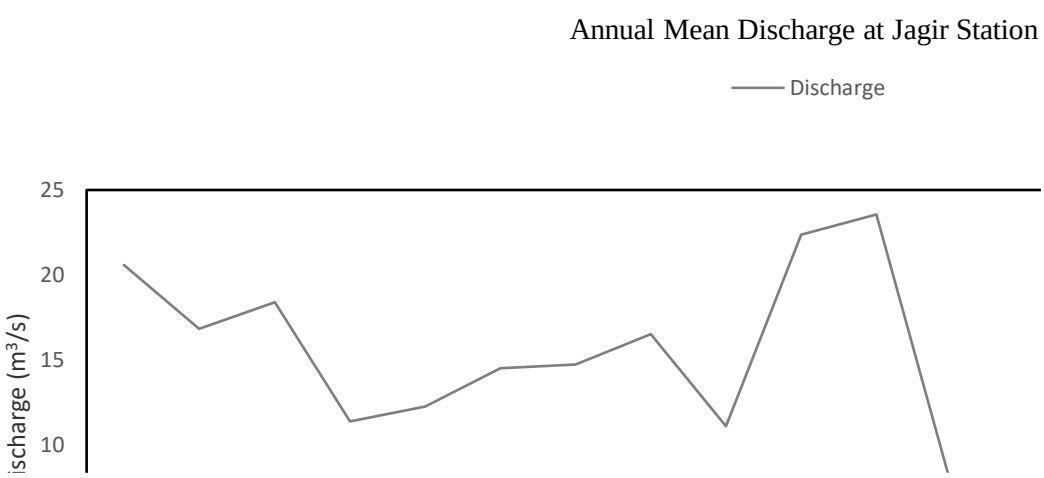

Figure 2: Annual mean discharge at jagir station

3.2 Trend is seasonal mean discharge

The range of months of summer is from March to May and monsoon is from June to October and winter is from November to February. Time period of data considered as from 1998 to 2018 for summer, monsoon and winter. Table 2 indicates that Mann-Kendall test value of summer, monsoon and winter are -0.54, -1.00 and 1.60 respectively. These values clearly indicate that trend of discharge in summer and monsoon is downward. Winter trend is upward. Sen's slope values of summer, monsoon and winter are -0.042, -0.595 and 0.099 respectively.

Table 2: Mann-Kendall and sen's slope values of seasonal mean discharge

Station (jagir)	Mann-kendalls slope (z)	Sen's slope
Summer	-0.54	-0.042
Monsoon	-1.00	-0.595
Winter	1.60	0.099

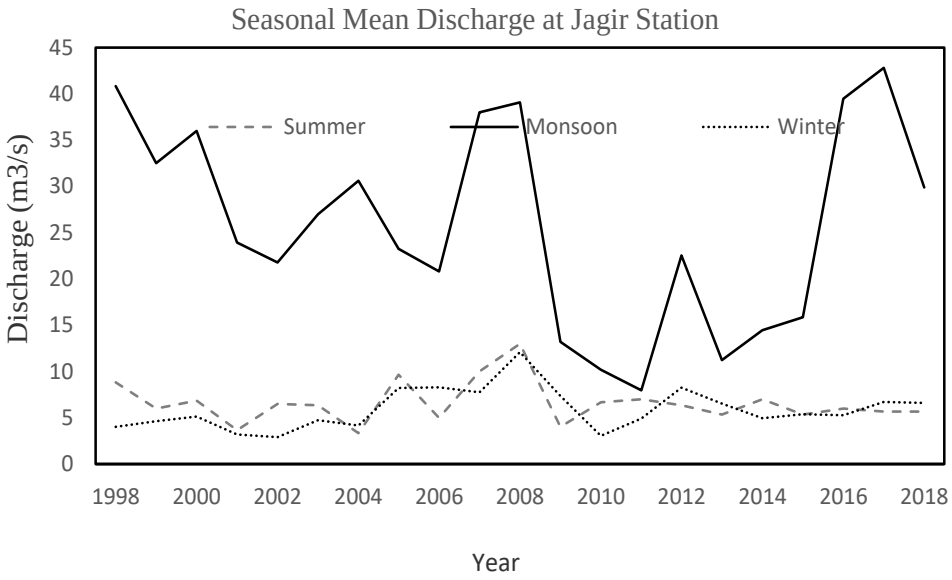

Figure 3: Seasonal mean discharge at jagir station

Graphical representation has been clearly indicated that there is little difference between summer and winter stream flow. Discharge rate in some years are higher in winter than summer. In 2011, very low discharge appeared in monsoon.

3.3 Trends in rainfall at savar station

Rainfall trend is the annual, seasonal, monthly, etc variability of rainfall. Trend of rainfall during time period of rainfall data is from 1998 to 2018 has been studied here. To detect trend, non-parametric test (Mann-Kendall test, sen's slope estimator) has been used in this study.

3.4 Annual rainfall trend at savar station

21 years of rainfall at savar station has been studied here. Trend condition has been determined by non-parametric tests which are Mann-Kendall test and sen's slope estimator. From table 3, it has been showed that annual rainfall is upward or increasing trend. Value of the Mann-Kendall test is 0.27 which is positive value. Sen's slope value of annual rain is 5.258 that mean magnitude of rainfall change is 5.258 per year.

Table 3: Mann-Kendall and sen's slope statistics of trend in rainfall at savar station.

Station	Mann-kendall test, z value	Sen's slope
Savar	0.27	5.258

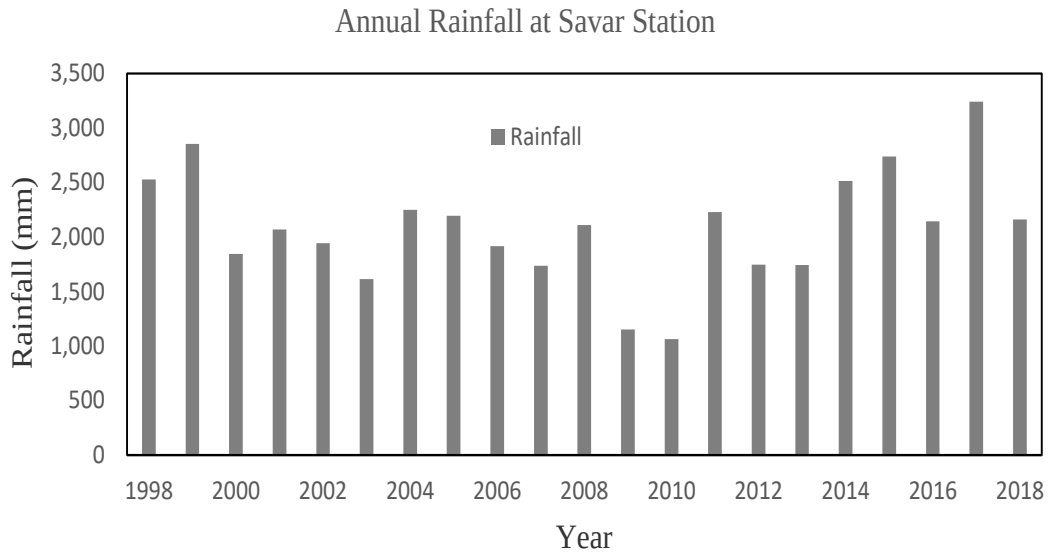

Figure 4: Annual rainfall at savar station

3.5 Seasonal rainfall trend at savar station

There are three seasons in total which are summer, monsoon and winter. Summer consists of March to May and monsoon is June to October and winter is November to February. Monsoon considers as rainy season and summer and winter are considered as dry season.

Seasonal rainfall trend has been analysed here. From table 4, Mann-Kendall test values of summer, monsoon, and winter are 0.96, -0.03 and -0.36 respectively. So, it clearly indicates that summer trend of rainfall is upward. On the other hand, monsoon and winter rainfall trends are downward because their z values are negative. Sen's slope values of summer, monsoon, and winter are 8.907, -4.340 and -1.183 respectively. Downward trend of monsoon rainfall is higher than winter rainfall. Graphical presentation of seasonal rainfall trend has been shown by bar diagram in figure 5.

Table 4: Mann-Kendall And Sen's Slope Test Of Seasonal Trend Of Rainfall At Savar Station

Season	Z value	Sen's slope
Summer	0.96	8.907
Monsoon	-0.03	-4.34
Winter	-0.36	-1.183

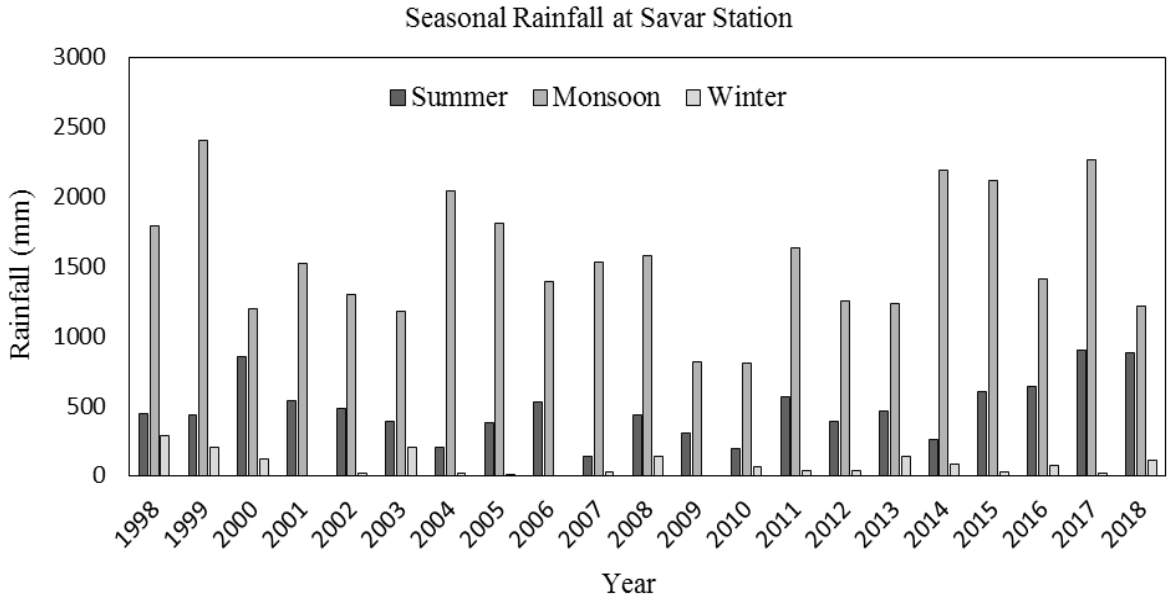

Figure 5: Seasonal rainfall at savar station

3.6 Relation between two stations

In river catchment area, some portions of discharge of river are fed by precipitation. Precipitation considered as rainfall. So, discharge of a river must depend on precipitation (rainfall). In Bangladesh, 75% of rainfall occurs in monsoon region (Islam, et al, 2007). For Pearson's coefficient of correlation, rainfall considered as an independent variable and discharge considered as dependent variable. Table 5 shows the correlation and dependency rate between discharge at jagir station and rainfall at savar station. In this table, it appears that "r" is positive. There was positive correlation between discharge and rainfall. The positive value of "r" indicates positive relationship and negative value of "r" indicates negative relationship. Value of "r" is 0.3776 is close to 0.5 that results significant relationship between two station.

Table 5: Correlation between Rainfall at Savar Station and Discharge at Jagir Station

Independent variable	Dependent variable	r	r^2	r^2 (%)
Rainfall	Discharge	0.3776	0.14258	14.2

From table 5, it has been indicated that relationship between annual rainfall and discharge is 14.2%. That means 14.2% of annual discharge is fed by annual rainfall. Rest of discharge is contributed by others sources like runoff, tributaries, etc. Three different seasons have been considered here which are summer (March – May), monsoon (June – October), and winter (November – February). Winter season comprise with November, December, January and February.

Table 6 shows the correlation between rainfall at savar station and discharge at jagir station. Where rainfall is independent variable and discharge is dependent variable. Pearson's coefficient of

correlation exhibits the dependence rate of dependent variable on independent variable. From table 6 it seems that "r" value of correlation of summer, monsoon and winter is -0.16855, 0.299655 and -0.11885 respectively. Value of "r" is positive in monsoon. So, there has positive relationship between rainfall at savar station and discharge at jagir station in monsoon time. Negative value of "r" shows negative relation between rainfall and discharge in summer and wintertime.

Dhalesshori river in summer depends on rainfall at savar. The rest of discharge is fed by other sources. In monsoon and winter discharge is contributed by rainfall is 8.97% and 1.41% respectively. Upstream flows are the main contributor to Dhalesshori river's discharge.

Table 6: Correlation between Rainfall at Savar Station and Discharge at Jagir Station at different seation

Duration	R	R^2	R^2 (%)
Summer	-0.16855	0.0284	2.84%
Monsoon	0.299655	0.089793	8.97%
Winter	-0.11885	0.0141	1.41%

4. CONCLUSIONS

Annual discharge within these time periods is 14.2% that means 14.2% of annual discharge is fed by annual rainfall. Rest of discharge is contributed by others sources like runoff, tributaries, etc. In 2011, very low discharge appeared in monsoon. The mean discharge and rainfall during this period are negative whereas recent years' rainfall increasing in summer season and for monsoon opposite trend. There was positive correlation between discharge and rainfall. The positive value of "r" indicates positive relationship and negative value of "r" indicates negative relationship. Value of "r" is 0.3776 is close to 0.5 that results significant relationship between two station.

ACKNOWLEDGEMENTS

The authors wish to acknowledge administration of Flood Processing and Forecasting Circle (FPEC) of Bangladesh Water Development Board (BWDB) for providing necessary data to conduct this research.

REFERENCES

Aziz, M. A. (2008). "Business Statistics." 4th edition, Dhaka: The angle Publication.

Baskerville, R. (1991). "Risk Analysis as a Source of Professional Knowledge." *Computer & Security*, Vol. 10 (8), 749-764.

Coscarelli, R. and Caloiero, T. (2012). "Analysis of daily and monthly rainfall concentration in Southern Italy – Calabria region." *Journal of Hydrology*, Vol. 416, 145–156.

EPA- United States Environmental Protection Agency (2014), "Annual report" USA.

Helsel, D. R. & Hirsch, R.M. (1992). "Statistical Methods in Water Resources." Amsterdam: *Elsevier Science Publications*.

Islam M. N. & Uyeda H. (2007). "Use of TRMM in determining the climatic characteristics of rainfall over Bangladesh." *Remote Sensing of Environment*, Vol. 108, 264-276.

Islam, S. M. & Sikder, B. M. (2017). "Detection of Trend in Hydrologic Variables Using NonParametric Test: A Study on Surma River in Northeastern Bangladesh." *Journal of Scientific Research*, Vol. **9** (3), 277-284.

IPCC (2007). "Climate change: climate change impacts, adaptation and vulnerability. Contribution of the Working Group II to the Fourth Assessment Report of Intergovernmental Panel on Climate Change." Summary for policy makers, 23.

Kothari, C. R. (2004). "Research Methodology: Methods and Techniques." Second edition. New Delhi: New Age International (p) Limited.

Mann, H.B. (1945). "Non-parametric tests against trend." *Econometrica*, Vol. 13, 163-171.

Mitchell, J. M., Dzerdzeevskii, B., Flohn, H., Hofmeyr, W. L., Lamb, H. H., Rao, K. N., Walle'n, C. C. (1966). "Climate change." WMO Technical Note No. 79. World Meteorological Organization, 79.

Shiklomanov, A. I., Yakovleva, T. I., Lammers, R. B., Karasev, I. Ph., V. Osmarty, C. J. and Linder E., 2006 "Cold region river discharge uncertainty- estimates from large Russian rivers." *Journal of Hydrology*, Vol. 326, 231-56.

Uddin, E.M., Akter, A. S., Uddin, J. M., Diganta, M. T. M., (2018). "Trend Analysis Variations and Relation Between Discharge and Rainfall: a Study on Kushiyara River." *Journal of Environmental Science & Natural resources*, Vol. 10(2), 121–132.

Proceedings of the 5th International Conference on Civil Engineering for Sustainable Development (ICCESD 2020), 7~9 February 2020, KUET, Khulna, Bangladesh (ISBN-978-984-34-8764-3)

DREDGING AND DREDGED MATERIAL MANAGEMENT: A CASE STUDY OF MONGLA PORT

Md. Motiur Rahman*[1] and Md. Shahjahan Ali[2]

[1]Executive Engineer, Mongla Port Authority, Bagerhat, Bangladesh, e-mail: khan.motiur06@gmail.com
[2]Professor, Department of Civil Engineering, Khulna University of Engineering and Technology, Khulna-9203, Bangladesh, e-mail: bablu41@yahoo.com

***Corresponding Author**

ABSTRACT

Dredging is the relocation of earth which is mainly under or with water. This operation normally done to create or improve waterways and sometimes to improve the environment. There are several types of dredger such as cutter suction dredger, trailing suction hopper dredger, grab dredger, backhoe dredger, bucket dredger etc. Types of dredgers selected based on the location and soil properties. Dredged material normally disposed in open water or confined area. In some cases management of dredged material is a very complicated issue.

Mongla Port is situated on the left bank of Pussur River at about 130 km upstream of Bay of Bengal. At establishment time of the port depths of Pussur River at present location were satisfactory for average 8.5 m draft ships. But, since 1970 the depths in this area started to deteriorate rapidly. Since then, regular maintenance dredging has been required to provide sufficient depth alongside the berths and in the approaches to the berths. Till now Mongla Port has carried out 172.28 lac cu.m dredging which is about 4.30 lac cu.m/year. In the year 2019-20, Mongla Port is implementing the 117 lac cu.m dredging at outer bar and food silo area. In 2020-2022, Mongla Port is planning to dredge the approach channel upto 8.5 m CD and the quantity will be about 216 lac cu.m.

Mainly Cutter Suction Dredger and Trailing Suction Hopper Dredger used at Mongla Port dredging works. All the dredged material was dumped on land and all of the low land of port area has filled up. To keep the port operational in connection with the market demand, huge amount of dredging will be required in upcoming years. Dredged material management will be a serious issue in future. Now Mongla Port doesn't have sufficient land for disposal of dredged material from any major dredging project. At this context disposal in water at suitable location could be an alternative. About 3,84,50,000.00 cu.m can be accommodated in shallow areas, deep pockets and deep channels.

But the present regulatory conditions of MPA as well as Bangladesh don't allow open disposal. The government is now preparing "Dredging and dredged material management policy-2018". The draft policy also recommended only confined disposal on land only. Considering the international practice in dredging field, open disposal need to permit in exceptional cases such as MPA. However the movement pattern of sediment and its effect on river need to assess through mathematical model and some case study.

Keywords: *Navigability, Pussur river, Dredging, Dumping, Mongla Port.*

1. INTRODUCTION

Mongla Port (MP) is situated on the left bank of Pussur River at about 130 km upstream of Bay of Bengal. The Pussur River forms part of a very big and complex river system. Numerous tributaries and channels connect the Pussur River with other rivers like Sibsa, the Ganges and Jamuna Rivers. Flow conditions in all these rivers determined the current and morphological condition in the Pussur River. At establishment time the depths of the Pussur River at present location were satisfactory for average 8.5 m draft ships. But, since 1970 the depths in this area started to deteriorate rapidly. When the construction of the berth was completed in 1978 the depths in the area had already been reduced significantly. Since then, regular maintenance dredging has been required to provide sufficient depth alongside the berths and in the approaches to the berths.

The navigation channel at the Pussur River entrance crosses a wide bar known as outer bar. The bar is relatively stable with sea bed elevation of -6.4 m Chart Datum (CD). This outer bar also needs to dredge up to 8.5 m CD at least. Till now MP has carried out 172.28 lac cu.m dredging which is about 4.30 lac cu.m/year. In the year 2019-20, MP is implementing the dredging at outer bar and food silo area. Quantity of those areas are 104 and 13 lacs respectively. In 2020-2022, MP is planning to dredge the approach channel upto 8.5 m CD and the quantity will be about 216 lac cu.m.

Mainly Cutter Suction Dredger (CSD) and Trailing Suction Hopper Dredger (TSHD) used at MP dredging works. All the dredged material was dumped on land and all of the low land of port area has filled up.The Port is well protected by the largest mangrove forest known as the Sundarbans, part of which has been declared as "World Heritage" in 1997 by UNESCO. Sundarban has covered about 100 km of bank of the channel and there is no scope of dumping on that 100 km bank.

To keep the port operational in connection with the market demand, about 320 lac cu.m to be dredged in next 05 years and after that yearly 30-40 lac cu.m dredging will be required. Since the financial capability of Bangladesh in increasing day by day, financing for dredging may not be a problem but dredged material management will be a serious issue in future.

2. DREDGING

Dredging is the activity to remove material from one part of the water body and replacing it to another. In most of situations the excavation is undertaken by a specialist floating plant, known as a dredger. Dredging is carried out in many different locations and for many different purposes, but the main objectives are usually to recover material that has some value or use, or to create a greater depth of water.

2.1 Types of dredging equipment

Dredging equipment can be divided in Mechanical Dredgers and Hydraulic Dredgers. The differences between these two types are the way that the soil is excavated, either mechanical or hydraulic (Emermanand & White, 2017).

2.1.1 Mechanical Dredgers

Mechanical dredgers work by mechanically digging or gathering sediment from the bottom surface of a body of water, typically through use of a bucket. Mechanical dredging takes place at the shoreline or working off of a barge. The most common types of mechanical dredgers are:

2.1.1.1 Bucket Dredger

Bucket Dredger is a stationary dredger, fixed on anchors and moved while dredging along semi-arcs by winches. The bucket dredger is one of the oldest types of dredging equipment. It has an endless chain of buckets that fill while scraping over the bottom. The buckets are turned upside down and empty moving over the tumbler at the top. The dredged material is loaded in barges.

2.1.1.2 Grab Dredger

Grab Dredger is a stationary dredger, moored on anchors or on spud-poles. A spud is a large pole that can anchor a ship while allowing a rotating movement around the point of anchorage. The dredging tool is a grab normally consisting of two half-shells operated by wires or hydraulically. The grab can be mounted on a dragline or on a hydraulic excavator of the backhoe type. Many modifications of grabs have been constructed like open grab, closed grabs and watertight grabs. The dredged material is loaded in barges.

2.1.1.3 Backhoe Dredger

Backhoe Dredger is a stationary dredger, moored on anchors or on spud-poles. A spud is a large pole that can anchor a ship while allowing a rotating movement around the point of anchorage. Small backhoe dredgers can be track mounted and work from the banks of ditches. A backhoe dredger is a hydraulic excavator equipped with a half open shell. This shell is filled moving towards the machine. Usually the dredged material is loaded in barges. This machine is mainly used in harbors and other shallow waters.

2.1.2 Hydraulic Dredger

Hydraulic dredgers work by sucking up a mixture of sediment and water from the bottom surface and then transferring the mixture through a pipeline to another location. This dredger acts like a giant floating vacuum, removing sediment.

2.1.2.1 Suction Dredger

Suction Dredger is a stationary dredger used to mine for sand. The suction pipe is pushed vertically into a sand deposit. If necessary, water jets help to bring the sand up. It is loaded into barges or pumped via pipeline directly to the reclamation area.

2.1.2.2 Cutter Suction Dredger

Cutter Suction Dredger is a stationary dredger which makes use of a cutter head to loosen the material to be dredged. It pumps the dredged material via a pipeline ashore or into barges. While dredging, the cutter head swing around the spud-pole powered by winches. The cutter head can be replaced by several kinds of suction heads for special purposes, such as environmental dredging.

2.1.2.3 Trailing Suction Hopper Dredger

Trailing Suction Hopper Dredger is a self-propelled ship which fills its hold or hopper during dredging, while following a pre-set track. The hopper can be emptied by opening bottom doors or valves or by pumping its load off ashore. This kind of dredger is mainly used in open water such as rivers, canals, estuaries and the open sea.

2.1.2.4 Reclamation Dredger

Reclamation Dredger is a stationary dredger used to empty hopper barges. A suction pipe is lowered into the barge. Extra water can be added by water by water jets to facilitate the suction process. The dredged material is pumped by pipeline ashore, to a reclamation area, or to a storage depot.

2.1.2.5 Barge unloading dredgers

Barge unloading dredgers are used to transfer material from hopper barges to shore, usually for reclamation. A barge unloader is basically a pontoon supporting a suction pump for the unloading, and a high-pressure water pump used to fluidize the barge contents by jetting. The mixture is then pumped through a pipeline to the point of reclamation or relocation.

2.2 Locations and Quantities for Dredging

When dredging projects are planned, the locations and quantities of material are the most important considerations that need to be addressed. The biggest problem is usually the disposal of the dredged material, which means that long-term projections are essential. Before the project commences,

hydrographic surveys carried out to determine the existing depths as well as the depths that will be attained after the dredging operation. The process requires the use of proper equipment and both vertical and horizontal controls to ensure accurate calculations.

2.2.1 Physical Properties of Sediments

If there is a specialized problem with the dredging operations, then field testing is required to determine the quantities, characteristics, and location of the material that needs to be removed. Sediment samples normally collected down to the depth that will be targeted. At the same time, a pre-dredge survey carried out. Once the characteristics are well known based on multiple samples, then a smaller number of samples can be used for future work. When soft materials are present, then grab sampler (using a bucket or scoop) or push tube sampler (using an open-ended tube that is thrust vertically into the sediment) are used for sample collection.

2.2.2 Sampling for new Project

When samples are taken for new work, then conventional boring techniques are usually used. These samples obtained in the major work zones for a full representation of site samples. These samples go through laboratory testing to determine the proper dredge plant, disposal alternatives, the design of retention dikes and channel slopes, and the estimation of long-term storage capacity when the disposal areas are confined. These sample tests normally include:

- Natural Water Content Test
- Plasticity Analysis
- Specific Gravity Test
- In Situ Density
- Grain size distribution

2.2.3 Selection of Dredging Equipment

Sometimes limitations are placed on equipment depending on the circumstances. Avoid of specifications whenever possible is helpful to avoid restriction to the competitive bidding process. The goal of equipment selection is to reduce the environmental impact that occurs due to the operation. This protection is an adequate justification for managing the selection and control of the dredging equipment.

2.3 Disposal of Dredged Material

Before selecting any dredging equipment, it is important to consider the options for disposal alternative, especially from technical and environmental point of view. Three common disposal alternatives might be used:

- Open-water disposal
- Confined disposal
- Beneficial Use

The operation for dredging and dredged material disposal needs to cover both short-term and long-term management goals. Typically, short-term focus is on the channels that are needed for existing navigation, but it doesn't necessarily need to be based on the project dimensions. Ideally, the dredging process done using the best technical options that are both economically feasible and environmentally compatible. On the other hand, long-term goals are focused on the operation and management of the disposal areas. Preliminary data collection for a dredging and dredged material disposal project includes:

- Assessing the location as well as the amount that needs to be dredged.
- Determining the chemical and physical characteristics of the sediments.
- Identifying potential alternatives for the disposal.
- Considering the applicable environmental, social, and institutional factors.
- Evaluating the dredge plant requirements.

2.3.1 Open water Disposal

Open water disposal can be in the ocean, estuarine waters, lakes and rivers, all of which are highly regulated. Although open-water disposal may be inexpensive, it gives the least amount of control over hydrodynamic and environmental aspects. The suitability of the open-water option normally carefully determined by taking sediment samples which are then evaluated for chemical and biological composition. Both the dredged material itself and the placement area evaluated for compatibility. In sensitive open-water environments, for instance, where there are coral reefs and other marine flora and fauna, placement of sediment, even if it is clean and compatible, may be deemed unsuitable.

2.3.2 Confined Disposal

Confined disposal takes place in a structure which isolates the dredged material from the surroundings, e.g., within a diked area either in water or on land. When the dredged material is contaminated and cannot be cleaned, then placing it in a confined disposal area, be it on land or at sea, is the only choice. In water or underwater confined disposal can be complex. Space is not an issue but ensuring complete control over the isolation of the materials may not be possible. Confined disposal options can be controlled better but options are limited by the space available.

2.3.3 Beneficial Use

Also, the benefits of disposal area reuse shouldn't be overlooked. When the dewatered fine-grained material and coarse-grained material are removed from the site, then partial or total reuse of the disposal area is available. This strategy basically turns the disposal area into a transfer station, where the dredged materials are collected, processed, and then moved to another location for inland disposal or productive use. Examples of productive use include:

- Construction or landfill material
- Low land reclamation
- Material for sanitary landfill cover
- Enhancement of agricultural land

3. DREDGING OF MONGLA PORT

3.1 Dredging Activity

Mongla Port was designed for berthing ships having 8.50 m draft. Up to 1980 there was not any siltation problem either in Jetty front or Channel area. But after 1980 siltation started in Jetty front Area (Rahman and Ali, 2018). From that time regular maintenance dredging was performed in jetty front area. In the meantime, it was seen that siltation has started in Harbor Area (About 13 Km downstream from Port Jetty). Due to this siltation, 04 times capital dredging project has implemented in the year of 1994 - 1995, 2004 - 2005, 2013-2014& 2017-2019. For regular maintenance dredging, Mongla Port Authority has 02 nos 18" dia Cutter Suction Dredger. Moreover, MPA carried out maintenance dredging every year at different location of the channel. Table 1.1 presented a brief dredging history of Mongla Port Authority.

Table 1.1: Dredging History of MPA

Dredging period	Dredger Authority	Dredging Area	Dredging Quantity (Lac cu.m)	Total expenditure (CroreTaka)	Dredger Type
1979-1981	Water Dev. Board	Jetty front(J5-J9)	3.25	0.896	CSD
1983-1987	BIWTA	Jetty front(J5-J9)	6.95	3.094	CSD
1988-1990	Water Dev. Board	Jetty front(J5-J9) & Confluence	5.23	2.856	CSD
1991-1992	China Harbour Engineering Company, China	Harbour Area	35.51	30.88	CSD
1993-1996	Khanak dredger of Ctg. Port. (Trailing Suction Hopper Dredger)	Southern Anchorage confluence & Sabur Beacon	2.26	2.989	TSHD
1994-2001	Water Dev. Board	Jetty front (J5-J9)	8.13	9.714	CSD
2000-2004	PT. Rukindo- Basic Dredging Partnership	Harbour Area	27.9	45.480	CSD & TSHD
2003-2004	Water Dev. Board	Jetty no- 8 & 9	0.69	0.805	CSD
2004-2005	Basic dredging Co.	Jetty no- 8 & 9	0.54	0.724	CSD
2005-2006	Water Dev. Board	Jetty no- 8 & 9	0.69	0.905	CSD
2007-2008	Water Dev. Board	Jetty no- 8 & 9	1.08	1.941	CSD
2009-2010	Water Dev. Board	Jetty no- 8 & 9	0.71	1.576	CSD
2012-2013	MPA's own Dredger	Jetty no- 8 & 9	0.17	-	CSD
2013-2014	China Harbour Engineering Company, China	Harbour Area	34.06	111.85	CSD
2015-2016	AZ dredging Company Ltd	Approach and Pontoon front of Nil Komol	1.55	3.197	CSD
2017-2018	Banga Dredgers Ltd	Jetty Front	1.40	3.560	CSD
	Dredging Corporation of India	Mongla Port to Rampal Power Plant	4.10	11.90	CSD
	Bangladesh Navy	Approach to Nil Komol	0.38	1.20	CSD
2018-2019	Banga Dredgers Ltd	Jetty Front	1.25	3.240	CSD
	Dredging Corporation of India	Mongla Port to Rampal Power Plant	34.7	107.10	CSD & TSHD
	Bangladesh Navy	Approach to Nil Komol	0.48	1.70	CSD
	Asian Dredgers Ltd.	Food Silo Area	1.25	2.80	CSD
Total			**172.28**	**348.407**	

Among the above 29 lac cu.m was dredged by TSHD and 143 lac cu.m by CSD. In 2019-2020, another two dredging projects will be completed at outer bar and food silo area. Approximate quantity of those projects is 117 lac cu.m, among them 104 lac cu.m will be dredged by TSHD and 13 lac cu.m will be dredged by CSD.

Upto 2017-18, average dredging at MP is 4.3 lac cu.m/year which will be 7.05 lac cu.m/ year at the end of 2010-2020. MP is also planning a long-term dredging project to handle 9 m draft vessel in first phase and 11 m draft vessel at second phase. That project includes capital dredging, river training and maintenance dredging. Approximate quantity of capital dredging will be 216 lac cu.m in 1st phase, 1470 lac cu.m in 2nd phase and yearly maintenance dredging will be at least 150 lac cu.m.

3.2 Sediment Characteristics

DHI (1993) has collected a large quantity of data on this river, based on which the governing physical processes and the nature of the sediment transport processes in the Pussur River can be understood.

From the suspended samples analysis, DHI concluded that the main part of the suspended sediment material consists of silt which is only represented in the bed material by approximately 5 percent. Consequently, the suspended sediment picked up in the measurements for the main part consists of wash load. Silt is generally not found in the bed along the main flow of Pussur River indicates that suspended silt contributes in any significant way to the erosion/deposition processes along the river. The bed material along the main flow areas of the bigger rivers is fine sand. Closer to the banks it is often mainly silt. The suspended fine material does not contribute significantly to erosion/sedimentation processes in the main flow regions of the bigger rivers including the navigation channel of Mongla Port.

3.2.1 Bed Load Characteristics

To know the characteristics of river bed material near the Mongla Port area, 4 (four) bed samples were collected and analyzed. Sieve analysis of the bed material shows that the Fineness Modulus (FM) of the collected samples are 0.30, 0.60, 0.48 and 0.49, i.e. the bed material is mostly sandy. Figure 1 shows the average grain size distribution of bed material, where d_{50} is found as 0.052 mm.

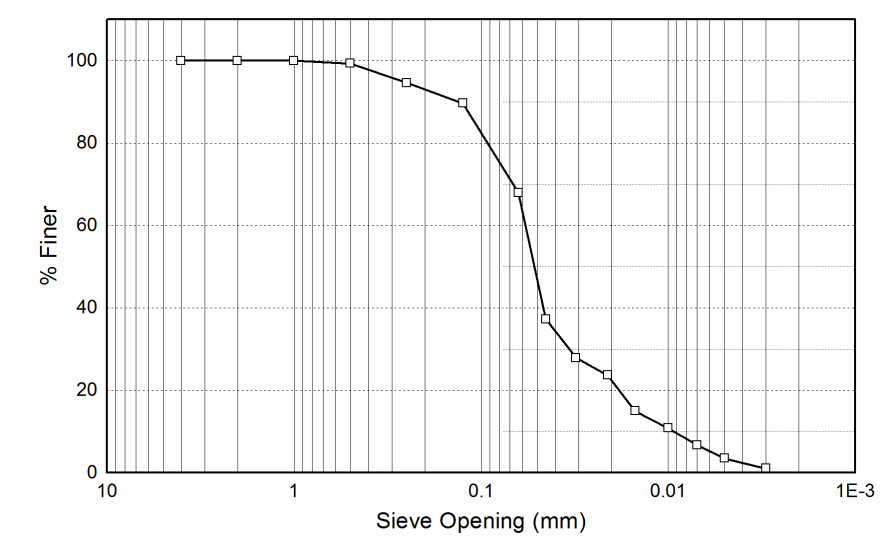

Figure 1: Average grain size distribution of bed material

3.3 Disposal of MP Dredged Material

Initially, the land area of MP was 2068 acre. Within this land EPZ, BEZA, and Navy was established later on. Most of this 2068-acre land was low land, which has developed by the dredged material of MP. Some industries in Mongla area, Road construction project of Rampal power plant, partial development of Block-B of Rampal power plant has also done by dredging material. Now all of MP land has developed and private upcoming industries along the river side already developed their land. Due to Sundarban, DoE is not giving permission for any industrialization at south side of Mongla River up to Joymonirgol and this reach of Pussur River is mainly siltation prone area which require huge dredging.

MP is not getting any land for dumping the dredge material at south side of Mongla River upto Joymonirgol because all the land is mainly using for fish pond. In 2014-15, MP has filled about 250-acre private lands at Chilla and Joymonirgol area. Till now, there is no use of those land, neither agriculture nor fishing. Due to the saline content of dredged material, even any plantation is not possible there upto certain years. To implement the dredging project at Joymonirgol area, MP is now thinking to get some private land by giving compensation. Present dredging project is small quantity of only 13 lac cu.m and compensation may not be a problem. But in future, if MP implement project to handle higher draft vessel then the dumping area for 1686 lac cu.m from capital dredging and yearly 150 lac cu.m from maintenance dredging will be the main challenge of MP. Only the capital dredging material will need 10,000-acre land and maintenance dredging may need 900 acre/year. This amount of land is totally impossible and alternative solution should be found out before planning any of this project.

3.4 Alternatives of Disposal Area

Considering the future dredging demand of MP, alternative disposal method should be considered. In most of the worldwide sea ports, open discharge in deep pockets of channel is very common. Most of the seaports in the world are near to sea and disposal of dredged material in sea is economical and easiest solution there. But the ports like MP which are very far from sea, carrying the material to sea is not economical. In these cases, deep pocket in channel and very shallow area could be an alternative. Length of Pussur Channel is 130 km from sea, within which only 22 km from port to Harbaria and 11 km at the entrance of channel requires dredging. Dredged material from entrance channel which is known as outer bar, can be dumped either in sea or land. Sea is about 15 km and nearest islands such as Dubla Island, Bangabondhu Island is within 10 km of dredging area. Channel between Harbaria to outer bar has sufficient depth more than 10 m which never requires dredging. For disposal of dredged material of port to Harbaria, following areas can be considered:

- Shallow area at west side of port
- Shallow area at downstream of Mongla river
- Deep water pocket at danger khal area
- Deep water pocket at Joymonirgol
- Deep channel at downstream of Joymonirgol
- Deep channel at upstream of monkey point
- Deep water pocket at monkey point

The possible disposal areas have indicated in figure 2. The shallow areas are mainly situated on the convex end and deep pockets are on concave side. The details of these areas are stated in following articles.

3.4.1 Shallow area at west side of port

The width of river near port area is about 1000 m, within which only 200 – 300 m at east side is used as navigation channel. The velocity of flow is strong in this portion only. Depth at remain 700-800 m varies between 1-4 m. Length of shallow area between Digraj to Mongla river is 7000 m. If half of the shallow area i.e 400 m is considered then the area will be 28,00,000.00 sq.m. This area can accommodate about 70,00,000.00 cu.m at a filling height of 2.5 m which is also below the water level. Material of maintenance dredging from port area can be dumped in this shallow area.

3.4.2 Shallow area at downstream of Mongla river

The width of river at downstream of Mongla is about 1500 m, within which only 200 – 300 m at west side is used as navigation channel. The velocity of flow is strong in this portion only. Depth at remain 1200-1300 m varies between 1-4 m. Length of shallow area at downstream of Mongla River is 7000 m. If half of the shallow area i.e 650 m is considered then the area will be 45,50,000.00 sq.m. This area can accommodate about 1,13,75,000.00 cu.m at a filling height of 2.5 m which is also below the water level. Material of maintenance dredging from inner bar area can be dumped in this shallow area.

3.4.3 Deep water pocket at danger khal area

The confluence of Pussur river and danger khal is very deep due to scouring effect of water. The length of deep area is 500 m and width 200 m. Depth at this area varies between 12 ~ 18 m. The navigation channel is adjacent to this deep area. Dredged material is possible to dispose in this deep area during slag tide. This area can accommodate at least 4,00,000.00 cu.m.

3.4.4 Deep water pocket at Joymonirgol

The confluence of Pussur River and shella river is very deep due to scouring effect of water. The length of deep area is 1200 m and width 400 m. Depth at this area varies between 15 ~ 30 m. The navigation channel is adjacent to this deep area. Dredged material is possible to dispose in this deep area during slag tide. This area can accommodate at least 38,00,000.00 cu.m.

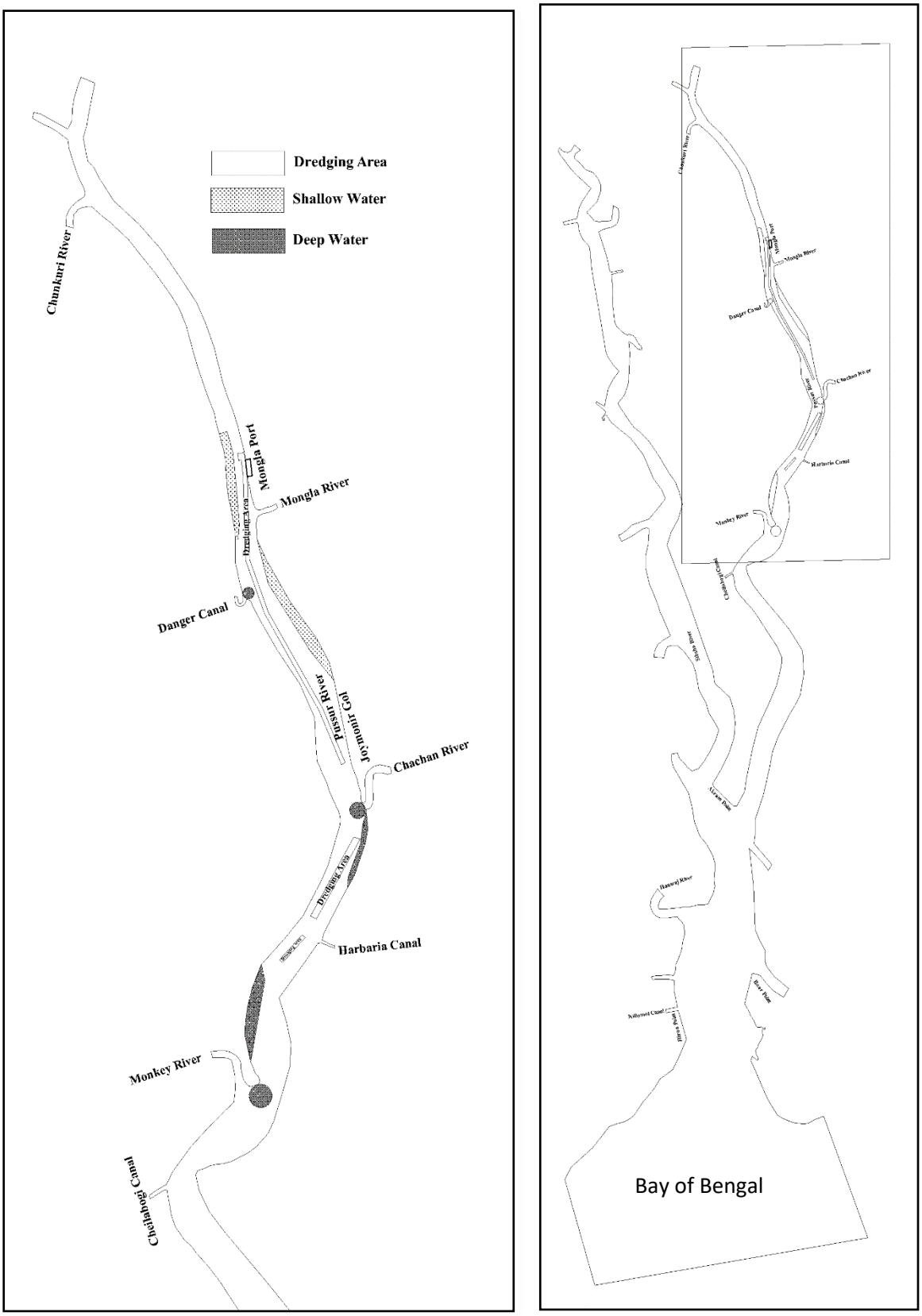

Figure 2: Disposal options of dredged material

3.4.5 Deep channel at downstream of Joymonirgol

The navigation channel at downstream of Joymonirgol is 10-14 m deep. If MP wants to maintain the channel at a minimum depth of 8 m CD then this area also can be considered as disposal area like a lot of sea ports in the world. The length of this deep channel portion is about 5000 m. This area can accommodate about 40,00,000.00 cu.m which have possibilities to spread in the deeper channels at further downstream.

3.4.5 Deep channel at upstream of monkey point

The navigation channel at upstream of monkey point is 10-14 m deep. If MP wants to maintain the channel at a minimum depth of 8 m CD then this area also can be considered as disposal area. The length of this deep channel portion is about 6000 m. This area can accommodate about 50,00,000.00 cu.m which have possibilities to spread in the deeper channels at further downstream.

3.4.6 Deep water pocket at monkey point

The confluence of Pussur River and Monkey River is very deep due to scouring effect of water. The length of deep area is 2700 m and width 500 m. Depth at this area varies between 15 ~ 30 m. The navigation channel is adjacent to this deep area. Dredged material is possible to dispose in this deep area during slag tide. This area can accommodate at least 70,00,000.00 cu.m of dredged material.

3.4.7 Summary of disposal options

The shallow and deep areas adjacent to the dredging sections in Pussur channel can accommodate at least 3,84,50,000 cu.m dredged material. But the present regulatory conditions of MPA as well as Bangladesh don't allow open disposal. The government is now preparing "Dredging and dredged material management policy-2018". The draft policy also recommended only confined disposal on land only. Considering the international practice in dredging field, open disposal needs to permit in exceptional cases such as MPA.

4. CONCLUSIONS

Pussur River requires huge amount of dredging to meet up the future demand. Proper management of dredged material will be the main challenge for implementing the dredging projects. Now MPA and the government must have to consider the open disposal options. If government allows open disposal, then may be a sustainable solution of dredged material management. However, the movement pattern of sediment and its effect on river need to assess through mathematical model and some case study.

REFERENCES

Emerman, D., and White, J. 2017. "Sustainable solutions for dredged material management in Ohio." Western Dredge Association – Midwest Chapter, Omaha, Nebraska

Rahman, M.M. and Ali, M.S. 2018. "Hydrological Characteristics of Pussur River and its Navigability." Proceedings of the 4th International Conference on Civil Engineering for Sustainable Development, Khulna, Bangladesh

Rahman, M.M. and Ali, M.S. 2018. "Potential causes of navigation problem in Pussur River and interventions for navigation enhancement." Proceedings of the 4th International Conference on Civil Engineering for Sustainable Development, Khulna, Bangladesh

US Army Corps of Engineers, 2015. "Dredging and Dredged Material Management, Engineering and Design", EM 1110-2-5025

Proceedings of the 5th International Conference on Civil Engineering for Sustainable Development (ICCESD 2020), 7~9 February 2020, KUET, Khulna, Bangladesh (ISBN-978-984-34-8764-3)

PERFORMANCE EVALUATION OF DRAINAGE NETWORK USING HEC-HMS UNDER DIFFERENT CLIMATIC AND LAND USE CONDITIONS, A CASE STUDY

M.H. Masum*[1], J. Hossen[2] and S.K. Pal[3]

[1]Student, Chittagong University of Engineering & Technology, Bangladesh, e-mail: mehedi.ce.cuet@gmail.com
[2]Student, Chittagong University of Engineering & Technology, Bangladesh, e-mail: jobayathfd@gmail.com
[3]Professor, Chittagong University of Engineering & Technology, Bangladesh, e-mail: sudip@cuet.ac.bd

***Corresponding Author**

ABSTRACT

Unplanned urbanization along with city's changed landscape causes urban drainage changes and also fall short maintaining its capacity. The situation gets even worse because of today's climate change. Urban drainage design and its performance depends on hydro metrological conditions. Because of climatic change, it is already evident that temperature and rainfall pattern changes with increased magnitude is a harsh reality now. So this is necessary to evaluate the consequences and to design the drainage pattern in accordance to climatic change.

This study therefore aims to evaluate the performance of drainage pattern under different land use and climatic conditions. Mahesh khal is taken as a study area, a major drainage canal connected with Karnaphuli River. This study analyses land use pattern of the study area with the data collected through field investigation and also gathered from the secondary sources using ArcGIS 10.4. Chattogram city holds monthly average rainfall of 243.26 mm and therefore totalling 2919.1 mm in a year which is about to increase 5% - 6% by 2030. Out of total 8.59 square kilometres of total land areas 5.12 square kilometres areas of land occupied as vegetation and open areas which was about 59.64% of the total area in 1988 but unfortunately within the 30 years of time span the areas lost its 28.12% of the vegetation and open. Moreover the peak discharge found for 2, 5, 10, 25, 50 and 100 years return period were 19.8, 29.4, 35.8, 44.1, 50.4 and 56.5 m^3/sec.

The study also evaluate the performances varying Curve Number (CN) value, percent (%) impervious, canal bottom materials etc. It has been found that the actual capacity of the canal is 103.85 m^3/sec of which 87.34 m^3/sec discharge contributed due to tidal effect of average peak tidal height of about 3.75 m. The peak discharge decreases with the increase of Roughness Coefficient (Manning's n) values because the canal with high n values indicates high weeds which will give more resistance than a clear canal. But peak discharge increases with the increase of CN value and percent (%) impervious as amount of direct surface runoff increases with the increase of CN value and percent (%) impervious. Rainwater harvesting, recharge well, retention pond etc. may be effectively implemented in mitigation of problematic issues related with urban drainage.

Keywords: *CN, HEC-HMS 4.2, ArcGIS 10.4, Runoff.*

1. INTRODUCTION

Hydrologic cycle is greatly affected with the growth of urbanization in many ways such as increases percent impervious areas(Lee & Chung, 2007;Schuelet, 2000), surface runoff, decreases vegetation and open space, infiltration of runoff into soils and base flow, withdrawing water (Chung, Park & Lee, 2011),water quality replacing indigenous vegetation with irrigated ornamental vegetation etc. This conversation leads to change in physical, chemical and biological disturbance of the watershed of a drainage system. Urban drainage is considered as an essential tools to human being as it contributes to prevent the floods and provides a better way to discharge the surface runoff . Moreover climate also contributes in increasing precipitation, rising temperature and sea levels resulting multiplying the effects of the events (Walega, 2013). Therefore understanding the relation between land development and climate change on storm water runoff is particularly essential from practical point of view and is socially justified (Paule-mercado, Salim, Lee & Memon, 2018; Walega, 2013). Monitoring, analysis and subsequent implementation of the preventive measures in order to integrated management of the urban drainage runoff (Paule-mercado & Lee, 2017; Tsihrintzis & Rizwan, 1998).

Chittagong city is the second largest city of Bangladesh comprising hills formed during tertiary time. Majority of the people along coastal areas living between 0 to 5 meter elevation from mean sea level. It lies at the coastal area and the most prominent natural hazards are cyclone with storm surge, water logging, landslide, earthquake and flash flood are the dominant ones. But at present water logging and landslides are the most burning issues (Islam & Das, 2014). Due to rapid urbanization along with climate change, Chittagong city dwellers are facing water logging problem in last few years. The average rainfall of Chittagong is 3378 mm which is quite high than other locations in Bangladesh. Mostly rainfall occurs between May to October. In July, the rainfall reaches its peak, with an average of 743 mm (BMD, 2017).Naturally hydrological condition of an area comes first as it directly involve in water logging events (Zhang & Pan, 2014). The land use patterns of an area have influences over the hydrological condition while the increasing urbanization reduces water body and natural streams. Chittagong city saw at least 12 canals vanish in the last 48 years, during which time the waterlogging problem accelerated. A mere 22 canals were found to be emptying into the Karnaphuli River and there was no trace of 12 canals in the premier port city where 8 of the 22 existing canals are also dying (Chowdhury, 2017). In recent years, major canals lost 42% carrying capacity due to siltation, with 87% of the existing silt traps being dysfunctional (Hussain, 2017). Over 14,000 ponds and other water bodies have disappeared is last 18 years in Chittagong. According to a survey conducted by District Fisheries Department in 1991, the number of water bodies in Chittagong city was 19,250 while the Featured Survey conducted by CDA in 2006-2007 indicated existence of 4,523 water bodies there. About 100 sq. km. water of Chittagong city is pumped out through five canals- Chaktai khal, Mahesh khal, Sub area khal, Monohar khal and Hizra khal.

The study has undertaken three objectives to know the changes of the urban drainage under different changed climate and land use pattern.

a. To evaluate the changes of drainage network in different land use and climatic conditions
b. To simulate the existing drainage network by using primary data to replicate real scenario.
c. To evaluate the performances of the existing drainage network in different land use and climatic conditions.

2. METHODOLOGY

2.1 Study Area

Mahesh Khal, one of the major khal in Chattagram city connected with the Karnaphuli River is taken as study area as shown in Figure 1. The catchment lies between latitude ($22°17'49.751"N - 22°20'22.2612"N$) and ($91°46'30.6948"E - 91°48'45.2412"E$) and occupies the area about 8.578 Km^2 (857.8 ha) with 16.37% inclination. The canal is located between Sadarghat and Khal 10 station. The study area is classified in 17 catchment (Sub-Basin) and these area is mainly used for commercial and residential purposes. 31.52% of the area is vegetation and open space, 14.97% is

water body and 53.51% is build up area. The length of the canal is about 6.3 Km considered for this study and divided into 6 reaches.

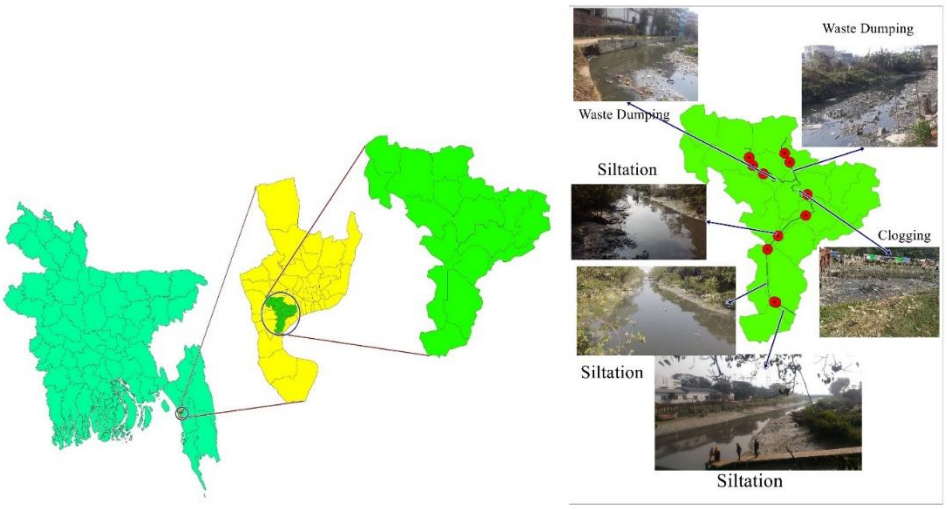

Figure 1: Area showing Mahesh Khal and its physical conditions in different places.

The canal collects the natural flow along with water draining from Sub-Basin area at the upstream and finally discharges into Karnaphuli River at downstream. Total 11 points have been selected for collecting data i.e. cross section, bottom materials, tide table, discharge etc.

2.2 Analogous of Methodology

The methodology as shown in Figure 2 starts with collection of primary and secondary data. Primary data include cross section, side slope, bottom slope, bottom materials, tide level, discharge of the canal also types of land use land cover (LULC), flow path etc. Due to lack of data, the cross sections of the canal were taken manually. Total 11 study points were selected for data collection. The bottom width of the canal was divided into several strips and depth of the bottom of the canal was determined by a rope with a mass attached at the bottom of the rope.

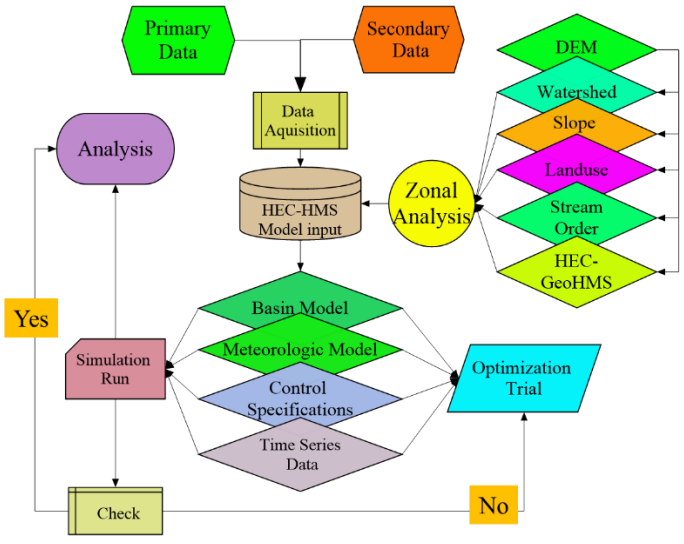

Figure 2: Details Methodology

The length of the canal was determined by ArcGIS 10.4 using field calculator. The average bottom slopes were determined using GPS and adjusted with data found from HEC-GeoRAS. Bottom materials were investigated physically and recorded for the selection of Manning's n. Field land use

and land cover data were recorded in different locations for accuracy assessment of the land use map prepared from DEM by ArcGIS 10.4. Field investigation was done for problem identification, flow pattern of the canals, causes of overflow etc. Secondary data are collected from different sources. Digital Elevation Model (DEM), Land use map, soil data map, precipitation, tide tables, discharge etc. are the main secondary data used for the study. Secondary data and their sources are given in Table 1.

Table 1: Necessary Data Sources of the Study

Data	**Source**	**Address**	**Resolution /Periods /Others**
DEM	United States geological Survey (USGS)	https://earthexplorer.usgs.gov/	30m
Land Use Map	GlobeCover	http://due.esrin.esa.int/page_globcover.php	1 : 500000
Soil Data Map	Food and Agricultural Organization (FAO)	http://www.fao.org/geonetwork/srv/en/metadata.show?id=14116	1000m
Precipitation	National Aeronautics and Space Administration (NASA) Bangladesh meteorological department (BMD)	https://earthdata.nasa.gov/ www.bmd.gov.bd	2018
Water tide table	Chittagong Port Authority (CPA) Bangladesh Navy Hydrographic & Oceanographic Centre (BNHOC)	http://www.cpa.gov.bd/site/view/commondoc/Tide%20Table/ http://bnhoc.navy.mil.bd/?pageid=77	2017, 2018
Discharge	Bangladesh Water Development Board (BWDB)	https://www.bwdb.gov.bd/	2018

The USDA Natural Resources Conservation Service (NRCS) method previous known as SCS has been used for the computation of storm water runoff rates, volumes and hydrograph. The NRCS Curve Number (CN) is the key component of NRCS method which depends on soil permeability, surface cover, hydrologic condition etc. The most commonly used are the June, 1986 Technical release 55 – Urban Hydrology for small watershed (TR-55)(USDA, 1986).

3. RESULTS AND DISCUSSION

3.1 Land Use Analysis

Remote sensing and GIS technique is the most important tool for studying the land use and land cover analysis. Large land area can be mapped with low cost and rapidly with high accuracy. Major three land use classification have been identified for the study area and results are presented in the Table 2 and Figure 3.

The classification process was repeated for respective year. The generated classified land cover map was verified using ground truth data and Google earth. The Figure 3 shows the Land use maps of the Mahesh khal watershed area from the year 1988 to 2018 with different interval. Results obtained from the land cover classification of three types of land use analysis have been shown in Table 2. The results clearly shows that built up areas are increasing in an alarming rate whereas open and vegetation areas are decreasing day by day.

Table 2: Land use analysis of the study area

Type of land use	Area-1988 (%)	Area (sq Km)	Area-2008 (%)	Area(sq Km)	Area-2012 (%)	Area(sq Km)	Area-2018 (%)	Area (sq Km)
Vegetation & open area	59.64	5.1219	48.85	4.19	36.71	3.15	31.52	2.7072
Water	15.34	1.3176	14.37	1.2339	14.41	1.24	14.97	1.2852
Built up	25.02	2.1483	36.78	3.159	48.88	4.20	53.51	4.5954

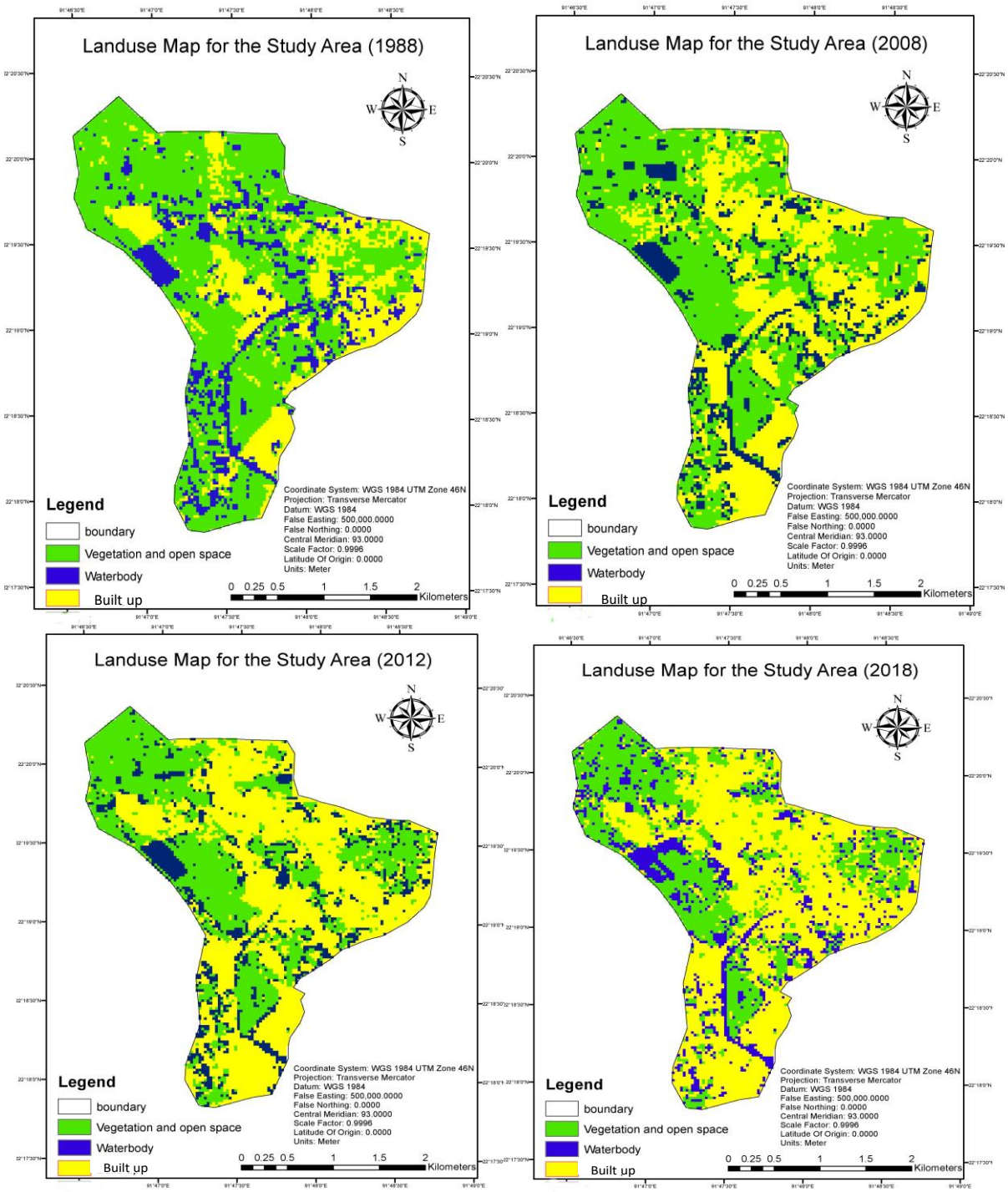

Figure 3: Land use maps of the study area (1988-2018)

From the year 1988 to 2018 the build-up area increased about 28.49%. Initially in the year of 1988 the build-up area was about 2.15 square kilometres which was 25.02% of the total area of 8.59 square kilometres. The trend of change in build-up areas was slower up to 2008 as compared with the changes found later years. The build-up area was about 3.16, 4.20, 4.60 square kilometres for the year of 2008, 2012 and 2018 which is 36.78%, 48.88% and 53.51% of the total area. Out of total 8.59 square kilometres of total land areas 5.12 square kilometres areas of land occupied as vegetation and open areas which posed the highest portion of the total area and was about 59.64% of the total area in 1988. Within the 30 years of time span the areas lost its 28.12% of the vegetation and open areas which can be termed as alarming.

3.2 Data Preparation

The basin and canal parameters were extracted from the attributes table for 17 sub-basins and for canal from ArcGIS 10.4 as prepared earlier and summarized in Table 6.3. Area, slope, percent (%) impervious are directly derived from ArcGIS 10.4. Hydraulic length, initial abstraction, lag time are derived using respective equation's mentioned in methodology chapter. Curve Number (CN) for each sub-basin was used from TR-55 Curve number Tables. The corrected curve number (CN*) found after optimization trials in HEC-HMS.

Table 3: Physical properties of Sub- basins used in model

Basin ID	Basin Area, A (ha)	Slope, H (%)	Hydraulic Length, L (m)	Curve Number, CN	Corrected Curve Number, CN*	Initial abstraction, Ia (mm)	Percent impervious (%)	Lag Time, (min)
S0	30.20	18.85	1523.36	84	79.06	13.45	37	16.38
S1	40.01	22.53	1675.36	80	76.83	15.32	4	17.29
S2	47.46	12.49	1114.83	87	83.56	10.00	63	13.57
S3	48.88	16.59	1134.61	82	78.75	13.71	43	13.92
S4	31.97	13.06	879.52	86	75.85	16.17	73	13.95
S5	32.03	13.74	880.46	87	76.73	15.40	68	13.27
S6	58.89	13.11	1268.81	86	82.59	10.71	56	15.16
S7	35.65	16.99	938.91	82	78.75	13.71	44	11.82
S8	48.87	16.75	1590.26	83	79.71	12.93	38	17.62
S9	19.02	18.11	1044.10	86	82.59	10.71	62	11.04
S10	44.53	16.51	1072.89	85	81.63	11.43	75	12.19
S11	37.32	16.13	965.10	85	81.63	11.43	45	11.33
S12	33.91	21.98	911.22	87	76.73	15.40	37	10.78
S13	40.93	14.30	1019.99	86	82.59	10.71	56	12.19
S14	68.07	13.82	1384.08	83	79.71	12.93	42	17.36
S15	44.13	17.22	1067.12	87	83.56	10.00	78	11.16
S16	74.71	17.78	1463.55	85	81.63	11.43	45	15.06

Reach parameters shown in Table 4 were found through field survey. Length, top width, depth, bottom width, side slope are determined direct measurement in the field. Bottom slopes have been determined using GPS instrument with respect to reduced level and finally validated and adjusted with the data extracted from DEM using 3D analyst in ArcGIS 10.4. Manning's n value used for the canal found from TR-55 Manning's n table and validated in optimization trials in HEC-HMS.

Table 4: Reach parameters used in the model

Reach Name	Length (m)[a]	Top width (m)[b]	Depth (m)[b]	Bottom width (m)[b]	Bottom Slope (m/m)[b]	Side slope (1:z)[b]	Manning's n[c]
R1	557.18	39.01	5.63	6.67	0.0011430	0.35	0.04000
R2	935.75	34.51	4.80	11.57	0.0021100	0.42	0.04500
R3	1196.06	39.22	3.51	10.57	0.0045000	0.24	0.04500
R4	1118.85	33.05	3.71	19.56	0.0051300	0.55	0.07750
R5	1601.93	17.27	3.34	8.06	0.0065400	0.73	0.10000
R6	896.04	10.82	2.87	7.20	0.0063700	1.59	0.07000

[a]DEM
[b]Field Survey
[c]Manning's n chart

Rainfall depths for different return periods have been shown in columns (2), (3), (4), (5), (6) of the Table 5 for the 2, 5, 10, 25, 50 and 100 year respectively. The storm depths are adopted from IDF curve. Others parameter includes total catchment area for the catchment, overland slope, total length of the canal and the time of concentration etc.

Table 5: Parameters used for rainfall depth and watershed in the model

Rainfall depth (mm)[a]						
Present	**2 year**	**5 year**	**10 year**	**25 year**	**50 year**	**100 year**
74.13	91.06	122.62	143.57	169.99	189.58	209.06
Parameters for watershed						
Properties					Value	Unit
Catchment Area, A[b]					8.58	Km^2
Overland Slope, S[b]					16.37	%
Overland Slope, S[b]					163.70	m/Km
Length of the stream, L[b]					6.30	Km
Time of Concentration, Tc[c]					107.24	min

[a]IDF curve
[b]DEM
[c]Rational method

3.3 Validation of the model

Successful implementation of hydrological models mainly depends on how accurately the model is calibrated. Model calibration is done to match the values of runoff volume, peak discharge and time of hydrograph among observed and simulated values. The model calibration can be conducted both automatically and manually. In the present study, automatic calibration known as "Trial Optimization" was used to obtain the optimum parameter values that gives the more similar values among observed and simulated values as manual calibration could be erroneous. The assumed parameters undergoes an iterative adjustments under certain boundary conditions. The calibration was done between simulated and observed discharge. HEC-HMS model basically calibrated using event based simulation.

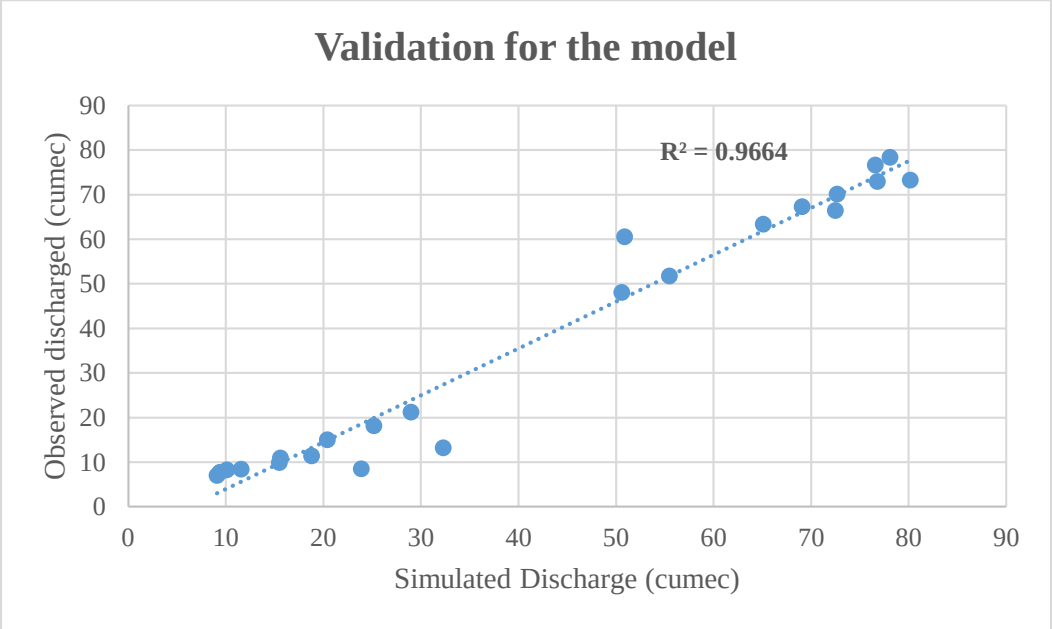

Figure 4: Observed and simulated discharge after calibration

A particular event (24 July, 2018) was selected for calibration of the HEC-HMS model parameters. The hydrograph generated from the model is compared with the observed direct runoff. Two important parameters Curve Number (CN) and manning's n were selected for calibration. Initial and corrected parameter values are show in Table 3. The corrected and calibrated values are considered for the further analysis and performance evaluation of the drainage system. The observed and simulated values were assessed using R^2 indicator and the R^2 value obtained after implementation of all calibrated values for this particular event is 0.9664 which indicates good accuracy of the calibration.

3.4 Performance evaluation based on present situation

For the simplicity, all the performance evaluation was conducted considering metrological effect only. Tidal effect, metrological effect, backwater effect and inflow were not considered. The reasons behind this approach are not availability of sufficient data set, no future master plan for the study area, limitations of the HEC-HMS model, uncertainties etc. The capacity of the canal has been considered subtracting the average peak tide discharge from actual capacity. Hence the capacity for the canal with respect to metrological consider for further performance evaluation. The cross section considered for determination of the actual capacity is the average cross section of the whole canal. The discharge due to tidal effect have considered the average peak discharge available of the canal throughout the year. The result found that the actual capacity of the canal is 103.85 m^3/sec whereas the average peak tidal height along with inflow has been found 3.75m and corresponding discharge due to tidal effect and inflow has been found 87.34 m^3/sec. Hence the capacity with respect to metrological effect is only 16.51 m^3/sec. Such kind of tidal effect cause frequent flooding in these area with limited rainfall.

3.4.1 Performance evaluation for different Curve Number (CN)

Figure 5 illustrates the change of discharge with different CN number varying from 30 to 98 in different return periods. Basically Curve Number (CN) value is a hydrological parameter that used to predict the direct surface runoff. Considering water present in canal for tidal effect, the peak discharge would be within the capacity in present condition and also in 2 years return period for CN values up to 30, 40, 50 respectively but for further increased values of CN, it has found to exceed the carrying capacity limit of the canal. As with the increase of CN values, more direct surfaces runoff occurs and hence the discharge has been found higher for higher values of CN.

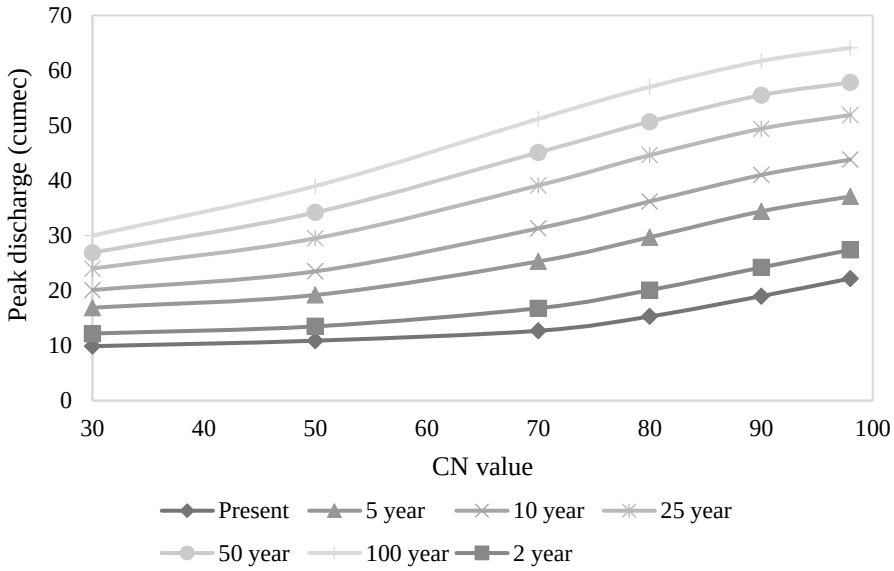

Figure 5: Variation of discharge with CN value in different return periods

The deviation changes at a constant rate in different return periods for a particular CN value. The average values found for 2 and 100 year return periods are 26 m^3/sec and 50.5 m^3/sec respectively with respect to different CN value. The result also shows that the deviation changes more rapidly up to CN value 70 and for further increase of CN value the deviation is almost same. The average discharge value found for CN value 30 and 90 are 20 26 m^3/sec and 43.47 26 m^3/sec respectively.

3.4.2 Performance evaluation for different Percentage impervious

The following graph illustrates the change of discharge with different % impervious land varying from 30% to 98% in different return periods. Percent (%) impervious indicates the area which will contribute 100% surface runoff without any loss (i.e. infiltration, percolation etc.). The discharge increase linearly with the increase of the % impervious as shown in Figure 6. The more impervious areas increases, there will be more surface runoff and hence the discharge would be higher that's why the value increases with the increase of % impervious.

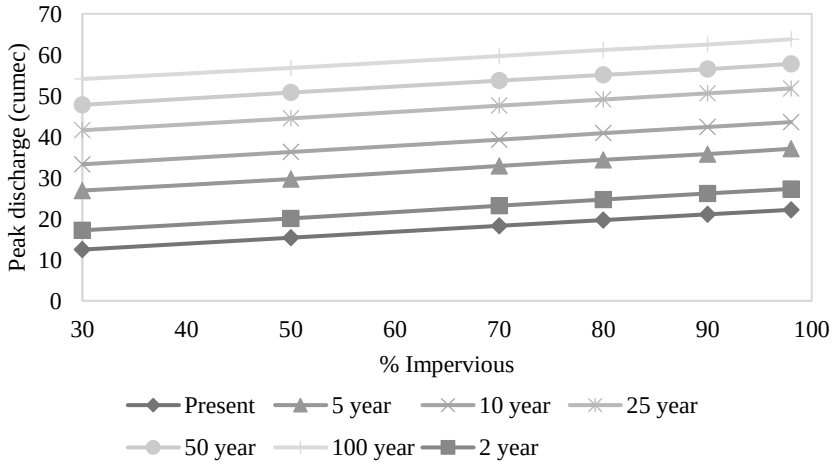

Figure 6: Variation of discharge with % impervious in different return periods

The study also found that average value of discharge for 2 year and 100 year return period have been found 18.2m^3/sec and 59.68m^3/sec respectively. The standard deviation found almost same for all return periods and the value is about 3.78. On the other hand, the average value changes from 33.34 to 43.37 m^3/sec for the % impervious value of 30 and 98. The standard deviation value found almost

same for different % impervious value and the value is about 15.48. The carrying capacity of the canal exceeds almost every values of % impervious for any return periods considering back flow from river.

3.4.3 Performance evaluation in different return periods

The change of discharge with time has been found in the figure 7 for different return periods. For a day period, the maximum discharge has been found from 9am to 2pm. In present situation the maximum discharge value is about 15cumec which increase with the increase of return period and become 55cumec in 100years return period.

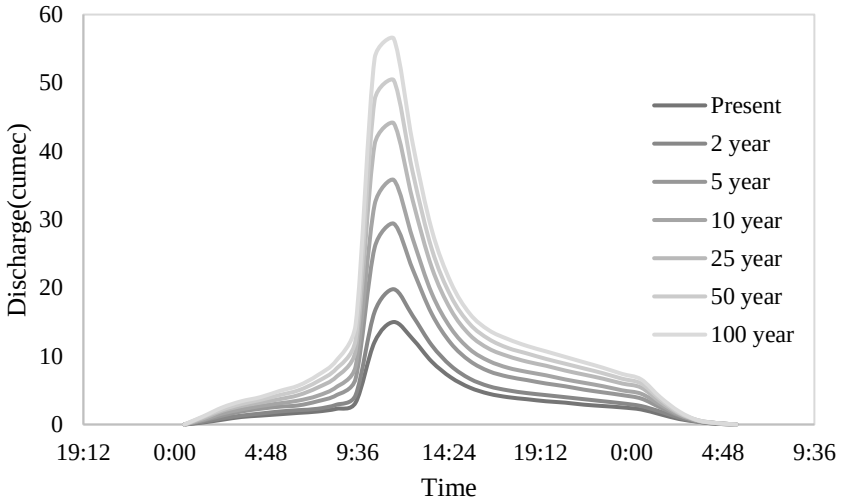

Figure 7: Variation of discharge in return periods.

4. CONCLUSIONS

Rapid growth of urbanization and dense population has great effect on every sector of environment including increased percent impervious areas, surface runoff, decreased vegetation, open space, water quality, and also in physical, chemical and biological disturbance of the watershed of a drainage system. The major findings of this study are given below :

1. The build-up area has increased about 28.49% from the year 1988 to 2018 and lost its 28.12% of the vegetation and open areas. Therefore it can be easily predicted that the build-up areas will increase and reach to above 90% of the total area within short time span if no measures are taken and checked back to ensure sustainable urban planning.
2. Maximum discharge has been found from 9am to 2pm. In present situation the maximum discharge value is about 15cumec which increase with the increase of return period and become 55cumec in 100years return period.
3. The peak discharge found within the capacity in present condition and also in 2 years return period for CN values up to 30, 40, 50 respectively but for further increased values of CN, it has found to exceed the carrying capacity limit of the canal considering water present in canal for tidal effect.
4. The discharge increases linearly with the increase of the % impervious and the carrying capacity of the canal exceeds almost every values of % impervious for any return periods considering back flow from river.
5. Thus, few more improvement required of the next phase of this study incorporating quality of the discharged water and susceptibility of sustainable urban drainage system in Chattogram drainage basin.

REFERENCES

BMD. (2017). Bangladesh Meteorological Department. Retrieved from http://www.bmd.gov.bd/

Chowdhury, M. (2017). Freeing Chittagong of waterlogging is not an easy task: Mayor Nasir. Retrieved November 25, 2019, from https://bdnews24.com/

Chung, E., Park, K., & Lee, K. S. (2011). The relative impacts of climate change and urbanization on the hydrological response of a Korean urban watershed. In *Hydrol. Process.* (Vol. 25, pp. 544–560). https://doi.org/10.1002/hyp.7781

Hussain, A. (2017). Ctg canals on their deathbed, 12 have vanishe. Retrieved December 3, 2019, from http://www.dhakatribune.com/

Islam, R., & Das, S. (2014). *Assessment of Waterlogging and Landslide Vulnerability using CVAT Tool in Chittagong City Corporation area*. Chittagong University of Engineering and Technology. https://doi.org/10.13140/RG.2.2.14575.94885

Lee, K. S., & Chung, E. (2007). Development of integrated watershed management schemes for an intensively urbanized region in Korea. *Journal of Hydro-Environment Research*, *1*, 95–109. https://doi.org/10.1016/j.jher.2007.07.004

Paule-mercado, M. C. A., & Lee, C. (2017). Calibration of the SWMM for a mixed land use catchment in Yongin , South Korea Calibration of the SWMM for a mixed land use and land cover catchment in Yongin , South Korea, (January). https://doi.org/10.5004/dwt.2017.11441

Paule-mercado, M. C. A., Salim, I., Lee, B., & Memon, S. (2018). Monitoring and quanti fi cation of stormwater runo ff from mixed land use and land cover catchment in response to land development. *Ecological Indicators*, *93*(June), 1112–1125. https://doi.org/10.1016/j.ecolind.2018.06.006

Schuelet, T. (2000). The Importance of Imperviousness. *Watershed Protection Technique*, *1*(3), 100–111.

USDA. (1986). Urban Hydrology for Small Watersheds. *United States Department of Agriculture*, *TR-55*.

Tsihrintzis V.A., & Rizwan, H. (1998). Runoff quality prediction from small urban catchments using SWMM. *Hydrological Processe Process*, *12*, 311–329.

Walega, A. (2013). Application of HEC-HMS programme for the reconstruction of a flood event in an uncontrolled basin. *J. Water Land Dev*, *18*(March), I–VI. https://doi.org/10.2478/jwld-2013-0002

Zhang, S., & Pan, B. (2014). An urban storm-inundation simulation method based on GIS. *Journal of Hydrology*, *517*, 260–268. https://doi.org/10.1016/j.jhydrol.2014.05.044

Proceedings of the 5th International Conference on Civil Engineering for Sustainable Development (ICCESD 2020), 7~9 February 2020, KUET, Khulna, Bangladesh (ISBN-978-984-34-8764-3)

A POSITIVE KRIGING APPROACH FOR MISSING RAINFALL ESTIMATION

Nafisa Israt Jaman*[1] and Sajal Kumar Adhikary[2]

[1]Assistant Engineer, Local Government Engineering Department (LGED), Bagerhat Sadar, Bagerhat, Bangladesh, e-mail: nafisajaman29@gmail.com
[2]Professor, Department of Civil Engineering, Khulna University of Engineering & Technology, Khulna-9203, Bangladesh, e-mail: sajal@ce.kuet.ac.bd

***Corresponding Author**

ABSTRACT

Rainfall data provide fundamental input for various water resources management applications such as design of hydraulic structures, water budget analysis, streamflow estimation, flood frequency analysis and flood forecasting. Hydrologists are often required to estimate areal average rainfall over the catchment and/or point rainfall values at ungauged locations from observed sample measurements at neighbouring locations. Conventionally, stochastic spatial interpolation methods such as kriging are the most commonly used methods for estimating missing point rainfall values at any desired locations based on the available recorded values at neighbouring gauges. However, traditional kriging offers a major weakness because it requires a priori definition of the mathematical function for the variogram model that represents spatial correlations among data points and thus significantly impacts the performance of the methods. The robustness of kriging methods heavily depends on how the variogram model is constructed. Another limitation of traditional kriging is that negative kriging weights are often obtained as a part of the solution for satisfying the requirement of unbiased constraints in the kriging algorithm. It is the variogram that determines the magnitudes of negative weights based on the degree of continuity of the variable. Since positive weights cannot be obtained based on the solutions of kriging algorithms in many cases and thereby positive estimates of desired variables (rainfall in this study) in target locations cannot be ensured in many hydrological applications. In such case, negative weights (when assigned to high rainfall values) lead to negative estimates of rainfall values at the target or base station, which does not make any physical sense. Therefore, in this study, a positive kriging approach is presented where negative kriging weights can be eliminated through a technique called 'positive kriging' in the current study. The proposed positive kriging confirms the estimation of positive weights in the traditional ordinary kriging and hence positive estimates in the target or base station. The approach is applied to estimate missing rainfall values at a rain gauge station (Faridpur station in this study) through spatial interpolation using the historical rainfall data from a network of sixteen raingauge stations for a case study area in Bangladesh. The results indicate that Gaussian variogram is identified as the best fitted variogram model and ordinary kriging with the Gaussian variogram model gives the best estimates of the missing rainfall at the base station. This study conclusively proves that the missing rainfall estimation through spatial interpolation by the proposed positive kriging approach could be a viable option to estimate missing rainfall data in the field of hydrology and water resource engineering.

Keywords: *Positive kriging, Variogram model, Base station, Missing rainfall, Raingauge network.*

1. INTRODUCTION

Rainfall is the key climatic variable for most hydrologic analyses for the effective management of water resources systems. However, in practice, missing values frequently occur in rainfall data and the hydrologic analysis is thus hampered by the shortage of consecutive data (De Silva et al., 2007; Simolo et al., 2010). The presence of missing values in the rainfall data in different countries of the world is a common problem for data analysis. Rainfall data may be missing for various reasons such as loss of yearbooks, human errors, wars, fire accidents, occurrence of high floods, occasional interruptions of automatic stations, instrument malfunctions, and network reorganizations etc. (Simolo et al., 2010).

In order to carry out the effective hydrologic analysis, it is essential to estimate the messing value of daily rainfall data. For this purpose, different authors have suggested suitable methods for estimating the missing values for specific countries or regions using several techniques. Because the performance of any method for estimating missing values generally depends on the nature of the missing mechanism, nature of consecutive occurrences of rainfall, nature of neighboring stations, other intrinsic characteristics of the climate variables, etc. (Little and Rubin, 1987).

Conventionally, variance-dependent stochastic interpolation methods, belonging to the general family of kriging, have been widely applied in hydrological sciences for spatial interpolation of hydrologic variables such as rainfall. These methods are based on the principle of minimizing estimation variances at locations where no measurements are available (Adhikary et al., 2016). Kriging in various forms has been used for estimating missing rainfall data at ungauged locations from point measurements available at surrounding stations (Ashraf et al., 1997). Among the various kriging methods, ordinary kriging (OK) remains one of the most preferred stochastic interpolation methods, which has been adopted for estimating missing rainfall values at an ungauged location in a catchment or a region. The performance of OK is highly influenced by the variogram model that represents spatial correlations among data points.

In general, OK does not make sure of getting positive weights and thereby positive estimates of target variable (rainfall in this case) through spatial interpolation. Negative weights can be obtained in OK as a part of the solution for satisfying the requirement of unbiasedness constraints of kriging algorithm (Isaaks and Srivastava, 1989). In case of OK based missing rainfall estimation, negative weights (when assigned to high rainfall values) may lead to the negative estimates of rainfall values at the target or base station, which does not make physical sense. Szidarovszky et al. (1987) and Deutsch (1996) suggest that negative kriging weights should be corrected if it is obtained as a part of the solution. Therefore, a positive kriging approach is presented in the current study where negative kriging weights can be eliminated through a technique called ‘positive kriging’. The proposed positive kriging confirms the estimation of positive weights in the traditional OK and hence positive estimates in the target or base station.

2. POSITIVE KRIGING APPROACH

Kriging, the best linear unbiased estimator, in geostatistics refers to a family of generalized least-square regression methods (Isaaks and Srivastava, 1989; Webster and Oliver, 2007). It helps to estimate the unknown variable values at unobserved locations based on the observed known values at surrounding locations. The general expression of ordinary kriging (OK) to estimate missing value of variable Z in space is given by:

$$Z_{OK}^{m}(x_0) = \sum_{i=1}^{n} w_i^{OK} Z(x_i) \qquad (1)$$

where, $Z_{OK}^{m}(x_0)$ refers to the estimated missing value of variable Z (rainfall in this study) at desired location x_0; w_i^{OK} is the kriging weights associated with the observation at location x_i with respect to

x_0; and n indicates the number of observed data points. The kriging weights w_i^{OK} mainly depend on the fitted variogram model.

The unbiasedness condition in the kriging estimates is ensured by enforcing a constraint on the kriging weights that is expressed by:

$$\sum_{i=1}^{n} w_i^{OK} = 1 \tag{2}$$

However, the unbiasedness condition indicated in Eq. (2) cannot ensure of getting positive kriging weights in the solution of kriging algorithm. Szidarovszky et al. (1987) suggests that inclusion of an additional non-negative constraint for weights, w_i (i.e., $w_i \geq 0$ where i = 1, 2, 3,……., n) in the kriging process confirms the estimation of positive kriging weights.

In this study, a variant of positive kriging technique (Teegavarapu, 2007; Adhikary et al., 2016) was adopted to restrict the kriging weights to non-negative values. The objective function was the difference between the observed and estimated rainfall values by the OK method (using the OK-derived weights) over a given time period. The optimization approach used in the proposed positive kriging technique based on mathematical programming formulation can be expressed as:

Minimize

$$\sum_{j=1}^{n} \left[\sum_{i=1}^{N} \left(w_i Z_i^j \right) - Z_m^j \right]^2 \tag{3}$$

Subject to

$$\sum_{i=1}^{N} w_i = 1 \tag{4}$$

$$w_i \geq 0 \tag{5}$$

where Z_m^j is the observed rainfall value at the target or base station (where estimation is desired), Z_i^j is the observed rainfall at individual stations, *j*, *N* is the number of stations excluding the base station, *n* is the number of days (i.e. the specific time period for which data used in individual stations, *j*).

The objective function described by Eq. (3) minimizes the difference between the observed and kriging based estimates of rainfall values over a period of *n* days. The constraint expressed by Eq. (4) makes sure that the estimate is unbiased whereas the additional inequality constraint defined by Eq. (5) will ensure the computation of non-negative kriging weights. The optimization formulation expressed in Eqs. (3) - (5) was solved using the Microsoft Excel Solver with initial weights obtained by the traditional OK method. The solver uses a generalized reduced gradient (GRG) non-linear optimization algorithm for the optimal solution.

The proposed 'positive kriging' approach is applied to estimate missing rainfall values at a rain gauge station (Faridpur station in this study) through spatial interpolation using the historical rainfall data from a network of sixteen raingauge stations for a case study area in Bangladesh, which is shown in Figure 1. As can be seen from the figure, the study area is located in the central part of Bangladesh and there are seventeen (17) rainfall stations operated by Bangladesh Meteorological Department (BMD) enclosed by the large circle. These 17 stations are considered for the analysis and missing rainfall estimation. Details of these rainfall stations are presented in Table 1. Among all these stations, Faridpur station is taken as a base station, where estimation of missing rainfall values will be carried

out using the known rainfall values of the remaining sixteen (16) rainfall stations. The base station can be defined as a station where it is assumed that rainfall data are missing but rainfall data are actually available in the location (Adhikary et al., 2016). In this way, the estimated rainfall using kriging technique and the observed rainfall data in the base station can be compared to evaluate the efficacy of the method.

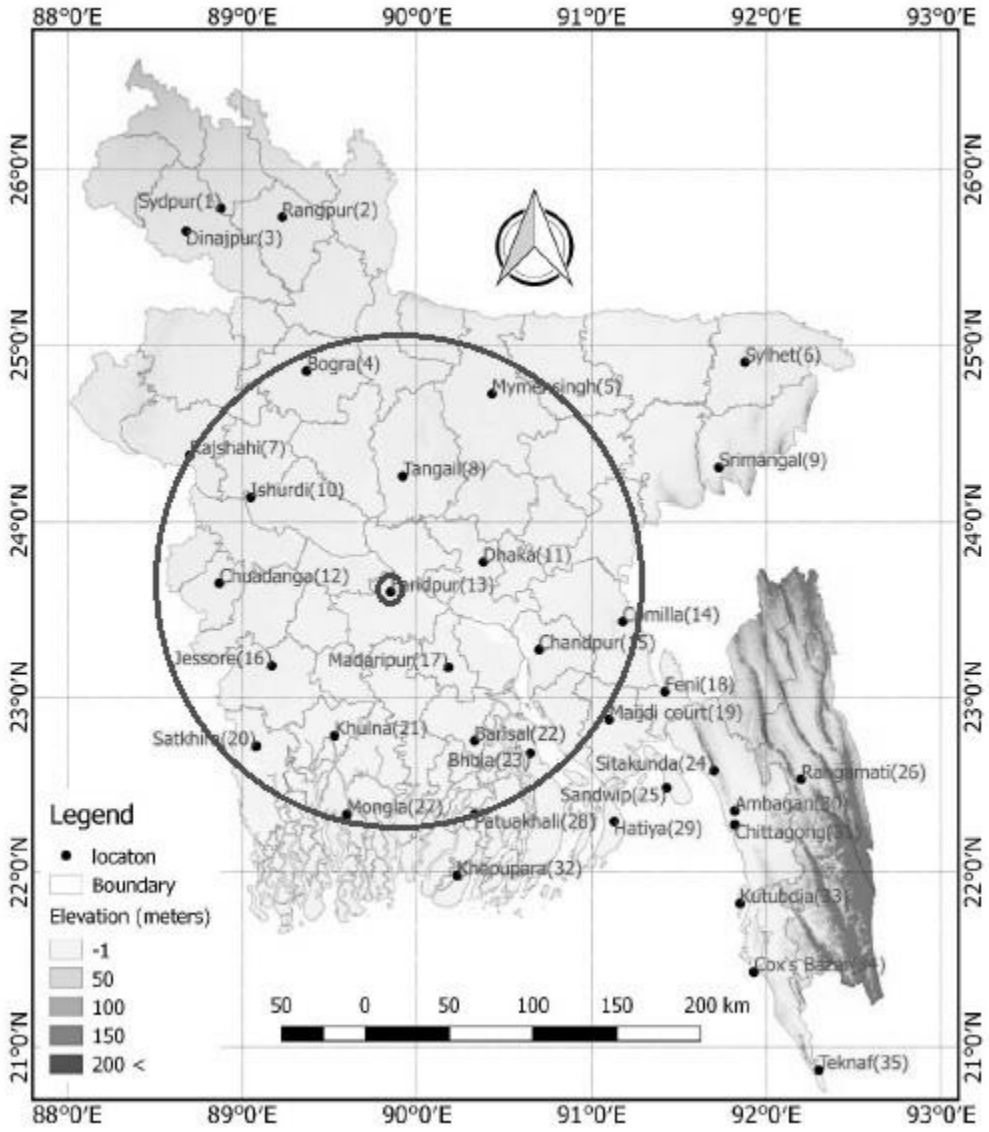

Figure 1: The case study area (enclosed by the large circle) showing the location of rainfall stations (Faridpur is the base station (enclosed by the small circle) at which missing rainfall is to be estimated)

Table 1: Details of raingauge station used in this study

Sl. No.	Station Name	Latitude (Deg)	Longitude (Deg)	UTMX (m)	UTMY (m)
1	Barishal	22.75	90.33	225802.973	2518317.125
2	Bhola	22.68	90.65	258556.565	2510006.493
3	Bogra	24.85	89.37	739490.028	2750420.964
4	Chandpur	23.27	90.70	264720.137	2575275.519
5	Chuadanga	23.65	88.87	690733.691	2616726.444
6	Comilla	23.43	91.18	314058.126	2592296.490
7	Dhaka	23.77	90.38	232982.262	2631224.617
8	**Faridpur***	23.60	89.85	790847.540	2612839.729
9	Ishurdi	24.13	89.05	708327.510	2670143.497
10	Jessore	23.18	89.17	722125.849	2565102.189
11	Khulna	22.78	89.53	759756.056	2521387.708
12	Madaripur	23.17	90.18	211284.241	2565136.011
13	Mongla	22.33	89.60	767814.674	2471663.874
14	Mymensingh	24.72	90.43	240020.327	2736383.727
15	Rajshahi	24.37	88.70	672427.673	2696247.395
16	Satkhira	22.72	89.08	713631.854	2514022.525
17	Tangail	24.25	89.92	796505.415	2685010.465

Note: Faridpur* station is assumed as the base station in the current study, where missing rainfall estimation is to be done.

3. ESTIMATION OF MISSING RAINFALL

3.1 Variogram Modelling

Daily rainfall records from 1980 to 2013 for all seventeen (17) rainfall stations (as shown in Figure 1) are collected from BMD, which are used for the analysis. Summary statistics of collected rainfall data are presented in Table 2. Based on the mean daily rainfall values obtained for all 17 stations, estimation of experimenal variogram is done. Initially, a variogram cloud is carried out and then the variogram cloud is averaged for different lag distances to obtain the experimental variogram.

Table 2: Summary of statistics of collected daily rainfall data

Sl. No.	Station Name	Mean	Std. Dev.	Skewness	Kurtosis
1	Barishal	5.698	15.219	5.112	39.924
2	Bhola	6.208	16.602	5.056	38.674
3	Bogra	4.803	14.330	5.697	49.015
4	Chandpur	5.942	16.790	6.202	65.721
5	Chuadanga	4.057	12.594	6.618	70.911
6	Comilla	5.669	15.768	5.377	47.464
7	Dhaka	5.704	15.809	5.560	54.226
8	**Faridpur**	5.006	14.308	6.098	67.931
9	Ishurdi	4.097	12.050	5.232	39.157
10	Jessore	4.641	13.603	6.190	61.782
11	Khulna	4.963	14.226	7.076	105.753
12	Madaripur	5.396	15.007	5.073	36.572
13	Mongla	5.272	14.071	4.737	31.419
14	Mymensingh	6.196	16.725	5.342	43.926
15	Rajshahi	3.983	12.358	5.971	54.760
16	Satkhira	4.756	13.559	5.859	57.753
17	Tangail	4.950	14.420	5.844	57.526

Finally, the experimental variogram is fitted to a modeled variogram. The most commonly used variogram model included exponential, Gaussian and spherical variogram model functions (Adhikary et al., 2016). They are used to fit the experimental variogram in order to obtain the variogram model. All the best fitted variogram models with the experimental variogram are shown in Figures 2.

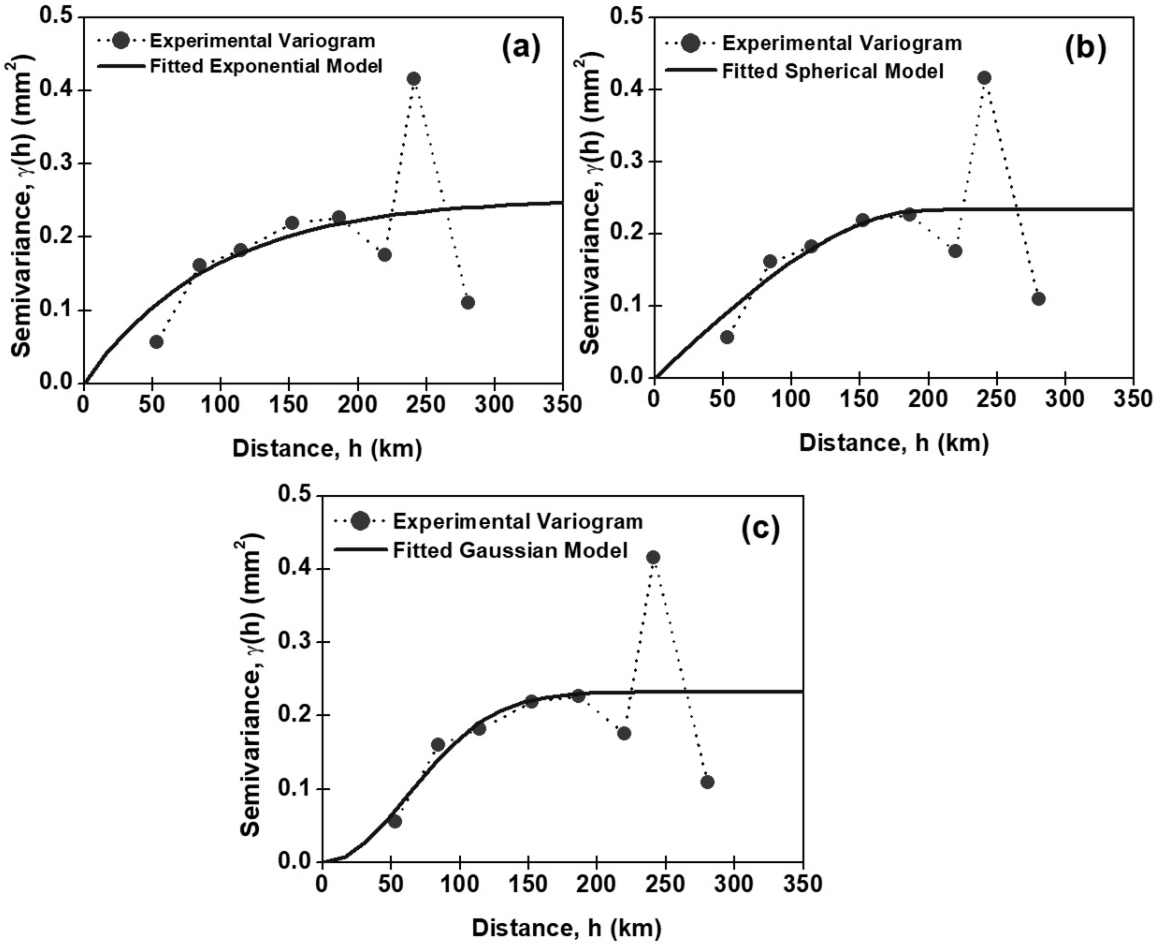

Figure 2: Experimental variogram and best fitted exponential, spherical and Gaussian variogram models for the mean daily rainfall data

While fitting and finding the best fitted variogram models, the corresponding variogram parameters namely, sill, nugget and range are also calculated. Details of the variogram parameters are presented in Table 3. In order to fit the variogram model with the experimental variogram, minimizing the residual sum of squares (RSS) are considered as an objective function. The model which gives the lowest RSS value, is identified as the best fitted model. The variogram modelling and parameters estimation is carried out in the GS+ software platform. As can be seen from Table 3, the Gaussian variogram model gives the lowest RSS value and hence gives the best fitted variogra model. This is also justified from figure 2 and it is seen that the gaussian variogram best fits the first five points of the experimental variogram compared to the remaining variogram models.

Table 3: Summary of variogram parameters of variogram models

Variogram Model	**Nugget (mm^2)**	**Sill (mm^2)**	**Range (Km)**	**RSS**
Exponential variogram	0.0001	0.2532	282.000	0.0562
Spherical variogram	0.0001	0.2332	198.300	0.0536
Gaussian variogram	0.0001	0.2322	150.861	0.0526

Note: RSS = Residual sum of squares

3.2 Estimation of Kriging Weights

After estimating the variogram parameters and identifying all three variogram models including exponential, spherical and Gaussian variogram models, kriging weights are computed by solving the system of simultaneous linear equations in the kriging process. To accomplish this, a spreadsheet application is developed in the Microsoft Excel platform. The estimated kriging weights by different kriging methods including ordinary kriging with exponential variogram model, ordinary kriging with spherical variogram model, and ordinary kriging with Gaussian variogram model are shown in Figures 3.

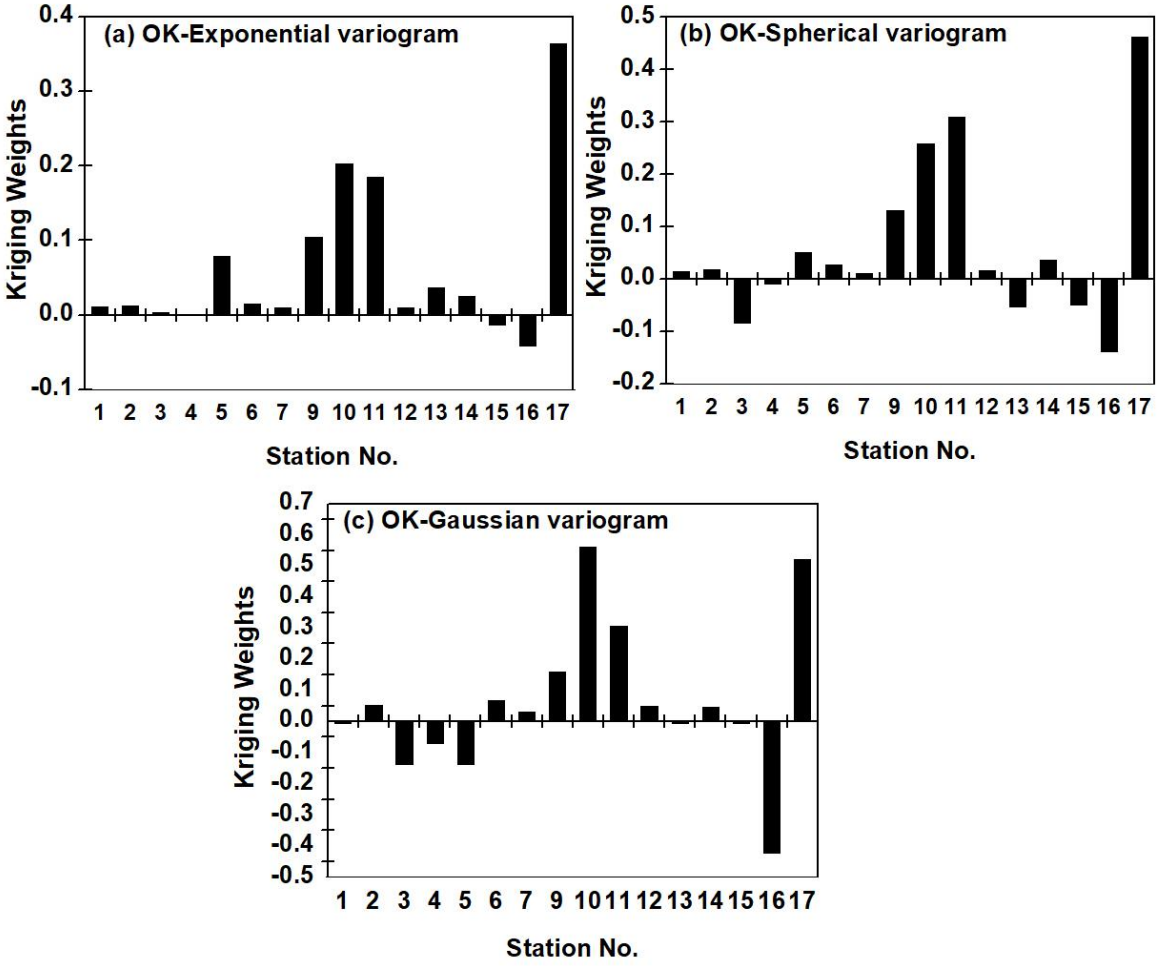

Figure 3: Estimated kriging weights with respect to the base station, rainfall station no. 8 (Faridpur station in this study) using different kriging methods

It is seen from the figure that kriging weights obtained for some of the rainfall stations are negative, which should be made positive before missing rainfall estimation. Since there is no non-negativity constraints in the kriging algorithm, these negative kriging weights are obtained in order to maintain the unbiasedness constraints expressed in Eq. (2). This justifies the development of a new kriging technique, which is referred to as the postive kriging in the current study. In the positive kriging technique detailed in Section 2 and optimization formulation expressed in Eqs. (3) – (5), the inclusion of an additional non-negative constraint for weights, w_i (i.e., $w_i \geq 0$ where i = 1, 2, 3,……., n) in the kriging process confirms the elimination of all negative kriging weights (as shown in Figure 3) and thereby ensures the estimation of positive kriging weights. These positive kriging weights will be used to estimate missing rainfall at the base or target station (Faridpur rainfall station in the current study).

3.3 Estimation of Missing Rainfall

Now, the missing rainfall values at the base station (Faridpur station in this study) are estimated using the positive kriging weights obtained as a solution of the optimization formulation given in Eqs. (3) – (5). The conceptual framework for missing rainfall estimation is presented in Figure 4, where it is assumed that rainfall values are missing at the base station (rainfall station no. 8) although rainfall values are available for that station along with remaining sixteen (16) surrounding rainfall stations. The reason is that in this way the estimated rainfall values by different kriging techniques can be compared with the observed rainfall values to check the efficiency of the different positive kriging techniques in missing rainfall estimation.

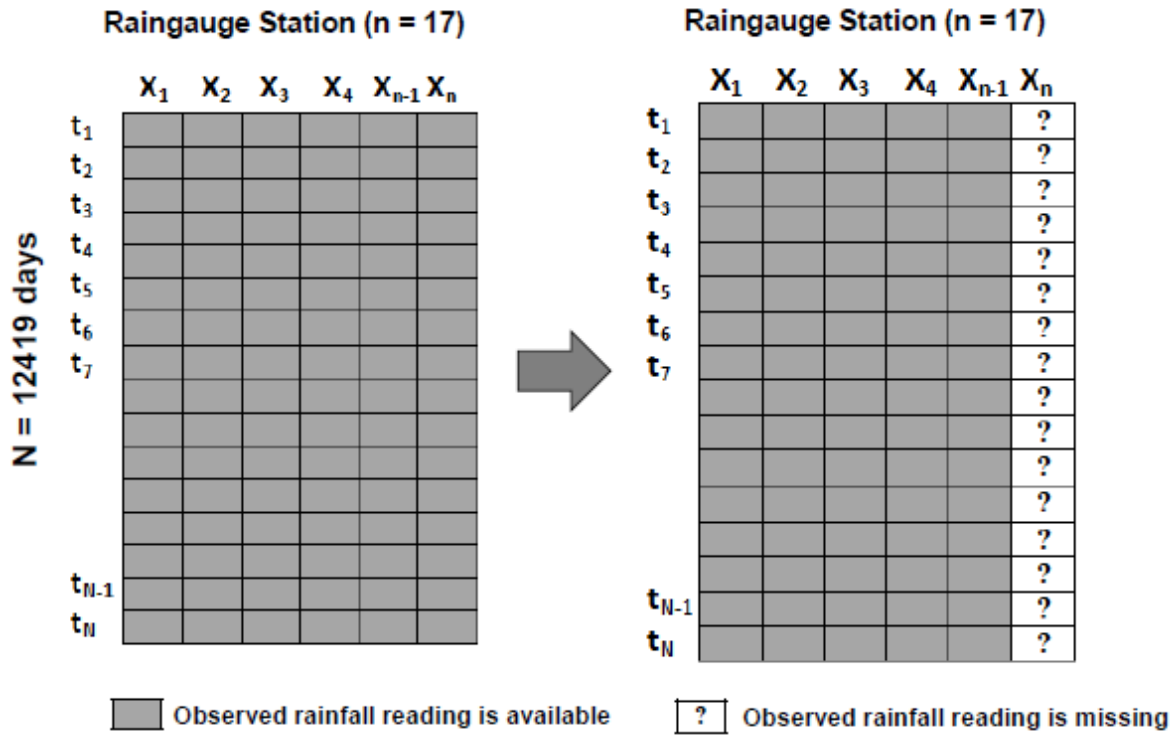

Figure 4: Conceptual framework for missing rainfall estimation at the base station

Now, the observed and estimated rainfall values using different kriging techniques are compared and different error indices are calculated including root mean squared error (RMSE), mean absolute error (MAE) and coefficient of determination (R), which are presented in Table 4. The results presented in Table 4 indicate that ordinary kriging with Gaussian variogram model gives the best estimation with the lowest error and the highest coefficient of determination. Therefore, ordinary kriging with Gaussian variogram model is identified as the best kriging technique for missing rainfall estimation at Faridpur station in this study.

Table 4: Performance of different kriging methods for missing rainfall estimation

Method of Estimation	RMSE	MAE	R
OK-Exponential variogram model	11.747	4.559	0.576
OK-Spherical variogram model	11.775	4.581	0.579
OK-Gaussian variogram model	11.637	4.538	0.591

The estimated and observed rainfall values using different kriging techniques at Faridpur rainfall station is also plotted, which are shown in Figure 5. As can be seen from the figure, a reasonably good

agreement between the observed and the estimated rainfall values is obtained. This ultimately proves the efficacy of the kriging technique for estimating missing rainfall values at ungauged locations.

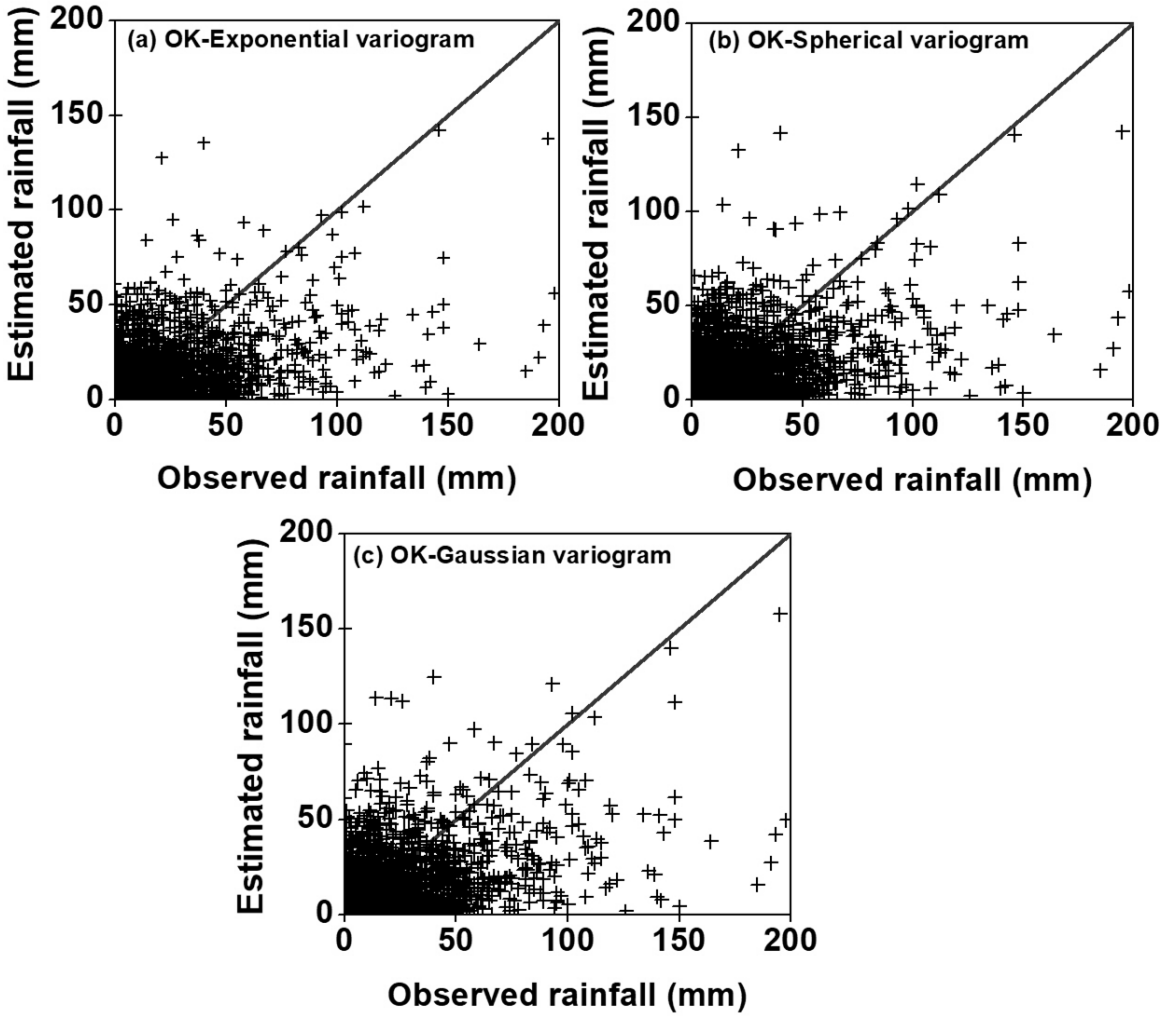

Figure 5: Estimated and observed rainfall values at the base station (Faridpur station in this study) using different kriging methods

4. CONCLUSIONS

In this study, a new variant of kriging called the positive kriging is proposed and adopted to estimate missing rainfall data at the base or target station in a selected area in Bangladesh. Since the traditional kriging does not ensure of getting positive kriging weights, an additional non-negativity constraint has been included and an optimization formulation is developed to achieve the positive kriging weights. The positive kriging weights are used to estimate the missing rainfall values at the base station (Faridpur rainfall station in this study) based on the available rainfall values from sixteen rainfall stations located around the base station. From the experiment, it is obvious that Gaussian variogram is the best fitted variogram model and ordinary kriging (OK) with Gaussian variogram model gives the best estimates of the missing rainfall at the base station. This study conclusively proves that the missing rainfall estimation through spatial interpolation by kriging technique could be a viable option for missing data estimation in the field of hydrology and water resources engineering.

REFERENCES

Adhikary, S.K., Nitin M., & Yilmaz, A.G. (2016). Genetic programming-based ordinary kriging for spatial interpolation of rainfall. *Journal of Hydrologic Engineering*, 21(2), 04015062. DOI: 10.1061/(ASCE)HE.1943-5584.0001300.

Ashraf, M., Loftis. J. C., & Hubard, K. G. (1997). Application of geostatistics to evaluate partial weather station network. *Agricultural and Forest Meteorology*, 84(3-4), 255-271.

De Silva, R.P., Dayawansa, N.D.K., & Ratnasiri, M.D. (2007). A comparison of methods used in estimating missing rainfall data. *Journal of Agricultural Sciences – Sri Lanka*, 3(2), 101–108.

Deutsch, C. V. (1996). Correcting for negative weights in ordinary kriging. *Computers & Geosciences*, 22(7), 765-773.

Isaaks, H. E., & Srivastava, R. M. (1989). *An Introduction to Applied Geostatistics*, Oxford University Press, New York, USA.

Little, J.R.A., & Rubin, D.B. (1987). *Statistical Analysis with Missing Data*. Wiley, New York.

Simolo, C., Brunetti, M., Maugeri, M., & Nanni, T. (2010). Improving estimation of missing values in daily precipitation series by a probability density function-preserving approach. *International Journal of Climatology*, 30: 1564–1576.

Szidarovszky, F., Baafi, E. Y., & Kim, Y. C. (1987). Kriging without negative weights. *Mathematical Geology*, 19(6), 549-559.

Teegavarapu, R. S. V. (2007). Use of universal function approximation in variance-dependent surface interpolation method: an application in hydrology. *Journal of Hydrology*, 332(1-2), 16-29.

Webster, R., & Oliver, M. A. (2007). *Geostatistics for Environmental Scientists* (2nd Ed.), John Wiley & Sons, Chichester, UK.

Proceedings of the 5th International Conference on Civil Engineering for Sustainable Development (ICCESD 2020), 7~9 February 2020, KUET, Khulna, Bangladesh (ISBN-978-984-34-8764-3)

PREDICTION OF GROUNDWATER LEVEL USING ARTIFICIAL NEURAL NETWORK AND MULTIVARIATE TIME SERIES MODELS

Md. Abrarul Hoque*[1] and Sajal Kumar Adhikary[2]

[1]Undergraduate Student, Department of Civil Engineering, Khulna University of Engineering & Technology, Khulna-9203, Bangladesh, e-mail: milon16khan@gmail.com
[2]Professor, Department of Civil Engineering, Khulna University of Engineering & Technology, Khulna-9203, Bangladesh, e-mail: sajal@ce.kuet.ac.bd

***Corresponding Author**

ABSTRACT

Groundwater is the major source of potable water supply in Bangladesh. The overextraction of groundwater and as a consequence, the continued depletion of groundwater level are causes numerous problems such as reducation in freshwater supply, increase in water scarcity, reduction in crop yields, degradation of water quality and impact on human health. Therefore, accurate prediction of grounwater level is of great importance for the efficient management of groundwater resources in Bangladesh. In this study, a framework of predicting the groundwater level fluctuations in the shallow aquifer of Bangladesh using is presented and demonstrated through a case study (Kushtia district of Bangladesh). For this purpose, a groundwater level observation station in each upazilla (sub-district) is selected under the study area. The time series groundwater level data collected on a weekly basis during the period from 1999 to 2006 from the observation station is used for the analysis, model development and prediction. Since most shallow aquifers in Bangladesh is unconfined in nature, the fluctuation of groundwater level is highly influenced by rainfall. With this consideration, both groundwater level and rainfall information are required to be taken into account for accurate prediction of groundwater level fluctuations.

In the current study, artificial neural network (ANN) and autoregressive integrated moving average with exogenous variable (ARIMAX) time series models are adopted in MATLAB platform for modelling and prediction of groundwater level fluctuations. In order to develop ANN and autoregressive integrated moving average (ARIMA) based univariate time series models, only groundwater level data is used. However, the rainfall data is used as an exogenous input to both ANN and ARIMAX based multivariate time series models. Finally, one-week-ahead groundwater level prediction is carried out using the adopted models and the performance of each model is checked through a number of performance evaluation criteria. The results indicate that ANN and ARIMAX based multivariate models give better prediction compared to the ANN and ARIMA based univariate time series models. It is also found that ANN based models generate the best prediction over the ARIMA and ARIMAX time series models and proves its superiority over the time series models for groundwater fluctuation modelling and prediciton. Overall, this study proves the fact that the inclusion of exogenous input is highly effective to achieve the enhanced prediction of groundwater level fluctuations in the field of groundwater hydrology.

Keywords: *Artificial Neural Network, ARIMAX, Time Series, Exogenous Input, Groundwater Level.*

1. INTRODUCTION

Groundwater is one of the major sources of potable water supply all over the world and also used in many purposes such as domestic, agricultural, industrial purposes but this resource is not unlimited. The continuous depletion of groundwater due to its excessive utilization and the fluctuations of ground water are major issues, which causes numerous problems such as water scarcity, impact on crop yields, degradation of water quality etc. In some areas, groundwater can be the only usable sources of water. Prediction of groundwater level could be supportive for the proper management and utilization of this resource in an efficient way and for the design of suitable groundwater improvement projects (Adhikary et al, 2012).

Predicting the groundwater level is vital for the effective planning of the conjunctive use of any aquifer with groundwater and surface water (Nayak et al., 2006). By ensuring the conjunctive use of groundwater and surface water one can get many benefits such as storage of the water will be economical, famine or drought can be easily overcome by the storage of groundwater. Furthermore, it ensures the sustainable utilization of this valuable resource for future generation (Taweesin et al, 2018). At present, Bangladesh is facing extreme pressures on its groundwater resource due to the rapid growth of population, and fast increase of the industrialization, where 80% of population is dependent on the groundwater source for their freshwater supplies. The presence of arsenic in groundwater makes it more challenging. Therefore, detailed analysis and prediction of this resource is indispensable for Bangladesh.

Artificial neural network (ANN), an evolutionary data-driven technique, is frequently used to forecast the fluctuations of groundwater level. An important advantage of ANN models is their capability to adjust recurring alterations and also identify patterns of a complex natural system. ANN models are fast and dependable, also produce results analogous to conceptual models, and these models can mine the complex nonlinear relationships between the inputs and outputs, in a process deprived of the physics being explicitly provided (Adhikary et al., 2018). It has been proven to be effective in modelling any nonlinear function with an arbitrary degree of accuracy and the main advantage of this method over traditional methods is that it does not need the complex nature of the process under consideration to be explicitly defined in mathematical form, this makes ANN model is a good tool for modelling water level fluctuations (Nayak et al., 2006).

Forecasting of groundwater level by ANN technique is carried out by several researchers (e.g., Daliakopoulos et al, 2005; Sreekanth et al, 2009; Taormina et al, 2012). Due to its several advantages, ANN models have been applied in many fields including water table depth fluctuation forecasting (Patle et al, 2015; Coulibaly et al., 2001), rainfall forecasting (Luk et al., 2001), salinity estimation and forecasting in rivers (Maier & Dandy, 1996), streamflow forecasting (Adhikary et al., 2018), and rainfall-runoff modelling (Dawson and Wilby, 1998; Hsu et al., 1995). It is widely recognized that like many other factors, the groundwater level in shallow unconfined aquifer is highly influenced by rainfall and thus, rainfall should be considered as an exogenous input for grounwater level modelling and prediction. Therefore, the aim of the current study is to use ANN and multivariate time series models using groundwater level and rainfall variables for groundwater level fluctuation modelling and prediciton in Kushtia district of Bangladesh. In this study, a feed-forward multilayer perceptron (MLP) ANN model and and autoregressive integrated moving average with exogenous variable (ARIMAX) multivariate time series models are adopted for modelling and prediction of groundwater level fluctuations.

2. METHODOLOGY

2.1 Study Area and Datasets

Kushtia district of Bangladesh is selected as a study area in this study, which is showin in Figure 1. A larger part of the Ganges-Kobadak irrigation project (also known as the G-K project) is located in this area. Five groundwater (GWL) monitoring wells with a rainfall station in the study area are selected

from each upazila (sub-district) of Kushtia to carry out the study. The frequency of GWL data collection is a week. So, weekly time series GWL data from 1999 to 2006 with 414 data points are collected from the Bangladesh Water Development Board (BWDB). As mentioned earlier, the rainfall will be used as an exogenous input for model development, rainfall data for the same period is collected from the BWDB. Details of the collected are presented in Table 1 and the locations of the GWL monitoring stations are shown in Figure 1.

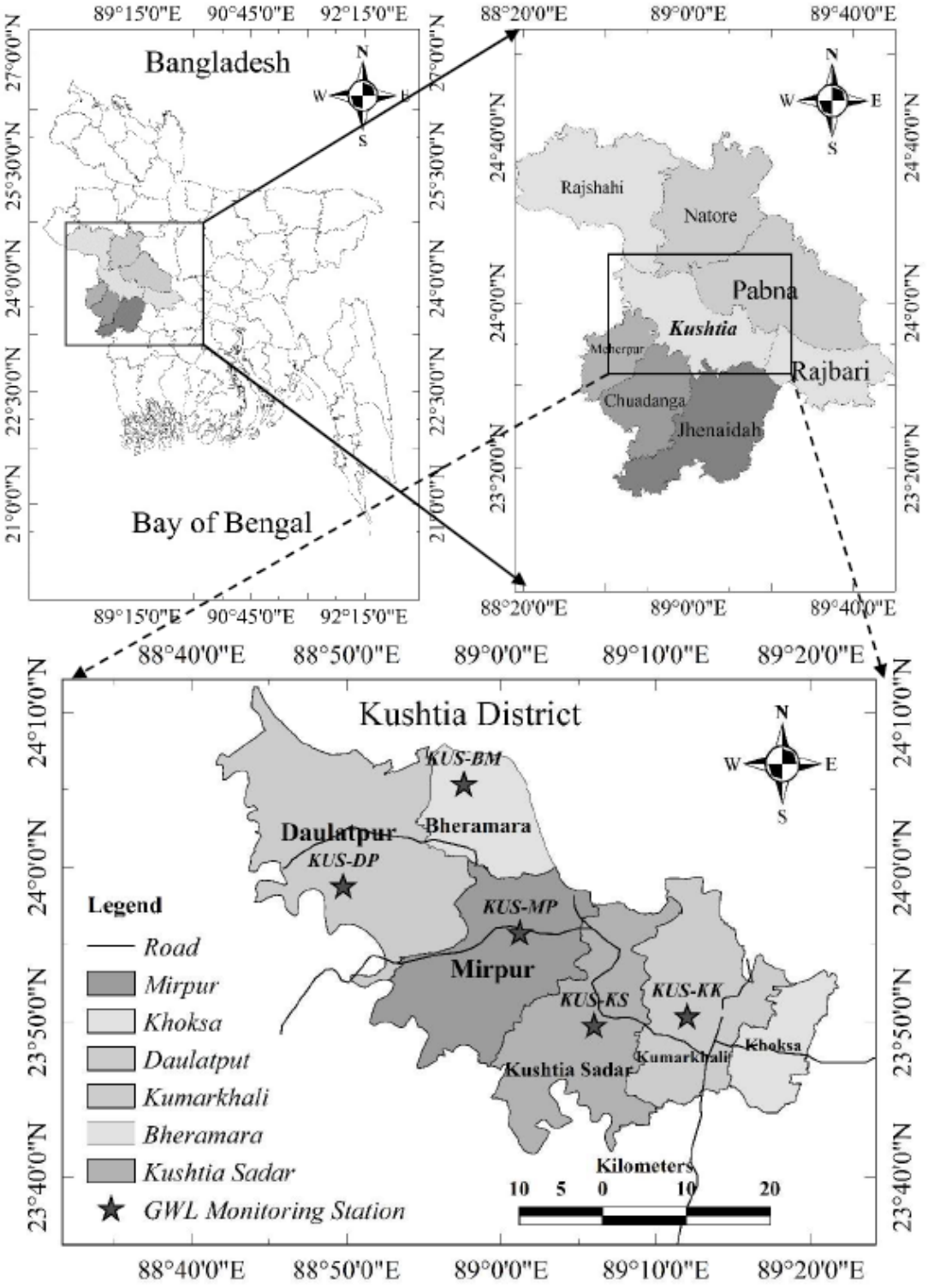

Figure 1: Study area with the location of GWL monitoring stations

Table 1: Details of GWL and Rainfall monitoring stations

ID	Latitude	Longitude	Location
Well ID			
KUS-BM	24.09	88.96	Bheramara, Kushtia
KUS-DP	23.98	88.83	Daulatpur, Kushtia
KUS-KS	23.83	89.10	KushtiaSadar Kushtia,
KUS-KK	23.84	89.20	Kumarkhali, Kushtia
KUS-MP	23.93	89.02	Mirpur, Kushtia
Rainfall Station ID			
RF	24.05	88.99	Mirpur, Kushtia

2.2 ANN Model

In this study, one week ahead GWL modelling and prediction is carried out using the ANN model. The steps involved are preparation of datasets, division of data for model training, validation and testing purposes, selection of the best ANN architectures and finally validation and testing of the developed ANN model. Different ANN architectures have been analyzed to identify the best ANN architecture for modeling testing and evaluation of the model performance. The GWL data is used for developing univariate ANN model whereas rainfall data is used as an exogenous variable along with the GWL data to develop the multivariate ANN model in the current study. Finally, the performance of each model is evaluated through some model performance criteria. The ANN model development is performed in the neural network toolbox of MATLAB platform.

In this study, a multilayer perceptron (MLP) feed forward ANN model is adopted. The architecture of a typical ANN model consists of an input layer, a hidden layer and an output layer, which is shown in Figure 2. In this study, sigmoid activation function is used in the hidden layer of ANN model with the linear activation function in the output layer. The input and output variables are standardized between 0 and 1, to make them fall within a specified range following the ANN modelling framework.

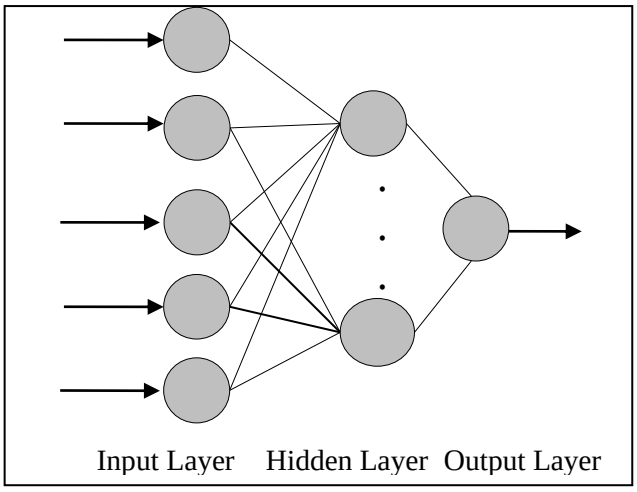

Figure 2: A typical architecture of an ANN model

In ANN modelling, data are generally divided into three categories including training, validation and testing. In this study, the data are divided in the proportion of 70% for training the ANN model, 15% for the ANN model validation and the remaining 15% for testing of the ANN model. The training dataset is used to train the ANN model and the validation dataset is used during the training process to avoid overtraining problem in the model, while validation error rises for a specified number of iterations then the training is stopped (Adhikary et al., 2018). In general, large numbers of data points are used in training because it can capture the patterns exist in the dataset. ANN models are trained by

adjusting the values of the connection weights between the network components (Sreekanth et al., 2009). Back-propagation algorithm is used to train the ANN model, it adjusts the weights and biases in the backward direction, which are fixed random value to the same results every time. There are many training algorithms have been developed for back propagation. The widely used Levenberg-Marquardt (LM) back propagation algorithm is used in this study. To stop the back-propagation 1000 epochs are used.

2.3 ARIMAX Model

An ARIMAX multivariate time series model is simply a combinaton of a univariate autoregressive integrated moving average (ARIMA) time series model and exogenous variables, X. Since ARIMA model is a univarate model, it does not contain any exogenous variable. On the other hand, the ARIMAX models contain one or more exogenous variables. The ARIMAX model has some certain advantages over ARIMA model and thus widely used for model development and prediction purposes. It is suitable for forecasting when data is multivariate, stationary or non-stationary, contains any type of data form such as seasonality, periodicity, trend etc. A few studies have been conducted for grounwater level modelling and prediction in Bangladesh (e.g., Adhikary et al., 2012) but no studies have been found using ARIMAX model for prediciton purpose. Therefore, an attemp has been made in the current study to adopt ARIMAX model for modelling and prediciton of groundwater level fluctuations. The development of ARIMA and ARIMAX models are performed in the econometric toolbox of MATLAB platform.

In this study, one week ahead GWL modelling and prediction is also carried out using the ARIMA and ARIMAX models. The GWL data is used for developing univariate time series model using ARIMA modelling technique whereas rainfall data is used as an exogenous variable along with the GWL data to develop the multivariate time series model using the ARIMAX modelling technique in this study. Finally, the performance of each model is evaluated through some model performance criteria.

2.4 Model Evaluation Criteria

Different performance evaluation criteria have been used to assess the efficacy of the adopted modelling techniques. The mean squared error (MSE) and Nash-Sutcliffe efficiency (NSE) expressed in Eqs. (1)-(2) are used in this study to evaluate the performance of the adopted ANN and ARIMAX models in groundwater level modelling and prediction. The model with the lowest MSE and with the highest NSE is selected as the best model in each case.

$$NSE = 1 - \frac{\sum_{q=1}^{n}[Y_{obs}(q) - Y_{est}(q)]^2}{\sum_{q=1}^{n}[Y_{obs}(q) - \overline{Y}_{est}(q)]^2} \qquad (1)$$

$$MSE = \frac{\sum_{q=1}^{n}[Y_{obs}(q) - Y_{est}(q)]^2}{n} \qquad (2)$$

Where Y_{obs} is the observed data, Y_{est} is the estimated data, $\bar{Y}_{est}$ is the mean value of the estimated data and n is the number of observations.

In order to evaluate the ARIMA and ARIMAX models, two commonly used criteria such the Akaike information criterion (AIC) and Bayesian information criterion (BIC) are additionally used along with the MSE. The model with the lowest MSE, AIC and BIC gives the best model.

3. RESULTS AND DISCUSSION

In this study, the GWL and rainfall data are prepared with a five weeks lag, which generates a total of ten inputs for multivariate case and five inputs for univariate case and by using that data, one week ahead GWL modelling and prediction is carried out using the ANN, ARIMA and ARIMAX models. The model can be characterized by the structure (architecture), training methods or algorithms, neurons, number of layers, inputs, weights, outputs and activation functions. In this study, only one single layer is used because it is often adequate for fitting multi-dimensional mapping problems with satisfactory neurons (Wu et al., 2005). Large number of neurons in the hidden layer may cause over fitting (Adhikary et al, 2018). Hence, the optimum number of hidden neurons should be determined during the ANN model development. The optimum number of neurons in the hidden layer is determined by trial and error method by varying the number of hidden neurons from 2 to 10, which was found satisfactory in this study.

For all five stations, ANN models with exogenous input (rainfall in this study) are developed. The models are trained and validated and finally, tested. The performance of each model is evaluated based on the evaluation criteria indicated above. The best ANN models identified for all GWL monitoring stations for both multivariate and univariate cases with their performance measures is presented in Table 2. It can be seen from the table that the best ANN model for KUS-BM, KUS-DP, KUS-KK, KUS-KS and KUS-MP are 10-6-1, 10-3-1, 10-2-1, 10-4-1 and 10-6-1, respectively.

Table 2: Details of the ANN multivariate models for all five GWL stations in the study area

Well ID	**ANN model architecture**	**Model performance**	
		MSE	**NSE**
Multivariate ANN models			
KUS-BM	10-6-1	**0.0316**	**0.9848**
KUS-DP	10-3-1	0.0595	0.9567
KUS-KK	10-2-1	0.0849	0.9817
KUS-KS	10-4-1	0.0538	0.9653
KUS-MP	10-6-1	0.0326	0.9843
Univariate ANN models			
KUS-BM	5-9-1	**0.0291**	**0.9860**
KUS-DP	5-7-1	0.0392	0.9714
KUS-KK	5-9-1	0.0702	0.9849
KUS-KS	5-10-1	0.0754	0.9515

The models developed for all five selected GWL stations in the study area using the ARIMA or ARIMAX techniques are presented in Table 3. As can be seen from the table, the best time series model for multivariate case is ARIMAX (3,0,2) whereas the best univariate time series model is ARIMA (2,0,1). It is also identified that the performance of the ANN models are better than the ARIMA or ARIMAX models. This justifies the application of ANN modelling technique in the current study.

Table 3: Details of the ARIMAX and ARIMA time series models for all five GWL stations

Well ID	Model structure	Model performance		
		MSE	AIC	BIC
ARIMAX multivariate time series models				
KUS-BM	ARIMAX (3,0,3)	0.03738	-166.485	-130.318
KUS-DP	ARIMAX (3,0,2)	0.04555	-87.1871	-55.0384
KUS-KK	ARIMAX (2,0,1)	0.15456	411.9365	436.0627
KUS-KS	ARIMAX (1,0,3)	0.06162	35.10959	63.27372
KUS-MP	ARIMAX (3,0,2)	0.03685	-174.354	-142.206
ARIMA univariate time series models				
KUS-BM	ARIMA (2,0,1)	0.04159	-131.619	-111.491
KUS-DP	ARIMA (2,0,1)	0.06493	52.7996	72.929
KUS-KK	ARIMA (3,0,1)	0.15599	417.701	441.856
KUS-KS	ARIMA (2,0,3)	0.06813	76.755	104.936
KUS-MP	ARIMA (2,0,1)	0.04006	-147.101	-126.971

4. CONCLUSIONS

In this current study, an attempt has been made for modelling and prediction of groundwater level fluctuation for five selected monitoring wells in Kushtia district of Bangladesh. For this purpose, artificial neural network (ANN) and autoregressive integrated moving average (ARIMA) with exogenous variable (ARIMAX) multivariate time series models are adopted. Model development and analysis are carried out in the neural network toolbox for ANN model and in the econometric toolbox for the ARIMA and ARIMAX models in MATLAB platform. In order to develop ANN and autoregressive integrated moving average (ARIMA) based univariate time series models, only groundwater level data is used. However, the rainfall data is used as an exogenous input to both ANN and ARIMAX based multivariate time series models. Finally, one-week-ahead groundwater level prediction is carried out using the adopted models and the performance of each model is checked through a number of performance evaluation criteria. The results indicate that ANN and ARIMAX based multivariate models generate better prediction compared to the ANN and ARIMA based univariate time series models. It is also found that ANN based models give the best prediction over the ARIMA and ARIMAX time series models and proves its superiority over the time series models for modelling and prediction of groundwater level fluctuations.

REFERENCES

Adhikary, S. K., Muttil, N., & Yilmaz, A. G. (2018). Improving streamflow forecast using optimal rain gauge network-based input to artificial neural network models, *Hydrology Research*, 49(5), 1559-1577.

Adhikary, S. K., Rahman, M., & Gupta, A. D. (2012). A stochastic modelling technique for predicting groundwater table fluctuations with time series analysis, *International Journal of Applied Science and Engineering Research*, 1(2), 238-249.

Coulibaly, P., Anctil, F., Aravena, R., & Bobée, B. (2001). Artificial neural network modeling of water table depth fluctuations, *Water resources research*, 37(4), 885-896.

Daliakopoulos, I. N., Coulibaly, P., &Tsanis, I. K. (2005). Groundwater level forecasting using artificial neural networks, *Journal of hydrology*, 309(1-4), 229-240.

Dawson, C. W., &Wilby, R. (1998). An artificial neural network approach to rainfall-runoff modelling, *Hydrological Sciences Journal*, 43(1), 47-66.

Hsu, K. L., Gupta, H. V., &Sorooshian, S. (1995). Artificial neural network modeling of the rainfall-runoff process, *Water resources research*, 31(10), 2517-2530.

Luk, K. C., Ball, J. E., & Sharma, A. (2001). An application of artificial neural networks for rainfall forecasting, *Mathematical and Computer modelling*, 33(6-7), 683-693.

Maier, H. R., & Dandy, G. C. (1996). The use of artificial neural networks for the prediction of water quality parameters, *Water resources research*, 32(4), 1013-1022.

Nayak, P. C., Rao, Y. S., & Sudheer, K. P. (2006). Groundwater level forecasting in a shallow aquifer using artificial neural network approach, *Water resources management*, 20(1), 77-90.

Patle, G. T., Singh, D. K., Sarangi, A., Rai, A., Khanna, M., &Sahoo, R. N. (2015). Time series analysis of groundwater levels and projection of future trend, *Journal of the Geological Society of India*, 85(2), 232-242.

Sreekanth, P. D., Geethanjali, N., Sreedevi, P. D., Ahmed, S., Kumar, N. R., &Jayanthi, P. D. (2009). Forecasting groundwater level using artificial neural networks, *Current Science*, 96(7), Paper ID: 00113891.

Taormina, R., Chau, K. W., &Sethi, R. (2012). Artificial neural network simulation of hourly groundwater levels in a coastal aquifer system of the Venice lagoon, *Engineering Applications of Artificial Intelligence*, 25(8), 1670-1676.

Taweesin, K., Seeboonruang, U., &Saraphirom, P. (2018). The influence of climate variability effects on groundwater time series in the lower central plains of Thailand, *Water*, 10(3), 290.

Proceedings of the 5th International Conference on Civil Engineering for Sustainable Development (ICCESD 2020), 7~9 February 2020, KUET, Khulna, Bangladesh (ISBN-978-984-34-8764-3)

ANALYZING LONG-TERM TRENDS IN MONTHLY AND ANNUAL RAINFALL OVER WESTERN PART OF BANGLADESH

Zarin Tasnim*[1] and Sajal Kumar Adhikary[2]

[1]Undergraduate Student, Department of Civil Engineering, Khulna University of Engineering & Technology, Khulna, Bangladesh, e-mail: zarintasnim.zt3@gmail.com
[2]Professor, Department of Civil Engineering, Khulna University of Engineering & Technology, Khulna, Bangladesh, e-mail: sajal@ce.kuet.ac.bd

***Corresponding Author**

ABSTRACT

Rainfall is the key climatic variable that governs the regional hydrologic cycle and availability of water resources. The climatic variability is referred to the long-term changes in rainfall, temperature, humidity, evaporation, wind speed and other meteorological parameters. In order to identify the change, quantification of environmental change is necessary that will be supportive to make forecast for future. This will result into a better planning and awareness for natural disasters. The objective of the study is to examine the rainfall variability over the western part of Bangladesh. This will give an understanding about trends or changes in rainfall over the studied region. In the current study, trend analysis has been carried out on monthly and annual rainfalls for the selected eleven rainfall stations located within the western part of Bangladesh. The well-known statistical trend analysis techniques including Mann-Kendall test and Sen's slope estimator are used to detect trends at the 5% significance level on time series data of the study area for the time period from 1948 to 2014. These tests are adopted to identify the change in magnitude and direction of existing trend over time. The analysis for trend detection using the Mann-Kendall test and Sen's slope estimator is undertaken in the XLSTAT 2016 platform. Trend detection of rainfall using the adopted techniques over 65 years shows increasing trend in monthly rainfall for four rainfall stations, namely Satkhira, Khulna, Jessore and Ishurdi stations. Three of them are located in the southwest coastal part of the study area. Furthermore, the analysis indicates similar trend in annual rainfall and the increasing trend is evidenced for three rainfall stations, namely Satkhira, Khulna and Ishurdi stations in which two are located in the coastal part. The findings of this analysis would be of interest to water resources managers and policy makers for the effective planning and management of water resources in Bangladesh.

Keywords: *Ranfall trend, Rainfall variability, Mann-Kendall test, Sen's slope, XLSTAT.*

1. INTRODUCTION

Water resource has become a major concern for any change and development including food manufacture, effective management and controlling of floods. Potential changes in climate might impact rainfall trend, which ultimately affects the overall water availability along with the drought risk as well as floods increases. Intergovernmental Panel on Climate Change (IPCC) demonstrates that the temperature has increased by 0.74°C ± 0.18°C throughout the most recent 100 years. In additiona, rainfall is expected to increase by 0.2 to 0.3% every period over zones of land in 21st century (IPCC, 2007). To address environmental changes and its effects on the various parts, the impact of climate change on agriculture, increased water shortages, rapid melting of glaciers and decrease in streamflows should be properly assessed.

Rainfall is the key climatic variable that governs the regional hydrologic cycle and availability of water resources. This is also an important parameter that can indicate the evidence of climate change. The climatic variability is referred to the long-term changes in rainfall, temperature, humidity, evaporation, wind speed and other meteorological parameters. In order to identify the change, quantification of environmental change is necessary that will be supportive to make forecast for future. This will result into a better planning and awareness for natural disasters.

Rainfall and its intensity are vital factors on the climate of Bangladesh for agricultural production (Shahid, 2010a). The total economy of this country highly depends on rainfall. A slight change in rainfall patterns can cause a blessing or misfortune for this country. The variability and trends in rainfall and temperature patterns have been documented by many researchers in Bangladesh (Bhuyan et al., 2018; Shahid, 2010a; Shahid, 2010b). However, none of the studies have been found specific to the western part of Bangladesh, which is an important region of the country from the socio-economic point of view.

The objective of the study is to examine the rainfall variability and trends over the western part of Bangladesh. Detection of trends in rainfall in various scales will give an improved understanding to the issues related with flood inundations and scarcities of water for utilizing in different climatic conditions. Assessment of rainfall and analysis of annual maximum daily rainfall would upgrade the management of water resources as well as the viable utilization of water resources (Mondal et. al., 2013). In the current study, trend analysis has been carried out on monthly and annual rainfalls for the selected eleven (11) rainfall stations located within the western part of Bangladesh. Since the impact of climate change on rainfall is also a serious concern to water resources managers and policy makers, a trend analysis of the extreme rainfall events is also undertaken in the current study.

2. STUDY AREA AND DATA USED

The rainfall is highly variable in the western part of Bangladesh. Particularly, this part of the country experiences the shortages of rainfall compared to other parts of the country and thus frequent droughts occur in this region (Shahid & Behrawan, 2008). Furthermore, the coastal belt in this part of the country faces severe problems of water salinity and freshwater shortages. The potential impact of climate change may aggravate the problems in this part of the country (Hossain, 2014). Therefore, the western part of Bangladesh is selected as a case study area in this study for long-term rainfall trend analysis. It could be helpful for setting up future water management plans and strategies.

In the trend analysis, one of the limitations is the use of short dataset to assess the variability of rainfall in time. If the dataset is not long enough it is difficult to determine whether the observed trends in rainfall data series are due to natural fluctuations in the weather and climate or whether the atmospheric forcing has experienced (anthropogenic/deterministic) a change (Hajani et al., 2017). Therefore, daily rainfall data for a period of 65 years from 1948 to 2014 for eleven (11) rainfall stations located in the study area is obtained from the Bangladesh Meteorological Department (BMD). Details of those stations are presented in Table 1. Table 1 also presents the duration of records used for trend analysis for each rainfall station. This daily rainfall data is used to calculate the monthly and

annual rainfall data series, which is finally used for estimating long-term trend in the monthly and annual rainfall series. The locations of the selected eleven rainfall stations in the study area are shown in Figure 1.

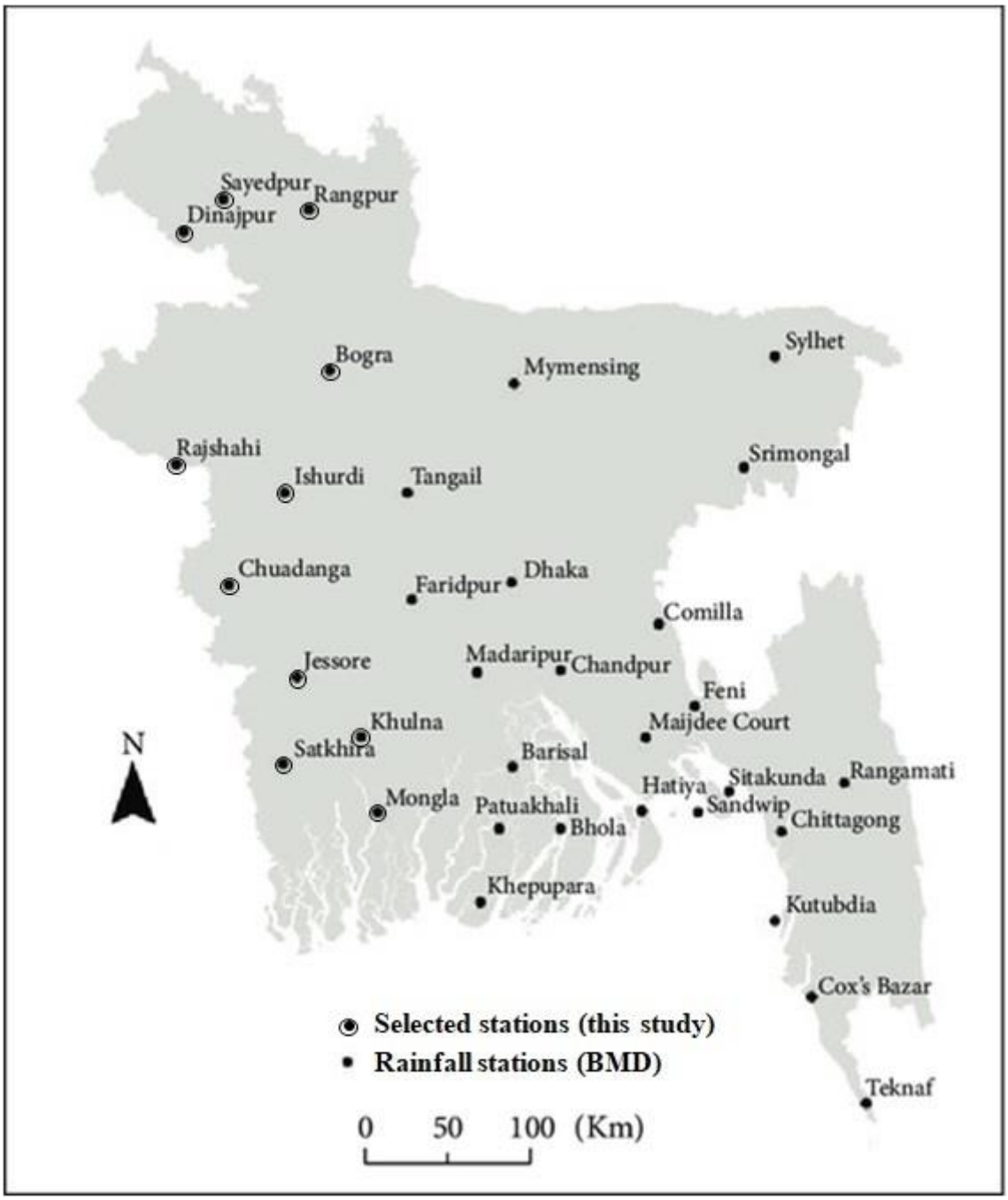

Figure 1: The study area (western part of Bangladesh) with location of rainfall stations

Table 1: Details of rainfall stations used for trend analysis in this study

SN	Station Name	Latitude (N)	Longitude (E)	Elevation (m)	Data Period
1	Bogra	24˚51′	89˚22′	17.9	1948-2014
2	Chuadanga	23˚39′	88˚49′	11.58	1989-2014
3	Dinajpur	25˚39′	88˚41′	37.58	1948-2014
4	Ishurdi	24˚09′	89˚02′	12.9	1961-2014
5	Jessore	23˚12′	89˚20′	6.1	1948-2014
6	Khulna	22˚47′	89˚32′	2.1	1948-2014
7	Mongla	22˚28′	89˚36′	1.8	1991-2014
8	Rajshahi	24˚22′	88˚42′	19.5	1964-2014
9	Rangpur	25˚44′	89˚16′	32.61	1954-2014
10	Satkhira	22˚43′	89˚05′	3.96	1948-2014
11	Sayedpur	25˚45′	88˚55′	39.6	1991-2014

3. METHODOLOGY

In the current study, the long-term trend analysis is performed for the monthly and annual rainfall data series for the selected eleven (11) rainfall stations located in the western part of Bangladesh. The generic framework of methodology adopted in this study for the rainfall trend analysis is shown in Figure 2. A non-parametric trend estimation technique, widely known as the Mann-Kendall's test (Panda & Sahu, 2018) is adopted in this study to obtain the trends in monthly and annual rainfall data series in the study area. Generally, the parametric (distribution-dependent) or non-parametric (distribution-free) statistical tests can be used to decide whether there is a statistically significant trend in the data series. This non-parametric test is taken into consideration over the parametric one because it can avoid the problem roused by the skewed data. The trend analysis rainfall in the current study is carried out in the XLSTAT 2016 software platform. The main advantage of this software is that it allows taking into account and removing the effect of autocorrelation in the data series.

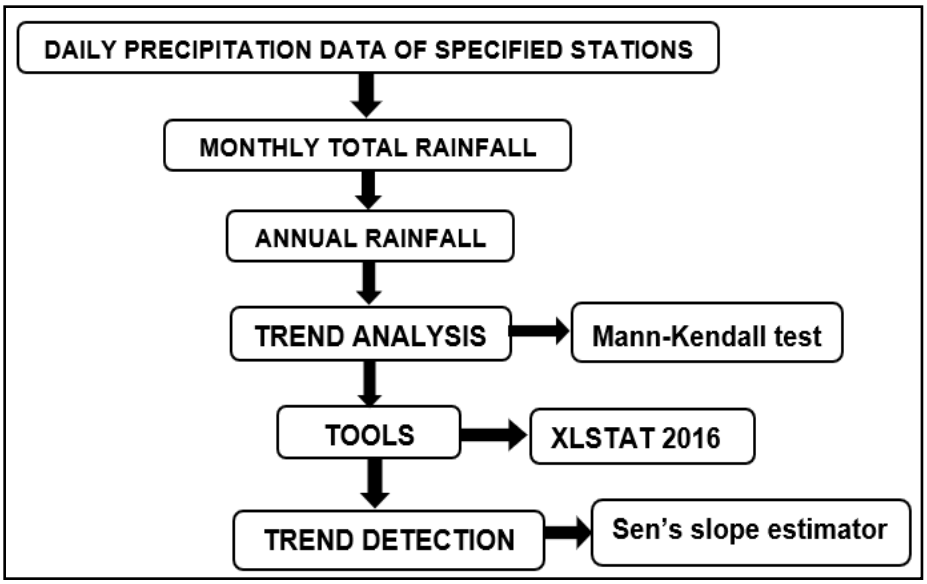

Figure 2: Framework of methodology adopted in this study for trend analysis

3.1 Mann Kendall Test

The initial value of Mann-Kendall's statistic, S, is assumed to be 0 (e.g., indicating no trend). A very high positive value of S is an indicator of an increasing trend and a very low negative value indicates a decreasing trend (Khambhammettu, 2005). The three alternative hypotheses are that there is a negative, non-null, or positive trend. According to this test, the null hypothesis H_0 assumes that there

is no trend (the data is independent and randomly ordered) and this is tested against the alternative hypothesis H_1, which assumes that there is a trend. Kendall's tau (Hollander et al., 2014) is used to identify strength of the trend and alpha (α) indicates the level of significance. The null hypothesis is tested at 95% confidence level for the monthly and annual rainfall data series for all selected station in this study. In order to calculate the p-value of this test, a normal approximation is used. If the p-value is less than the significance level α (alpha = 0.05), H_0 is rejected. The rejection of H_0 indicates that there is a trend in the time series, while accepting H_0 indicates that there is no trend present in the data series. On rejecting the null hypothesis, the result is said to be statistically significant.

3.2 Sen's Slope Estimator

The Sen's Slope method (Sen, 1968) involves the calculation of slopes for all the pairs of ordinal time points and then using the median of these slopes as an estimation of the overall slope. The Sen's method assumes that the trend is linear (Shahid, 2010b). In the current study, the magnitude of the trend is estimated by the Sen's slope method, which have been widely used for estimating the magnitude of the trend (e.g., Kamal & Pachauri, 2019).

4. RESULTS AND DISCUSSION

4.1 Trends in Monthly and Annual Rainfall Data

Initially, the statistical analysis is carried out for the monthly and annual rainfall data series for all the selected eleven (11) rainfall stations in the western part of Bangladesh, which is presented in Table 2.

Table 2: Summary of statistics of monthly and annual rainfall data in the study area

SN	Station Name	Mean (mm)	Max (mm)	Min (mm)	Std. Dev (mm)
Monthly Rainfall					
1	Bogra	139.4	835.0	0.0	164.616
2	Chuadanga	122.3	818.0	0.0	143.682
3	Dinajpur	153.4	1196.0	0.0	193.102
4	Ishurdi	120.2	1167.0	0.0	149.024
5	Jessore	131.0	917.0	0.0	147.383
6	Khulna	139.5	846.0	0.0	159.114
7	Mongla	159.1	983.0	0.0	169.142
8	Rajshahi	122.2	763.0	0.0	140.247
9	Rangpur	174.2	1314.0	0.0	208.372
10	Satkhira	133.8	728.0	0.0	151.695
11	Sayedpur	177.1	951.0	0.0	214.904
Annual Rainfall					
1	Bogra	1607.8	2516.0	751.0	408.243
2	Chuadanga	1380.0	1951.0	381.0	345.869
3	Dinajpur	1742.3	3179.0	479.0	510.346
4	Ishurdi	1448.5	2742.0	525.0	436.474
5	Jessore	1505.0	2444.0	494.0	376.341
6	Khulna	1571.0	2762.0	271.0	464.171
7	Mongla	1506.5	2786.0	569.0	415.449
8	Rajshahi	1248.0	2241.0	429.0	332.658
9	Rangpur	1958.8	3748.0	427.0	596.806
10	Satkhira	1413.6	2251.0	297.0	460.246
11	Sayedpur	1978.0	3145.0	562.0	586.905

As can be seen from Table 2, mean monthly rainfall in the study area varies from 120.2 mm at Ishurdi station to 177.1 mm at Sayedpur station whereas mean annual rainfall in the study area varies from 1248.0 mm at Rajshahi station to 1978.0 mm at Sayedpur station. It is worth mentioning that Ishurdi

and Rajshahi stations are close to each other and thus the lowest rainfall occurs in those areas. However, the highest monthly and annual rainfall occurs at Sayedpur station located in the furthest north-western part of the study area. The higher elevation combined with the effect of the Himalayan located north of the country boundary line may cause this increase rainfall in the furthest north-western part of the study area. Another interesting finding is that the rainfall is relatively lower in the coastal belt (including the area covered by Jessore, Khulna, Mongla and Satkhira stations), particularly in the south-west part of the study area. Overall, it can be concluded based on the statistical analysis of monthly and annual rainfall that there is a great variation of rainfall patterns in the western part of Bangladesh from north to south.

In order to estimate the trend in rainfall data series, the Mann-Kendall test is performed using the XLSTAT 2016 software. After performing the Mann-Kendall test on the monthly rainfall data series for the selected eleven (11) rainfall stations in the study area, the trend analysis results for monthly rainfall data is obtained, which is presented in Table 3. The results given in Table 3 indicate that the null hypothesis is accepted for seven (7) rainfall stations (e.g., Bogra, Chuadanga, Dinajpur, Mongla, Rajshahi, Rangpur and Sayedpur). On the other hand, the null hypothesis is rejected for remaining four (4) rainfall stations (e.g., Ishurdi, Jessore, Khulna and Satkhira). The rejection of null hypothesis indicates that the p-value of this test is less than the significance level of alpha. The initial value of Mann-Kendall statistic S is positive for the aforementioned four stations. Since the positive value of S remains for the increasing trend, these four stations show the signs of having the increasing trend. Ishurdi station, which is located in the north-western region of Bangladesh, shows the increasing trend. It is also found that the other three stations, Jessore, Khulna and Satkhira, which are located in the south-western coastal belt of Bangladesh, exhibit the increasing trend. The results of Sen's slope estimator also indicate that the magnitude of trend for these four stations is positive. It is interesting to see from the results that Mongla station does not show any trend although it is located near to Khulna and Satkhira stations. This may be due to the fact that the duration of available data is much lower than the aforementioned two stations. It is important to note that it is difficult to determine the non-parametric trends or may give fake results if the dataset is not long enough (Hajani et al., 2017).

Table 3: Trend analysis results for monthly rainfall data in the study area

SN	Station Name	Kendall's tau	S	p-value	alpha	Decision	Sen's slope	Trend Interpretation
1	Bogra	0.020	6385	0.395	0.05	Accept	0	Not Significant
2	Chuadanga	-0.004	-164	0.927	0.05	Accept	0	Not Significant
3	Dinajpur	0.049	11707	0.057	0.05	Accept	0	Not Significant
4	**Ishurdi**	0.077	15487	0.004	0.05	Reject	0.007	**Increasing**
5	**Jessore**	0.048	14662	0.046	0.05	Reject	0.006	**Increasing**
6	**Khulna**	0.054	15371	0.028	0.05	Reject	0.004	**Increasing**
7	Mongla	-0.024	-923	0.559	0.05	Accept	0.006	Not Significant
8	Rajshahi	-0.015	-2471	0.597	0.05	Accept	0	Not Significant
9	Rangpur	0.045	10898	0.078	0.05	Accept	0.004	Not Significant
10	**Satkhira**	0.059	17337	0.015	0.05	Reject	0.004	**Increasing**
11	Sayedpur	-0.007	-277	0.861	0.05	Accept	0	Not Significant

Table 4 presents the results of the Mann-Kendall test on the annual rainfall data series for the selected eleven (11) rainfall stations in the western part of Bangladesh. As can be seen from the table, three stations including Ishurdi, Khulna and Satkhira exhibit the sign of increasing trends whereas the remaining eight (8) rainfall stations show the non-significant trend. Furthermore, the magnitude of trend for these three stations is found positive based on the results of Sen's slope estimator on the annual rainfall data. It is also seen from the results that the trend results of the annual rainfall data are consistent with the trend results of the monthly rainfall data.

Table 4: Trend analysis results for annual rainfall data in the study area

SN	Station Name	Kendall's tau	S	p-value	alpha	Decision	Sen's slope	Trend Interpretation
1	Bogra	0.021	7672	0.365	0.05	Accept	0	Not Significant
2	Chuadanga	0.004	237	0.906	0.05	Accept	0	Not Significant
3	Dinajpur	0.046	12851	0.065	0.05	Accept	0	Not Significant
4	**Ishurdi**	0.08	18917	0.002	0.05	Reject	0.009	**Increasing**
5	Jessore	0.045	16171	0.051	0.05	Accept	0.007	Not Significant
6	**Khulna**	0.051	16964	0.032	0.05	Reject	0.005	**Increasing**
7	Mongla	-0.012	-539	0.763	0.05	Accept	0	Not Significant
8	Rajshahi	-0.01	-1905	0.718	0.05	Accept	0	Not Significant
9	Rangpur	0.043	12228	0.080	0.05	Accept	0.005	Not Significant
10	**Satkhira**	0.057	19481	0.016	0.05	Reject	0.006	**Increasing**
11	Sayedpur	0.001	67	0.970	0.05	Accept	0	Not Significant

4.2 Trends in Extreme Rainfall Events

In the recent past, it has been suggested that the extreme rainfall events are becoming more intense due to the impact of climate change. An attempt is made to identify if there are any differences in the intensities of extreme rainfall events for the stations showing increasing trend of rainfall (e.g., Ishurdi, Jessore, Khulna and Satkhira) as identified in the non-parametric trend analysis. The index adopted to measure the intensity of rainfall events is the 'maximum 1-day rainfall' in a year for those stations. Figure 3 shows the bar plots for the maximum 1-day rainfall at Ishurdi, Jessore, Khulna and Satkhira stations.

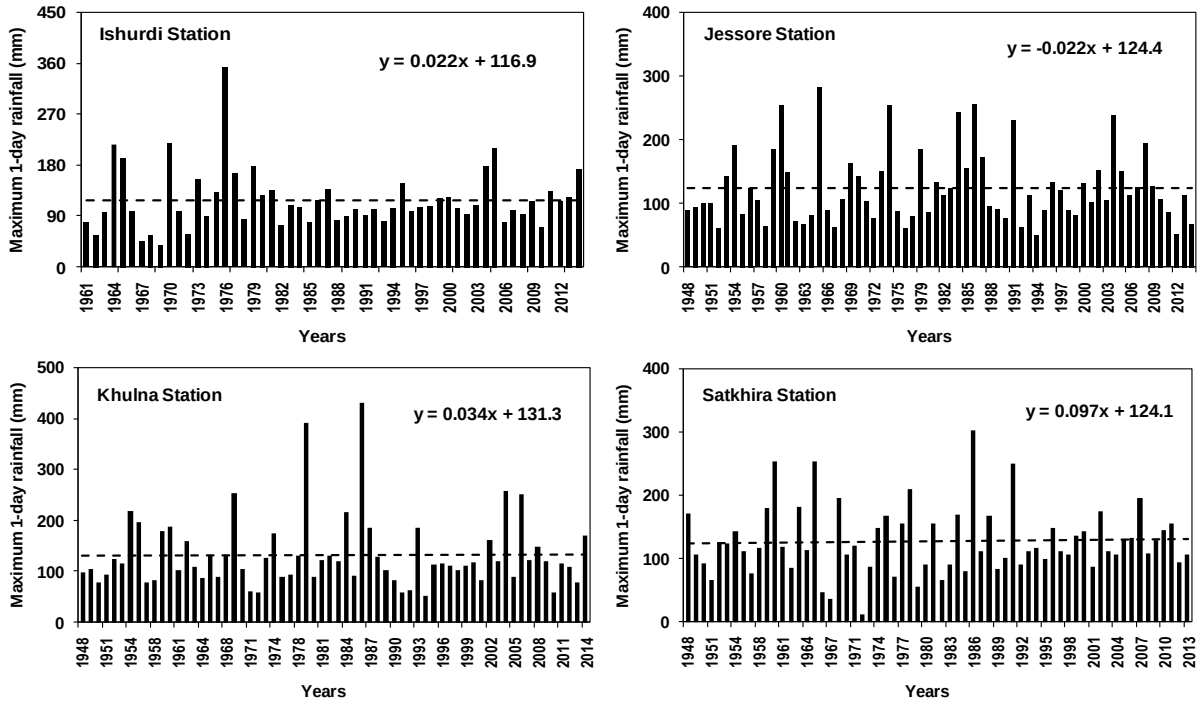

Figure 3: Maximum 1-day rainfall at stations showing increasing trend of rainfall

It can be seen from Figure 3 that the trends of maximum 1-day rainfall is increasing for Ishurdi, Khulna and Satkhira stations whereas for Jessore station, the trend of maximum 1-day rainfall is decreasing. It is worth mentioning that this result is consistent with the results obtained by the non-parametric trend analysis using the Mann-Kendall test based on the annual rainfall data series. Thus, it is clearly observed that the storm events are becoming more intense along with the long-term increasing trend of rainfall. This has serious implications on the water management in those areas

where these stations are located. Specifically, the low-lying coastal belt could be severely affected due to the increasing trend of extreme rainfall events combined with the potential impact of climate change.

5. CONCLUSIONS

This study focuses on the analysis and detection of trends of long-term trend monthly and annual rainfall data series for selected eleven (11) rainfall stations located within the western part of Bangladesh. For this purpose, the widely used Mann-Kendall's test and Sen's slope estimator is adopted at 5% significance level on monthly and annual rainfall time series data for each of the eleven stations for the time period, 1948 to 2014. The results of Mann-Kendall's test statistic (S) indicate how strong the trend in rainfall data is and whether it is increasing, stable or decreasing. Trend detection of rainfall using the adopted techniques over 65 years shows increasing trend in monthly rainfall for four rainfall stations, namely Satkhira, Khulna, Jessore and Ishurdi stations. Three of them are located in the southwest coastal part of the study area. The trend analysis results for annual rainfall data also demonstrate similar patterns and the increasing trend is evidenced for three rainfall stations, namely Satkhira, Khulna and Ishurdi stations in which two are located in the coastal part. On the other hand, linear trend line plotting of the maximum 1-day rainfall for Satkhira, Khulna, Jessore and Ishurdi stations indicates an increasing trend of rainfall in Ishurdi, Khulna and Satkhira stations and a decreasing trend of rainfall in Jessore station. This finding is consistent with the trend analysis results for the annual rainfall data series obtained by the non-parametric Mann-Kendall test. The findings of this analysis would be of interest to water resources managers and policy makers for the effective planning and management of water resources in Bangladesh.

REFERENCES

Bhuyan, M.D. I., Islam, M.M., & Bhuiyan, M.E.K. (2018). A trend analysis of temperature and rainfall to predict climate change for northwestern region of Bangladesh. *American Journal of Climate Change*, 7, 115-134.

Hajani, E., Rahman, A., & Ishak, E. (2017). Trends in extreme rainfall in the State of New South Wales, Australia, *Hydrological Sciences Journal*, 62(13), 2160-2174.

Hossain, M. F. (2014). Impact of climate change in Bangladesh: Rainfall. *International Journal of Agriculture Innovations and Research*, 2(5), 2319-1473.

Intergovernmental Panel on Climate Change (IPCC) (2007). *Climate Change 2007: The Scientific Basis. Contribution of Working Group I to the Fourth Assessment Report of the Intergovernmental Panel on Climate Change*, edited by S. Solomon et al., Cambridge University Press, New York.

Kamal, N., & Pachauri, S. (2019). Mann-Kendall, and Sen's Slope estimators for precipitation trend analysis in north-eastern states of India. *International Journal of Computer Applications*, 177(11), 7-16.

Khambhammettu, P. (2005). *Mann-Kendall Analysis for the Fort Ord site*. HydroGeoLogic, Inc., California, USA.

Mondal, M.S., Jalal, M.R., Khan, M.S.A., Kumar, U., Rahman, R., & Huq, H. (2013). Hydro-meteorological trends in southwest coastal Bangladesh: Perspectives of climate change and human interventions. *American Journal of Climate Change*, 2(1), 62-70.

Panda, A. & Sahu, N. (2018). Trend analysis of seasonal rainfall and temperature pattern in Kalahandi, Bolangir and Koraput districts of Odisha, India. *Atmospheric Science Letters*, 20(2), e932, DOI: 10.1002/asl.932.

Sen, P. K. (1968). Estimates of the Regression Coefficient Based on kendall's Tao. *Journal of the American Statistical Association*, 63(324), 1379-1389.

Shahid, S. (2010a). Recent trends in the climate of Bangladesh. *Climate Research, 42(3)*, 185-193.

Shahid, S. (2010b). Rainfall variability and the tends of wet and dry periods of Bangladesh. *International Journal of Climatology*, 30(15), 2299–2313.

Shahid, S. & Behrawan, H. (2008). Drought risk assessment in the western part of Bangladesh. *Natural Hazards*, 46(3), 391-413.

Proceedings of the 5th International Conference on Civil Engineering for Sustainable Development (ICCESD 2020), 7~9 February 2020, KUET, Khulna, Bangladesh (ISBN-978-984-34-8764-3)

FINANCIAL FEASIBILITY ASSESSMENT OF RAINWATER HARVESTING SYSTEM IN COASTAL BANGLADESH CONSIDERING PRECIPITATION VARIABILITY DUE TO CLIMATE CHANGE

Mohammad Maksimul Islam*[1] and Sadia Afrin[2]

[1]Assistant Professor, Bangladesh University of Engineering and Technology (BUET), Bangladesh, e-mail: maksimulislam075@gmail.com
[2]Assistant Professor, Bangladesh University of Engineering and Technology (BUET), Bangladesh, e-mail: sadiaafrin9888@gmail.com

***Corresponding Author**

ABSTRACT

Rainwater harvesting system (RWH) is considered an environmentally sound solution to provide safe drinking water. It is particularly suitable for Bangladesh because of its having tropical monsoon with a large seasonal cycle in rainfall. Although few studies dealt with the technical feasibility of the RWH system, reliability based cost-benefit analyses are still scarce. This study aims at assessing the financial feasibility of RWH system in Khulna, a coastal district in Bangladesh. We apply a mass balance based behavioral model named 'Yield-After-Spillage (YAS)' to conduct reliability analysis. We use historical as well as future predicted rainfall data in the model to explore the effect of climate change on reliability and financial feasibility. We conducted a social survey to collect necessary information related to RWH system including roof area, roof material, water demand, existing water supply system and cost of materials. Cost-benefit analysis reveals that 85-95% of total RWH installation cost is for the storage reservoir, making it the most expensive unit of the system. We find 'net present value (NPV)' of a typical RWH system positive indicating that RWH is a financially viable solution in the study area. Payback period varies between 3-13 years depending on the precipitation variability. For 100 litre/day demand, predicted rainfall for the 2041-2070 period showed 1.5 times larger storage tank requirement compared to that for historical precipitation scenario to attain 90% volumetric reliability, which results in a substantial increase in cost, and 20% reduction in NPV. However, for 200 litre/day demand, historical precipitation scenario cannot provide more than 53% reliability.

Keywords: *Cost-benefit, Rainwater, Harvesting, Reliability, Climate-change.*

1. INTRODUCTION

Globally around 1.1 billion people do not have access to safe water (Shaw & Thaitakoo, 2010). However, a safe and reliable source of water is imperative for leading a healthy life (Hunter, MacDonald, & Carter, 2010). According to the Safe Drinking Water Foundation (SDWF, 2018), unsafe drinking water and waterborne diseases cause 80% of all illness in developing countries. Water-related diseases also attributes to 3 million death annually, majority of which are the children under the age of five (World Bank, 2002). Water scarcity is expected to increase in the near future due to climate change (Umetsu, Donma, Nagano & Coşkun, 2019). Especially in coastal Bangladesh, sea level and temperature are predicted to rise along with more frequent extreme events (e.g. floods, droughts, storms) due to climate change (Khan, Xun, Ahsan & Vineis, 2011), which will make scarcity of potable water acute there as coastal people rely on either fresh surface water bodies (rivers, ponds) or ground water (tube well). Around 30 million people there do not have access to safe drinking water and half of them are forced to drink saline water (Hoque, 2009). However, suitable rainfall pattern in coastal areas in Bangladesh makes rainwater harvesting (RWH) system a potential source of potable water, and a medium to fight against water scarcity (Islam, Afrin, & Rahman, 2015b; Islam, Afrin, Redwan, & Rahman, 2015; Islam, Chou, Kabir & Liaw, 2010)

RWH system has many aspects to explore. Some studies focused on assessing reliability (Bashar, Karim, & Imteaz 2018; Islam, Afrin, Redwan, et al., 2015; Islam, Afrin & Rahman, 2015), financial feasibility (Karim, Bashar, & Imteaz, 2015) and water quality (Islam, Akber, Rahman, Islam & Kabir, 2019); some investigated its applicability in urban and rural areas, in irrigation (Ghimire & Johnston, 2019) and in water sensitive water designs (Wahab, Mamtaz & Islam, 2016). However, few studies focused on coastal Bangladesh. For example, Islam (Islam, Afrin, & Rahman, 2015b, 2016) applied behavioral, and storm water management model (SWMM) to calculate reliability of RWH for available roof areas in coastal Bangladesh. Water quality measurement of rainwater to assess its viability for coastal schools is explored in some studies (Islam et al., 2019). However, cost-benefit analysis of RWH, which is a main concern for poor coastal people, has not been explored adequately. There are some studies (Akter & Ahmed, 2015; Bashar et al., 2018; Islam, Chou, & Kabir, 2011; Karim et al., 2015) that conducted economic analysis of RWH system for urban cities in Bangladesh only. Therefore, there is a need of financial feasibility assessment of RWH in coastal Bangladesh.

In this paper, we assess the financial feasibility of RWH system in a typical household in coastal Bangladesh. We also conduct reliability analysis of the RWH to provide a complete picture of it to coastal people. This study is a part of a big study focusing on reliability and economic analysis of a community based RWH system in coastal Bangladesh.

2. METHODOLOGY

2.1 Study Area

Since this study intends to explore reliability and financial feasibility of rainwater harvesting system in a water scarce coastal area of Bangladesh, we chose Paikgacha pourashava under Khulna district as the study area. Paikgacha is about 67.2 km from Khulna city corporation and very near to Kobadak River. This river and tube wells here are contaminated with high saline water. Pond water is available and comparatively less saline but during cyclone or flood disaster, sea water enters into the ponds and makes the water saline.

2.2 Site survey

We conducted a site survey to get acquainted with the study area and also to collect necessary data for the study. We collected information regarding family size, roof catchment, water demand and existing water supply systems. We also visited local markets to gather information about the cost of different components required for RWH system. We did not discuss outcomes of the site study in this paper.

For this paper, we used the information from the site survey needed for the reliability and economic analysis.

2.3 Mass balance model and inputs

We applied mass balance model (supply vs demand) to calculate reliability of RWH system. I also adopted yield after spillage (YAS) behavioral approach in the mass balance (Fewkes & Butler, 2000). In this paper, we calculated volumetric reliability as a performance indicator that is the fraction of total demand met by the RWH system (Islam, Afrin & Rahman, 2015a; Islam et al., 2016; Karim et al., 2015; Liaw & Tsai, 2004). In the mass balance, I calculated supply matrix using the rational formula that provides the volume of water harvested from a roof catchment (Islam, Afrin, & Rahman, 2015b). Demand matrix is calculated as the product of per capita water demand and family size. The inputs of the supply and demand matrices are discussed in the following sections.

2.3.1 Rainfall Intensity and runoff coefficient

Since we wanted to see how reliability and cost-benefit of RWH system would change under precipitation variability (Islam, Afrin, Ahmed & Ali, 2014, 2015) and future precipitation scenario due to climate change (Rajib, Rahman, Islam & McBean, 2011), we used both historical observed and future predicted precipitation data in this study. We collected historical observed data of the study area from Bangladesh Meteorological Department (BMD). We used future predicted data from a previous study (Rajib et al., 2011) in which a regional climate model PRECIS was used. This data was monthly data predicted up to 2100. We divided the future predicted data into three time periods (2011-2040, 2041-2070 and 2071-2100) to understand clearly the future precipitation trend. Among the three time periods in future, average monthly predicted rainfall was higher during 2071-2100 in all twelve months. For the runoff coefficient (Gould & Nissen-Petersen, 1999), we applied a value of 0.80 that was used in some studies for the study area (Islam, Afrin & Rahman, 2014; Islam, Afrin, Redwan, et al., 2015).

2.3.2 Catchment Area

As mentioned earlier, this paper is a part of a study aiming at exploring reliability and feasibility of community RWH. We obtained roof areas of the study area from the Local Government Engineering Department (LGED). Study area comprises roofs of residential, commercial, educational and other community buildings. For this paper, we used 400 ft2 as the roof area that is the average of all residential households in that community.

2.3.3 Water demand and family size

Water demand is a critical part of the mass balance needed to calculate the appropriate tank size of a household. Household water demand is the product of family size and per capita water demand. During the site survey, we got an idea of the range of water demand and family size of different households. For this paper, we used three household water demand scenarios: 100, 150 and 200 litre per day. We used a family size of 5 members for the inter-period and inter-demand comparison analysis.

2.4 Cost-benefit analysis and inputs

The cost of a rainwater harvesting system is basically dependent on four elements: roof catchment, guttering, first flush device and storage tank (Islam et al., 2010). Moreover, there are some auxiliary elements such as treatment, pump, overhead tank, operation and maintenance etc. Of these, the roof and the tank are critical in terms of costing. Since most people will have a roof on their house, this may not immediately be the biggest cost, except when it is necessary to improve the roof for water quality reasons. On the other hand, the cost of a storage tank is often high. Table 1 summarizes the installation cost elements of individual rainwater harvesting system.

Table 1: Cost elements of individual rainwater harvesting system

Installation		Operation and Maintenance	Treatment
Storage	**Collection**		
Storage Tank	Gutter	Electricity	UV disinfection
Pump	Coarse filter	Replacing pump	
Riser pipe	Downpipe		
Overhead tank			

2.4.1 Collection System

Collection system involves collection of rainwater from roof to storage tank through gutter, coarse filter and downpipe. The roof materials of the buildings of the study area were satisfactory for a rainwater harvesting system. Therefore, no costs associated with the roof material were considered. Usually UPVC (Unplasticized polyvinyl chloride) pipes are used for making gutter and downpipe. The local market price of 4" standard UPVC pipe is 52 BDT/ft. Coarse filter is placed at the entrance of the rainwater collection system as a primary treatment system that costs 150 BDT/piece.

2.4.2 Storage System

Storage system involves storage reservoir, pump, riser pipe and overhead water tank. Through downpipe water comes from roof and finally accumulates in the storage tank. After that, water is lifted up to overhead water tank by pumping to distribute with enough pressure. Storage tank is the costliest part of rainwater harvesting system. Prior to cost estimation, design had to be done for the storage tank. Conventionally reinforced concrete tanks have been used as storage tank for several decades. The Portland Cement Association (PCA) has publications for designing rectangular tanks, which is comprised of tables of coefficients for calculating moment and shear in two-way slabs (Portland Cement Association, 1996).

After designing the tank, cost was calculated for each tank. Local market price of brick, cement, sand, and rod was collected and summarized in Table 2. Labour cost and transportation cost were also considered while calculating cost.

Table 2: Local market price of cement, sand, brick and rod

Item Description	Unit	Per Unit Cost (BDT)
Best Quality Brick	nos.	7.5
1st class Brick chips	cft	75
Kushtia Sand	cft	30
Cement	bags	410-450
Rebar	ton	57500

Price of pump varies with capacity (HP). There are many pump manufacturing companies in Bangladesh and almost all companies provide two years' warranty for the pumps. We collected the market price of pumps of some prominent companies available in local market and used it in cost-benefit analysis. Different companies have different rates for various HP. We chose the most reasonable price for pump depending on required HP. Desired pump capacity depends on demand and total head to be supplied. Higher the demand and head, higher would be the desired capacity. The formula for determining the pump capacity is as follows:

$$Pump\ Capacity\ (HP) = \frac{H \times Q}{3960 \times Efficiency} \quad (1)$$

Where,
H= Total Head (ft)
Q= water demand (gpm)

Food grade plastic water tanks are popular now as overhead water tank (OHT) and it is comparatively less costly than RCC tank. The price of tanks varies with capacity; however, for a particular specification, price does not vary much among the manufacturing companies. In addition, overhead tank height is an important parameter to supply water to households at adequate pressure. For individual household-based community system, OHT will be above the roof by an elevated structure. We calculated from pressure requirement of the fixtures that tank height above the roof should be minimum 14 ft.

2.4.3 Operation, maintenance and treatment system

Operation cost is the cost of electricity required to run the pump. Since warranty period of pumps is two years, price of pump is also included as maintenance cost for every two year. There are three sequential options of the treatment of rainwater for harvesting: filtration, first flush and disinfection (Kloss, 2008). Coarse filter at the entrance of the rainwater collection system works as a filter. The first flush of rainwater after a dry period helps to clean dust, bird droppings etc. from roof (Rashid & Ahmed, 2012). Locally PVC pipes are used for making first flush device as low-cost technology. Local market price of 4" standard UPVC pipe is 76 BDT/ft. Nowadays UV disinfection process is being used for rainwater harvesting system as UV inactivates general bacteria, total Coliform and E. coli (Redwan, Ghosh & Rahman, 2014) and it is not a costly method. It should be mentioned that to be effective, the water passing though the UV system must be relatively clear and free of particles. The coarse filter and first flush prior to UV system fulfil this criterion. The UV bulbs are of different power. Higher the power, higher the amount of treated water or lower the time required for deactivation of pathogens. The cost of bulbs also varies with power. The capacity, deactivation time and costing are provided on Table 3

Table 3: Capacity, deactivation time and costing (without jacket) of UV disinfection process (adapted from Redwan et al., 2014)

Power of UV bulb (W)	Water treatment capacity (Liter)	Required Deactivation Time (min)	Cost (BDT)
6W	100	30	2500
16W	500	30-45	3500
25W	500	20	4500
55W	3000	30	6000

2.4.4 Benefit element

Local people buy jar water to fulfil the demand. Different NGOs of the study area supply this jar water and each jar contains 10-30 litre water. Benefits of operating RWH facility is altering of charge of this jar water with rainwater. The jar water charge is BDT 0.8 per litre, so by multiplying it with annual rainwater usage, annual benefit was calculated.

2.4.5 Parameters of cost-benefit analysis

We used net present value (NPV) and payback period as the financial indicators for assessing financial feasibility of RWH system under different precipitation and demand scenarios. RWH system has start-up expenditures, operational expenditures (outflow), and incoming cash (inflows) over its economic life. In this paper, we considered an economic life of 20 years, although storage tank and PVC pipes can last more than that. We converted all costs and benefits to present values using a

discount rate of 5% as established as an average by the Central Bank of Bangladesh. This rate is also used by Department of Public Health Engineering (DPHE) for evaluation of their long term projects.

3. ILLUSTRATIONS

3.1 Reliability

As mentioned earlier, precipitation data are available from 1950 to 2100 of the study areas in which 1950-2010 are historical observed data. To assess the effect of climate change, we consider four consecutive time periods (1950-2010, 2011-2040, 2041-2070 and 2071-2100), and calculate volumetric reliability for each period applying the behavioural model for a typical household in the study area having a roof area of 360 ft2 and family size of 5 members for different tank sizes. Figure 1 shows the volumetric reliability (Rv) curves for four time periods for two daily household demand of 100 and 200 litre. Highest Rv (99.7%) can be achieved for historical precipitation data at a tank size of 20 m3 for 100 litre/day demand (Figure 1-a). 2011-2040 and 2071-2100 time periods show similar trend of Rv. In both cases, maximum achievable Rv (91.7) occurs at a tank size of 15 m3. 2041-2070 scenario also gives same maximum Rv as the other two predicted scenarios; however, for a larger tank size (25 m3). Higher precipitation in 2011-2040 & 2071-2100 compared to 2041-2070 seems the reason for this. Rv curves for the future predicted scenarios for the water demand of 200 litre/day (Figure 1-b) are similar to lower demand of 100 litre/day (Figure 1-a), although the tank sizes required to attain maximum Rv were larger for the higher household demand. Interestingly, Rv shows a drastic change between higher and lower demand for the historical observed period. Although maximum achievable Rv is the highest for 100 litre/day demand, it is the lowest for 200 litre/day demand for 1951-2010 period indicating that both demand and precipitation scenario play a major role in sizing storage tank for RWH

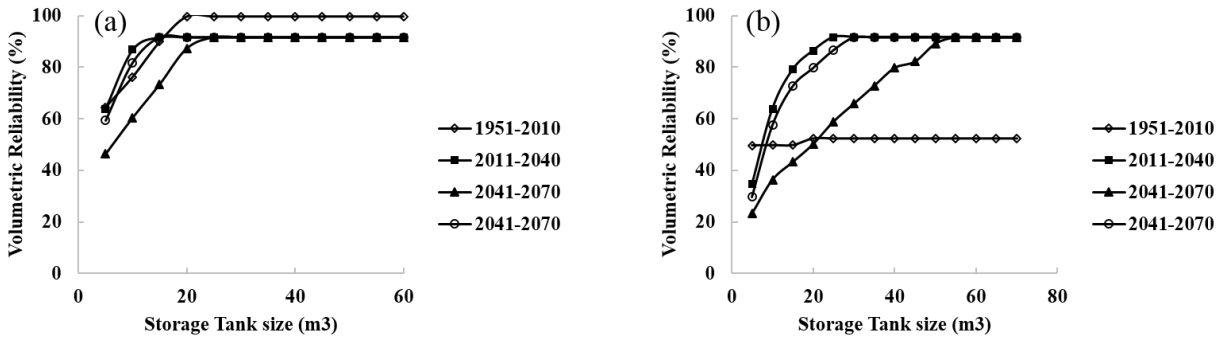

Figure 1: Volumetric reliability curves considering four different precipitation scenarios for (a) 100 litre/day and (b) 200 litre/day household water demand

Volumetric reliability appears to be significantly higher for two time periods in future (2011-2040 & 2071-2100) compared to historical period whereas reliability in 2041-2070 seems lower (Figure 4.10). Higher precipitation in 2011-2040 & 2071-2100 compared to other two periods is the reason for this. However, in each case, maximum reliability that could be achieved is about 91% and increase in tank size cannot increase the reliability. The main difference among the curves is the minimum tank size for which that maximum reliability is achieved. These minimum tank sizes corresponding to highest volumetric reliability are 2000, 2200, 1200 and 1400 m³ for 1950-2010, 2011-2040, 2041-2070 and 2071-2100 time periods respectively.

3.2 Cost-benefit analysis

3.2.1 Cost of different component of RWH

As a part of the cost benefit analysis, we want to compare the cost of all major components of a RWH system in the study area. Figure 2 shows the proportion of cost of different components for 100 and

200 litre/day demand for the 2011-2040 scenario. Storage tank sizes associated with 90% Rv are considered for the cost calculation. In both cases, storage system is the costliest part of the entire system (94-97%). In storage system, costing of central storage tank is the highest. Cost of operation & maintenance (O & M), collection and treatment system are lower but close to each other.

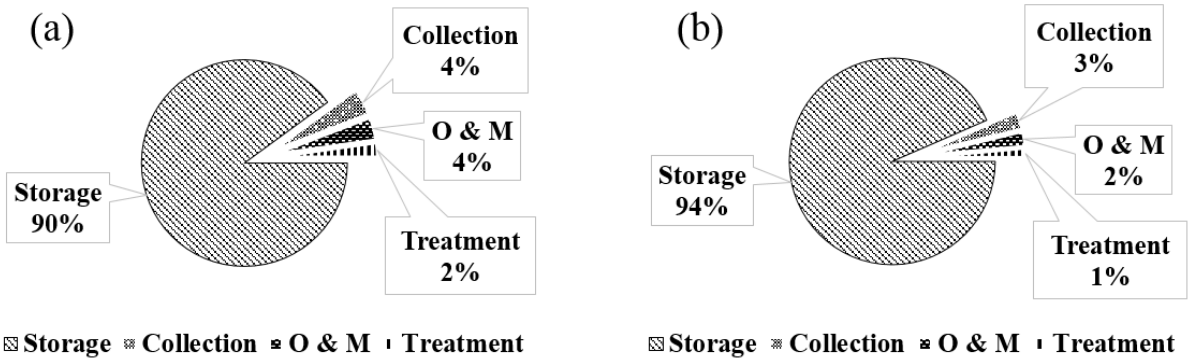

Figure 2: Proportion of cost of major components of RWH system for (a) 100 litre/day and (b) 200 litre/day household water demand

3.2.2 Net present value (NPV)

Figure 3 shows NPV associated with the RWH system for four time periods, and three household demands. As mentioned earlier, storage tank required for 90% Rv was considered for the cost-benefit analysis for each scenario. Since, 90% Rv is not achievable for 1951-2010 period, NPV is not calculated and shown in the figure. For each time period, a higher water demand shows a reduction in NPV. Increase in storage tank size associated with 90% Rv with increased household demand makes the overall cost of the system higher and thus NPV lower. Note that, reduction in NPV with higher water demand is substantially higher for 2041-2070 period compared to other two predicted precipitation scenario suggesting that household water demand should be chosen based on the precipitation scenario of the area to get a profitable RWH system.

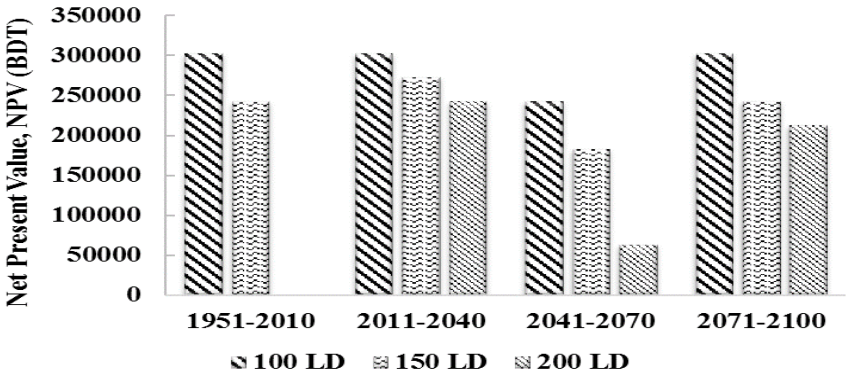

Figure 3: NPV of RWH systems considering four different precipitation scenarios for three different household water demands. Storage tank sizes associated with 90% R_v are considered for this calculation.

3.2.3 Payback period

Figure 4 shows the cumulative NPV at each successive year of the economic life of RWH system to indicate the payback period for the 2011-2040 scenario. Three water demands are considered as before to see the effect of water demand on payback period. When demand is 100 liter/day, payback period is 4 year indicating that it takes 4 year to recover initial investment for the RWH system. If the water demand doubles (200 liter/day), payback period also almost doubles (7 year). This figure

indicates that for a typical household in the study area, RWH system is profitable; however, it takes years to get back the initial cost depending on the water demand to be met.

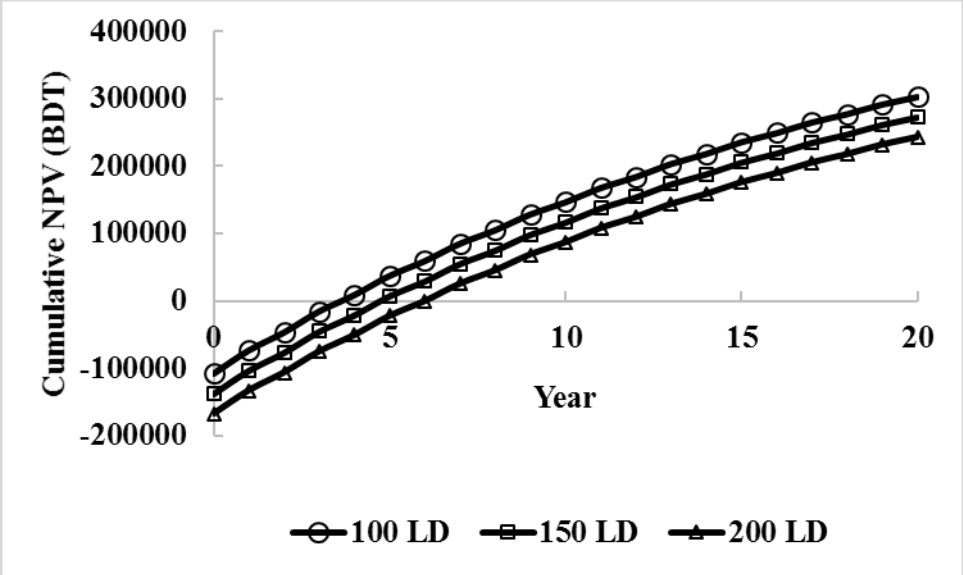

Figure 4: Cumulative NPV in each successive year of the economic life of RWH systems for three different household water demands. Storage tank sizes associated with 90% R_v are considered for this calculation.

4. CONCLUSIONS

This study assesses financial feasibility of RWH system in a typical household in a coastal district in Bangladesh. Results show that RWH is financially viable in the study area. However, for a higher water demand scenario, NPV decreases and payback period increases. Relative proportion of costs of major components of RWH does not change with water demand though. This study also conducts reliability analysis. Precipitation variability under future climate change scenario seems to affect reliability of RWH of the study area. For 100 litre/day demand, predicted rainfall for the 2041-2070 period showed 1.5 times larger storage tank requirement compared to that for historical precipitation scenario to attain 90% volumetric reliability. However, for 200 litre/day demand, maximum 53% reliability can be achieved for historical precipitation scenario.

REFERENCES

Akter, A., & Ahmed, S. (2015). Potentiality of rainwater harvesting for an urban community in Bangladesh. Journal of Hydrology, 528, 84–93. https://doi.org/10.1016/j.jhydrol.2015.06.017

Bashar, M. Z. I., Karim, Md. R., & Imteaz, M. A. (2018). Reliability and economic analysis of urban rainwater harvesting: A comparative study within six major cities of Bangladesh. Resources, Conservation and Recycling, 133, 146–154. https://doi.org/10.1016/j.resconrec.2018.01.025

Fewkes, A., & Butler, D. (2000). Simulating the performance of rainwater collection and reuse systems using behavioural models. Building Services Engineering Research and Technology, 21(2), 99–106. https://doi.org/10.1177/014362440002100204

Ghimire, S. R., & Johnston, J. M. (2019). Sustainability assessment of agricultural rainwater harvesting: Evaluation of alternative crop types and irrigation practices. PLOS ONE, 14(5), e0216452. https://doi.org/10.1371/journal.pone.0216452

Gould, J., & Nissen-Petersen, E. (1999). Rainwater Catchment Systems for Domestic Supply. https://doi.org/10.3362/9781780445694

Hoque, M. R. (2009). Access to safe drinking water in rural Bangladesh: Water governance by DPHE. Retrieved from http://dspace.bracu.ac.bd/xmlui/handle/10361/279

Hunter, P. R., MacDonald, A. M., & Carter, R. C. (2010). Water Supply and Health. PLoS Medicine, 7(11). https://doi.org/10.1371/journal.pmed.1000361

Islam, M. A., Akber, Md. A., Rahman, Md. A., Islam, Md. A., & Kabir, Md. P. (2019). Evaluation of harvested rainwater quality at primary schools of southwest coastal Bangladesh. Environmental Monitoring and Assessment, 191(2), 80. https://doi.org/10.1007/s10661-019-7217-6

Islam, M. M., Afrin, S., Ahmed, T., & Ali, M. A. (2015). Meteorological and seasonal influences in ambient air quality parameters of Dhaka city. Journal of Civil Engineering (IEB), 43(1), 67–77.

Islam, M. M., Afrin, S., & Rahman, M. M. (2015a). A comparative analysis between the application of rational formula and SWMM model for modeling community rainwater harvesting system. Proceedings of International Conference on Recent Innovation in Civil Engineering for Sustainable Development (IICSD-2015). Gazipur, Bangladesh.

Islam, M. M., Afrin, S., & Rahman, M. M. (2015b). Reliability Analysis of Community Rainwater Harvesting System Considering Precipitation Variability Due to Climate Change. Proceedings of International Conference on Recent Innovation in Civil Engineering for Sustainable Development (IICSD-2015). Gazipur, Bangladesh.

Islam, M. M., Afrin, S., Redwan, A., & Rahman, M. M. (2015). Impact of Climate Change on Reliability of Rainwater Harvesting System: A case Study in Mongla, Bangladesh. Proceedings of 10th Global Engineering, Science and Technology Conference. Dhaka, Bangladesh.

Islam, M. M., Chou, F. N.-F., & Kabir, M. R. (2011). Feasibility and acceptability study of rainwater use to the acute water shortage areas in Dhaka City, Bangladesh. Natural Hazards, 56(1), 93–111. https://doi.org/10.1007/s11069-010-9551-4

Islam, M. M., Chou, F. N.-F., Kabir, M. R., & Liaw, C.-H. (2010). Rainwater: A Potential Alternative Source for Scarce Safe Drinking and Arsenic Contaminated Water in Bangladesh. Water Resources Management, 24(14), 3987–4008. https://doi.org/10.1007/s11269-010-9643-7

Islam, M. M., Afrin, S., Ahmed, T., & Ali, M. A. (2014). THE INFLUENCE OF METEOROLOGY ON PARTICULATE MATTER CONCENTRATION IN THE AIR OF DHAKA CITY. Proceedings of 2nd International Conference on Advances in Civil Engineering 2014 (ICACE-2014). Chittagong, Bangladesh.

Islam, M. M., Afrin, S., & Rahman, M. M. (2014). Development of a Design Tool for Sizing Storage Tank of Rainwater Harvesting System in Coastal Areas of Bangladesh Under Future Climatic Scenario. Proceedings of 2nd International Conference on Advances in Civil Engineering 2014 (ICACE-2014). Chittagong, Bangladesh.

Islam, M. M., Afrin, S., & Rahman, M. M. (2015). Correlation Between The Performance Indicators of Community Rainwater Harvesting System. Proceedings of International Conference on Recent Innovation in Civil Engineering for Sustainable Development (IICSD-2015). Gazipur, Bangladesh.

Islam, M. M., Afrin, S., & Rahman, M. M. (2016). RUNOFF SIMULATION USING SWMM MODEL AND RELIABILITY ASSESSMENT OF COMMUNITY RAINWATER HARVESTING SYSTEM. Proceedings of 8th International Perspective on Water Resources and the Environment. Colombo, Sri Lanka.

Karim, Md. R., Bashar, M. Z. I., & Imteaz, M. A. (2015). Reliability and economic analysis of urban rainwater harvesting in a megacity in Bangladesh. Resources, Conservation and Recycling, 104, 61–67. https://doi.org/10.1016/j.resconrec.2015.09.010

Khan, A. E., Xun, W. W., Ahsan, H., & Vineis, P. (2011). Climate Change, Sea-Level Rise, & Health Impacts in Bangladesh. Environment: Science and Policy for Sustainable Development, 53(5), 18–33. https://doi.org/10.1080/00139157.2011.604008

Kloss, C. (2008). Managing Wet Weather with Green Infrastructure Municipal Handbook Rainwater Harvesting Policies.

Liaw, C.-H., & Tsai, Y.-L. (2004). Optimum Storage Volume of Rooftop Rain Water Harvesting Systems for Domestic Use1. Journal of the American Water Resources Association; Middleburg, 40(4), 901–912.

Portland Cement Association. (1996). Underground Concrete Tank. Retrieved from https://www.cement.org/docs/default-source/th-buildings-structures-pdfs/design-aids/is071-underground-concrete-tanks.pdf?sfvrsn=4&sfvrsn=4

Rajib, M. A., Rahman, M. M., Islam, A. K. M. S., & McBean, E. A. (2011). Analyzing the Future Monthly Precipitation Pattern in Bangladesh from Multi-Model Projections Using Both GCM and RCM. Proceedings of World Environmental and Water Resources Congress 2011@ SBearing Knowledge for Sustainability.

Rashid, R., & Ahmed, M. H. B. (2012). Roof Top Rain Water Harvesting System in Dhaka City. Proceedings of the Global Engineering, Science and Technology Conference. Presented at the Dhaka, Bangladesh. Dhaka, Bangladesh.

Redwan, A., Ghosh, S., & Rahman, M. M. (2014). Effectiveness of UV-Technique for Water Disinfection in Dhaka City. International Journal of Scientific & Engineering Research, 5(1).

SDWF. (2018). Water and Human Health. Retrieved October 27, 2019, from Safe Drinking Water Foundation website: https://www.safewater.org/fact-sheets-1/2017/1/23/water-and-human-health

Shaw, R., & Thaitakoo, D. (2010, June 7). Chapter 1 Water communities: Introduction and overview [Book-part]. https://doi.org/10.1108/S2040-7262(2010)0000002004

Umetsu, C., Donma, S., Nagano, T., & Coşkun, Z. (2019). The Role of Efficient Management of Water Users' Associations for Adapting to Future Water Scarcity Under Climate Change. In T. Watanabe, S. Kapur, M. Aydın, R. Kanber, & E. Akça (Eds.), Climate Change Impacts on Basin Agro-ecosystems (pp. 319–342). https://doi.org/10.1007/978-3-030-01036-2_15

Wahab, S. T., Mamtaz, R., & Islam, M. M. (2016). Applicability of Water Sensitive Urban Design (WSUD) in Dhaka City. Proceedings of the 3rd International Conference on Civil Engineering for Sustainable Development (ICCESD2016). Khulna, Bangladesh.

World Bank. (2002). Linking poverty reduction and environmental management—Policy challenges and opportunities (No. 24824; p. 1). Retrieved from The World Bank website: http://documents.worldbank.org/curated/en/347841468766173173/Linking-poverty-reduction-

Proceedings of the 5th International Conference on Civil Engineering for Sustainable Development (ICCESD 2020), 7~9 February 2020, KUET, Khulna, Bangladesh (ISBN-978-984-34-8764-3)

INUNDATION PROBLEM AND DRAINAGE SYSTEM ANALYSIS OF BUET USING EPA SWMM

Abdullah Mohammad Taher[1] and Akramul Haque*[2]

[1]M.Sc Engineering Student, Dept. of Water Resources Engineering, Bangladesh University of Engineering and Technology, Dhaka-1000, Bangladesh, e-mail: abdullahtaher997@gmail.com
[2]M.Sc Engineering Student, Dept. of Water Resources Engineering, Bangladesh University of Engineering and Technology, Dhaka-1000, Bangladesh, e-mail: akramul109183@gmail.com

***Corresponding Author**

ABSTRACT

Dhaka, Capital of Bangladesh, is known for water-logging and drainage congestion, losing its past glory of natural khals and wetlands full of fresh water. The situation is seriously provoked during the monsoon. BUET is not exceptional in this case. The main reason behind the water logging in BUET is the lacking of organized drainage network and capacity of it. There is no valid data on, how much water, BUET area does carry to the outlet of Education Board area, Bakshi Bazar, Dhaka. This study mainly focuses on determining the total outfall at the outlet of that area and the pipe capacity to extract water from it or not.A study area of 69.65 acres (0.288 sq. km) of BUET is chosen for the study.The study area has been divided into three parts. West Palashi campus is not included in this study, as the outlet of that campus is different. The water logging problem is severe in the main campus and the Southern side of the campus.After assessing the drainage network, it was found that some network is mixed with the sewer system. Also, some new network is not modified in the main drawing. As the study area is small, DEM was not used, rather the area was extracted from the Google Earth. A stream network was added later. After that, the model was simulated using EPA SWMM and find out the basic reason for inundating the area in high intensity rainfall.As the Southern part of BUET is lower than the Eastern side, a lot of stormwater comes outside of the catchment area and goes through the main BUET WASA line of stormwater. That's why an extra flow is assumed in this study at the first junction point. Peak discharge at two outlets have been determined considering 50 years rainfall data for 5 year return period.

Keywords: *Drainage problem, BUET area, EPA SWMM, Stream network, Peak discharge.*

1. INTRODUCTION

The surface water area of Dhaka Central Region is about 13% of the total land area. Our drainage has two aspects: Flood protection and storm-water discharge, which are interrelated. The capital's water resources are threatened by both human activity as well as natural causes. Climate change is affecting our city, in particular, in three ways: Increased frequency of floods, drainage congestion, and heat stress. Because of its geographic location, Dhaka suffers from river floods annually. The city also suffers from frequent storm water flooding. The illegal encroachment of rivers, water bodies, lands filling, and indiscriminate dumping of domestic and industrial waste into rivers and canals are accelerating the drainage congestion (Ahammad, 2018).

As a result, Dhaka faces severe storm water flooding during heavy rainfall. The local surface water hydrology around Dhaka is complex -- the Dhaleswari River, a tributary of the Jamuna River, flows by the south-eastern part of the North Central Region of Bangladesh, close to the confluence of the Padma River and Upper Meghna River. The Lakhya River joins Dhaleswari at 11km downstream of the Buriganga confluence. About 5km below the Dhaleswari-Lakhya confluence, the Dhaleswari meets the Meghna River, which in turn flows into the Padma River, a further 20km downstream (Ahmed, 2019).

All of these results with the city's drainage system being under the influence of backwater effects from surrounding rivers. The city has been experiencing a gradual increase in water-logging over the last decade, of course. Moderate-to-heavy rain causes serious drainage problems in many parts of the city. The process of rapid urbanization is not focusing enough on adequate drainage facilities, which causes water-logging and temporary inundation in parts of Dhaka for several days during monsoon.

The inundation problem in BUET has been deteriorating in the recent years because of poor drainage system. One of the basic reasons behind this, the campus is in a natural depression because of the surroundings ground elevation has been increased by the authority of municipality and this campus is also situated low-lying area compare to the surroundings. When a moderate or high intensity rainfall occurs, storm runoff from inside and outside the campus comes together in the low-lying southern part of the campus. And it creates drainage congestion. This issue has become more serious when the drainage system of the education Board area has become worsen. Most of the water from BUET area generally passes through the Education Board outlet and their final outlet is in Buriganga River. But, two final outlets are being found according to DWASA Design. One outlet is in Gabtoli-Sadarghat Outlet & another is Babubazar Outlet (Ahmed, 2008).

Dhaka city experiences a deluge every time it rains heavily. Every time major floods occur in the country and every time it rains; the city of Dhaka faces acute drainage problem. Parts of the city go under water. In the densely populated city, woes of people know no bounds.

In spite of huge investment over the years, particularly after 1988 floods when almost whole city of Dhaka went under water, the 1998 floods appeared most devastating. About Dhaka city, drainage situation aggravated due to silted-up, blocked drainage channels. WASA's limited storm water drainage is too inadequate for a city of 850 sq.km. (Abdullah, 2017).

In this study, ArcGIS is basically used for the assessment and analysis of Drainage system and inundation problem identification through some data which are basically made in ArcGIS. SWMM Model also has been used for the calibration of the surface runoff coefficient and the analysis of actual surface runoff in this area. The specific objectives of the study are:

(i) Review the major causes, extent of the severity and management approaches of the past storm water flooding in the BUET drainage area.
(ii) Develop a Model using SWMM for the coordination approach to improve the urban flood management and drainage system.

(iii) Study of the existing storm water drainage facilities and maintenance system of the BUET zone of Dhaka city.

This study is expected to provide significant insight to find out the causes addressing its effects of waterlogging due to storm water flooding. Developing guidelines of integrated management approach will provide effective storm water flood mitigation and management.

2. METHODOLOGY

2.1 Study area

BUET is located at the southern part of Dhaka which is shown in Figure 1-1. It is located in Zone-3 of Dhaka South City Corporation. The natural slope of BUET campus is from north to south. There is a natural depression in the southern part of the campus, the Bakshibazar residential area, Dr. Fazley Rabbi Hall and education board. Consequently, the runoff is driven under gravity to the southern part of the campus. It has some large academic and residential building in both sides. There is a big play ground at the eastern end of the BUET. The area is drained by the surface and sub-surface and underground drains. The drainage is slow due to blockage of the underground sewer and a major drainage system under BUET central road have been deactivated before years. Even a few years back, flooding in the campus usually did not occur during early monsoon under average rainfall condition. But it is observed in recent years that even an average rainfall is causing a big water logging.

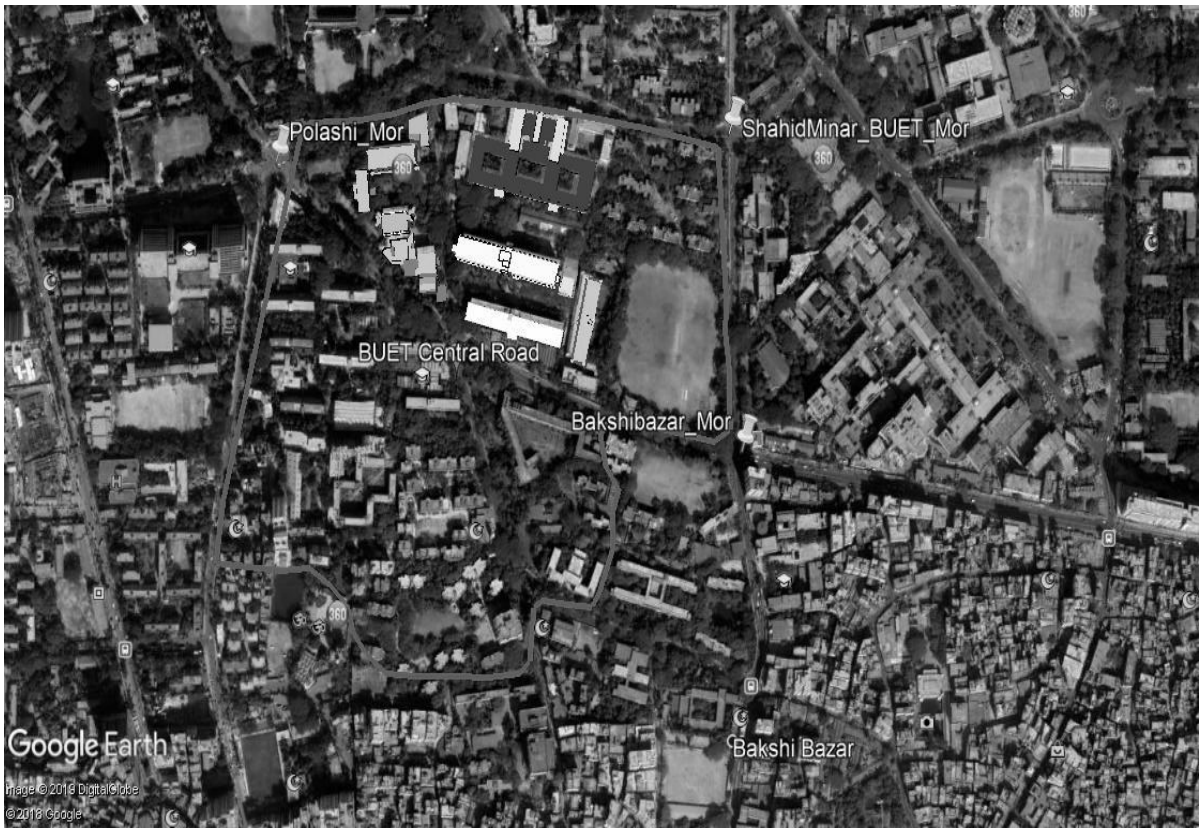

Figure 1-1: Map of Study Area of BUET (Source: Google Earth Pro).

2.2 Data collection

For the analysis of the Storm water Drainage System, rainfall and drainage network data of the study area is required which are shown in Table 1-1. Rainfall data for Dhaka city has been collected from Bangladesh Meteorological Department (BMD). As the study area is a part of Dhaka city, the rainfall

should be same for both cases. Moreover, there is no special station to capture the rainfall of BUET area. So, the overall rainfall of Dhaka city has been considered in this study.

Table 1-1: Data collection

Data type	Source	Data location	Period
Rainfall	BMD	Dhaka	1965-2015
Conduit invert elevation	DWASA	Buet	
Buet area image	GOOGLE EARTH	Buet	

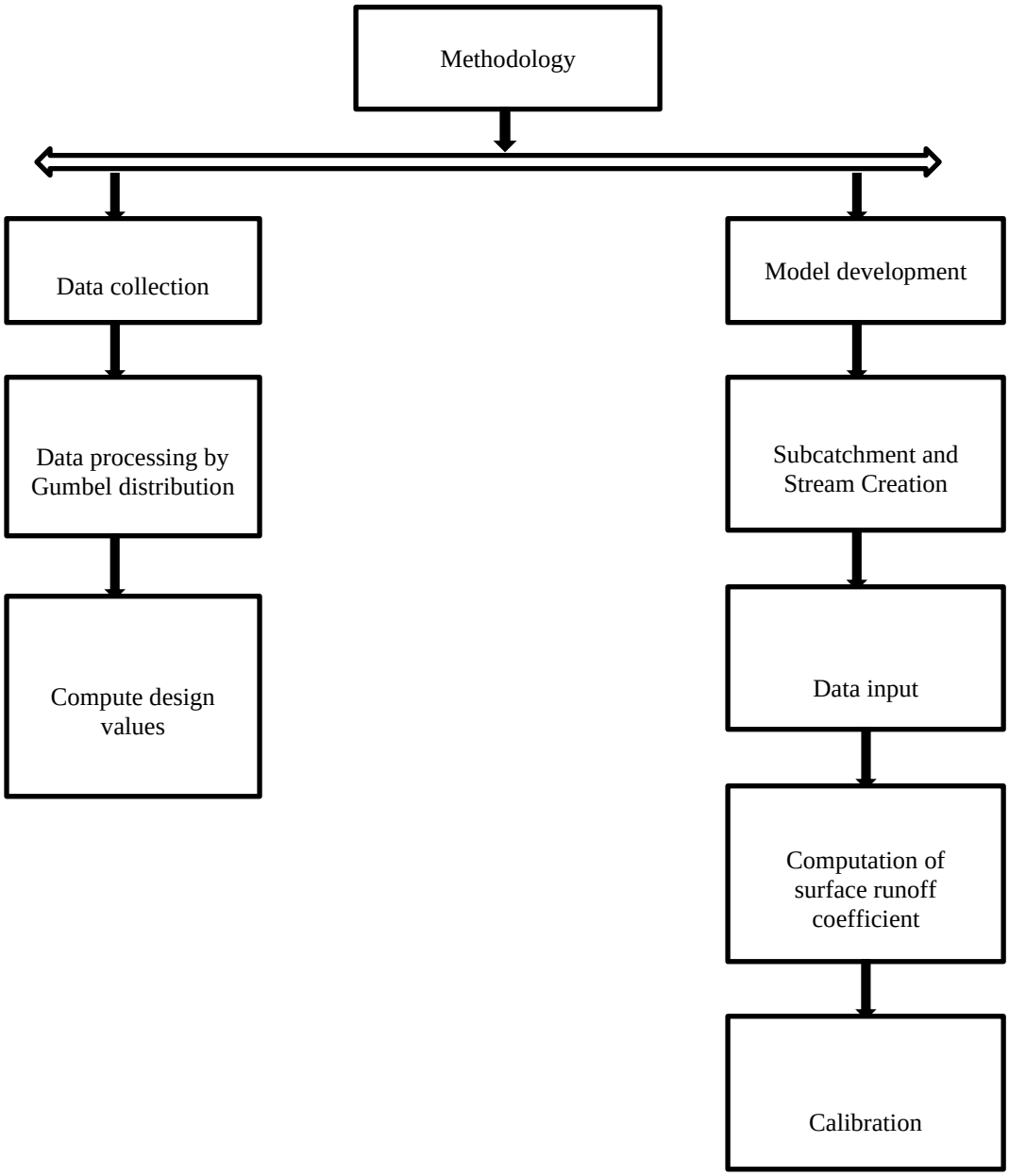

Figure 2-1: Diagram of methodology

3. DATA ANALYSIS AND RESULTS

EPA SWMM provides runoff quantity generated within each sub-catchment. The Watershed (Study area) is divided according to the elevation and it is plotted in ARC-GIS. Hydrological analysis is done

to determine 5 years return period rainfall. This analysis is done by Gumbel's distribution. Annual maximum rainfall data is shown in Table 3-1. Table 3-2 is for percentage of rainfall for different time steps.

3.1 Manhole Data Analysis

An analysis of invert elevation and ground elevation over distance between manholes from BUET main gate to the final outlet in Buriganga was observed and also the main outlet of BUET area near Education Board data also attached to understand the volume of water passing from manhole.

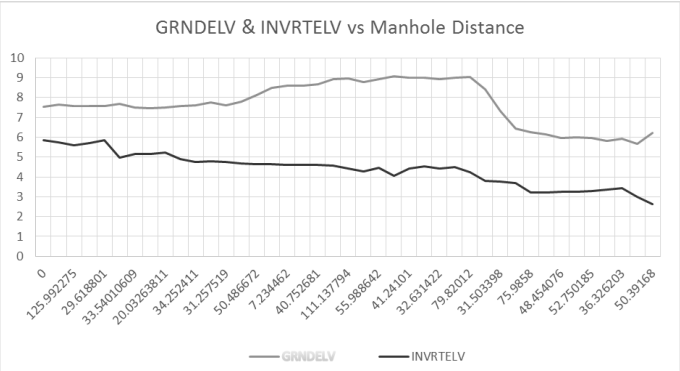

Figure 3-1: Ground Elevation, Invert elevation of manhole over manhole distance observation

3.2 Hydrological Analysis

The collected rainfall data from BMD data are analysed which is shown in Table 3-1

Table-3.1: Annual Maximum Daily Rainfall Data in Dhaka City from year 1965-2015

Year	Max daily rainfall(mm)	Year	Max daily rainfall(mm)
1965	177	1992	90
1966	257	1993	140
1967	125	1994	74
1968	145	1995	83
1969	86	1996	150
1970	152	1997	121
1971	251	1998	122
1972	231	1999	141
1973	168	2000	158
1974	143	2001	71
1975	163	2002	88
1976	100	2003	93
1977	128	2004	341
1978	108	2005	125
1979	91	2006	185
1980	81	2007	152
1981	81	2008	190
1982	146	2009	333
1983	133	2010	87
1984	151	2011	94
1985	92	2012	62
1986	176	2013	122
1987	138	2014	75
1988	135	2015	90
1989	118	2016	
1990	94	2017	
1991	123	2018	

By Gumbel's distribution, it has been found that for 5 yr.'s return period, rainfall is 187.26 mm which means this rainfall will occur at least once in 5 years in Dhaka City. BUET experiences same amount of rainfall as BUET is within the main Dhaka city.

Table 3.2: For 5-year return period, Percentage of Rainfall for Different Time Steps

Time step	Percentage	5-yr return period
0-4	9%	16.86
4-8	15%	28.09
8-12	44%	82.41
12-16	16%	29.97
16-20	9%	16.86
20-24	7%	13.11

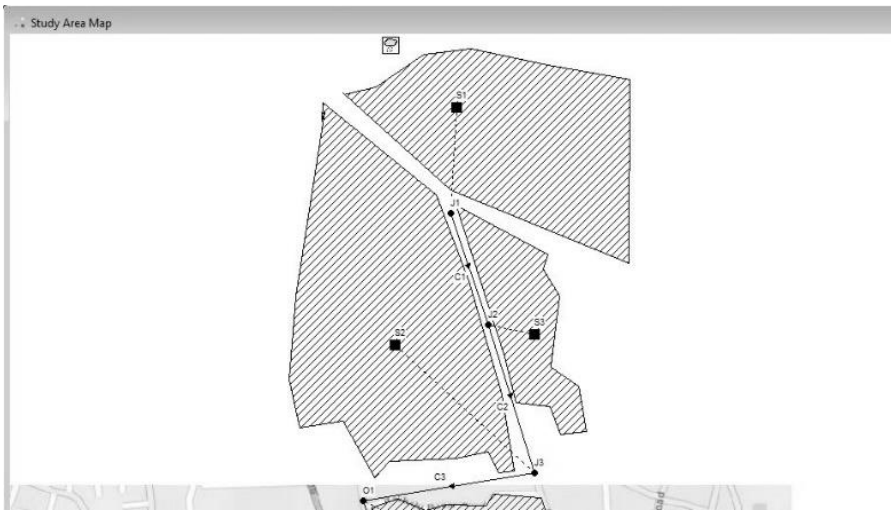

Figure 3-2: Delineated Watershed of Study Area using EPA SWMM

3.3. Model results

Watershed delineation using EPA SWMM gives 3 sub-catchments (Figure 3-2). In Table 3-3, the runoff values of each sub-catchment are given. The peak runoff is 332.03 CFS in S1 sub-catchment for 5-year return period. Flow rate, flow velocity (ft/sec), Time of maximum flow occurence of link such as conduit, outlets are obtained from EPA SWMM simulation are shown in Table 3-4.

Table 3-3: Sub catchment runoff coefficient in SWMM Model

Sub-catchment	Total Precipitation(mm)	Total Runoff (mm)	Peak runoff (CFS)	Runoff coefficient
S3	187.26	5.82	125.23	0.777
S2	187.26	4.72	269.55	0.630
S1	187.26	4.56	332.03	0.609

Table 3-4: Conduit flow summary, simulated by GeoSWMM for 5 years return period

Link	Type	Maximum flow (CFS)	Day of maximum flow	Hour of max flow	Max velocity (ft/sec)
C1	CONDUIT	2.78	0	01:50	1.79
C2	CONDUIT	0.74	0	02:28	0.58
C3	CONDUIT	6.75	0	01:12	4.20

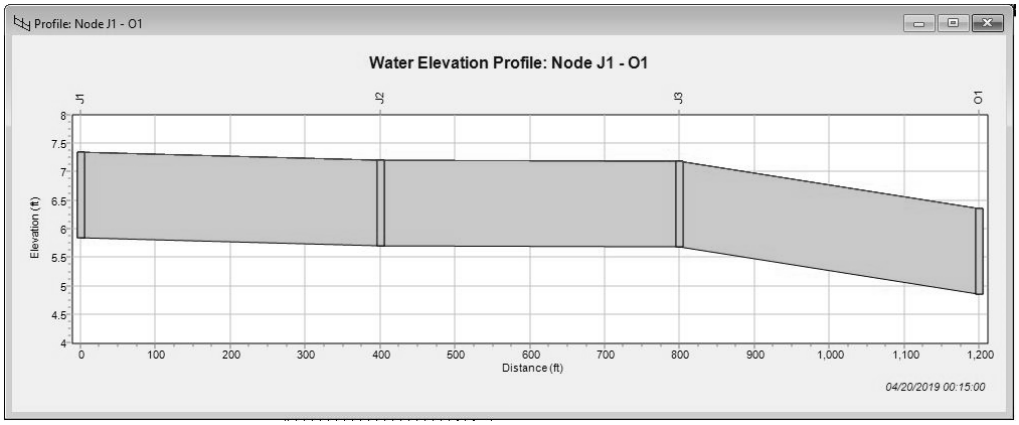

Figure 3-3 : Water elevation profile plot of Study Area

The water profile plot is obtained for conduits from node J1 to O1 is as shown in Fig. 3-3. The simulation status report shows that sections between these nodes are surcharged (flooded). The depth of surcharging at node J1,at node J2 and at node J3 is 1.5 ft above crest level, whereas for node O1 is 1.8 ft.

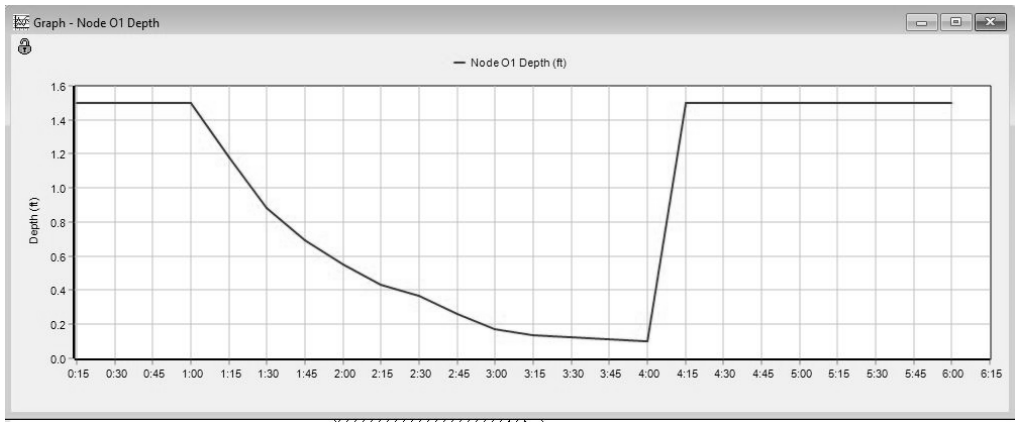

Figure 3-4 : Node O1 depth plot of the study area

In outfall Node in Figure 3-4, Depth is variable for certain time but before flooding node depth decreased and after flooding node depth again increased.

Table 3-5 : Node flooding at different locations

Summary Results

Topic: Node Flooding — Click a column header to sort the column.

Node	Hours Flooded	Maximum Rate CFS	Day of Maximum Flooding	Hour of Maximum Flooding	Total Flood Volume 10^6 gal	Maximum Ponded Volume 1000 ft3
J1	3.77	323.10	0	04:10	4.026	0.000
J2	4.33	124.92	0	04:10	1.435	0.000
J3	3.17	259.03	0	04:10	2.905	0.000
O1	3.95	346.35	0	04:10	4.762	0.000

The Table 3-5 is shown for Node flooding.The maximum rate at Node J1,J2,J3,O1 are 323.1 CFS,124.92 CFS,259.03 CFS and 346.35 CFS respectively.

3.3.1 Calibration

According to New Neighbourhood Design and development standard manual (2012),

In this study, the total area of the study is 0.288 km^2 or 65.69 acres.

In this study, Runoff Coefficient for Roofs and streets are almost 0.75 to 0.95

Runoff Coefficient for Playgrounds/Residential is almost 0.20 to 0.40

From ArcGIS, from 34.9 acres, 46% playground (Around 16.12 acres) and 54% building (Around 18.78 acres), 26.97 acres 74% building (17.202 acres) and 36% playground (Around 9.768 acres), 7.78 acres 28% playground (Around 2.189 acres) and 72% building(around 5.591 acres).

The value of runoff co-efficient, C

$$= \frac{(34.9(0.54 * 0.75 + 0.46 * 0.25) + 26.97(0.74 * 0.75 + 0.36 * 0.25) + 7.78(0.28 * 0.75 + 0.72 * 0.25))}{(34.9 + 26.97 + 7.78)}$$

$$= 0.553$$

From Model,the average value of runoff co-efficient,C = 0.672
From the Calibration, it can be said that the model has shown about 77.52% accuracy found in 5 year return period.

3.4 The outlet pipe size calculation:

From Model,the average value of runoff co-efficient,C = 0.672

Runoff Coefficient of the study area, C = 0.553

Rainfall Intensity for 5-yr 1-hr Rainfall, i = 2.59 inch/hr =65.786 mm/hr

Total area of the study, A = 65.69 acres = 0.288 sq. km

So, Peak Discharge, Q = 0.278 CiA = 2.917 m3/s

From Model, Peak Discharge, Q= 0.278 CiA= 6.56 m3/s where, C=0.672
From rational method, D = 1.726 m = 5.66 ft.
According to model discharge, D= 2.55 m = 8.38 ft.

So, 8.5 ft diameter pipe needed for the total flow passing which is generated in total area but now, at present, 5.5 ft diameter pipe exists there. Though, A manhole with 13.21 m^3 volume generated there but still pipe size isn't enough to flow the total runoff

4. CONCLUSIONS

It has been seen from the field visit that the sewer system and storm water drainage system has been mixed at various places and the catchment outside BUET area (BUET to Buriganga outlet), pipe size isn't enough to remove the city's excess water completely. That's why BUET area is inundated. As moving forward, discharge will be increased spontaneously. Final outlet pipe diameter is 5.5 ft. but it needs min. 8.5 ft. diameter pipe to runoff the stormwater completely. Natural depression is another cause but if the drainage is being properly maintained, that's not create any problem.

- A few maintenance occur in BUET drainage and drainage system is very poor in condition.
- Behind the reduction in the drain capacity, Dumping wastages and blockage in the drains are important reasons.
- One of the system which starts from BUET shahid minar to BUET teachers quarters (Education board) has been disabled in recent years. So, this is one of the major cause for water logging in this area.

ACKNOWLEDGEMENTS

I would like to express my sincere gratitude to Dr. Md. Mostafa Ali, Professor, Department of Water Resources Engineering, BUET and then to Md. Touhid Hossain, Consultant, Eden Green Environmental Ltd. for their wonderful guidance in teaching and guiding.

REFERENCES

A.S. Islam, S.K. Bala and M.A. Haque, 2009, Flood inundation map of Bangladesh using MODIS time-series images, Journal of Flood Risk Management.

Abdullah, F., 2017, Design of Stormwater Drainage Network with Limited Data Using GeoSWMM: a Case Study for Tangail Sadar Upazilla, B.Sc. thesis, Department of Water Resources Engineering, Bangladesh University of Engineering and Technology, Dhaka.

Afrin, S. (2015). Drainage Capacity Assessment of Hatirjheel Beguenbari Khal System Considering Climate Change. M.Sc. thesis, Department of Water Resources Engineering, Bangladesh University of Engineering and Technology, Dhaka.

Ahammad, M., 2018, Analysis of Stormwater Runoff for a Selected Catchment of Eastern Dhaka using Hydrological Model, M.Sc. thesis, Department of Water Resources Engineering, Bangladesh University of Engineering and Technology, Dhaka.

Ahmed, N., 2008, Management of Storm Water for Drainage of Azimpur, BUET, and Lalbag Area of Dhaka City. M.Sc. Thesis, Institute of Water and Flood Management, BUET.

Ahmed,T.,2019. Dhaka's water problems.Dhaka Tribune .

Google Earth Engine. (n.d.). Retrieved 2019, from https://www.google.com/earth/

Kibria,S. and Biswas,R.,2019. Design Of Stormwater Drainage Network With Limited Rainfall Data Using GeoSWMM: Case Study For Dinajpur City, Proceedings on International Conference on Disaster Risk Management, Dhaka, Bangladesh, January 12-14, 2019 .

Waiker, M.L. and Namita,U.,2015. Urban Flood Modeling by using EPA SWMM 5. SRTM University's Research Journal of Science.

Proceedings of the 5th International Conference on Civil Engineering for Sustainable Development (ICCESD 2020), 7~9 February 2020, KUET, Khulna, Bangladesh (ISBN-978-984-34-8764-3)

NUMERICAL INVESTIGATION OF CHARACTERISTICS OF FLOW AROUND SPUR DIKES WITH IPSILATERAL LAYOUT

Nur-E-Jannat Pollen *[1] and Md. Shahjahan Ali[2]

[1]Postgraduate Student, Institute of Disaster Management, Khulna University of Engineering & Technology, Bangladesh, e-mail: pollen.kuet@gmail.com
[2]Professor, Department of Civil Engineering, Khulna University of Engineering & Technology, Bangladesh, e-mail: babul41@yahoo.com

***Corresponding Author**

ABSTRACT

In a group of dikes, water flow varies with the number of dikes, their position and orientations as well as the space between the dikes. This study represents the results from the numerical simulation of flow around a group of dikes with ipsilateral layout (two dikes and three dikes in a group, installed on same side of the bed) for installed condition in different orientations. In the study, iRICNays2DH based on 2D model is used to simulate the flows in a straight open channel with groins of 90º, 60º, 120º angled with the direction of flow. A fixed bed, uniform flow with depth-averaged k-epsilon model is used for the simulation. The model has been used to simulate the pattern of flow around the dikes and the basic flow features are reproduced. The general flow features around a group of dikes is reproduced successfully in this simulation. From the simulation it is seen that the flow is deviated towards the opposite bank than the groin mounted bank due to obstruction of flow by groin. From the simulation it is observed that one vortex was generated for the groin spacing to groin length ratio L/l=1-3, two vortices were generated at L/l=4-9, three vortices were found to be generated at the ratio L/l=10-9. The simulated results are compared with the previous experimental data. A good agreement is shown between the numerical and experimental results. From the compared results it may conclude that the present model can be used for simulating the flow around an individual and group of dikes.

Keywords: *Dike, iRICNays2DH, k-epsilon model, Numerical result.*

1. INTRODUCTION

In the field of hydraulic engineering and river engineering the most commonly used structure is spur dikes (Cao et al. 2013). Dikes are used for various purposes, like river erosion, protection, river diversion, navigation, flood control (Kang et al. 2012). Dikes are like elongated obstruction which have one end into the current and other end on the bank of the tide (Ali et al. 2017) Spur dikes decreases the width of river and increase velocity and causes flow separation aligned with the flow of the river and recirculation of downstream streamlines and results in extensive scour and scour hole (Yazdi et al. 2010). Construction of dikes can protect neighbouring river bank by guiding flow to a relevant direction from scour (Fang et al. 2014). The ability of sediment transport of water flow increases with the velocity. This may help to prompt bed erosion in the main channel and the area around groin head (Fang et al. 2014). These studies were accomplished by different conditions like groin length, number of groins, installation angle towards the river flow, permeable or impermeable states, submerged or non-submerged conditions, etc. (Yeo et al. 2005). It is a challenge for the applications of numerical models due to the variation of groin flow. Separation and recirculating length may greatly different (Quanhong & Pengzhi, 2007). The groin with perpendicular directions at the river main flow, may give a complex three dimensional form of flow around the groin because of narrowing and deviation of flow (Tingsanchali & Maheswaran, 1990). For total understanding of the flow pattern, use of numerical techniques is important (Fang et al. 2014). Traditionally, the Reyolds-averaged Navier-Stokes model is used for both research and engineering (Fang & Rodi, 2003). Many cases which have complex flow boundaries may face difficulties to solve the equation of motion (Zhou et al. 2004).

In groin flow study, groin field is the dead-water zone between groins. One or more vortices influenced over the flow and secondary flow produces and develops. (Fang et al. 2014). When the width of the flow is large then depth, compared to the gravitational acceleration, vertical acceleration of water is neglected at the free surface flows (Zarrati et al. 2005). A two-dimensional depth-averaged model, was used by Tingsanchali and Maheswaran (1990), introducing a three-dimensional correction factor and incorporating a correction factor used in k-epsilon model to improve the computed bottom stresses. To solve the unsteady two-dimensional depth averaged equations Molls et al. (1995) developed a general mathematical model by combining it with a constant eddy viscosity turbulent model (Ettema and Muste, 2004). A great deal of research has been carried out in recent years, especially by Chinese researchers such as Fang et al. (2014), Tang and Ding (2007), Quanhong and Pengzhi (2007), Zhanfeng and Xiaofeng (2006). They studied the model and the scouring around the groin using various models of turbulence under different conditions of flow and groin dimension.

Groins under clear water scour conditions have been a rapid expension of literatures in both laboratory experiments and numerical simulations (Rahman and Muramoto 1999, Raudhivi and Ettema 1997. Again, research about local scour formulates around piers and groins (Anawaruzzaman 1998); River course stabilization by groin like structures (Khaleduzzaman 2004); Exchanging process between river and its groin fields etc. (Uijttewaal et al. 2001). The local scour at the toe of protected embankment was investigated by Hasan (2003). In this study iRIC Nays2DH, 2D software based on Navier-Stokes (available in www.i-ric.org) is used to simulate the flow in an open channel around the groin structure.

2. BASIC EQUATIONS OF THE MODEL

The International River Interface Cooperative (iRIC) is an informal organization made up of academic faculty and government scientists with the goal of developing, distributing, and providing education for a public-domain software interface for river modeling. Formed in late 2007, the group released the first version of this interface, iRIC, in 2009. The iRIC software interface includes models for two- and three-dimensional flow, sediment transport, bed evolution, groundwater-surface-water interaction, topographic data processing, and habitat assessment, as well as comprehensive data and model output visualization, mapping, and editing tools. All of the tools within iRIC are specifically designed for use in river reaches and utilize common river data sets. The models are embedded within a single

graphical user interface so that many different models can be made available to users without requiring them to learn new pre and post-processing tools. iRIC provides a comprehensive, unified environment in which data that are necessary for river analysis solvers (hereafter: solvers) can be compiled, rivers can be simulated and analytical results can be visualized. The highly flexible iRIC interface allows various solvers to be imported, or you can use one of the iRIC solvers. Upon selecting the solver, iRIC selects functions suitable for the solver and prepares the optimal simulation environment. Because the iRIC functions vary depending on the solver, the method of using the iRIC application depends on the solver. The basic equations in an orthogonal coordinate system (x, y) before transformation (mapping) into a general curvilinear coordinate system are as follows:
[Equation of continuity]

$$\frac{\partial h}{\partial t} + \frac{\partial (hu)}{\partial x} + \frac{\partial (hv)}{\partial y} = 0 \quad (1)$$

[Equations of motion]

$$\frac{\partial (uh)}{\partial t} + \frac{\partial (hu^2)}{\partial x} + \frac{\partial (huv)}{\partial y} = -hg\frac{\partial H}{\partial x} - \frac{\tau_x}{\rho} + D^x + \frac{F_x}{\rho} \quad (2)$$

$$\frac{\partial (vh)}{\partial t} + \frac{\partial (huv)}{\partial x} + \frac{\partial (hv^2)}{\partial y} = -hg\frac{\partial H}{\partial y} - \frac{\tau_y}{\rho} + D^y + \frac{F_y}{\rho} \quad (3)$$

$$\frac{\tau_x}{\rho} = C_f u\sqrt{u^2 + v^2} \quad (4)$$

$$\frac{\tau_y}{\rho} = C_f v\sqrt{u^2 + v^2} \quad (5)$$

$$D^x = \frac{\partial}{\partial x}\left[v_t \frac{\partial (uh)}{\partial x}\right] + \frac{\partial}{\partial y}\left[v_t \frac{\partial (uh)}{\partial y}\right] \quad (6)$$

$$D^y = \frac{\partial}{\partial x}\left[v_t \frac{\partial (vh)}{\partial x}\right] + \frac{\partial}{\partial y}\left[v_t \frac{\partial (vh)}{\partial y}\right] \quad (7)$$

$$C_f = \frac{gn_m^2}{h^{\frac{1}{3}}} \quad (8)$$

where h is water depth, t is time, u is velocity in the x direction, v is velocity in the y direction, g is gravitational acceleration, H is water depth, τ_x is riverbed shearing force in the x direction, τ_y is riverbed shearing force in the y direction, C_f is riverbed shear coefficient, ν_t is eddy viscosity coefficient, and hv is minimum value of water depth and height of vegetation.

2.1 K-ε Model

The eddy viscosity coefficient νt in the standard k-ε model is expressed by the following equation:

$$v_t = C_\mu \frac{k^2}{\epsilon} \quad (9)$$

Where, Cμ is a model constant. k and ϵ are obtained by the following equations:

$$\frac{\partial k}{\partial t} + u\frac{\partial k}{\partial x} + v\frac{\partial k}{\partial y} = \frac{\partial}{\partial x}\left(\frac{v_t}{\sigma_k}\frac{\partial k}{\partial x}\right) + \frac{\partial}{\partial y}\left(\frac{v_t}{\sigma_k}\frac{\partial k}{\partial y}\right) + P_h + P_{kv} - \epsilon \quad (10)$$

$$\frac{\partial \epsilon}{\partial t} + u\frac{\partial \epsilon}{\partial x} + v\frac{\partial \epsilon}{\partial y} = \frac{\partial}{\partial x}\left(\frac{v_t}{\sigma_\epsilon}\frac{\partial \epsilon}{\partial x}\right) + \frac{\partial}{\partial y}\left(\frac{v_t}{\sigma_\epsilon}\frac{\partial \epsilon}{\partial y}\right) + C_{1\epsilon}\frac{\epsilon}{k}P_h + P_{\epsilon v} - C_{2\epsilon}\frac{\epsilon^2}{k} \quad (11)$$

where C1ε, C2ε, σk and σε are model constants whose respective values are shown in Table 2.

C_μ	$C_{1\varepsilon}$	$C_{2\varepsilon}$	σ_k	σ_ε
0.09	1.44	1.92	1.0	1.3

$$P_{kv} = C_k \frac{u_*^3}{h} \quad (12)$$

$$P_{\epsilon v} = C_{\epsilon} \frac{u_*^4}{h^2} \quad (13)$$

3. METHODOLOGY

3.1 Numerical Tests

3.1.1 Hydraulic Parameter

The simulated hydraulic parameters are shown in table 1 for different test cases. The parameters were taken same as the experiments by Kang et al. (2012) for series-1 (case-1) which flows in a straight open channel with groin 90º angle to the direction flow. The hydraulic parameters for the 60º (case-2) and 120º (case-3) angled groin are the same as case-1.
Again, the parameters for series-2 (case-1) flows in a straight open channel with groin 90º angled to the direction of flow were taken same as the experiments by Fang et al. (2014).
Both cases the groins are installed on the same side to make a ipsilateral layout.

Table 1: Hydraulic parameters for the simulated cases

Simulation conditions	**Series 1 (Case 1-3)**	**Series 2 (Case 1)**
Space of the groins, *L/l*	1m to 12m	5.2m
Channel length between two groins, *L*	0.3m to 3.6m	1.25m
Channel langth	8.6m to 15.2m	2.6m
Channel width, *B*	1m	1.8m
Dike length, *l*	0.3m	0.5m
Constant upstream discharge, *Q*	0.09m^3/s	0.001m^3/s
Constant depth, *h*	0.15m/s	0.046m/s
Longitudinal mesh size, *Δx*	0.06m	0.05m
Traverse mesh size, *Δv*	0.03m	0.05m
Manning's roughness equation, *n*	0.015	0.01
Time step, *Δt*	0.01sec	0.01sec

3.1.2 Flow Domain

Figure 3-2 shows the sketch of the flow domain for flows in a straight open channel with groin of 90^0 angled to the direction of flow which was performed under the same conditions of the experiments conducted by Kang et al. (2012). Figure 3-3 and Figure 3-4 show the sketch of the flow domain for 60^0 and 120^0 which were performed under the same conditions as series-1 (case-1). For all these cases 172 x 33 grids were used and the bed of the channel was fixed. Figure 3-5 shows the sketch of the flow domain for flows in a straight open channel with groin of 90^0 angled to the direction of flow which was performed under the same conditions of the experiments conducted by Fang et al. (2014). For this case 54 x 38 grids were used and the bed of the channel was fixed.

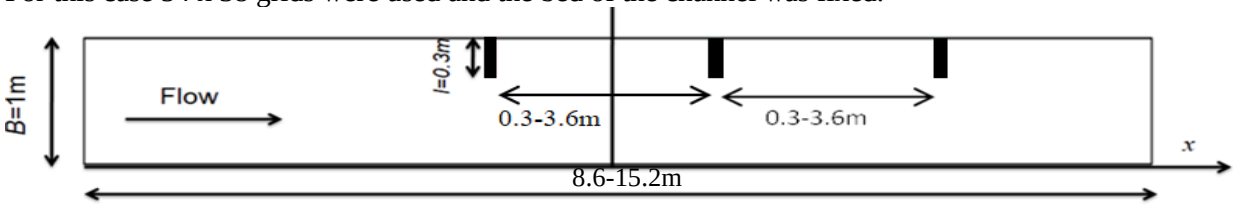

Figure 1: Groin Orientation for 90º angled to the direction of flow (series-1, case-1).

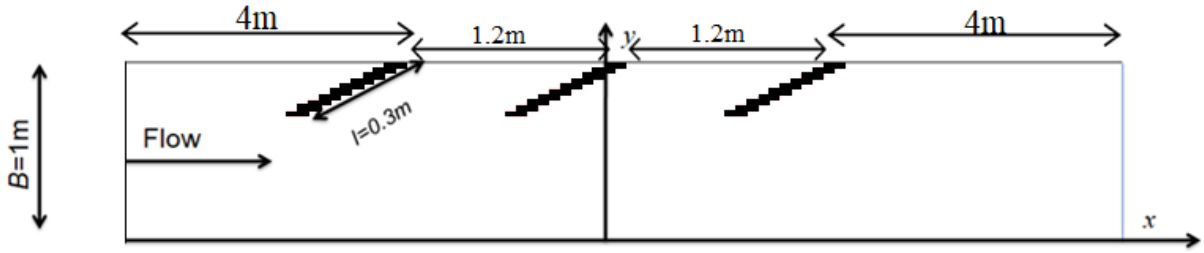

Figure 2: Groin Orientation for 60º angled to the direction of flow (series-1, case-2).

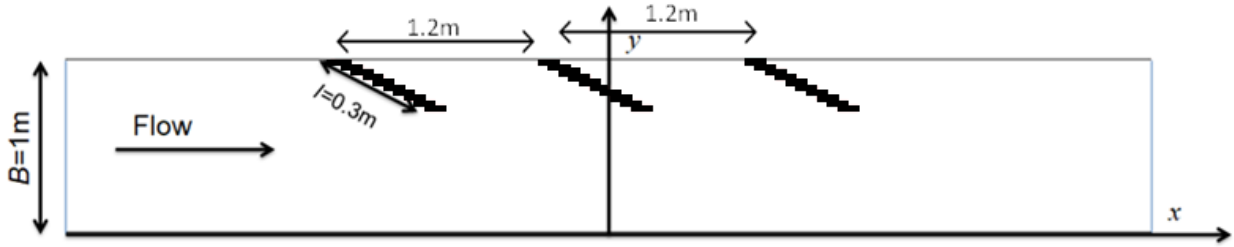

Figure 3: Groin Orientation for 120º angled to the direction of flow (series-1, case-3).

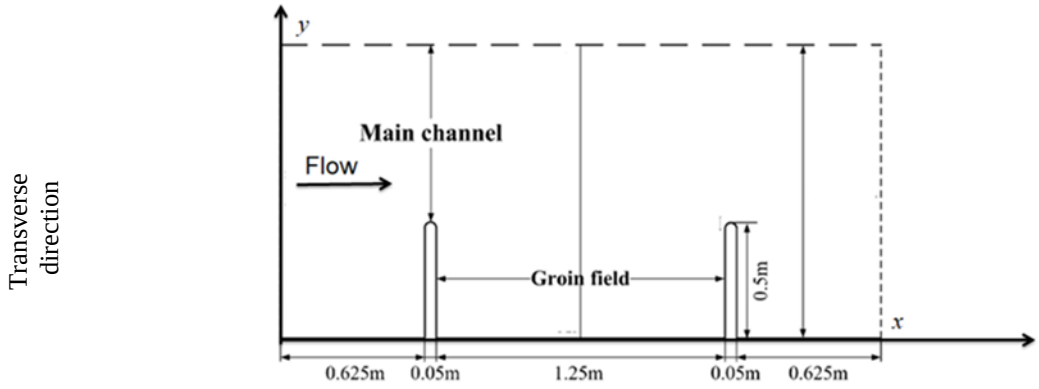

Figure 4: Groin orientation for 90º angled to the direction of flow (series-2).

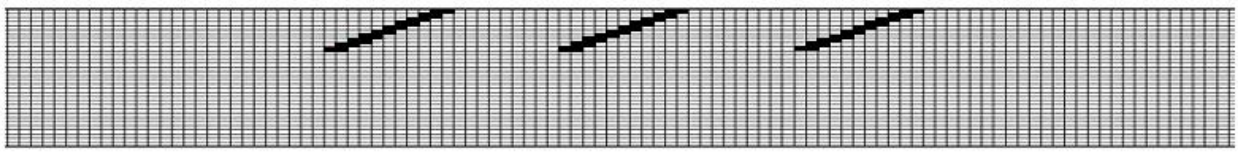

Figure 5: Grid preparation for Groin with 60º angle (Series-1, case-2)

3.2 Computational Scheme

For mean velocities governing equations are separated with the finite difference method based on full staggered boundary fitted coordinate system. The basic equations are separated as fully explicit forms and solved with the time increment. At each time step interactive procedure is used to solve it. Constant discharge at upstream and constant depth with zero velocity gradients was given as downstream boundary conditions. Finite difference scheme, whereas the nonlinear convection terms with an upwind scheme was used for the solution of the equations. 2D grid, Q, h, and initial flow conditions were given as input.

4. SIMULATED RESULTS

4.1 Numerical Setup

In the analysis, the computational domain is 8.4m to 15.2m in length and 1m in width for series-1, case-1 to-3 and 2.6m in length and 1.8m in width for series-2 (case-1). The groin length, l is 0.3m for series-1 (case-1 to case-3) and 0.5m for series-2 case-1. In series-1 (for case-1 to case-3) the upstream and downstream boundaries was 4m and in series-2 (case-1) the upstream and downstream boundaries was 0.625m. Spaces between two groins are 0.3m to 3.6m for series-1 (case-1 to case-3) and 1.25m for series-2 (case-1) respectively. Upstream discharge was 0.09m3/s for series-1 (case-1 to case-3) and 0.0132m3/s for series-2 (case-1). Manning's roughness coefficient was 0.015 and 0.01 for series-1 (case-1 to case-3) and series-2 (case -1) respectively. Ratio of channel width, l/B=0.15 for series-1 (case-1 to case-3) and 0.28 for series-2 (case-1). Calculation time setup was, Δt = 0.01sec. Flow velocity v was 0.3m/s for series-1 (case-1 to case-3) and 0.016m/s for series-2 (case-1). The simulations were performed at fixed bed.

4.2 Flow Velocity Distribution of The Groin Field By iRIC

Figure 6 represents the reproduced velocity vector for series-1 (case-1). This showed the change of shape of flow at the groin field at different ratio of L/l. From the figure, it is observed that, one vortex was generated at the ratio L/l=1-3 because of the channel rotation of the flow at the back of the upstream groin of segment fluid. For L/l=4-9 two vortices were to be generated because of the clockwise backward flow with downstream groin which made a border with segment fluid at the back of upstream groin. At the ratio L/l=10-12 three vortexes were generated because of the downstream groin and recirculation zone. The results are found to be well agreed with the experimental result of Kang et al. (2012).

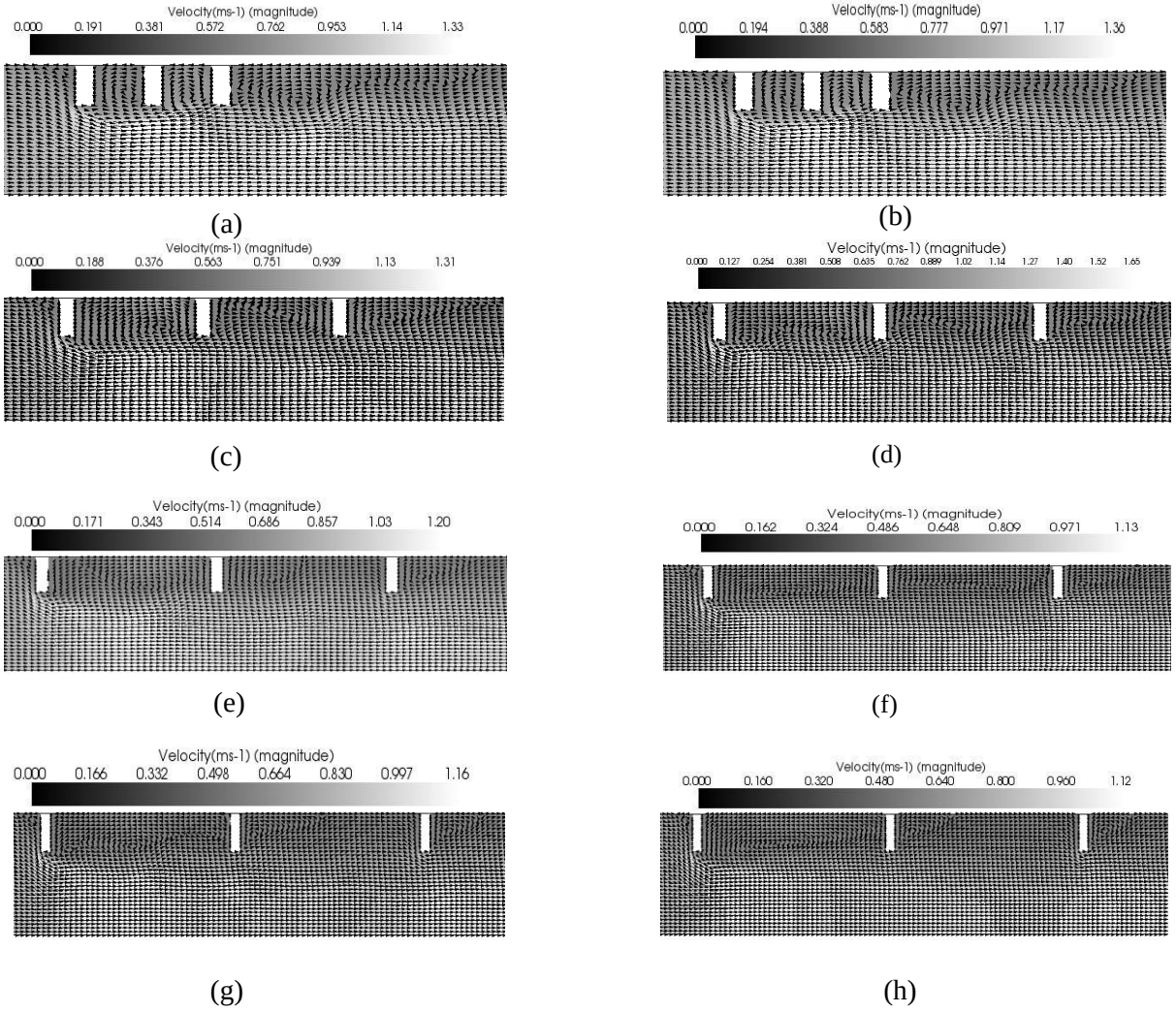

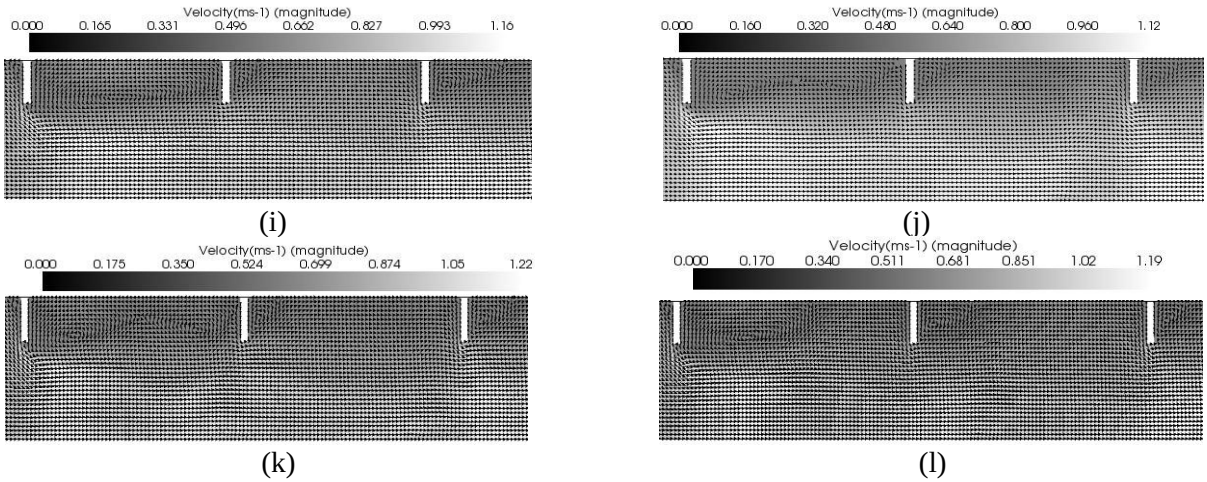

Figure 6: Velocity field of groin field measured by iRIC for series-1, case-1. (a)L/l=1; (b)L/l=2; (c)L/l=3; (d)L/l=4; (e)L/l=5; (f)L/l=6; (g)L/l=7; (h)L/l=8; (i)L/l=9; (j)L/l=10; (k)L/l=11; (l)L/l=12.

4.3 Flow Velocity Distribution of The Groin Field by Surfer

Figure 7 represents the reproduced velocity field of groin for series-1, case-1. This showed the change of shape of flow at the groin field at different ratio of L/l. Figure 4-3 shows the reproduced velocity field for L/l=1-12. The results are found to be well agreed with the experimental result of Kang et al. (2012).

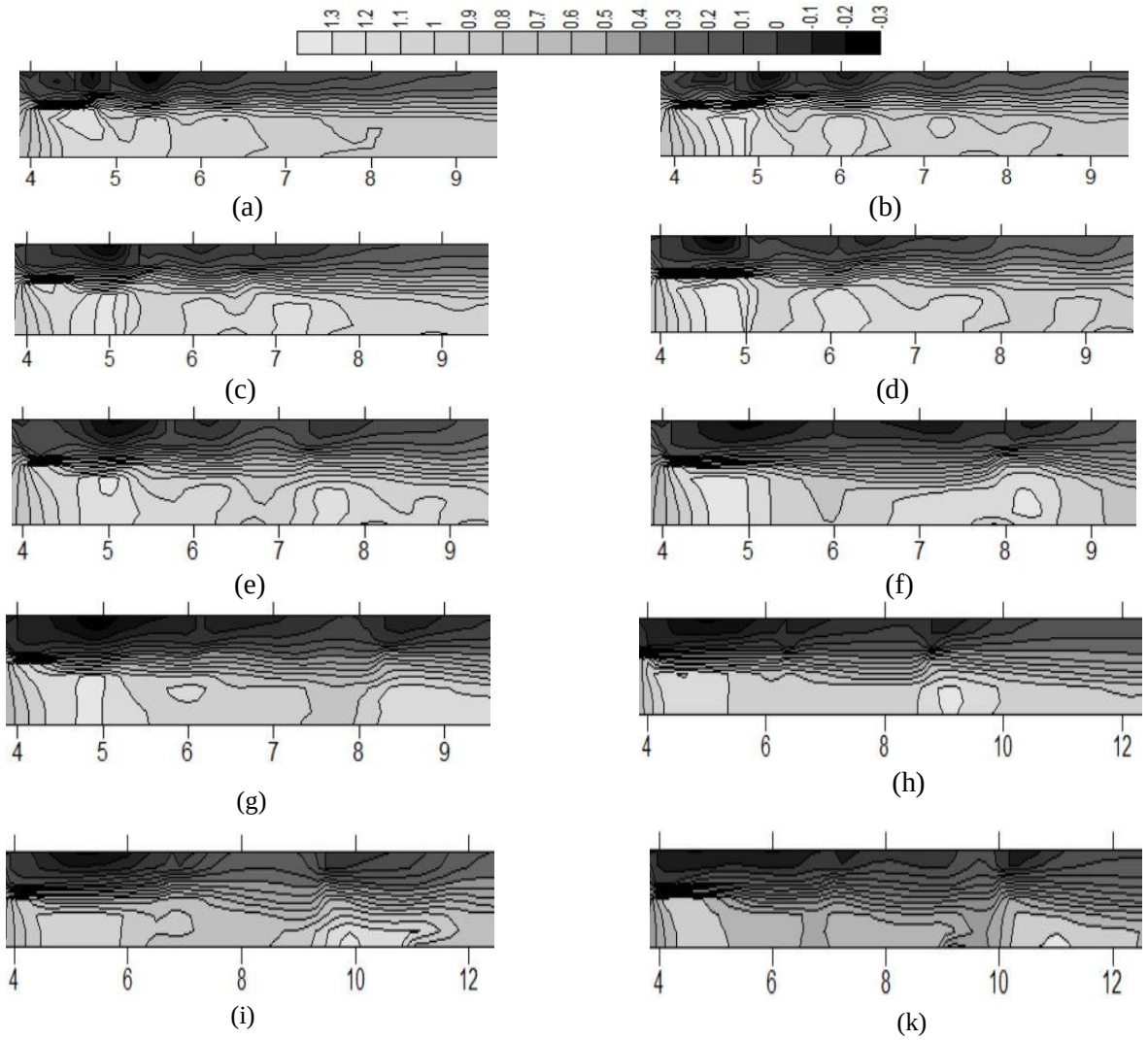

(k) (l)

Figure 7: Velocity field of groin field measured by Surfer for series-1, case-1. (a)L/l=1; (b)L/l=2; (c)L/l=3; (d)L/l=4; (e)L/l=5; (f)L/l=6; (g)L/l=7; (h)L/l=8; (i)L/l=9; (j)L/l=10; (k)L/l=11; (l)L/l=12.

4.4 Velocity Field for *L/l*=4

The space between the groins is two times bigger than length for l/l=4 in series-1. In upstream groin two vortices are shown. Figure 4-4 shows the velocity vector for groins space of L/l=4 which are reproduced form Kang et al. (2012).

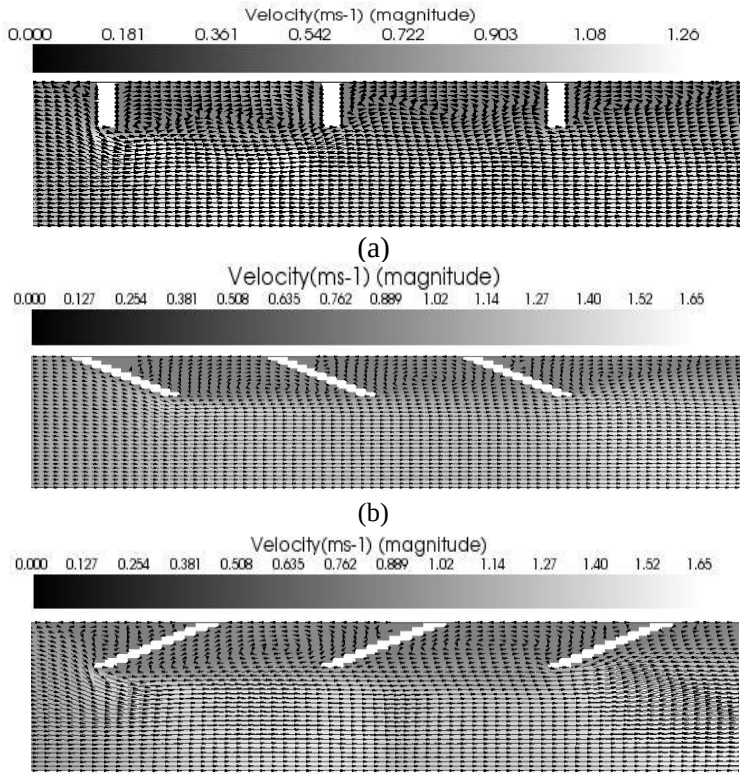

Figure 8: Velocity field of groin field measured by iRIC for L/l=4 for series-1, (a) for 90º (case-1), (b) for 60º (case-2), (c) for 120º (case-3).to the direction of the flow.

Figure 9 shows the velocity fields for L/l=4 which are reproduced from Kang et al. (2012)

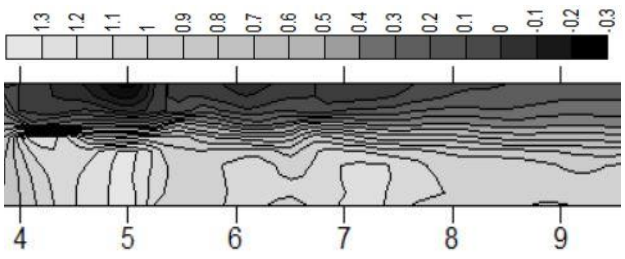

(a)

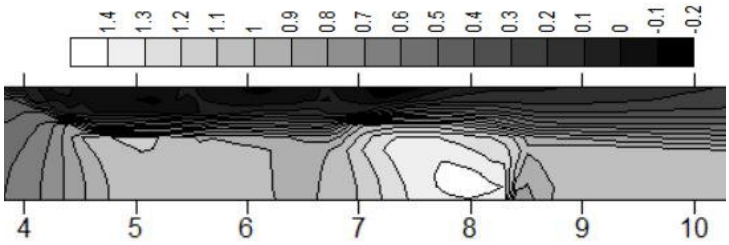

(b)

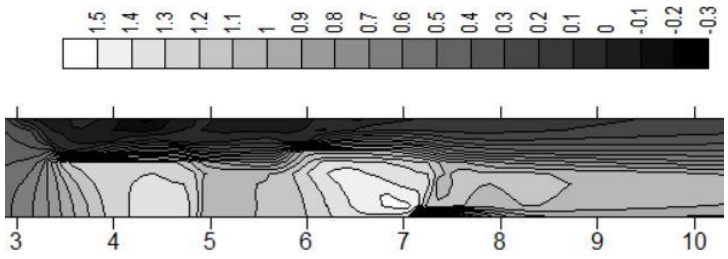

(C)

Figure 9: Velocity field of groin field for *L/l*=4 measured by Surfer for series-1, (a) case-1 (for 90º), (b) case-2 (or 60º), (c) case-3 (for 120º), to the direction of the flow.

4.5 Flow Analysis at The Groin Field

The relationship between the groin's interval with the tip velocity of 2nd groin is shown in figure 4-6. The graph indicates that the downstream groin vertical flow increases with the increase of space between the groins. Figure 4-6 shows the comparison between the experimental results of Kang et al. 2012 with reproduced numerical results.

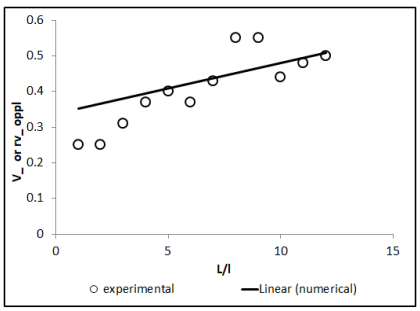

Figure 10: Comparison of experimental and numerical relationship between groins interval with tip velocity of 2nd groin (Series-1, case-1).

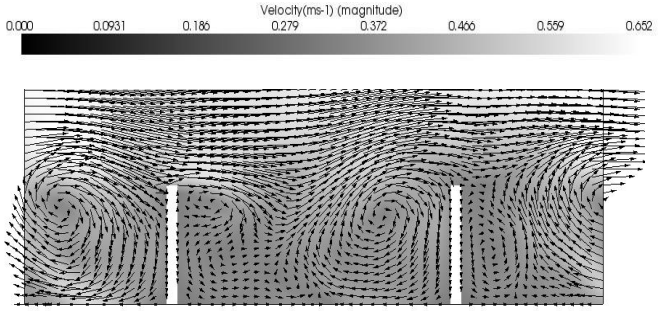

Figure 11: Computed velocity field for series-2, case-1.

4.6 Predicted Velocity Field (Series-2)

Figure 11 shows the predicted velocity field for the groin field for the experiments performed by Fang et al. (2014). A primary clockwise and a counterclockwise vortex was developed in the groin area.

4.7 Streamlines

Figure 12 shows the streamlines around the groin which is reproduced form the experimental data of Fang et al. (2014). From the streamline contour it is found that streamlines was not exactly parallel to the x-direction and the flow was oriented to the main channel or to the groin field at the water surface.

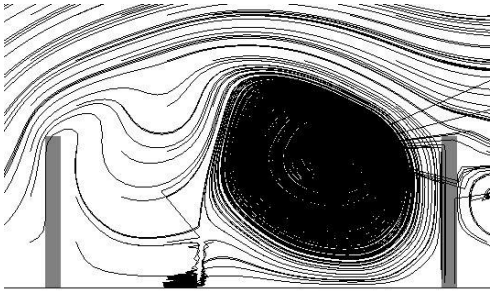

Figure 12: Depth averaged streamline for series-2, case-1.

4.8 Flow Analysis at The Groin Field

Figure 4-9 presents the comparison between the streamwise velocities by Fang et al. (2014) and experimental measurement in the lateral direction at the mid-section between two groins.

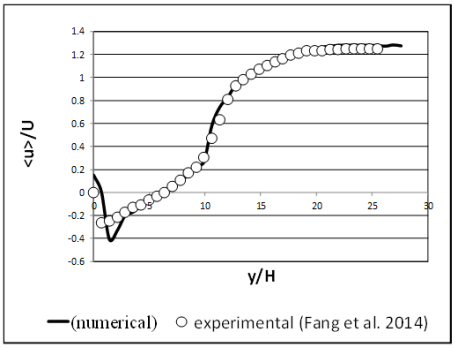

Figure 13: Comparisons of results of streamwise, time-averaged velocities in lateral direction at mid-section between two groins by experiment (Fang et al., 2014) and computed numerical results.

5. CONCLUSIONS

The simulated results provide us with detailed information about the flow pattern, velocity and streamlines around a groin. This adds to the results of work which was done by others on different kinds of groins. The general flow features around a group of groins is reproduced successfully in this simulation. From the simulated result it is seen that the flow is deviated towards the opposite bank than the groin mounted bank due to obstruction of flow by groin. A recirculation zone is observed just downstream region of groin for all cases. The computed velocities of present study are compared among the cases of series-1 and series-2. The change of flow around the space of the groins in the channel seems to be influenced by the recirculation zone. This zone is created by the upstream groin and downstream groin installed position. The maximum flow velocity at the groin area continuously appeared from the upstream, vertical and downstream groins. More dominant changes are found in the mean flow velocity in the groin area. That denotes an active fluid movement around the groin area. Comparisons among the results show that the aspect ratio of *L/l* influenced the flow structure

significantly. When the ratio is small, one or no vortex is composed. The number of vortexes increase with the increase of *L/l* ratio.

In order to confirm the present model, the computed results of the study are compared with previous experimental and numerical results. A good agreement is shown between the numerical and experimental results.

ACKNOWLEDGEMENTS

All praises goes to Almighty, the most merciful, most benevolent to man. The authors would like to Acknowledge the iRIC software. I wish my profound gratitude and heartiest thanks to Professor Dr. Md. Shahjahan Ali, Department of Civil Engineering, KUET, for his careful supervision, indefatigable guidance, valuable suggestion throughout the study period and for the successful completion of the report. Without his generous advice, encouragement, guidance and support at every step of this project, it would not have been possible.

REFERENCES

Ali, M. S., Hasan, M. M., & Haque, M. (2017). Two-Dimensional Simulation of Flows in an Open Channel with Groin-Like Structures by iRIC Nays2DH. (J. G. Zhou, Ed.) Mathematical Problems in Engineering, Volume 2017 (2017), Article ID 1275498, 10.

Anwaruzzaman, S. M. (1998). Evaluation of Selected Local Scour Formulae Around Piers and Groins. M.Engg. Thesis, Department of Water Resources Engg., BUET, Dhaka.

Cao, X., Gu, Z., & Tang, H. (2013). Study on Spacing Threshold of Nonsubmerged Spur Dikes with Alternate Layout. Journal of Aplied Mathematics, 8.

Ettema, R, Muste, M. (2004). Scale Effects in Flume Experiments on Flow around a Spur Dike in Flatbed channel J. Hydraulic Eng., ASCE, 130: 635-646.

Fang, H. W., & Rodi, W. (2003). Three-Dimentional calculations of flow and suspended sediment transport in the nieghborhood of the dam for the Three Gorges Project(TGP) reservoir in the Yangtze River. Hydraul. Res., 41(4), 379-394.

Fang, H., M.ASCE, Bai, J., He, G., & Zhao, H. (2014). Calculations of Nonsubmerged Groin Flow in a Shallow Open Channel by Large-Eddy Simulation. American Society of Civil, 11.

Hasan, R.M.M. (2003). Experimental Study of Local Scour at the Toe of Protected Embankment. M.Engg. Thesis, Department of Water Resources Engg., BUET, Dhaka.

Kang, J., Yeo, H., & Kim, C. (2012). An Experimental Study on a Characteristics of Flow around Groyne Area by Install Conditions. Scientific Research, Engineering, 2012, 4, 636-645, 10.

Khaleduzzaman, A.T.M. (2004). Experimental Study on River Course Stabilization and Restoration by using Groin-like Structures. Master thesis Kyoto University, Japan.

Molls, T., Chaudhry, M.H., Khan, K.W. (1995). Numerical simulation of two- dimensional flow near a spur dike. J. Advance in Water Res., ASCE, 118(4): 227-236.

Quanhong, L., & Pengzhi, L. (2007). Numerical Simulation of Recirculating Flow Near a Groyne. The 2nd International Conference on Marine Research and Transportation, pp. 61-68. Naples,Italy.

Rahman, M.M., Muramoto, Y. (1999). Prediction of Maximum Scour Depth around Spur-Dike-Like Structures. Annual Journal of Hydraulic Engineering, JSCE, 43: 623-628.

Tingsanchali, T., & Maheswaran, S. (1990). Depth-Averaged Flow Computation Near a Groin. Hydraulic Eng., ASCE, 116(1):71-96.

Uijttewaal, W. S. J., Lehmann, D., Mazijk, A. (2001). Exchange processes between a river and its groyne fields: Model experiments. J. Hydraul. Eng., ASCE, 127(11): 928–936.

Yazdi, J., Sarkardeh, H., Azamathulla, H. M., & Ghani, A. A. (2010). 3D simulation of flow around a single spur dike with free-surface flow. international Journal of River Basin Management, 8:1, 55-62.

Yeo, H. K., Kang, J. G., & S.J. (2005). An Experimental Study on Tip Velocity and Downstream Recirculation Zone of Single Groyne of Permeablity Change. KSCE J Civil Eng., 9(1): 29-38.

Zarrati, A.R., Tamai, N., Jin, Y.C. (2005). Mathematical Modeling of Meandering Channels with a Generalized Depth Averaged Model. J. Hydraul. Eng., ASCE, 131:467–475.

Proceedings of the 5th International Conference on Civil Engineering for Sustainable Development (ICCESD 2020), 7~9 February 2020, KUET, Khulna, Bangladesh (ISBN-978-984-34-8764-3)

A DEMAND-DRIVEN WATER MANAGEMENT FRAMEWORK FOR RAJSHAHI CITY CORPORATION IN BANGLADESH

Md. Masud Rana*[1] and Sajal Kumar Adhikary[2]

[1]Postgraduate Student, Department of Civil Engineering, Khulna University of Engineering & Technology, Khulna-9203, Bangladesh, e-mail: masudrana2k14@gmail.com
[2]Professor, Department of Civil Engineering, Khulna University of Engineering & Technology, Khulna-9203, Bangladesh, e-mail: sajal@ce.kuet.ac.bd

***Corresponding Author**

ABSTRACT

Globally, the major concern of a water supply system is to provide sufficient quantity of water with acceptable quality to ensure the safe health and well-being of the consumers. However, the continued growth of population and increasing urbanization coupled with the reduction in freshwater supplies makes the demand management quite challenging. Furthermore, the increasing cost of water supply and management infrastructures and the potential impact of climate change on water resources impose additional burdens over the water supply authority all over the world. In Bangladesh, groundwater is a major source of potable water supply as it is available abundantly in the shallow depth and surface water sources are highly polluted. About 80% of drinking water supply comes from the groundwater source. However, increasing population and uncontrolled urbanization combined with natural arsenic pollution causes increasing demand for freshwater which causes serious impact on this finite water resource of the country.

Rajshahi City Corporation (RCC) of Bangladesh is currently facing the shortages in freshwater supplies, which is being caused by the fluctuations of pressure in the water distribution networks. In 2018, the freshwater demand for RCC is estimated to be 118 million liters per day (MLD) and only 72 MLD is supplied by the Rajshahi Water Supply and Sewerage Authority (RWASA) authority. Water shortage is estimated to be about 46 MLD, which is expected to be about 67 MLD in 2031. Therefore, an optimal water management framework is indispensable for RCC of Bangladesh. Hence, an attempt is made in this study to develop an optimal water management framework for Rajshahi City Corporation of Bangladesh by considering existing water demand, supply and consumption patterns. The performance of the water supply network of RCC is analyzed in the ArcGIS platform. Based on the analysis, necessary improvements and/or modifications of the existing water supply network as well as the mode of operation for quantity and quality improvement are identified. It is found that there is a large variation in pressure head and the pressure supplied in the supply network and thus it is not adequate to satisfy the water demand of RCC at the consumer level. The results also indicate that a number of pipe sections and nodal points have been identified where modifications and/or improvements are required for optimum operation of the water supply network in the Rajshahi City Corporation of Bangladesh.

Keywords: *Demand, Supply, Water management, ArcGIS, Water quality, Rajshahi City Corporation.*

1. INTRODUCTION

Development activity in a country is currently associated with its water consumption. Globally, the demand for freshwater is continuously increasing with the growing population and uncontrolled development activities. The situation is more complex particularly in the urban part of a country (Garcia et al., 2008). However, the increasing trend in water consumption in Bangladesh during the last decades has been counteracted by a decrease in available water resources due to the impact of climate change, mainly in summer and uncontrolled human interventions. Urban population is growing rapidly in the country due to the natural urban growth and disaster-induced migration from rural areas (Karim and Mohsin, 2009). The current urban population in Bangladesh is about 38 million and is expected to be reached to about 74 million by 2035 (BBS, 2005). This fact has put an obligation to establish an appropriate management policy that can ensure a stability of both water resources as well as development activities. It is also highlighted in the National Water Polity (NWP) of Bangladesh, which states that all required means and measures should be adopted to manage water resources of the country in a comprehensive, integrated and equitable manner (NWP, 1999).

Establishing sustainable water source is an indispensable component in any urban water supply scheme. In Bangladesh, municipal water supply mainly comes from the surface water and groundwater sources. About 85% of the freshwater comes from the groundwater sources and in some rural areas, increasing demand for irrigation water affects the availability of drinking water (Haque et al., 2012). The reason behind this is that most of the SW sources in Bangladesh is usually polluted with different degrees and thus requires appropriate treatment prior to consumption (Das Gupta et al., 2005). As a result, the associated cost of operation and supply of the water supply systems increases and causes a huge burden on consumers. In recent years, there is a declining trend in the groundwater table due to the uncontrolled abstraction of groundwater, mainly for irrigation purposes in Bangladesh in order to support its huge amount of population (Ahmed et al., 1999). Therefore, the optimal management and supply system is essential for the sustainable development and the existence of the future generation.

Rajshahi City Corporation (RCC) of Bangladesh, located in the north-west region of the country, is currently facing the shortages in freshwater supplies, which is being caused by the fluctuations of pressure in the water distribution networks. In 2018, the freshwater demand for RCC is estimated to be 118 million liters per day (MLD) and only 72 MLD is supplied by the Rajshahi Water Supply and Sewerage Authority (RWASA). Water shortage is estimated to be about 46 MLD, which is expected to be about 67 MLD in 2031. Every year, the groundwater table in RCC is declining by 2 to 3m. This causes the management of water supply and/or demand satisfaction more challenging since domestic or residential water demand from the system is the highest during the dry season (Ahmed et al., 1999). Therefore, an optimal water management framework is indispensable for RCC of Bangladesh. Hence, the objective of the current study is to develop an optimal water management framework for Rajshahi City Corporation of Bangladesh by considering existing water demand, supply and consumption patterns.

2. MATERIALS AND METHODS

2.1 Study Area

Rajshahi City Corporation (RCC) is selected as a case study area to carry out this study, which is situated in between 24°20′ and 24°25′ north latitudes and between 88°32′ and 88°40′ east longitudes. The city is bounded by Paba Upazila on all sides as shown in Figure 1, which consists of 30 wards. Geographically, the city is located within the Barind Tract that lies approximately 23 m above the mean sea level. The city is located on the alluvial plains of the Padma River that runs through southern side of the city. RCC covers an area about 95 sq. km with a total population of about 2.3 million. The city has a hot tropical climate where most of the rainfall occurs in the summer and monsoon seasons. The average annual rainfall of the city varies from 1542.1 mm to 2235.8 mm. The

annual temperature in RCC varies from 18.5°C to 29.4°C and June is identified as the hottest month in most cases.

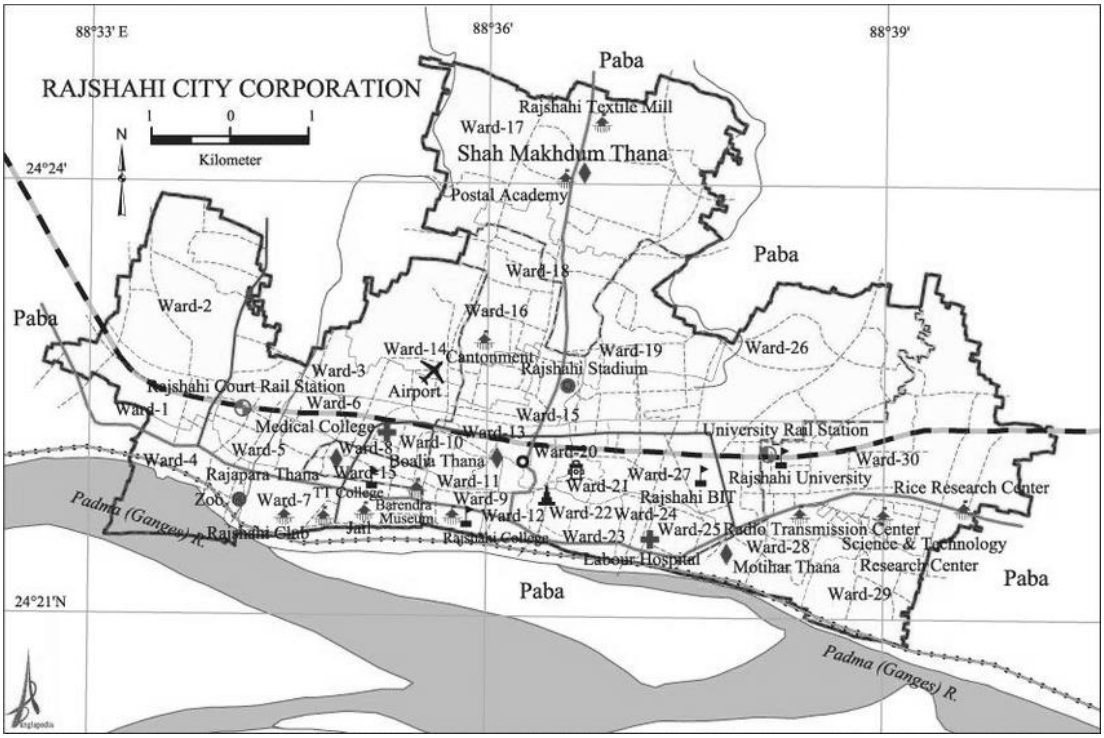

Figure 1: Location of Study Area in the North East Region of Bangladesh

2.2 Methods

The framework of methodology to develop a demand-driven water management framework for RCC of Bangladesh is given in Figure 2. As can be seen from the figure, different secondary data related to water demand and consumption are collected from the various data providing agencies. The agencies include RCC authority, Bangladesh Water Development Board (BWDB), Rajshahi Water Supply and Sewerage Authority (RWASA), Rajshahi Barind Area Authority, Bangladesh Meteorological Department (BMD) and Bangladesh Bureau of Statistics (BBS). Primary data such as water quality of surface water and groundwater are obtained through the lab test results. The water supply network is simulated based on the existing water demand and available pressure in the different nodes of the network. The network is also simulated for the projected population and increased demand for water supply. The simulation is undertaken on the ArcGISv10.5 platform and results are analyzed for decision making.

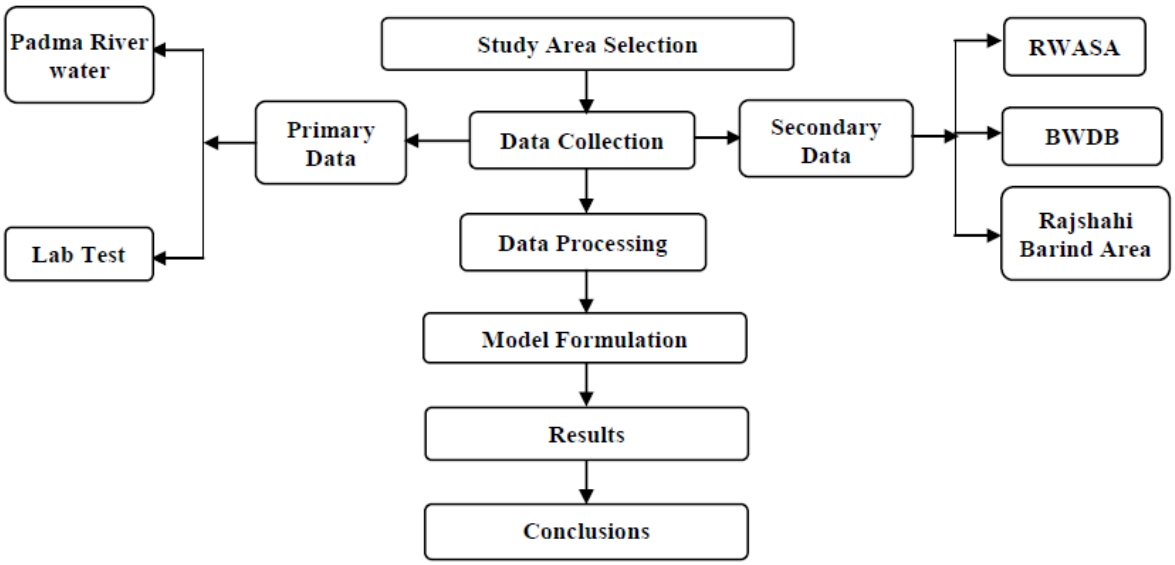

Figure 2: Methodological framework adopted in the current study

3. RESULTS AND DISCUSSION

For analyzing the water supply network system of RCC, hydraulic design of the network is undertaken using the Loop software and then the network is simulated and analyzed on the ArcGIS and MSExcel platform. The network modeling with various pipe network and nodes are shown in Figure 3.

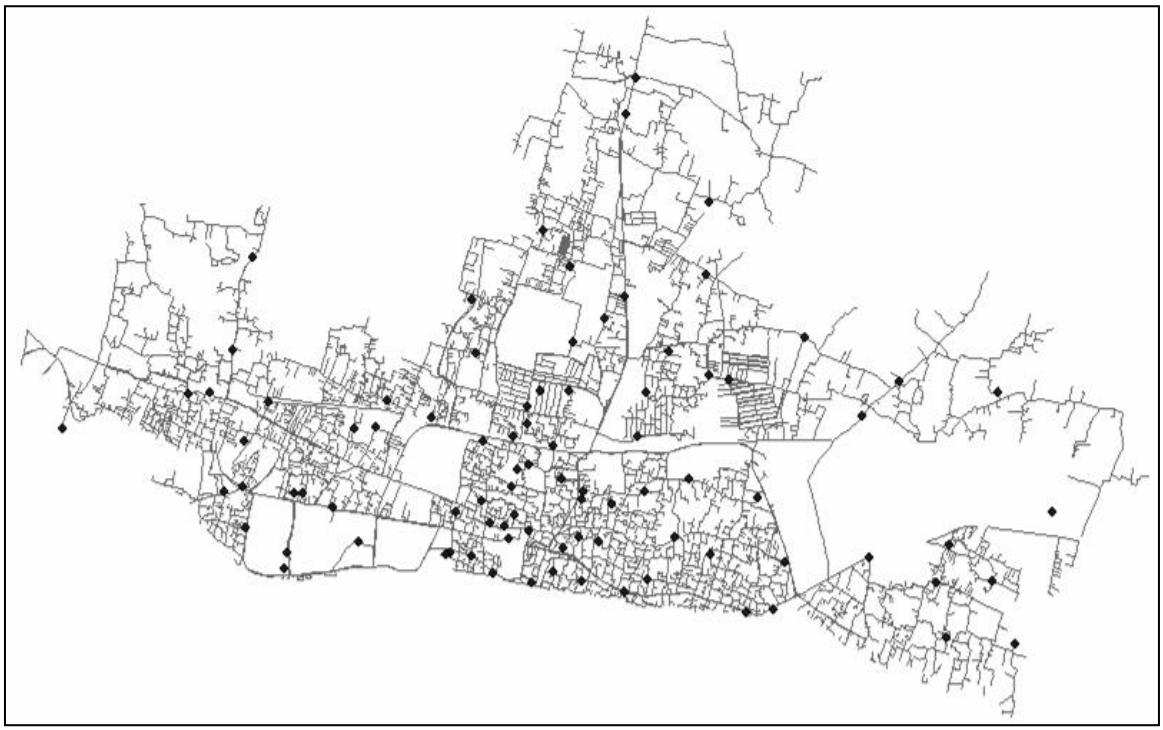

Figure 3: Branched networks of existing water distribution network of RCC

For efficient and equitable distribution of water, a grid pattern is recommended where different mains are interconnected keeping dead ends to a minimum. This system facilitates supplying of water to any one point in the grid at least from two different directions. The water supply network system is

designed for future demand in such a way to supply water from the adjacent grid to the later developments where the growth of the city has not been orderly planned, with several pockets just in developing stage and some areas still remaining agricultural and/or unused lands. Theoretical future demand is estimated based on the projection of present population for the feeders where streets are not formed. Hence the supply and distribution pipes can be extended as and when development takes place in future. The system is designed for the projected population for the year 2021 and 2031 and for the per capita water supply at 215 lpcd.

Daily demand is increased day by day due to the increase in population of RCC and decrease in the quantity of groundwater supply. Surface water supply is also limited by the uncertainty in regular supply from the nearby Padma River due to the upstream diversion (Farakka Barrage) located outside the country. Population growth rate is remarkably responsible for the proposition. The projection of population for the design period of 10 years is calculated by the geometric progression method, which can be expressed by Eq. (1) as follows.

$$P_n = P_0(1 + r)^{\ n} \ldots\ldots\ldots\ldots\ldots\ldots\ldots\ldots\ldots\ldots\ldots (1)$$

Where,

P_n = Projected population in 'n' year
P_0 = Present population
r = Growth rate of population
n = Projected year

For population projection, the base year is taken as 2011 and intermediate and final design year are taken as 2018 and 2031, respectively. The projection of the population in RCC obtained by the geometric progression method is presented in Table 1. Increased population directly influences the water supply and demand patterns. In the current study, water demand is estimated for future years by multiplying the current unit demand design values in lpcd by the projected number of future users in the water system. The project water demand in RCC computed in this way is also given in Table 1. It is assumed that new users added to the water supply system will consume water at the same rate as the current users. Taking per capita supply of water as 215 lpcd (185 lpcd + 15% for the unaccounted flow), the water demand for the years 1991, 2001, 2011, 2018, 2021 and 2031 is estimated to be 63.21, 83.64, 96.75, 118.25, 125.35 and 169.48 MLD, respectively. The zoning of the supply coverage is done geometrically with reference to the locations of the head works.

Table 1: Projected population and the corresponding water demand in RCC

Year	1981	1991	2001	2011	2018	2021	2031
Population (Lakh)	2.54	2.94	3.89	4.50	5.50	5.84	7.88
Water demand (MLD)	54.61	63.21	83.64	96.75	118.25	125.35	169.48

The demand and supply at each nodal point (total 88 nodal points) of the water distribution network is shown in Figure 4. As can be seen from the figure, there is a high variation in water supply according to the nodal point values, which also influences the demand and supply for the consumers. There are active 88 nodal points in the distribution network with 30 wards of RCC and population growth rate in each ward is directly responsible for satisfying the demand and supply of the users. To perform hydraulic modeling, the water demand from each defined sub-region is assigned to the corresponding demand nodes in the hydraulic model of the water distribution network. There are 95 nodal points for extracting water and overall 88 points are active for the whole time and thus total nodal points are considered 88 in the analysis. The daily demand for RCC is 118 million liter per day (MLD) and 88 nodal points try to collect the water to meet the demand from the nodal point.

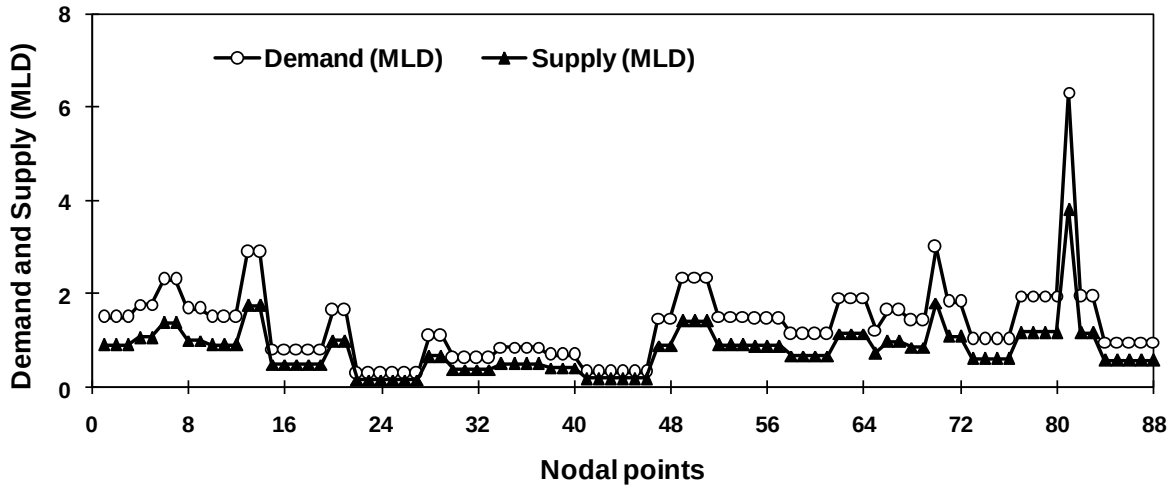

Figure 4: Water demand and supply in each nodal point of total active 88 nodal points of RCC water distribuiton network

The demand and supply curve is shown in Figure 5, which clearly indicates reasonable deficit between demand and supply in 30 wards of RCC area. The daily water demand and supply curves indicate that the existing and future water demand are increasing day by day. The demand curve is always increased upward and supply curve is always lacking. In order to fulfill the increasing demand in such situation, necessary modification in the supply strategy of RCC water supply is required and also alternative sources of water need to be identified and developed. Figure 5 shows that the maximum demand is 7.85 MLD and supply is 4.76 MLD in 27 no. ward of RCC. The population of 27 no. ward is also the maximum among all 30 wards and here the number of pump is bounded by Adorsho School, Tikapara, Baliapukur Upavadra and Seiculture gate pumps.

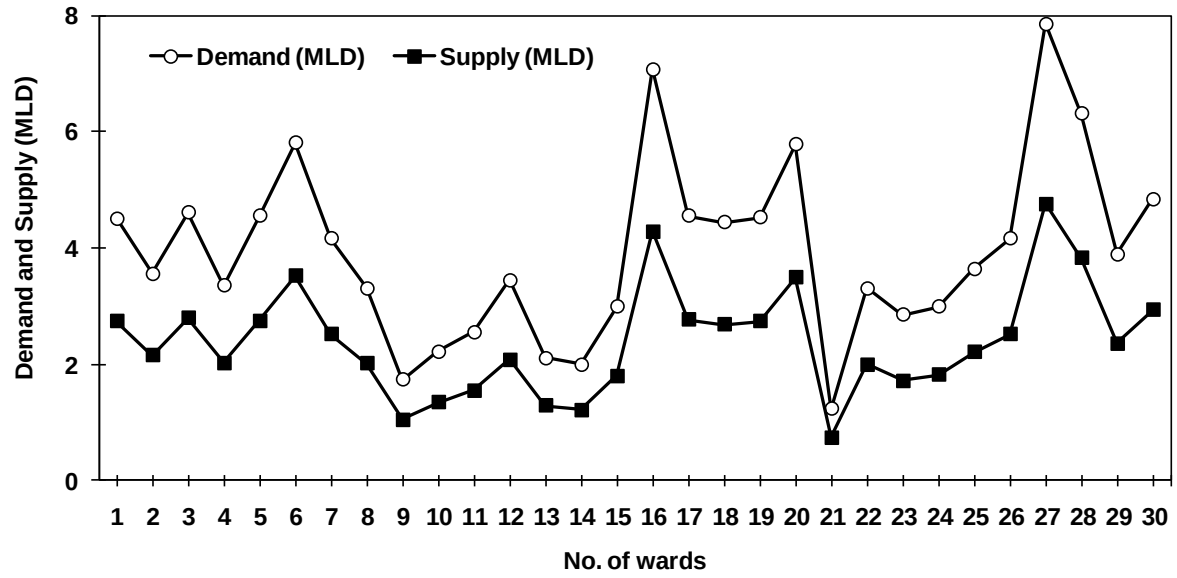

Figure 5: Ward wise demand and supply in RCC area

The water distribution network of RCC area consists of three types of pipelines. They include PVC pipelines of 495.5 km, GI pipelines of 1.5 km, and AC pipelines of 37.5 km, respectively. The fluctuation of head loss and velocity in different nodes of the AC pipelines of RCC area is shown in Figure 6. As can be seen from the figure, the maximum velocity is 2.298 m/s whereas the maximum head loss is 0.84 m, respectively.

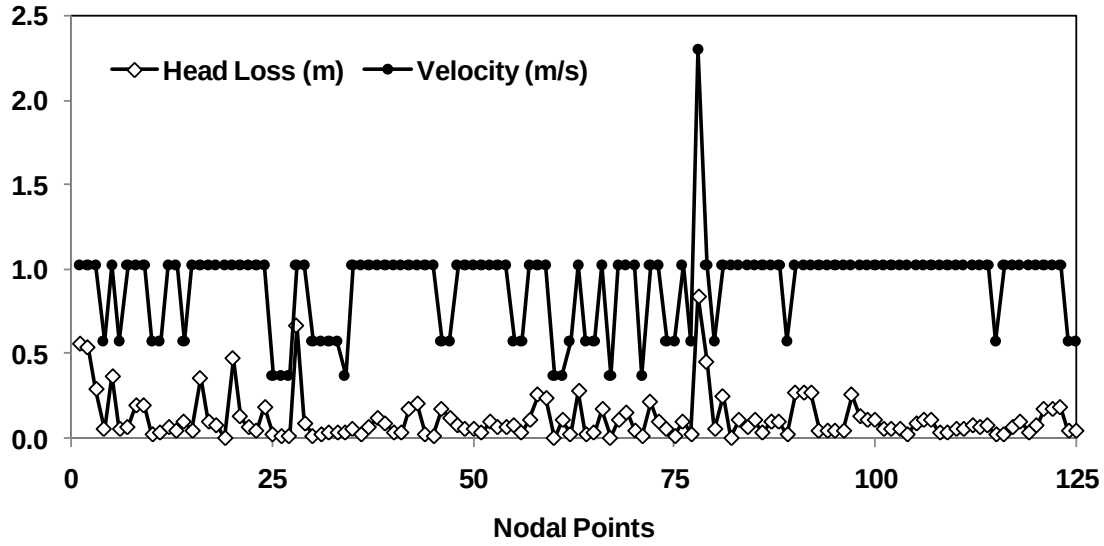

Figure 6: Variations of head loss and velocity distribution for AC pipe in the RCC area

Figure 7 shows the velocity distribution in various points of the water supply network in RCC area. The maximum velocity is found to be 2.4 m/s, which exists only in the PVC pipelines. The maximum velocity in GI pipelines is found to be 1.9 m/s whereas for the AC pipelines, the maximum velocity is obtained as 2.298 m/s, respectively.

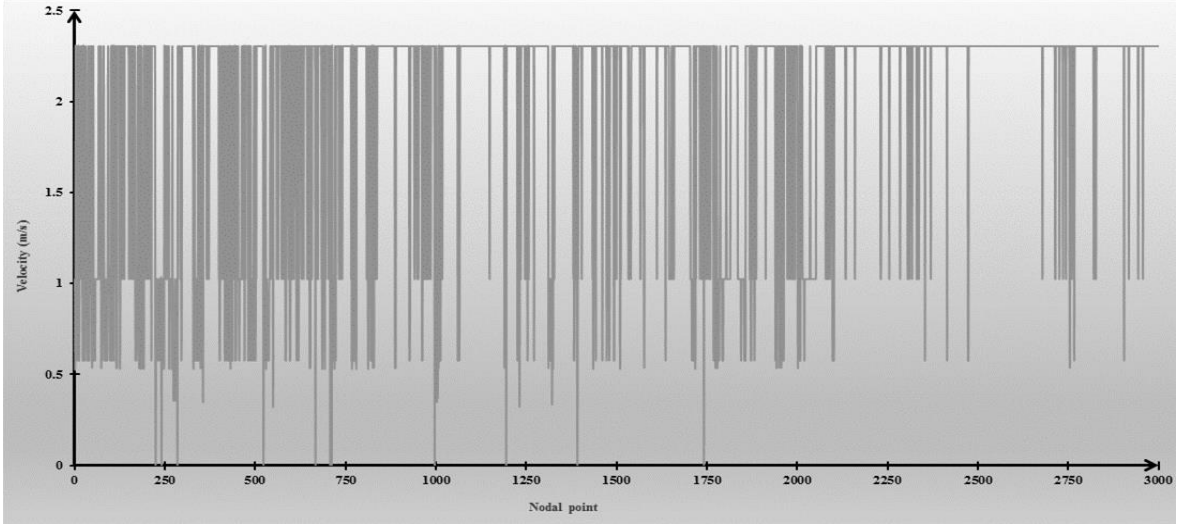

Figure 7: Velocity distribution in pipelines in various sections of RCC water supply network

4. CONCLUSIONS

Rajshahi City Corporation (RCC) of Bangladesh is currently facing the shortages in freshwater supplies, which is being caused by the fluctuations of pressure in the water distribution networks. Therefore, an optimal water management framework is indispensable for RCC of Bangladesh. In the current study, an attempt is made to develop an optimal demand-driven water management framework for RCC by considering existing and projected water demand, supply and consumption patterns. The performance of the water supply network of RCC is analyzed in the ArcGIS platform. Based on the analysis, necessary improvements and/or modifications of the existing water supply network as well as the mode of operation for quantity and quality improvement are identified. It is also identified that there is a great variation in pressure head, velocity and head loss in different nodes of the water distribution network of RCC. Thus, it is not adequate to satisfy the water demand of RCC at the

consumer level. The results also indicate that a number of pipe sections and nodal points have been identified where modifications and/or improvements are required for optimal operation of the water supply network in the Rajshahi City Corporation of Bangladesh.

REFERENCES

Ahmed, S.S., Mazumder, Q.H., Jahan, C.S., Ahmed, M. and Islam, S. (1999). Qualitative analysis of groundwater resource, Rajshahi City Corporation area, Bangladesh. *Rajshahi University Studies*, Part-B, v.27.

BBS (Bangladesh Bureau of Statistics), 2005. Statistical yearbook of Bangladesh-2005. Bangladesh Bureau of Statistics (BBS). Government of Bangladesh (GoB).

Das Gupta, A; Babel, MS, Albert, X and Mark, O. 2005. Water sector of Bangladesh in the context of integrated water resources management: a review. Water Resources Development, 21(2): 385-398.

Garcia, A; Sainz, A, Revilla, JA, Alvarez, C, Juanes, JA and Puente, A. 2008. Surface water resources assessment in scarcely gauged basins in the north of Spain. Journal of Hydrology, 356(3-4): 312-326.

Haque, M.A.M., Jahan, C.S., Mazumder, Q.H., Nawaz, S.M.S., Mirdha, G.C., Mamud, P., & Adham, M.I. (2012). Hydrogeological condition and assessment of groundwater resource using Visual Modflow modelling, Rajshahi city aquifer, Bangladesh, *Journal of the Geological Society of India*, 79(1), 77-84.

Karim, MR; and Mohsin, GM. 2009. Assessment of urban water supply situation: a case study in Khulna city corporation area. Proc. of the 2nd Int. Conf. on Water and Flood Man. (ICWFM-2009), Dhaka, Bangladesh, 1: 235-242.

NWP (National Water Policy), 1999. Draft report of Bangladesh national water policy, Water Resources Planning Organization (WARPO), Dhaka, Bangladesh.

Proceedings of the 5th International Conference on Civil Engineering for Sustainable Development (ICCESD 2020), 7~9 February 2020, KUET, Khulna, Bangladesh (ISBN-978-984-34-8764-3)

LAND USE CHANGE PREDICTION OF CUMILLA CITY USING GIS AND REMOTE SENSING TECHNIQUE WITH CELLULAR AUTOMATA MARKOV ANALYSIS

M. F. Hasan*[1], M. A. Rashid[2] and N. Mostofa[3]

[1]Assistant Engineer, Bangladesh Water Development Board, Bangladesh, email: fahimhasan107@gmail.com
[2]Student, Department of Civil Engineering, Bangladesh University of Engineering and Technology, Bangladesh, email: marcextreme09@gmail.com
[3]Student, Department of Civil Engineering, Bangladesh University of Engineering and Technology, Bangladesh, email:nomanbuet14@gmail.com

***Corresponding Author**

ABSTRACT

Assessment of urban growth pattern is a priority in transportation and urban planning as land use change and transportation network closely interact with each other. The objectives of this research are to develop a land use prediction model and analyse the future urban growth of Cumilla, a major city in Bangladesh. In the study, ArcGIS has been used as a data processing and Multi Criteria Evaluation (MCE) analysis platform, and mathematical modules like Markov and Cellular Automata Markov (CA Markov) have been run on IDRISI Selva edition. Three major parts of the land use prediction model on this research are 1) Markov analysis; 2) MCE; and 3) CA Markov analysis. Markov analysis predicts future temporal changes in land use classes based on two previous land use images but only determines magnitude of change, not direction. MCE analysis determines areas which are most likely to change based on various user defined criteria. These criteria might be socio-economic, demographic or spatial data and depends on the objective of the research. CA Markov analysis combines the result of Markov and MCE analysis to predict future land use pattern. Also, it overcomes the limitation of Markov analysis and adds direction to the model. First, Landsat images of 2001 and 2011 have been classified as water, trees, agricultural field and urban classes by remote sensing. From these classified imageries, an intermediate prediction of land use of 2018 has been performed through Markov analysis. Markov analysis generates a probability matrix that defines the probability of each land type turning into other types over the year. Multi-criteria evaluation (MCE) analysis has been incorporated in the process, which included factors and constraints like road, railway network, population, slope, waterbody etc. Based on these factors and constraints, most suitable areas for each land class's growth have been determined. MCE generated suitability maps for each land use type. Then, using transition probability matrix of 2018 and suitability images from MCE , CA Markov model have been run to predict final land use of 2018. This prediction of 2018 has been checked with classified land use of 2018 for validation. Afterwards, using the validated model, land use classification of 2030 has been predicted. Analyses shows that urban area will increase by almost 145% in 2030 than 2001 (Urban area was 2405 and will be 5893 hectares in 2001 and 2030 respectively). Result also shows decreased percentage of agricultural field and trees while percentage of waterbody remains almost the same. The Land use prediction model developed for Cumilla in this research can work as a framework for a more robust integrated land use transportation model for the region.

Keywords: *Land use prediction podel, CA markov, Multi-criteria evaluation, Urban growth, GIS.*

1. INTRODUCTION

Rapid urban development has exerted heavy pressure on land and resources in and around the cities as well as caused various environmental and socio-economic problems. So, prediction of urban growth and forecasting land use change pattern carry a lot of significance to the planners and policy makers (Kashem, 2008). Developing countries lack comprehensive decision making process and planning regarding urban development. As a result, they are experiencing rapid and unplanned urban sprawl (Kashem & Maniruzzaman, 2008).

Bangladesh possesses few fast growing cities like Dhaka, Chattogram, Cumilla, Bagura, Gazipur etc. Among them Dhaka, the capital of Bangladesh, has already faced a lot of geospatial changes over the decades. Previously, land cover changes and urban expansion of Dhaka between 1975 and 2003 have been analyzed using satellite images and socio-economic data by Dewan and Yamaguchi (2009). Also, Ahmed (2011) has examined spatio-temporal growth dynamics of Dhaka between 1989 to 2009, using remote sensing and GIS techniques.

Prediction of land use change is a complex process, dependent on many variables. For developing countries, scarcity of detail historical and socio-economic data is also a setback. In such cases, combination of Markov Chain (MC) model and Cellular Automata (CA) model presents the best outcome. Markov Chain model is a probabilistic model which predicts how a land will change from one mutually exclusive state to another (Thomas & Laurence, 2006). It calculates the change between two previous time periods 't' and 't-1'. Based on the past change, it predicts future change at time 't+1'. The MC model analyzes two historical land cover images and generates a transition probability matrix, a transition area matrix, and some conditional probability images (Eastman, 2006; Takada et al., 2010). Yet, a stochastic Markov model isn't accurate as it only gives right magnitude of change but not the right direction (Boerner et al. 1996). Cellular Automata (CA) adds direction to the model by incorporating spatial component (Soe & Le, 2006). The combined Markov-CA model overcomes the limitations of markov model. Multi Criteria Evaluation (MCE) analysis adds an element of spatial contiguity, specific decision, and also the knowledge of dynamic distribution in the model (Sang et al., 2011). MCE analysis is also known as suitability analysis. The MCE analysis uses various user-defined criteria, which can either be a factor or a constraint (Eastman 2006), to develop suitability images for each land class.

Based on this method, a model to predict land use change of Cumilla, a major city along the Dhaka-Chattogram highway , has been developed in this study. The Dhaka-Chattogram highway is known as principle economic corridor of Bangladesh, connecting the port city Chattogram to capital city Dhaka. Recently, the highway has been developed into a four lane corridor. In addition, major development works are underway along this route which makes Cumilla a potential study area to analyze future land use change.

Principle objectives of this research are:

1. To develop a land use prediction model for Cumilla
2. To quantify the rate of urban growth of Cumilla

In this study, ArcGIS has been used as a data processing and Multi Criteria Evaluation analysis platform, and IDRISI Selva has been used as a mathematical module. The IDRISI Selva is an integrated GIS and image processing software which facilitates not only format conversion between data sets, map composition, and map display but also provides statistical analysis, time-series analysis, spatial land use analysis, and decision support analysis.

2. METHODOLOGY

2.1 Study Area

Cumilla district is under Chattogram Division of Bangladesh, having an area of 3146 km^2. The district is well connected with the whole country with rail and road network. Focus of this study is the city area of Cumilla, which is along the Dhaka-Chattogram highway. Therefore, 3 upazillas of Cumilla District: Cumilla Adarsha Sadar, Cumilla Sadar Dakshin and Burichang have been selected as Study area (Figure 1). The selected portion of Cumilla District covers a large urban agglomeration and is the central part of Cumilla city in terms of social and economic aspects. As a result, it is undergoing rapid unplanned urbanization.

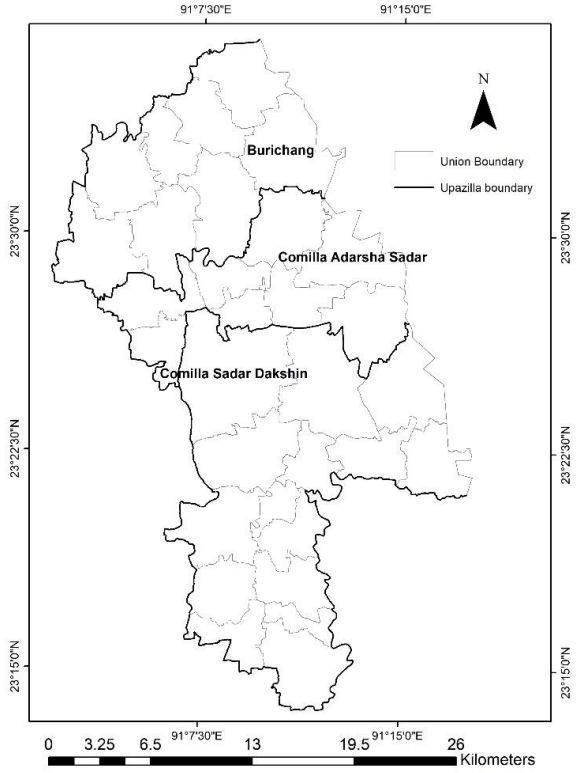

Figure 1: Study Area

2.2 Data Collection

Three types of data have been used to develop the model. Data types along with their sources are mentioned below-

1. Satellite Images of year 2001, 2011 and 2018: USGS
2. Historic Google Earth Images as Reference Data: Google Earth
3. Socio-economic, demographic and spatial data: Survey of Bangladesh (SoB)

Satellite images have been collected from official website of United States Geological Survey (USGS). Depending on availability, images from Landsat 4-5, 7 and 8 satellites have been downloaded. Landsat 4-5 and 7 images of 2001 and 2011 have 7 spectral bands and Landsat 8 image of 2018 have 8 spectral bands. From these bands, False Color Composite (FCC) of Red, Green and Blue (RGB) bands 4-3-2 has been used in this research. For avoiding the effect of seasonal variation in remote sensing, the images are of the same season (March and April).

2.3 Image classification

Two basic methods of image classification are used for remote sensing: supervised and unsupervised. For supervised classification, one need to know about the terrain of the concerned area. Therefore, for

this research, a supervised classification method has been used. ArcGIS 10.5.3 has been used as remote sensing platform for classification.

Each Landsat images were classified into four land use classes: Water, Trees, Agricultural Field and Urban Area. In RGB 4-3-2 combination, urban areas appear blue, vegetation red, water bodies from dark blue to black, soils with no vegetation from white to brown (Geospatial Data Service Centre, 2008). First, several training sites were developed for each land class. More than one training sites were defined for each class. The vector files of the similar training sites indicated pixels which were used to develop signature files. These signature files consist statistical information about reflectance value of the pixels of each land cover type (Eastman, 2009). After that, Fisher Classifier was used to classify the images based on the signature files. Fisher classifier works best when there are very few unknown areas in an image and representative training sites are available (Eastman, 2009). In this research the satellite images have been classified into four land classes as shown in the Table 1 below-

Table 1: Details of the land Cover Classes

Land Cover Classes	Description
Water	River, permanent open water, lakes, ponds, canals and reservoirs.
Trees	Trees, shrub lands and semi natural vegetation, deciduous, coniferous and mixed forest, palms, orchard, herbs, climbers.
Agricultural Field	Agricultural field, Fallow land, earth and sand land in-fillings, open space, bare and exposed soils, grasslands and vegetable lands.
Urban	All residential, commercial and industrial areas, villages, settlements and transportation infrastructure.

The final stage of image classification process is accuracy assessment. For accuracy assessment, random points were chosen from the classified images. Land class of each point was added to its attribute. Next, the points were placed on google earth historic images i.e. points from classified 2001 Landsat images were placed on 2001 google earth image of that area. The land class type from google earth was given input as another attribute in these points and compared with the previous attributes. The accuracy for 2001, 2011 and 2018 images were found 86%, 87% and 91% respectively. Classified Land Use images of 2001 and 2011 are shown in Figure 2.

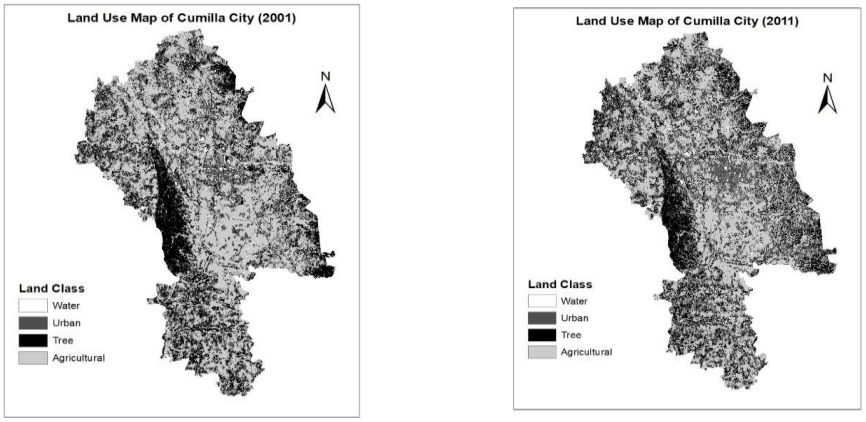

Figure 2: Classified Images of 2001 and 2011 of Cumilla City

2.4 Markov Analysis

Markov Analysis is a stochastic process that predicts future land use change at time 't+1' based on the change between two previous land use at time 't' and 't-1' respectively. In this research, Markov model has been run on IDRISI Selva 17.0 edition. Land use images of 2001 and 2011 were used as base years to predict land use change in year 2030. But first for validation purpose, land use map of 2018 was predicted with Markov model. Markov analysis produces a transition matrix (Table 2), a transition area matrix, and a set of conditional probability images for each land class. The transition matrix shows the probability at which one category will change into other categories in future. Table 3 shows the number of cells that will transform into other land types over time.

Table 2: Markov Probability of Changing Land Cover Types

	Waterbody	**Trees**	**Agricultural Field**	**Urban**
Waterbody	0.4629	0.2912	0.0897	0.1562
Trees	0.0291	0.4887	0.4011	0.0811
Agricultural Field	0.0378	0.2269	0.6980	0.0374
Urban	0.0902	0.1873	0.1732	0.5529

Table 3: Expected Cell Transition to Different Land Classes

	Waterbody	**Trees**	**Agricultural Field**	**Urban**
Waterbody	15852	99973	3073	5350
Trees	5109	85954	70545	14264
Agricultural Field	13283	79727	245284	13134
Urban	4363	8891	8382	26755

2.5 Multi Criteria Evaluation (MCE) Analysis

Performing a Cellular Automata-Markov (CA Markov) analysis requires suitability images. Suitability image of a land class shows which areas are suitable for that particular land class's future growth. In this way, suitability images add direction to CA Markov analysis. Suitability images are developed through Multi Criteria Evaluation analysis. In this study, ArcGIS has been used as MCE analysis platform.

Each land class requires a separate suitability image. And for that, MCE analysis had to be performed separately for each land class. It uses various user-defined criteria which can either be a factor or a constraint. A factor facilitates growth while a constraint impedes development. Road and rail network, waterbodies, slope, population density and urban developed sites were used as various criteria for MCE analysis. The factors were assigned with weighted values based on various literature review and authors' judgement. The constrains were assigned as Null value which restricted any growth in those regions. Table 4 shows weighted values for developing Urban suitability image.

Table 4: Weighted Value of Criteria Assigned to Urban Suitability Analysis

Factor/Constraint	**Criteria**	**Weighted Value (%)**
Factor	Distance from Road	15%
	Distance from existing Urban Area	25%
	Slope	10%
	Population	20%

	Classified base map of 2011	30%
Constraint	Water Body	Null value
	Road Network	Null value
	Rail Network	Null value

Figure 3 presents the suitability image for each land class. The higher the value (from 0 to 6), higher the chance of that cell to turn into that land class.

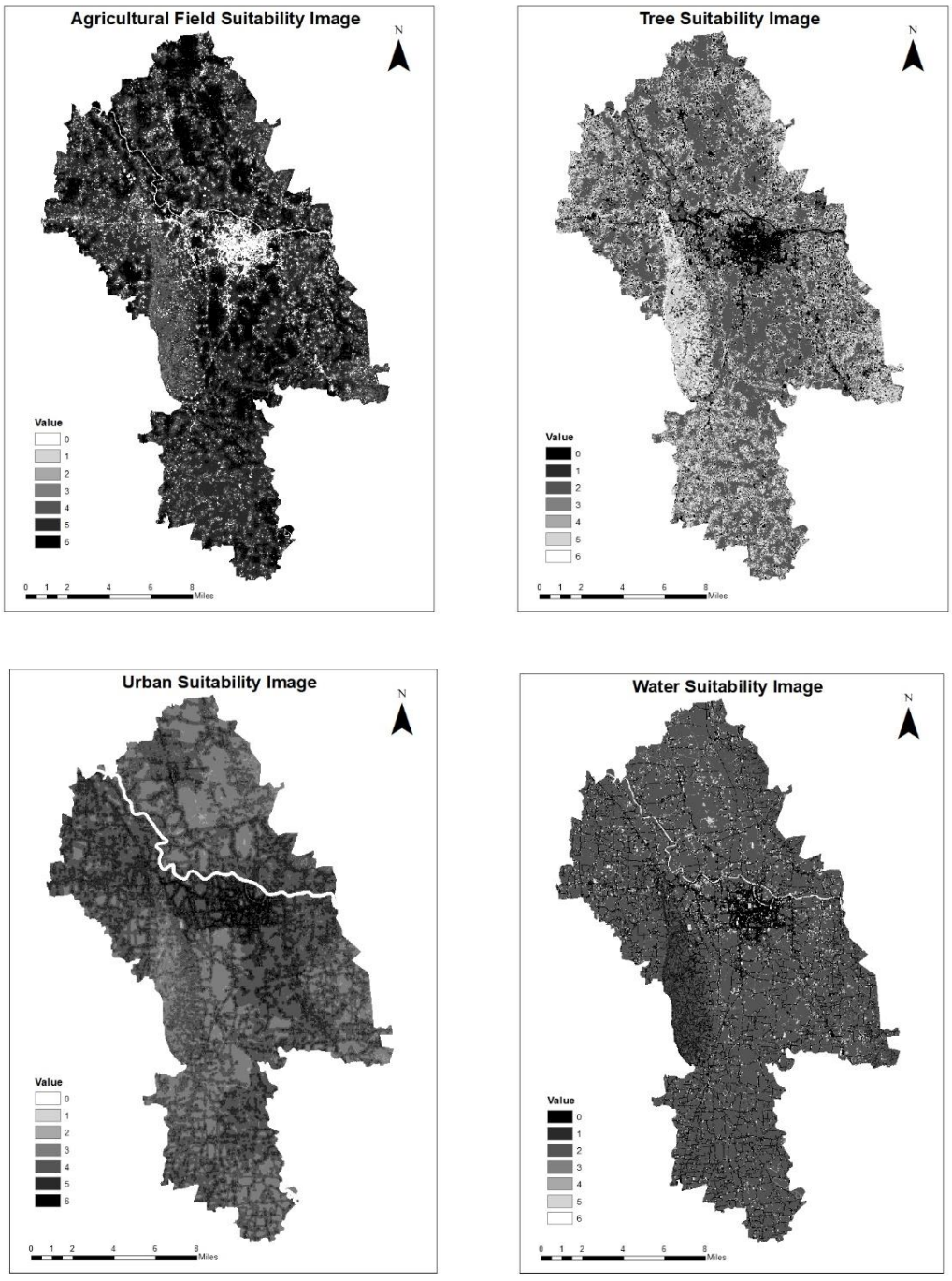

Figure 3: Suitability Map of different Classes (Higher Value indicates Higher Suitability)

2.6 Model Validation

For model validation, first Markov analysis was used for predicting 2018 land use which generated a transitional probability matrix for year 2018 specifiaclly. After that, suitability images were developed by MCE analysis. Then, CA Markov module was run with the transitional probability matrix of 2018 and four suitability images. CA Markov module also needs a basis land cover image which is the later land use images of the two base images (in this case image of 2011). From this predicted land use image of 2018 was obtained. The predicted image was compared with the classified Landsat image of 2018. The comparison is presented in Table 5 which shows that the model is validated.

Table 5: Statistical Comparison between Classified and Simulated Map

Land Cover Type	Classified Map (2018)		Simulated Map (2018)		Change in
	Area (km^2)	%	Area (km^2)	%	Area (%)
Water body	28.417	5.17745	32.4656	5.92087	0.74%
Trees	171.339	31.2172	167.404	30.5301	0.7%
Agricultural Land	295.752	53.8847	294.791	53.7621	0.12%
Urban	53.3528	9.72064	53.0436	9.67375	0.05%

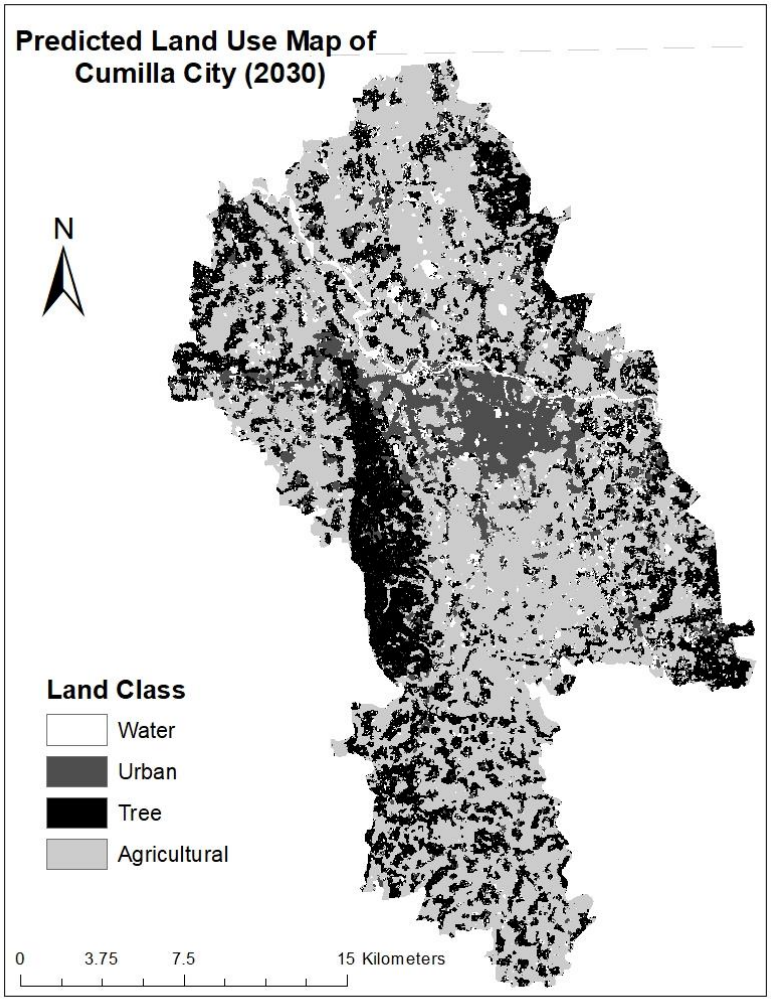

Figure 4: Predicted Land Use Map of 2030 of Cumilla City

2.7 Final Prediction

With the validated model, land use of 2030 was predicted for Cumilla city. First, Makrov analysis was performed to obtain a transition probability matrix for 2030. Suitability images for each classes remained same. Afterwards, CA Markov analysis was done with the transition probability matrix of 2030, suitability images, and basis year image of 2011. Figure 4 shows the predicted image of 2030.

3. RESULT ANALYSIS

Figure 5 represents the area (hectare) under each land class type of predicted 2030 land use map. Area under Urban Class in 2030 is 5893 ha, which was 2405 ha in 2001. So, there is an 145% increase in Urban land class type.

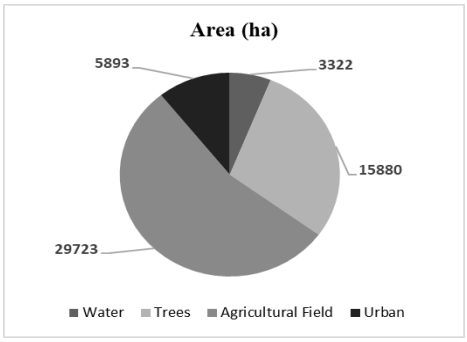

Figure 4: Area Occupied by Different Land Cover Type in 2030

Area occupied by water land class (3322 ha) will stay almost the same as 2001 (54.23% in 2030 and 54.45% in 2001) while there is a loss of area in tree and agricultural field land classes. A comparison of different land classes over the year is presented in Figure 5.

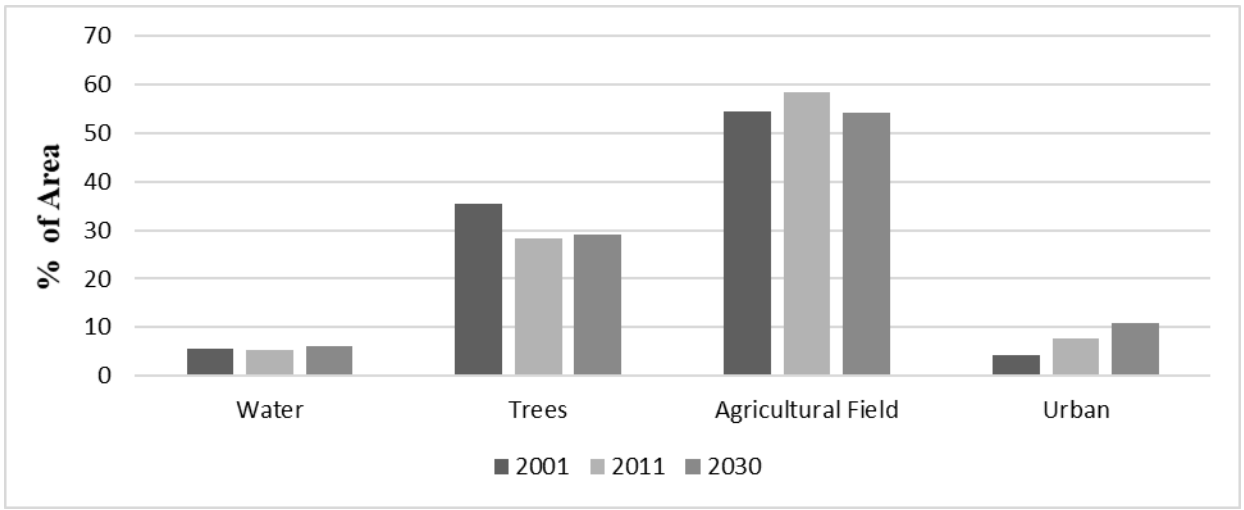

Figure 5: Comparison between Various Land Classes for year 2001, 2011 and 2030

4. DISCUSSION

Land Use Prediction model developed though this study shows a growing pattern of Cumilla city. There will be an almost 145% rise in urban area in 2030 compared to 2001. Meanwhile, other land classes will be losing their parts. This depicts the widely seen picture of rapid urban development around the world. However, the model has some limitations. Satellite data has been collected from

free sources, therefore, contains a coarse resolution of 30m×30m cell size. It might have affected the accuracy of remote sensing. Also, various socio-economic and spatial data for specific area like Cumilla are rarely available. So, the authors had to limit themselves in choosing criteria for MCE analysis depending on available data. MCE analysis is a crucial part of land use prediction. In case of availability of sufficient data, this analysis could be done more precisely by adding more criteria.
However, this model is one of the first land use prediction models developed for a crucial city like Cumilla. In future, this model might be used as a framework model in developing a robust land use prediction model for the region. Overcoming the constraints might help to develop a complete integrated land use and transportation planning tool for engineers, planners and policy makers to help them make befitting decisions.

REFERENCES

Ahmed, B. (2011). Urban land cover change detection analysis and modeling spatio-temporal growth dynamics using remote sensing and GIS techniques: a case study of Dhaka, Bangladesh (Masters Dissertation, Erasmus Mundus Program). Retrieved from

Boerner, R. E. J., Demers, M. N., Simpson, J. W., Artigas, F. J., Silva, A., & Berns, L. A. (1996). Markov models of inertia and dynamic on two contiguous Ohio landscapes. Geographical. Analysis, 28(1) 56–66.

Dewan, A. M., & Yamaguchi, Y. (2009). Landuse and land cover change in greater Dhaka, Bangladesh: using remote sensing to promote sustainable urbanization. Journal of Applied Geography, 29, 390–401.

Eastman, J. R. (2006). IDRISI Andes Tutorial. Clark Labs, Worcester, MA, USA. Retrieved from http://gis.fns.uniba.sk/vyuka/DTM_ako_sucast_GIS/Kriging/1/Andes_Tutorial.pdf

Eastman, J. R. (2009). IDRISI Taiga Guide to GIS and Image Processing, Clark Labs, Clark University, Worcester. Retrieved from https://www.scirp.org/(S(i43dyn45teexjx455qlt3d2q))/reference/ReferencesPapers.aspx?ReferenceID=1826143

Geospatial Data Service Centre, Netherlands. (2008) Retrieved on http://gdsc.nlr.nl/gdsc/information/earth_observation/band_combinations

Kashem, M. S. B. (2008). Simulating urban growth dynamics of Dhaka metropolitan area: a Cellular Automata based approach (Masters Dissertation, Department of Urban and Regional Planning, Bangladesh University of Engineering and Technology, Dhaka, Bangladesh). Retrieved from http://lib.buet.ac.bd:8080/xmlui/handle/123456789/2126

Kashem, M.S, B, & and Maniruzzaman, K. M. (2008). A critical review of some selected urban land use change models and evaluating their transferability 10 developing countries. Paper presented at 10th Pacific Regional Science Conference Organization (PRSCO) Summer Institute. Dhaka, Bangladesh.

Sang, L., Zhang, C., Yang, J., Zhu, D., & Yun, W. (2011). Simulation of land use spatial pattern of towns and villages based on CA-Markov model. Mathematical and Computer Modelling, 54(3-4), 938-943. Retrieved from https://www.sciencedirect.com/science/article/pii/S0895717710005108

Soe, W. M., & Le, W. (2006). Multicriteria decision approach for land use and land cover change using Markov chain analysis and a cellular automata approach. Canadian Journal of Remote Sensing. 32(6), 390–404.

Takada, T., Miyamoto, A., & Hasegawa, S. F. (2010). Derivation of a yearly transition probability matrix for land-use dynamics and its applications. Landscape Ecology, 25, 561-572.

Thomas, H., & Laurence, H. M. (2006). Modeling and projecting land-use and land-cover changes with a cellular automaton in considering landscape trajectories: an improvement for simulation of plausible future states. EARSeL eProceedings, European Association of Remote Sensing Laboratories, 5(1), 63-76. Retrieved from https://halshs.archives-ouvertes.fr/halshs-00195847

Proceedings of the 5th International Conference on Civil Engineering for Sustainable Development (ICCESD 2020), 7~9 February 2020, KUET, Khulna, Bangladesh (ISBN-978-984-34-8764-3)

PREDICTING LOW FLOW THRESHOLDS OF HALDA-KARNAFULI CONFLUENCE IN BANGLADESH

Aysha Akter*[1] and Ahad Hasan Tanim[2]

[1]Professor, Department of Civil Engineering, Chittagong University of Engineering & Technology (CUET) Chittagong-4349, Bangladesh. e-mail: aysha_akter@cuet.ac.bd
[2]Lecturer, Center for River, Harbor& Landslide Research, Chittagong University of Engineering and Technology, Chittagong-4349, Bangladesh. e-mail: ahtanim@cuet.ac.bd

***Corresponding Author**

ABSTRACT

Eco-hydraulic modeling for flow assessment has increased in recent years due to complex hydraulic factors that control different life stages of ecological habitat. Both the Halda and Karnafuli Rivers play a vital role in the south-eastern part of Bangladesh. In almost every dry season they experience lower inflow. In this study, a 1D eco-hydraulic model, which is representing a Physical Habitat Simulation System (PHABSIM), and a 2D eco-hydraulic model for inflow regimes (CASiMiR), are applied to selected areas. To study low and minimum flow regimes two key factors, the Weighted Usable Area (WUA) and the Habitat Suitability Index (HSI) were applied. Based on the flow during flood tide and long term flow variability, a flow series was investigated to simulate suitable environmental flow regimes. Both models predicted similar trends in incremental discharge variation during minimum inflow and average minimum inflow operating in the in a range of 25 - 30.1 m3/s. Although, difficulties arise while acquiring river bed topography data in the 2D eco-hydraulic model set up, reasonable prediction accuracy and geometry of regime could be obtained. However, insufficient bathymetric data necessitated the application of 1D eco-hydraulic simualtion which yielded reasonable performance while taking suitable eco-hydraulic factors into account.

Keywords: *CASiMiR2D, Low flow, Karnafuli river, PHABSIM, Physical habitat.*

1. INTRODUCTION

Low flow is the minimum flow requirement to sustain the ecological habitat of a riverine ecology. Since 1980, river managers have tried to correlate habitat change with flow using the inflow habitat model that can define a minimum flow while maintaining a healthy ecology. Usually, a habitat model that is based on predefined flow of a hydraulic model can predict water velocity and depth. In terms of velocity, size and depth of a certain range might be suitable for biota (Leclerc et al., 2003, Pasternack et al., 2004, Smakhtin, 2001). A 2D or 3D hydraulic model can be sensitive to river geometry, if one considers depth, magnitude, and velocity distribution in X, Y (2D) or X, Y, Z (3D) direction. 1D models only predict mean velocities. To yield progress in modelling, the assessment of low flow regimes can be based on four major methods: a) hydrological methods (Mathews and Richter, 2007), b) hydraulic methods (Lamouroux and Capra, 2002), c) physical habitat methods (Muñoz-Mas et al., 2014), and d) holistic methods (McClain et al., 2014). All of those methods require hydrological, hydraulic, and biological data that maybe statistically or data driven. Physical habitat methods have a wider applicability due to consideration of alternative management methods, restoration actions, and climate change effects (Yi et al., 2014). This also allows the identification of habitats, which are exposed to flow changes. Main key assumptions include and refer to river velocity, river depth, river temperature, etc. They can become limiting factors and determine the distribution of habitats, which can be considered in the model in terms of Weighted Usable Area (WUA) (Milhouse and Waddle, 2012). Based on those key assumption, model developments like PHABSIM (Nagaya et al., 2008), RHYHABSIM (Jowett, 1996), EVHA (Ginot, 1995), and Mesohabitat (Parasiewicz and Dunbar, 2001), or 2D model like Hydro2de, River 2D (Muñoz-Mas et al., 2014) were possible. However, few of these models hardly consider factors related to habitat availability and environmental factors like water quality and nutrient availability. In order to consider these factors, fuzzy logic based Computer Aided Simulation Models for inflow regimes (CASiMiR) (Yao et al., 2015) were developed to take 1D and 2D habitat modeling, environmental, and biotic and abiotic factors into account. In this study, preference curve methods used by PHABSIM and CASiMiR2D were used to assess low flow regimes and thresholds of selected areas of Karnafuli River.

2. MATERIAL AND METHODS

2.1 Study Area

The study area is situated in the downstream part of Halda River where joining Karnafuli River (Figure 1). This restoration site is located along Karnafuli River, 27 km away from the delta (Bay of Bengal). The restoration site is 3 km long. The study reach has 450~700 m width; the water depth varies from 3.28 to 7.5 m. Since 1980, researchers have started investigating ecological responses of Carp fish spawning ground at natural flow regimes, including the loss of suitable ecological factors, species and disruption of habitat for spawning fish (Tsai et al., 1981, Akter and Ali, 2012). Fish monitoring revealed that three species Catla (*Catlacatla*), Mrigala (*Cirrhinusmrigala*), and Rohi (*Labeorohita*) dominate in this area. Low flow regimes are vital for a healthy and intact spawning environment.

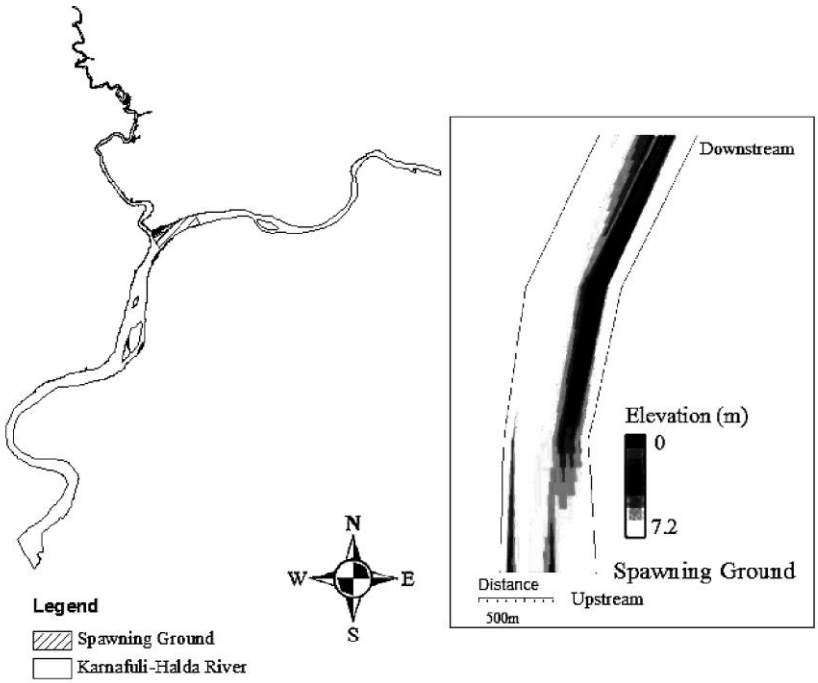

Figure 1: Study Area

2.2 Data Collection

The Halda-Karnafuli confluence represents a natural spawning site. Spawning duration for three native fish species ranges from April to June (Akter and Ali, 2012). During the spawning season, they migrate from upper to the lower parts of the Halda River due to suitable spawning environment. Thus, the carp fish was considered as critical ecological indicator, and establishment of minimum inflow regime was most important to sustain those ecological habitats. For the 1D PHABSIM model, a setup of total 4 cross-sections (i.e. transects obtained from Bangladesh Water Development Board in 2006 and Chittagong Port Authority in 2004 survey) were applied. Thus, acquired database was classified to establish symmetry of the CASiMiR 2D and PHABSIM model based on lateral cell boundaries. Totally, 231 surveyed points were used for the CASiMiR 2D model grid setup. Long-term flow characteristics (2010-2015) of the selected critical reach were taken from the flow pattern study of selected study sites conducted by Akter and Tanim (2017). The Habitat Suitability Curve (HSC) method was developed from comprehensive studies (Tsai et al., 1981). Microhabitat variables (depth, velocity, and substrate) were considered in this study as important factors of carp fish spawning. Different bed roughness coefficients were estimated in accordance with observations of bed material and bed form size. Substrate size was visually determined and a three-substrate type consisting of silt, sand, and vegetation type substrate was identified. The recommended channel index (Table 1) as per Schneider et al. (2010) is assigned in PHABSIM and CASiMiR 2D model.

Table 1: Channel Index code (Schneider et al., 2010)

Code	Substrate type	Sizes (mm)	Code for model input	Substrate type	Sizes (mm)
0	Organic material, detritus	Visually identifiable	5	Large Gravel	20-60
1	Silt clay, loam	0.00024~0.062	6	Small stones	60-120
2	Sand	0.062~2	7	Large stones	120-200
3	Fine Gravel	2-6	8	Boulders	>200
4	Medium Gravel	6-20	9	Rock	Visually identifiable

2.3 Flow characteristics of restoration site

Tides are the major driving force in Karnafuli River, along with freshwater outflow and saline water inland flow. Tides entering from upstream (where the river joins at mouth) are gradually distorted with distance, and increasingly extinct due to channel bottom friction (Devkota and Fang, 2015). Thus, overall flow pattern prominently depends on tidal process of the river. Due to diurnal tide fluctuations, usually two tide cycles are observed in Karnafuli River and thus two directions of flow occur. During flood tide, saline water flow from the sea to the inland and direction changes in reverse order during ebb tide. Flow hydrograph and its nature changes with tide cycle and water level fluctuations. To determine low flow thresholds, the flood tide is considered and analysed as a unidirectional river. Based on the percentage of flow that exceeded the threshold during the flood tide, several incremental discharges were selected to cover the entire flow range (Table 2).

Table 2: Description of the selected discharge to assess habitat suitability

Discharge (m^3/s)	Description
15.8	Minimum flow of flood tide in Karnafuli River during winter season(Akter and Tanim, 2017)
25	10% of flow of annual runoff reported as per Tennant method (Tennant, 1976)
30.1, 35.6	Minimum discharge of flood tide during monsoon season(Akter and Tanim, 2017)
60.7	Q_{95} reported according to Q_{95} method obtained from flow duration curve (Arthington and Zalucki, 1998)
75	30% of mean annual runoff as per Tennant method (Tennant, 1976)
100, 153, 175	Discharges were selected in incremental order based on the change of stage
200, 225	Flooding discharge (Akter and Tanim, 2017)

2.4 Habitat Simulation method based on preference curve

The habitat simulation method considers physical components of river hydraulics and predicts the optimum flow regime while analysing maximum suitability of factors like depth, velocity, temperature, and substrate size. From a global perspective, among 207 methodologies of inflow assessment in 44 countries the habitat simulation method is the second most frequently applied method (Tharme, 2003). This method is employed in the habitat simulation model throughout several modules like hydraulic module, hydrologic module, and habitat module. In the hydraulic module flow, components like geometric cross sections, depth, discharge, and velocity need to be introduced in the model interface through either manual input (PHABSIM) or developing algorithm (CASiMiR 2D). The hydrologic module consists of suitable ecological factors like substrate size and habitat preference curve. Finally, the habitat module takes decision of suitable minimum inflow based on univariate preference function in terms of WUA and Habitat suitability Index (HSI).

2.5 Habitat Suitability Curve

Due to lack of ecological data, the generation of proper Habitat Suitability Curves (HSC) is quite challenging while conducting eco-hydraulic modeling. During the study period (i.e., 2010-2015), an expert judgement was applied to work out proper HSC. In doing so, also data from literature are assessed (Akter and Ali, 2012; Tsai et al., 1981). In the habitat simulation method, HSCs correlate the hydraulic module and the habitat module. However, HSC development usually needs comprehensive biological and environmental data collection. In Figure 2, typical habitat suitability curves are shown for carp fish species.

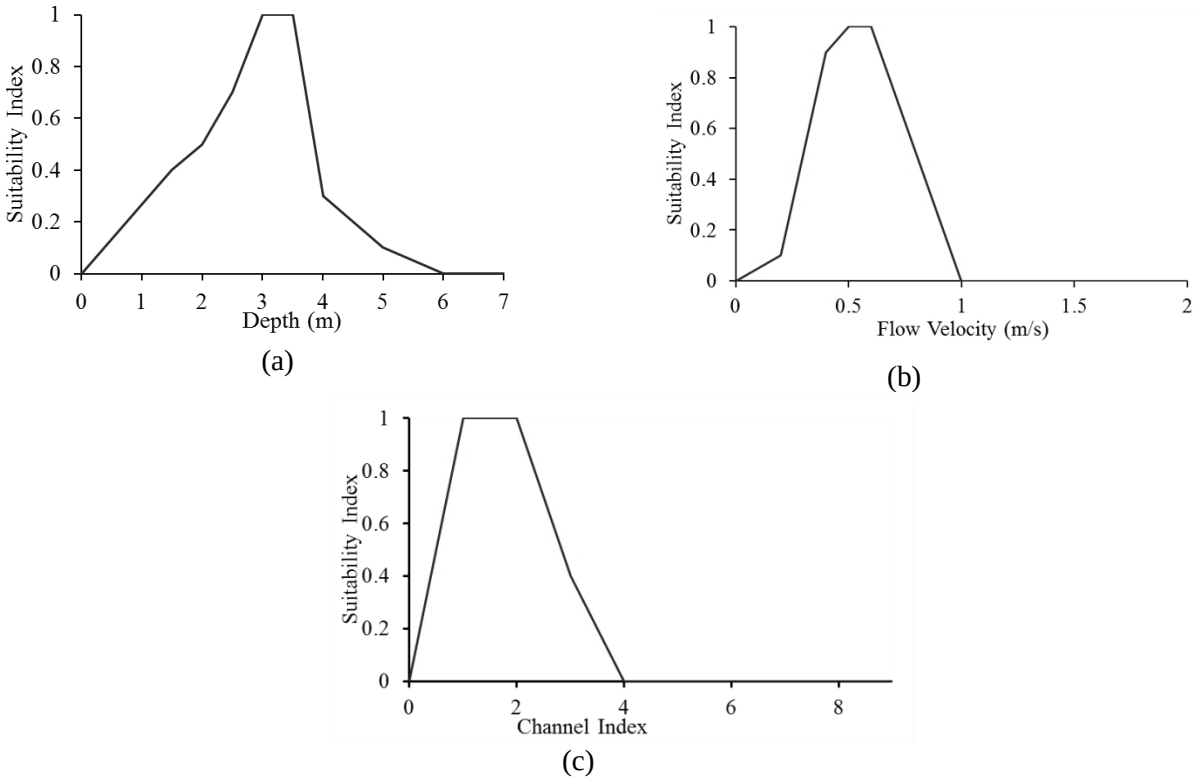

Figure 2: HSC curves of major carp fishes based on (a) depth, (b) flow velocity, and (c) channel index (Schneider et al., 2010)

2.6 PHABSIM model setup

To study low flow regimes in incremental discharge, the 1D eco-hydraulic model PHABSIM is the most widespread and preferred habitat model. It integrates a habitat simulation model with a biological model of habitat selection and relies on habitat suitability criteria like WUA using a discharge function (Ayllón et al., 2012). In this study, all of the 4 transects were placed along 1000 m intervals from the upstream consisting boundary conditions of defined flow and mean column velocity. Fish and other aquatic organisms can tolerate a certain range of stream velocity, water depth and bed substrate. An eco-hydraulic model like PHABSIM has key assumptions that reflect a habitat suitability of a regime based on velocity, depth, and substrate size, i.e., the Habitat Suitability Index (HSI). HSI has preference curves of targeted species on a scale of 0 to 1. The water level in the 1D eco-hydraulic model is usually predicted by three methods, whereas the Water Surface Profile (WSP) method is one of them. The WSP code uses a standard step-backwater method to determine the water surface elevations on a cross section and adjust manning's "n" (roughness coefficient for channels, closed conduits flowing partially full, and corrugated metal pipes) from the calculated discharge. Further, boundary conditions for the individual discharge can be provided. Based on predefined flow and discharge ranges, the WSP method - in this study – was modified for hydraulic modelling purposes.

The inflow is provided at upstream hydraulic section of restoration site. For 1D-HEC-RAS hydraulic simulations, the acquired water surface elevation was used as downstream boundary condition. During the HEC-RAS model setup, the average velocity ($\bar{V}$) was modified for application in each of the PHABSIM model cells. In order to minimize field survey for average velocity collection, Nikghalb et al. (2016) developed a relevant approach in the PHABSIM model. The cell velocity $(Vi)_{mod}$ obtained from the average velocity (Eq. 2) depends on the Manning's roughness coefficient (n), the hydraulic radius of each cell (HD), and the weighted discharge (Q') of each cell as shown in Eq. (3).

$$(V_i)_{mod} = V_i + \frac{\Delta Q}{nA_i} \quad (1)$$

$$V_i = \overline{V} \times \left(\frac{\overline{HD}}{HD_i}\right)^{\frac{2}{3}} \quad (2)$$

Where $HD = R = \frac{A}{P} \approx \frac{A}{b} \approx \frac{A}{T}$

$\Delta Q = Q' \sim Q_{actual}$

$$Q' = \sum_{i=1}^{n} V_i \times A_i \quad (3)$$

2.7 CASiMiR2D model setup

CASiMiR (Schneider et al., 2010) is a fuzzy logic based eco-hydraulic model, developed by a group at the University of Stuttgart, Germany, to assess habitat suitability. The sub-model consisting of hydrodynamic parts can execute 1D, 2D and 3D hydraulic computation. It can calculate inflow values for the habitat using preference functions and fuzzy rules (Ahmadi-Nedushan et al., 2008). In this study, the CASiMiR 2D model was applied as 2D eco-hydraulic model using same univariate preference functions as for the PHABSIM model. The boundary conditions (discharge and water surface elevation) were established from HEC-RAS simulations. An algorithm in ASCII (American Standard Code for Information Interchange) languages was developed, which is based on Schneider et al. (2010). The algorithm consists of 231 numbers of X, Y, Z coordinates and channel indices to create a grid for hydraulic sub-model input. This was further interpolated in longitudinal scale (100 m) and vertical scale (0.3 m) to remove abrupt topography as well as to improve hydraulic performance of the channel. The WSP method was employed for the PHABSIM model, in which the boundary condition provides discharge throughout the water surface elevation at each sub-section. However, this boundary condition is limited between two adjacent transects. Another algorithm based on the WSP method (HEC-RAS 1D hydraulic simulation model) was developed to set the upstream and downstream boundary condition.

2.8 Low flow thresholds establishment

In the Habitat Simulation Method (HSM), the Weighted Usable Area (WUA) and the Habitat Suitability Index (HSI) can be used to describe the integrated habitat suitability and low flow threshold of the whole river investigated. The WUA value can be obtained by multiplying the area of each grid (CASiMiR) or cell (PHABSIM) by its HSI value. Suitable environmental flow or low flow thresholds will be achieved at maximum WUA. The WUA (m^2) function can be described as:

$$WUA = \sum_{i=1}^{i=n} A_i HS_i = f(Q), \quad (4)$$

where, i is the order number of cell; n is the number of all cells; A_i is the area of the i^{th} cell; $SI_i$is HSI value of the i^{th} cell; Q is discharge (m^3/s).

3. RESULTS AND DISCUSSION

3.1 Habitat suitability assessment

Due to the topographic variation and sand bar formation, flow diversion occurred within the first kilometer (Figure 3). PHABSIM predicts this zone as most suitable area of carp fish spawning, due to river confluence and less turbulence. The habitat suitability criteria assumed that habitat suitability could be ascribed in a weightage scale of 0 to 1. The effect of substrate size shows less prominent effect rather than flow components (depth and velocity). The overall habitat diversity obtained was relatively low in comparison to the total area. Spawning suitability of carp fish shows more heterogeneity near the bank and around the place where flow contraction occurred. Thus, the flow velocity is relatively low and makes the velocity most dominant. The habitat simulation model was developed based on a calibrated hydraulic model HEC-RAS, and the boundary condition was

incorporated from the previously applied hydraulic model. The HSI variability makes the difference in WUA computation between 1D and 2D models that influence environmental flow prediction (Figure 4). This result is expected because the hydraulic modules of both, the 1D and 2D eco-hydraulic model, have different approaches of considering transverse flow (Ayllón et al., 2012). However, the results might be influenced by optimum PHABSIM cross-section that depends on data availability. The PHABSIM hydraulic module is usually unstable in turbulent flow (Kondolf et al., 2000). However, the CASiMiR2D model was used to handle unstable turbulent flow. To maintain the required regime condition in a tidal river, the spatial flow variability is one of the common characteristics of tidal rivers.

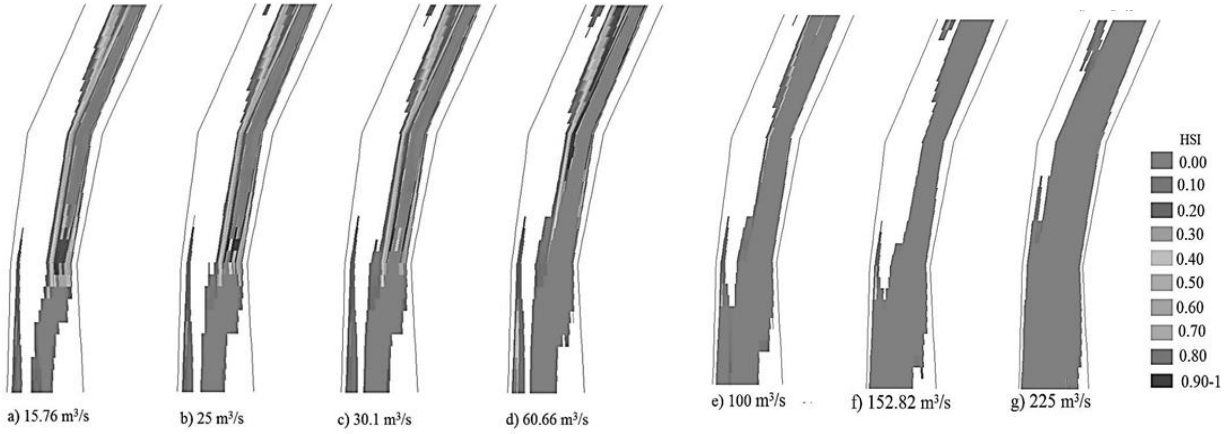

Figure 3: Habitat Suitability Index obtained from CASiMiR 2D

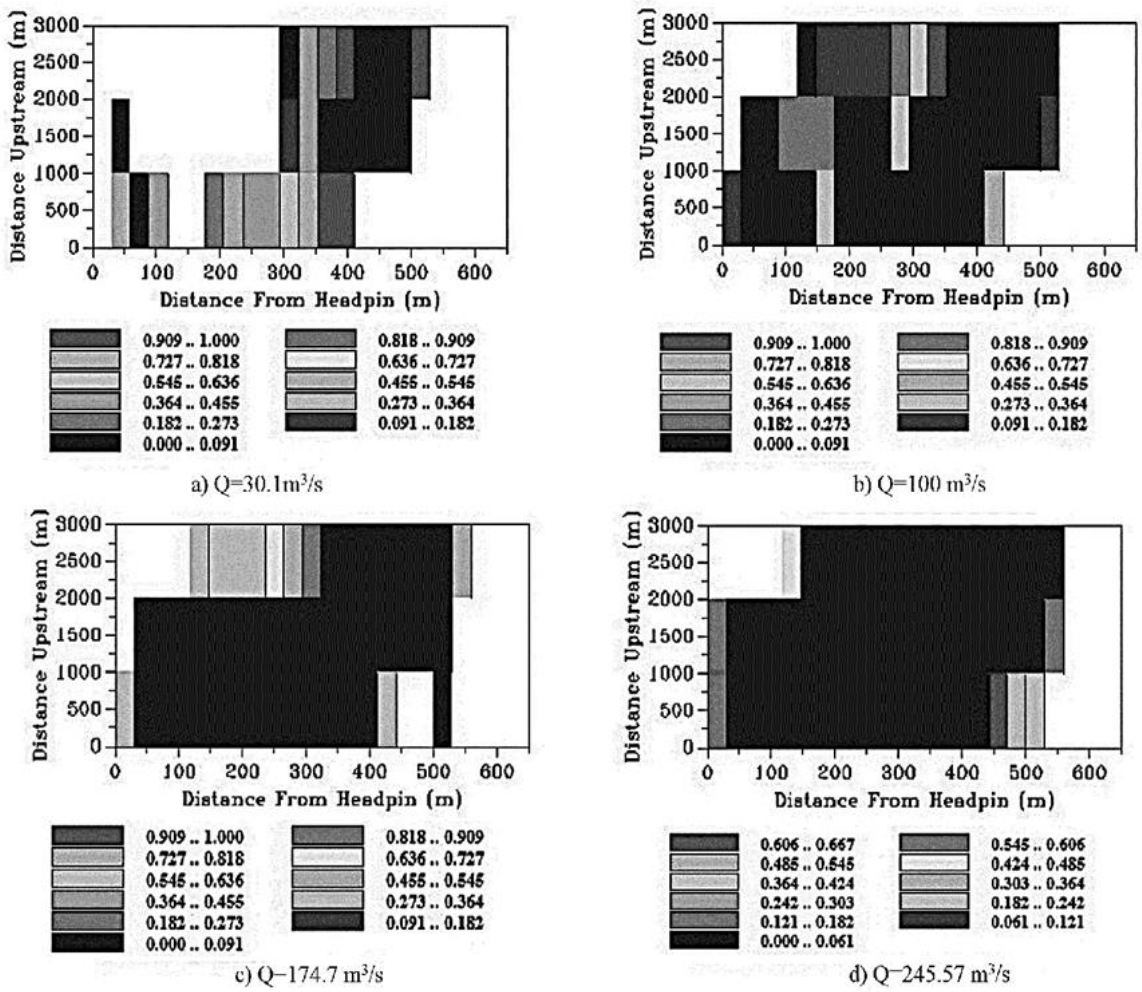

Figure 4: Habitat Suitability Index obtained from PHABSIM

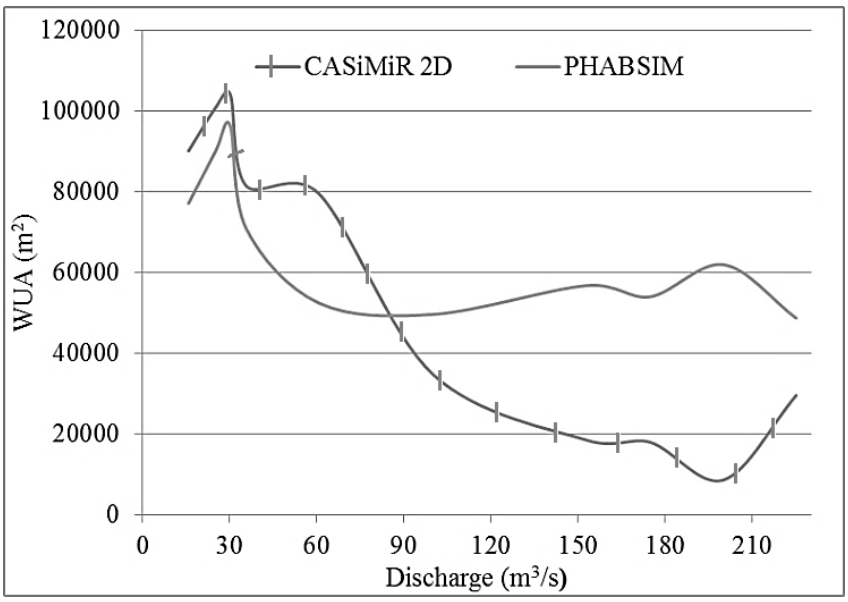

Figure 5: WUA vs. Discharge Relationship

3.2 Low flow thresholds

The WUA and flow relationships were obtained from model simulation (Figure 5). Both models predict that 30.1 m^3/s discharge can be established as low flow threshold. WUA in view of the flow relationship shows that low flow regime is sensitive to flow influencing parameters. The CASiMiR 2D model predicts that during flood tide the habitat suitability of carp fishes can maintain sufficient discharge between 15 m^3/s and 60.7 m^3/s. By increasing the discharge, the HSI reduces rapidly and reveals that spawning suitability is sensitive to flow parameters. In any hydraulic model, the accuracy of results relies on the topographic and hydrographical data that are influenced by river velocity and depth. Thus, related to the HIS, the variation of depth and velocity differed from 1D to 2D. This also resulted in variation of the WUA. Waddle et al. (2000) found that a 2D model can capture complex flow situations while significant transverse flow regimes are present. A significant variation of WUA in the 2D model was observed after 90 m^3/s (Figure 5). This indicates that the velocity and discharge prediction significantly vary when exceeding this threshold.

4. CONCLUSIONS

In this study, low flow threshold was established using the WUA concept, 1D, and 2D eco-hydraulic simulations for the Karnafuli-Halda river confluence. It was found that spawning conditions for carp fish relied on flow velocity and depth. Further, climate changes (storm surges or sea level rise) will influence the tidal flow and negatively affects the spawning ground. Migration and spawning of fish might occur in upper less turbulent parts of the Halda or Karnafuli River.

With respect to the spatial variability during the habitat and flow simulation, the CASiMiR 2D model is more coherent than the 1D PHABSIM model. The 2D eco-hydraulic model is suited for rapidly varying river topographies and tidal regimes with complex flow patterns. The improved interpolation techniques of the CASiMiR 2D model allows any 3D or 2D simulation at desired scales.

ACKNOWLEDGEMENTS

This research was supported by the funds provided for Potentialities of Flow Restoration in Karnafuli-Halda River (FRKR) research project (CUET/DRE/2016-17/CRHLSR/001), Chittagong University of Engineering and Technology (CUET), Bangladesh. We express our gratitude to BWDB, CPA, BMD for providing bathymetric, meteorological and validation data during the study.

REFERENCES

Ahmadi-Nedushan, B., St-Hilaire, A., Bérubé, M., Ouarda, T. B. M. J. & Robichaud, É.: *Instream flow determination using a multiple input fuzzy-based rule system: a case study*. River Research and Applications, 24**,** 279-292 (2008).

Akter, A. & Ali, M. H.: *Environmental flow requirements assessment in the Halda River, Bangladesh*. Hydrological Sciences Journal, 57**,** 326-343 (2012).

Akter, A. & Tanim, A. H.: *Environmental flow assessment of diurnal tidal river using synthetic streamflow* (submitted) (2017).

Arthington, A. H. & Zalucki, J. M.: *Comparative Evaluation of Environmental Flow Assessment Techniques: Review of Methods.* Occasional Paper No. 27/98. Land and Water Resources Research and Development Corporation: Canberra (1998).

Ayllón, D., Almodóvar, A., Nicola, G. G. & Elvira, B.: *The influence of variable habitat suitability criteria on PHABSIM habitat index results.* River Research and Applications, 28**,** 1179-1188 (2012).

Devkota, J. & Fang, X.: *Numerical simulation of flow dynamics in a tidal river under various upstream hydrologic conditions.* Hydrological Sciences Journal, 60**,** 1666-1689 (2015).

Ginot, v. (1995). EVHA, A Windows software for fish habitat assessment instreams B. Fr. PechePiscic. .

Jowett, I. G. (1996). RHYHABSIM, River Hydraulics and Habitat Simulation. ComputerManual. National Institute of Water and Atmospheric Research (NIWA) Report, Hamilton ,50. .

Kondolf, G. M., Larsen, E. W. & Williams, J. G. (2000). Measuring and Modeling the Hydraulic Environment for Assessing Instream Flows. *North American Journal of Fisheries Management,* 20**,** 1016-1028.

Lamouroux, N. & Capra, H.: *Simple predictions of instream habitat model outputs for target fish populations.* Freshwater Biology, 47**,** 1543-1556 (2002).

Leclerc, M., Saint-Hilaire, A. & Bechara, J.: *State-of-the-Art and Perspectives of Habitat Modelling for Determining Conservation Flows.* Canadian Water Resources Journal / Revue canadienne des ressources hydriques, 28**,** 135-151 (2003).

Mathews, R. & Richter, B. D. *Application of the Indicators of Hydrologic Alteration Software in Environmental Flow Setting*. JAWRA Journal of the American Water Resources Association, 43**,** 1400-1413 (2007).

Mcclain, M. E., Subalusky, A. L., Anderson, E. P., Dessu, S. B., Melesse, A. M., Ndomba, P. M., Mtamba, J. O. D., Tamatamah, R. A. & Mligo, C.: C*omparing flow regime, channel hydraulics, and biological communities to infer flow–ecology relationships in the Mara River of Kenya and Tanzania.* Hydrological Sciences Journal, 59**,** 801-819. (2014).

Milhouse, R. T. & Waddle, T. J.: Physical Habitat Simulation (PHABSIM) Softwarefor Windows Fort Collins, CO: FortCollins Science Centre (2012).

Muñoz-Mas, R., Martínez-Capel, F., Garófano-Gómez, V. & Mouton, A. M.: *Application of Probabilistic Neural Networks to microhabitat suitability modelling for adult brown trout (Salmo trutta L.) in Iberian rivers.* Environmental Modelling & Software, 59**,** 30-43. (2014).

Nagaya, T., Shiraishi, Y., Onitsuka, K., Higashino, M., Takami, T., Otsuka, N., Akiyama, J. & Ozeki, H.: *Evaluation of suitable hydraulic conditions for spawning of ayu with horizontal 2D numerical simulation and PHABSIM.* Ecological Modelling, 215**,** 133-143(2008).

Nikghalb, S., Shokoohi, A., Singh, V. P. & Yu, R.: E*cological Regime versus Minimum Environmental Flow:Comparison of Results for a River in a Semi Mediterranean Region.* Water Resources Management**,** 1-16 (2016).

Parasiewicz, P. & Dunbar, M. J.: *Physical habitat modelling for fish: a developing approach.* Arch. Hydrobiol., 135**,** 1–30 (2001).

Pasternack, G. B., Wang, C. L. & Merz, J. E.: *Application of a 2D hydrodynamic model to design of reach-scale spawning gravel replenishment on the Mokelumne River, California.* River Research and Applications, 20**,** 205-225 (2004).

Schneider, M., Noack, M., Gebler, T. & Kopecki, L.: *Handbook for the Habitat Simulation Model CASiMiR*, http://www.casimir-software.de/data/CASiMiR_Fish_Handb_EN_2010_10.pdf. , (2010).

Smakhtin, V. U.: *Low flow hydrology: a review*. Journal of Hydrology, 240**,** 147-186 (2001).

Tennant, D. L.: *Instream flow regimens for fish, wildlife, recreation and related environmental resources.* Fisheries, 1**,** 6-10 (1976).

Tharme, R. E.: *A global perspective on environmental flow assessment: emerging trends in the development and application of environmental flow methodologies for rivers.* River Research and Applications, 19**,** 397-441 (2003).

Tsai, C., Islam, M. N. & Rahman, K. U. M. S.: *Spawning of major carps in the lower Halda River. Bangladesh.* Estuaries, 4**,** 127-138. (1981).

Waddle, T. J., Steffler, P., Ghanem, A., Katopodis, C. & Locke, A.: *Comparison of one and two-dimensional open channel flow models for a small habitat stream.* Rivers, 7**,** 205-220 (2000).

Yao, W., Rutschmann, P. & Sudeep: *Three high flow experiment releases from Glen Canyon Dam on rainbow trout and flannelmouth sucker habitat in Colorado River.* Ecological Engineering, 75**,** 278-290 (2015).

Yi, Y., Cheng, X., Wieprecht, S. & Tang, C.: *Comparison of habitat suitability models using different habitat suitability evaluation methods.* Ecological Engineering, 71**,** 335-345 (2014).

Proceedings of the 5th International Conference on Civil Engineering for Sustainable Development (ICCESD 2020), 7~9 February 2020, KUET, Khulna, Bangladesh (ISBN-978-984-34-8764-3)

WATER VULNERABILITY AND SUSTAINABILITY SCENARIO OF A TYPICAL POPULUS CITY OF LEAST DEVELOPED COUNTRY

Emon Roy*[1], Md Salman Rahman[2], Nadia Sultana Nisha[3] and Amlan Majumder[4]

[1]Graduate Student, Chittagong University of Engineering & Technology, Bangladesh, e-mail: emonroy.cuet@gmail.com
[2]Graduate Student, Chittagong University of Engineering & Technology, Bangladesh, e-mail: u1301099@student.cuet.ac.bd
[3]Graduate Student, University of Chittagong, Bangladesh, e-mail: nadiasultana1612@gmail.com
[4]Graduate Student, Ahsanullah University of Science & Technology (AUST), Dhaka, Bangladesh, e-mail: amlanmajumderrupai21@gmail.com

***Corresponding Author**

ABSTRACT

Problems related to water and environmental sector like scarcity of pure and safe water are becoming a major concern particularly in large densely populous cities as a result of rapid growth of population and unplanned urbanization. This research focuses on the present situation of water security and vulnerability scenario in the poor urban area of Sylhet, Bangladesh and finds out the consequences of impure water along with the present and future peoposed role of public and private organizations to improve water security and vulnerability at the study area. Survey data were collected from face to face questionare, telephone interview, mail completion, online survey, observation and focused group discussion. A questionnaire survey was also conducted in 16 wards of Sylhet City Corporation where water crisis is severe. The major environmental problems are inappropriate solid waste disposal system, inadequate water supply, water logging etc. WASA provides water for only 18.87% of total respondents and the role of NGO is not satisfactory too. Almost half of total residents collect water around 10-meter distance from water source, meaning water security management plan is not good enough for urban people. Scarcity of water leads to unhygienic sanitation problem in the city causing degradation of health condition of people day by day. Some organizations are working now to reduce this problem but due to lack of planning, their hard work goes in vain. This research work will help to find out the problem that the people of this zone are facing and what kind of measures are needed to be taken to mitigate this kind of challenging problem.

Keywords: *Vulnerability, WASA, Water, Environment, Sylhet.*

1. INTRODUCTION

Safe drinking water, good sanitation and hygiene are fundamental to people's health, survival, growth and development. Yet, roughly one-sixth of the world's population lacks access to safe water, and around two-fifths lack adequate sanitation (Alam, Nishat, & Siddiqui, 1999). According to a WHO report, around 780 million people globally do not have access to adequate water supply sources (Sakai, Kataoka, & Fukushi, 2013). Use of contaminated water has its health and financial cost. In terms of health cost, it is reported that 80% of all diseases in developing countries may be attributed to the use of contaminated water (Haydar, Nadeem, Hussain, & Rashid, 2016). Industrial waste discharges into the natural environment can deteriorate surface water (Nguyen & Westerhoff, 2019) which is also a major concern regarding urbanization. Access to drinking water which is a global objective of sustainable development is increasingly threatened by the pressure of uses on all resources (Lanmandjèkpogni, Codo & Hountondji, 2019).

Surface and near-surface drinking water in the coastal areas of the mega-deltas in Vietnam and Bangladesh-India are most vulnerable, putting more than 25 million people at risk of drinking 'saline' water (Haque, Vineins, Scheelbeek & Khan, 2016). The country being located on a geotectonically active sedimentary basin; it experiences subsidence almost all over the delta. Subsidence of land, however, not only affects the mean sea level, it might result in changes of water level as a relative measure over the surrounding lands and thus in the depth of inundation (Alam et al., 1999). In most city areas of Bangladesh, people suffer from scarcity of pure and safe water. The difficulties with drinking water collection in normal situations are mainly caused by the spatially varied availability of drinking water sources (Sarkar & Vogt, 2015). Especially in the urban poor area people are affected various waterborne diseases due to impure water. In the rural areas, it has been found that the groundwater extracted by hand tube wells is contaminated with arsenic in many places (Choudhury, Quadir & Ahmed, 1990).

This research work focuses on depicting the overall scenario of Sylhet urban areas where poor people are having trouble finding a safe and hygienic water source for them. Residents of Sylhet city are suffering from acute water crisis as the city corporation is supplying only 2.5 crore liters of water per day while the demand for water is 7.9 crore liters daily. Due to high population density and lack of adequate housing facilities, slums and squatters are increasing every year in Sylhet City. People who live in slums and such other places do not have access to safe drinking water and they are easy casualties to water-borne diseases (Alam et al., 2012). Slums are not homogeneous, and there many diverse vested interests that exist in slums. Slum upgrading is not simply about water or drainage or housing. It is about putting into motion the economic, social, institutional and community activities that are needed to turn around downward trends in an area. These activities should be undertaken cooperatively among all parties involved residents, community groups, businesses as well as local and national authorities if applicable.

2. METHODOLOGY

Demographic description of the study area is discussed and then the overall data collection method is described in the methodology section. To understand present situation of water security in the poor urban area of Sylhet and to find out consequence of impure water, and also to know about the role of public and private organization to improve water security at the study area, the study area is surveyed through questionnaire method. After the field work, the primary data that were collected by the questionnaires, were analyzed and well arranged in lists and figures.

2.1 Study Area

Sylhet is located in the north-eastern of Bangladesh at 24°32'0? N, 91°52'0 E, on the northern bank of the Surma River consisting of 27 wards and 210 mahallas. Sylhet experiences a hot, wet and humid tropical climate. The city is within the monsoon climate zone, with annual average highest

temperatures of 23°c (Aug-Oct) and average lowest temperature of 7°c (Jan). Nearly 80% of the annual average rainfall of 3,334 mm occurs between May and September. A total of nine natural drainage channels (locally called chara) are responsible for draining storm water from city area to the Surma and Khushiara River (Rahman, Zafor & Rahman, 2013). The city corporation is supplying 22,500 Gallons of water where the demand is about 65000 Gallons. The major sources of water to the city is the tube wells and the Surma River. Tests of tube wells in Sylhet District by the Bangladesh University of Engineering & Technology in 1997 found that about 27.6% contained more arsenic than the acceptable limit set by Bangladesh of 50 micrograms per litre.

2.2 Data Collection Method

The data collection phase of the survey process is absolutely vital and not only needs careful planning, but careful monitoring as well. Choosing a method of data collection depends on a number of quite complex factors. Such as amount of time, budget of money and the complexity or nature of the question. The collected data during the year of 2017 and 2018 through the survey method will be depicted in this paper.

2.2.1 Social data collection method

There are different ways of collect data from field or other sources. Social data collection work is the primary survey work that is considered the study and various ways of social data collection methods are discussed below.

2.2.1.1 Face to Face Interviews

In face to face data collection; a team of interviewers especially trained to collect data for surveying work are sent out to respondent's residence to conduct the questionnaire. This is preceded by an 'advance letter' sent out by the survey organization to inform the respondents that they have been selected for the survey, what the survey is about, why they have been selected and that an interviewer will be calling.

2.2.1.2 Telephone Interviews

In a telephone survey the interviewer sits in a call center and reads a structured questionnaire to the respondent keying in their answers to a computer screen. Computer Assisted Telephone Interviewing as this is known, allows the researchers to have more complex questions, although the questionnaire must be kept shorter on the telephone than in face to face encounters. In a telephone survey questions need to be short and are generally attitudinal or behavioral. This is because people are much less inclined to answer personal questions over the telephone when they have not met the interviewer. Response categories also need to be short as respondents will not be able to see show cards and are unlikely to remember a long list of responses read out to them.

2.2.2 Mail Surveys

Mail surveys or postal questionnaires which are filled in by respondents and then sent back to the researcher are relatively cheap method of surveying a large sample, especially if that sample is widely geographically dispersed Generally, a questionnaire is sent out with a covering letter and a stamped addressed envelope. Follow up postcards can be sent several times to boost the response rate**.** Self-completion questionnaires can also be given out to certain groups of people at key event.

2.2.3 Observation

Participant observation is the process of learning through exposure to or involvement in the day-to-day or routine activities of participants in the researcher setting. One is expected to become a part of and turn to the observer for information about how the group is operating. It helps the researcher to get the feel for how things are organized and prioritized, how people interrelate, and what are the cultural parameters.

2.2.4 Secondary Data

Secondary data were collected through thorough analysis of previous research work along with proper scrutiny of NGO and Government organization report. All these facts helped to find out to visualize the actual water vulnerability scenario of the regarding area.

3. RESULTS AND DISCUSSIONS

Socio-economic status of a slum area is mostly depended on education, income and occupation and this entire trio always influences on the nutritional health of slum dwellers. Water security is a prime issue connecting and ensuring the safety of this trio. Not only health but also lifestyle and livelihood status also been tracked by socio economic condition. Here all socio-economic condition is depicted over a marginalized urban slum area of Sylhet. The results obtained following the outlined methodology are organized into four sub-sections. Section 3.1& 3.2 are for demographic data analysis and water contamination scenarios; Section 3.3 explains role of Government and NGOs and Section 3.4 listed the role that can be played by civil society.

3.1 Demographic Survey

The age of respondents is a major concern of the study as the authors had to rely mostly on the questionare survey and people of young to middle aged were targeted most beacuse they were mostly answering the questions than others. From figure 3.1 it is clear that people of age 18-48 are the main target of the study as they are the person who have idea of the whole area and have connections with almost every member of the locatlity along with the possibility of getting most response from them.

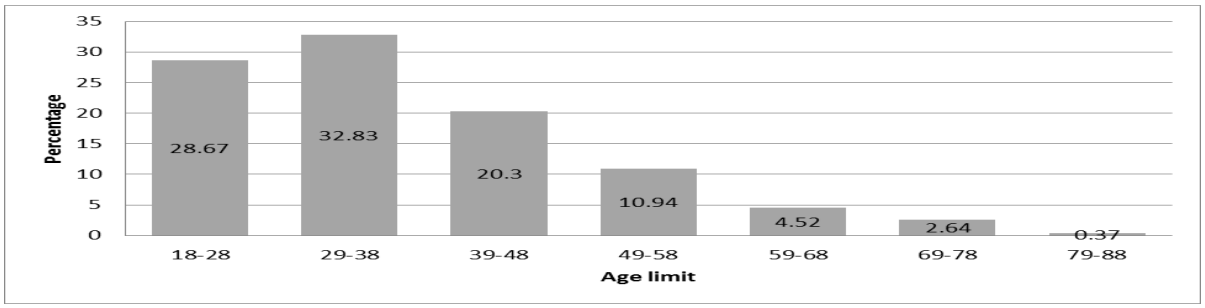

Figure 3.1: Age of the Respondents
Source: Field survey 2017-18

Table 3.1 depicts is the acutal scenario of urbanization happening in Sylhet. Where we found 73% respondents whose actual birthplace is Dhaka but now they are living in the study area. Some of them moved afrter marriage, some of them moved to earn their livelihood. But the fact is they are making the city a much conjusted place which is one of the reasons why the authority is screwing up things.

Table 3.1: Birthplace of Respondents

Area	Sylhet	Chittagong	Dhaka	Khulna	Rajshahi	Rangpur	Barisal
Percentage	58	14	212	2	2	2	1

Occupation of the respondents is clear from figure 3.2. Businessmen and the housewives were asked most questions as the housewives know best about the quality of water they serve to their family and the businessmen were willing to help as well as they were concerned about leading a healthy life. People of other occupation were not asked much as they might not get interested about the water quality due to lack of knowledge.

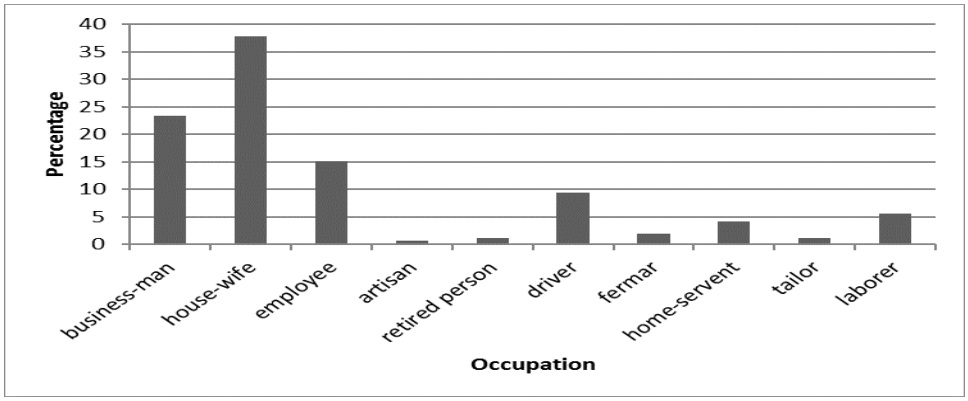

Figure 3.2: Occupation of the Respondents
Source: Field survey 2017-18

Sanitation problem is also a major concern in our regarding study area. Only 17% of the respondents having a cemented house indicates that other 83% of the respondents are having a certain amout of trouble in terms of hygenic questions. People living other than cemented house is causing problems for other people as they are polluting the area which is harmfull for all in the end. This problem needs to taken care of as soon as possible other wise all the steps taken to provide adequate water supply will never be fruitful.

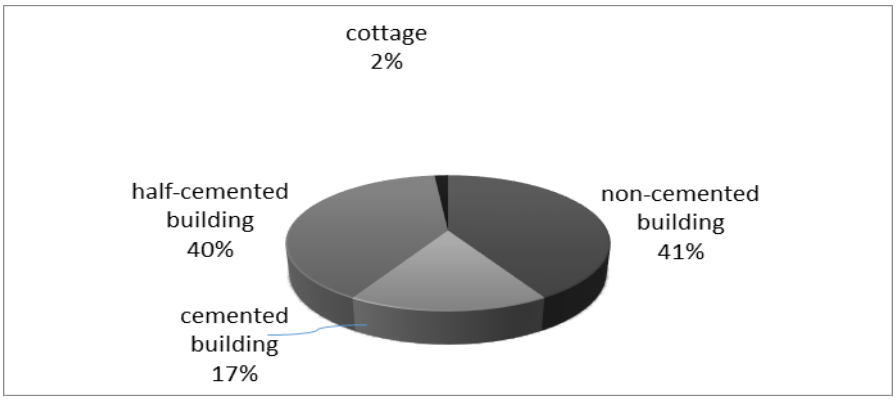

Figure 3.3: Type of Respondent's Houses
Source: Field Survey 2017-18

Table 3.2 and Figure 3.4 represents the distance of water sources from respondent houses and daily amount of household water required. Almost 45% of people collecting water from 5-10 metre indicates that the supply system from the source isn't good enough to reach door to door which creates trouble for the users. On the other hand almost 35% of people having a water demand of 10-20 litre per day indicates that by taking adequate steps in the water supply field will clearly going solve the current problems that the residents are facing as providing supply of 10-20 litre water per day is not an enormous task which cannot be resolved by taking adequate steps. Government along with NGOs and with the help of civil society need to take necessary steps and their perspective steps will be discussed in the upcoming sections.

Table 3.2: Distance of the water sources from respondent houses

Distance(meter)	Frequency	Percentage(%)
5-10	120	45.28
11-15	27	10.188
16-20	22	8.3
21-25	21	7.92
26-30	17	6.42
31-35	0	0
36-40	0	0
41-45	10	3.77
46-50	48	18.11
Total	265	100

Source: Field survey 2017-18

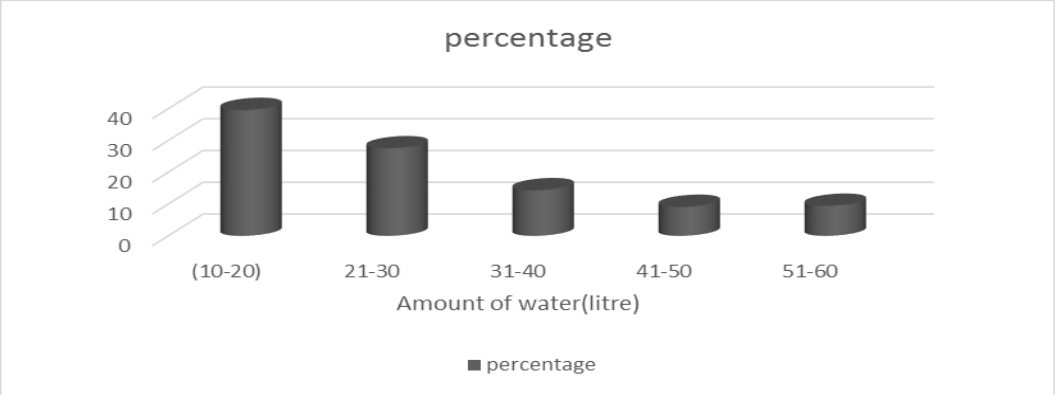

Figure 3.4: Daily amount of water required for cooking and house hold usage
Source: Field survey 2017-18

3.1 Water Contamination Scenario

Household water security will be achieved when reliable and safe household water supply and proper sanitation will be ensured for all communities. It is an essential foundation to support sustainable economic development. Household water security index can be rendered with three sub-indices: access to piped water supply, access to improved sanitation and hygiene condition as indicated by age-standardized Disability Adjusted Life Years (DALY).

Figure 3.5 and table 3.3 shows the water contamination scenario clearly. From figure 3.5 it is clear that more than 50% repondents have no knowledge about their watrer quality which calls for a serious investigation on the water supply management system. And table 3.3 describes the the scenario of disceases regarding water pollution. People are suffering from many water brone diseases like dirraohea, dyscentry etc. 25.08% people affected by diarrohea clearly indicates that the supplied water quality is bad enough to cause problems to human health. Necessary steps should be taken to improve the water quality in the repective area.

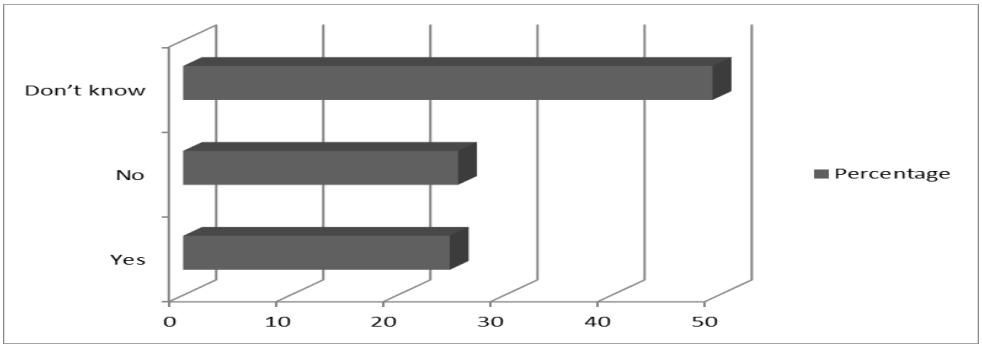

Figure 3.5: Whether the tube well used as a water source by Respondent's family is Examined and Certified as free from Arsenic or not
Source: Field Survey 2017-18

Table 3.3: Problem due to water scarcity and water contamination

Diseases type	Frequency	Percentage(%)
Diarrhoea	66	25.08
Cholera	11	4.1
Jaundice	9	3.3
Dysentery	28	10.64
Skin diseases	19	7.22
Arsenic poisoning	3	1.14
Hair fall	2	0.76
Typhoid	11	4.151
No diseases	74	28.12
No answer	42	15.54
Total	265	100

Source: Field survey 2017-18

3.2 Role of Government

Slum dwellers are part of the urban populace, with the same democratic rights to environmental health and basic living conditions as all residents. These rights are often limited by a government's ability to realize them. Water scarcity is one of the greatest problem in the slum area that Government failure to ensure water security for the poor. Government should take proper steps to reduce this type of problem. 56% of the respondents had no comment on steps taken by the Goverenment; which actually indicates the drastic failure of the authority to provide the sufficient water supply to all its people. Some steps that can be taken by the Government are listed in table 3.4:

Table 3.4: Steps that can be taken by Government to Solve water related problems

Step	Frequency	Percentage (%)
Placement of tube well	70	26.32
Providing water by WASA	50	18.87
No comment	145	54.72
Total	265	100

Source: Field Survey 2017-18

3.3 Role of NGOs

To develop water security, NGOs can help in many ways. NGOos should play a critical part in developing society, improving communities and promoting citizen participation. Local NGOs often have the knowledge and experience needed for practicing good governance. The following steps can be taken by the NGOs to make a sustainable future for the locality:

1. NGOs can help them with money to develop their economic condition.
2. Can help to set up tube well and other equipments required for safe drinking water.
3. NGOs can also create consciousness among poor people.
4. NGO can also contribute in government programs.
5. They can provide water purification tablet and train the illiterate people how contaminated water can be preapared for safe drining purpose.

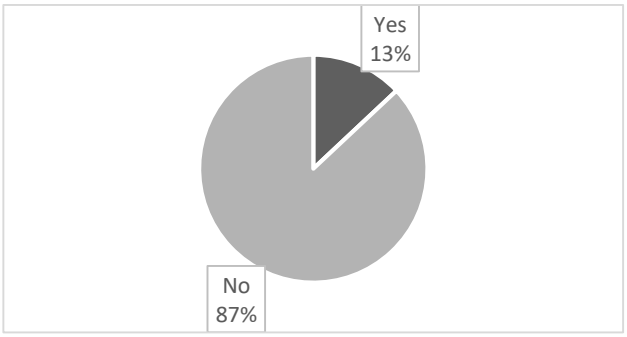

Figure 3.7: Whether any NGO is currently working on water survey at survey area or not
Source: Field survey 2017-18

3.4 Role of Civil Society

Civil society can take valuable steps for poor urban people to make the city more attracted. One important role the city alliance can play, is to help cities or countries share experiences with slum upgradation. Additionally, the city alliances have the ability to access governments and community organizations and can help them to perceive the importance of managing urban development as well as water security for the slum dwellers. The world is becoming increasingly urbanized, and managing urban development must involve identifying strategies to deal with the urban poor. Some noteworthy steps that can be taken by civil society are:

1. To make the poor people conscious about water security.
2. To help them develop their economic condition.
3. To play role with governmental policy.
4. To help slum dwellers understand importance of pure and hygienic water.
5. To supply water if there is no proper water source to use.

4. CONCLUSIONS

This survey work is conducted on water security in urban poor area of Sylhet which indicates the unhealthy, unhygienic, impure, unsafe, contaminated and poisonous supply and source of water which affects the socio economic condition of the poor urban people . The research work will help the policy maker and government to take proper action for future strategy and planning. The demographic survey conducted in this study will help the authorities to get an overall idea on which necessary educational and infrastructural steps can be taken. The water vulnerability study shall help the Government as well as people to be conscious about water security and enjoy their life. It is high time the authority needs to take actions to reduce rural –urban migration. Government should encourage NGOs and other private organizations to play role regarding this matter. Local NGOs can help in various ways such as supplying pure water and giving knowledge on negative impact of unhygienic

water along with arranging semeners for local people on local process of water purification. Lack of knowledge, uncertainties, priorities and reasons for those priorities needs to be identified. Therefore, it is imperative to involve local stakeholders from all levels, ranging from the household to the district and city level, as early on as possible. Civil and alliance society of city area must create consciousness among slum people besides Government and NGOs as stated in the research work. Future study on this topic can include the Strategic Choice Approach (SCA), which can be used to guide efforts to choose sustainable water and wastewater systems in an iterative process that includes: shaping the problem focus, designing potential strategies for addressing problems, comparing those strategies, and finally choosing a strategy to be implemented.

REFERENCES

Alam, Mozaharul, Nishat, Ain-Ul, Siddiqui, S. M. (1999). Water Rresources Vulnerability to Climate Change With Special Reference to Inundation. In S. Huq, Z. Karim, M. Asaduzzaman & F. Mahtab (1999); Vulnerability and Adaptation to Climate Change for Bangladesh (pp 22-28). SPRINGER-SCIENCE+BUSINESS MEDIA, B.V.

Alam, R., Munna, G., Chowdhury, M. A. I., Sarkar, M. S. K. A., Ahmed, M., Rahman, M. T., Jesmin, F., Toimoor, M. A. (2012). Feasibility study of rainwater harvesting system in Sylhet City. Environmental Monitoring and Assessment, 184(1), 573–580.

Choudhury, a. M., Quadir, D. a., & Ahmed, a. U. (1990). Socio-Economic and Physical Perspectives of Water-related Vulnerability to Climate Change: Results of Field Study in Bangladesh. Science and Culture 71 (7).

Haque, Md. A.; Vineins, Paolo; Scheelbeek, Pauline; Khan, E. U. (2016). Drinking water vulnerability to climate change and alternatives for adaptation in coastal South and South East Asia (January). Article in Climatic Change · January 2016 DOI: 10.1007/s10584-016-1617-1.

Haydar, S., Nadeem, O., Hussain, G., & Rashid, H. (2016). Drinking Water Quality in Urban Areas of Pakistan : A Case Study of Gujranwala City. Pakistan Journal of Scientific and Industrial Research Series A: Physicl Sciences 59(3): 157-166.

Lanmandjèkpogni, M.P.S., De Paule Codo, F., Hountondji, B. and Yao, B.K. (2019) Accessibility Index of Aquatic Environments as an Indicator of Surface Water Vulnerability in Urban Areas: Case of the Okpara Basin (Benin). Open Journal of Modern Hydrology , 9, 103-112.

Nguyen, T., & Westerhoff, P. K. (2019). Drinking water vulnerability in less-populated communities in Texas to wastewater-derived contaminants. Nature Partner Journals Clean Water,(2019) 2:19.

Rahman, A., Zafor, M. A., & Rahman, M. (2013). Surface water quality and risk assessment in the vicinity of Sylhet City. International Journal of Water Resources and Environmental Engineering Vol. 5(1), pp. 29-34, January 2013.

Sakai, H., Kataoka, Y., & Fukushi, K. (2013). Quality of Source Water and Drinking Water in Urban Areas of Myanmar. The Scientific World Journal 2013 (4): 854261.

Sarkar, R., & Vogt, J. (2015). Drinking water vulnerability in rural coastal areas of Bangladesh during and after natural extreme events. International Journal of Disaster Risk Reduction, 14, 411–423.

Proceedings of the 5th International Conference on Civil Engineering for Sustainable Development (ICCESD 2020), 7~9 February 2020, KUET, Khulna, Bangladesh (ISBN-978-984-34-8764-3)

MORPHOLOGICAL CHARACTERICTICS OF INNER BAR AREA OF PUSSUR RIVER IN BANGLADESH

Md. Inzamul Haque Prince*[1], Md. Motiur Rahman[2], and Md. Shahjahan Ali[3]

[1]*UG Student, Department of Civil Engineering, Khulna University of Engineering & Technology, Khulna-9203, Bangladesh, email:* inzamulhaque2k14@gmail.com
[2]*PhD Student, Department of Civil Engineering, Khulna University of Engineering & Technology, Khulna-9203, email:* khan.motiur06@gmail.com
[3]*Professor, Department of Civil Engineering, Khulna University of Engineering & Technology, Khulna-9203, Bangladesh, email: bablu41@yahoo.com*

***Corresponding Author**

ABSTRACT

The Pussur is a distributaries of the Ganges river flowing in southwestern region of Bangladesh. This river is at the downstream side of Bhairab river, which is originated from Gorai river. The scouring and siltation phenomenon of a river affects the navigation facility for the transport of products from different firms, factories, mills situated at its bank. In this study, the morphological characteristics of inner bar area of Pussur river has been analyzed. The study area covers from Mongla to Base creek (9.476 Km) which is very important route of national and international trading. Hydrographic charts have been collected from Mongla Port Authority for the years from 2006 to 2017. From the hydrographic chart, 4 longitudinal and 21 cross sectional bed profiles have been analyzed. From those bed profiles, topographical variation in river bed has been studied for different years. This study presents the comparison of erosion and deposition between different years. From 2006 to 2010, the navigation route of inner bar area was siltation dominating that found to be changed to scour dominating from 2010 to 2014. This is probably due to increase of upstream flow in Gorai river because of the dredging in Gorai mouth. After 2014, the navigation route from Mangla to Karamjal area are found to be siltation prone and Sultan Khal to Farid khal area are found to be scour dominating region.

Keywords: *Morphological change; Deposition and Erosion rate; Change in bed elevation; Pussur River.*

1. INTRODUCTION

Southwestern region of Bangladesh is encompassed by the Ganges and the Lower Meghna in the east and by the Indian Border in the west and by the Bay of Bengal in the south. The coastal region of Bangladesh and the rivers in this region exposes a continuing process of siltation progressing generally from northwest to southeast. The significant source of upstream freshwater at Mongla Port is flow through Ganges to Pussur. Pussur River is situated in South Western part of Bangladesh and Mongla Port is established on left bank of this river. Bangladesh is a riverain country. It is a low-lying flat country with significant inland water bodies, including some of the biggest rivers in the world (Kamal et al. 1999). About 700 rivers including tributaries flow through the country constituting a waterway of total length around 24,140 kilometers (15,000 mi). Most of the country's land is formed through silt brought by the rivers. River pollution and degradation occurs, when river water is adversely affected due to the addition of large amounts of external materials to the water and is unfit for its intended use. When due to anthropogenic activities its changes its natural states, river degradation occurs (Rahman et al. 2009). The Pussur river is a continuation of the Rupsa, which is formed of the union of the Bhairab and Atrai rivers. At present, much of its water is from the Gorai diverted through the Nabaganga. From near Batiaghata upazila the Rupsa changes its name to Kazibacha, which is given up near Chalna in favour of Pussur. Near the Mongla port, the Pussur receives Mongla river, and near the forest outpost at Chandpai it receives the Mirgamari cross-channel from the Bhola, both on the leftbank. On the rightbank the Manki, Dhaki and Bhadra are connected with the Shibsa system. In the lower delta, the Rupsa-Pussur is second only to the Meghna in size. Formerly it was third, after the Madhumati, but with the considerable diversion of the Gorai flow through Nabaganga, it is now bigger than that river. From its junction with the Mongla, it is no less than a kilometer and a half in width. Thirty-two kilometres from the open sea, it joins the Shibsa to form the five to eight kilometres wide Morzal river, which empties into the bay of bengal by the Marjat and Pussur estuaries. It continues the Rupsa River. All its distributaries are tidal. It meets the Shibsa River within the Sundarbans, and near to the sea the river becomes the Kunga River. It is the deepest river in Bangladesh. This river is at the downstream side of Bhairav river, which is originated from Gorai river. Moreover, in the developing world, urban rivers are used as endpoints of industrial effluents and municipal sewage discharges (Bhuiyan et al., 2015). The scouring and siltation phenomenon of this river affects the navigation facility for the transport of products from different firms, factories, mills situated at its bank.

Figure 1: Study reach of Pussur river

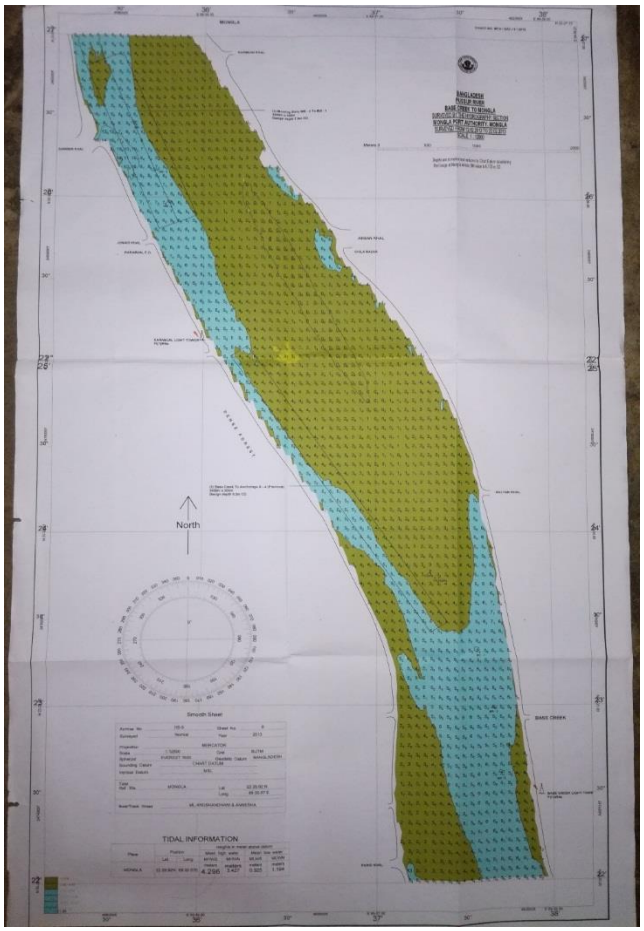

Figure 2: Sample of hydrographic chart (Source: MPA, 2017)

Besides this, river is an important route of international trading. Mongla Port situated at the confluence of Pussur River and Mongla Nulla, approximately 71 nautical miles (about 131 km) upstream from the Fairway buoy (approaches to the Pussur River) of the Bay of Bengal. The Port is well protected by the largest mangrove forest known as the Sundarbans. The Port provides facilities and services to the international Shipping lines and other concerned agencies providing shore based facilities like 5 (five) Jetty berths (total length 914 m), have a capacity of about 6.5 million tones general cargo/break bulk and 50,000 TEUS. The midstream berth (7 buoys & 14 anchorages) have a capacity of about 6.00 million tones. Total 33 ships can take berth in the Port (in the Jetties, buoys & anchorage) at a time. However, alike other modern port of the world Mongla Port is keen to provide highest port facilities, so that bigger draft ships can enter into the port channel safely. The objective of this study is to evaluate the temporal and spatial change in bed topography of the Inner bar area of Pussur river and to determine the erosion-deposition phenomena.

2. METHODOLOGY

The study area covers about 9.476 km of Pussur River from Mongla to Base creek area, which is called inner bar area. Mongla Port is situated on the east bank of Pussur River about 131 km upstream from the fairway buoy. Figure 1 shows the study reach of Pussur River. In this study, hydrographic charts for the year of 2006, 2010, 2013, 2014, 2015 and 2017 has been collected from Mongla port authority. Figure 2 shows one of the hydrographic chart collected from Mongla port authority.

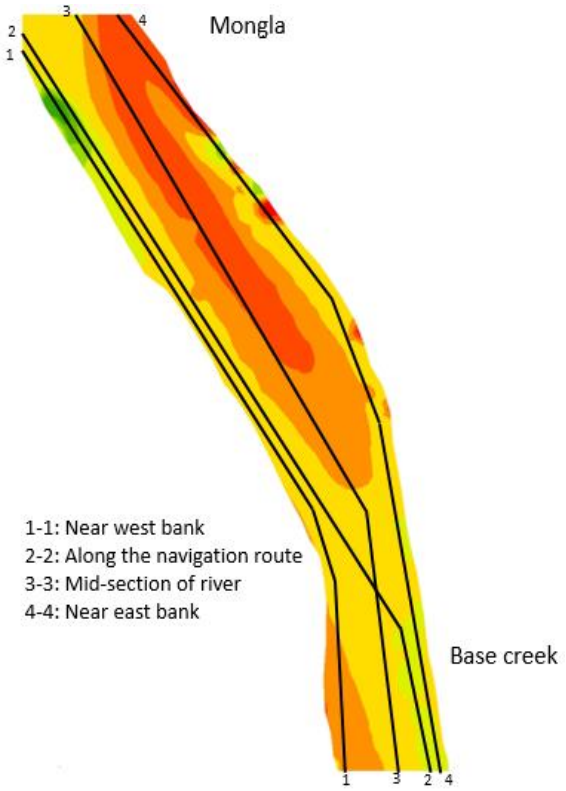

Figure 3: Location selected for longitudinal bed profile

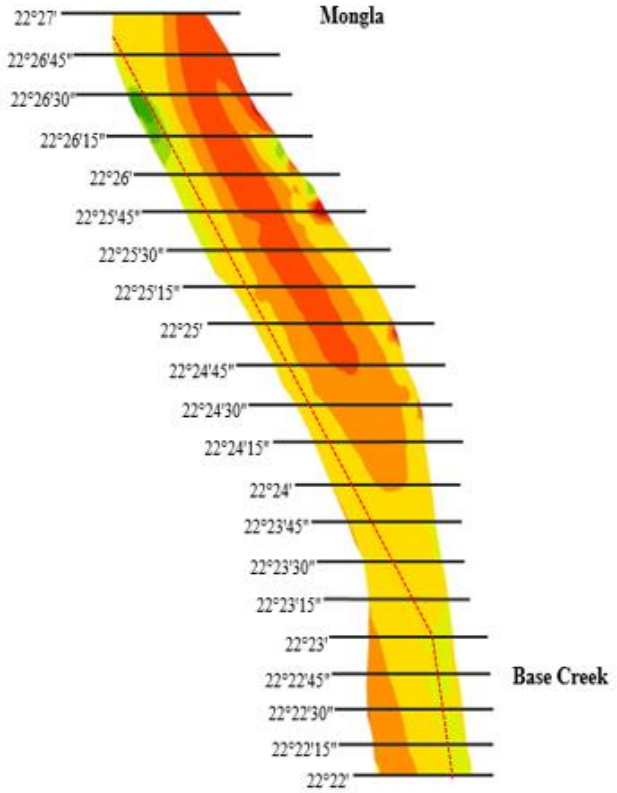

Figure 4: Location selected for cross sectional bed profiles

To determine the longitudinal flow profile, 4 Longitudinal sections (near west bank, along the navigation route, along the center and near west bank) are studied. The sections are shown in Figure 3. 21 cross sectional bed profiles (0°0'15" apart) have been considered over the study area of 9.476 km from Mongla to Base creek. The sections are shown in Figure 4. From those bed profiles, temporal changes of scouring and siltation phenomena have been analyzed. It is observed that the navigation route is near the west bank side of the river for the region 22°27' to 22°24' and then from 22°24' to 22°23'15" it is the near the cross over area. The route is shifted to near the east side from 22°23'15" to further downstream.

3. RESULTS AND DISCUSSIONS

The main purpose of this study is to analysis the scouring and siltation phenomena of inner bar area of Pussur river as well as to investigate the temporal change of morphological characteristics of the study area. Longitudinal and cross-sectional bed profiles for different sections are presented and based on that the morphological change of inner bar area is explained below.

3.1 Longitudinal Bed Profiles

Four longitudinal sections of bed topography have been considered, which are near the west bank, near the east bank, at the center of the river and along the center of the navigation route. Each of them was evaluated for the years of 2006, 2010, 2013, 2014, 2015 and 2017. Figures 5(a), 5(b), 5(c) and 5(d) show the comparison among the bed profiles for Section 1-1 (near west bank), Section 2-2 (at the centerline of the navigation route of the river), Section 3-3 (Mid-section of the river) and Section 4-4 (near east bank) for different years.

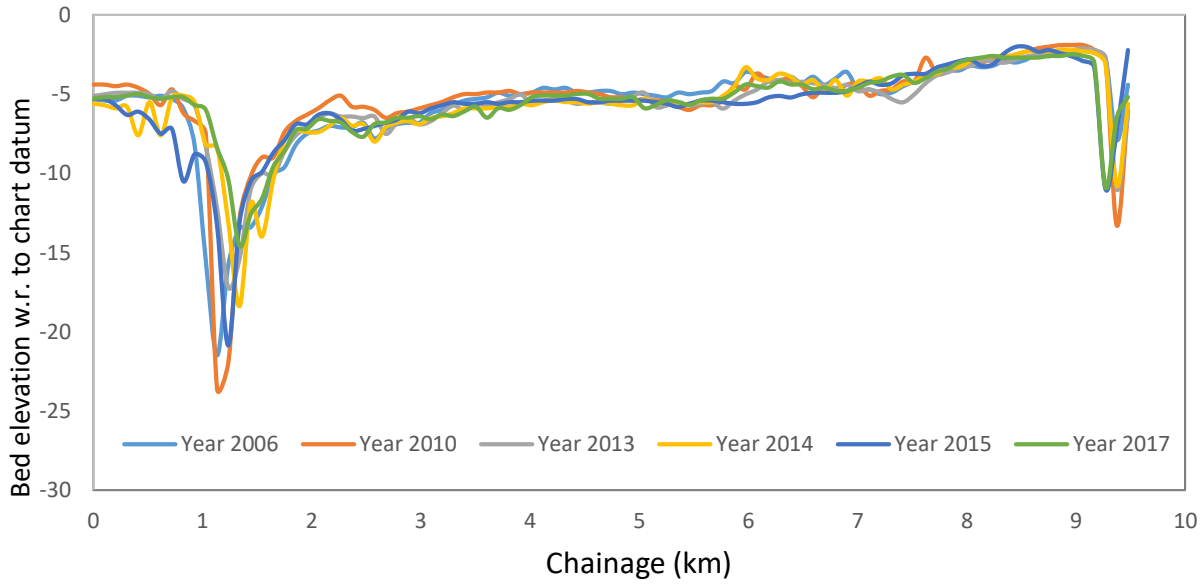

(a) bed profile near west bank of the river (Section 1-1)

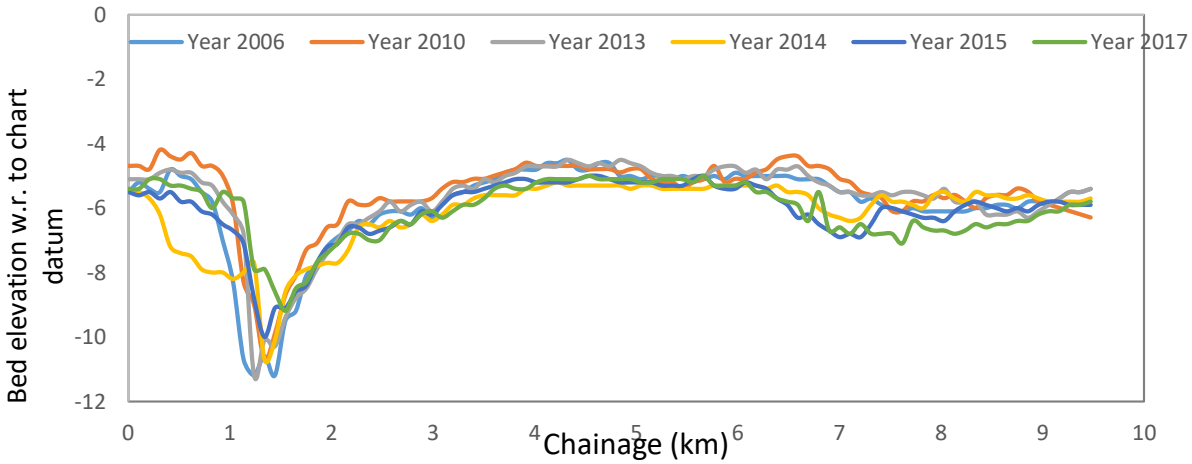

(b) bed profile along the center of navigation route (Section 2-2)

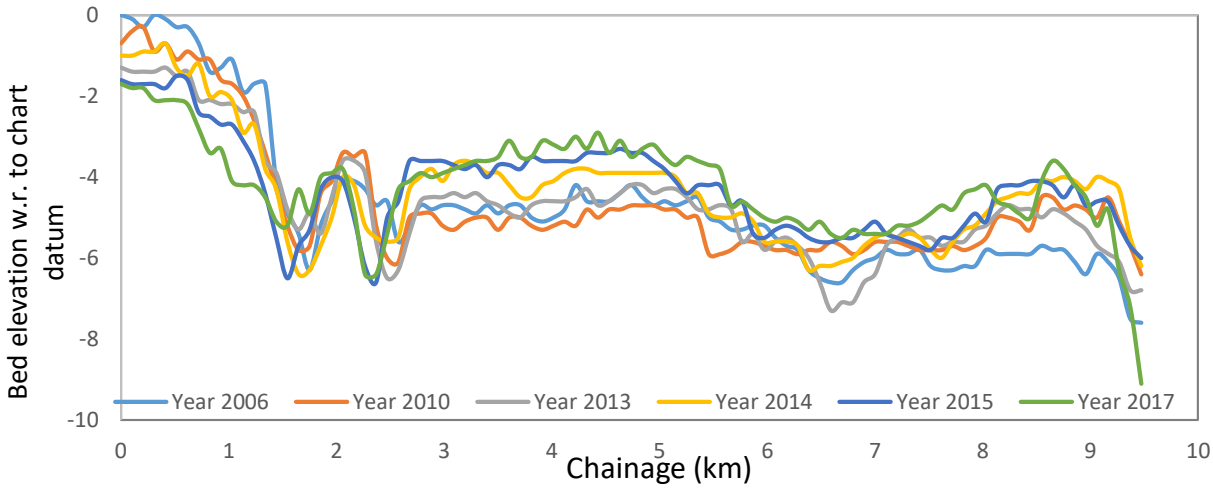

(c) bed profile along the center of the river (Section 3-3)

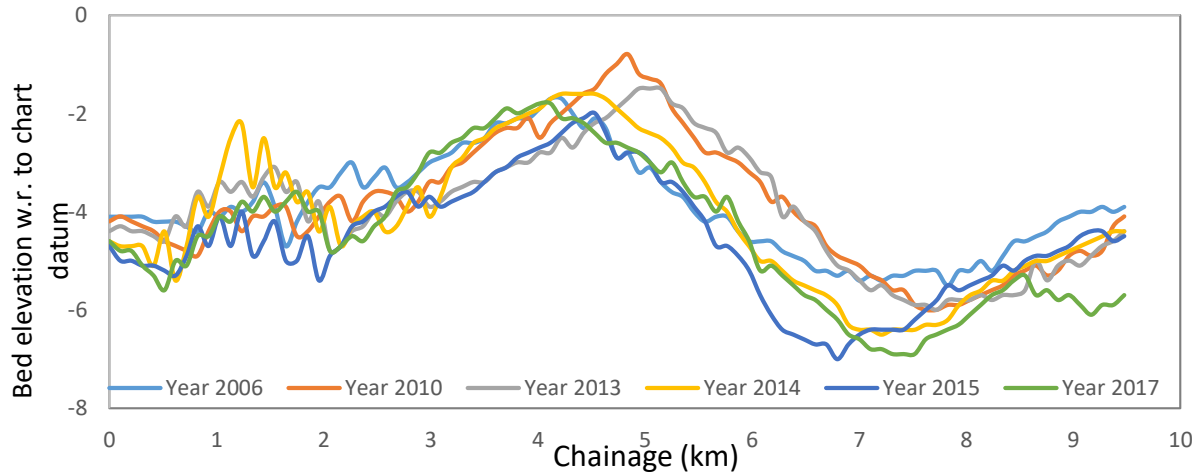

(d) bed profile near east bank of the river (Section 4-4)

Figure 5: Comparison of bed profile along different longitudinal sections for different years

It is observed that section 3-3 and 4-4 are passed over the shallower bar area and the bed profile fluctuates highly year to year. However, the temporal variations of bed profiles are minimum in the deeper part of the channel as observed in sections 1-1 and 2-2.

3.2 Cross Sectional Bed Profiles

21 cross-sections each of 0°0'15" apart have been calculated for the cross sectional bed profiles. In a bed profile, the variation of river bed with respect to the year 2006, 2010, 2013, 2014, 2015 and 2017 are illustrated and the navigation channel of 200 m width is also shown in the figures. It can be noted that the width of the river in the studied portion is varied from 100 m to 1900 m. From the 21 different sections of bed profiles some sample sections located at 22°27', 22°25', 22°24', 22°22' are shown in Figure 6. In Figures (a), (b) and (c), the navigation route is located at west bank side and in Figure (d) the route is near the east bank of the river.

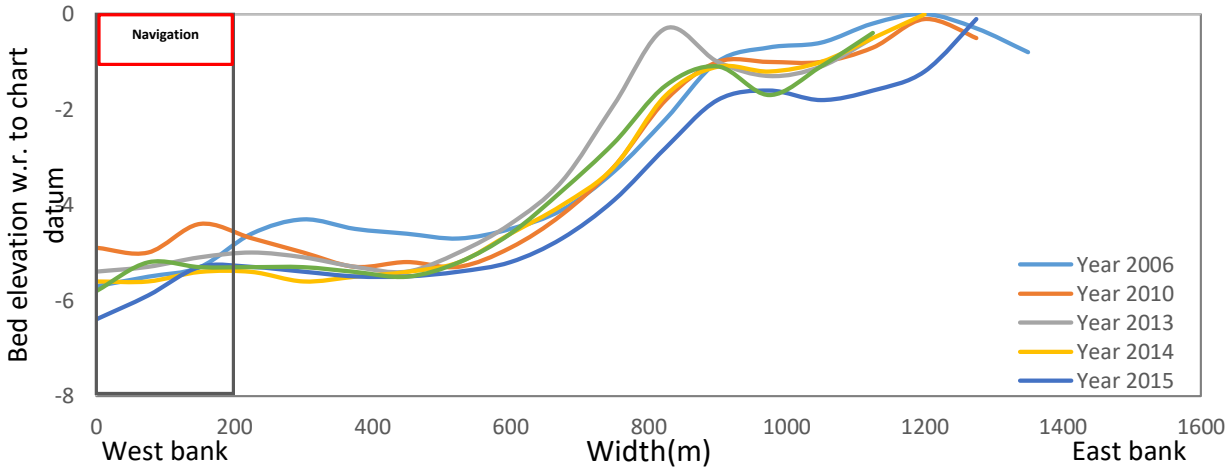

(a) Cross sectional bed profile at 22°27'

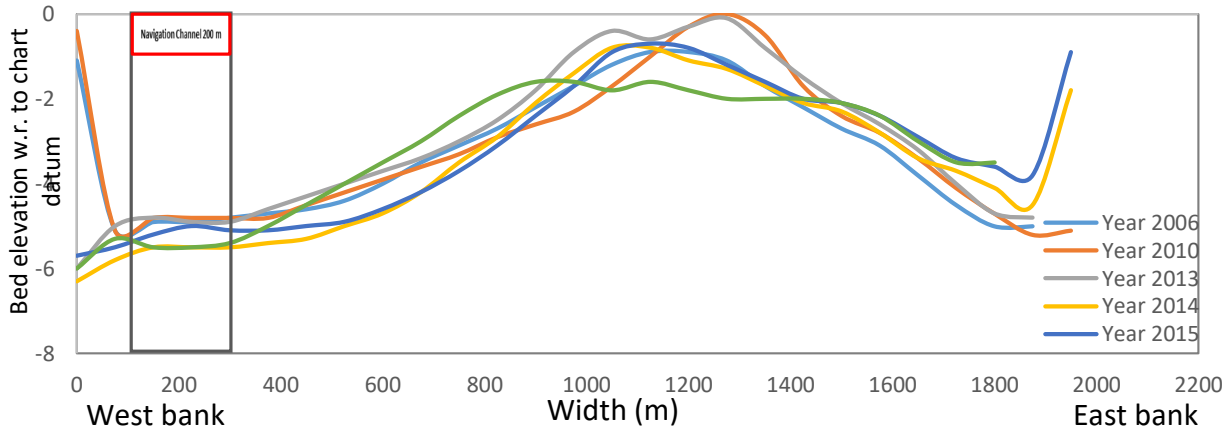

(b) Cross sectional bed profile at 22°25'

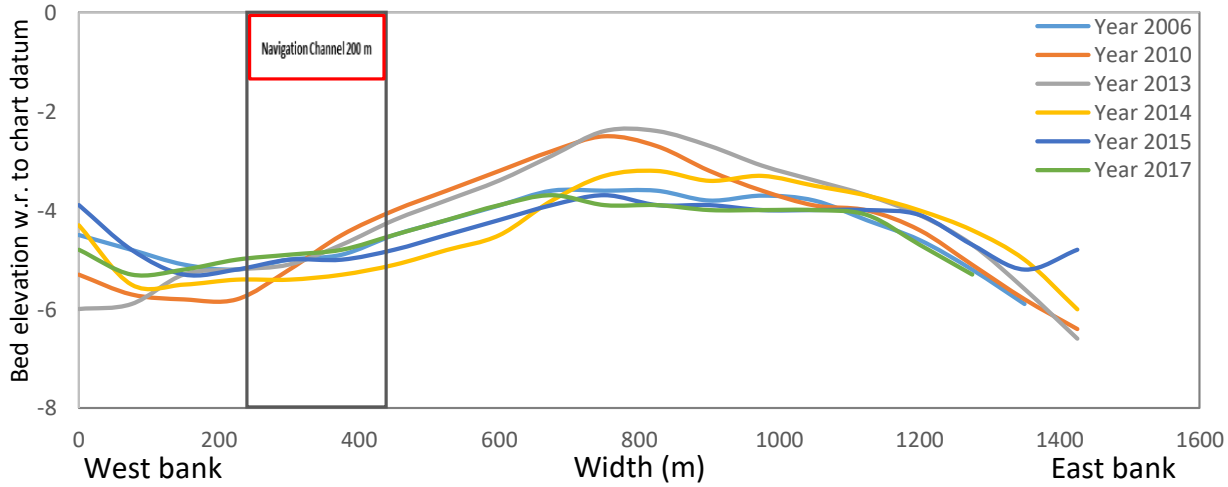

(a) Cross sectional bed profile at 22°24'

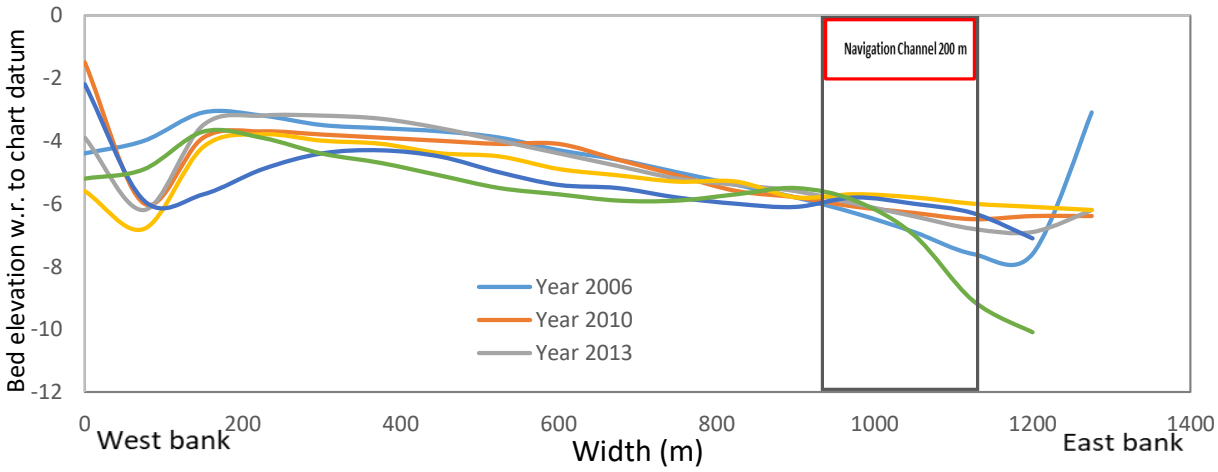

(a) Cross sectional bed profile at 22°22'

Figure 6: Temporal change in cross-sectional bed profile for different years

3.3 Morphological Changes in the Navigation Channel

The width of the navigation channel is 200 m. From the analysis, a comparison between the amount of siltation-erosion volume for different years have been prepared and the net change is presented in Tables 1 to 5.

Table 1: Changes of sedimentation in navigation channel with respect to year 2006

Sedimentation Pattern	Changes between years (m^3)				
	2006-2010	**2006-2013**	**2006-2014**	**2006-2015**	**2006-2017**
Deposition	1437880	848720	298700	263680	407880
Erosion	-98880	-74160	-1324580	-964080	-1124760
Net change	1339000	774560	-1025880	-700400	-716880

Table 2: Changes of sedimentation pattern with respect to year 2010

Sedimentation Pattern	Changes between years (m^3)			
	2010-2013	**2010-2014**	**2010-2015**	**2010-2017**
Deposition	220420	100940	96820	195700
Erosion	-784860	-2465820	-2136220	-2251580
Net change	-564440	-2364880	-2039400	-2055880

Table 3: Changes of sedimentation pattern with respect to year 2013

Sedimentation Pattern	Changes between years (m^3)		
	2013-2014	**2013-2015**	**2013-2017**
Deposition	199820	121540	203940
Erosion	-2000260	-1596500	-1695380
Net change	-1800440	-1474960	-1491440

Table 4: Changes of sedimentation pattern with respect to year 2014

Sedimentation Pattern	Changes between years (m3)	
	2014-2015	**2014-2017**
Deposition	640660	793100
Erosion	-315180	-484100
Net change	325480	309000

Table 5: Changes of sedimentation pattern with respect to year 2017

Sedimentation Pattern	Changes between years (m3)
	2015-2017
Deposition	286340
Erosion	-302820
Net change	-16480

4. DEPOSITION OR EROSION RATE

For the calculation of deposition or erosion rate, the longitudinal bed profile of different years along the center of the navigation route have been considered. The center of the navigation route are taken into account by averaging three bed profile along the navigation route. From longitudinal bed profiles of two different years the erosion and deposition rate have been calculated. .From the 6 different years bed profile here only one deposition or erosion in the year 2014 is shown below. The erosion or deposition is shown in the Table 6. Where "-'' sign represents erosion and "+" sign represents deposition. Table 4.6 shows that the deposition rate varies from 2.2 m to 0.1 m and the erosion rate varies from -0.1 m to -0.7 m between the year 2006 to 2010; the deposition rate and erosion rate are varied from 1.5 m to 0.1 m and -2.2 m to -0.1 m between the year 2010 and 2013, from 3.5 m to 0.1 m and -2.7 m to -0.1 m between the year 2013 and 2014; from 1.8 m to 0.1 m and -1.2 m to -0.1 m between the year 2014 and 2015; from 2.1 m to 0.1 m and -1.0 m to -0.1 m between the year 2015 and 2017.

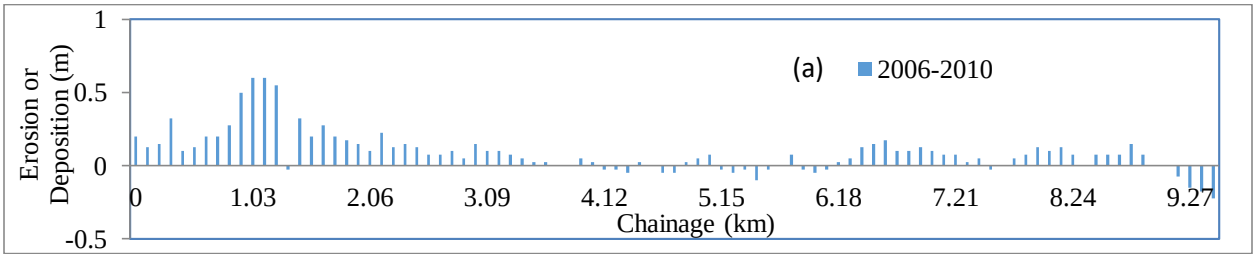

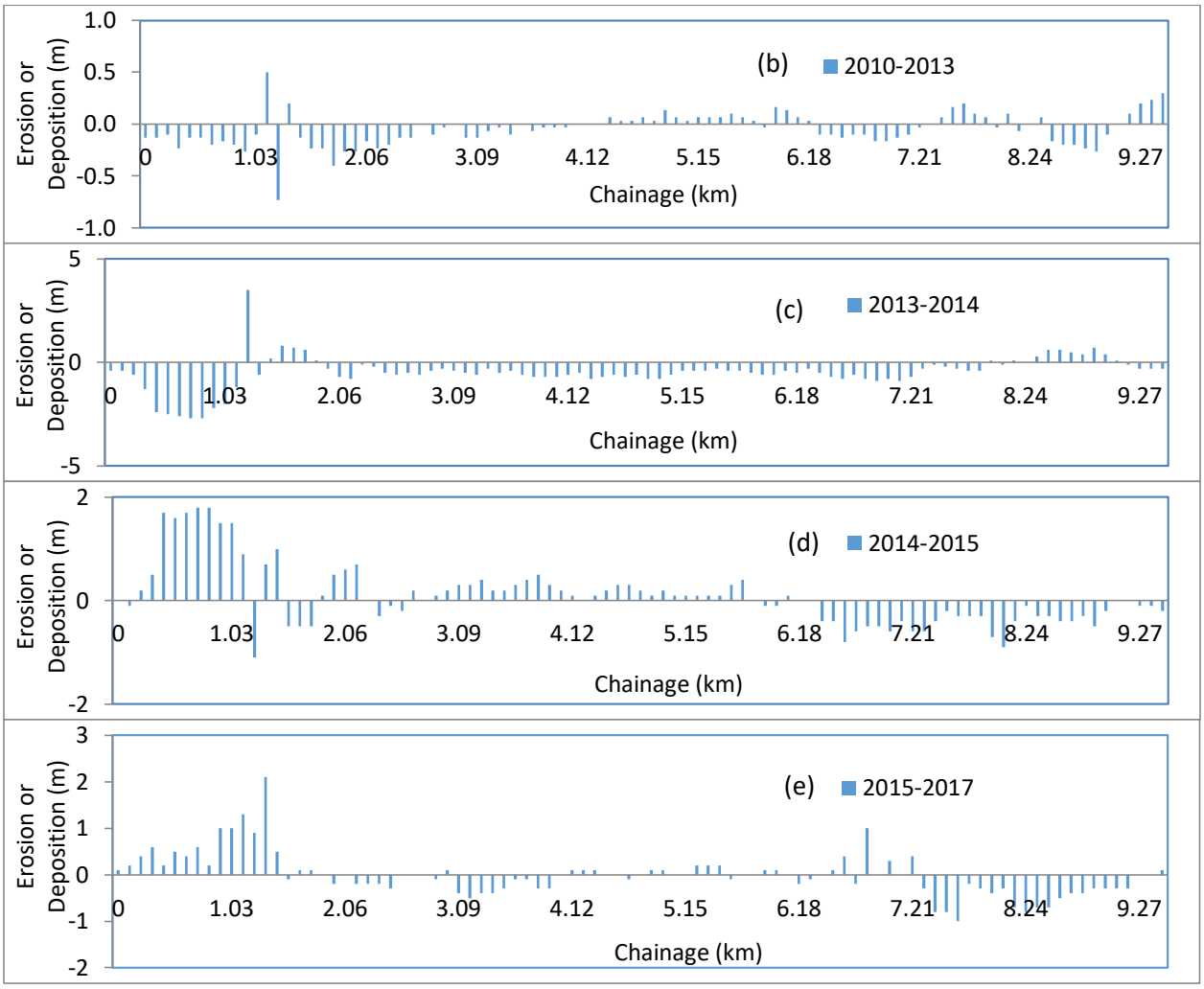

Figure 7: Yearly erosion (negative value) and deposition (Positive value) at different chainages of the inner bar area considering different time spans: (a) 2006 to 2010 (b) 2010-2013 (c) 2013-2014 (d) 2014-2015) (e) 2015-2017.

Figure 7 shows the graphical representation of yearly erosion (negative value) and deposition (Positive value) rate at different chainages of the inner bar area considering different time spans. The study area can be divided into five different locations such as Mongla to Danger khal, Danger khal to Karamjal, Karamjal to Sultan khal, Sultan khal to Base creek, Base creek to Farid khal area. In Table 7, the calculated erosion-deposition are presented for different time spans for those five regions. From 2006 to 2010, the navigation route of inner bar area was siltation dominating that found to be changed to scour dominating from 2010 to 2014. This is probably due to increase of upstream flow in Gorai river because of the dredging in Gorai mouth. After 2014, the navigation route from Mangla to Karamjal area are found to be siltation prone and Sultan Khal to Farid khal area are found to be scour dominating region.

Table 7: Defining Siltation and scouring prone area of inner bar for different time spans.

No.	Location	2006-2010	2010-2013	2013-2014	2014-2015	2015-2017
1.	Mongla to Danger khal	Siltation (1.13 m/yr)	Scouring (-0.39 m/yr)	Scouring (-1.19 m/yr)	Siltation (0.91 m/yr)	Siltation (0.66 m/yr)
2.	Danger khal to Karamjal	Siltation (0.44 m/yr)	Scouring (-0.39 m/yr)	Scouring (-0.29 m/yr)	Siltation (0.12 m/yr)	Scouring (-0.15 m/yr)
3.	Karamjal to Sultan khal	Scouring (-0.01 m/yr)	Siltation (0.12 m/yr)	Scouring (-0.63 m/yr)	Siltation (0.16 m/yr)	Siltation (0.02 m/yr)
4.	Sultan khal to Base creek	Siltation (0.16 m/yr)	Scouring (-0.008 m/yr)	Scouring (-0.52 m/yr)	Scouring (-0.23 m/yr)	Souring (-0.03 m/yr)
5.	Base creek to Farid khal	Siltation (0.08 m/yr)	Scouring (-0.01 m/yr)	Siltation (0.10 m/yr)	Scouring (-0.30 m/yr)	Scouring (-0.36 m/yr)

5. CONCLUSIONS

In this study, the temporal and spatial change in bed topography of the Inner bar area of Pussur river was evaluated and the erosion-deposition phenomena is studied. The depth of the Pussur river over the study area of 9.476 km was found to be varied from 0 m to 7.9 m with a deep pocket varies from 23.3 m to 11.2 m near west bank close to Base creek. It is found that, from 2006 to 2010, the navigation route of inner bar area was siltation dominating that found to be changed to scour dominating from 2010 to 2014. This is probably due to increase of upstream flow in Gorai river because of the dredging in Gorai mouth. After 2014, the navigation route from Mangla to Karamjal area are found to be siltation prone and Sultan Khal to Farid khal area are found to be scour dominating region.

REFERENCE

Kamal, M.M., Hansen, A.M., Badruzzaman, ABM., 1999. Assessment of pollution of the River Buriganga, Bangladesh, using a water quality model. Water Science and Technology 40(2), 129-136.

Rahman, S.H., Tareq, S.M., Ahmed, T., 2009. Degrading Riverine Ecology: Causes, States, and Impacts. River Pollution Concerns and Expectations, Chapter 2, pp 21-76.

Bhuiyan, MAH., Samuel, B., Damper, Islam, M.A., Suzuki, S., 2015. Source apportionment and pollution evaluation of heavy metals in water and sediments of Buriganga River, Bangladesh, using multivariate analysis and pollution evaluation indices. Environmental Monitoring and Assessment, 187, 4075 DOI 10.1007/s10661-014-4075-0.

Proceedings of the 5th International Conference on Civil Engineering for Sustainable Development (ICCESD 2020), 7~9 February 2020, KUET, Khulna, Bangladesh (ISBN-978-984-34-8764-3)

CHANGE IN TRANSVERSE SLOPE OF WATER SURFACE AT RIVER BEND: A NUMERICAL STUDY

Priyata Rahman *[1], MD. Shahjahan Ali[2]

[1] *Postgraduate Student, Institute of Disaster Management, Khulna University of Engineering & Technology, Bangladesh. e-mail: priyata2214.pr@gmail.com*
[2] *Professor, Department of Civil Engineering, Khulna University of Engineering & Technology, Bangladesh, e-mail: babul41@yahoo.com*

***Corresponding Author**

ABSTRACT

In recent years, the CFD (Computational Fluid Dynamics) models application is considered to be efficient tool to study the river processes and outdoor channels. Generation of secondary current in a meandering river flow due to the centrifugal force acting on the river is obviously three dimensional (3D) in nature. But in case of practical problems like alluvial geomorphic processes, 3D models are not proved to be efficient. Hence, two dimensional (2D) models are generally adopted for such problems. This study offers a presentation of numerical simulation results for turbulent flows around bends of a meandering channel for different meander angles. 2D models were built by the use of iRIC Nays2DH for flow simulation for 45˚, 90˚, 135˚, 180˚ meandering bends with varying widths of 0.15m, 0.25m, 0.75m, 1.00m, 1.25m, 1.50m considering constant Froude number, with constant meandering length (M_L/W) and constant radius of curvature (R/W). Zero equation model was used as turbulence closure model with finite differential advections as upwind scheme. The flow behavior had been studied at the apex and cross over portions of bends. From the simulation, the velocity at outer bank was found to be lower than that of the inner bank while the water surface elevation was found to be higher than that of the inner bank. Increase in transverse slope of water surface at bend was observed for increasing meander angles, Froude numbers and decreasing channel widths. The simulation of flow at bend of meandering channel was successfully carried out by using iRIC Nays2DH.

Keywords: *Meandering river, two dimensional flow, bend, channel width, Froude number, iRIC, Nays2DH.*

1 INTRODUCTION

The classification of river includes a large number of classes. They can be classified according to topography of river basin, flood hydrograph, origin, discharge, sinuosity etc. The term sinuosity describes an index which is used to elaborate the channel platform. It is mainly defined as the ratio of channel length to straight line distance of the river. In general, rivers of a straight planform having sinuosity value of 1, are uphill to find and are rare in nature. Most of the rivers in general are of meandering pattern which is most common in the river morphology. By the term meandering pattern it concludes rivers having a sinuosity value greater than 1.5, holding alternate bends. They are generated by the combined actions of the sediment transport in rivers and the water flow. The water flow simulation in meandering river has been a popular topic for research work purpose in river engineering and water resources engineering field. Flow through bends includes three dimensional (3D) patterns as secondary current is produced in a meandering river. When flow approaches to bends, water current flows from the convex side towards the concave. This phenomenon is mainly created by the centrifugal forces acting on the water. In contrast, the water surface in the outer bank rises and makes the inner bank lower thus balances the centrifugal force acting on water surface. Thus produces variation in flow rate along different portion of the river. This elevation change between the outer and inner banks creates transverse slope in water surface. The study of such a flow involves 3D hydrodynamic model. But for the practical application like the alluvial geomorphic processes, the 3D model does not provide much efficiency. For this reason, generally two-dimensional (2D) model is adopted to simulate the flow in a meandering river. The study and analysis of flow through meandering channels hold extensive interest in the field of river engineering for the construction of flood retention structures as rivers play a vital role in influencing the environment. Meandering rivers are formed when sediment erosion occurs, comprising an outer concave bank which is followed by deep scour holes and deposition of sediments are executed on an inner convex curve at downstream creating shallow depth. The creation of inner bank is encouraged by the development of vegetation at low flow stages and consequently stabilizing the point bar (the submergence of zone of minimum flow depth). And the transport of sediments from the outer bank to the inner bank brings changes in the shape of the river. Thus enhances the creation of meander channels. The continuous migration of meander channels can be a reason of many practical problems such as bank erosion, shifting of center line and boundaries, loss of fertile soil, heterogeneous sediment stratigraphy etc.

In the past, many researchers have taken initiative to explain the flow pattern in a meander by considering different meander angles and discharges with varying geometric conditions. Kim and Choi (2003) performed an experiment to simulate the open channel flows in meandering bend. By considering the finite element method they evaluated the 2D numerical algorithm to complete the simulation. Rozovskii (1961) considered a completely smooth and rough bed of a rectangular channel with 180˚ meander bends where the channel width was taken to be 80 cm and the radius of curvature for the 180˚ bend was 80 cm on the centerline. A value for discharge was taken to be 12.3 l/sec while the flow depth, Froude number and Reynolds number were chosen as 5.8 cm, 0.35 and 14000 respectively. He conducted an exploration for trapezoidal channels also. He gave an extensive discussion on the flow mechanism of the meander and explained the generation of secondary current through bends and also interpreted the change of tangential secondary current of flow while traversing a bend. A numerical model in harmony of Rozovskii tests was formed by Leschziner and Rodi (1974) for a 90˚ strongly curved bend where the ratio of average radius to width was considered as 1. In this research, he found the external bank surface slope to be lower than the inner bank surface slope and did not get a linear surface slope along the cross section. De Vriend and Geoldof (1983) constructed a model with 90˚ central angle, 6m channel width, 0.25m channel depth, 0.25 Froude number, 50m radius of curvature with a discharge value of 0.61 m^3/sec. From this hypothesis, the surface transversal profile was found to be linear but the calculation of water surface elevation along the upstream and downstream bends were not done. Ali *et al.*, (2017) worked on the flow pattern around a bend in an open channel for different bend angles of 45˚, 90˚, 135˚ and 180˚. The simulation was done by using the iRIC software. Sharply and mildly curved channels were constructed for predicting the

simulation of the flow field. Constant discharge at upstream and constant depth with zero velocity gradients was given as downstream boundary conditions. The length of the high velocity zone in inner bank and low velocity zone in outer bank along stream-wise direction was found higher for 135˚ bend and gradually decreasing with the decrease of bend angle. Ahmadi *et al.* (2009) worked on a 2D depth-average model for simulating the unsteady flow norms in bends of an open channel. The impression of the secondary flow occurrence was considered in the calculation of dispersion stresses. The actual and mean velocity distributions are inconsistent. Due to which, the product integration is generated and influence the creation of dispersion stresses. These phenomena are considered while performing the momentum equation. In the experiment, orthogonal curvilinear co-ordinate system was used for the simulation of flow with irregular boundary conditions. Finite volume projection method was used in case of staggered grid for evolving the governing equation. They concluded the experimental results by showing a good arrangement of the water surface elevation measurements. They also illustrated a good simulation result with improved dispersion terms.

Due to the generation of secondary current of flow in a meandering channel because of the effect of centrifugal force acting on the water surface, the flow through bends involve three dimensional flow nature. But for the application in the practical engineering problems such as- alluvial geomorphic processes, generally two dimensional models are evaluated to get proper efficiency level of the work. In this study, a 2D model based software named iRIC Nays2DH is used for the simulation of flows for bend angles of 45˚, 90˚, 135˚ and 180˚ considering channels widths of 0.15m, 0.25m, 0.50m, 0.75m, 1.00m, 1.25m and 1.50m of the river and for Froude number of 0.25 and 0.50.

2 SIMULATION TECHNIQUE

In this study the iRIC Nays2DH software is used to simulate the flow fields. The iRIC software provides a vast scope for evaluating the flow in a domain such as- transport of sediment, evaluation of bed, two and three dimensional flow simulation, processing of topographic data, ground-surface-water interrelation, assessment of dwelling, model output visualization, editing tools, mapping, extracting data etc (Shimizu & Takebayashi, 2014). This software is made suitable for exploiting the sets of river data from the river reaches. An advantage is that a user can readily use the software as the models are adorned with single graphical user interface and hence there is no need for the user to learn the pre and post processing tools. This approach is made available for the users by supporting all documentation in public domain. Nays2DH comprises an analytical model for the simulation of two-dimensional (2D) horizontal flow, morphological variation of beds and banks of river, transport of sediment. The basic equations used in this model are obtained from the transformation of the basic equations in an orthogonal co-ordinates system (x, y) into a general curvilinear co-ordinate system as follows.

Continuity Equation

$$\frac{\partial}{\partial t}\left(\frac{h}{J}\right)+\frac{\partial}{\partial \xi}\left(\frac{hu^{\xi}}{J}\right)+\frac{\partial}{\partial \eta}\left(\frac{hu^{\eta}}{J}\right)=0$$

Momentum Equations

$$\frac{\partial u^{\xi}}{\partial t}+u^{\xi}\frac{\partial u^{\xi}}{\partial \xi}+u^{\eta}\frac{\partial u^{\eta}}{\partial \eta}+\alpha_1 u^{\xi}u^{\xi}+\alpha_2 u^{\xi}u^{\eta}+\alpha_3 u^{\eta}u^{\eta}$$
$$=-g\left[(\xi_x^2+\xi_y^2)\frac{\partial H}{\partial \xi}+(\xi_x\eta_x+\xi_y\eta_y)\frac{\partial H}{\partial \eta}\right]$$
$$-\left(C_f+\frac{1}{2}C_D\alpha_s h\right)\frac{u^{\eta}}{hJ}\sqrt{(\eta_y u^{\xi}-\xi_y u^{\eta})^2+(-\eta_x u^{\xi}-\xi_x u^{\eta})^2}+D^{\eta}$$

$$\frac{\partial u^{\xi}}{\partial t} + u^{\xi}\frac{\partial u^{\xi}}{\partial \xi} + u^{\eta}\frac{\partial u^{\eta}}{\partial \eta} + \alpha_4 u^{\xi}u^{\xi} + \alpha_5 u^{\xi}u^{\eta} + \alpha_6 u^{\eta}u^{\eta}$$
$$= -g\left[(\eta_x\xi_x + \eta_y\xi_y)\frac{\partial H}{\partial \xi} + (\eta_x^2 + \eta_y^2)\frac{\partial H}{\partial \eta}\right]$$
$$-\left(C_f + \frac{1}{2}C_D\alpha_s h\right)\frac{u^{\eta}}{hJ}\sqrt{(\eta_y u^{\xi} - \xi_y u^{\eta})^2 + (-\eta_x u^{\xi} - \xi_x u^{\eta})^2} + D^{\eta}$$

Where,

$\alpha_1 = \xi_x\frac{\partial^2 x}{\partial \xi^2} + \xi_y\frac{\partial^2 y}{\partial \xi^2}$, $\alpha_2 = 2\left(\xi_x\frac{\partial^2 x}{\partial \xi \partial \eta} + \xi_y\frac{\partial^2 y}{\partial \xi \partial \eta}\right)$, $\alpha_3 = \xi_x\frac{\partial^2 x}{\partial \eta^2} + \xi_y\frac{\partial^2 y}{\partial \eta^2}$

$\alpha_4 = \eta_x\frac{\partial^2 x}{\partial \xi^2} + \eta_y\frac{\partial^2 y}{\partial \xi^2}$, $\alpha_5 = 2\left(\eta_x\frac{\partial^2 x}{\partial \xi \partial \eta} + \eta_y\frac{\partial^2 y}{\partial \xi \partial \eta}\right)$, $\alpha_6 = \eta_x\frac{\partial^2 x}{\partial \eta^2} + \eta_y\frac{\partial^2 y}{\partial \eta^2}$

$D^{\xi} = \left(\xi_x\frac{\partial}{\partial \xi} + \eta_x\frac{\partial}{\partial \eta}\right)\left[v_t\left(\xi_x\frac{\partial u^{\xi}}{\partial \xi} + \eta_x\frac{\partial u^{\eta}}{\partial \eta}\right)\right] + \left(\xi_y\frac{\partial}{\partial \xi} + \eta_y\frac{\partial}{\partial \eta}\right)\left[v_t\left(\xi_y\frac{\partial u^{\xi}}{\partial \xi} + \eta_y\frac{\partial u^{\eta}}{\partial \eta}\right)\right]$

$D^{\eta} = \left(\xi_x\frac{\partial}{\partial \xi} + \eta_x\frac{\partial}{\partial \eta}\right)\left[v_t\left(\xi_x\frac{\partial u^{\eta}}{\partial \xi} + \eta_x\frac{\partial u^{\eta}}{\partial \eta}\right)\right] + \left(\xi_y\frac{\partial}{\partial \xi} + \eta_y\frac{\partial}{\partial \eta}\right)\left[v_t\left(\xi_y\frac{\partial u^{\eta}}{\partial \xi} + \eta_y\frac{\partial u^{\eta}}{\partial \eta}\right)\right]$

$\xi_x = \frac{\partial \xi}{\partial x}$, $\xi_y = \frac{\partial \xi}{\partial y}$, $\eta_x = \frac{\partial \eta}{\partial x}$ $\eta_y = \frac{\partial \eta}{\partial y}$

$u^{\xi} = \xi_x u + \xi_y v, u^{\eta} = \eta_x u + \eta_y v$ b

$J = \frac{1}{x_\xi y_\eta - x_\eta y_\xi}$

$k - \varepsilon$ model is used for turbulent closure. In the standard $k - \varepsilon$ model, the eddy viscosity co-efficient can be evolved by the following expression-

$$v_t = C_\mu\frac{k^2}{\epsilon}$$

Where, C_μ= model constant,

k and ϵ are attained by the following equations-

$$\frac{\partial k}{\partial t} + u\frac{\partial k}{\partial t} + v\frac{\partial k}{\partial t} = \frac{\partial}{\partial x}\left(\frac{v_t}{\sigma_k}\frac{\partial k}{\partial x}\right) + \frac{\partial}{\partial y}\left(\frac{v_t}{\sigma_k}\frac{\partial k}{\partial y}\right) + P_h + P_{kv} - \epsilon$$

$$\frac{\partial \epsilon}{\partial t} + u\frac{\partial \epsilon}{\partial t} + v\frac{\partial \epsilon}{\partial t} = \frac{\partial}{\partial x}\left(\frac{v_t}{\sigma_\epsilon}\frac{\partial \epsilon}{\partial x}\right) + \frac{\partial}{\partial y}\left(\frac{v_t}{\sigma_\epsilon}\frac{\partial \epsilon}{\partial y}\right) + C_{1_\epsilon}\frac{\epsilon}{k}P_h + P_{\epsilon v} - C_{2_\epsilon}\frac{\epsilon^2}{k}$$

Table 1: Model constants.

C_μ	C_{1_ϵ}	C_{2_ϵ}	σ_k	σ_ϵ
0.09	1.44	1.92	1.00	1.30

Where, C_{1_ϵ}, C_{2_ϵ}, σ_k and σ_ϵ are the model constants having the particular values given in Table 1.

The terms P_{kv} and $P_{\epsilon v}$ are obtained by-

P_{kv}= $C_k\frac{u_*^3}{h}$ = 0.33

$$P_{\epsilon v} = C_k \frac{u_*^4}{h^2}$$

2.1 Numerical test cases

The hydraulic parameters for numerical test cases that were adopted in this study for flow simulation are given in Table 2. Figure 1 shows the meander geometry for series S_1. In the simulation cases, the width of the channel varies from 0.15 to 1.50m and meander length varies from 4.5 to 45m having a constant meandering length M_L/W =30 and for a constant radius of curvature R/W=7.5. 56 numbers of numerical test cases for flow simulations were run within the seven series (S_1 to S_7) of numerical test cases as shown in Table 3. The simulations were performed for bend angles of 45˚, 90˚, 135˚ and 180˚ and for Froude number of 0.25 and 0.50.

Table 2: Meander parameters.

Series No.	Width of Channel, w (m)	Meander Length, M_L (m)	$\frac{M_L}{w}$	Meander Belt (m)	Length of Channel (m)	Radius of Curvature R, (m)
S_1	0.15	4.5	30	2.41	12	1.13
S_2	0.25	7.5	30	4.01	20	1.88
S_3	0.50	15.0	30	8.00	40	3.75
S_4	0.75	22.5	30	12.01	60	5.63
S_5	1.00	30.0	30	16.00	80	7.50
S_6	1.25	37.5	30	20.01	100	9.38
S_7	1.50	45.0	30	24.00	120	11.25

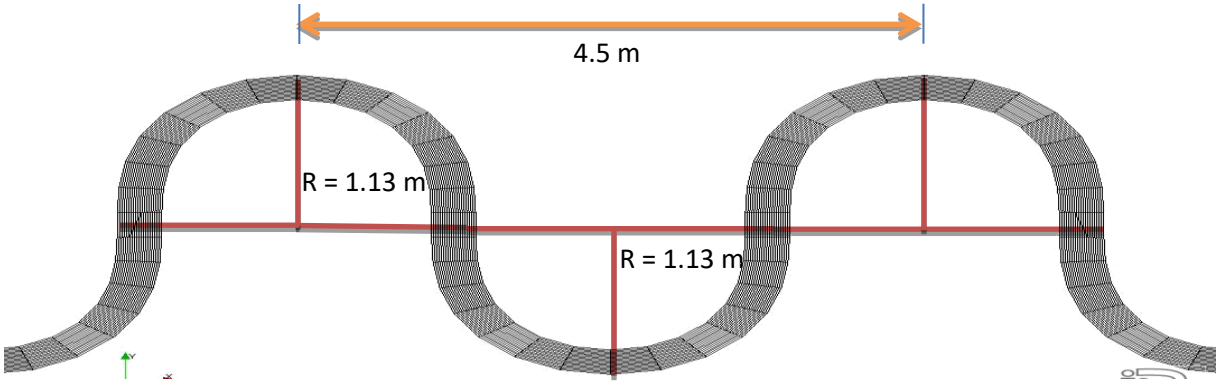

Figure 1: Meander geometry for series S_1.

Table 3: Hydraulic parameters for numerical test cases.

Series No.	Case No.	Bend Angle	Fr	Width of Channel (m)	Discharge, Q (m^3/s)
S_1	$S_1C_1R_1 \sim S_1C_1R_4$	45˚, 90˚, 135˚, 180˚	0.25	0.15	0.05459
	$S_1C_2R_1 \sim S_1C_2R_4$	45˚, 90˚, 135˚, 180˚	0.50	0.15	0.10918
S_2	$S_2C_1R_1 \sim S_2C_1R_4$	45˚, 90˚, 135˚, 180˚	0.25	0.25	0.09098
	$S_2C_2R_1 \sim S_2C_2R_4$	45˚, 90˚, 135˚, 180˚	0.50	0.25	0.18195
S_3	$S_3C_1R_1 \sim S_3C_1R_4$	45˚, 90˚, 135˚, 180˚	0.25	0.50	0.18196
	$S_3C_2R_1 \sim S_3C_2R_4$	45˚, 90˚, 135˚, 180˚	0.50	0.50	0.36390
S_4	$S_4C_1R_1 \sim S_4C_1R_4$	45˚, 90˚, 135˚, 180˚	0.25	0.75	0.27294
	$S_4C_2R_1 \sim S_4C_2R_4$	45˚, 90˚, 135˚, 180˚	0.50	0.75	0.54585
S_5	$S_5C_1R_1 \sim S_5C_1R_4$	45˚, 90˚, 135˚, 180˚	0.25	1.00	0.36392
	$S_5C_2R_1 \sim S_5C_2R_4$	45˚, 90˚, 135˚, 180˚	0.50	1.00	0.72780
S_6	$S_6C_1R_1 \sim S_6C_1R_4$	45˚, 90˚, 135˚, 180˚	0.25	1.25	0.45490
	$S_6C_2R_1 \sim S_6C_2R_4$	45˚, 90˚, 135˚, 180˚	0.50	1.25	0.90975
S_7	$S_7C_1R_1 \sim S_7C_1R_4$	45˚, 90˚, 135˚, 180˚	0.25	1.50	0.54588
	$S_7C_2R_1 \sim S_7C_2R_4$	45˚, 90˚, 135˚, 180˚	0.50	1.50	1.09170

Here, in Table 3, R_1, R_2, R_3 and R_4 represents simulation run for 45˚, 90˚, 135˚ and 180˚ bend angles of meanders, respectively. S_1, S_2, S_3, S_4, S_5, S_6 and S_7 stands for the series numbers having channel widths of 0.15m, 0.25m, 0.50m, 0.75m, 1.00m, 1.25m and 1.50m, respectively. C_1 and C_2 are the cases of simulation for Froude numbers of 0.25 and 0.50.

3 RESULTS AND DISCUSSIONS

The meander length of models varied with channel widths, as the ratio of meander length to width of the channel was taken to be a constant value of 30. Number of grids in the longitudinal and transverse direction was 161 and 21 respectively. At the sidewall locations, the logarithmic law was encountered in the numerical solution. Boundary conditions were set up by inserting a constant discharge at upstream and a constant depth at the downstream end. Seven sections of 1-1, 2-2, 3-3, 4-4, 5-5, 6-6 and 7-7 were considered as illustrated in Figure 2.

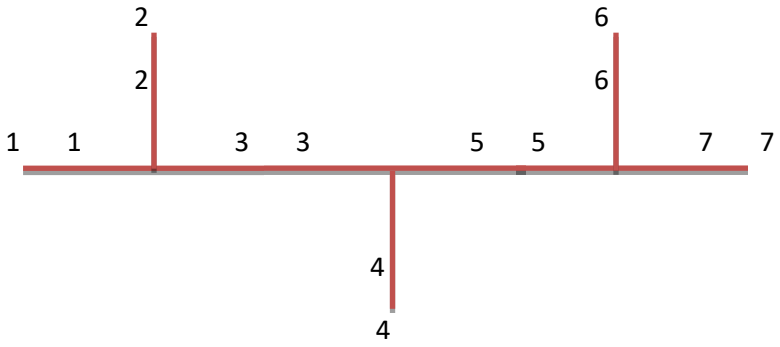

Figure 2: Sections taken for simulation.

3.1 Simulated Flow Profiles

Figure 3 shows that the value of depth was high for the outer concave end in comparison with the inner convex end and the center of the channel. Thus it developed a transverse water surface slope. And from the velocity vectors in Figure 3, it is evident that the velocity vectors were high in inner convex end and low in outer concave end. The value range of water surface elevation was higher for higher Froude number (0.50) than lower Froude number (0.25).

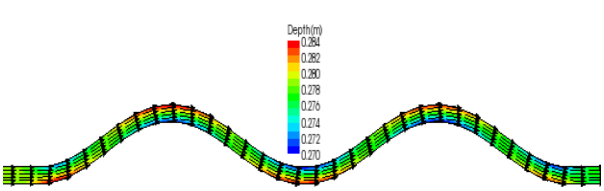

(a) (Case $S_1C_1R_1$).

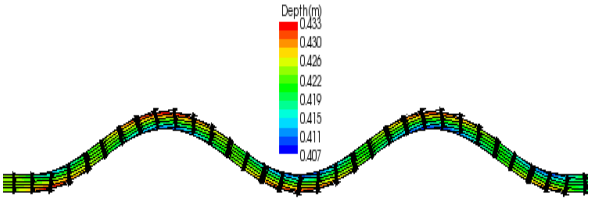

(b) (Case $S_1C_2R_1$).

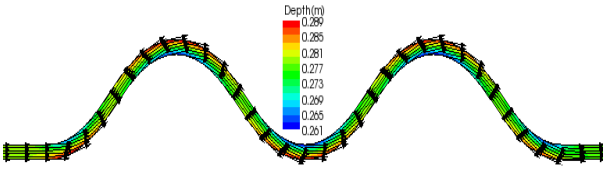

(c) (Case $S_1C_1R_2$).

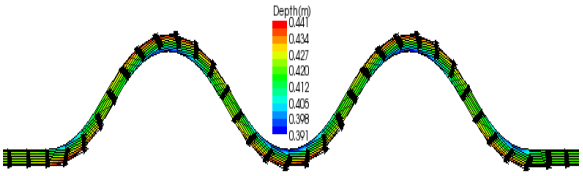

(d) (Case $S_1C_2R_2$).

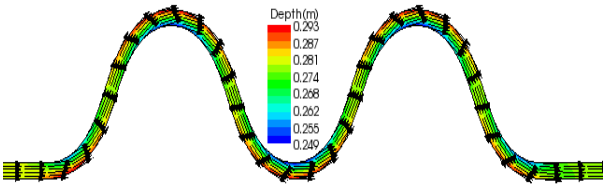

(e) (Case $S_1C_1R_3$).

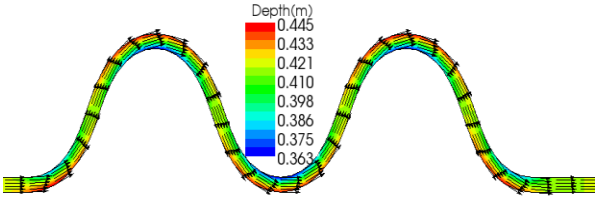

(f) (Case $S_1C_2R_3$).

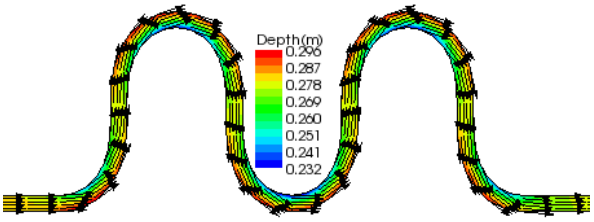

(g) (Case $S_1C_1R_4$).

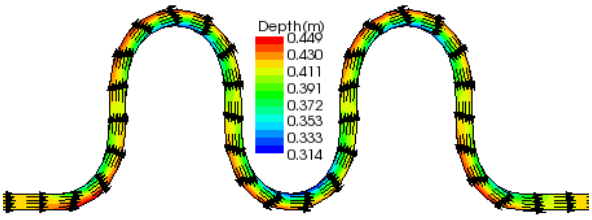

(h) (Case $S_1C_2R_4$).

Figure 3: Simulated velocity vectors superimposed with depth contour for cases $(S_1C_1R_1 \sim S_1C_1R_4)$ and $(S_1C_2R_1 \sim S_1C_2R_4)$.

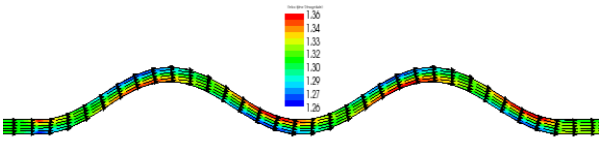

(a) (Case $S_1C_1R_1$).

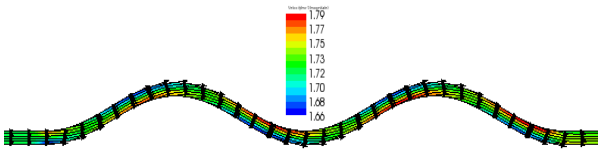

(b) (Case $S_1C_2R_1$).

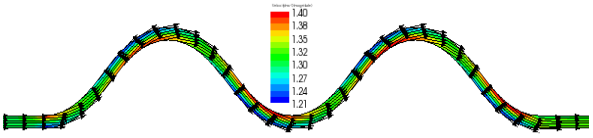

(c) (Case $S_1C_1R_2$).

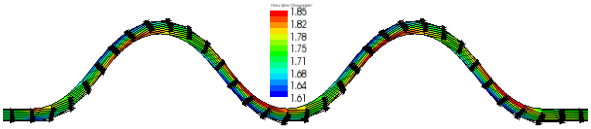

(d) (Case $S_1C_2R_2$).

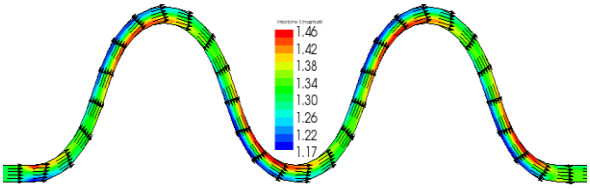

(e) (Case $S_1C_1R_3$).

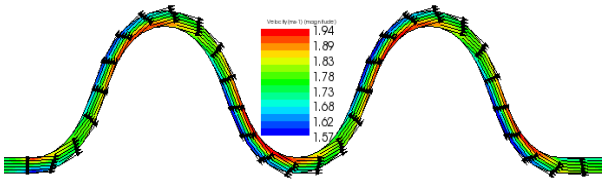

(f) (Case $S_1C_2R_3$).

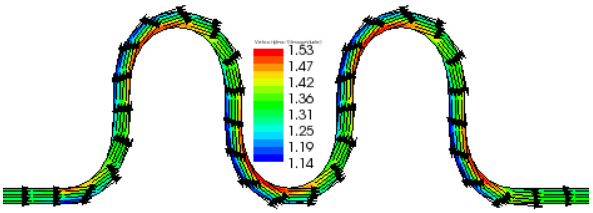

(g) (Case $S_1C_1R_4$).

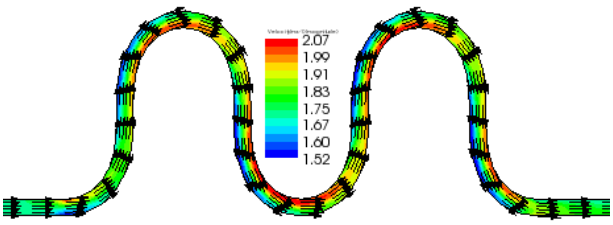

(h) (Case $S_1C_2R_4$).

Figure 4: Simulated velocity vectors superimposed with velocity contour for cases ($S_1C_1R_1$~$S_1C_1R_4$) and ($S_1C_2R_1$~$S_1C_2R_4$).

Figure 4 shows that the velocity in the outer bank was lower while the velocity at the inner bank was higher. The velocity at the center of the channel was higher than that of the velocity magnitude at the outer bank. And from the velocity vectors in Figure 4, it is evident that the velocity vectors were high in inner convex end and low in outer concave end. The value range of velocity magnitude was higher for 0.50 Fr number than 0.25 Fr number.

3.2 Transverse Slope in Water Surface

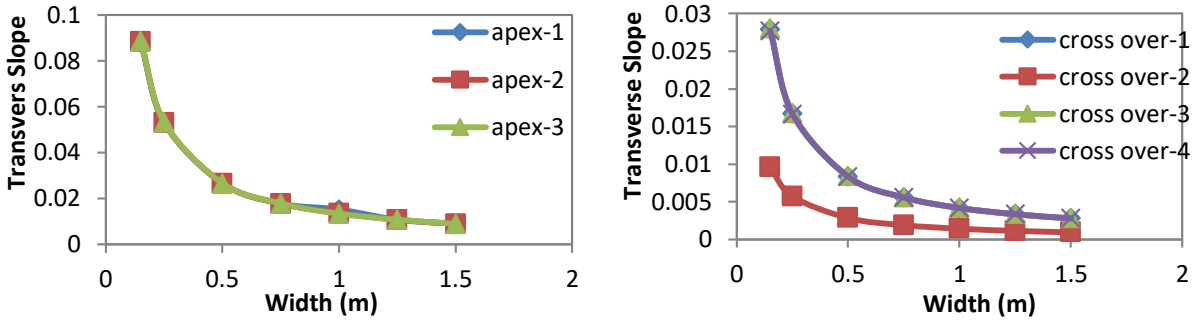

(a) $(S_1C_1R_1 \sim S_7C_1R_1)$. (b) $(S_1C_1R_1 \sim S_7C_1R_1)$.

Figure 5: Transverse slope at apex points and cross-over points for different values of widths having meandering length (M_L/W), Radius of Curvature (R/W) and Froude numbers are constant.

From Figure 5, it was found that the transverse slope of water surface at the cross over sections of a meander was lower than that of the apex points The transverse slope was found to decrease with the increase of width of the channel. It was found out that the change in transverse slope of water surface varied rapidly for channel widths between (0.15-0.75)m while the change in transverse slope was gradual for width of channel greater than 0.75m.

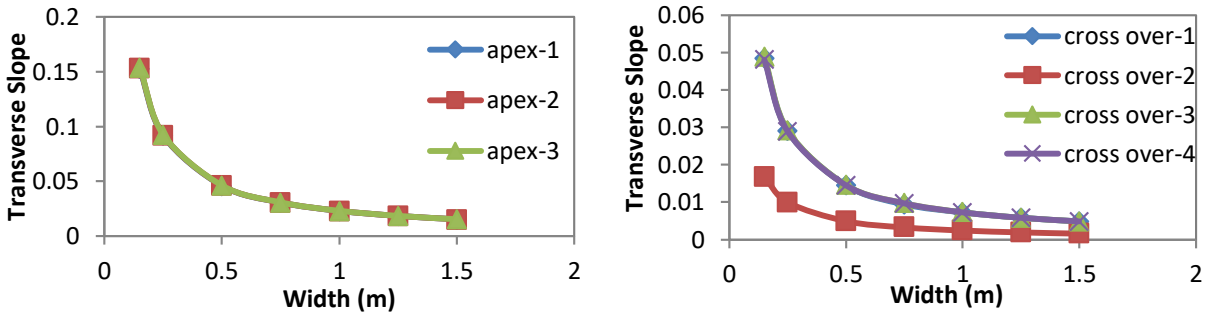

(a) $(S_1C_2R_1 \sim S_7C_2R_1)$. (b) $(S_1C_2R_1 \sim S_7C_2R_1)$.

Figure 6: Transverse slope-width graph at apex points and cross over points of meander bend.

Figure 6 shows that the transverse slope of water surface at the cross over points of a bend was lower than that of the apex points. The transverse slope was found to decrease with the increase of width of the channel. It was found out that the change in transverse slope of water surface varied rapidly for channel widths between (0.15-0.75)m while the change in transverse slope was gradual for width of channel greater than 0.75m.

It was also observed that the transverse slope of water surface at the apex points and cross over points of a meander bend for Froude number 0.50 was higher than that of the transverse slope of water surface with Froude number value of 0.25.

Table 4 shows the value range of transverse slope of water surface for the numerical test cases that were run for simulation of flow.

Table 4: Change in transverse slope of water surface for different test cases.

Case No.	At apex point-1	At apex point-2	At apex point-3	At cross over point-1	At cross over point-2	At cross over point-3	At cross over point-4
$S_1C_1R_1$ ~ $S_7C_1R_1$	0.0881 ~ 0.00883	0.08835 ~ 0.00884	0.08856~ 0.00885	0.0279 ~ 0.0028	0.00961~ 0.00095	0.02803~ 002795	0.02771~ 0.00278
$S_1C_2R_1$ ~ $S_7C_2R_1$	0.15269 ~ 0.01536	0.15337 ~ 0.15337	0.15394 ~ 0.0154	0.04842 ~ 0.00485	0.01679 ~ 0.00165	0.0488 ~ 0.00486	0.04804 ~ 0.00483
$S_1C_1R_2$ ~ $S_7C_1R_2$	0.17873 ~ 0.01771	0.17962 ~ 0.01776	0.17998 ~ 0.01784	0.05581 ~ 0.00553	0.01921 ~ 0.00189	0.05613 ~ 0.00556	0.05555 ~ 0.00554
$S_1C_2R_2$ ~ $S_7C_2R_2$	0.31267 ~ 0.03077	0.31457 ~ 0.03089	0.31494 ~ 0.03107	0.09763 ~ 0.00957	0.03385 ~ 0.00326	0.09826 ~ 0.00965	0.0966 ~ 0.00961
$S_1C_1R_3$ ~ $S_7C_1R_3$	0.27699 ~ 0.02672	0.27901 ~ 0.0269	0.27879 ~ 0.02714	0.08439 ~ 0.00816	0.02903 ~ 0.00278	0.08478 ~ 0.00825	0.08388 ~ 0.00827
$S_1C_2R_3$ ~ $S_7C_2R_3$	0.49898 ~ 0.04635	0.50246 ~ 0.04678	0.49752 ~ 0.04737	0.15123 ~ 0.01406	0.05234 ~ 0.00481	0.15121 ~ 0.01431	0.14703 ~ 0.01431
$S_1C_1R_4$ ~ $S_7C_1R_4$	0.36906 ~ 0.03586	0.39402 ~ 0.03631	0.39139 ~ 0.03688	0.11405 ~ 0.01063	0.0392 ~ 0.00361	0.11439 ~ 0.01082	0.11302 ~ 0.01093
$S_1C_2R_4$ ~ $S_7C_2R_4$	0.72637 ~ 0.0619	0.74847 ~ 0.06297	0.73319 ~ 0.06438	0.20847~ 0.01814	0.07385~ 0.01866	0.22014 ~ 0.01866	0.20205~ 0.01883

4 CONCLUSIONS

The flow fields of the channels with 45˚, 90˚, 135˚ and 180˚ bend angles with 0.15m, 0.25m, 0.50m, 0.75m, 1m, 1.25m and 1.5m channel widths were successfully simulated by using the two dimensional flow simulation software of iRIC Nays2DH. The changes of transverse slope, velocity and water surface elevation due to different geometric conditions of the channels were found out by using this software. The simulation results showed that the water surface elevation at the outer bank was higher than the inner bank. From the velocity profiles, it was observed that velocity at outer bank was lower than the inner bank. It is found that, there is an increase in transverse slope of water surface due to the increase in meandering angles and Froude numbers while it decreased with increasing channel widths having meandering length (M_L/W), Radius of Curvature (R/W) and Froude numbers are constant. It was also observed that the transverse slope of water surface at the apex and cross over points of a meander was higher for Froude number 0.50 than that of the transverse slope of water surface with Froude number value of 0.25. It can be concluded that the iRIC Nays2DH software is suitable for simulating the flow field at bends and as well as at straight portions.

REFERENCES

Ahmed, M. M., Ayyoubzadeh, S.A., Namin, M. M. and Samani, J.M.V. (2009). "A 2D depthaveraged model for simulating and examining unsteady flow patterns in open channel bend". Department of Water Structures Engineering, College of Agriculture, Tarbiat Modares University, P.O. Box: 14115-336, Tehran, Islamic Republic of Iran.

Ali, M. S. Lemon, M. H. R., and Talukder, M. A. Q. (2014) "Two dimensional simulation of flows in bends of an open channel by iRIC Nays2D", Proceedings of the 2nd International Conference on Civil Engineering for Sustainable Development (ICCESD-2014), 14~16 Feb., KUET, Bangladesh, pp. 103-104 of Ext. Abstract Proc. (Full paper in CD-ROM).

De-Vriend, H.J. and H.J. Geoldof, (1983). "Main flow velocity in Short River bends". Journal of Hydraulic Engineering, ASCE, 109: 991-1011.

Kim, T.B. and Choi, S.U. (2003). "Experiment on numerical simulations of open-channel flows in a bend using the finite element method". School of Civil and Environmental Engineering, Yonsei University, Seoul, Korea.

Leschziner, M.A. and Rodi, W. (1979). "Calculation of strongly curved open channel flow". Journal of Hydraulic Engineering, ASCE, 105: 1297-1314.

Rozovskii, I.L. (1961). "Flow of water in bends of open channels". Academy of Sciences of the Ukrainian SSR, Kiev, Israel Program for Scientific Translation, Jerusalem.

Science, C. R. (2014) 'iRIC Software Nays2DH Solver Manual'.

Shimizu, Y. and Takebayashi, H. (2014). "iRIC software Nays2DH solver manual", Nays2DH development team, Japan.